frontiers | Research Topics

Investigating novel mechanisms and treatments of metabolic disorders associated with cardiovascular disease

Edited by
Wei Liu, Jian Shi and Han Xiao

Published in
Frontiers in Cardiovascular Medicine

ISSN 1664-8714
ISBN 978-2-83251-543-3
DOI 10.3389/978-2-83251-543-3

About Frontiers

Frontiers is more than just an open access publisher of scholarly articles: it is a pioneering approach to the world of academia, radically improving the way scholarly research is managed. The grand vision of Frontiers is a world where all people have an equal opportunity to seek, share and generate knowledge. Frontiers provides immediate and permanent online open access to all its publications, but this alone is not enough to realize our grand goals.

Frontiers journal series

The Frontiers journal series is a multi-tier and interdisciplinary set of open-access, online journals, promising a paradigm shift from the current review, selection and dissemination processes in academic publishing. All Frontiers journals are driven by researchers for researchers; therefore, they constitute a service to the scholarly community. At the same time, the *Frontiers journal series* operates on a revolutionary invention, the tiered publishing system, initially addressing specific communities of scholars, and gradually climbing up to broader public understanding, thus serving the interests of the lay society, too.

Dedication to quality

Each Frontiers article is a landmark of the highest quality, thanks to genuinely collaborative interactions between authors and review editors, who include some of the world's best academicians. Research must be certified by peers before entering a stream of knowledge that may eventually reach the public - and shape society; therefore, Frontiers only applies the most rigorous and unbiased reviews. Frontiers revolutionizes research publishing by freely delivering the most outstanding research, evaluated with no bias from both the academic and social point of view. By applying the most advanced information technologies, Frontiers is catapulting scholarly publishing into a new generation.

What are Frontiers Research Topics?

Frontiers Research Topics are very popular trademarks of the *Frontiers journals series*: they are collections of at least ten articles, all centered on a particular subject. With their unique mix of varied contributions from Original Research to Review Articles, Frontiers Research Topics unify the most influential researchers, the latest key findings and historical advances in a hot research area.

Find out more on how to host your own Frontiers Research Topic or contribute to one as an author by contacting the Frontiers editorial office: frontiersin.org/about/contact

Investigating novel mechanisms and treatments of metabolic disorders associated with cardiovascular disease

Topic editors

Wei Liu — The University of Manchester, United Kingdom
Jian Shi — University of Leeds, United Kingdom
Han Xiao — Peking University Third Hospital, China

Citation

Liu, W., Shi, J., Xiao, H., eds. (2023). *Investigating novel mechanisms and treatments of metabolic disorders associated with cardiovascular disease*.
Lausanne: Frontiers Media SA. doi: 10.3389/978-2-83251-543-3

Table of contents

frontiers in Cardiovascular Medicine

BRIEF RESEARCH REPORT
published: 02 February 2022
doi: 10.3389/fcvm.2022.840358

Targeting ApoC3 Paradoxically Aggravates Atherosclerosis in Hamsters With Severe Refractory Hypercholesterolemia

Yitong Xu[1†], Jiabao Guo[2†], Ling Zhang[2†], Guolin Miao[2], Pingping Lai[2], Wenxi Zhang[2], Lili Liu[3], Xinlin Hou[3], Yuhui Wang[2], Wei Huang[2], George Liu[2], Mingming Gao[1] and Xunde Xian[2,4*]*

[1] Laboratory of Lipid Metabolism, Institute of Basic Medicine, Hebei Medical University, Shijiazhuang, China, [2] Institute of Cardiovascular Sciences and Key Laboratory of Molecular Cardiovascular Sciences, Ministry of Education, School of Basic Medical Sciences, Peking University, Beijing, China, [3] Department of Pediatrics, Peking University First Hospital, Beijing, China, [4] Beijing Key Laboratory of Cardiovascular Receptors Research, Peking University Third Hospital, Beijing, China

OPEN ACCESS

Edited by:
Wei Liu,
The University of Manchester, United Kingdom

Reviewed by:
Yue Wu,
The First Affiliated Hospital of Xi'an Jiaotong University, China
Linzhang Huang,
Fudan University, China

***Correspondence:**
Mingming Gao
g.m0515@163.com
Xunde Xian
xianxunde@bjmu.edu.cn

† These authors have contributed equally to this work

Specialty section:
This article was submitted to Cardiovascular Metabolism, a section of the journal Frontiers in Cardiovascular Medicine

Received: *21 December 2021*
Accepted: *03 January 2022*
Published: *02 February 2022*

Citation:
Xu Y, Guo J, Zhang L, Miao G, Lai P, Zhang W, Liu L, Hou X, Wang Y, Huang W, Liu G, Gao M and Xian X (2022) Targeting ApoC3 Paradoxically Aggravates Atherosclerosis in Hamsters With Severe Refractory Hypercholesterolemia. Front. Cardiovasc. Med. 9:840358. doi: 10.3389/fcvm.2022.840358

Rationale: ApoC3 plays a central role in the hydrolysis process of triglyceride (TG)-rich lipoproteins mediated by lipoprotein lipase (LPL), which levels are positively associated with the incidence of cardiovascular disease (CVD). Although targeting ApoC3 by antisense oligonucleotide (ASO), Volanesorsen markedly reduces plasma TG level and increase high-density lipoprotein cholesterol (HDL-C) in patients with hypertriglyceridemia (HTG), the cholesterol-lowering effect of ApoC3 inhibition and then the consequential outcome of atherosclerotic cardiovascular disease (ASCVD) have not been reported in patients of familial hypercholesterolemia (FH) with severe refractory hypercholesterolemia yet.

Objective: To investigate the precise effects of depleting ApoC3 on refractory hypercholesterolemia and atherosclerosis, we crossed ApoC3-deficient hamsters with a background of LDLR deficiency to generate a double knockout (DKO) hamster model (LDLR$^{-/-}$, XApoC3$^{-/-}$, DKO).

Approach and Results: On the standard laboratory diet, DKO hamsters had reduced levels of plasma TG and total cholesterol (TC) relative to LDLR$^{-/-}$ hamsters. However, upon high-cholesterol/high-fat (HCHF) diet feeding for 12 weeks, ApoC3 deficiency reduced TG level only in female animals without affecting refractory cholesterol in the circulation, whereas apolipoprotein A1 (ApoA1) levels were significantly increased in DKO hamsters with both genders. Unexpectedly, loss of ApoC3 paradoxically accelerated diet-induced atherosclerotic development in female and male LDLR$^{-/-}$ hamsters but ameliorated fatty liver in female animals. Further analysis of blood biological parameters revealed that lacking ApoC3 resulted in abnormal platelet (PLT) indices, which could potentially contribute to atherosclerosis in LDLR$^{-/-}$ hamsters.

Conclusions: In this study, our novel findings provide new insight into the application of ApoC3 inhibition for severe refractory hypercholesterolemia and ASCVD.

Keywords: ApoC3, atherosclerosis, LDLR, Syrian golden hamster, hypertriglyceridemia

HIGHLIGHTS

- ApoC3 deficiency reduces plasma triglyceride and total cholesterol levels in female and male LDLR$^{-/-}$ hamsters on a standard laboratory diet.
- Loss of ApoC3 only lowers circulating triglyceride level in female LDLR$^{-/-}$ hamsters without affecting severe refractory hypercholesterolemia after high-cholesterol/high-fat diet feeding.
- Targeting ApoC3 paradoxically exacerbates diet-induced atherosclerosis in LDLR$^{-/-}$ hamsters independent of gender, but only protects against fatty liver in female animals.

INTRODUCTION

Elevated triglyceride (TG) levels caused by genetic or environmental factors are positively associated with the increased incidence of atherosclerotic cardiovascular disease (ASCVD) and acute pancreatitis (AP) (1). Lipoprotein lipase (LPL) is a key rate-limiting enzyme that plays a central role in modulating TG metabolism. Loss-of-function mutations in the *LPL* gene cause severe hypertriglyceridemia (HTG) (2). To our knowledge, several important regulators of LPL enzymatic activity have been identified in the past decades, including activators such as apolipoprotein C-II (ApoC2) and apolipoprotein A-V (ApoA5), and inhibitors such as apolipoprotein C-III (ApoC3) and angiopoietin-like 3/4/8 (ANGPTL3/4/8). Although functional studies show that ApoC2 and ApoA5 are required for LPL-mediated TG hydrolysis process *in vitro* and *in vivo*, overexpression of human ApoC2 in mice unexpectedly elicits HTG and ApoA5-deficient mice have no obvious HTG under the condition of regular standard diet (3), implying that TG metabolism is complicated *in vivo* and HTG cannot be solved when only targeting activators involved in LPL activity.

Unlike the contradictory data from the LPL activator, abrogating the inhibitory effects of ApoC3 and ANGPTLs on LPL activity consistently reduces circulating TG levels, thus yielding promising outcomes of dyslipidemia in different experimental animal models (4). Recently, ANGPTL3 and ApoC3 have been reported to be potential therapeutic targets for the treatment of HTG in clinical trials. For example, evinacumab, an antibody that inhibits ANGPTL3 not only reduces TG level in circulation by enhancing LPL activity but also significantly decreases low-density lipoprotein cholesterol (LDL-C) in patients with familial hypercholesterolemia (FH) in two independent phase 3 trials (5, 6). However, although targeting ApoC3 by antisense oligonucleotide (ASO), volanesorsen, markedly reduces plasma TG level in patients with HTG (7, 8), the cholesterol-lowering effect of ApoC3 inhibition and then the consequential outcomes of atherosclerotic cardiovascular disease (ASCVD) have not been reported yet in patients with FH so far.

Previously, using CRISPR/Cas9 editing our group deleted the *Apoc3* gene from the Syrian golden hamster model that replicates human metabolic features, and we found that lack of ApoC3 significantly decreased plasma TG and total cholesterol (TC) levels, meanwhile increased high-density lipoprotein cholesterol (HDL-C) in hamsters fed with high-cholesterol/high-fat (HCHF) diet (9), suggesting that ApoC3 deficiency ameliorates diet-induced combined dyslipidemia. However, in agreement with the observations from the clinical trials, whether the beneficial effect of lacking ApoC3 relies on the presence of low-density lipoprotein receptor (LDLR) and whether ApoC3 inhibition can be applied for the treatment of severe refractory hypercholesterolemia and atherosclerosis due to LDLR deficiency still needs to be elucidated. In this study, we crossed ApoC3-deficient hamsters with a background of LDLR deficiency to generate a double knockout (DKO) hamster model (LDLR$^{-/-}$ XApoC3$^{-/-}$, DKO) and investigated the role of ApoC3 inhibition in lipid metabolism and atherosclerosis in the hamster model of FH. Our experimental evidence provides new insight into the possibility that ApoC3 will be a potential therapeutic target for the treatment of FH and atherosclerosis.

MATERIALS AND METHODS

Animals

Golden Syrian hamsters were purchased from Vital River Laboratories (Beijing, China). Homozygous LDLR-deficient (LDLR$^{-/-}$) hamsters and ApoC3$^{-/-}$ hamsters were generated by CRISPR/ Cas9 genetic editing system in our laboratory as described previously (9, 10). In this study, ApoC3$^{-/-}$ hamsters were crossed with LDLR$^{-/-}$ hamsters to obtain homozygous double mutant animals (DKO), and LDLR$^{-/-}$ hamsters were used as a control. The animals were maintained on a 14-h light/10-h dark cycle at 24°C and fed either a standard laboratory diet or HCHF diet (0.5% cholesterol and 20% fat) with water *ad libitum*. Both male and female animals were used in our study. All procedures were followed to the guidelines of Laboratory Animal Care (NIH Publication No. 85Y23, revised 1996), and the experimental protocol was approved by the Animal Care Committee, Peking University Health Science Center (LA2015-012).

The Assays of Plasma Lipids and (Apo)Lipoproteins

Blood samples were collected from the retro-orbital plexus of the hamsters after 12-h fasting under isoflurane anesthesia. The plasma TC and TG levels were determined enzymatically using commercially available kits (Zhongsheng Beikong, Beijing) as described previously (9).

To analyze the lipid distribution, fast protein liquid chromatography (FPLC) of plasma lipoproteins was performed using 200 μl of pooled plasma samples from 6 animals with indicated genotypes, which were filtered by 0.22-mm filters and then applied to Tricorn high-performance Superose S-6

Abbreviations: ApoA1, apolipoprotein A1; ApoB, apolipoprotein B; ApoE, apolipoprotein E; ApoC3, apolipoprotein C3; HDL, high-density lipoprotein; LDL, low-density lipoprotein; LDLR, low-density lipoprotein receptor; VLDL, very low-density lipoprotein; FH, familial hypercholesterolemia; HCHF, high cholesterol/high fat; LPL, lipoprotein lipase; TG, triglyceride; HTG, hypertriglyceridemia; ASCVD, atherosclerotic cardiovascular disease.

10/300GL columns (Amersham Biosciences), eluting with PBS at a constant flow rate of 0.25 ml/min. Eluted fractions (500 μl per fraction) were assessed for TG and cholesterol concentrations using the same TG and cholesterol kits as described above.

Western Blots

The concentrations of apolipoprotein B (ApoB), apolipoprotein E (ApoE), and apolipoprotein A1 (ApoA1) in eluted fractions were detected by western blots. Briefly, every 3 consecutive fractions were equally pooled together, and 15 μl of pooled fractions was mixed with 4X SDS loading buffer (0.1 M Tris-HCl, 724 pH 6.8, 2% SDS, 5% β-mercaptoethanol, 10% glycerol, and 0.05% bromophenol blue). The mixtures were boiled at 95°C for 10 min. Proteins were separated by 4–20% SDS-PAGE and transferred to a nitrocellulose membrane for western blotting using different antibodies against ApoB, ApoE, and ApoA1. The following antibodies were used: ApoA1 (sc-30089, Santa Cruz Biotechnology, USA, rabbit polyclonal IgG, 1:1,000), ApoE (178479, Millipore, goat polyclonal IgG, 1:5,000), and ApoB (178467, Millipore, goat polyclonal IgG, 1:5,000).

Pathological Analysis

To investigate atherosclerotic lesions and lipid accumulation in different tissues, all animals fed with HCHF diet for 16 weeks were perfused with cold (phosphate-buffered saline) PBS and then fixed by 4% paraformaldehyde PFA. The whole aorta, heart, and liver were harvested and embedded in OCT solution. A total of 10 μm of frozen cross-sectioned slices of aortic root and liver was used for morphological analysis. The atherosclerotic plaques in whole aortas (en-face) and cross-sectioned slices were visualized using 0.3% oil red O (ORO) solution (Sigma-Aldrich, St. Louis, MO, USA).

For immunofluorescence staining, the cluster of differentiation 68 (CD68) and ApoB in aortic root and liver were analyzed using primary antibodies against CD68 (1:100 rabbit polyclonal IgG; BA3638, BOSTER, California, USA) and ApoB antibody (1:100 goat polyclonal IgG; 178467, Millipore, Massachusetts, USA), respectively. The slices were then incubated with appropriate biotinylated second antibodies [1:100, Donkey anti-Goat IgG (H+L) Cross-Adsorbed Secondary Antibody, Alexa Fluor 633; Alexa Fluor 555; Thermo Fisher, Massachusetts, USA).

Test of Blood Biochemical Parameters

A total of 20 μl of fresh blood samples was used for the measurement of the following biochemical parameters: the count platelet (PLT) count, mean platelet volume (MPV), platelet distribution width (PDW), and plateletcrit (PCT).

Lecithin–Cholesterol Acyltransferase Activity Assays

Lecithin–cholesterol acyltransferase (LCAT) activity was performed using a commercial kit (Sigma, MAK107-1KT). The fluorometric substrates were incubated with 4 μl plasma from LDLR$^{-/-}$ and DKO hamsters at 37°C for 2.5 h. The heat-inactivated plasma was used as a negative control to eliminate endogenous autofluorescence interference. The emission spectrum of the substrate reagent showed two distinct peaks at 390 and 470 nm, respectively. After hydrolysis of the substrate by LCAT, the fluorescence signal of 390/470 was increased. LCAT activity was evaluated by a change in the ratio of fluorescence intensity at 390 to 470 nm after excluding the value of endogenous autofluorescence.

STATISTICAL ANALYSIS

All data were expressed as the mean ± SEM and evaluated using two-tailed Student's *t*-test for two groups with one variable tested and equal variances, one-way ANOVA with Dunnett's *post-hoc* or Tukey's *post-hoc* for multiple groups with only variable tested, or two-way ANOVA with Sidak's *post-hoc* for plaque quantification. The differences were considered to be significant at $p < 0.05$. The software used for data analysis was ImageJ (NIH) and Prism 8.0 (GraphPad Software).

RESULTS

Effects of Depleting ApoC3 on Plasma Lipid Metabolism in LDLR$^{-/-}$ Hamsters Under Different Dietary Conditions

To investigate the cholesterol-lowering effect of depleting ApoC3 in hamsters, in this study, we crossed ApoC3-deficient hamsters with a background of LDLR deficiency to generate a DKO hamster model (**Figures 1A,B**). At the age of 12 weeks, both LDLR$^{-/-}$ hamsters and DKO hamsters with different genders on standard laboratory diet were switched to the HCHF diet for another 16 weeks to study diet-induced obesity, dyslipidemia, and atherogenesis (**Figure 1C**). We found that ApoC3 deficiency did not accelerate obesity in DKO hamsters when compared to controls (**Figure 1D**). Before the HCHF diet challenge, both female and male DKO hamsters on standard laboratory diet showed lower levels of TG and TC in plasma (754 mg/dl vs. 1272 mg/dl in females, 868 mg/dl vs. 1453 mg/dl in males). Consistently, lipoprotein distribution analysis by FPLC demonstrated that the contents of TG and cholesterol in VLDL particles were significantly reduced in DKO hamsters compared to LDLR$^{-/-}$ hamsters (**Supplementary Figure 1**). However, there were no significant differences in plasma TC levels between two genotypes on the HCHF diet for 12 weeks, but only TG level was partially decreased by 85% in female DKO relative to corresponding controls (**Figure 1E**). Next, to avoid the obstruction of FPLC by very large TG-rich lipoprotein particles caused by HCHF diet application, we removed chylomicrons from our pooled plasma samples and found that only female DKO hamsters consistently showed reduced contents of TG in VLDL fractions but no changes in LDL and HDL fractions (**Figure 1F**). Additionally, western blots demonstrated that compared to LDLR$^{-/-}$ hamsters, lacking ApoC3 significantly increased ApoA1 levels; however, ApoB and ApoE were not altered in both female and male DKO hamsters (**Figure 1F**). ApoC3 has been reported to be an inhibitor of LCAT activity in the previous study (11). Therefore, we measured the LCAT activity in our hamster model after HCHF diet feeding. We found

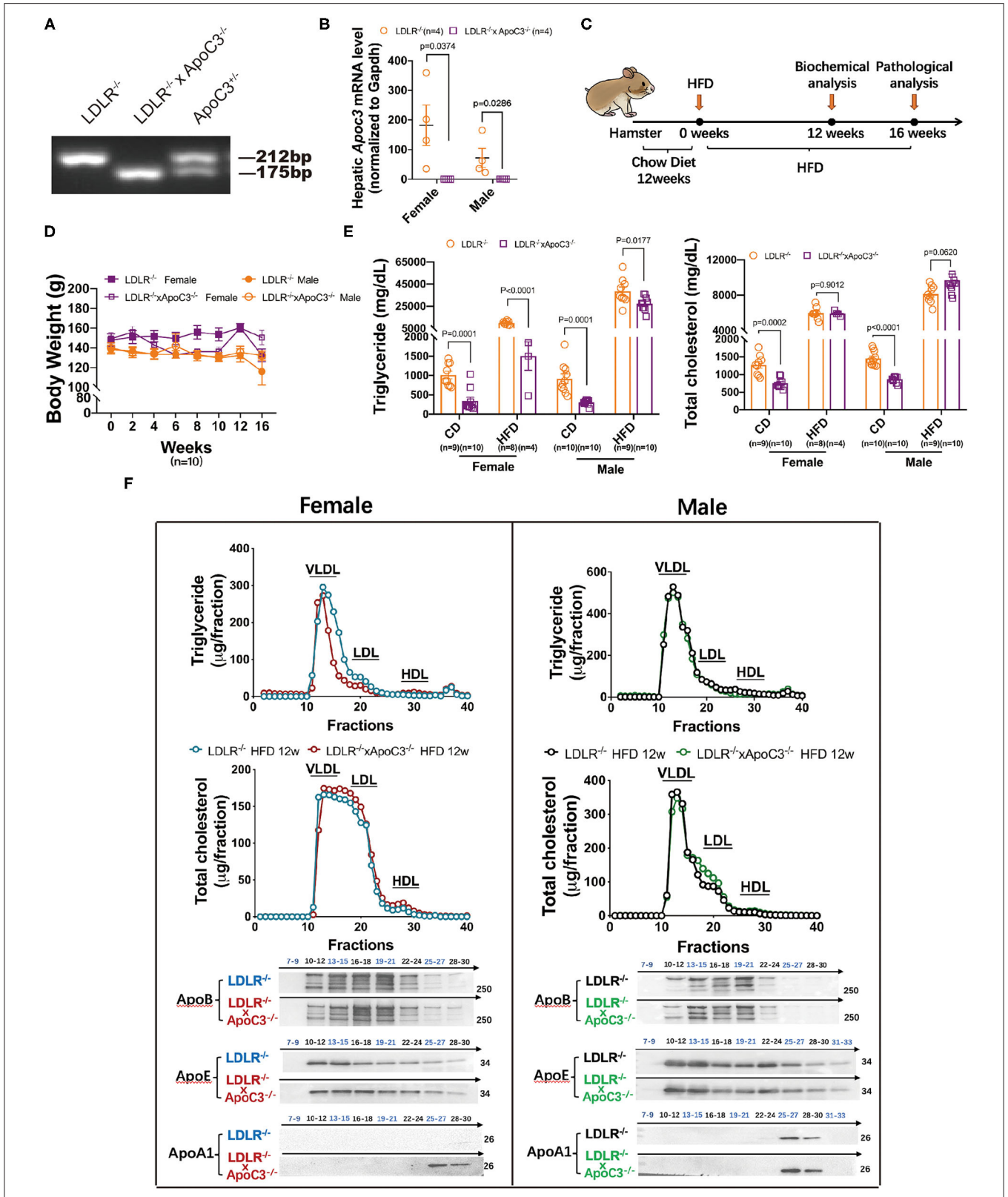

FIGURE 1 | Effects of ApoC3 deficiency on lipid metabolism in LDLR$^{-/-}$ hamsters. **(A)** Generation of DKO hamster model. **(B)** Hepatic *Apoc3* mRNA expression levels were determined in indicated animals on chow at 12 weeks old. **(C)** Timeline of the whole experiments in this study. High-cholesterol/high-fat diet (HCHF) contains 0.5% cholesterol and 20% fat. **(D)** Measurement of body weight during the 16-week experiment. **(E)** Fasting plasma TG and TC levels in the indicated animal

(Continued)

FIGURE 1 | on chow or HCHF diet. **(F)** The distribution of TG and cholesterol in pooled plasma samples from the indicated animals after 12-week HCHF diet feeding and representative western blots of ApoB, ApoE, and ApoA1 in eluted fractions. $n = 4$–5/group. Data are expressed as mean ± SEM, analyzed by two-way ANOVA or Student's *t*-test after D'Agostino–Pearson's normality test using Prism 8.0.

that compared to the corresponding LDLR$^{-/-}$ hamsters, female and male DKO hamsters showed an increase in LCAT activity by 1.23 and 1.25 (ratio of fluorescence intensity at 390–470 nm), respectively. These data suggested that targeting ApoC3 could differentially influence lipid metabolism depending on gender and dietary intervention.

ApoC3 Deficiency Aggravates HCHF Diet-Induced Atherosclerosis in LDLR$^{-/-}$ Hamsters but Protects Against Fatty Liver Only in Female LDLR$^{-/-}$ Hamsters

Previously, our group found that ApoC3 deficiency generated favorable lipoprotein profiles, then protecting against diet-induced atherosclerosis in hamster (9); however, whether ApoC3 inhibition still executed long-term beneficial function in atherosclerosis, a major event in FH with hypercholesterolemia due to lacking LDLR. Surprisingly, in HCHF-fed animals, we found that both female and male DKO hamsters developed more atherosclerotic plaques in the whole aorta when compared to the corresponding LDLR$^{-/-}$ hamsters (46.04 vs. 16.25% in females; 27.14 vs. 10.64% in males; **Figures 2A,B**). Consistent with the results of atherosclerotic plaques observed in the whole aorta, the areas of atherosclerotic lesions in aortic roots were also significantly increased in DKO hamsters relative to control animals (6.7×10^5 μm vs. 1.9×10^5 μm in females; 3.5×10^5 μm vs. 1.7×10^5 μm in males; **Figures 2C,D**). To better understand the composition of atherosclerotic lesions, we performed immunofluorescence staining to analyze ApoB and CD68, two key markers of lipid-loaded macrophages accumulated in atherosclerotic lesions (**Figure 2E**). Our data showed that more ApoB and CD68 were discovered in the lesions of DKO hamsters regardless of gender, demonstrating that loss of ApoC3 paradoxically accelerated atherosclerotic development in both female and male DKO hamsters in a lipid-independent manner, accompanied by abnormal infiltration of lipid-loaded macrophages. Recently, the approach trial using volanesorsen showed thrombocytopenia in patients of familial chylomicronemia syndrome (FCS), who received ASO-mediated inhibition of ApoC3. Thus, it was rational for us to determine PLT indices in our animal model, which have been reported to play an essential role in atherosclerosis. We measured the number of PLT, MPV, PDW, and PCT and found that platelet indices were abnormal to some extent in both female and male DKO hamsters when compared to the corresponding LDLR$^{-/-}$ hamsters, implying that abnormal platelet function could be a potential contributor to atherosclerosis in our study.

Since the relationship between ApoC3 and fatty liver is still elusive in different mouse models, we also studied the hepatic morphology in our hamster model. ORO staining revealed that hepatic lipid accumulation was markedly increased in female DKO hamsters compared to LDLR$^{-/-}$ hamsters with the same gender, but no obvious difference was observed in male animals (**Figures 2F,G**). In agreement with the findings of lipid contents stained by ORO, immunoflurorescent detection of ApoB and CD68 in the liver showed that hepatic ApoB and CD68 levels were significantly reduced in only female DKO hamsters (**Figures 2H,I**), accompanied by a reduced level of aspartate aminotransferase (AST), one of the predictors of liver injury (**Figure 2J**).

DISCUSSION

Although ApoC3 inhibition has been applied for the treatment of HTG in different clinical trials, however, unlike ANGPTL3, an inhibitory regulator of LPL activity was recently accepted as a potential therapeutic target for both HTG and hypercholesterolemia, whether targeting ApoC3 has beneficial effects on refractory hypercholesterolemia and consequential outcome of atherogenesis in the context of FH due to dysfunctional LDLR is still elusive. In this study, we developed a DKO hamster model lacking both ApoC3 and LDLR. Our data showed that depleting ApoC3 by CRISPR/Cas9 gene editing significantly reduced circulating TG and TC levels in LDLR$^{-/-}$ hamsters on standard laboratory diet, but only lowered plasma TG concentration in HCHF diet-fed female LDLR$^{-/-}$ hamsters without affecting severe refractory hypercholesterolemia. Unexpectedly, diet-induced atherosclerosis was aggravated in DKO hamsters independent of gender, whereas female DKO hamsters were protected from fatty liver. Our findings indicate that complete loss of ApoC3 plays favorable effects on HTG and fatty liver in the setting of severe refractory hypercholesterolemia only in female LDLR$^{-/-}$ hamsters, but paradoxically elicits atherosclerotic development regardless of gender.

A growing body of evidence demonstrates that increased plasma ApoC3 levels are positively associated with elevated circulating TG concentration and increased incidence of CVD in independent population-based studies (12). Consistently, transgenic mice overexpressing human ApoC3 also show HTG and accelerated diet-induced atherosclerotic development in atherosclerosis-prone LDLR$^{-/-}$ mice (13). However, whether reduced plasma ApoC3 levels are cardioprotective is still under debate because the results from both human and experimental animal studies are contradictory. Human knockouts of ApoC3 study revealed that ApoC3 deficiency decreased plasma TG and cholesterol levels, and increased HDL-C levels, suggesting an atheroprotective lipoprotein profile (14). But recent Mendelian randomization studies led by Goyal et al. discovered that only one rare loss-of-function variant (rs138326449) was correlated with reduced plasma TG levels and lower risk of cardiovascular heart disease (CHD) in Europeans but not in Asian Indians. Of note, another five common loss-of-function variants of ApoC3, including rs373975305 (IVS1-2G-A), rs76353203

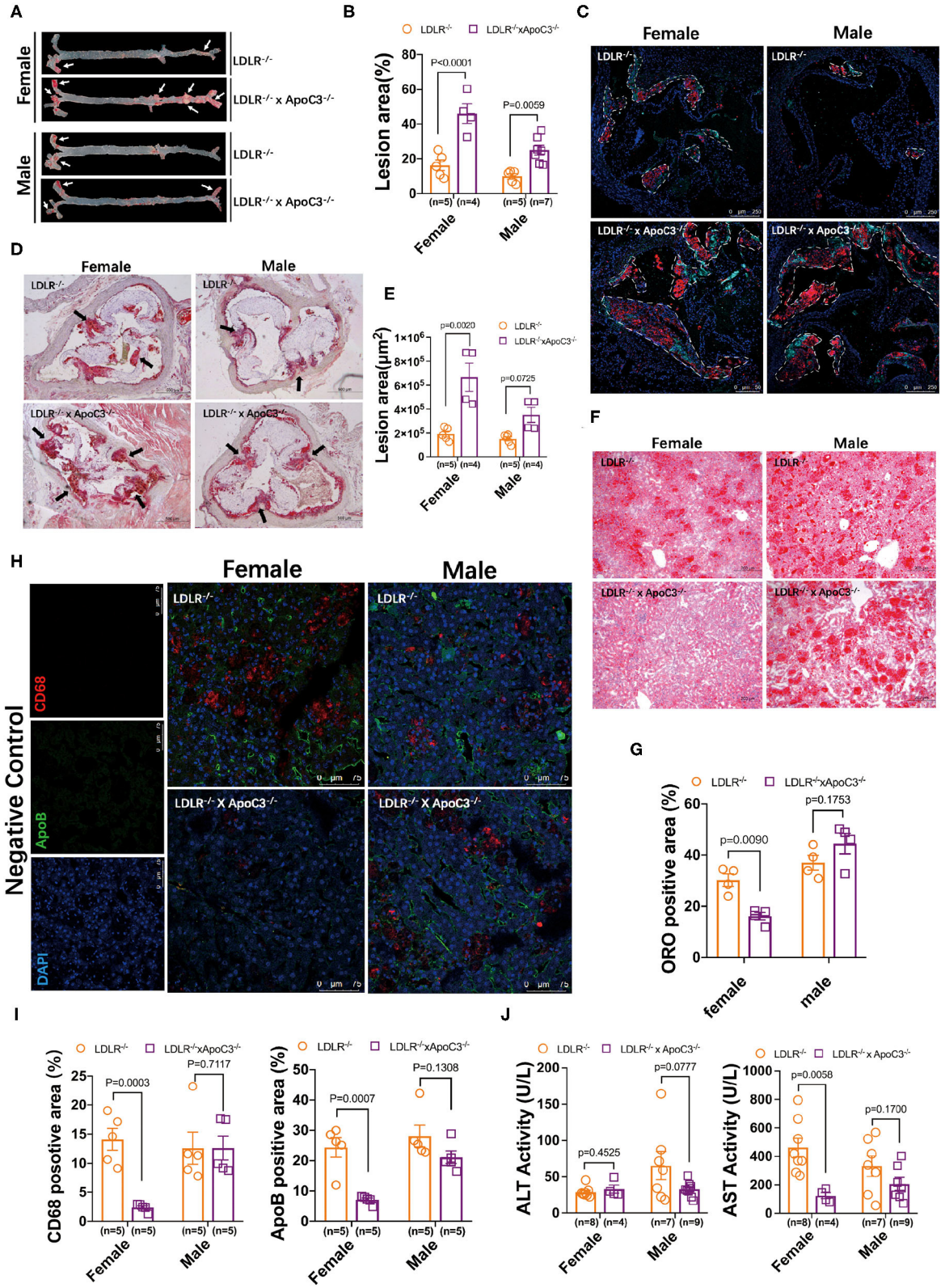

FIGURE 2 | Morphological analysis of atherosclerosis and fatty liver in LDLR$^{-/-}$ and DKO hamsters on HCHF diet. **(A)** Representative en-face images of the whole aorta. Arrows indicate positive staining. **(B)** Quantification of the lesion sizes in the whole aorta. **(C)** Analysis of the components in atherosclerotic plaques by immunofluorescence in HCHF diet-fed animals. Representative staining of ApoB and CD68 in the atherosclerotic lesions of the aortic root. The areas enclosed by

(Continued)

FIGURE 2 | white-dotted lines show the plaques in the aortic root. **(D)** Representative ORO staining of the aortic root. Black arrows indicate ORO-positive staining. **(E)** Quantification of the lesion areas in the aortic root. **(F)** Representative images of ORO-stained cryosections from liver samples. *n*=4/group. **(G)** Quantification of the ORO positive areas in the aortic root from **(F)**. **(H)** Immunofluorescence analysis of macrophage infiltration (CD68) in the liver. $n = 4$/group. **(I)** Quantification of the positive sizes in the liver. **(J)** Fasting plasma ALT and AST levels after 12-week HCHF diet feeding. Data are expressed as mean ± SEM, analyzed by two-way ANOVA or Student's *t*-test after D'Agostino–Pearson's normality test using Prism 8.0.

(R19X), rs138326449 (IVS2+1G-A), rs147210663 (A43T), and rs140621530 (IVS3+1G-T), did not show cardioprotective property even though they differentially influenced plasma TG levels in Asian Indians (15). In addition, Li et al. found that deletion of ApoC3 from LDLR$^{-/-}$ mice has no impact on lipid metabolism and atherogenesis, indicating that targeting ApoC3 to treat hyperlipidemia and CVD needs to be further validated.

In our study, our results showed that ApoC3 deficiency improved combined hyperlipidemia with elevated TG and cholesterol in LDLR$^{-/-}$ hamsters on a standard laboratory diet, which was consistent with the lipid-lowering effect observed in HCHF diet-fed wild-type hamsters (10). Unfortunately, upon HCHF diet feeding, severe refractory hypercholesterolemia was not ameliorated in DKO hamsters, whereas partial reduction in TG was observed in only female DKO hamsters. These findings demonstrated that loss of ApoC3 still attenuated severe HTG in the setting of severe refractory hypercholesterolemia in female FH hamster model after lipid-rich diet challenge, indicating that sex hormone could potentially contribute to lowering TG. Interestingly, in patients with FCS caused by loss-of-function mutation P207L/P207L in *LPL* gene, TG reduction was more prominent in females than in male patients after receiving ISIS304801, an inhibitor of *Apoc3* messenger RNA (mRNA) (16). However, the molecular mechanism by which sex hormones, including estrogen and testosterone, regulate TG metabolism through ApoC3/LPL pathways has not been fully understood yet. It will be tempting to perform ovariectomy in female hamsters or castration in male hamsters to solve this unanswered issue in future studies.

Although ApoC3 deficiency did not alter severe refractory cholesterol levels in LDLR$^{-/-}$ hamster on HCHF diet, we observed an obvious increase in plasma ApoA1 concentration in HDL fractions separated by FPLC in both female and male animals. We speculated that the elevated ApoA1 levels could be attributed to increased LCAT activity because a previous study reported that LCAT activity was significantly reduced in human ApoC3 transgenic mice, suggesting that ApoC3 was an inhibitor of LCAT activity (11). In accordance with the results gained from the mice overexpressing human ApoC3, we found that LCAT activity was increased in DKO hamsters when compared to LDLR$^{-/-}$ hamsters after HCHF diet feeding. However, although ApoA1 levels were elevated in LDLR$^{-/-}$ hamsters lacking ApoC3, TC and HDL-C levels did not change, which was similar to the observations that overexpression of LCAT in LDLR$^{-/-}$; ob/ob mice only increased LCAT activity by 64%, but did not affect total lipid levels in plasma (17). Thus, we speculated that a 24% increase in LCAT activity in our FH model with ApoC3 deficiency was sufficient to elevate ApoA1 levels but could not influence plasma cholesterol levels, including HDL-C.

Surprisingly, contrary to what was expected from TG-lowering effect of ApoC3 deficiency in the context of severe refractory hypercholesterolemia, our findings showed that DKO hamsters displayed accelerated atherosclerotic plaques with more lipid-load macrophage accumulation in the lesions, which was independent of gender. This paradoxical result raised a possibility that ApoC3 deficiency might enhance the uptake of lipid-rich lipoprotein particles at the surface of the local vascular wall through LPL activity dependent or independent manner because the LPL-mediated catabolism of ApoC3-containing lipoproteins was lower than ApoC3-deficient lipoproteins (16). Adenovirus overexpressing active or non-active LPL in the endothelial-intact artery caused lipid deposition in HTG mice with LPL deficiency and hypercholesterolemic mice lacking ApoE (18), which did not affect plasma lipid levels, suggesting that endothelial-associated LPL was proatherosclerotic *in vivo*. Moreover, another independent study led by Ferna'ndez-Hernando from Yale reported that lack of hematopoietic cell-derived ANGPTL4, one of the inhibitors of LPL, also promoted atherosclerosis by regulating monocyte expansion in LDLR$^{-/-}$ mice (19). Collectively, these data demonstrated that suppressing the inhibitory effect of LPL inhibitors at the vascular wall might trigger atherosclerotic development. Importantly, thrombocytopenia has been reported in FCS patients with volanesorsen treatment; however, this study showed that depleting ApoC3 by CRIPSR/Cas9 resulted in abnormal platelet indices without thrombocytopenia, indicating that genetically targeting ApoC3 could not significantly cause decreased platelet number; however, the abnormal platelet function due to ApoC3 deletion would be considered as another potential contributor to atherosclerosis in our study. It should be noted that in this study, we only investigated atherosclerosis under the HCHF diet condition, which predisposed LDLR$^{-/-}$ hamsters and DKO hamsters to severe refractory hypercholesterolemia that could not be improved by the absence of ApoC3; however, ApoC3 deficiency generates a favorable plasma lipoprotein profile by reducing both TG and cholesterol levels in LDLR$^{-/-}$ hamsters, suggesting that currently, we cannot exclude the long-term beneficial effect of ApoC3 inhibition on spontaneous atherosclerosis in LDLR$^{-/-}$ hamsters on standard laboratory diet, which should be validated in future.

Non-alcoholic fatty liver disease (NAFLD) is the consequence of hyperlipidemia in humans and experimental animals. Our data clearly showed that ApoC3 inhibition obviously reduced lipid contents in female LDLR$^{-/-}$ hamsters after HCHF diet feeding, which was consistent with plasma lipid levels, suggesting that the TG-lowering effect of ApoC3 inhibition effectively ameliorated fatty liver by reducing macrophage infiltration, then protecting from liver damage. Again, although we still do not understand

why TG was reduced only in female DKO, our data suggest the need for future investigation of the effect of sex hormones in our model.

In conclusion, we have demonstrated that targeting ApoC3 could reduce TG levels and ameliorate fatty liver only in female FH hamsters with severe refractory hypercholesterolemia after HCHF diet feeding, but paradoxically accelerated diet-induced atherosclerotic development in dependent on gender. Our unexpected findings provide new insight into the possibility that targeting ApoC3 will be a potential therapeutic approach for the treatment of FH with severe refractory hypercholesterolemia and atherosclerosis.

DATA AVAILABILITY STATEMENT

The datasets presented in this study can be found in online repositories. The names of the repository/repositories and accession number(s) can be found in the article/**Supplementary Material**.

ETHICS STATEMENT

The animal study was reviewed and approved by the Animal Care Committee, Peking University Health Science Center (LA2015-012).

AUTHOR CONTRIBUTIONS

XX conceived and designed the study. YX, JG, LZ, GM, PL, and WZ performed the experiments. YX, JG and XX wrote the original manuscript. YX, JG, LL, XH, YW, WH, and XX interpreted the data. YW, GL, and XX acquired the funding. GL and XX supervised the study. MG and XX reviewed and edited the manuscript. All authors approved the final manuscript.

FUNDING

This study was supported by the National Natural Science Foundation of China (NSFC) 31520103909 and 91739105 to GL, 81770449 to YW, and 82070460 to XX. GL is a fellow at the Collaborative Innovation Center for Cardiovascular Disease Translational Medicine, Nanjing Medical University.

SUPPLEMENTARY MATERIAL

The Supplementary Material for this article can be found online at: https://www.frontiersin.org/articles/10.3389/fcvm.2022.840358/full#supplementary-material

REFERENCES

1. Laufs U, Parhofer KG, Ginsberg HN, Hegele RA. Clinical review on triglycerides. *Eur Heart J.* (2020) 41:99–109c doi: 10.1093/eurheartj/ehz785
2. Han P, Wei G, Cai K, Xiang X, Deng WP Li YB, et al. Identification and functional characterization of mutations in lpl gene causing severe hypertriglyceridaemia and acute pancreatitis. *J Cell Mol Med.* (2020) 24:1286–99. doi: 10.1111/jcmm.14768
3. Sakurai T, Sakurai A, Vaisman BL, Amar MJ, Liu C, Gordon SM, et al. Creation of apolipoprotein c-ii (apoc-ii) mutant mice and correction of their hypertriglyceridemia with an apoc-ii mimetic peptide. *J Pharmacol Exp Ther.* (2016) 356:341–53. doi: 10.1124/jpet.115.229740
4. Kumari A, Kristensen KK, Ploug M, Winther AL. The importance of lipoprotein lipase regulation in atherosclerosis. *Biomedicines.* (2021) 9:782. doi: 10.3390/biomedicines9070782
5. Rosenson RS, Burgess LJ, Ebenbichler CF, Baum SJ, Stroes ESG, Ali S, et al. Evinacumab in patients with refractory hypercholesterolemia. *N Engl J Med.* (2020) 383:2307–19. doi: 10.1056/NEJMoa2031049
6. Raal FJ, Rosenson RS, Reeskamp LF, Hovingh GK, Kastelein JJP, Rubba P, et al. Evinacumab for homozygous familial hypercholesterolemia. *N Engl J Med.* (2020) 383:711–20. doi: 10.1056/NEJMoa2004215
7. Gaudet D, Alexander VJ, Baker BF, Brisson D, Tremblay K, Singleton W, et al. Antisense inhibition of apolipoprotein c-iii in patients with hypertriglyceridemia. *N Engl J Med.* (2015) 373:438–47. doi: 10.1056/NEJMoa1400283
8. Witztum JL, Gaudet D, Freedman SD, Alexander VJ, Digenio A, Williams KR, et al. Volanesorsen and triglyceride levels in familial chylomicronemia syndrome. *N Engl J Med.* (2019) 381:531–42. doi: 10.1056/NEJMoa1715944
9. Guo M, Xu Y, Dong Z, Zhou Z, Cong N, Gao M, et al. Inactivation of apoc3 by crispr/cas9 protects against atherosclerosis in hamsters. *Circ Res.* (2020) 127:1456–8. doi: 10.1161/CIRCRESAHA.120.317686
10. Guo X, Gao M, Wang Y, Lin X, Yang L, Cong N, et al. Ldl receptor gene-ablated hamsters: A rodent model of familial hypercholesterolemia with dominant inheritance and diet-induced coronary atherosclerosis. *EBioMedicine.* (2018) 27:214–24. doi: 10.1016/j.ebiom.2017.12.013
11. Zvintzou E, Lhomme M, Chasapi S, Filou S, Theodoropoulos V, Xapapadaki E, et al. Pleiotropic effects of apolipoprotein c3 on hdl functionality and adipose tissue metabolic activity. *J Lipid Res.* (2017) 58:1869–83. doi: 10.1194/jlr.M077925
12. Borén J, Packard CJ, Taskinen MR. The roles of apoc-iii on the metabolism of triglyceride-rich lipoproteins in humans. *Front Endocrinol.* (2020) 11:474. doi: 10.3389/fendo.2020.00474
13. Li H, Han Y, Qi R, Wang Y, Zhang X, Yu M, et al. Aggravated restenosis and atherogenesis in apociii transgenic mice but lack of protection in apociii knockouts: the effect of authentic triglyceride-rich lipoproteins with and without apociii. *Cardiovasc Res.* (2015) 107:579–89. doi: 10.1093/cvr/cvv192
14. Reyes-Soffer G, Sztalryd C, Horenstein RB, Holleran S, Matveyenko A, Thomas T, et al. Effects of apoc3 heterozygous deficiency on plasma lipid and lipoprotein metabolism. *Arterioscler Thromb Vasc Biol.* (2019) 39:63–72. doi: 10.1161/ATVBAHA.118.311476
15. Goyal S, Tanigawa Y, Zhang W, Chai JF, Almeida M, Sim X, et al. Apoc3 genetic variation, serum triglycerides, and risk of coronary artery disease in asian Indians, Europeans, and other ethnic groups. *Lipids Health Dis.* (2021) 20:113. doi: 10.1186/s12944-021-01531-8
16. Gaudet D, Brisson D, Tremblay K, Alexander VJ, Singleton W, Hughes SG, et al. Targeting apoc3 in the familial chylomicronemia syndrome. *N Engl J Med.* (2014) 371:2200–6. doi: 10.1056/NEJMoa1400284
17. Mertens A, Verhamme P, Bielicki JK, Phillips MC, Quarck R, Verreth W, et al. Increased low-density lipoprotein oxidation and impaired high-density lipoprotein antioxidant defense are associated with increased macrophage homing and atherosclerosis in dyslipidemic obese mice: Lcat gene transfer decreases atherosclerosis. *Circulation.* (2003) 107:1640–6. doi: 10.1161/01.CIR.0000056523.08033.9F
18. Wang J, Xian X, Huang W, Chen L, Wu L, Zhu Y, et al. Expression of lpl in endothelial-intact artery results in lipid deposition and vascular cell adhesion molecule-1 upregulation in both lpl and apoe-deficient mice. *Arterioscler Thromb Vasc Biol.* (2007) 27:197–203. doi: 10.1161/01.ATV.0000249683.80414.d9
19. Aryal B, Rotllan N, Araldi E, Ramírez CM, He S, Chousterman BG, et al. Angptl4 deficiency in haematopoietic cells promotes monocyte

expansion and atherosclerosis progression. *Nat Commun.* (2016) 7:12313. doi: 10.1038/ncomms12313

Conflict of Interest: The authors declare that the research was conducted in the absence of any commercial or financial relationships that could be construed as a potential conflict of interest.

Publisher's Note: All claims expressed in this article are solely those of the authors and do not necessarily represent those of their affiliated organizations, or those of the publisher, the editors and the reviewers. Any product that may be evaluated in this article, or claim that may be made by its manufacturer, is not guaranteed or endorsed by the publisher.

frontiers in Cardiovascular Medicine

ORIGINAL RESEARCH
published: 08 February 2022
doi: 10.3389/fcvm.2022.826861

Metabolomic Profile Reveals That Ceramide Metabolic Disturbance Plays an Important Role in Thoracic Aortic Dissection

Hang Yang[1†], Fangfang Yang[1†], Mingyao Luo[2], Qianlong Chen[1], Xuanyu Liu[1], Yinhui Zhang[1], Guoyan Zhu[1], Wen Chen[1], Tianjiao Li[1], Chang Shu[2] and Zhou Zhou[1]*

[1] State Key Laboratory of Cardiovascular Disease, Beijing Key Laboratory for Molecular Diagnostics of Cardiovascular Diseases, Diagnostic Laboratory Service, Fuwai Hospital, National Center for Cardiovascular Diseases, Chinese Academy of Medical Sciences and Peking Union Medical College, Beijing, China, [2] State Key Laboratory of Cardiovascular Disease, Center of Vascular Surgery, Fuwai Hospital, National Center for Cardiovascular Diseases, Chinese Academy of Medical Sciences and Peking Union Medical College, Beijing, China

OPEN ACCESS

Edited by:
Jian Shi,
University of Leeds, United Kingdom

Reviewed by:
Chen Gao,
UCLA Department of Anesthesiology and Perioperative Medicine, United States
Jian Xia,
Central South University, China

***Correspondence:**
Zhou Zhou
zhouzhou@fuwaihospital.org

[†]These authors have contributed equally to this work

Specialty section:
This article was submitted to Cardiovascular Metabolism, a section of the journal Frontiers in Cardiovascular Medicine

Received: *01 December 2021*
Accepted: *04 January 2022*
Published: *08 February 2022*

Citation:
Yang H, Yang F, Luo M, Chen Q, Liu X, Zhang Y, Zhu G, Chen W, Li T, Shu C and Zhou Z (2022) Metabolomic Profile Reveals That Ceramide Metabolic Disturbance Plays an Important Role in Thoracic Aortic Dissection. Front. Cardiovasc. Med. 9:826861. doi: 10.3389/fcvm.2022.826861

Aims: Thoracic aortic dissection (TAD) is a life-threatening disease with no effective drug therapy thus far. New therapeutic targets and indications for timely surgical intervention are urgently needed. Our aim is to investigate new pathological mechanisms and potential biomarkers of TAD through global metabolomic profiling of aortic aneurysm and dissection patients.

Methods and Results: We performed untargeted metabolomics to determine plasma metabolite concentrations in an aortic disease cohort, including 70 thoracic aortic aneurysm (TAA) and 70 TAD patients, as well as 70 healthy controls. Comparative analysis revealed that sphingolipid, especially its core metabolite C18-ceramide, was significantly distinguished in TAD patients but not in TAA patients, which was confirmed by subsequent quantitative analysis of C18-ceramide in a validation cohort. By analyzing our existing multiomics data in aortic tissue in a murine TAD model and TAD patients, we found that an enhanced ceramide *de novo* synthesis pathway in macrophages might contribute to the elevated ceramide. Inhibition of the ceramide *de novo* synthesis pathway by myriocin markedly alleviated BAPN-induced aortic inflammation and dissection in mice. *In vitro* studies demonstrated that exogenous C18-ceramide promoted macrophage inflammation and matrix metalloprotein (MMP) expression through the NLRP3-caspase 1 pathway. In contrast, inhibition of endogenous ceramide synthesis by myriocin attenuated lipopolysaccharide (LPS)-induced macrophage inflammation.

Conclusions: Our findings demonstrated that ceramide metabolism disturbance might play a vital role in TAD development by aggravating aortic inflammation through the NLRP3 pathway, possibly providing a new target for pharmacological therapy and a potential biomarker of TAD.

Keywords: thoracic aortic dissection, metabolomics, ceramide, macrophage, NLRP3

INTRODUCTION

Thoracic aortic dissection (TAD) is usually an acute onset and life-threatening disease, characterized by any intimal tear in the thoracic aorta that allows blood flow to enter the aortic media. If untreated, its mortality is up to 33% within the first 24 h and rises to 50% by the first 48 h. An epidemiological survey of aortic dissection in China shows that the incidence rate in urban Chinese adults is 2.78 per 100,000 person-years (1). Current pharmacological therapy can only delay the expansion of aortic aneurysms rather than prevent aortic dissection or aneurysm rupture. To date, prophylactic surgical repair is so far the only effective strategy to avoid the occurrence of malignant events. Most of the time, preventive surgical intervention is recommended when the aorta diameter reaches 5.0–5.5 cm. However, studies have shown that up to 60% of acute type A aortic dissections occur when the diameter is <5.5 cm (2). Therefore, there remains an urgent need to explore new pathological mechanisms in the pathogenesis of TAD and biomarkers for timely surgical intervention.

In recent years, metabolomics has emerged as a useful tool for deciphering new disease pathogenesis and identifying novel biomarkers, as it situates downstream of physiological and pathological changes and therefore reflects cellular processes more directly and unbiasedly than genomic, transcriptomic, and proteomic variations. This approach has provided valuable insight into novel pathologic pathways and potential biomarkers in several cardiovascular diseases (3), such as cardiac hypertrophy, heart failure, coronary artery disease, and cardiovascular risk prediction. To the best of our knowledge, only a few studies (4–7) have focused on thoracic aortic diseases, and the findings have suggested that several bioactive lipids, such as glycerophospholipids, sphingolipids and lysophosphatidylcholines (7), as well as some other metabolites, such as fumarate (8) and succinate (9), are significantly altered in aortic disease.

Bioactive lipids can play a variety of roles in regulating cellular processes and functions, of which sphingolipids have emerged as molecules of special interest. In recent years, sphingolipids, especially their core metabolite ceramides, have attracted much attention for their association with cardiovascular diseases (10). Studies have shown that specific ceramides are positively correlated with the incidence of cardiovascular disease (11), secondary cardiovascular events (12), and mortality (13) and may become a potential biomarker for predicting the risk of atrial fibrillation (14) and poor prognosis of coronary artery disease (15). Although the exact mechanisms underlying these observations remain largely unknown, several studies have implicated that ceramdies might promote cardiovascular pathological progress through multiple pathways, such as exacerbating the inflammatory response (16–18), promoting cell apoptosis (17), and producing superoxide anions (16), as well as some other pathways (10).

In this study, we performed untargeted metabolomics analysis to delineate the metabolic landscape of patients with thoracic aortic aneurysm and dissection and explored potential biomarkers and novel mechanisms underlying TAD. The results indicated that the specific C18-ceramide was significantly increased in aortic dissection, but not in aortic aneurysm. Subsequently, we further investigated the source and pathological significance of excessive ceramides.

MATERIALS AND METHODS

Human Subjects and Specimens

Syndromic and non-syndromic thoracic aneurysm and Stanford type A aortic dissection patients were enrolled from Fuwai Hospital between August 2017 and December 2020. Aneurysms and dissections were evaluated and diagnosed by echocardiography or computed tomography (CT). Thoracic aortic aneurysm (TAA) was defined as a localized dilation of the thoracic aorta that was more than 50% of predicted, and Stanford type A aortic dissection referred to dissections involving any part of the aorta proximal to the origin of the left subclavian artery. Patients with aortic trauma, pseudoaneurysm, or arteritis were excluded. Healthy control subjects were recruited from physical examination individuals at Fuwai Hospital, who had neither significant systemic disease nor aortic dilation evaluated by echocardiography. Two datasets were established to identify the plasma metabolite features. In the discovery cohort, 140 patients (70 TAA, 70 TAD) and age- and sex- matched healthy individuals were enrolled. The validation cohort included 269 aortic disease patients (183 TAAs, 86 TADs) with aortic diameters $\leq$ 5.5 cm. Blood samples were collected during outpatient service or after anesthesia induction and before heparin during surgery. 3–4 ml venous blood was collected in ethylene diamine tetraacetic acid (EDTA)-anticoagulated tubes, and plasma was separated by centrifuging at 3,000 rpm for 10 min at room temperature within 1 h and stored at −80°C until analysis.

This study conformed to the Declaration of Helsinki principles and was approved by the ethics committee of the institutional review board at Fuwai Hospital (Approval No.:2017-877). All of the patients and healthy control subjects included in this study assigned a consent form.

Untargeted Metabolomics Analysis

Plasma metabolomics was performed by Metabolon (Durham, NC, USA) using a multiplatform system encompassing tandem ultrahigh-performance liquid chromatography-mass spectrometry as well as tandem gas chromatography-mass spectrometry systems with different column ionization parameters.

Plasma samples were prepared using the automated MicroLab STAR system (Hamilton Company). Several recovery standards were added before the first step in the extraction process for quality control purposes. Plasma proteins were precipitated with methanol under vigorous shaking for 2 min (Glen Mills GenoGrinder 2000) followed by centrifugation. The resulting extract was divided into five fractions: two for analysis by two separate reverse phase/ultra-performance liquid chromatography (UPLC)-tandem mass spectrometry (MS/MS) methods with positive ion mode electrospray ionization (ESI), one for analysis by reverse phase/UPLC-MS/MS with negative ion mode ESI, one for analysis by hydrophilic interaction liquid chromatography

(HILIC)/UPLC-MS/MS with negative ion mode ESI and one sample reserved for backup. Samples were placed briefly on a TurboVap (Zymark) to remove the organic solvent. The sample extracts were stored overnight under nitrogen before preparation for analysis.

Several types of controls were analyzed in concert with the experimental samples: a pool of well-characterized human plasma served as a technical replicate throughout the dataset; extracted water samples served as process blanks; and a cocktail of quality control standards that were carefully chosen not to interfere with the measurement of endogenous compounds were spiked into every analyzed sample, allowed instrument performance monitoring and aided chromatographic alignment. Instrument variability was determined by calculating the median relative s.d. for the standards that were added to each sample before injection into the mass spectrometers. Overall process variability as determined by calculating the median relative s.d. for all endogenous metabolites (that is, non-instrument standards) present in 100% of the pooled matrix samples was 10%. Experimental samples were randomized across the platform run with quality control samples spaced evenly among the injections.

All methods utilized an ACQUITY ultra-performance liquid chromatography (UPLC; Waters, Milford, MA, USA), a Q-Exactive high resolution/accurate mass spectrometer interfaced with a heated electrospray ionization (HESI-II) source (Thermo Scientific, Waltham, MA, USA) and Orbitrap mass analyzer operated at 35,000 mass resolution. The sample extract was dried and reconstituted in solvents compatible with each of the four methods. Each reconstitution solvent contained a series of standards at fixed concentrations to ensure injection and chromatographic consistency. One aliquot was analyzed using acidic positive ion conditions, chromatographically optimized for more hydrophilic compounds. The extract was gradient eluted from a C18 column (Waters UPLC BEH C18−2.1 × 100 mm, 1.7 μm) using water and methanol, containing 0.05% perfluoropentanoic acid (PFPA) and 0.1% formic acid. Another aliquot was also analyzed using acidic positive ion conditions, which was chromatographically optimized for more hydrophobic compounds. The extract was gradient eluted from the C18 column using methanol, acetonitrile, water, 0.05% PFPA and 0.01% formic acid and was operated at an overall higher organic content. Another aliquot was analyzed using basic negative ion optimized conditions using a separate dedicated C18 column. The basic extracts were gradient eluted from the column using methanol and water with 6.5 mM Ammonium Bicarbonate at pH 8. The fourth aliquot was analyzed *via* negative ionization following elution from a HILIC column (Waters UPLC BEH Amide 2.1 × 150 mm, 1.7 μm) using a gradient consisting of water and acetonitrile with 10 mM ammonium formate, pH 10.8. The MS analysis alternated between MS and data-dependent MSn scans using dynamic exclusion. The scan range covered 70–1,000 m/z.

Raw data were extracted, peak-identified and QC processed by Metabolon (Metabolon, Inc., Morrisville, NC, USA). Compounds were identified by comparison to library entries of purified standards or recurrent unknown entities. Biochemical identifications are based on three criteria: retention index within a narrow RI window of the proposed identification, accurate mass match to the library ±10 ppm, and the MS/MS forward and reverse scores between the experimental data and authentic standards. The MS/MS scores are based on a comparison of the ions present in the experimental spectrum to the ions present in the library spectrum. Peaks were quantified by Metabolon, Inc. using the area-under-the-curve with a data normalization step was performed to correct variation resulting from instrument inter-day tuning differences.

Statistical analysis was performed by Metabolon as well as using MetaboAnalyst 5.0 (https://www.metaboanalyst.ca, accessed date on 6 June 2021) for pathway and enrichment analyses. Following log transformation and imputation of missing values, if any, with the minimum observed value for each compound, Welch's two-sample *t*-test was used to identify biochemicals that differed significantly between experimental groups, while outliers were identified using the ROUT method. Biochemicals that achieved statistical significance ($p \leq 0.05$) and demonstrated a low estimate of false discovery rate ($q > 0.10$) were included in this analysis.

Statistical analysis was performed by Metabolon as well as using online MetaboAnalyst 5.0 (https://www.metaboanalyst.ca) for pathway and enrichment analyses. Following log transformation and imputation of missing values, if any, with the minimum observed value for each compound, Welch's two-sample *t*-test was used to identify biochemicals that differed significantly between experimental groups, while outliers were identified using the ROUT method. Biochemicals with fold change (FC) > 1.3 or FC $< 1/1.3$ that achieved statistical significance ($p \leq 0.05$) and demonstrated a low estimate of false discovery rate ($q > 0.10$), were included in this analysis.

Quantitative Measurement of Plasma C18-Ceramide

The SHIMADZU Prominence UPLC system (Kyoto, JAPAN) equipped with an Applied Biosystems 4500 Q-Trap mass spectrometer (Foster City, CA, USA) with electrospray ionization source was used. Chromatographic separation was achieved by using a Phenomenex Kinetex C8 column, 50 mm × 2.1 mm, 5 μm (phenomenex, USA). Mobile phase A was made of a 2-mM ammonium acetate aqueous solution with 0.1% formic acid by volume and mobile B 70:30 (v:v) acetonitrile: isopropanol with 0.1% formic acid by volume. The column temperature was set at 40°C, and the flow rate was 0.3 ml/min. The gradient elution program was set as follows, 0–1 min 65% B; 1–1.5 min 65–75% B; 1.5–3.5 min 75–95% B; 3.6–4.5 min 65% B.

The mass detection and quantification was performed in a positive electrospray ionization mode using multiple reactions monitoring (MRM) method. The mass spectrometer working parameters were optimized as follows: curtain gas at 35 psi, Gas 1 at 55 psi, Gas 2 at 55 psi and a turbo ion spray temperature of 550°C. The MRM transitions for C18-ceramide and the isotope internal standard C18-ceramide-d7 was 548.5–264.5 and 555.5–271.5. Data acquisition and procession was

performed with Analyst 1.6.1 software version (AB SCIEX, Concord, Ontario, Canada).

To get the precise concentration, a standard curve was performed. An aliquot of 100 ul various concentration standards (10–500 ng/ml) were analyzed with the same procedure. The calibration curve was constructed by plotting the peak area ratios of each analyte/IS vs. its nominal concentrations in standards, using a linear regression. Standard curves were acceptable when coefficient of determination (R2) exceeded 0.990. Five replicates ($n = 5$) of QC samples were analyzed in the same batch assay to determine the intra-day precision and accuracy and in three different batch assays to determine the inter-day precision and accuracy of the method. The precision is expressed by relative standard deviation (RSD) between the replicate measurements. Accuracy is defined as relative error (RE) which is calculated using the formula RE% = [(measured value–theoretical value)/theoretical value] ×100. The intra-day precision (RSD) ranged between 1.08 and 13.20%, and accuracy (RE) ranged between −11.83 and 5.78%. The inter-day precision (RSD) ranged between −10.89 and 2.11%, and accuracy (RE) ranged from 0.05 to 11.10%, respectively. All inter- and intra-day precision and accuracy were acceptable for working in biological media.

The quantitative detection limit (LOQ) of the method was investigated by detecting the linear lowest point of the standard curve. The lowest-concentration standard (10 ng/ml) was tested for 6 consecutive times, and coefficient of variation (CV) and accuracy (RE) were 4.00 and −1.17%, respectively, which was acceptable.

Animal Model and Treatment

Wild-type (WT) mice on a C57B/L6 background were obtained from Vitalstar in Beijing. Three-week-old male mice were fed a normal diet and administered with freshly prepared β-aminopropionitrile (BAPN) solution (0.5 g/kg/day) dissolved in the drinking water for 4 weeks. Myriocin (0.5 mg/kg; APExBIO Inc.) or its solution was injected intraperitoneally from the beginning of BAPN administration every other day for 4 weeks. Then the mice were anesthetized to harvest the aortas. Anesthetization and euthanasia were performed by intraperitoneal injection of sodium pentobarbital (50 and 150 mg/kg, respectively).

All animal studies conformed to the NIH Guide for the Care and Use of Laboratory Animals and were approved by the Institutional Animal Care and Use Committee (IACUC) at Fuwai Hospital (Approval No.: FW-2019-0008).

HE Stating and Elastin Van Geison Staining

HE staining and elastin Van Geison (VG) staining were conducted using kits (Zhongshan Golden Bridge Biotechnology, Beijing, China) according to routine protocols. Briefly, for HE staining, after deparaffinization and rehydration, aorta sections were stained with hematoxylin solution for 3–5 min followed by 5 dips in 1% acid ethanol (1% HCl in 70% ethanol) and then rinsed in distilled water. Then, the sections were stained with eosin solution for 3 min, dehydrated with graded alcohol and cleared in xylene. For elastin VG staining, potassium permanganate was oxidized for 5 min and bleached with oxalic acid for 5 min. Then, the sections were washed with 95% alcohol and stained with elastin dyeing at room temperature for 8–24 h. Differentiation was then performed with 95% alcohol or 1% hydrochloric acid, followed by washing with distilled water. Contrasting staining was performed with Van Gieson staining for 1 min, and rapid differentiation was performed with 95% alcohol for a few seconds. Then 100% alcohol dehydration was performed, followed by the use of transparent xylene and sealing with neutral gum.

Immunohistochemistry (IHC)

Tissues were fixed in 4% paraformaldehyde (PFA) and embedded in paraffin. Six-μm sections were deparaffinized and rehydrated in an ethanol series, and antigen retrieval was performed in a steamer. Non-specific binding was blocked by 5% BSA in PBS. The sections were probed with primary antibody, washed and then probed with secondary antibody. Primary antibody: CD68 (Abcam, ab201340). IHC staining was developed using DAB (Vector Laboratories) followed by hematoxylin counterstaining. After mounting, the slips were visualized by microscopy.

Cell Culture and Treatment

RAW 264.7 cells were cultured in Dulbecco's modified Eagle's medium (DMEM; Gibco, 10569044) supplemented with 10% fetal bovine serum (FBS), 100 U/mL penicillin and 100 μg/mL streptomycin and incubated at 37°C under 5% CO_2. For ceramide treatment, cells were starved for 24 h and then primed by 100 ng/ml LPS for 16 h. After the pretreatment, cells were incubated in Cer18 (GlpBio Inc.) at a concentration of 10 μmol/L for 24 h. For LPS and myriocin treatment, cells were starved for 24 h and then incubated in 1 μg/ml LPS (Sigma) with or without 10 μmol/L myriocin.

RNA Isolation and Quantitative Real-Time PCR

Total RNA from aortic tissues or RAW264.7 cells was extracted with TRIzol reagent (Invitrogen, 15596018). Real-time PCR samples were prepared by mixing cDNAs, power-SYBR Mix (ABI, A25742) and specific primer sets (**Supplementary Table 1**). The initial denaturation step of PCR amplification was 95°C for 10 min, followed by 40 cycles of 95°C for 15 s and 55°C for 1 min, then 95°C for 15 s and 60°C for 1 min, and last at 95°C for 1 s. Gene expressions were normalized against *Gapdh*.

Western Blot

Cells were lysed with RIPA (Beyotime P0013B) lysis buffer. Equal amounts of protein were separated by SDS–PAGE, transferred to nitrocellulose membranes, blocked in 5% skimmed milk, and incubated with the primary antibodies against NLRP3 (1:1000, CST 15101S), Caspase1 (1:150,), IL-1β (1:500, CST), MMP9 (1:500, Abcam), and β-actin (1:50000, Proteintech) overnight at 4°C, followed by detection with Horseradish enzyme labeled goat anti-rabbit IgG (H+L; ZSGB-BIO, ZB-2301). Visualization was performed with Chemiluminescence imaging system (Bio Rad, ChemiDocXRS+).

Statistical Analysis

Data were analyzed using GraphPad Prism version 5.01 (GraphPad Software, San Diego, CA) and SPSS version 22.0 (IBM SPSS Statistics, Armonk, NY). The continuous variables were described as the means and standard deviations (SDs) with a normal distribution or as medians and interquartile ranges (IQRs) with an abnormal distribution, and the categorical variables were described as proportions. Statistical analysis was performed by unpaired or paired *t*-test for two groups of data and by one-way ANOVA for multiple comparisons. Statistical significance among multiple groups was determined by *post-hoc* analysis (Tukey honestly significant difference test). Proportions were compared using the Chi-square test. Values of $p < 0.05$ were considered statistically significant.

RESULTS

Global Metabolic Profiles Revealed a Significant Increase in C18-Ceramide in TAD Patient Plasma and Quantitative Analysis Verified It

To explore novel mechanisms and potential biomarkers of thoracic aortic aneurysm/dissection, 70 thoracic aortic aneurysm (TAA) patients and 70 type A aortic dissection (TAD) patients, as well as 70 age- and sex- matched controls, were subjected to untargeted metabolomics by using ultrahigh performance liquid chromatography-tandem mass spectrometry (UPLC–MS/MS) method (Metabolon, USA). The demographic and clinical information of all patients and healthy controls was listed in (**Supplementary Table 2**). A total of 866 named biochemicals in plasma were determined. Principal component analysis (PCA) revealed that both TAA and TAD separated from controls, but TAD showed more distant separation (**Figure 1A**), suggesting that TAA and TAD display related metabolic signatures, with TAD exhibiting the more extreme metabolic phenotype.

A total of 373 significantly differentiated metabolites were observed between TAA and TAD (**Supplementary Table 3**), of which 145 were elevated while 228 were decreased. Pathway analysis of differentiated metabolites between TAA and TAD was presented in **Supplementary Figure 1**. Metabolite set enrichment analysis demonstrated that sphingolipid metabolism was one of the most distinguished enriched pathways (**Figure 1B**). Notably, its core metabolite, N-stearoyl-sphingosine (d18:1/18:0; C18-ceramide), was ∼2-fold higher in TAD patients than in healthy controls, but not significantly changed in TAA patients (**Figure 1C**), suggesting that it might be a distinguished biomarker between TAA and TAD. After excluding the 10 TAD patients who had already a history of aortic surgeries before the dissection onset, the remaining 60 TAD patients were divided into three groups based on the tirtile valule of C18-ceramide relative amount (low, moderate, high) and we observed that the rate of early-onset dissection in moderate- and high-level ceramide group was higher than in low-level group (**Table 1**) (90, 85 vs. 45%, $n = 20$, $p = 0.002$).

To confirm the association between C18-ceramide content and ealry-onset aortic dissection, we subsequently enrolled 269 TAAD patients (183 TAA and 86 TAD) with aortic diameters ≤ 5.5 cm and quantitatively detected their plasma C18-ceramide content. The demographic and clinical information of all patients was listed in **Supplementary Table 4**. The results showed that C18-ceramide concentrations were elevated in ealry-onset TAD patients (66.3 ± 30.9 ng/ml, $n = 86$) compared with those in TAA patients (39.3 ± 16.3 ng/ml, $n = 183$) (**Figure 1D**).

Multiomics Data Suggested That Macrophage-Derived Ceramide *de novo* Synthesis Contributed to the Increased Ceramide Content

To investigate the source of elevated ceramide in plasma in TAD, we tried to find clues from our two existing RNA-sequencing (RNA-seq) datasets (19). In our previous study, we had performed time-series single-cell RNA-seq of thoracic aortic cells from β-aminopropionitrile (BAPN)-induced TAAD mouse models. Genes in the ceramide *de novo* synthesis pathway, such as *Sptlc*, *Cers*, and *Degs*, were significantly upregulated in the proinflammatory macrophage subpopulation c13 (*Il1rn*$^{+}$) in BAPN-induced mice for 21 days (**Figure 2A**). Genes in the sphingomyelin hydrolysis and salvage pathways were not significantly altered (data not shown). In addition, our other aortic bulk RNA-Seq dataset from humans demonstrated that higher expression of *CERS6* (ceramide synthesis gene) and *ASAH1* (ceramide hydrolysis gene) was observed in CD11b^{+} macrophages than CD11b^{-} cells in aortic tissues from TAAD patients (**Figure 2B**). Combining these two RNA-seq results, we speculated that elevated ceramide content was due to an enhanced ceramide *de novo* synthesis pathway in aortic macrophages. Furthermore, we quantified the expression of all major genes involved in ceramide synthesis in aortic tissues from TAD mice and found that only *de novo* pathway genes, *Sptlc2* and *Cers6*, were significantly upregulated under BAPN-induced TAD conditions (**Figure 2C**).

Inhibition of Ceramide *de novo* Synthesis With Myriocin Prevented BAPN-Induced Thoracic Aortic Dissections and Aortic Inflammation in Mice

To determine the role of ceramide in TAD, we examined the effect of the ceramide *de novo* synthesis inhibitor myriocin on a BAPN-induced TAD mouse model. Forty-eight mice were randomly divided into three groups: WT, BAPN, and BAPN+myriocin. The results showed that BAPN-induced aortic dissection and related death occurred in 68.75% (11/16) of mice, while the rate in the BAPN+myriocin group was 12.5% (2/16), suggesting that myriocin effectively prevented BAPN-induced TAD (**Figure 3A**). HE and elastin VG staining staining demonstrated that myriocin mitigated BAPN-induced aortic damage and elastic fiber degradation (**Figure 3B**). Histochemical staining of CD68^{+} in the aorta revealed that BAPN promoted the accumulation of macrophages and that myriocin suppressed this phenomenon (**Figure 3C**). Moreover, myriocin alleviated BAPN-induced aortic inflammatory cytokine (IL-1β, TNF-α, and IL-6) expression and NLRP3 inflammasome-related

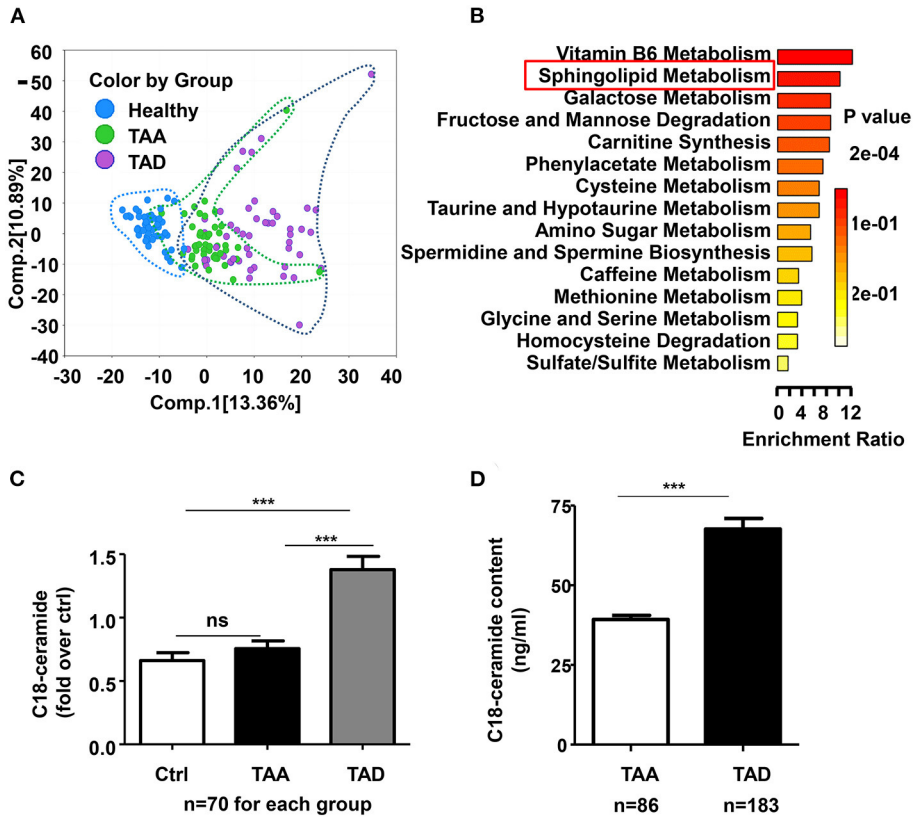

FIGURE 1 | The global metabolic profile revealed a significant change in sphingolipid metabolism, especially C18-ceramide in TAD patients. **(A)** Principal component analysis (PCA) demonstrated distinguished metabolic signatures among TAA, TAD and healthy controls. **(B)** Metabolite set enrichment analysis showed the top 15 significantly altered enrichment pathways between TAAs and TADs. **(C)** Untargeted metabolomics result demonstrated that C18-ceramide was significantly elevated in TAD patients but not significantly changed in TAA patients (ctrl, $n = 70$; TAA, $n = 70$; TAD, $n = 70$), One-way ANOVA, $^{***}p < 0.001$. **(D)** Quantitative analysis confirmed the increase in C18-ceramide in early-onset TAD patients (TAA, $n = 183$; TAD, $n = 86$), unpaired t-test, $^{***}p < 0.001$.

TABLE 1 | The proportion of early-onset TAD in each group of TAD patients with different amount of C18-ceramide level.

	C18-ceramide group			
	Low	**Moderate**	**High**	***p*-value**
Numbers	20	20	20	
Age (year-old)	52 (39–62.75)	54.5 (47.25–64.75)	49 (43–57.25)	0.2926
Male (%)	11 (55%)	12 (60%)	16 (80%)	0.2147
Hypertension (%)	14 (70%)	16 (80%)	16 (80%)	0.689
Hyperlipidemia (%)	12 (60%)	12 (60%)	15 (75%)	0.5171
Diabetes (%)	0 (0%)	1 (5%)	3 (15%)	0.1534
Early onset aortic dissection	9 (45%)	17 (85%**)	18 (90%**)	0.0020

$^{**}p < 0.01$ when compared to the low-level C18-ceramide group.

gene expression and protein (**Figures 3D,E**). Altogether, the present results suggested that inhibition of ceramide *de novo* synthesis could alleviate BAPN-induced aortic inflammation and dissection.

Ceramide Accelerated Inflammation Through the NLRP3-Caspase1 Pathway in Macrophages

To further investigate the underlying mechanism of ceramide in inflammation, we performed *in vitro* studies in the mouse macrophage cell line RAW264.7. Treatment of RAW 264.7 cells with exogenous C18-ceramide at 10 μmol/L for 24 h upregulated the expression of NLRP3, Caspase 1, Il1b, and Mmp9 and coincidingly promoted IL-1β and MMP9 cleavage (**Figures 4A,B**). Conversely, myriocin impeded LPS-induced NLRP3–caspase 1 cascade activation and subsequent IL-1β and MMP9 cleavage (**Figures 4C,D**).

DISCUSSION

TAD is often a life-threatening condition with high morbidity and mortality, and is characterized by smooth muscle cell loss, extracellular matrix degradation and increased vascular inflammation. Metabolomics has developed rapidly and offers an opportunity to explore new advances and potential biomarkers underlying TAD. Several lipid species alterations,

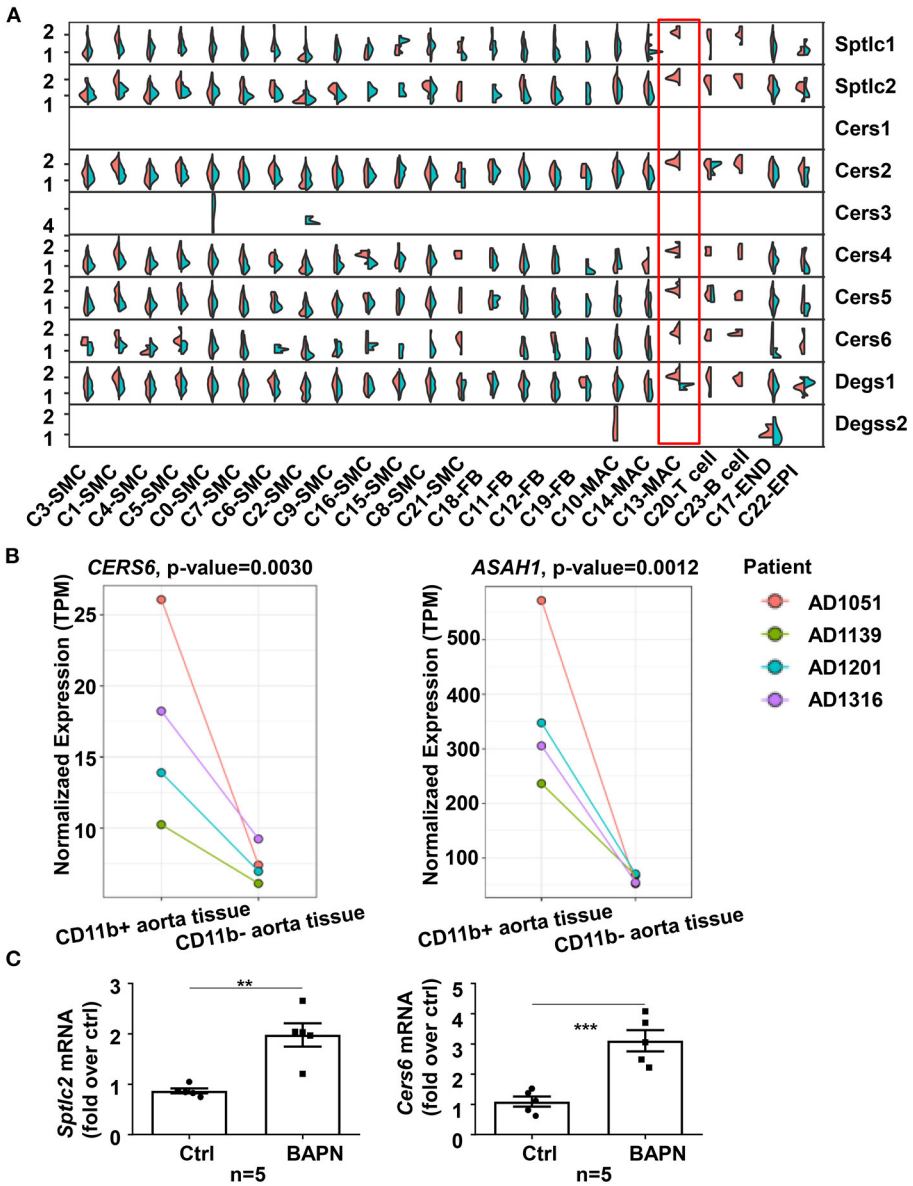

FIGURE 2 | Enhanced ceramide *de novo* synthesis in macrophages contributed to the increased ceramide content in plasma. **(A)** Split violin plot showed the expression of genes involved in ceramide synthesis pathways in mouse aortic cell subpopulations of the BAPN and CTRL groups in the 21-day mouse model. **(B)** Expression of ceramide synthesis and hydrolysis genes, *CERS6* and *ASAH1*, was higher in CD11b$^+$ aortic cells from TAAD patients than in CD11b$^-$ cells ($n = 4$). The statistical threshold of the differential expression test was set to be a q-value < 0.05. **(C)** Expression of ceramide *de novo* synthesis genes, *Sptlc2* and *Cers6*, was elevated in aortas from BAPN-induced TAD mice ($n = 5$), unpaired t-test, $^{**}p < 0.01$, $^{***}p < 0.001$.

such as increased phosphatidylcholine (4, 6) and decreased lysophosphatidylcholines and sphingolipids (5), were observed in aortic dissection patients and were regarded as potential biomarkers. However, these studies had some limitations. First, they had relatively small datasets and the results were not verified in larger cohorts. Second, they were observational studies, and the causal relationship between altered metabolites and the disease was not investigated. Therefore, the relationship needs to be further confirmed. In the present study, we aimed to explore the differentiated metabolites in TAA and TAD patients using an untargeted metabolomics approach. To our knowledge, this was the largest untargeted metabolomic study on thoracic aortic disease so far. It allowed for investigating the distinguished metabolites between TAA and TAD, so as to explore the specific pathophysiological process in TAD and potential biomakers.

From metabolite set enrichment analysis of differentiated metabolites between TAA and TAD, we observed vitamin B6 metabolism was the most enriched pathway. Its metabolite pyridoxate was significantly decreased in TAA, but not in

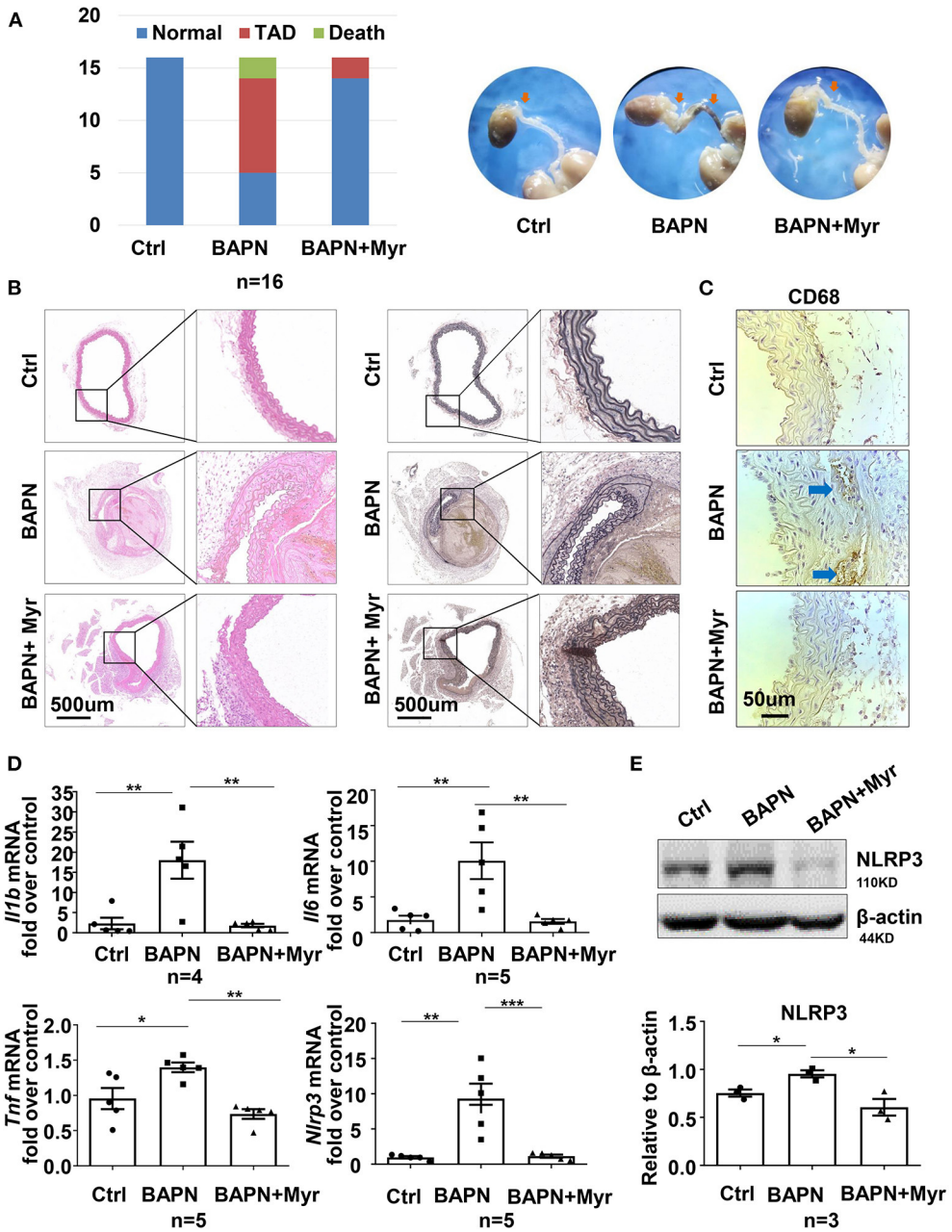

FIGURE 3 | Inhibition of ceramide *de novo* synthesis with myriocin alleviated BAPN-induced aortic dissection and inflammation. Three-week-old mice were administered with BAPN (0.5 g/kg/day) for 4 weeks, with or without intraperitoneally injected myriocin (0.5 mg/kg). **(A)** Incidence of TAD events and related death for each group and representative aorta images ($n = 16$). **(B)** Representative HE and VG staining images for each group ($n = 3$). **(C)** Representative immunohistochemical staining for macrophage marker CD68 ($n = 3$). **(D)** Quantification of the mRNA expression of *Il1b*, *Il6*, Tnf, and *Nlrp3* in the aorta by RT-qPCR ($n = 5$), One-way ANOVA, $^{*}p < 0.05$, $^{**}p < 0.01$, $^{***}P < 0.001$. **(E)** Representative western blot of NLRP3 in the aorta ($n = 3$), One-way ANOVA, $^{*}p < 0.05$. Myr, myriocin.

TAD (**Supplementary Table 3**). Vitamin B was reported to be associated with abdominal aortic aneurysm (20) and to mitigate thoracic aortic dilation in Marfan syndrome mice (21). Whether it was involved in aortic dissection remained unclear. Beyond that, we were more interested in another enriched pathway, sphingolipids, which were recently focused as a variety of cardiovascular diseases drivers and biomarkers. Consistent with previous studies, most sphingolipids including various sphingomyelins were significantly decreased in TAD (**Supplementary Figure 2**) (5, 7). However, we noticed significantly increased C18-ceramide content in the plasma of TAD patients, but not in TAA, from which we hypothesized that ceramide might play a role in TAD incidence.

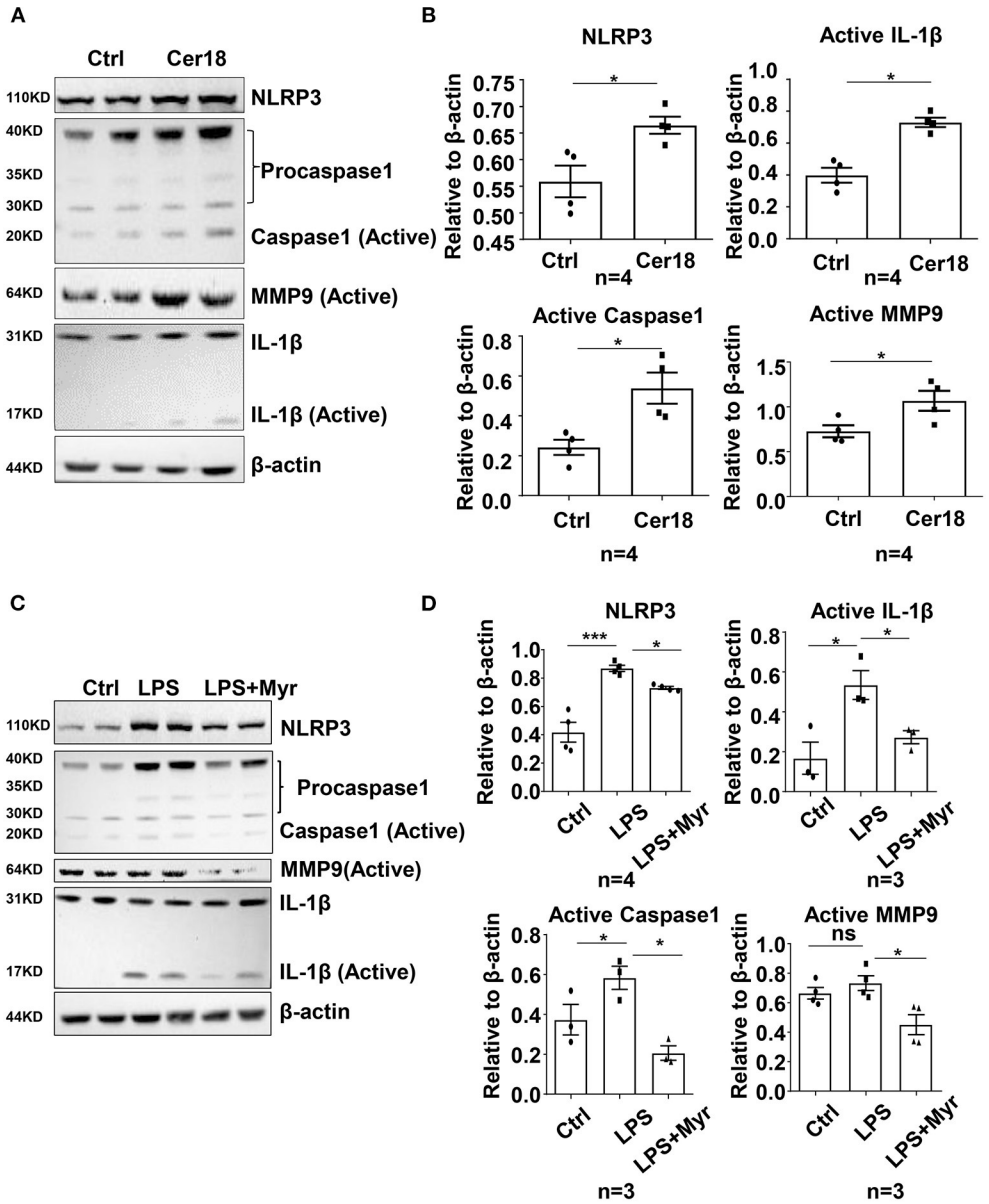

FIGURE 4 | Ceramide was involved in the activation of IL-1β and MMP9 by the NLRP3-caspase1 cascade in mouse macrophage RAW264.7. **(A,B)** Representative western blots and their quantification showed that C18-ceramide induced the activation of IL-1β and MMP9 by the NLRP3-caspase1 cascade, $n = 4$, unpaired *t*-test, $^{*}p < 0.05$, $^{**}p < 0.01$, $^{***}p < 0.001$. **(C,D)** Representative western blots and their quantification showed that myriocin prevented LPS-induced the activation of IL-1β and MMP9 by the NLRP3-caspase1 cascade, $n \geq 3$, One-way ANOVA, $^{*}p < 0.05$, $^{**}p < 0.01$, $^{***}p < 0.001$. Myr, myriocin; Cer18, C18-ceramide.

Ceramides are the central core of sphingolipid metabolism. They can be synthesized by different pathways: (1) the *de novo* synthesis pathway; (2) the complex sphingolipid (such as sphingomyelin) hydrolysis pathway; and (3) the salvage pathway (22). The former two contribute mostly to ceramide production. Once generated, ceramides can participate in numerous physiological and pathological processes, such as cellular proliferation and migration, inflammatory responses, apoptosis and senescence. Our existing single-cell RNA-Seq data from a murine aortic dissection model revealed specifically high expression of *Sptlc*, *Cers*, and *Degs* in a subpopulation of macrophages, suggesting that elevated ceramide might contribute to the enhanced *de novo* synthesis pathway in macrophages. Therefore, we focused on the inflammatory impact of ceramide in aortic dissection.

Aortic dissection is closely related to inflammatory processes. A variety of inflammatory cells can invade the vascular wall and cause arterial inflammation, among which

macrophages are the core cells (23). Activated macrophages secrete matrix metalloproteinases (MMPs), interleukins and vascular endothelial cell growth factors to further magnify the inflammatory response, matrix destruction and smooth muscle cell dysfunction, resulting in aortic injury and ultimately aortic dissection. After dissection, a large number of inflammatory cells enter the site of dissection, aggravating the local inflammatory response and participating in later aortic remodeling. Lian et al. (8) and Cui et al. (9) Both revealed that macrophage metabolic reprogramming was involved and played a vital role in aortic dissection. Some metabolites in the tricarboxylic acid (TCA) cycle, such as fumarate (8) and succinate (9), were substantially elevated in aortic dissection patients and aortic dissection mouse models induced by BAPN or AngII stimulation. Reprogrammed macrophages exaggerated vascular inflammation through the HIF1α-ADAM17 pathway and excessive ROS production, ultimately leading to aortic dissection.

Ceramides can promote inflammation through a variety of pathways (24). They can induce the expression or activation of NF-κB, a ubiquitous transcription factor involved in inflammatory and immune responses, and then upregulate many proinflammatory genes, including the cytokine genes IL-1β, IL-6, and IL-8, and chemokine genes, such as monocyte chemoattractant protein-1 (MCP-1). Deficiency of serine palmitoyltransferase subunit 2, a key enzyme involved in the ceramide *de novo* synthesis pathway, could reduce murine atherosclerosis partly by attenuating TLR4 recruitment and downstream NF-κB-mediated inflammation (25). In addition, the NOD-like receptor pyrin domain containing 3 (NLRP3) inflammasome is another important pathway that is involved in ceramide-mediated inflammation. Ceramides activate the Nlrp3 inflammasome and IL-1β secretion through caspase-1 activation in a Nlrp3-dependent manner in various tissues, including adipose (26), thymus (27) and brain microglia (28), suggesting that the Nlrp3 inflammasome could sense intracellular elevated ceramide.

Recent studies have suggested that the NLRP3 inflammasome plays an important role in TAD development (29–31). The Nlrp3-caspase 1 complex is activated in the condition of aortic dissection and participates in the process of aortic damage by degrading smooth muscle cell contractile protein (29), promoting macrophage inflammation and *MMP9* expression and intensifying extracellular matrix degradation. The NLRP3 inhibitor MCC950 effectively prevented aortic aneurysm and dissection induced by AngII in mice (30). However, the relationship between ceramide and inflammasome activation in TAD development remains unknown. Therefore, the present study sought to determine whether ceramide promotes TAD development by inducing NLRP3 inflammasome formation.

Our *in vivo* study demonstrated that inhibition of ceramide *de novo* synthesis by myriocin significantly alleviated BAPN-induced aortic dissection, and NLRP3 mRNA and protein levels were both decreased in BAPN-treated mouse aortae. Consistently, *in vitro* studies in the murine macrophage cell line RAW264.7 indicated that myriocin impeded the LPS-induced NLRP3-caspase 1 pathway, while exogenous C18-ceramide promoted this pathway, suggesting that the NLRP3-caspase 1 pathway might be involved in ceramide-induced inflammation and aortic injury.

Nevertheless, our present study had some limitations. First, it was still a cross-sectional study, and further investigations in prospective and longitudinal cohorts were needed to confirm the association between ceramide and early-onset aortic dissection risk. Second, ceramides in aortic tissues in human and mice were neither determined in this study. Further, alleviating BAPN-induced TAD through inhibition of ceramide *de novo* synthesis pathway might be better proved using *Sptlc2* deficient mouse models.

In summary, our current study first revealed that ceramide metabolism disturbance might play a vital role in TAD development by aggravating aortic inflammation through the NLRP3 pathway, possibly providing a new target for pharmacological therapy and a potential biomarker of TAD.

DATA AVAILABILITY STATEMENT

The original contributions presented in the study are included in the article/**Supplementary Material**, further inquiries can be directed to the corresponding author/s. The scRNA-seq data presented in the study are deposited in the Genome Sequence Archive (http://bigd.big.ac.cn/gsa/), accession number CRA003013.

ETHICS STATEMENT

The studies involving human participants conformed to the Declaration of Helsinki principles and were reviewed and approved by Ethics Committee of the Institutional Review Board at Fuwai Hospital (Approval No.: 2017-877). The patients/participants provided their written informed consent to participate in this study. The animal study was reviewed and approved by Institutional Animal Care and Use Committee (IACUC) at Fuwai Hospital (Approval No.: FW-2019-0008). Written informed consent was obtained from the individual(s) for the publication of any potentially identifiable images or data included in this article.

AUTHOR CONTRIBUTIONS

HY designed the project, carried out experiments, and drafted the manuscript together with FY. ML and CS were in charge of patient enrollment and clinical evaluation. QC and YZ participated in clinical data collection and the follow-up study. XL contributed to bioinformatics analysis of existing RNA-seq data. GZ, WC, and TL participated in animal experiments and cell experiments, respectively. ZZ was in charge of the project

design and revised the manuscript. All authors had read and approved the final manuscript.

FUNDING

This work was supported by the grant of CAMS Initiative for Innovative Medicine, China (No. 2016-I2M-1-016) and the grant of Initiative Research Program from State Key Laboratory of Cardiovascular Disease (SKL2021008).

ACKNOWLEDGMENTS

We thank all subjects who participated in this study.

SUPPLEMENTARY MATERIAL

The Supplementary Material for this article can be found online at: https://www.frontiersin.org/articles/10.3389/fcvm.2022.826861/full#supplementary-material

REFERENCES

1. Tang X, Lu K, Liu X, Jin D, Jiang W, Wang J, et al. Incidence and survival of aortic dissection in Urban China: results from the National Insurance Claims for Epidemiological Research (NICER) study. *Lancet Regional Health Western Pacific.* (2021) 17:100280. doi: 10.1016/j.lanwpc.2021.100280
2. Pape LA, Tsai TT, Isselbacher EM, Oh JK, O'Gara PT, Evangelista A, et al. Aortic diameter >or = 55 cm is not a good predictor of type A aortic dissection: observations from the International Registry of Acute Aortic Dissection (IRAD). *Circulation.* (2007) 116:1120–7. doi: 10.1161/CIRCULATIONAHA.107.702720
3. McGarrah RW, Crown SB, Zhang GF, Shah SH, Newgard CB. Cardiovascular metabolomics. *Circ Res.* (2018) 122:1238–58. doi: 10.1161/CIRCRESAHA.117.311002
4. Doppler C, Arnhard K, Dumfarth J, Heinz K, Messner B, Stern C, et al. Metabolomic profiling of ascending thoracic aortic aneurysms and dissections - implications for pathophysiology and biomarker discovery. *PLoS ONE.* (2017) 12:e0176727. doi: 10.1371/journal.pone.0176727
5. Zhou X, Wang R, Zhang T, Liu F, Zhang W, Wang G, et al. Identification of lysophosphatidylcholines and sphingolipids as potential biomarkers for acute aortic dissection *via* serum metabolomics. *Eur J Vasc Endovasc Surg.* (2019) 57:434–41. doi: 10.1016/j.ejvs.2018.07.004
6. Zeng Q, Rong Y, Li D, Wu Z, He Y, Zhang H, et al. Identification of serum biomarker in acute aortic dissection by global and targeted metabolomics. *Ann Vasc Surg.* (2020) 68:497–504. doi: 10.1016/j.avsg.2020.06.026
7. Huang H, Ye G, Lai S, Zou H, Yuan B, Wu Q, et al. Plasma lipidomics identifies unique lipid signatures and potential biomarkers for patients with aortic dissection. *Front Cardiovasc Med.* (2021) 8:757022. doi: 10.3389/fcvm.2021.757022
8. Lian G, Li X, Zhang L, Zhang Y, Sun L, Zhang X, et al. Macrophage metabolic reprogramming aggravates aortic dissection through the HIF1alpha-ADAM17 pathway. *EBioMedicine.* (2019) 49:291–304. doi: 10.1016/j.ebiom.2019.09.041
9. Cui H, Chen Y, Li K, Zhan R, Zhao M, Xu Y, et al. Untargeted metabolomics identifies succinate as a biomarker and therapeutic target in aortic aneurysm and dissection. *Eur Heart J.* (2021) 42:4373–85. doi: 10.1093/eurheartj/ehab605
10. Choi RH, Tatum SM, Symons JD, Summers SA, Holland WL. Ceramides and other sphingolipids as drivers of cardiovascular disease. *Nat Rev Cardiol.* (2021) 18:701–11. doi: 10.1038/s41569-021-00536-1
11. de Carvalho LP, Tan SH, Ow GS, Tang Z, Ching J, Kovalik JP, et al. Plasma ceramides as prognostic biomarkers and their arterial and myocardial tissue correlates in acute myocardial infarction. *JACC Basic Transl Sci.* (2018) 3:163–75. doi: 10.1016/j.jacbts.2017.12.005
12. Hilvo M, Meikle PJ, Pedersen ER, Tell GS, Dhar I, Brenner H, et al. Development and validation of a ceramide- and phospholipid-based cardiovascular risk estimation score for coronary artery disease patients. *Eur Heart J.* (2020) 41:371–80. doi: 10.1093/eurheartj/ehz387
13. Peterson LR, Xanthakis V, Duncan MS, Gross S, Friedrich N, Volzke H, et al. Ceramide remodeling and risk of cardiovascular events and mortality. *J Am Heart Assoc.* (2018) 7:7931. doi: 10.1161/JAHA.117.007931
14. Jensen PN, Fretts AM, Hoofnagle AN, Sitlani CM, McKnight B, King IB, et al. Plasma ceramides and sphingomyelins in relation to atrial fibrillation risk: the cardiovascular health study. *J Am Heart Assoc.* (2020) 9:e012853. doi: 10.1161/JAHA.119.012853
15. Poss AM, Maschek JA, Cox JE, Hauner BJ, Hopkins PN, Hunt SC, et al. Machine learning reveals serum sphingolipids as cholesterol-independent biomarkers of coronary artery disease. *J Clin Invest.* (2020) 130:1363–76. doi: 10.1172/JCI131838
16. Reforgiato MR, Milano G, Fabrias G, Casas J, Gasco P, Paroni R, et al. Inhibition of ceramide *de novo* synthesis as a postischemic strategy to reduce myocardial reperfusion injury. *Basic Res Cardiol.* (2016) 111:12. doi: 10.1007/s00395-016-0533-x
17. Hadas Y, Vincek AS, Youssef E, Zak MM, Chepurko E, Sultana N, et al. Altering sphingolipid metabolism attenuates cell death and inflammatory response after myocardial infarction. *Circulation.* (2020) 141:916–30. doi: 10.1161/CIRCULATIONAHA.119.041882
18. Lallemand T, Rouahi M, Swiader A, Grazide MH, Geoffre N, Alayrac P, et al. nSMase2 (type 2-neutral sphingomyelinase) deficiency or inhibition by GW4869 reduces inflammation and atherosclerosis in Apoe(-/-) mice. *Arterioscler Thromb Vasc Biol.* (2018) 38:1479–92. doi: 10.1161/ATVBAHA.118.311208
19. Liu X, Zhu CW, Yang G, Li H, Luo W, Shu M, et al. Single-cell RNA-seq identifies a Il1rn+/Trem1+ macrophage subpopulation as a cellular target for mitigating the progression of thoracic aortic aneurysm and dissection. *Cell Discov.* doi: 10.1038/s41421-021-00362-2
20. Takagi H, Umemoto T. Vitamins and abdominal aortic aneurysm. *J Clin Invest.* (2013) 123:1784–97. doi: 10.23736/S0392-9590.16.03618-X
21. Huang T, Chang H, Guo Y, Chang W, Chen Y. Vitamin B mitigates thoracic aortic dilation in marfan syndrome mice by restoring the canonical TGF-β pathway. *Int J Mol Sci.* (2021) 22:11737. doi: 10.3390/ijms222111737
22. Borodzicz S, Czarzasta K, Kuch M, Cudnoch-Jedrzejewska A. Sphingolipids in cardiovascular diseases and metabolic disorders. *Lipid Health Dis.* (2015) 14:55. doi: 10.1186/s12944-015-0053-y
23. Wang X, Zhang H, Cao L, He Y, Ma A, Guo W. The role of macrophages in aortic dissection. *Front Physiol.* (2020) 11:54. doi: 10.3389/fphys.2020.00054
24. Maceyka M, Spiegel S. Sphingolipid metabolites in inflammatory disease. *Nature.* (2014) 510:58–67. doi: 10.1038/nature13475
25. Chakraborty M, Lou C, Huan C, Kuo MS, Park TS, Cao G, et al. Myeloid cell-specific serine palmitoyltransferase subunit 2 haploinsufficiency reduces murine atherosclerosis. *J Clin Invest.* (2013) 123:1784–97. doi: 10.1172/JCI60415
26. Youm YH, Grant RW, McCabe LR, Albarado DC, Nguyen KY, Ravussin A, et al. Canonical Nlrp3 inflammasome links systemic low-grade inflammation to functional decline in aging. *Cell Metab.* (2013) 18:519–32. doi: 10.1016/j.cmet.2013.09.010
27. Youm YH, Kanneganti TD, Vandanmagsar B, Zhu X, Ravussin A, Adijiang A, et al. The Nlrp3 inflammasome promotes age-related thymic demise and immunosenescence. *Cell Rep.* (2012) 1:56–68. doi: 10.1016/j.celrep.2011.11.005
28. Scheiblich H, Schlutter A, Golenbock DT, Latz E, Martinez-Martinez P, Heneka MT. Activation of the NLRP3 inflammasome in microglia: the role of ceramide. *J Neurochem.* (2017) 143:534–50. doi: 10.1111/jnc.14225
29. Wu D, Ren P, Zheng Y, Zhang L, Xu G, Xie W, et al. NLRP3 (nucleotide oligomerization domain-like receptor family, pyrin domain containing 3)-caspase-1 inflammasome degrades contractile proteins: implications for aortic biomechanical dysfunction and aneurysm

and dissection formation. *Arterioscler Thromb Vasc Biol.* (2017) 37:694–706. doi: 10.1161/ATVBAHA.116.307648
30. Ren P, Wu D, Appel R, Zhang L, Zhang C, Luo W, et al. Targeting the NLRP3 inflammasome with inhibitor MCC950 prevents aortic aneurysms and dissections in mice. *J Am Heart Assoc.* (2020) 9:e014044. doi: 10.1161/JAHA.119.014044
31. Le S, Zhang H, Huang X, Chen S, Wu J, Chen S, et al. PKM2 activator TEPP-46 attenuates thoracic aortic aneurysm and dissection by inhibiting NLRP3 inflammasome-mediated IL-1beta secretion. *J Cardiovasc Pharmacol Ther.* (2020) 25:364–76. doi: 10.1177/1074248420919966

Conflict of Interest: The authors declare that the research was conducted in the absence of any commercial or financial relationships that could be construed as a potential conflict of interest.

Publisher's Note: All claims expressed in this article are solely those of the authors and do not necessarily represent those of their affiliated organizations, or those of the publisher, the editors and the reviewers. Any product that may be evaluated in this article, or claim that may be made by its manufacturer, is not guaranteed or endorsed by the publisher.

frontiers in Cardiovascular Medicine

MINI REVIEW
published: 10 March 2022
doi: 10.3389/fcvm.2022.861110

Comorbidity of Type 2 Diabetes Mellitus and Depression: Clinical Evidence and Rationale for the Exacerbation of Cardiovascular Disease

Mengmeng Zhu[1†], *Yiwen Li*[1†], *Binyu Luo*[1], *Jing Cui*[1], *Yanfei Liu*[2*] and *Yue Liu*[1*]

[1] National Clinical Research Centre for Chinese Medicine Cardiology, Xiyuan Hospital of China Academy of Chinese Medical Sciences, Beijing, China, [2] Second Department of Geriatrics, Xiyuan Hospital of China Academy of Chinese Medical Sciences, Beijing, China

OPEN ACCESS

Edited by:
Han Xiao,
Peking University Third Hospital, China

Reviewed by:
Weiguang Li,
Beijing Normal University, China
Yibo Wang,
Huangpu Branch of Ninth People's Hospital Affiliated to Medical School of Shanghai Jiaotong University, China

***Correspondence:**
Yue Liu
liuyueheart@hotmail.com
Yanfei Liu
yanfeitcm@163.com

[†] These authors share first authorship

Specialty section:
This article was submitted to Cardiovascular Metabolism, a section of the journal Frontiers in Cardiovascular Medicine

Received: 24 January 2022
Accepted: 07 February 2022
Published: 10 March 2022

Citation:
Zhu M, Li Y, Luo B, Cui J, Liu Y and Liu Y (2022) Comorbidity of Type 2 Diabetes Mellitus and Depression: Clinical Evidence and Rationale for the Exacerbation of Cardiovascular Disease. Front. Cardiovasc. Med. 9:861110. doi: 10.3389/fcvm.2022.861110

Depression is a common comorbidity of type 2 diabetes mellitus (T2DM). T2DM with comorbid depression increases the risk of cardiovascular events and death. Depression and T2DM and its macrovascular complications exhibited a two-way relationship. Regarding treatment, antidepressants can affect the development of T2DM and cardiovascular events, and hypoglycemic drugs can also affect the development of depression and cardiovascular events. The combination of these two types of medications may increase the risk of the first myocardial infarction. Herein, we review the latest research progress in the exacerbation of cardiovascular disease due to T2DM with comorbid depression and provide a rationale and an outlook for the prevention and treatment of cardiovascular disease in T2DM with comorbid depression.

Keywords: type 2 diabetes mellitus (T2DM), depression, cardiovascular disease, clinical evidence, outlook

INTRODUCTION

According to the 2021 International Diabetes Federation data (1), the global incidence of diabetes is 10.5% and is expected to increase to 12.2% by 2,045, making it one of the fastest growing global major health events of the 21st century. Depression is a common comorbidity of type 2 diabetes mellitus (T2DM). The International Prevalence and Treatment of Diabetes and Depression (INTERPRET-DD) study (2) found that the incidence of major depressive disorder (MDD) in patients with T2DM was approximately 10.6%. Depression also has a high incidence in patients with cardiovascular disease (CVD) and is an important risk factor for CVD (3). Several clinical studies have shown that T2DM with comorbid depression increases the risk of CVD morbidity and mortality and is associated with secondary composite outcomes such as CVD mortality, myocardial infarction (MI), and cardiovascular surgery (4–6). The view that "diabetes is a cardiovascular disease risk equivalent" is now considered a consensus, and many studies have been conducted on the relationship and mechanism between the two. However, as an adverse psychological factor that affects T2DM and CVD, the effect of depression on T2DM with comorbid CVD remains to be determined.

In this mini review, the keywords "depression," "depressive symptoms," "depressive disorders," "major depressive disorder," "type 2 diabetes," "type 2 diabetes mellitus," "diabetes," "cardiovascular disease," "cardiovascular events," "cardiovascular risk," and "cardiovascular outcomes" were searched in the PubMed, MEDLINE, EMBASE, and Web of Science databases. Clinical studies on the effect of T2DM with comorbid depression on CVD published in the past 5 years (from January 1, 2017, to January 1, 2022) were reviewed, and the effects of T2DM with comorbid depression on cardiovascular disease were summarized, providing a clinical reference for future studies on the prevention and treatment of cardiovascular disease due to diabetes with comorbid depression.

COMORBIDITY CHARACTERISTICS

T2DM With Comorbid Depression Increases the Risk of Cardiovascular Events and Mortality

T2DM with comorbid depression increases the risk of cardiovascular morbidity and mortality. A cohort study of 192,685 diabetic patients with or without depression showed that the risk of macrovascular complications, such as acute coronary syndrome and stroke, was 1.35-fold higher in diabetic patients with depression than in those without depression. This correlation was stronger in females than in males, and the severity of depression had different effects on the outcome of patients with T2DM. The correlation between recurrent MDD and macrovascular complications was stronger than that of isolated MDD and mild depression (7). A longitudinal study evaluating the two-way relationship between depression and macrovascular and microvascular complications of diabetes found that depression increases the risk of MI, coronary artery disease (CAD), congestive heart failure, cardiovascular surgery, and other composite T2DM-associated macrovascular events (8). A meta-analysis of 17 studies and over 1 million participants (5) found that depression was strongly associated with the risk of nonfatal and fatal CVD in patients with T2DM, providing evidence for the relationship between depression in patients with T2DM and cardiovascular events. Furthermore, depression was associated with an increased risk of major adverse cardiovascular events such as atherosclerotic cardiovascular disease (ASCVD), heart failure (HF), and MI in patients with early-onset T2DM. This association was not related to ethnic groups or age, and the correlation was stronger in females than in males (9).

These studies have underlined the association between T2DM with comorbid depression and composite cardiovascular events, and studies on the effects of T2DM with comorbid depression on coronary heart disease, MI, HF, and other diseases have also shown significant correlations. In patients with T2DM and comorbid depression, the risk of coronary heart disease and stroke increases by 36.8 and 32.9%, respectively, compared to patients with T2DM without depression (4). T2DM with comorbid depression increases the risk of MI compared to T2DM without depression, and persistent depression has a greater impact on the risk of MI than transient depression (10). This study not only demonstrated that T2DM with comorbid depression was associated with the development of MI but also confirmed that the course of depression was positively correlated with the risk of MI. Depression is prevalent in asymptomatic elderly patients with T2DM. In a study of the new-onset HF outcomes of 274 patients with asymptomatic T2DM followed up for a median period of 1.5 years, Cox regression analysis showed that comorbid depression increased the risk of HF in patients with asymptomatic T2DM by 2.5-fold. Furthermore, depression was a predictor of the incidence of HF in conjunction with poor glycemic control, left ventricular hypertrophy (LVH), and diastolic dysfunction (11).

In addition to predicting HF, depression can also be a predictor of cardiac ischemia in T2DM. In a 2-year follow-up study of asymptomatic T2DM patients with and without a history or symptoms of CAD, patients underwent myocardial perfusion single-photon emission computed tomography (MPS) and a depression and anxiety questionnaire. The results showed that depression and anxiety scores were predictors of cardiac ischemic events in patients with asymptomatic T2DM (12). However, due to the small number of new-onset cardiac ischemic events ($n = 11$) in the study, conclusions must still be verified through large-scale clinical trials. Depression can also be an independent predictor of all-cause mortality in T2DM. A large-scale prospective cohort study of 3,923 patients with T2DM in 56 primary health care centers (13) showed that the all-cause mortality in patients with depression was 1.4-fold that in patients without depression. The results of another large-scale cohort study in the T2DM population (14) also confirmed that depression increases the risk of mortality in patients with T2DM. In addition, depression can affect all-cause mortality in patients with prediabetes. Increased symptoms of depression increased all-cause mortality not only in patients with diabetes but also in patients with prediabetes; this correlation was stronger in patients with prediabetes (15).

T2DM with comorbid depression not only increases the risk of all-cause mortality but is also closely associated with increased cardiovascular mortality. The results of a meta-analysis (4) showed that patients with T2DM and comorbid depression had a 47.9% increase in cardiovascular mortality compared to patients with T2DM alone. A follow-up study of 1,495 patients over a median follow-up period of 7.7 years showed that patients with diabetes and depressive symptoms 1 year after enrollment were associated with increased eventual cardiovascular mortality (16).

The Two-Way Relationship Between T2DM and Depression

Several clinical studies have shown that depression increases the risk of T2DM (17, 18) and that T2DM also increases the risk of depression (19); more severe depression is associated with a higher risk of T2DM (19). The 2020 guidelines of the Chinese Diabetes Society (20) clearly cited a possible two-way relationship between T2DM and depression and anxiety; T2DM exacerbates the development of depression and anxiety, and depression

and anxiety increase the risk of T2DM. In addition, the guidelines also mentioned that specific populations of patients with gestational diabetes or postpartum diabetes have a higher risk of depression and anxiety. Gestational diabetes significantly increases the risk of postpartum depression and may be a risk factor for postpartum depression. Therefore, pregnant women with gestational diabetes must be screened for postpartum depression (21). Another prospective cohort study (22) found that women with prenatal depression were more likely to develop gestational diabetes than those without depressive symptoms. Thus, gestational diabetes mellitus and perinatal depression can also have a two-way relationship. Studies have shown that gestational diabetes increases the risk of future CVD in mothers (23). Currently, most studies have focused on the effect of gestational diabetes mellitus or depression alone on CVD or the effect of both on adverse pregnancy outcomes, and there have been relatively few studies on the effect of gestational diabetes mellitus with comorbid perinatal depression on CVD. Therefore, high-quality clinical studies are needed to investigate the effect of gestational diabetes mellitus with comorbid perinatal depression on cardiovascular outcomes in this specific population of pregnant women.

Depression increases the risk of macrovascular complications of T2DM. In addition, macrovascular complications of diabetes can also lead to an increased risk of depression (8). There are two-way effects between depression and macrovascular complications of diabetes, and the two are mutually influencing factors.

Potential Mechanisms

The exact mechanism by which depression affects the risk of CVD in T2DM is unclear. Currently, it is believed to be associated with multiple pathways, such as neuroendocrine disorders and the vascular endothelial inflammatory response; these mechanisms are interrelated and not isolated (24, 25). Depression overstimulates the hypothalamic-pituitary-adrenal (HPA) axis, leading to excessive cortisol secretion, which aggravates vascular endothelial damage and promotes insulin resistance. In patients with depression, poor adherence to medications and poor lifestyle increase vulnerability of hyperglycemia and hyperinsulinemia, thus, promoting coagulopathy and fibrinolysis. Depression is also associated with elevated levels of inflammatory factors such as C-reactive protein (CRP), tumor necrosis factor-alpha (TNF-α), and interleukin 6 (IL-6). Hyperglycemia and insulin resistance in diabetes are known to promote endothelial dysfunction, inflammation, and abnormalities of coagulation and fibrinolysis, thus accelerating the development of atherosclerosis and CVD. Depression promotes these mechanisms to accelerate the development of CVD. Other studies have analyzed the association between mood disorders and diabetes and CVD (including hypertension and CAD) from a genetic perspective (26), finding that depression, diabetes, and CVD may have multiple shared potential pleiotropic genes, thus affecting multiple signaling pathways such as corticotropin-releasing hormone (CRH), adenosine monophosphate activated protein kinase (AMPK), and 5 hydroxytryptamine (5-HT) pathways.

TREATMENT

Pharmacological Treatments

Antidepressants

Patients with depression who received selective serotonin reuptake inhibitors (SSRIs), tricyclic antidepressants (TCAs), heterocyclic antidepressants, and other antidepressants have a significantly reduced the risk of developing T2DM (27). Moreover, long-term use of SSRIs (≥120 days) or TCAs (≥35 days) was associated with a lower risk of developing T2DM. Some researchers have studied the antidepressant dosage (28) and found that in diabetic patients with poor glycemic control with baseline hemoglobin A1c (HbA1c) of 9.29%, those treated with the optimal therapeutic dosage of antidepressants were more likely to achieve better glycemic control (HbA1c $< 7\%$) after 12 months. Therefore, optimizing antidepressant dosage in patients with T2DM may be beneficial for glycemic control.

Different classes of antidepressants have different effects on mortality and cardiovascular events in T2DM with comorbid depression. In a study of 36,276 patients with newly diagnosed diabetes and depression treated with different classes of antidepressants for 6 months, regular use of antidepressants was associated with a reduced risk of macrovascular complications and/or all-cause mortality (29). Another cohort study (30) also reached the same conclusion of reduced mortality in diabetic patients with comorbid depression with SSRIs and tricyclic/tetracyclic antidepressant treatment. Furthermore, the study also found that serotonin-norepinephrine reuptake inhibitors (SNRIs), norepinephrine-dopamine reuptake inhibitors, mirtazapine, and trazodone also significantly decreased the mortality risk, but the use of reversible inhibitors of monoamine oxidase-A (RIMA) increased mortality risk.

Oral Hypoglycemic Agents

Currently, numerous clinical studies have confirmed that sodium-glucose cotransporter 2 (SGLT2) inhibitors and glucagon-like peptide 1 (GLP-1) receptor agonists reduce the risk of CVD, and their clinical indications have also been included in treatment guidelines (31). However, few studies have investigated the effects of hypoglycemic agents on depression and no guidelines are available. Different classes of hypoglycemic agents have different effects on the risk of depression in patients with T2DM. The results of a retrospective cohort study of 40,214 adult patients with T2DM who were not treated or treated with single or combined oral hypoglycemic agents where depression was used as an outcome measure (32) showed that dipeptidyl peptidase 4 (DPP-4) inhibitors and SGLT-2 inhibitors were both significantly associated with a reduced risk of depression, while biguanides, sulfonylureas, α-glucosidase inhibitors, thiazolidinediones, and glinides did not show to be associated with a reduced risk of depression. Because only one patient in the study was treated with SGLT-2 inhibitors, and the study was a non-randomized retrospective study with many confounding factors, the conclusions must be further verified. There have also been different conclusions regarding the effects of metformin on depression. In a case-control study of 550 elderly diabetic patients in nine communities, Chen et al.

(33) found that the risk of depression in patients treated with metformin was decreased compared with those not treated with metformin. However, this was a case-control study with a small sample size; hence, it cannot be concluded that metformin reduces depression in elderly patients with diabetes, but it only shows that metformin may be a protective factor for depression in elderly patients with diabetes. Danish researchers (34) tracked patients receiving antidiabetic drugs or insulin therapy between 2005 and 2015 through Danish population-based registers and found that continued use of metformin and combinations of drugs were associated with decreased rates of depression.

Antidepressants and Hypoglycemic Agents

In the last 5 years, studies on the effects of antidepressants combined with antidiabetic drugs on CVD remain lacking. However, in 2016, a Swedish study investigating the risk of first MI in patients undergoing antidiabetic and/or antidepressant

TABLE 1 | Guidelines for depression screening and interventions for patients with diabetes.

Guideline for the Prevention and Treatment of Type 2 Diabetes Mellitus in China (2020 edition) (20)	The mental status of patients with diabetes mellitus and depression and anxiety disorders should always be evaluated throughout the treatment. Early screening, evaluation, and monitoring of psychological status, especially in diabetic patients with a history of depression and anxiety, should emphasize emotional assessment when conditions change (e.g., development of complications) or when other psychosocial factors are present.	The collaborative care model can significantly improve depression and glycemic control in patients with diabetes and depression and reduce medical costs. Diabetic patients with depression should be referred to a psychiatrist with familiarity and knowledge of diabetes. Selective serotonin reuptake inhibitors and serotonin and norepinephrine reuptake inhibitors are often the first-line drugs of choice for diabetic patients with depression and anxiety and can improve glycemic control.
Standards of Medical Care in Diabetes—2022 (45)	Providers should consider the annual screening of all patients with diabetes, especially those with a self-reported history of depression, for depressive symptoms with age-appropriate depression screening measures, recognizing that further evaluation will be necessary for individuals who have a positive screening.	Referrals for the treatment of depression should be made to mental health providers who have experience using cognitive behavioral therapy, interpersonal therapy, or other evidence-based treatment approaches in conjunction with collaborative care with the patient's diabetes treatment team.
Precision Medicine in Diabetes: A Consensus Report from the American Diabetes Association (ADA) and the European Association for the Study of Diabetes (EASD) (46)	Providers must assess symptoms of depression using appropriate standardized and validated tools at the initial visit, at periodic intervals.	Psychological counseling can help patients understand and manage their emotional reactions to major events by developing a more optimistic outlook and more realistic, modulated, and adaptive emotional reactions.
Diabetes Self-management Education and Support in Adults with Type 2 Diabetes: A Consensus Report of the American Diabetes Association, the Association of Diabetes Care & Education Specialists, the Academy of Nutrition and Dietetics, the American Academy of Family Physicians, the American Academy of PAs, the American Association of Nurse Practitioners, and the American Pharmacists Association (47)	The identification of diabetes-related complications or other individual factors (e.g., psychosocial factors such as depression and anxiety) that may influence self-management should be considered a critical indicator of the need for DSMES that requires immediate attention and adequate resources.	Focused emotional support may be needed for depression. Additional mental health resources are generally required to address clinical depression.
Consensus statement of the American Association of Clinical Endocrinologists and American College of Endocrinology on the comprehensive type 2 diabetes management algorithm—2020 Executive Summary (48)	Healthcare professionals should assess the mood and psychological well-being of patients.	Healthcare professionals should refer patients with mood disorders to a mental healthcare facility.
Japanese Clinical Practice Guideline for Diabetes 2019 (49)	After at-risk patients with diabetes are screened for depression, systematically coordinated care is essential for both diabetes and depression.	An intervention that addresses both depressive symptoms and diabetes-related mental distress and anxiety is required to improve self-care ability and glycemic control in affected patients.
Diabetes Canada 2018 Clinical Practice Guidelines for the Prevention and Management of Diabetes in Canada: Diabetes and Mental Health (50)	Individuals with diabetes should be regularly screened for psychiatric disorders (e.g., depression) using validated self-report questionnaires or clinical interviews. Children and adolescents with diabetes should be screened for major depressive disorder and screened regularly for psychosocial difficulties, family distress, or mental health disorders.	Depression with diabetes should be referred to specialized mental healthcare professionals. Collaborative care by interprofessional teams should be provided for individuals with diabetes and depression. Antidepressant medications should be used to treat acute depression in people with diabetes and as a maintenance treatment to prevent recurrence of depression. Cognitive behavior therapy can be used to treat depression in individuals with depression alone or in combination with antidepressant medication.

treatment (35) found that the combination of antidepressants and antidiabetic drugs significantly increased the risk of first MI compared to drugs alone or without drugs. This risk was greater in middle-aged females (45–64 years) than in middle-aged males.

Non-pharmacological Treatments

Non-drug therapies for diabetes with comorbid depression, such as psychosocial intervention and self-management, have proven to be effective. A randomized controlled trial found that a collaborative care model of behavioral activation and skills to support self-management, such as adherence to diet plans, exercise, medication, tobacco cessation, and follow-up visits with physicians, improved depressive symptoms and resulted in fewer cardiovascular events or hospitalizations than usual care (36). A meta-analysis of 31 randomized controlled studies (37) also indicated that psychosocial interventions could significantly improve depressive symptoms in patients with T2DM and depression, as well as improve glycemic control. Therefore, including psychosocial interventions in the management of T2DM may also be beneficial for glycemic control, but the impact on CVD outcomes may have a lack of evidence from large RCTs. In addition, another interesting study (38) suggest that rural residence may have a protective effect on veterans' mental health, indicating that the environment is also an important aspect of psychological influence, but the effect on T2DM is not yet known. In recent years, neuromodulation methods such as transcranial magnetic stimulation (TMS) (39, 40) and transcranial direct current stimulation (tDCS) (41) have also been proved to be effective treatments for depression. In the treatment of diabetes, deep repetitive TMS can promote weight loss in obesity and thus prevent T2DM (42), and tDCS treatment can improve the quality of life and physical function of patients with diabetic polyneuropathy (43). The results of a single-blind cross-over trial showed that double tDCS improved both glucose tolerance and stress axes activity in healthy men, so repetitive tDCS may be a promising non-pharmacological treatment option for improving glucose tolerance in patients with T2DM (44).

PERSPECTIVE

T2DM with comorbid depression has an increased risk of cardiovascular events and death. Depression and T2DM and its macrovascular complications influence each other and exhibit a two-way relationship. Depression is involved in and accelerates the development and progression of cardiovascular disease in diabetic patients. Therefore, it is particularly important to screen for depression in diabetic patients to provide further intervention or psychological treatment to reduce the risk of CVD. Several guidelines have recommended screening and intervention for depression in patients with diabetes (**Table 1**) (20, 45–50), but most of the guidelines lack uniform standards for populations requiring screening and associated tools and interventions.

Different classes of hypoglycemic agents have different effects on depression, and different classes of antidepressants have different effects on macrovascular complications and mortality in T2DM. In cases of T2DM with comorbid depression, there is no uniform conclusion on the impact of the simultaneous selection of hypoglycemic agents and antidepressants on the subsequent risk and prognosis of CVD. The effect of newly available hypoglycemic agents on depression is also a future research direction. The peroxisome proliferator-activated receptors (PPAR) pan-agonist Chiglitazar sodium (Bilessglu) was officially approved for the Chinese market as a novel hypoglycemic agent. Animal studies have shown that PPAR-δ is associated with depression-like behavior in a mouse model of chronic social defeat stress (CSDS) (51). Future clinical trials may determine whether Chiglitazar sodium can be used to improve depressive symptoms in diabetic patients. Due to the low side effects and low cost of neuromodulatory treatment, it can avoid the adverse reactions caused by the combination of multiple oral drugs, future studies on the clinical effects of T2DM with depression co-morbidities could also be conducted, thus enriching the options for its adjunctive therapies.

AUTHOR CONTRIBUTIONS

MZ and YiL formed the reference collection, conducted the reference analysis, and wrote the manuscript. YuL and YaL contributed to the topic conception, manuscript revision, and decision to submit for publication. JC and BL contributed to reference analysis and helped in the revision of the manuscript. All authors contributed to the article and approved the submitted version.

FUNDING

This work was supported by the Outstanding Youth Foundation of National Natural Science Foundation (82022076) and the Special Project for Outstanding Young Talents of China Academy of Chinese Medical Sciences (ZZ15-YQ-017).

REFERENCES

1. Sun H, Saeedi P, Karuranga S, Pinkepank M, Ogurtsova K, Duncan BB, et al. IDF diabetes Atlas: Global, regional and country-level diabetes prevalence estimates for 2021 and projections for 2045. *Diabetes Res Clin Pract*. (2021) 109119. doi: 10.1016/j.diabres.2021.109119
2. Lloyd CE, Nouwen A, Sartorius N, Ahmed HU, Alvarez A, Bahendeka S, et al. Prevalence and correlates of depressive disorders in people with Type 2 diabetes: results from the International Prevalence and Treatment of Diabetes and Depression (INTERPRET-DD) study, a collaborative study carried out in 14 countries. *Diabet Med.* (2018) 35:760–9. doi: 10.1111/dme.13611
3. Jha MK, Qamar A, Vaduganathan M, Charney DS, Murrough JW. Screening and management of depression in patients with cardiovascular disease: JACC state-of-the-art review. *J Am Coll Cardiol.* (2019) 73:1827–45. doi: 10.1016/j.jacc.2019.01.041
4. Farooqi A, Khunti K, Abner S, Gillies C, Morriss R, Seidu S. Comorbid depression and risk of cardiac events and cardiac mortality in people with diabetes: A systematic review and meta-analysis. *Diabetes Res Clin Pract.* (2019) 156:107816. doi: 10.1016/j.diabres.2019.107816
5. Inoue K, Beekley J, Goto A, Jeon CY, Ritz BR. Depression and cardiovascular disease events among patients with type 2 diabetes: A systematic review and meta-analysis with bias analysis. *J Diabetes*

Complications. (2020) 34:107710. doi: 10.1016/j.jdiacomp.2020.107710
6. Hazuda HP, Gaussoin SA, Wing RR, Yanovski SZ, Johnson KC, Coday M, et al. Long-term association of depression symptoms and antidepressant medication use with incident cardiovascular events in the look AHEAD (Action for Health in Diabetes) clinical trial of weight loss in type 2 diabetes. *Diabetes Care.* (2019) 42:910–8. doi: 10.2337/dc18-0575
7. Wu CS, Hsu LY, Wang SH. Association of depression and diabetes complications and mortality: a population-based cohort study. *Epidemiol Psychiatr Sci.* (2020) 29:e96. doi: 10.1017/S2045796020000049
8. Nouwen A, Adriaanse MC, Van Dam K, Iversen MM, Viechtbauer W, Peyrot M, et al. Longitudinal associations between depression and diabetes complications: a systematic review and meta-analysis. *Diabet Med.* (2019) 36:1562–72. doi: 10.1111/dme.14054
9. Dibato JE, Montvida O, Zaccardi F, Sargeant JA, Davies MJ, Khunti K, et al. Association of cardiometabolic multimorbidity and depression with cardiovascular events in early-onset adult type 2 diabetes: a multiethnic study in the US. *Diabetes Care.* (2021) 44:231–9. doi: 10.2337/dc20-2045
10. Jung I, Kwon H, Park SE, Han K-D, Park Y-G, Kim Y-H, et al. Increased risk of cardiovascular disease and mortality in patients with diabetes and coexisting depression: a nationwide population-based cohort study. *Diabetes Metab J.* (2021) 45:379–89. doi: 10.4093/dmj.2020.0008
11. Wang Y, Yang H, Nolan M, Burgess J, Negishi K, Marwick TH. Association of depression with evolution of heart failure in patients with type 2 diabetes mellitus. *Cardiovasc Diabetol.* (2018) 17:19. doi: 10.1186/s12933-018-0664-5
12. Haaf P, Ritter M, Grize L, Pfisterer ME, Zellweger MJ. Quality of life as predictor for the development of cardiac ischemia in high-risk asymptomatic diabetic patients. *J Nucl Cardiol.* (2017) 24:772–82. doi: 10.1007/s12350-016-0759-x
13. Salinero-Fort MA, Gómez-Campelo P, Cárdenas-Valladolid J, San Andrés-Rebollo FJ, De Miguel-Yanes JM, De Burgos-Lunar C. Effect of depression on mortality in type 2 diabetes mellitus after 8 years of follow-up. The DIADEMA study diabetes. *Res Clin Pract.* (2021) 176:108863. doi: 10.1016/j.diabres.2021.108863
14. Naicker K, Johnson JA, Skogen JC, Manuel D, Øverland S, Sivertsen B, et al. Type 2 diabetes and comorbid symptoms of depression and anxiety: longitudinal associations with mortality risk. *Diabetes Care.* (2017) 40:352–8. doi: 10.2337/dc16-2018
15. Liwo ANN, Howard VJ, Zhu S, Martin MY, Safford MM, Richman JS, et al. Elevated depressive symptoms and risk of all-cause and cardiovascular mortality among adults with and without diabetes: The REasons for Geographic And Racial Differences in Stroke (REGARDS) study. *J Diabetes Complications.* (2020) 34:107672. doi: 10.1016/j.jdiacomp.2020.107672
16. Inoue K, Mayeda ER, Nianogo R, Paul K, Yu Y, Haan M, et al. Estimating the joint effect of diabetes and subsequent depressive symptoms on mortality among older latinos. *Ann Epidemiol.* (2021) 64:120–6. doi: 10.1016/j.annepidem.2021.09.007
17. Meng R, Liu N, Yu C, Pan X, Lv J, Guo Y, et al. Association between major depressive episode and risk of type 2 diabetes: A large prospective cohort study in Chinese adults. *J Affect Disord.* (2018) 234:59–66. doi: 10.1016/j.jad.2018.02.052
18. Graham EA, Deschênes SS, Khalil MN, Danna S, Filion KB, Schmitz N. Measures of depression and risk of type 2 diabetes: A systematic review and meta-analysis. *J Affect Disord.* (2020) 265:224–32. doi: 10.1016/j.jad.2020.01.053
19. Chireh B, Li M, D'arcy C. Diabetes increases the risk of depression: A systematic review, meta-analysis and estimates of population attributable fractions based on prospective studies. *Preventive medicine reports.* (2019) 14:100822. doi: 10.1016/j.pmedr.2019.100822
20. CDS. Guideline for the prevention and treatment of type 2 diabetes mellitus in China (2020 edition). *Chin J Diabetes Mellitus.* (2021) 13:315–409. doi: 10.3760/cma.j.cn115791-20210221-00095
21. Azami M, Badfar G, Soleymani A, Rahmati S. The association between gestational diabetes and postpartum depression: A systematic review and meta-analysis. *Diabetes Res Clin Pract.* (2019) 149:147–55. doi: 10.1016/j.diabres.2019.01.034
22. Minschart C, De Weerdt K, Elegeert A, Van Crombrugge P, Moyson C, Verhaeghe J, et al. Antenatal depression and risk of gestational diabetes, adverse pregnancy outcomes, and postpartum quality of life. *J Clin Endocrinol Metab.* (2021) 106:e3110–24. doi: 10.1210/clinem/dgab156
23. Li J, Song C, Li C, Liu P, Sun Z, Yang X. Increased risk of cardiovascular disease in women with prior gestational diabetes: A systematic review and meta-analysis. *Diabetes Res Clin Pract.* (2018) 140:324–38. doi: 10.1016/j.diabres.2018.03.054
24. Hackett RA, Steptoe A. Psychosocial factors in diabetes and cardiovascular risk. *Curr Cardiol Rep.* (2016) 18:95. doi: 10.1007/s11886-016-0771-4
25. Singh P, Khullar S, Singh M, Kaur G. Mastana S. Diabetes to cardiovascular disease: is depression the potential missing link? *Med Hypotheses.* (2015) 84:370–8. doi: 10.1016/j.mehy.2015.01.033
26. Amare AT, Schubert KO, Klingler-Hoffmann M, Cohen-Woods S, Baune BT. The genetic overlap between mood disorders and cardiometabolic diseases: a systematic review of genome wide and candidate gene studies. *Transl Psychiatry.* (2017) 7:e1007. doi: 10.1038/tp.2016.261
27. Fang Y-J, Wu T-Y, Lai J-N, Lin C-L, Tien N, Lim Y-P. Association between depression, antidepression medications, and the risk of developing type 2 diabetes mellitus: a nationwide population-based retrospective cohort study in Taiwan. *Biomed Res Int.* (2021) 2021:8857230. doi: 10.1155/2021/8857230
28. Grisham-Takac C, Lai P, Srinivasa M, Vasquez L, Rascati KL. Correlation of antidepressant target dose optimization and achievement of glycemic control. *Ment Health Clin.* (2019) 9:12–7. doi: 10.9740/mhc.2019.01.012
29. Wu C-S, Hsu L-Y, Pan Y-J, Wang S-H. Associations between antidepressant use and advanced diabetes outcomes in patients with depression and diabetes mellitus. *J Clin Endocrinol Metab.* (2021) 106:e5136–46. doi: 10.1210/clinem/dgab443
30. Chen H-M, Yang Y-H, Chen K-J, Lee Y, Mcintyre R S, Lu M-L, et al. Antidepressants reduced risk of mortality in patients with diabetes mellitus: a population-based cohort study in Taiwan. *J Clin Endocrinol Metab.* (2019) 104:4619–25. doi: 10.1210/jc.2018-02362
31. Cui J, Liu Y, Li Y, Xu F, Liu Y. Type 2 diabetes and myocardial infarction: recent clinical evidence and perspective. *Frontiers in cardiovascular medicine.* (2021) 8:644189. doi: 10.3389/fcvm.2021.644189
32. Akimoto H, Tezuka K, Nishida Y, Nakayama T, Takahashi Y, Asai S. Association between use of oral hypoglycemic agents in Japanese patients with type 2 diabetes mellitus and risk of depression: A retrospective cohort study. *Pharmacol Res Perspect.* (2019) 7:e00536. doi: 10.1002/prp2.536
33. Chen F, Wei G, Wang Y, Liu T, Huang T, Wei Q, et al. Risk factors for depression in elderly diabetic patients and the effect of metformin on the condition. *BMC Public Health.* (2019) 19:1063. doi: 10.1186/s12889-019-7392-y
34. Kessing LV, Rytgaard HC, Ekstrøm CT, Knop FK, Berk M, Gerds TA. Antidiabetes agents and incident depression: a nationwide population-based study. *Diabetes Care.* (2020) 43:3050–60. doi: 10.2337/dc20-1561
35. Rådholm K, Wiréhn AB, Chalmers J, Östgren CJ. Use of antidiabetic and antidepressant drugs is associated with increased risk of myocardial infarction: a nationwide register study. *Diabet Med.* (2016) 33:218–23. doi: 10.1111/dme.12822
36. Ali MK, Chwastiak L, Poongothai S, Emmert-Fees KMF, Patel SA, Anjana R M, et al. Effect of a collaborative care model on depressive symptoms and glycated hemoglobin, blood pressure, and serum cholesterol among patients with depression and diabetes in india: the independent randomized clinical trial. *JAMA.* (2020) 324:651–62. doi: 10.1001/jama.2020.11747
37. Xie J, Deng W. Psychosocial intervention for patients with type 2 diabetes mellitus and comorbid depression: a meta-analysis of randomized controlled trials. *Neuropsychiatr Dis Treat.* (2017) 13:2681–90. doi: 10.2147/NDT.S116465
38. Boscarino JJ, Figley CR, Adams RE, Urosevich TG, Kirchner HL, Boscarino JA. Mental health status in veterans residing in rural versus non-rural areas: results from the veterans' health study. *Military Med Res.* (2020) 7:44. doi: 10.1186/s40779-020-00272-6
39. Cash RFH, Weigand A, Zalesky A, Siddiqi SH, Downar J, Fitzgerald PB, et al. Using brain imaging to improve spatial targeting of transcranial magnetic stimulation for depression. *Biol Psychiatry.* (2021) 90:689–700. doi: 10.1016/j.biopsych.2020.05.033
40. Cappon D, Den Boer T, Jordan C, Yu W, Metzger E, Pascual-Leone A. Transcranial magnetic stimulation (TMS) for geriatric depression. *Ageing Res Rev.* (2022) 74:101531. doi: 10.1016/j.arr.2021.101531

41. Chase HW, Boudewyn MA, Carter CS, Phillips ML. Transcranial direct current stimulation: a roadmap for research, from mechanism of action to clinical implementation. *Mol Psychiatry.* (2020) 25:397–407. doi: 10.1038/s41380-019-0499-9
42. Devoto F, Ferrulli A, Zapparoli L, Massarini S, Banfi G, Paulesu E, et al. Repetitive deep TMS for the reduction of body weight: Bimodal effect on the functional brain connectivity in "diabesity". *Nutr Metab Cardiovasc Dis.* (2021) 31:1860–70. doi: 10.1016/j.numecd.2021.02.015
43. Ferreira G, Silva-Filho E, De Oliveira A, De Lucena C, Lopes J, Pegado R. Transcranial direct current stimulation improves quality of life and physical fitness in diabetic polyneuropathy: a pilot double blind randomized controlled trial. *J Diabetes Metab Disord.* (2020) 19:327–35. doi: 10.1007/s40200-020-00513-4
44. Wardzinski EK, Friedrichsen L, Dannenberger S, Kistenmacher A, Melchert UH, Jauch-Chara K, et al. Double transcranial direct current stimulation of the brain increases cerebral energy levels and systemic glucose tolerance in men. *J Neuroendocrinol.* (2019) 31:e12688. doi: 10.1111/jne.12688
45. American Diabetes Association Professional Practice C, American Diabetes Association Professional Practice C, Draznin B, Aroda VR, Bakris G, Benson G, et al. 5. facilitating behavior change and well-being to improve health outcomes: standards of medical care in diabetes-2022. *Diabetes Care.* (2022) 45:S60–S82. doi: 10.2337/dc22-S005
46. Chung WK, Erion K, Florez JC, Hattersley AT, Hivert M-F, Lee CG, et al. Precision medicine in diabetes: a consensus report from the American Diabetes Association (ADA) and the European Association for the study of diabetes (EASD). *Diabetes Care.* (2020) 43:1617–35. doi: 10.2337/dci20-0022
47. Powers MA, Bardsley JK, Cypress M, Funnell MM, Harms D, Hess-Fischl A, et al. Diabetes self-management education and support in adults with type 2 diabetes: A Consensus Report of the American Diabetes Association, the Association of Diabetes Care & Education Specialists, the Academy of Nutrition and Dietetics, the American Academy of Family Physicians, the American Academy of PAs, the American Association of Nurse Practitioners, and the American Pharmacists Association. *Diabetes Care.* (2020) 43:1636–49. doi: 10.2337/dci20-0023
48. Garber AJ, Handelsman Y, Grunberger G, Einhorn D, Abrahamson MJ, Barzilay JI, et al. Consensus statement by the American association of clinical endocrinologists and American college of endocrinology on the comprehensive type 2 diabetes management algorithm. *Endocr Pract.* (2020) 26:107–39. doi: 10.4158/CS-2019-0472
49. Araki E, Goto A, Kondo T, Noda M, Noto H, Origasa H, et al. Japanese clinical practice guideline for diabetes 2019. *J Diabetes Investig.* (2020) 11:1020–76. doi: 10.1111/jdi.13306
50. Robinson DJ, Coons M, Haensel H, Vallis M, Yale J-F. Diabetes and Mental health. *Can J Diabetes.* (2018) 42:S130–41. doi: 10.1016/j.jcjd.2017.10.031
51. He J-G, Zhou H-Y, Xue S-G, Lu J-J, Xu J-F, Zhou B, et al. Transcription factor TWIST1 integrates dendritic remodeling and chronic stress to promote depressive-like behaviors. *Biol Psychiatry.* (2021) 89:615–26. doi: 10.1016/j.biopsych.2020.09.003

Conflict of Interest: The authors declare that the research was conducted in the absence of any commercial or financial relationships that could be construed as a potential conflict of interest.

Publisher's Note: All claims expressed in this article are solely those of the authors and do not necessarily represent those of their affiliated organizations, or those of the publisher, the editors and the reviewers. Any product that may be evaluated in this article, or claim that may be made by its manufacturer, is not guaranteed or endorsed by the publisher.

frontiers | Frontiers in Cardiovascular Medicine

ORIGINAL RESEARCH
published: 07 April 2022
doi: 10.3389/fcvm.2022.851905

Metabolomics Fingerprint Predicts Risk of Death in Dilated Cardiomyopathy and Heart Failure

Alessia Vignoli[1,2†], Alessandra Fornaro[3†], Leonardo Tenori[1,2], Gabriele Castelli[3], Elisabetta Cecconi[4], Iacopo Olivotto[3], Niccolò Marchionni[5], Brunetto Alterini[4] and Claudio Luchinat[1,2*]*

[1] Department of Chemistry "Ugo Schiff", Magnetic Resonance Center (CERM), University of Florence, Sesto Fiorentino, Italy, [2] Interuniversity Consortium for Magnetic Resonance of Metalloproteins, Sesto Fiorentino, Italy, [3] Cardiomyopathy Unit, Careggi University Hospital, Florence, Italy, [4] Division of Cardiovascular and Perioperative Medicine, Careggi University Hospital, Florence, Italy, [5] Division of General Cardiology, Department of Experimental and Clinical Medicine, Careggi University Hospital, University of Florence, Florence, Italy

OPEN ACCESS

Edited by:
Han Xiao,
Peking University Third Hospital, China

Reviewed by:
Yuan Wang,
Capital Medical University, China
Chen Chen,
Huazhong University of Science and Technology, China

***Correspondence:**
Brunetto Alterini
alterinib@aou-careggi.toscana.it
Claudio Luchinat
luchinat@cerm.unifi.it

[†]These authors have contributed equally to this work

Specialty section:
This article was submitted to Cardiovascular Metabolism, a section of the journal Frontiers in Cardiovascular Medicine

Received: 10 January 2022
Accepted: 01 March 2022
Published: 07 April 2022

Citation:
Vignoli A, Fornaro A, Tenori L, Castelli G, Cecconi E, Olivotto I, Marchionni N, Alterini B and Luchinat C (2022) Metabolomics Fingerprint Predicts Risk of Death in Dilated Cardiomyopathy and Heart Failure. Front. Cardiovasc. Med. 9:851905. doi: 10.3389/fcvm.2022.851905

Background: Heart failure (HF) is a leading cause of morbidity and mortality worldwide. Metabolomics may help refine risk assessment and potentially guide HF management, but dedicated studies are few. This study aims at stratifying the long-term risk of death in a cohort of patients affected by HF due to dilated cardiomyopathy (DCM) using serum metabolomics *via* nuclear magnetic resonance (NMR) spectroscopy.

Methods: A cohort of 106 patients with HF due to DCM, diagnosed and monitored between 1982 and 2011, were consecutively enrolled between 2010 and 2012, and a serum sample was collected from each participant. Each patient underwent half-yearly clinical assessments, and survival status at the last follow-up visit in 2019 was recorded. The NMR serum metabolomic profiles were retrospectively analyzed to evaluate the patient's risk of death. Overall, 26 patients died during the 8-years of the study.

Results: The metabolomic fingerprint at enrollment was powerful in discriminating patients who died (HR 5.71, $p = 0.00002$), even when adjusted for potential covariates. The outcome prediction of metabolomics surpassed that of N-terminal pro b-type natriuretic peptide (NT-proBNP) (HR 2.97, $p = 0.005$). Metabolomic fingerprinting was able to sub-stratify the risk of death in patients with both preserved/mid-range and reduced ejection fraction [hazard ratio (HR) 3.46, $p = 0.03$; HR 6.01, $p = 0.004$, respectively]. Metabolomics and left ventricular ejection fraction (LVEF), combined in a score, proved to be synergistic in predicting survival (HR 8.09, $p = 0.0000004$).

Conclusions: Metabolomic analysis *via* NMR enables fast and reproducible characterization of the serum metabolic fingerprint associated with poor prognosis in the HF setting. Our data suggest the importance of integrating several risk parameters to early identify HF patients at high-risk of poor outcomes.

Keywords: metabolomics, heart failure, prognosis, NMR spectroscopy, precision medicine

INTRODUCTION

Dilated cardiomyopathy (DCM), one of the leading causes of heart failure (HF) worldwide (1), is generally considered as a "final phenotype," resulting from miscellaneous genomic or phenomic insults *via* activation of diverse DCM disease-causing cascades (2). The DCM may remain asymptomatic for years (3), eventually leading to progressive ventricular dilatation and both systolic and diastolic dysfunctions, arrhythmias, sudden death, and HF. The prevalence of DCM in observational studies of HF patients varied between 8 and 47%, while in trials of Heart Failure with Reduced Ejection Fraction (HFrEF), DCM etiology accounted for 12–35% of individuals (4).

Heart failure is a complex clinical syndrome in which heart function is inadequate to meet physiological demands and it constitutes a massive health problem, with a considerable residual disease burden due, at least in part, to a broad range of disease courses and responses to therapy (5). Several studies have aimed at defining the underlying pathophysiology of HF using recent advances in system biology approach as well as at discovering possible biomarkers to achieve a better prognostic stratification of cardiac failure (6, 7), beyond left ventricular ejection fraction (LVEF) evaluation. With this regard, several survival prediction models have been created using clinical risk scores and biomarkers, such as natriuretic peptides (8), but important knowledge gaps remain regarding the complex biological pathways determining individual variability. This limitation hinders the identification of specific patient subsets with different needs and fates.

In the era of precision medicine, Omics sciences could be the instrument to meet this need. Metabolomics is one of the latest omic technologies, broadly defined as the comprehensive measurement of the complete ensemble of endogenous and exogenous metabolites present in a biological specimen, which is the so-called metabolome (9). Metabolites represent, at the same time, the downstream output of the omics cascade, and the upstream input from various external factors, such as environment, lifestyle, diet, and drug administration (10). Thus, metabolites have been described as the most proximal reporters of any disease status or phenotype because their concentrations in biospecimens are directly related to the underlying pathophysiological landscape (11). Metabolomics applications in biomedical research are manifold (12–17), and this technology has already demonstrated its potentiality in the setting of cardiovascular diseases (18–23).

Metabolic impairment has long been identified as an intrinsic feature of HF pathophysiology and a detrimental self-perpetuating cycle involving heart failure and altered metabolism that promotes HF progression was postulated (24, 25). Energetic and structural metabolic failure is not limited to the myocardium, but it is reflected at a systemic level, and considerably contributes to major HF symptoms and disease progression (26, 27). Metabolomics has contributed to elucidating several systemic metabolic impairments that occur in patients with HF: insulin resistance, shift toward hyper-catabolism with blunting of anabolic pathways, impaired glucose oxidation and a switch toward glycolysis, impaired fatty acid β-oxidation, and urea cycle dysfunction (27–30). In our previous paper on the same cohort of patients, we showed that patients with HF were characterized by higher serum concentrations of phenylalanine, tyrosine, isoleucine, creatine, and low serum levels of lactate, citrate, lysine, and L-dopa (28). Moreover, metabolomics has been demonstrated to be a promising approach for the clinical prognosis of patients with HF (31–33).

Here, we propose a strategy for the prognostic evaluation of HF due to DCM based on the combination of serum nuclear magnetic resonance (NMR)-based metabolomics with traditional prognostic factors, such as N-terminal pro b-type natriuretic peptide (NT-proBNP) and LVEF. For this purpose, we retrospectively analyzed a well-defined, homogeneous, single-center cohort of patients with DCM with stable chronic HF diagnosed and monitored between 1982 and 2011 (median follow up time from DCM diagnosis: 15 years), and consecutively enrolled for this study between 2010 and 2012 (**Supplementary Figure S1**).

METHODS

Patient Recruitment

In this retrospective study, a cohort of 106 adult patients (74 men, 32 women, median age 49, 95% CI 49–53 years) with chronic heart failure (i.e., at least one previous heart failure event, comprising hospitalization for HF and/or an urgent visit resulting in intravenous therapy for HF due to DCM) was examined. The present cohort is a sub-group of the population analyzed in our previous publication (28). The HF has been defined as a clinical syndrome characterized by fundamental symptoms (e.g., breathlessness, ankle swelling, and fatigue) and/or signs (e.g., elevated jugular venous pressure, pulmonary crackles, and peripheral edema) related to a structural and/or functional abnormality of the heart that results in elevated intracardiac pressures and/or inadequate cardiac output at rest and/or during exercise (34). A period of clinical stability of at least 6 months in optimal medical therapy (OMT) was required for enrollment. Patients were diagnosed between 1982 and 2011 (t0). In the period 2010–2012 (t1), patients were re-examined or examined for the first time (only for patients diagnosed between 2010 and 2012), blood serum samples were collected and analyzed *via* NMR. Then, survival status was evaluated at the last follow-up in 2019 (t2). In patients who died or were transplanted, the end of follow-up was considered either the time of death or heart transplantation. In the minority of patients lost to follow-up (i.e., not traceable by June 2019), the last clinical evaluation or the last telephone contact was considered. The experimental design is graphically illustrated in **Figure 1**.

The enrolled patients were classified as idiopathic DCM, defined by the presence of left ventricular (LV) or biventricular dilatation and systolic dysfunction in the absence of abnormal loading conditions (hypertension, valve disease) or coronary artery disease sufficient to cause global systolic impairment (1, 35). The patients with HF, judged to be secondary to ischemic heart disease, systemic hypertension, chemotherapy, alcoholic abuse, diabetes mellitus, *cor pulmonalis*, valve disease, or other cardiac or systemic diseases, were excluded, as well

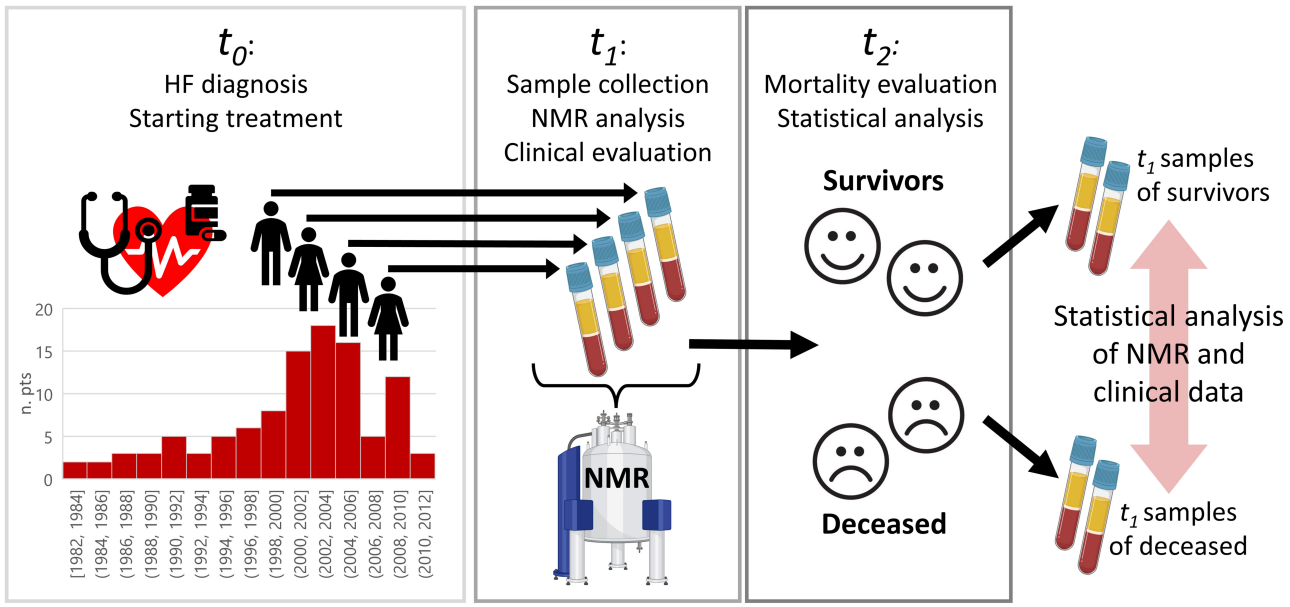

FIGURE 1 | Graphical overview of the study design to investigate differences between survived and deceased patients with HF. Patients were diagnosed at time t0, where t0 for each patient was in the range 1982–2011. Between 2010 and 2012 (t1), the patients were re-examined or examined for the first time, blood serum samples collected and analyzed *via* nuclear magnetic resonance (NMR). Survival status was evaluated in 2019 (t2). Patients were, then, retrospectively split in two groups according to the survival status (alive vs. deceased), and statistical analysis on NMR data was performed.

as patients for whom a coronary angiogram was not available. The patients were consecutively enrolled in the years 2010–2012 at the Careggi University Hospital Florence, Italy. They underwent half-yearly clinical assessments (median follow-up from enrollment 8 years). All study patients were evaluated and followed up by clinical history, physical examination, 12-lead ECG, standard chest radiograph, routine laboratory tests, M-mode, 2D, and Doppler echocardiography. For the entire study period, the patients were seen by the same cardiologists who assumed primary responsibility for their management.

Ethical Issues

This study was approved by the local Ethics Committee (Azienda Ospedaliero—Universitaria Careggi, Florence, Italy). Written informed consent was obtained from each participant at the time of blood sample collection. The study adheres to the principles of the Helsinki Declaration and its later amendments.

Collection of Samples

Each blood sample was collected through peripheral venous access in a 10-mL tube (BD P100, BD Diagnostics, Franklin Lakes, NJ). Subsequently, blood samples were centrifuged for 10 min at 4,000 rpm at the temperature of 4°C, then, the supernatant serum was aliquoted in sterile cryovials and stored at −80°C pending NMR analysis.

NMR Analysis

Serum samples were prepared for NMR experiments as described in our previous publications (28, 36). One-dimensional ^{1}H NMR spectra of each sample were acquired using a Bruker 600 MHz spectrometer (Bruker BioSpin) operating at 600.13 MHz proton Larmor frequency and equipped with a 5 mm CPTCI ^{1}H-^{13}C-^{31}P and ^{2}H-decoupling cryoprobe, including a z-axis gradient coil, an automatic tuning-matching, and an automatic sample changer. A BTO 2000 thermocouple served for temperature stabilization at the level of ∼0.1 K at the sample. Before measurement, samples were kept for at least 3 min inside the NMR probe-head, for temperature equilibration at 310 K. For each serum sample, a standard nuclear Overhauser effect spectroscopy pulse sequence NOESY 1Dpresat (noesygppr1d.comp; Bruker BioSpin)(37), using 64 scans, 98,304 data points, a spectral width of 18,028 Hz, an acquisition time of 2.7 s, a relaxation delay of 4 s and a mixing time of 0.01 s (total duration of the NMR experiment 7 min), was applied to obtain a spectrum in which both signals of low molecular weight metabolites and high molecular weight macromolecules (i.e., proteins, lipids, and lipoproteins) are detected.

Free induction decays were multiplied by an exponential function equivalent to 1.0 Hz line-broadening factor before applying Fourier transform. The transformed spectra were automatically corrected for phase and baseline distortions and calibrated to the anomeric glucose doublet at δ 5.24 ppm using TopSpin3.6.2 (Bruker Biospinsrl).

Each 1D spectrum was segmented into 0.02 ppm chemical shift bins in the range 0.2–10 ppm, and the corresponding spectral areas were integrated using the AssureNMR software (Bruker BioSpin). The regions of residual water signal (4.37–5.13 ppm) and the signals of ethanol (1.12–1.23 ppm and 3.53–3.73 ppm) were removed, and the dimension of the system was reduced to 438 bins. The probabilistic quotient

normalization (38) was applied on the remaining bins prior to statistical analysis.

Statistical Analysis

Data analyses were performed using the open-source software R. Multivariate analysis was performed on binned spectra (thus, on the whole spectra, considering both assigned and unassigned metabolites). Principal component analysis (PCA) was used as the first unsupervised analysis to visualize data. Metabolomics analysis was performed using a fingerprinting approach: the metabolomic fingerprint is a global, rapid evaluation of an NMR spectrum as a whole that considers all (assigned or unassigned) detectable metabolites present in that biological sample (39). Standard partial least square discriminant analysis (40) (PLS-DA) was applied to discriminate the metabolomic fingerprints of survivors and deceased patients using the first 7 PLS components, and the PLS-DA model was validated using a Leave-One-Out cross-validation scheme (LOOCV, R script developed in-house). Since the group size is unbalanced (survived 75.5%, deceased 24.5%), samples from 25 survivors and 25 deceased patients were randomly chosen from the full dataset and subjected to PLS-DA modeling. The resampling procedure was performed 100 times to account for variability in the sampling procedure, and each model was cross-validated each time. Samples were assigned to one of the two classes using the majority vote algorithm (R library "mclust") on the results obtained by the 100 iterations. Sensitivity, specificity, and accuracy were calculated according to the standard definitions. Variable importance in projections (VIP) was calculated using an R script developed in-house, variables with a VIP score higher than 1 were considered important in the PLS-DA model.

The predictive performance of the metabolomic PLS-DA classification was compared with that of LVEF and NT-proBNP. The LVEF classification followed the European Society of Cardiology guidelines (34), identifying three classes: reduced LVEF (<40%, high-risk: HiR), mid-range LVEF (40–49%, intermediate risk: IR), and preserved LVEF (≥50%, low risk: LR). Patients with a baseline level of NT-proBNP higher than 400 pg/ml were considered at high-risk of death. Moreover, the ability of the combination of metabolomics and LVEF in predicting poor prognosis was also tested. Metabolomics was used as the first screening method and then was adjusted using ejection fraction: patients predicted as survivors by the PLS-DA metabolomic model but with LVEF of <35% were reclassified as high-risk of death, while patients predicted as deceased but with LVEF of >50% were reclassified as low risk of death. All the above-mentioned analyses were performed using Kaplan–Meier (KM) curves, with the additional calculation of the hazard ratio (HR) and *p*-value assessed by the Log-Rank test (R library "survminer"). The performances and the independence of metabolomics were evaluated by calculating Cox proportional hazards regression models (41) (R library "Survival") and each model significance was assessed through a likelihood-ratio test. These analyses were performed in a univariate and multivariate fashion.

The untargeted quantification of 22 metabolites and 114 lipoprotein-related parameters was performed using the Bruker IVDr analysis platform (42). The non-parametric Wilcoxon Rank-Sum test was used to infer differences between the groups of interest. The *P*-values were adjusted for multiple testing using the false discovery rate (FDR) procedure with Benjamini and Hochberg (43) correction at $\alpha = 0.05$. Each metabolite/lipoprotein feature was divided into three tertiles and Cox regression models were calculated to estimate the association between metabolites/lipoproteins and prognosis. Additional models were calculated to adjust for additional covariates: sex, age at DCM diagnosis, time from DCM diagnosis and last follow up, NT-proBNP, LVEF, New York Heart Association (NYHA) class at enrollment, systolic blood pressure (SBP), end-diastolic diameter index (EDDi) at enrollment, and left atrial volume index (LAVi) at enrollment.

Robust correlations were calculated among metabolomic variables and clinical data following the 10% winsorized correlation approach (44) using the function "wincor" of the R package "WRC2." The *P*-values were adjusted for multiple testing using the FDR procedure.

RESULTS

Study Population

Baseline characteristics of the cohort are shown in **Table 1**. The median age at enrollment was 58.5 ± 14.1 years, with a median age at DCM diagnosis of 49 ± 11.9 years. The patients were predominantly men (69.8%). The median time from DCM diagnosis at last evaluation was 15 ± 5.9 years. The patients were mostly pauci-symptomatic at enrollment (85.8% NYHA class I-II). Median systolic blood pressure (SPB) was 120 ± 14.8 mmHg, while echocardiographic parameters showed a considerable LV (left ventricular) and LA (left atrial) enlargement in most patients, with median indexed LVEDDi and LAVi of 31.6 ± 4.9 and 41.9 ± 18 mm/m^2, respectively. Median LVEF at enrollment was 44.5 ± 8.15% with an NT-proBNP median value of 219.1 ± 237.8 pg/ml. All patients were on ACE-inhibitors or angiotensin receptor blockers inhibitors (ARBs) at enrollment, while 92.4% were receiving beta-blockers (BB). The introduction of Angiotensin Receptor Neprilysin Inhibitors (ARNIs) into clinical practice has become significant only in the last 2 years of the study follow-up, therefore, this agent has not been taken into consideration. Diuretic treatment was administered in 71% of patients at baseline.

At the last evaluation, 80 patients were alive, while 26 had died for HF-related causes (7 patients for sudden cardiac death and 19 patients for refractory heart failure). Demographic and clinical characteristics of the 106 patients with DCM depending on survival status at t2 are shown in **Table 1**: age, SBP, EDDi, LVEF, NT-proBNP, and diuretic administration at enrollment were significantly different between survivors and deceased patients.

NMR Metabolomics Prediction of HF Prognosis

Before any supervised approach, PCA was used as an exploratory analysis to visualize data. No outlier or relevant clustering

TABLE 1 | Baseline characteristics of enrolled patients.

	Overall at t_1 (106 pts)	Alive at t_2 (80 pts)	Deceased at t_2 (26 pts)	*p*-value[#]
Age at enrollment (yrs), median (mad)	58.5 (14.1)	56.0 (11.9)	67.5 (12.6)	0.004
Gender (M), *n* (%)	74 (69.8)	55 (68.8)	19 (73.1)	0.9
Age at DCM diagnosis (yrs), median (mad)	49 (11.9)	48.5 (11.1)	55.5 (17.0)	0.1
Time from DCM diagnosis and last follow up (yrs), median (mad)	15 (5.9)	15 (5.9)	15 (7.4)	0.9
NYHA class at enrollment				0.07
I, *n* (%)	38 (35.8)	31 (38.8)	7 (26.9)	
II, *n* (%)	53 (50.0)	41 (51.2)	12 (46.2)	
III, *n* (%)	13 (12.2)	8 (10.0)	5 (19.2)	
IV, *n* (%)	2 (2.0)	0 (0.0)	2 (7.7)	
SBP (mmHg) at enrollment, median (mad)	120 (14.8)	120 (14.8)	110 (14.8)	0.02
EDDi (mm/mq) at enrollment, median (mad)	31.6 (4.9)	30.8 (3.8)	36.9 (5.7)	0.004
LAVi (mL/mq) at enrollment, median (mad)	41.9 (18.0)	41.3 (16.3)	47.8 (26.9)	0.09
LVEF (%) at enrollment, median (mad)	44.5 (8.15)	46.0 (7.4)	37.5 (9.6)	0.001
NT-proBNP (pg/ml) at enrollment, median (mad)	219.1 (237.8)	180.6 (176.0)	613.3 (741.9)	0.005
BB* at enrollment, *n* (%)	98 (92.4)	73 (91.2)	25 (96.1)	0.8
ACE-I[§] at enrollment, *n* (%)	106 (100)	80 (100)	26 (100)	1
Diuretic at enrollment, *n* (%)	75 (70.7)	51 (63.8)	24 (92.3)	0.02

*DCM, dilated cardiomyopathy; NYHA, New York Heart Association Classification; SBP, systolic blood pressure; EDDi, indexed end diastolic diameter; LAVi, indexed left atrial volume; LVEF, left ventricular ejection fraction; NT-proBNP, N-terminal pro b-type natriuretic peptide; BB, beta blockers; ACE-I, Angiotensin-converting-enzyme inhibitors. *bisoprolol-equivalent; §ramipril-equivalent; #FDR adjusted with the Benjamini-Hochberg procedure. Data are reported for the overall population at enrollment (t1) and for alive and deceased patients at follow-up separated (t2).*

emerged from the score plot (**Supplementary Figure S2**). Then, the differences in serum metabolomics ^{1}H NMR fingerprints of survivors and deceased patients were analyzed using standard PLS-DA (**Figure 2A**). To ensure that the calculated PLS-DA model was statistically robust, an internal validation using a LOOCV was performed: the two groups show a good clustering, yielding 70.8% accuracy, 76.9% sensitivity, and 68.8% specificity (deceased patients wrongly classified as survivors present, on average, a longer survival time between enrollment and death: 5.7 vs. 4.3 years, see **Supplementary Figure S1**). Based on the VIP score analysis (**Figure 2B**) variables that mainly contributed to the PLS-DA model, and, thus, to the risk of stratification, were related to spectral regions of creatine, creatinine, lactate, trimethylamine-N-oxide, and lipoproteins.

Analyzing the metabolomic classification with KM curves (**Figure 2C**), clear discrimination resulted between patients who died and those who survived: *p*-value of 0.00002 and HR of 5.71 (95% CI 2.57–12.67). The use of the majority vote algorithm for patient classification produced a gray region in which patients were assigned to a class or another with a small margin (50 ± 10%). To verify the robustness of our model, we repeated the KM analyses after removing the 11 ambiguous patients that were classified with a margin <10%. Removing borderline patients did not significantly affect the overall model accuracy (**Supplementary Figure S3**).

Comparison of Metabolomics With Known Prognostic Factors: NT-ProBNP and Ejection Fraction

The prognostic significance of NT-proBNP natriuretic peptide, examined at enrollment, was analyzed. The results of the KM analyses are shown in **Supplementary Figure S4**. Compared to metabolomics results, NT-proBNP showed higher specificity (71.2%) in discriminating deceased and survivor patients, although with lower sensitivity (58.3%) and accuracy (68%). The combination of NT-proBNP and metabolomics provided only a slight improvement in the outcome prediction: 75% sensitivity, 68.5% specificity, and 70.1% accuracy.

The predictive performance of the metabolomic model was also compared with that of left ventricular ejection fraction, and the results are reported in **Figure 3**. Patients with reduced LVEF showed a significantly higher risk of death (HRs of 7.47 and 4.26 and *p*-values of 0.0001 and 0.0002 concerning LR and IR, respectively), whereas patients with mid-range and preserved LVEF were both associated with a lower risk (HR 1.79, *p*-value 0.38).

The potential of metabolomics in sub-stratifying LVEF classes was then tested: mid-range and preserved LVEF were considered

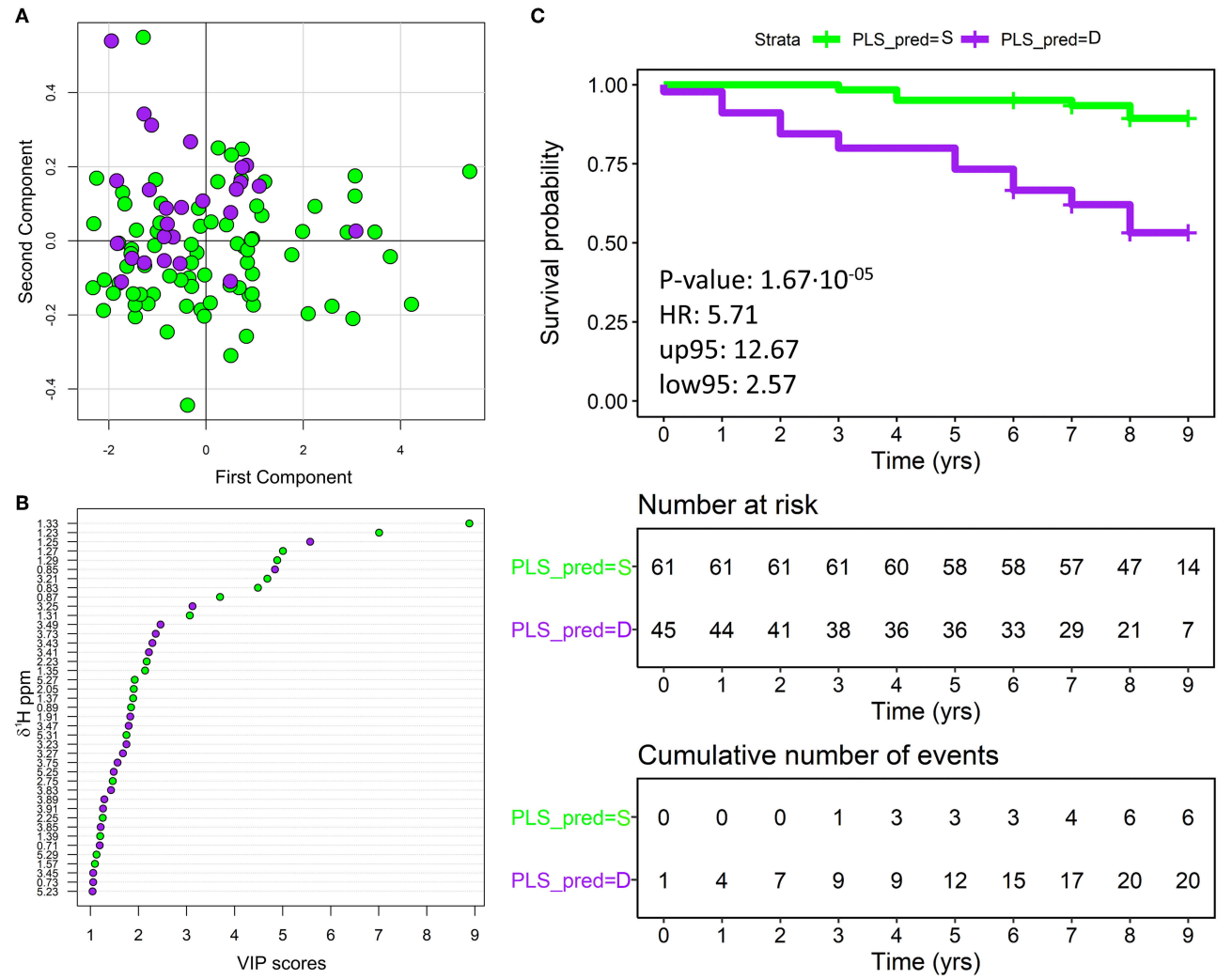

FIGURE 2 | (A) score plot of the first two components of the partial least square discriminant analysis (PLS-DA) model discriminating survivor (80 green dots) and deceased (26 purple dots) patients. **(B)** The variable importance in projections (VIP) score plot indicating the most discriminating bins in descending order of importance; only the bins that showed a VIP score>1 are reported in the plot. For each bin the starting ppm is reported. Green dots represent bins with intensity higher in survivor patients, conversely purple dots represent bins with intensity higher in deceased patients. **(C)** Overall patients with HF, plotting actual survival over time (in years) according to estimated metabolomic risk [Kaplan-Meier (KM) curves]. Low metabolomic risk (green) and high metabolomic risk (purple) patients are significantly clustered with a *p*-value of $1.67{\cdot}10^{-5}$ (calculated with the Log-Rank test) and an HR of 5.71. Censored events represent either the time of last recorded clinical follow-up, or the time of death. Number at risk: number of patients stratified according to the metabolomics classification at each time point. Cumulative number of events: total number of deceased patients at each time point for each metabolomics risk group. PLS_PRED = S, predicted by PLS as survivor; PLS_PRED = D, predicted by PLS as deceased.

as a single low-risk class, whereas reduced LVEF was considered as a high-risk class. Although metabolomics showed to effectively sub-stratify low- and high-risk patients in both classes (HRs 3.46 and 6.01, *p*-values 0.03 and 0.004, respectively), it showed the best performance in the high-risk class (**Figure 4**).

Finally, the outcome prediction of the combination of metabolomics and LVEF was tested. The resulting combined score relies on LVEF for <35 or >50% values (i.e., when LVEF appears highly prognostic), whilst it is based on metabolomics for intermediate LVEF values, for which LVEF shows the least predictive capacity. This combined approach led to an improved prediction, with 75.5% accuracy, 73.8% sensitivity, 80.8% specificity, HR 8.09, and *p*-value 0.0000004 as shown by KM analysis (**Figure 5**).

Analysis of Clinical Covariates

Possible covariates, such as advanced age at diagnosis (>60 years), sex, the time elapsed since the first diagnosis, NYHA functional class, SBP and echocardiographic parameters (EDDi and LAVi), were compared with the three main prognostic parameters (metabolomics, NT-proBNP, and LVEF) *via* univariate and multivariate Cox regression analyses (results

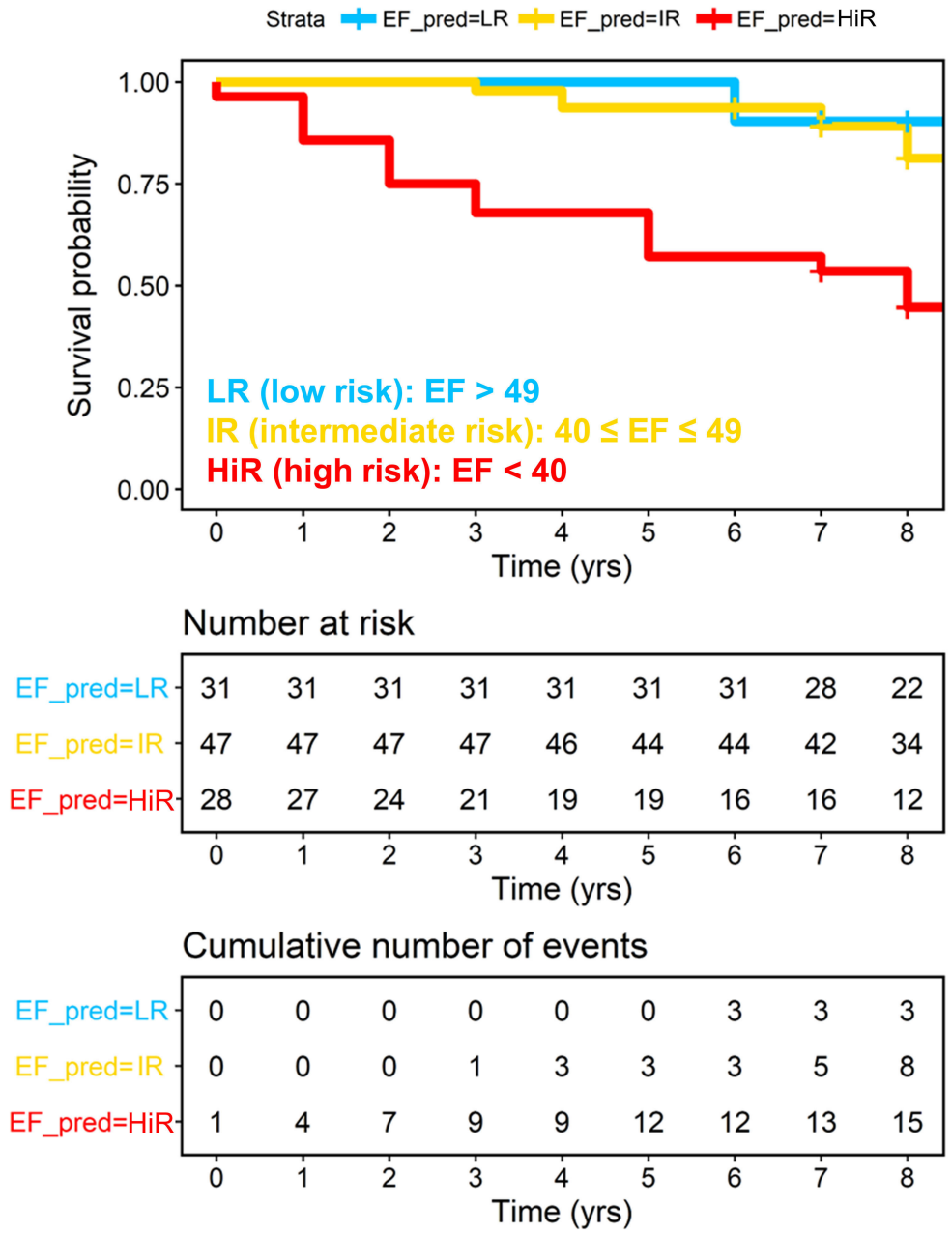

	p-value	HR	HR 95% CI
LR vs. IR	0.3767	1.79	0.54-5.98
IR vs. HiR	0.0002	4.26	1.75-10.34
LR vs. HiR	0.0001	7.47	2.91-19.17

FIGURE 3 | Overall patients with HF, plotting actual survival over time (measured in years) according to risk estimated based on ejection fraction (Kaplan-Meier curves). High-risk (red) group is significantly clustered with respect to both intermediate (yellow) and low (blue) risk groups with HR of 4.26 and 7.47, respectively.

(Continued)

FIGURE 3 | Censored events represent either the time of last recorded clinical follow up, or time of death. Number at risk: number of patients stratified according to the left ventricular ejection fraction (LVEF) at each time point. Cumulative number of events: total number of deceased patients at each timepoint for each risk group based on the LVEF. The *P*-values are calculated with the Log-Rank test. EF_PRED = LR: predicted by EF at low risk of death; EF_PRED = IR: predicted by EF at intermediate risk; EF_PRED = HR: predicted by EF at high-risk.

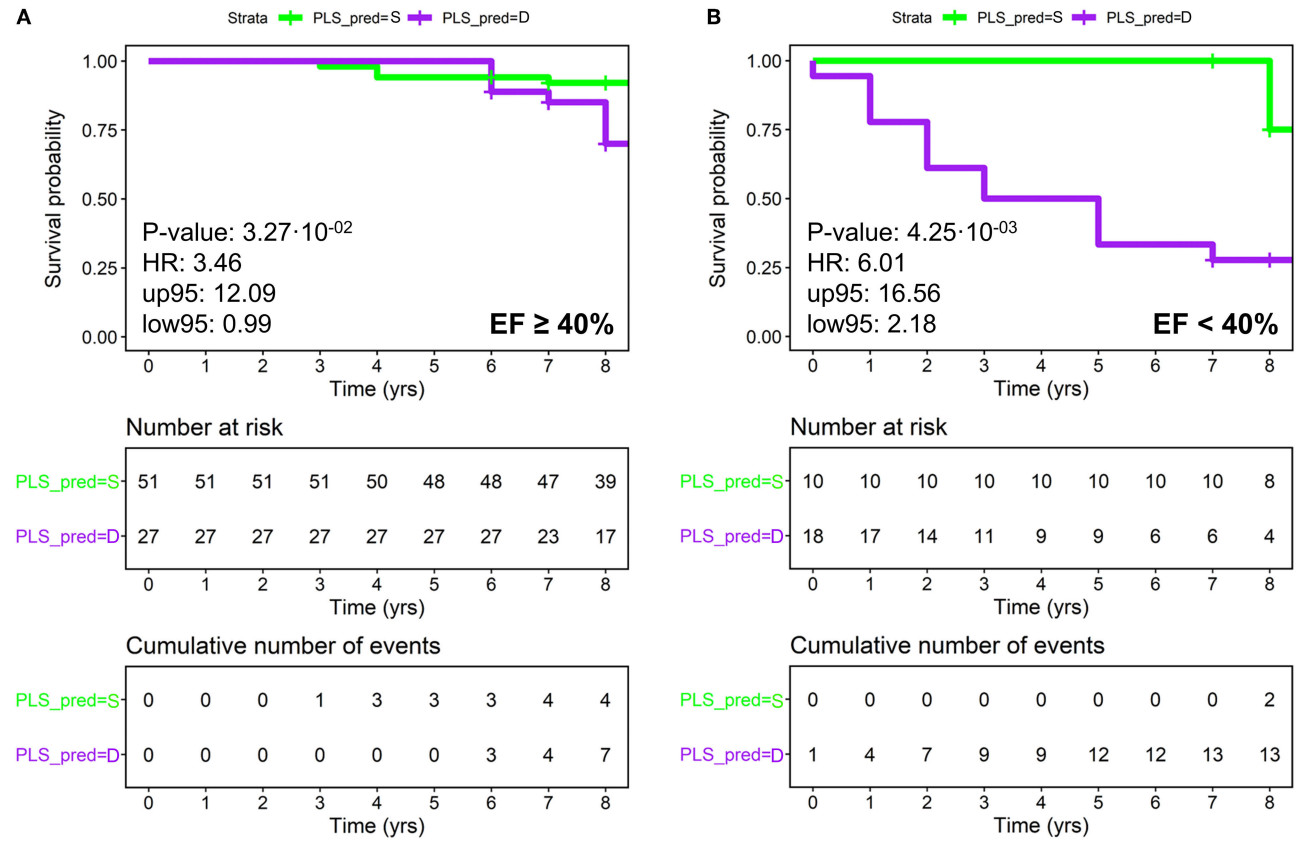

FIGURE 4 | Patients with HF divided according to LVEF subclasses **(A)** LVEF ≥ 40% (low risk), **(B)** LVEF < 40% (high-risk), plotting actual survival over time (measured in years) according to estimated risk based on metabolomics (KM curves). Low-risk patients are colored in green and high-risk in purple. The *P*-values are calculated using the Log-Rank test. Censored events represent either the time of last recorded clinical follow-up, or time of death. Number at risk: number of patients stratified according to metabolomics. Cumulative number of events: total number of deceased patients at each time point for each metabolomic group. **(A)** KM analysis on metabolomic classification of patients with LVEF ≥ 40%; **(B)** KM analysis on metabolomic classification of patients with LVEF < 40%. PLS_PRED = S, predicted by PLS as survivor; PLS_PRED = D, predicted by PLS as deceased.

displayed in **Table 2**). After univariate analysis, metabolomics, age at diagnosis, advanced NYHA classes (III-IV) at enrollment, NT-proBNP, and reduced LVEF resulted to be statistically associated with the outcome; however, after multivariate Cox regression model, only metabolomics (HR 6.72, *p* 0.0007), advanced age at diagnosis (HR 3.26, *p* 0.008), and reduced LVEF (HR 2.6, *p* 0.001) maintained their correlation with prognosis, regardless of other variables.

Correlations among metabolomics (metabolites and lipoprotein main parameters) and clinical variables are shown in **Supplementary Figure S5**. Several statistically significant correlations emerged from this analysis. In particular, succinic acid, acetone, and trimethylamine-N-oxide show a strong correlation pattern with NT-proBNP and with several echocardiographic (ECO) parameters (ECO left the atrial end-diastolic area, ECO left atrial end-diastolic diameter, ECO left atrial end-diastolic, and systolic volume). Also, glucose, lactic acid, and citric acid present correlations with the abovementioned echocardiographic parameters. Glycated hemoglobin (Hb1AC) significantly correlates with 12 metabolites. The LVEF anticorrelates with trimethylamine-N-oxide and correlates with creatine, Apo-A1, and Apo-2. Trimethylamine-N-oxide and creatine show the same trend of correlation with systolic blood pressure. Estimated glomerular filtration rate anticorrelates with creatinine and correlates with high-density lipo-protein (HDL) cholesterol, body mass index (BMI) correlates with phenylalanine and tyrosine, and electrocardiogram QT interval shows positive correlations with valine, pyruvic and citric acids.

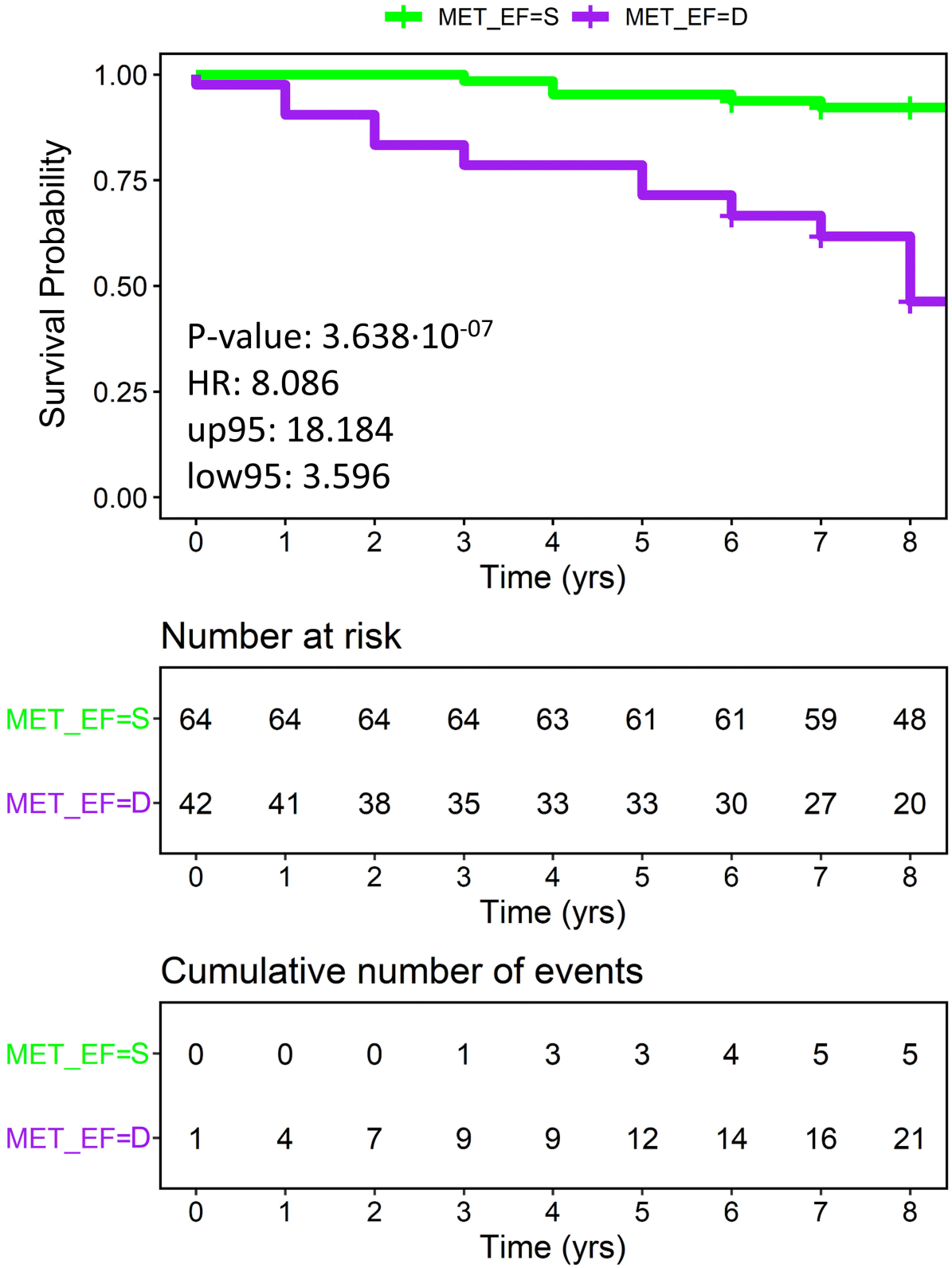

FIGURE 5 | Overall patients with HF, plotting actual survival over time (measured in years) according to risk estimated using a combination of metabolomics and ejection fraction (KM curves). Low metabolomic risk (green) and high metabolomic risk (purple) patients are significantly clustered with a *p*-value of $3.64 \cdot 10^{-7}$

(Continued)

FIGURE 5 | (calculated with the Log-Rank test) and an HR of 8.09. Censored events represent either the time of last recorded clinical follow-up, or the time of death. Number at risk: number of patients stratified according to the combined score at each time point. Cumulative number of events: total number of deceased patients at each time point for each risk group based on the combined score. MET_EF = S, predicted by the combined score of metabolomics and EF as survivor; MET_EF = D, predicted by the combined score of metabolomics and EF as deceased.

TABLE 2 | Association with the outcome: unadjusted and adjusted hazard ratios (HR).

	Hazard ratio (univariate)	*p*-value	Hazard ratio (multivariate)	*p*-value
Metabolomics				
High-risk	5.92 (2.37–14.76)	<0.001	7.00 (2.28–21.51)	<0.001
Sex				
Male	1.18 (0.49–2.80)	0.72	0.64 (0.24–1.73)	0.38
Age at DCM diagnosis				
>60 yrs	2.22 (1.01–4.90)	0.048	4.40 (1.64–11.79)	<0.01
Time from DCM diagnosis and last follow up				
>15 yrs	1.02 (0.47–2.20)	0.96	0.91 (0.36–2.31)	0.84
NT-proBNP				
>400 pg/mL	3.03 (1.34–6.82)	<0.01	1.30 (0.43–3.94)	0.64
LVEF				
40 ≤ EF ≤ 49 (IR)	1.80 (0.48–6.78)	0.39	1.80 (0.41–7.94)	0.44
<40 (HiR)	8.09 (2.34–27.99)	<0.001	9.35 (1.81–48.26)	<0.01
NYHA class at enrollment				
II	1.24 (0.49–3.14)	0.65	0.48(0.12–2.02)	0.32
III–IV	3.52 (1.23–10.06)	0.019	0.66(0.12–3.61)	0.63
SBP				
>130 mmHg	0.80 (0.28–2.33)	0.68	0.85 (0.26–2.72)	0.78
EDDi at enrollment				
>30 mm/mq	1.72 (0.69–4.28)	0.24	0.89 (0.28–2.84)	0.85
LAVi at enrollment				
>40 mL/mq	1.76 (0.77–4.06)	0.18	0.60 (0.18–1.98)	0.40

Correlation with the outcome for prognostic features and metabolomics score using univariate and multivariate Cox regression analysis. In the multivariate hazard ratios of all the variables were included together in the analysis.
DCM, dilated cardiomyopathy; NYHA, New York Heart Association Classification; SBP, systolic blood pressure; EDDi, indexed end diastolic diameter; LAVi, indexed left atrial volume; LVEF, left ventricular ejection fraction; NT-proBNP, N-terminal pro b-type natriuretic peptide.

Several statistically significant correlations also emerged among quantified metabolites and many lipoprotein-related parameters. In particular, amino acids, as well as lipoproteins, are shown to be highly intercorrelated. All results are presented in **Supplementary Figure S6**.

Association Between Metabolic Features and Prognosis

Univariate analysis of the quantified metabolomic features (**Supplementary Table S1**), using the Wilcoxon test, unraveled that deceased patients as compared with survivors were characterized at enrollment by lower levels of creatine, apolipoprotein (apo-)A2 HDL, apo-A2, phospholipids HDL-3, apo-A1 HDL-3, apo-A1 HDL-4, apo-A2 HDL-4, phospholipids VLDL, phospholipids HDL-4, apo-A2 HDL-3, free cholesterol VLDL-3, triglycerides HDL-4, cholesterol HDL-3, and by higher levels of trimethylamine-N-oxide, creatinine, lactate, LDL and HDL Cholesterol ratio, triglycerides LDL-3, and triglycerides LDL-2 (p-value <0.05 for all before FDR correction).

Concentrations of each metabolite/lipoprotein were used to build Cox regression models for the evaluation of their net effect on survived and deceased patients (**Table 3**). Multivariate models adjusted for sex, age at DCM diagnosis, time from DCM diagnosis and last follow up, NT-proBNP, LVEF, NYHA class at enrollment, SBP, EDDi at enrollment, and LAVi at enrollment were also calculated. In the univariate model, higher levels of trimethylamine-N-oxide (3rd tertile), creatinine (3rd tertile), acetic acid (2nd tertile), succinic acid (3rd tertile), triglycerides low-density lipoprotein (LDL) (2nd tertile), and triglycerides LDL-3 (3rd tertile) are associated with a higher risk of poor outcome, whereas higher levels of triglycerides very-low-density lipoprotein (VLDL) (3rd tertile), Apo-A2 HDL (2nd and 3rd tertiles), triglycerides, VLDL-3 (3rd tertile), phospholipids (VLDL-1 (3rd tertile), phospholipids VLDL-3 (3rd tertile), and triglycerides HDL-4 (3rd tertile) are associated with a good prognosis. Among them, only the associations related to trimethylamine-N-oxide (3rd tertile), triglycerides LDL (2nd tertile), phospholipids VLDL-3 (3rd tertile), triglycerides LDL-3 (3rd tertile), and triglycerides HDL-4 (3rd tertile) remain statistically significant in the multivariate model adjusted for clinical covariates. However, in addition to these variables, additional ones (that were not significant in the univariate model) related to various LDL subfractions 1, cholesterol HDL-2, and Apo-B100 Apo-A1 ratio resulted to be significant in the multivariate model (**Table 3**).

DISCUSSION

Heart failure is a complex syndrome and constitutes the ultimate result of several cardiovascular injuries. The DCM is one of the most frequent causes of HF and heart transplantation, and in turn, constitutes the final phenotype derived from multiple pathophysiological mechanisms that mainly involve the structure and the energetic metabolism of cardiomyocytes. Prognostic evaluation of patients with DCM, particularly when complicated by HF, is a crucial point in the clinical process. Among traditional risk factors, LVEF still represents the cornerstone of prognostic stratification and has an essential role in phenotyping and guiding the therapy of patients with chronic HF (45), albeit with limitations related to the operator-dependent variability and scarce precocity. As regards to natriuretic peptides, there is a considerable experience both in DCM and in HF (46): BNP or NT-proBNP levels increase the accuracy of diagnosis of HF in the emergency department (47), as well as the prognosis at the time of hospital discharge (48).

TABLE 3 | Association between metabolites/lipoproteins and the outcome: results of univariate and multivariate (adjusted for sex, age at DCM diagnosis, time from DCM diagnosis and last follow up, NT-proBNP, LVEF, NYHA class at enrollment, SBP, EDDi at enrollment, LAVi at enrollment) Cox regression analyses are reported.

	Hazard ratio (univariate)	*p*-value	Hazard ratio (multivariate)	*p*-value
Trimethylamine-N-oxide (2nd tertile)	3.33	0.0678	7.34	0.0148
Trimethylamine-N-oxide (3rd tertile)	5.94	0.0054	4.69	0.0323
Creatinine (2nd tertile)	1.28	0.6565	0.87	0.8352
Creatinine (3rd tertile)	2.69	0.0453	1.11	0.8673
Acetic acid (2nd tertile)	3.25	0.0414	2.39	0.1646
Acetic acid (3rd tertile)	2.90	0.0718	3.68	0.0534
Succinic acid (2nd tertile)	1.17	0.7895	0.67	0.5605
Succinic acid (3rd tertile)	4.24	0.0008	2.32	0.2101
Pyruvic acid (2nd tertile)	0.38	0.1000	0.09	0.0012
Pyruvic acid (3rd tertile)	1.24	0.6193	0.92	0.8852
Calculated Figures, Apo-B100/Apo-A1 (2nd tertile)	1.70	0.3048	3.26	0.0415
Calculated Figures, Apo-B100/Apo-A1 (3rd tertile)	1.97	0.1880	2.27	0.1732
Calculated Figures, LDL-1 Particle Number (2nd tertile)	1.21	0.7176	3.59	0.0494
Calculated Figures, LDL-1 Particle Number (3rd tertile)	1.78	0.2336	4.10	0.0192
Lipoprotein Main Fractions, Triglycerides, VLDL (2nd tertile)	0.98	0.9544	0.86	0.7625
Lipoprotein Main Fractions, Triglycerides, VLDL (3rd tertile)	0.32	0.0457	0.47	0.2199
Lipoprotein Main Fractions, Triglycerides, LDL (2nd tertile)	4.23	0.0110	4.02	0.0262
Lipoprotein Main Fractions, Triglycerides, LDL (3rd tertile)	2.30	0.1728	2.57	0.1579
Lipoprotein Main Fractions, Phospholipids, IDL (2nd tertile)	0.44	0.0967	0.42	0.1058
Lipoprotein Main Fractions, Phospholipids, IDL (3rd tertile)	0.53	0.1804	0.80	0.6833
Lipoprotein Main Fractions, Phospholipids, LDL (2nd tertile)	1.82	0.2466	3.22	0.0399
Lipoprotein Main Fractions, Phospholipids, LDL (3rd tertile)	1.77	0.2703	1.99	0.2403
Lipoprotein Main Fractions, Apo-A2, HDL (2nd tertile)	0.33	0.0222	0.41	0.1127
Lipoprotein Main Fractions, Apo-A2, HDL (3rd tertile)	0.28	0.0140	0.45	0.1562
VLDL Subfractions, Triglycerides, VLDL-3 (2nd tertile)	0.96	0.9173	0.93	0.8845
VLDL Subfractions, Triglycerides, VLDL-3 (3rd tertile)	0.24	0.0290	0.22	0.0573
VLDL Subfractions, Phospholipids, VLDL-1 (2nd tertile)	0.94	0.8898	0.48	0.1503
VLDL Subfractions, Phospholipids, VLDL-1 (3rd tertile)	0.32	0.0462	0.41	0.1622
VLDL Subfractions, Phospholipids, VLDL-3 (2nd tertile)	0.71	0.4346	0.84	0.7121
VLDL Subfractions, Phospholipids, VLDL-3 (3rd tertile)	0.30	0.0353	0.24	0.0358
LDL Subfractions, Triglycerides, LDL-1 (2nd tertile)	2.23	0.1435	3.44	0.0620
LDL Subfractions, Triglycerides, LDL-1 (3rd tertile)	2.65	0.0713	4.25	0.0243
LDL Subfractions, Triglycerides, LDL-3 (2nd tertile)	1.04	0.9447	0.55	0.3732
LDL Subfractions, Triglycerides, LDL-3 (3rd tertile)	2.88	0.0302	3.77	0.0418
LDL Subfractions, Triglycerides, LDL-6 (2nd tertile)	0.67	0.3796	0.32	0.0389
LDL Subfractions, Triglycerides, LDL-6 (3rd tertile)	0.49	0.1568	0.36	0.0859
LDL Subfractions, Cholesterol, LDL-1 (2nd tertile)	1.39	0.5176	2.95	0.0739
LDL Subfractions, Cholesterol, LDL-1 (3rd tertile)	1.55	0.3720	4.58	0.0161
LDL Subfractions, Cholesterol, LDL-2 (2nd tertile)	1.98	0.2112	2.15	0.2501
LDL Subfractions, Cholesterol, LDL-2 (3rd tertile)	2.23	0.1379	4.21	0.0287
LDL Subfractions, Free Cholesterol, LDL-1 (2nd tertile)	1.39	0.5176	2.84	0.1002
LDL Subfractions, Free Cholesterol, LDL-1 (3rd tertile)	1.55	0.3720	4.29	0.0251
LDL Subfractions, Free Cholesterol, LDL-2 (2nd tertile)	1.80	0.2938	3.55	0.0854
LDL Subfractions, Free Cholesterol, LDL-2 (3rd tertile)	2.43	0.0951	5.13	0.0211
LDL Subfractions, Phospholipids, LDL-1 (2nd tertile)	1.41	0.4965	3.47	0.0401
LDL Subfractions, Phospholipids, LDL-1 (3rd tertile)	1.60	0.3427	3.66	0.0460
LDL Subfractions, Phospholipids, LDL-2 (2nd tertile)	2.02	0.1998	2.05	0.2744
LDL Subfractions, Phospholipids, LDL-2 (3rd tertile)	2.25	0.1336	3.96	0.0374
LDL Subfractions, Apo-B, LDL-1 (2nd tertile)	1.21	0.7176	3.59	0.0494

(Continued)

TABLE 3 | Continued

	Hazard ratio (univariate)	*p*-value	Hazard ratio (multivariate)	*p*-value
LDL Subfractions, Apo-B, LDL-1 (3rd tertile)	1.78	0.2336	4.10	0.0192
HDL Subfractions, Triglycerides, HDL-4 (2nd tertile)	0.64	0.2996	0.45	0.1045
HDL Subfractions, Triglycerides, HDL-4 (3rd tertile)	0.28	0.0276	0.25	0.0433
HDL Subfractions, Cholesterol, HDL-2 (2nd tertile)	0.42	0.0830	0.26	0.0391
HDL Subfractions, Cholesterol, HDL-2 (3rd tertile)	0.62	0.2910	0.46	0.1834

For each variable the reference is the first tertile group.

Depending on LVEF, HF is currently classified into three subgroups: reduced (HFrEF), mildly-reduced (HFmrEF), and preserved ejection fraction (HFpEF) (34). The prognosis of HF subtypes appears to be similar, although patients with HFmrEF have higher readmission rates than patients with HFpEF, they share comparable mortality rates with patients with HFrEF and patients with HFpEF (49), even though ambulatory patients with HFmrEF show lower mortality than those with HFrEF, more akin to those with HFpEF. Moreover, patients with HFmrEF may include patients whose LVEF is increased from $\leq$40% or declined from $\geq$50% (50). Nonetheless, HF spans the entire range of LVEF (as an abnormally distributed variable), and measurement by echocardiography is subject to substantial variability, making the complexity of the phenotypes as well as their prognosis and management even more tricky. The level of neurohumoral activity and the response to medical therapies change among HF subtypes, suggesting differences in their underlying pathophysiology (51), which could be captured by the multiformity of the metabolomic fingerprints. Indeed, the metabolome represents what is happening in the body, providing the analysis of patients and their biological idiosyncrasies within the dynamic context of a disease process like HF.

Given these premises, our study aimed to evaluate the prognostic power of NMR metabolomic fingerprinting in predicting survival in a well-defined cohort of oligosymptomatic patients with HF with DCM over a median follow-up of 8 years. In our cohort, the overall mortality was 25%. Patients who deceased at baseline were older and showed larger LV, with lower LVEF and SBP values. Even if not reaching statistical significance, they tended to be more symptomatic and with larger LAVI. The NT-proBNP levels were significantly higher in patients who died. There were no differences in HF treatment among deceased patients concerning survivors. The NMR fingerprinting well-discriminated the survived and deceased patients with 70.8% accuracy (HR 5.71, $p < 0.0001$), and the metabolomic parameters that mainly contributed to the discrimination were trimethylamine-N-oxide, creatine, creatinine, lactate, and several lipoprotein-related parameters (**Table 3**; **Supplementary Table S2**).

Energetic metabolism plays a pivotal role in the onset and evolution of HF (52). Creatine is a key player in sustaining energy metabolism and functions of tissues with high energy demand, such as the myocardium (53). Indeed, the primary myocardial energy reserve pathway for generating ATP is the creatine kinase reaction (54). Several studies report a significant depletion of creatine, phosphocreatine, creatine kinase levels, and creatine transporter activities in heart tissues (55, 56), and this evidence has led to the hypothesis that the failing heart could be energy-starved (57). Our data show a reduction of the creatine levels in the sera of deceased patients with HF as compared with survivors. We can hypothesize that long-survival of patients with HF better compensates the heart's energetic demand by enhancing creatine synthesis and transport, whereas deceased patients could no longer cope with the myocardium energetic needs, and, thus, the decrease of creatine levels may indicate a state of energy depletion.

Creatine is non-enzymatically converted in creatinine by muscle at an almost constant rate depending on muscle mass, and, then, creatinine is excreted by the kidneys into the urine (53). Elevated levels of serum creatinine are associated with impaired kidney function and renal failure; thus, in clinical practice, it is routinely used as a marker of renal function. In our cohort, we observed higher serum creatinine levels in patients with HF with poor prognosis, despite, at the time of blood sample collection, only 4 (15.4%) out of the 26 deceased patients with HF presented overt chronic renal failure (whereas none of the survived patients with HF showed this comorbidity). The general increment of creatinine in deceased patients, although within the normal range for most of them, could be interpreted as a very early prodromal sign of future renal damage, and it can be associated with poor prognosis. This result is in line with the evidence that a loss of glomerular filtration rate independently predicts mortality and accelerates the overall progression of cardiovascular disease and HF (58). Indeed, the heart and kidneys interact in a complex, bidirectional, and interdependent manner in both acute and chronic settings, by sharing several inflammatory, metabolic, and hormonal pathways (59).

Interestingly, deceased patients with HF showed increased levels of trimethylamine-N-oxide (TMAO), a metabolite generated by gut microbiota from dietary precursors rich in choline, phosphatidylcholine, and l-carnitine. The altered intestinal function has long been associated with HF pathogenesis (60), and a positive correlation between blood levels of TMAO and 5-year risk of death in patients with HF was reported (61). Furthermore, within the cardiovascular setting, the TMAO accumulation has been linked with platelet hyperactivation, atherogenesis, and future adverse cardiac events (i.e., myocardial infarction, stroke, and cardiovascular death) (60).

The ability of the metabolomic fingerprint to distinguish deceased and survived patients with HF is also significantly affected by the levels of several HDL subfractions of apo-A1, apo-A2, cholesterol, and triglycerides. In particular, the patients

with HF with poor prognoses were associated with reduced levels of various HDL cholesterol subfractions and VLDL triglyceride subfractions. These data are in agreement with the evidence that low HDL-cholesterol, apo-A1, and triglycerides levels correlate with adverse prognosis in patients with heart failure independent of the etiology (62–64), probably because apo-A1 may exert an anti-inflammatory action in HF (65).

Although none of the just discussed metabolites has sufficient diagnostic power by itself, each of them contributes to the metabolic fingerprint of the patients with HF, and this is the most innovative point of the approach described here. The metabolic fingerprint can be thought of as a sort of holistic super-biomarker with a discriminative power higher than the simple sum of the few quantified metabolites because it takes into account all the detectable signals of endogenous and exogenous metabolites/lipoproteins present in the NMR spectra (66). The metabolomic fingerprint, as a whole, represents, therefore, a useful and innovative instrument that is able to accurately identify the patients with HF with good and poor prognosis, even when compared with more classical stratification approaches. After univariate analysis, metabolomic fingerprint, advanced (>60 years) age at DCM diagnosis, longer (>15 years) history of DCM, NT-proBNP values, and LVEF were significantly related to CV outcomes. With regards to the prognostic power of known risk factors compared with metabolomics results, our data showed higher specificity (71.2%) of NT-proBNP in discriminating deceased from survivor patients, despite lower sensitivity (58.3%) and accuracy (68%). Furthermore, only age, metabolomics, and LVEF have maintained their prognostic significance after multivariate analysis. As previously reported in the literature, younger age is a known protective factor in patients with HF (67, 68) and this finding is confirmed by our results. The importance of LVEF in the prognostic stratification of patients with HF is corroborated as well. In particular, LVEF remains one of the most powerful prognostic factors; indeed, patients with reduced LVEF were at higher risk of death (HRs 7.47 and 4.26, *p*-values 0.0001 and 0.0002 as compared with LR and IR, respectively), whereas patients with mid-range and preserved LVEF shared a lower risk (HR 1.79, *p*-value 0.38). When testing the potential of metabolomics in sub-stratifying LVEF classes, we considered mid-range and preserved LVEF as a unique low-risk class, whereas reduced LVEF was considered as a high-risk class; though metabolomics showed to effectively sub-stratify low and high-risk patients in both classes (HRs 3.46 and 6.01, *p*-values 0.03 and 0.004, respectively), it showed the best performance in the high-risk class. Furthermore, the outcome prediction of the combination of metabolomics and LVEF led to an excellent prognostic power with 75.5% accuracy, 73.8% sensitivity, and 80.8% specificity, (HR 8.09 and *p*-value 0.0000004), highlighting that metabolomic fingerprinting and LVEF provide complementary prognostic information, and, therefore, their combined use can improve poor outcome prediction beyond the use of LVEF only.

In conclusion, the results of this retrospective and proof-of-concept study demonstrate how metabolomic analysis *via* NMR enables a fast and reproducible characterization of the serum metabolic fingerprint associated with poor prognosis in a population of oligosymptomatic patients with HF, improving the cardiovascular risk assessment, and most likely identifying patients with HF who need to undergo more aggressive treatments. Thus, metabolomic fingerprinting could represent a valid addition to the established prognostic instruments, like LVEF. Furthermore, our results suggest that it would be advisable to integrate more risk parameters to identify earlier the patients with HF at high-risk of poor outcomes.

This study provides important insights into the HF setting by analyzing a well-defined, homogeneous, single-center, cohort of patients with DCM with stable chronic HF. As compared to other studies aimed at using metabolomics as a prognostic factor of mortality in patients with HF (31–33), in our study, the patients were monitored for follow up time significantly longer than the average follow ups time of clinical trials (median follow up from enrollment 8 years, median follow up from DCM diagnosis 15 years), most patients were pauci-symptomatic at enrollment (85.8% NYHA class I-II) and 68.8% of patients showed mid-range or preserved LVEF; this sub-group of patients with HF is probably the one that could gain more benefits from specific targeted therapies. However, some relevant limitations of our study should also be mentioned: the population sample was limited in size, the number of death events was low, and the study lacks an independent external validation cohort. These limitations prevent any definitive conclusion. However, the results obtained in this pilot study provide a rational basis for a future larger multi-center study, and further efforts in this direction are guaranteed.

DATA AVAILABILITY STATEMENT

The original contributions presented in the study are included in the article/**Supplementary Materials**, further inquiries can be directed to the corresponding authors.

ETHICS STATEMENT

The studies involving human participants were reviewed and approved by Ethics Committee (Azienda Ospedaliero—Universitaria Careggi, Florence, Italy). The patients/participants provided their written informed consent to participate in this study.

AUTHOR CONTRIBUTIONS

LT, GC, BA, and CL contributed to study conception and design. AF, GC, IO, NM, and BA contributed to patient enrollment and management. AF, GC, EC, IO, and BA contributed to collection of clinical data and serum samples. AV and LT performed NMR analysis, statistical analysis, biostatistics, and computational analysis. AV, AF, LT, GC, IO, BA, and CL contributed to results interpretation. AV and AF wrote the original draft. AV, AF, LT, GC, IO, and CL wrote, reviewed, and edited the manuscript. NM, BA, and CL contributed to supervision. All authors have read and agreed to the published version of the manuscript.

ACKNOWLEDGMENTS

The authors acknowledge Instruct-ERIC, a Landmark ESFRI project, and specifically the CERM/CIRMMP Italy Centre, for the use of NMR instrumentation.

SUPPLEMENTARY MATERIAL

The Supplementary Material for this article can be found online at: https://www.frontiersin.org/articles/10.3389/fcvm.2022.851905/full#supplementary-material

REFERENCES

1. Pinto YM, Elliott PM, Arbustini E, Adler Y, Anastasakis A, Böhm M, et al. Proposal for a revised definition of dilated cardiomyopathy, hypokinetic non-dilated cardiomyopathy, and its implications for the clinical practice: a position statement of the ESC working group on myocardial and pericardial diseases. *Eur Heart J.* (2016) 37:1850–8. doi: 10.1093/eurheartj/ehv727
2. Piran S, Liu P, Morales A, Hershberger RE. Where genome meets phenome: rationale for integrating genetic and protein biomarkers in the diagnosis and management of dilated cardiomyopathy and heart failure. *J Am Coll Cardiol.* (2012) 60:283–9. doi: 10.1016/j.jacc.2012.05.005
3. Burkett EL, Hershberger RE. Clinical and genetic issues in familial dilated cardiomyopathy. *J Am Coll Cardiol.* (2005) 45:969–81. doi: 10.1016/j.jacc.2004.11.066
4. Seferović PM, Polovina M, Bauersachs J, Arad M, Gal TB, Lund LH, et al. Heart failure in cardiomyopathies: a position paper from the Heart Failure Association of the European Society of Cardiology. *Eur J Heart Fail.* (2019) 21:553–76. doi: 10.1002/ejhf.1461
5. Talameh JA, Lanfear DE. Pharmacogenetics in chronic heart failure: new developments and current challenges. *Curr Heart Fail Rep.* (2012) 9:23–32. doi: 10.1007/s11897-011-0076-2
6. Ibrahim NE, Januzzi JL. Established and emerging roles of biomarkers in heart failure. *Circ Res.* (2018) 123:614–29. doi: 10.1161/CIRCRESAHA.118.312706
7. Shrivastava A, Haase T, Zeller T, Schulte C. Biomarkers for heart failure prognosis: proteins, genetic scores and non-coding RNAs. *Front Cardiovasc Med.* (2020) 7:601364. doi: 10.3389/fcvm.2020.601364
8. Pocock SJ, Ariti CA, McMurray JJV, Maggioni A, Køber L, Squire IB, et al. Predicting survival in heart failure: a risk score based on 39 372 patients from 30 studies. *Eur Heart J.* (2013) 34:1404–13. doi: 10.1093/eurheartj/ehs337
9. Wishart DS, Tzur D, Knox C, Eisner R, Guo AC, Young N, et al. HMDB: the Human Metabolome Database. *Nucleic Acids Res.* (2007) 35:D521–6. doi: 10.1093/nar/gkl923
10. Vignoli A, Ghini V, Meoni G, Licari C, Takis PG, Tenori L, et al. High-throughput metabolomics by 1D NMR. *Angew Chem-Int Edit.* (2019) 58:968–94. doi: 10.1002/anie.201804736
11. Clish CB. Metabolomics: an emerging but powerful tool for precision medicine. *Cold Spring Harb Mol Case Stud.* (2015) 1:a000588. doi: 10.1101/mcs.a000588
12. Vignoli A, Muraro E, Miolo G, Tenori L, Turano P, Di Gregorio E, et al. Effect of estrogen receptor status on circulatory immune and metabolomics profiles of HER2-positive breast cancer patients enrolled for neoadjuvant targeted chemotherapy. *Cancers (Basel).* (2020) 12:314. doi: 10.3390/cancers12020314
13. Wishart DS. Emerging applications of metabolomics in drug discovery and precision medicine. *Nat Rev Drug Discov.* (2016) 15:473–84. doi: 10.1038/nrd.2016.32
14. Albenberg LG, Wu GD. Diet and the Intestinal Microbiome: Associations, Functions, and Implications for Health and Disease. *Gastroenterology.* (2014) 146:1564–72. doi: 10.1053/j.gastro.2014.01.058
15. Vignoli A, Paciotti S, Tenori L, Eusebi P, Biscetti L, Chiasserini D, et al. Fingerprinting Alzheimer's disease by 1H nuclear magnetic resonance spectroscopy of cerebrospinal fluid. *J Proteome Res.* (2020) 19:1696–705. doi: 10.1021/acs.jproteome.9b00850
16. Calvani R, Brasili E, Praticò G, Sciubba F, Roselli M, Finamore A, et al. Application of NMR-based metabolomics to the study of gut microbiota in obesity. *J Clin Gastroenterol.* (2014) 48 Suppl 1:S5–7. doi: 10.1097/MCG.0000000000000236
17. Dani C, Bresci C, Berti E, Ottanelli S, Mello G, Mecacci F, et al. Metabolomic profile of term infants of gestational diabetic mothers. *J Maternal Fetal Neonatal Med.* (2014) 27:537–42. doi: 10.3109/14767058.2013.823941
18. Vignoli A, Tenori L, Giusti B, Takis PG, Valente S, Carrabba N, et al. NMR-based metabolomics identifies patients at high-risk of death within two years after acute myocardial infarction in the AMI-Florence II cohort. *BMC Med.* (2019) 17:3. doi: 10.1186/s12916-018-1240-2
19. Brindle JT, Antti H, Holmes E, Tranter G, Nicholson JK, Bethell HWL, et al. Rapid and noninvasive diagnosis of the presence and severity of coronary heart disease using 1H-NMR-based metabonomics. *Nat Med.* (2002) 8:1439–44. doi: 10.1038/nm1202-802
20. Shah SH, Kraus WE, Newgard CB. Metabolomic Profiling for identification of novel biomarkers and mechanisms related to common cardiovascular diseases: form and function. *Circulation.* (2012) 126:1110–20. doi: 10.1161/CIRCULATIONAHA.111.060368
21. Vignoli A, Tenori L, Giusti B, Valente S, Carrabba N, Baizi D, et al. Differential network analysis reveals metabolic determinants associated with mortality in acute myocardial infarction patients and suggests potential mechanisms underlying different clinical scores used to predict death. *J Proteome Res.* (2020) 19:949–61. doi: 10.1021/acs.jproteome.9b00779
22. DeFilippis AP, Trainor PJ, Hill BG, Amraotkar AR, Rai SN, Hirsch GA, et al. Identification of a plasma metabolomic signature of thrombotic myocardial infarction that is distinct from non-thrombotic myocardial infarction and stable coronary artery disease. *PLoS ONE.* (2017) 12:e0175591. doi: 10.1371/journal.pone.0175591
23. McGarrah RW, Crown SB, Zhang G, Shah SH, Newgard CB. Cardiovascular metabolomics. *Circ Res.* (2018) 122:1238–58. doi: 10.1161/CIRCRESAHA.117.311002
24. Neubauer S. The failing heart—an engine out of fuel. *N Engl J Med.* (2007) 356:1140–51. doi: 10.1056/NEJMra063052
25. Ashrafian H, Frenneaux MP, Opie LH. Metabolic mechanisms in heart failure. *Circulation.* (2007) 116:434–48. doi: 10.1161/CIRCULATIONAHA.107.702795
26. Doehner W, Frenneaux M, Anker SD. Metabolic impairment in heart failure: the myocardial and systemic perspective. *J Am Coll Cardiol.* (2014) 64:1388–400. doi: 10.1016/j.jacc.2014.04.083
27. Hunter WG, Kelly JP, McGarrah RW, Kraus WE, Shah SH. Metabolic dysfunction in heart failure: diagnostic, prognostic, and pathophysiologic insights from metabolomic profiling. *Curr Heart Fail Rep.* (2016) 13:119–31. doi: 10.1007/s11897-016-0289-5
28. Tenori L, Hu X, Pantaleo P, Alterini B, Castelli G, Olivotto I, et al. Metabolomic fingerprint of heart failure in humans: A nuclear magnetic resonance spectroscopy analysis. *Int J Cardiol.* (2013) 168:E113–5. doi: 10.1016/j.ijcard.2013.08.042
29. Deidda M, Piras C, Dessalvi CC, Locci E, Barberini L, Torri F, et al. Metabolomic approach to profile functional and metabolic changes in heart failure. *J Transl Med.* (2015) 13:297. doi: 10.1186/s12967-015-0661-3
30. Du Z, Shen A, Huang Y, Su L, Lai W, Wang P, et al. 1H-NMR-based metabolic analysis of human serum reveals novel markers of myocardial energy expenditure in heart failure patients. *PLoS ONE.* (2014) 9:e88102. doi: 10.1371/journal.pone.0088102
31. Lanfear DE, Gibbs JJ Li J, She R, Petucci C, Culver JA, et al. Targeted metabolomic profiling of plasma and survival in heart failure patients. *JACC Heart Fail.* (2017) 5:823–32. doi: 10.1016/j.jchf.2017.07.009
32. Desmoulin F, Galinier M, Trouillet C, Berry M, Delmas C, Turkieh A, et al. Metabonomics analysis of plasma reveals the lactate to cholesterol ratio as an independent prognostic factor of short-term mortality in acute heart failure. *PLoS ONE.* (2013) 8:e60737. doi: 10.1371/journal.pone.0060737
33. Cheng M-L, Wang C-H, Shiao M-S, Liu M-H, Huang Y-Y, Huang C-Y, et al. Metabolic disturbances identified in plasma are associated with outcomes in patients with heart failure: diagnostic and prognostic value of metabolomics. *J Am Coll Cardiol.* (2015) 65:1509–20. doi: 10.1016/j.jacc.2015.02.018

34. McDonagh TA, Metra M, Adamo M, Gardner RS, Baumbach A, Böhm M, et al. 2021 ESC Guidelines for the diagnosis and treatment of acute and chronic heart failure. *Eur Heart J.* (2021) 42:3599–726. doi: 10.1093/eurheartj/ehab368
35. Report of the 1995 World Health Organization/International Society and Federation of Cardiology Task Force on the Definition and Classification of Cardiomyopathies. *Circulation.* (1996) 93:841–2. doi: 10.1161/01.CIR.93.5.841
36. Bernini P, Bertini I, Luchinat C, Nincheri P, Staderini S, Turano P. Standard operating procedures for pre-analytical handling of blood and urine for metabolomic studies and biobanks. *J Biomol NMR.* (2011) 49:231–43. doi: 10.1007/s10858-011-9489-1
37. Mckay RT. How the 1D-NOESY suppresses solvent signal in metabonomics NMR spectroscopy: an examination of the pulse sequence components and evolution. *Concepts Magn Reson.* (2011) 38A:197–220. doi: 10.1002/cmr.a.20223
38. Dieterle F, Ross A. Schlotterbeck G+, Senn H. Probabilistic quotient normalization as robust method to account for dilution of complex biological mixtures application in 1H NMR metabonomics. *AnalChem.* (2006) 78:4281–90. doi: 10.1021/ac051632c
39. Griffiths WJ. *Metabolomics, Metabonomics and Metabolite Profiling.* Royal Society of Chemistry (2008). 336 p. doi: 10.1039/9781847558107
40. Barker M, Rayens W. Partial least squares for discrimination. *J Chemom.* (2003) 17:166–73. doi: 10.1002/cem.785
41. Cox DR. Regression models and life-tables. In: Kotz S, Johnson NL, editors. *Breakthroughs in statistics: methodology and distribution*. Springer Series in Statistics. New York, NY: Springer (1992). p. 527–41 doi: 10.1007/978-1-4612-4380-9_37
42. Jiménez B, Holmes E, Heude C, Tolson RF, Harvey N, Lodge SL, et al. Quantitative lipoprotein subclass and low molecular weight metabolite analysis in human serum and plasma by 1H NMR spectroscopy in a multilaboratory trial. *Anal Chem.* (2018) 90:11962–71. doi: 10.1021/acs.analchem.8b02412
43. Benjamini Y, Hochberg Y. Controlling the false discovery rate: a practical and powerful approach to multiple testing. *J Royal Stat Soc Ser B (Methodological).* (1995) 57:289–300. doi: 10.1111/j.2517-6161.1995.tb02031.x
44. Wilcox R. *Introduction to Robust Estimation and Hypothesis Testing.* 3rd ed. (2012). doi: 10.1016/B978-0-12-386983-8.00001-9
45. Ponikowski P, Voors AA, Anker SD, Bueno H, Cleland JGF, Coats AJS, et al. 2016 ESC Guidelines for the diagnosis and treatment of acute and chronic heart failure. The Task Force for the diagnosis and treatment of acute and chronic heart failure of the European Society of Cardiology (ESC) Developed with the special contribution of the Heart Failure Association (HFA) of the ESC. *Eur Heart J.* (2016) 37:2129–200. doi: 10.1093/eurheartj/ehw128
46. Daniels LB, Maisel AS. Natriuretic peptides. *J Am Coll Cardiol.* (2007) 50:2357–68. doi: 10.1016/j.jacc.2007.09.021
47. Maisel AS, Krishnaswamy P, Nowak RM, McCord J, Hollander JE, Duc P, et al. Rapid measurement of B-type natriuretic peptide in the emergency diagnosis of heart failure. *N Engl J Med.* (2002) 347:161–7. doi: 10.1056/NEJMoa020233
48. Felker GM, Hasselblad V, Hernandez AF, O'Connor CM. Biomarker-guided therapy in chronic heart failure: a meta-analysis of randomized controlled trials. *Am Heart J.* (2009) 158:422–30. doi: 10.1016/j.ahj.2009.06.018
49. Cheng RK, Cox M, Neely ML, Heidenreich PA, Bhatt DL, Eapen ZJ, et al. Outcomes in patients with heart failure with preserved, borderline, and reduced ejection fraction in the Medicare population. *Am Heart J.* (2014) 168:721–30. doi: 10.1016/j.ahj.2014.07.008
50. Tsuji K, Sakata Y, Nochioka K, Miura M, Yamauchi T, Onose T, et al. Characterization of heart failure patients with mid-range left ventricular ejection fraction-a report from the CHART-2 Study. *Eur J Heart Fail.* (2017) 19:1258–69. doi: 10.1002/ejhf.807
51. Hogg K, McMurray J. Neurohumoral pathways in heart failure with preserved systolic function. *Prog Cardiovasc Dis.* (2005) 47:357–66. doi: 10.1016/j.pcad.2005.02.001
52. Ingwall JS. Energy metabolism in heart failure and remodelling. *Cardiovasc Res.* (2009) 81:412–9. doi: 10.1093/cvr/cvn301
53. Wyss M, Kaddurah-Daouk R. Creatine and creatinine metabolism. *Physiol Rev.* (2000) 80:1107–213. doi: 10.1152/physrev.2000.80.3.1107
54. Gabr RE, El-Sharkawy A-MM, Schär M, Panjrath GS, Gerstenblith G, Weiss RG, et al. Cardiac work is related to creatine kinase energy supply in human heart failure: a cardiovascular magnetic resonance spectroscopy study. *J Cardiovasc Magn Res.* (2018) 20:81. doi: 10.1186/s12968-018-0491-6
55. Taegtmeyer H, Ingwall JS. Creatine—a dispensable metabolite? *Circ Res.* (2013) 112:878–80. doi: 10.1161/CIRCRESAHA.113.300974
56. Wallis J, Lygate CA, Fischer A. ten Hove M, Schneider JE, Sebag-Montefiore L, et al. Supranormal myocardial creatine and phosphocreatine concentrations lead to cardiac hypertrophy and heart failure. *Circulation.* (2005) 112:3131–9. doi: 10.1161/CIRCULATIONAHA.105.572990
57. Ingwall Joanne S, Weiss Robert G. Is the failing heart energy starved? *Circ Res.* (2004) 95:135–45. doi: 10.1161/01.RES.0000137170.41939.d9
58. Bagshaw SM, Cruz DN, Aspromonte N, Daliento L, Ronco F, Sheinfeld G, et al. Epidemiology of cardio-renal syndromes: workgroup statements from the 7th ADQI Consensus Conference. *Nephrol Dial Transplant.* (2010) 25:1406–16. doi: 10.1093/ndt/gfq066
59. Schefold JC, Filippatos G, Hasenfuss G, Anker SD, von Haehling S. Heart failure and kidney dysfunction: epidemiology, mechanisms and management. *Nature Reviews Nephrology.* (2016) 12:610–23. doi: 10.1038/nrneph.2016.113
60. Krack A, Sharma R, Figulla HR, Anker SD. The importance of the gastrointestinal system in the pathogenesis of heart failure. *Eur Heart J.* (2005) 26:2368–74. doi: 10.1093/eurheartj/ehi389
61. Tang WHW Li DY, Hazen SL. Dietary metabolism, the gut microbiome, and heart failure. *Nat Rev Cardiol.* (2019) 16:137–54. doi: 10.1038/s41569-018-0108-7
62. Mehra MR, Uber PA, Lavie CJ, Milani RV, Park MH, Ventura HO. High-density lipoprotein cholesterol levels and prognosis in advanced heart failure. *J Heart Lung Transpl.* (2009) 28:876–80. doi: 10.1016/j.healun.2009.04.026
63. Christ M, Klima T, Grimm W, Mueller H-H, Maisch B. Prognostic significance of serum cholesterol levels in patients with idiopathic dilated cardiomyopathy. *Eur Heart J.* (2006) 27:691–9. doi: 10.1093/eurheartj/ehi195
64. Kozdag G, Ertas G, Emre E, Akay Y, Celikyurt U, Sahin T, et al. Low serum triglyceride levels as predictors of cardiac death in heart failure patients. *Tex Heart Inst J.* (2013) 40:521–8.
65. Iwaoka M, Obata J-E, Abe M, Nakamura T, Kitta Y, Kodama Y, et al. Association of low serum levels of apolipoprotein A-I with adverse outcomes in patients with nonischemic heart failure. *J Card Fail.* (2007) 13:247–53. doi: 10.1016/j.cardfail.2007.01.007
66. Vignoli A, Rodio DM, Bellizzi A, Sobolev AP, Anzivino E, Mischitelli M, et al. NMR-based metabolomic approach to study urine samples of chronic inflammatory rheumatic disease patients. *Anal Bioanal Chem.* (2017) 409:1405–13. doi: 10.1007/s00216-016-0074-z
67. de Groote P, Fertin M, Duva Pentiah A, Goéminne C, Lamblin N, Bauters C. Long-term functional and clinical follow-up of patients with heart failure with recovered left ventricular ejection fraction after β-blocker therapy. *Circ Heart Fail.* (2014) 7:434–9. doi: 10.1161/CIRCHEARTFAILURE.113.000813
68. Park CS, Park JJ, Mebazaa A, Oh I-Y, Park H-A, Cho H-J, et al. Characteristics, outcomes, and treatment of heart failure with improved ejection fraction. *J Am Heart Assoc.* (2019) 8:e011077. doi: 10.1161/JAHA.118.011077

Conflict of Interest: The authors declare that the research was conducted in the absence of any commercial or financial relationships that could be construed as a potential conflict of interest.

Publisher's Note: All claims expressed in this article are solely those of the authors and do not necessarily represent those of their affiliated organizations, or those of the publisher, the editors and the reviewers. Any product that may be evaluated in this article, or claim that may be made by its manufacturer, is not guaranteed or endorsed by the publisher.

frontiers | Frontiers in Cardiovascular Medicine

REVIEW
published: 25 April 2022
doi: 10.3389/fcvm.2022.889743

Non-coding RNA-Associated Therapeutic Strategies in Atherosclerosis

Yuyan Tang[1,2], *Huaping Li*[1,2*] *and Chen Chen*[1,2*]

[1] Division of Cardiology, Tongji Hospital, Tongji Medical College, Huazhong University of Science and Technology, Wuhan, China, [2] Hubei Key Laboratory of Genetics and Molecular Mechanisms of Cardiological Disorders, Wuhan, China

Atherosclerosis has been the main cause of disability and mortality in the world, resulting in a heavy medical burden for all countries. It is widely known to be a kind of chronic inflammatory disease in the blood walls, of which the key pathogenesis is the accumulation of immunologic cells in the lesion, foam cells formation, and eventually plaque rupture causing ischemia of various organs. Non-coding RNAs (ncRNAs) play a vital role in regulating the physiologic and pathophysiologic processes in cells. More and more studies have revealed that ncRNAs also participated in the development of atherosclerosis and regulated cellular phenotypes such as endothelial dysfunction, leukocyte recruitment, foam cells formation, and vascular smooth muscle cells phenotype-switching and apoptosis. Given the broad functions of ncRNAs in atherogenesis, they have become potential therapeutic targets. Apart from that, ncRNAs have become powerful blueprints to design new drugs. For example, RNA interference drugs were inspired by small interfering RNAs that exist in normal cellular physiologic processes and behave as negative regulators of specific proteins. For instance, inclisiran is a kind of RNAi drug targeting PCKS9 mRNA, which can lower the level of LDL-C and treat atherosclerosis. We introduce some recent research progresses on ncRNAs related to atherosclerotic pathophysiologic process and the current clinical trials of RNA drugs pointed at atherosclerosis.

Keywords: non-coding RNA, atherosclerosis, inflammatory, biomarker, therapy

OPEN ACCESS

Edited by:
Han Xiao,
Peking University Third Hospital, China

Reviewed by:
Jinwei Tian,
The Second Affiliated Hospital of Harbin Medical University, China
Zhi Xin Shan,
Guangdong Provincial People's Hospital, China

***Correspondence:**
Huaping Li
lhp@tjh.tjmu.edu.cn
Chen Chen
chenchen@tjh.tjmu.edu.cn

Specialty section:
This article was submitted to Cardiovascular Metabolism, a section of the journal Frontiers in Cardiovascular Medicine

Received: *04 March 2022*
Accepted: *21 March 2022*
Published: *25 April 2022*

Citation:
Tang Y, Li H and Chen C (2022) Non-coding RNA-Associated Therapeutic Strategies in Atherosclerosis. Front. Cardiovasc. Med. 9:889743. doi: 10.3389/fcvm.2022.889743

INTRODUCTION

Cardiovascular diseases (CVDs) have been the main cause of death worldwide for decades, and atherosclerosis is a common etiology for various CVDs, such as myocardial infarctions and strokes (1). Therefore, it is of great value to figure out the pathophysiologic progression and the treatments for atherosclerosis. It is widely acknowledged that atherosclerosis is a chronic inflammatory disease characterized by the accumulation of plenty of immune cells, typically monocyte-derived macrophages, in the subendothelial space of arterial walls composed of three layers, namely intima, media, and adventitia (2).

The pre-atherosclerotic lesion in humans is thought to be diffuse intima thickening at the atherosclerosis-prone areas of arterials caused by disturbed blood flow, occurring even at an early age (3). The vascular smooth muscle cells from the media migrate into the intima and produce a negatively charged extracellular matrix that can interact with positively charged apoB-containing lipoproteins (4). The lipid retention in the subendothelial space initiates endothelial dysfunction and endothelial activation, resulting in a higher permeability of the endothelium and the production of inflammatory cytokines and adhesion molecules (5). Besides, the lipid stuck in the intima is susceptible to be modulated especially oxidation, resulting in oxidized lipid (6). Therefore, the monocytes in circulation are recruited to the lesion and enter the intima, where they differentiate into macrophages, take lipids, become foam cells, and are trapped here (2). The vascular smooth muscle cells continue to migrate into the intima and proliferate as well as synthesize collagen, which promotes the formation of fibrous cap (7). However, in advanced plaques, apoptosis and necrosis occur more frequently while proliferation and efferocytosis are suppressed, making the plaque an acellular lesion and easy to rupture.

The key cells in atherogenesis are endothelial cells, macrophages, and vascular smooth muscle cells. The vascular endothelium, composed of a single layer of endothelial cells (EC) and coating the inner surface of blood vessels, plays a vital role in the initiation of atherosclerosis. Studies have illustrated that high-risk factors for atherosclerosis lead to endothelial cell dysfunction and proinflammation activation eventually promoting atherogenesis. For example, the low shear stress at lesion-prone regions, arterial branches, and curvatures reduces eNOS expression and can also induce ROS by suppressing AT1R/eNOS/NO pathway (8, 9), both of which can impair endothelial permeability. The co-pathway of endothelial cell dysfunction is the activation of NF-κB (5, 10). It stimulates the synthesis of chemokines such as IL-8 and MCP-1 to trigger leukocyte recruitment (11). Furthermore, It can induce the expression of adhesion molecules on the surface of endothelial cells (12) such as VCAM-1 (13), ICAM1, and E-selectin (11) which initiate leukocyte adhesion. The key mechanism of atherosclerosis is the formation of foam cells in plaques as a result of macrophages' uptake of ox-LDL. The formation of foam cells is associated with impaired lipid metabolism and accumulation of lipid within macrophages. Scavenger receptor class A (SR-A), cluster of differentiation 36 (CD36), and lectin-like oxidized low-density lipoprotein receptor-1 (LOX-1) are upregulated in the atheroma (14, 15), mediating the uptake of oxLDL, promoting lipid accumulation within the macrophages, and finally exacerbating atherosclerosis (16, 17). In addition to increased intake of lipid, cholesterol efflux is also impaired in atherosclerosis contributed by lipid accumulation. The transporters mediating cholesterol efflux, such as ABCA1 and ABCG1, are decreased in the macrophage-derived foam cells (18). Consistently, deficiency of ABCA1 or ABCG1 contributes to damaged cholesterol efflux (19, 20), while their upregulation protects macrophages from forming foam cells and slows down plaques' enlargement (21, 22). The vascular smooth muscle cells (VSMCs) are normally located in the medial layer of blood vessels, whose functions are controlling vessels tone by contraction and producing extracellular matrix (ECM) (23). With the development of atherogenesis, VSMCs switch their phenotype from contractile to synthetic, partially because of oxLDL stimulation (24). At the early stage of atherosclerosis, VSMCs migrate from media and proliferate in the intima, but cell cycle and growth are arrested reversely at advanced plaques, which is termed as VSMC senescence (25, 26). Apart from decreased proliferation rate, VSMCs turn to senescence-associated secretory phenotype (SASP), characterized by secreting several pro-inflammatory mediators such as IL-6, IL-8, and producing metalloprotease, ending up with vulnerable atheroma and plaque rupture (27, 28). VSMCs apoptosis and necrosis are rare at the beginning but become common at advanced plaques (29, 30). Loss of VSMCs and their ability to synthesize ECM leads to plaque vulnerability (31).

Non-coding RNAs are RNAs that lack the ability to encode peptides or proteins, some of which function as regulators of other genes' expression. They have been potential therapeutic targets in the past few years because they can regulate protein production (32). Since ncRNAs play an important role in many diseases such as cancers, neurological diseases, and cardiovascular diseases involving atherosclerosis (33), pre-clinical studies and clinical trials for drugs targeting ncRNAs involved in atherogenesis are emerging currently (34).

NON-CODING RNAS IN ATHEROSCLEROSIS

With the development of full genome sequencing technology, it is found that although the major part of the human genome is transcriptionally active, only a little proportion of it can encode protein and the remaining comprises non-coding RNAs (ncRNAs) (35). Several ncRNAs are currently well studied, like microRNAs (miRNAs), long non-coding RNAs (lncRNAs), and circular RNA (circRNAs; **Table 1**). miRNAs are at the size of ∼22 nucleotides and regulate gene expression post-transcriptionally. In mammalian cells, they usually are incorporated into the RNA-induced silencing complex (RISC) and they guide the complex to the mRNA in which the 3′ UTR region is complementary to them, resulting in mRNA cleavage or translation regression (82). When it comes to lncRNAs, they are characterized as transcripts longer than 200 nt and without the ability to encode proteins. After being transcribed from either intergenic regions or protein-coding regions, both in the sense or antisense direction, they function in different ways. For example, they can act as a scaffold to help the assembly of protein complexes (83). They can also serve as a decoy for RNA-binding proteins or miRNAs such as transcription factors and prevent their functions. The ability to bind miRNA is called the "sponge effect". Besides, after binding target proteins, they can guide the complex to specific locations, which is called "guides" (84). CircRNAs are mostly generated from precursor mRNAs undergoing back splicing reactions where a downstream splice donor (5′ splice sites) is joined to a splice acceptor (3′ splice site) of the intron because of

TABLE 1 | Non-coding RNAs in atherosclerosis.

ncRNA name	Model	Functions	Pro-/anti-atherogenesis	Reference
hsa_circ_0003575	HUVECs	Suppressing ECs proliferation and promoting apoptosis	Not accessed	(36)
NEXN-AS1	ECs	Reducing endothelial inflammatory activation	Anti-atherogenesis	(37)
SENCR	HUVECs and HCAECs	Stabilizing membrane integrity and permeability of ECs	Anti-atherogenesis	(38, 39)
LncRNA-FA2H-2-MLKL	ECs and VSMCs	Inhibiting autophagy and inflammation	Anti-atherogenesis	(40, 41)
miR-1a-3p and miR-1b-5p	ECs	Activating endothelial inflammation	Pro-atherogenesis	(42)
miR-181a-5p and miR-181a-3p	ECs	Inhibiting endothelial inflammation	Anti-atherogenesis	(43)
miR-126-5p	ECs	Suppressing endothelial inflammatory activation and promoting ECs proliferation	Anti-atherogenesis	(44, 45)
circANRIL	VSMCs and macrophages	Preventing ribosome biogenesis by inhibiting proliferation	Anti-atherogenesis	(46–48)
circ_Lrp6	VSMCs	Inhibiting migration, proliferation and phenotype-switching	Anti-atherogenesis	(49)
circACTA2	VSMCs	Regulating SMCs contraction	Not accessed	(50)
SMILR	VSMCs	Promoting proliferation and mitosis	Pro-atherogenesis	(51, 52)
CARMN	VSMCs	Inhibiting VSMCs phenotype switching	Anti-atherogenesis	(53, 54)
miR-22	VSMCs	Suppressing VSMCs phenotyping switching	Not accessed	(55, 56)
miR-128	VSMCs	Suppress VSMCs proliferation, migration and phenotype switching	Anti-atherogenesis	(57)
miR-145	VSMC	Preventing VSMCs phenotype-switching	Anti-atherogenesis	(58–61)
MALAT1	Macrophages	Preventing inflammatory factors production and leukocytes retention	Anti-atherogenesis	(62–64)
MeXis	Macrophages	Promoting cholesterol efflux	Anti-atherogenesis	(65, 66)
MAARS	Macrophages	Inducing apoptosis and impairing efferocytosis	Pro-atherogenesis	(67, 68)
miR-181b	Macrophages	Stabilizing fibrous cap	Pro-atherogenesis	(69, 70)
miR-34a	Macrophages	Impairing cholesterol efflux	Pro-atherogenesis	(71–73)
miR-30c-5p	Macrophages	Promoting apoptosis	Anti-atherogenesis	(74)
miR-33	Macrophages and hepatocytes	Impairing cholesterol efflux	Pro-atherogenesis	(75–78)
miR-144	Macrophages and hepatocytes	Impairing cholesterol efflux	Not accessed	(79, 80)
CHROME	Macrophages and hepatocytes	Impairing cholesterol efflux	Not accessed	(81)

its slow slicing. Once generated, they are resistant to exonucleases cleavage and become stable in cells. The functions of circRNAs remain in research, but some of them can also serve as decoys or sponges for miRNAs. As a result, the number of free targeting miRNAs decreases, weakening their blocking functions (85).

NON-CODING RNAS IN ENDOTHELIAL CELLS

miR-1a-3p and miR-1b-5p

Non-alcoholic fatty liver disease (NAFLD), associated with increased triglycerides and decreased HDL in the blood, was identified to be related to subclinical atherosclerosis, regardless of traditional risk factors and metabolic syndrome (42). To clarify the relationship between the two diseases, the exosomes secreted from steatotic hepatocytes were analyzed by miRNA deep sequencing, among which the clusters of miR-1, miR-1a-3p, and miR-1b-5p were the most significantly raised miRNAs. ECs were confirmed to absorb miR-1 involved in exosomes from hepatocytes by co-culture. Subsequent experiments showed that miR-1 mimics were able to activate endothelial inflammation using the enhanced expression of E-selectin, ICAM-1, and VCAM-1 at both mRNA and protein levels. *In vivo* studies revealed that miR-1 knockdown by antagomiR-1 regressed endothelial inflammatory activation as well as the lesion areas, revealing a new therapeutic target for atherosclerosis (86).

miR-181a-5p and miR-181a-3p

Both miR-181a-5p and miR-181a-3p were found to descend in atherosclerotic lesions of $ApoE^{-/-}$ mice fed a high-fat diet as well as the plasma of patients with coronary arterial diseases, suggesting the potential role of the two miRNAs in atherogenesis. The overexpression of miR-181a-5p and miR-181a-3p in $ApoE^{-/-}$ mice attenuated the plaque size as expected. Further studies showed that the gain-of-function experiment

suppressed inflammatory genes, such as ICAM-1 and VCAM-1, as well as leukocytes infiltration in aortic intima rather than impacting lipid metabolism. To explore the molecular mechanism, algorithms were used to predict their potential targets, among which NEMO for miR-181a-3p and TAB2 for miR-181a-5p, involved in the NF-κB signaling pathway in ECs, were confirmed by luciferase reporter assay. As a result, miR-181a-5p and miR-181a-3p were decreased in atherogenesis to activate endothelial inflammation (43).

miR-126-5p

Previous studies exhibited that the pro-atherogenic triglyceride-rich lipoproteins from subjects having a high-fat meal suppressed miR-126 expression in ECs and promoted VCAM-1 expression as well as monocyte adhesion, suggesting the potential anti-atherosclerotic role of miR-126 (44). Another research showed that apart from suppression and endothelial inflammatory activation, miR-126-5p, rather than miR-126-3p, could promote ECs' proliferation by decreasing Notch1 inhibitor delta-like 1 homolog (Dlk1) expression so as to prevent plaque formation, which was identified in $Mir126^{-/-}ApoE^{-/-}$ mice. However, disturbed laminar flow downregulated miR-126 at atherosclerosis-prone areas, abolishing its protective effect (45).

hsa_circ_0003575

To identify circRNAs participating in atherosclerosis, a circRNA microarray analysis was performed in HUVECs stimulated by oxLDL, among which hsa_circ_0003575 was mostly upregulated. *In vitro*, loss-of-function experiments showed that hsa_circ_0003575 was able to suppress ECs' proliferation and promote apoptosis. The bioinformatic assays revealed that hsa_circ_0003575 might serve as a miRNAs sponge for miR-199-3p, miR-9-5p, miR-377-3p, and miR-141-3p. However, more *in vivo* evidence is still required for the precise mechanism of hsa_circ_0003575 in atherosclerosis (36).

NEXN-AS1

A microarray analysis was performed to identify dysregulated genes in atherosclerosis lesions, among which the NEXN gene, as well as the lncRNA gene, NEXN-AS1 was significantly decreased. *In vivo* experiment revealed that NEXN-AS1 lncRNA could enhance NEXN expression in ECs, and the overexpression of NEXN-AS1 reduced endothelial inflammatory activation by inhibiting the NF-κB pathway. Nevertheless, the protective functions of NEXN-AS1 disappeared when NEXN was knocked down. The anti-atherogenic role of NEXN was determined with the $NEXN^{+/-}$ $ApoE^{-/-}$ mice. After a Western diet for 12 weeks, the $NEXN^{+/-}$ $ApoE^{-/-}$ mice presented a heavier plaque burden and a stronger tendency to rupture than the controls. As a result, NEXN-AS1 plays a protective role in atherosclerosis and has the potential to be a treatment target (37).

SENCR

SENCR was found to be rich in the human coronary artery smooth muscle cells (HCASMC) by RNA-sequencing. Further studies showed that SENCR knockdown downregulated the contractile gene expression in HCASMCs and promoted proliferation and migration, on the contrary, revealing its influence on phenotype switching of VSMCs (38). Another research explored its impact on endothelial cells as the lncRNA was also expressed in them (38). Exposed to laminar shear stress, a protective factor for atherosclerosis, SENCR level was elevated in both human umbilical vein endothelial cells (HUVEC) and human coronary artery endothelial cells (HCAEC), but not reversely decreased when subjected to disturbed shear stress. The knockdown studies showed that the loss of SENCR impaired membrane integrity and the permeability of endothelial cells. Further experiments exhibited that SENCR was directly bound to cytoskeletal-associated protein 4 (CKAP4) and stabilized adherens junctions in ECs (39). Despite the lack of direct evidence, the results above illustrate there is a high possibility that SENCR is associated with atherogenesis.

lncRNA-FA2H-2-MLKL

It is broadly acknowledged that oxLDL is one of the strongest inflammatory triggers for atherosclerosis, and autophagy is the protective pathway of cells faced with stress to survive. Studies revealed that oxLDL decreased the activity of enzyme mature-Cathepsin D, as well as its number, accounting for decreased lysosome activity, which is partially contributed to impaired autophagic flux and less cell survival in atherogenesis. To figure out the molecular mechanism, a microarray analysis was carried out to find out dysregulated genes, among which MLKL, responsible for autophagy and inflammation (40), was overexpressed in ECs and SMCs. Subsequent analysis showed that lncRNA-FA2H-2, which was decreased in human advanced atherosclerotic plaque compared with normal arterial intima, was adjacent to MLKL. Dual-luciferase assays exhibited that lncRNA-FA2H-2 could directly bind to the MLKL promotor and downregulate it. Further lncRNA-FA2H-2 knockdown experiments in ApoE-deficient mice showed that the size of plaques was enlarged and the cell death was enhanced, followed by an increased level of MLKL protein, suggesting the protective effect of lncRNA-FA2H-2 in atherosclerosis (41).

NON-CODING RNAS IN VASCULAR SMOOTH MUSCLE CELLS

miR-22

Previous studies showed that miR-22 was identified to be upregulated in embryonic stem cells and adventitia progenitor cells, responsible for SMC differentiation through regressing MECP2 expression (55). The miRNA was found to be significantly decreased in atherosclerotic plaques, suggesting that it might function in atherogenesis by manipulating VSMC plasticity. Overexpression and silencing experiments revealed that miR-22 was able to suppress VSMC proliferation and migration as well as promote VSMC specific markers expression such as SMαA, SM22α, SM-myh11, and SMTN-B, suggesting its function for maintaining VSMC contractile phenotype. To access its therapeutic potential, miR-22 AgomiR and LNA-miR-22 were immediately transfected into mice with injured femoral arteries caused by the wire. The results exhibited that miR-22 could prevent arterials from neointima hyperplasia by suppressing

VSMC phenotyping switching (56). However, its direct protective effect on atherosclerosis remains to be explored.

miR-128

miR-128 was identified as a conversed miRNA modulated by VSMC DNA methylation status by miRNA profiling since it was highly expressed, strongly changed, and less investigated in VSMC biology. Overexpression experiments revealed that miR-128 was capable of suppressing VSMC proliferation, migration, as well as keeping VSMCs in contractile phenotype, suggesting its protective effect for VSMC de-differentiation. To explore the molecular mechanism, two different kinds of bioinformatic algorithms were taken advantage of to look for the targets of miR-128, with KLF4 identified by luciferase reporter assays. The therapeutic potential for it was subsequently investigated in ApoE$^{-/-}$ mice with a perivascular carotid collar to create stenosis. The results showed that miR-128 overexpression inhibited VSMC proliferation and neointima formation, identifying its protective role (57).

miR-145

miR-145 were identified to be expressed specifically in the heart and smooth muscle with the use of transgenic mice and Bluo-gal staining. *In vitro* experiments exhibited that miR-145 could determine the fate of the VSMC and keep them in a contractile phenotype rather than a proliferative and synthetic phenotype (58). Clinical studies revealed that miR-145 was significantly reduced in patients with coronary arterial diseases (59). Given its protective effects on the VSMC, several therapeutic strategies focused on raising the level of miR-145 in patients. In the beginning, the prevention effects of miR-145 were explored. ApoE$^{-/-}$ mice were injected with miR-145 lentivirus regulated by the SMC-specific promoter SM22α, followed by 12 weeks high-fat diet. As expected, SMC-specific miR-145 protected arteries from atherogenesis by reducing the size of the lesion, stabilizing the plaque, and hindering macrophage infiltration (60). Another study utilized a novel nanoparticles technology to ensure that miR-145 was precisely transfected into VSMCs, namely the miR-145 micelles. To figure out its therapeutic effect, both an early-stage and an advanced-stage atherosclerotic ApoE$^{-/-}$ mice were treated with the miR-145 micelles, resulting in the inhibition of phenotype switching of VSMCs and preventing atherosclerotic progression (61).

circANRIL

Previous research showed that linear ANRIL transcripts at chromosome 9p21 were strongly associated with chromosome 9p21 (46). As the gene locus at chromosome 9p21 was also transcribed as circANRIL, which was more highly expressed in cells than linANRIL RNA and also more stable, circANRIL was worthy of investigation in atherosclerosis. *In vitro* overexpression and knockdown experiments exhibited that circANRIL could promote apoptosis and suppress proliferation in HEK-293 cells, SMCs, and macrophages. Neither did circANRIL serve as a miRNA sponge nor was it bound to Argonaute 2 to degrade mRNAs mediated by miRNAs. It is directly bound to pescadillo homolog 1, which is responsible for 60S preribosomal assembly, preventing ribosome biogenesis. Further studies in human atherosclerotic plaques confirmed that high circANRIL levels were strongly correlated with the accumulation of 32S and 36S pre-rRNA (47). A recent study also showed that circANRIL was significantly negatively correlated with CAD risk and severity, suggesting its value for diagnosis and prognosis (48).

circ_Lrp6

It is widely known that circular RNAs can act as miRNAs sponges, which can downregulate miRNA expression, impacting cell biology as well. By RNA sequencing and bioinformatic analysis, circ_Lrp6 in VSMCs was identified because of the abundant binding sites for miR-145 and its conservation between humans and mice. With methods of RNA immunoprecipitation and competitive luciferase assays, circ_Lrp6 was confirmed to be a miRNA sponge for miR-145. *In vitro* silencing and overexpression experiments exhibited that circ_Lrp6 reversed miR-145-mediated inhibition of migration, proliferation, and VSMC phenotype switching. *In vivo* study further identified the pro-proliferative effect of circ_Lrp6. By injecting ApoE$^{-/-}$ with a perivascular carotid collar with circ_Lrp6-shRNA, the neointima hyperplasia was significantly attenuated (49).

circACTA2

In VSMCs, circACTA2 expression was induced by NRG-1-ICD, the intracellular domain of Neuregulins, that was able to bind to α-SMA and promote the cytoskeletal organization as a result. By luciferase assay and pulldown assay, circACTA2 was identified to bind to miR-548f-5p and reduce its expression. Subsequent experiments revealed that miR-548f-5p could bind to 3′-UTR of α-SMA and inhibit its expression. Therefore, the NRG-1-ICD/circACTA2/miR-548f-5p axis was built to regulate SMC contraction. Further *in vivo* studies exhibited that circACTA2 and its interaction with miR-548f-5p were decreased, while miR-548f-5p was increased in intimal hyperplastic arteries, suggesting the potential effect of circACTA2 in atherosclerosis (50).

SMILR

After being treated with IL1α and platelet-derived growth factor (PDGF) for 72 h to induce proliferation and inflammation in human saphenous vein-derived smooth muscle cells, RNA-seq was performed to identify subsequently varying lncRNAs. Among them, SMILR was the most differently expressed one with a particular location in the smooth muscle cells. *In vitro* experiments showed that SMILR was related to SMC proliferation and increased in human atherosclerotic lesions vs. neighboring artery tissues (51). Further molecular mechanisms were identified by fluorescence ubiquitin cell cycle indicator viral system and SMILR pulldowns, revealing that SMILR was able to promote mitosis by regulating late mitotic protein CENPF mRNA. Since SMILR was a human-specific lncRNA, the usage of animal models was limited. To access the therapeutic potential, a siRNA approach was used in vein grafts before grafting, resulting in reduced proliferation of SMCs (52).

CARMN

CARMN was identified as a strongly expressed SMC-specific lncRNA by transcriptome analysis and was highly conserved in mice as well, which was confirmed in the GFP KI Reporter Mouse Model that made the location of CARMN in cells visible. Analysis of scRNA-seq data from human atherosclerotic arteries showed that CARMN-positive cells, as well as CARMN levels, descended, suggesting its role in atherogenesis (53). The molecular mechanism was explored in another study. *In vivo* CARMN knockdown experiments combined with RNA sequencing analysis revealed that the dysregulated genes were strongly associated with VSMC phenotype switching, thereby promoting atherosclerosis. As CARMN was located exactly upstream of miR-143 and−145, experiments were carried out to figure out whether the effect of CARMN was dependent on the two miRNAs. On silencing CARMN by GapmeR strategy and overexpressing miR-143 and−145 by mimics at the same time, hCASMCs migration and VSMC identifying markers were observed to restore, whereas hCASMCs proliferation remained increased, revealing the independent role of the lncRNA in regulating VSMC proliferation. Further *in vivo* studies showed CARMN was a protective non-coding RNA in atherogenesis consistently (54).

NON-CODING RNAS IN MACROPHAGES

miR-181b

miR-181b was found to rise in unstable atherosclerotic plaques compared with stable ones, which was associated with an obvious fall in TIMP-3 protein. TIMP-3 was an inhibitor of matrix metalloproteinases (MMPs), a variety of proteases produced by macrophages. A previous study showed that in the fibrous cap of human atheroma, TIMP-3 was increased to prevent ECM from proteolysis by inhibiting MMPs (69). Thus, miR-181b may serve as a pro-atherogenic miRNA. To confirm the hypothesis, ApoE-deficient mice burdened with atherosclerotic lesions were treated with miR-181b inhibitor, and the TIMP-3 levels, proteolytic activity, and the lesion area were tested. As expected, macrophage TIMP-3 expression was enhanced after the inhibition of miR-181b, followed by attenuated lesion progression. However, this kind of protective effect was abolished when Timp3 was knocked out at the same time, revealing that miR-181b deteriorated atherosclerosis by suppressing TIMP-3 expression (70).

miR-34a

miR-34a is widely expressed in macrophages, endothelial cells, smooth muscle cells (SMCs), and hepatocytes. The previous study showed that miR-34a was highly induced in hepatocytes in NAFLD, which suppressed hepatic HNF4α in both mRNA and protein levels, resulting in a fatty liver by preventing VLDL from secreting but attenuating atherosclerotic plaques in both $ApoE^{-/-}$ and $Ldlr^{-/-}$ mice on the contrary (71). In addition, miR-34a was also induced in human and mice's atheroma, so its influence on atherogenesis was further explored later. In VSMCs, miR-34a was able to promote cell senescence and vascular calcification by decreasing Axl and SIRT1 (72). In macrophages, miR-34a was targeted to ABCA1 and ABCG1, which resulted in impaired cholesterol efflux and macrophage-specific miR-34a deletion, which could prevent atherogenesis. Given the contradictory effect on different tissues, a global miR-34a deficient model was introduced to access its impact in total. Dyslipidemia, atherosclerosis, and NAFLD were all reserved subsequently, suggesting that miR-34a mainly played a negative role in atherogenesis (73).

miR-30c-5p

To identify whether miRNAs were able to predict and promote atherosclerotic progression, 99 volunteers from the PLIC study free from atherosclerosis were randomly selected to measure their plasma miRNA levels at first, among whom 44 participants developed atherosclerosis after a 5-year follow-up and another 29 did after 6.5 years. Comparing the miRNA basal line at the beginning, a total of 7 miRNAs were picked, among which miR-30c-5p had the best ability to discriminate patients with plaque burden with the highest AUC and to predict atherosclerotic progression. Further, *in vitro* experiments revealed that plasma miR-30c-5p contained in microparticles secreted from macrophages was significantly reduced when treated with oxLDL, resulting from CD36 activation and inhibition of Dicer. Consequently, miR-30c-5p in cells fell, resulting in the upregulation of its target Caspase-3 and inducing IL-6β releasing, as well as the apoptosis of macrophages. *In vivo* study also showed that the lack of miR-30c-5p worsened endothelial healing response to injury, regarded as the first step of atherogenesis (74).

MALAT1

The previous study identified the association between the long non-coding RNA MALAT1 and cardiovascular innate immunity, showing its potential regulating effect on monocytes and macrophages (62). Two pieces of research revealed the protective function of MALAT1 in macrophages at the same time. One of the two utilized heterozygous MALAT1-deficient $ApoE^{-/-}$ mice to access the influence of the lncRNA on atherosclerosis. Even with a normal diet, the knockdown mice showed a progressive lesion and an increased level of inflammatory factors such as IFN-γ, TNF, and IL6, revealing that the function of MALAT1 is related to inflammation (63). The other study also measured the plaque burden of $ApoE^{-/-}$ $Malat1^{-/-}$ mice fed with a high-fat diet for 12 weeks. However, the lesion showed no significant difference compared with controls except for higher $CD45^{+}$ leukocytes retention, differing from the former study, partially because of compensatory upregulation of the adjacent lncRNA NEAT1. To identify the impact of MALAT1 on inflammatory cells, the bone marrow of $ApoE^{-/-}$ $Malat1^{-/-}$ was transplanted into $ApoE^{-/-}$ $Malat1^{+/+}$ mice, resulting in enlarged atherosclerotic plaques where more macrophage infiltrated. Further experiments showed that MALAT1 served as a microRNA sponge for miR-503 related to enhanced adhesion ability to activate endothelial cells. Moreover, MALAT1 is highly decreased in human atheroma, further demonstrating its anti-atherogenic function (64).

MeXis

The liver X receptors (LXRs) are transcriptional factors that promote the expression of genes related to reverse cholesterol transport containing Abca1 when intracellular cholesterol was elevated (65). It was noted that ABCA1 responsible for cholesterol efflux was particularly increased in macrophages in comparison with other cell types when treated with synthetic LXR agonist. By transcriptional profiling, several kinds of lncRNAs were also found to be increased, among which the lncRNA MeXis was most raised and of which the promoter was able to bind with LXRs, suggesting that LXRs could regulate cholesterol efflux in macrophage by controlling the transcription of MeXis. *In vitro* experiments exhibited that LXRs did induce the expression of ABCA1 by promoting MeXis transcription. To determine the effect of MeXis on cholesterol efflux and atherosclerosis, bone marrow from MeXis$^{-/-}$ was transplanted into Ldlr$^{-/-}$ mice, resulting in reduced Abca1 expression and enhanced atherosclerotic burden (66). According to the results above, MeXis was supposed to be a protective lncRNA in atherogenic progression.

MAARS

MAARS was a macrophage-specific lncRNA identified by RNA-Seq profiling in the aortic intima of Ldlr$^{-/-}$ mice. The level of MAARS gradually increased after the high-fat diet and descended strongly when the mice resumed a normal diet, suggesting its potential role in atherosclerosis. Knockdown studies proved MAARS to be a pro-atherogenic lncRNA due to the regression of atherosclerotic lesions. *In vitro* and *in vivo* overexpression and knockdown studies revealed that MAARS directly induced apoptosis and impaired efferocytosis of macrophages. The mechanism was that in atherosclerosis progression MAARS emerged to directly bind with HuR, an RNA-binding protein capable of stabilizing mRNA translation (67), resulting in the increase of HuR targeting genes such as p53, caspase-8,−9 related to apoptosis (68).

NON-CODING RNAS IN HEPATOCYTIC LIPID METABOLISM

miR-33

miR-33 is one of the key regulators of lipid metabolism in both macrophages and the liver and is observed to significantly rise in human atherosclerotic plaques. By reducing ABCA1 expression in the liver or macrophages, cholesterol efflux was impaired and plasma HDL was decreased, suggesting a pro-atherogenic effect of the miRNA (75). To access its particular impact on atherosclerosis, Ldlr$^{-/-}$ mice fed with a high-fat diet were treated with an antagonist of miR-33 for 4 weeks, resulting in reversed ABCA1 in the liver and plaque macrophages, improved plasma HDL level, and reduced lesion burden (76). In addition, miR-33 was identified to regulate mitochondrial metabolism by inhibiting mitochondrial regulatory genes related to mitochondrial respiration and ATP production, which was also contributed to cholesterol efflux in macrophages (77). Apart from the impact on lipid accumulation in macrophages, the capability of miR-33 to interfere with the balance between aerobic glycolysis and mitochondrial oxidative phosphorylation led to the suppression of M2 polarization as well as FOXP3^{+} Tregs accumulation (78). According to the results above, miR-33 would be a potential therapeutic target for atherosclerosis.

miR-144

Two independent studies almost revealed the important role miR-144 played in cholesterol metabolism in both the liver and macrophages at the same time (79, 80). The first one found that the expression of miR-144 in the mice liver and macrophages was significantly increased by the stimulation of liver X nuclear receptor (LXR) angonists. LXRs regulated cholesterol effluxes in hepatocytes and macrophages and the plasma HDL level by regulating ABCA1 and ABCG expression. *In vivo* experiments showed that the overexpression of miR-144 could suppress ABCA1 expression and cholesterol efflux in macrophages. Similarly, overexpressing miR-144 in male C57BL/6 mice could also decrease the ABCA1 protein level in the liver and reduce plasma HDL levels, while suppressing the microRNA showed the reverse result. The later study found that the expression of miR-144 in the liver could be activated by another receptor called Farnesoid-X-Receptor (FXR) which was also highly expressed in the liver. Given the negative correlation between plasma HDL levels and atherosclerosis, miR-144 was likely to play a pro-atherogenic role, but the accurate function still reminds to be answered.

CHROME

CHROME was a primate-specific long non-coding RNA that was found to be increased in the plasma of patients with atherosclerosis as well as in the atherosclerotic plaques. Suppression CHROME in human hepatic HepG2 cells revealed that the expression of cholesterol metabolism-related genes such as ABCA1 in hepatocytes was significantly decreased. Algorithm and *in vivo* experiments showed that CHROME could interact with miR-33, miR-27, and miR-128 and decrease their expression. These microRNAs had been proved to inhibit ABCA1 expression and promote atherogenesis (87). As a result, CHROME could promote cholesterol efflux in hepatocytes and increase plasma HDL levels. *In vivo* experiments using African green monkeys revealed that the expression of CHROME was regulated by excessive dietary cholesterol. The above results demonstrated the potential protective function of CHROME in atherosclerosis. However, the precise role it plays still needs to be evaluated (81).

RNA Therapeutics in Atherosclerosis

Apart from small molecules and proteins, RNA drugs nowadays are attached, thereby increasing their importance as they are easy to design, synthesize, and be absorbed into the cells (88). There are various types of RNA-targeted therapeutics in atherosclerosis, such as antisense oligonucleotides (ASO), small interfering RNA (siRNA), and microRNAs (**Table 2**) (89). Classical ASOs are short, single-stranded DNA-like molecules that are complementary to mRNA, forming a DNA–RNA duplex that can be hydrolyzed by the enzyme Ribonuclease H (RNase H) (90). ASOs can also be anti-miRs targeting miRNAs within cells and blocking their functions, two examples of which

TABLE 2 | RNA therapeutics in atherosclerosis.

Drug name	Chemistry	Target	Clinical status	NCT number
MRG-110	Antisense Oligonucleotides	miR-92a-3p	Phase I	[EudraCT]No.2017-004180-12
IONIS-ANGPTL3-L_{Rx}	Antisense Oligonucleotides	hepatic *ANGPTL3 mRNA*	Phase I	NCT02709850
AKCEA-APOCIII-L_{Rx}	Antisense Oligonucleotides	hepatic *APOC3* mRNA	Phase I/IIa	NCT02900027
Inclisiran	siRNA	hepatic *PCSK9* mRNA	Phase III	NCT03399370; NCT03400800

are antagomiRs and locked nucleic acid (LNA)-based anti-miRs (91). siRNA are double-stranded RNA molecules with a length of 20–25 nucleotides that can mediate the degradation of complementary mRNA by an RNA-induced silencing complex (RISC)-dependent pathway (92). miRNA mimics are double-stranded RNAs that imitate native miRNAs to reverse the protective molecules within cells (89).

Antisense Oligonucleotides

MRG-110

A previous study showed that miR-92a could directly bind to 3′UTR of KLF2 and KLF4, which could partially reverse endothelial inflammation in human arterial endothelial cells (HAECs) (93). miR-92a-3p was one of the atheromas in endothelial cells selected from large-scale miRNA profiling in human umbilical vein endothelial cells (HUVECs) stimulated by shear stress and oxLDL. miR-92a-3p was the most upregulated microRNAs subjected to low shear stress with oxLDL. Inhibition of it attenuates endothelial Inflammation *in vitro*. Consistently, blockade of miR-92a in Ldlr-deficient mice with a high-fat diet significantly reduced the atherosclerotic lesions (94).

According to the experimental results above, miR-92a-3p showed therapeutic potential. As a result, a locked nucleic acid-based anti-miR named MRG-110 targeting miR-92a-3p was developed to be utilized in a human study. A randomized, double-blinded clinical trial with a size of 49 persons at phase I (European Clinical Trials Database [EudraCT] No. 2017-004180-12) was conducted to estimate its functional efficiency to block miR-92a-3p. The volunteers were healthy men at 18–45 years of age without cigarette use for at least 3 months. The results showed that the amount of miR-92a-3p was decreased in the peripheral blood compartment with a low dose of MRG-110, revealing its high efficiency (95). However, the safety and its effects to treat atherosclerosis need to be accessed in later clinical trials.

IONIS-ANGPTL3-L_{Rx}

ANGPTL3 is the gene encoding angiopoietin-like 3 protein reported to inhibit the activation of lipoprotein lipase and endothelial lipase. Once produced in the liver, ANGPTL3 is secreted for circulation and absorbed by other cells where it is cleaved by furin and PACE4, and its N-terminal domain is released to suppress the activity of lipoprotein lipase (96). Using the exome sequencing, two nonsense mutations in two patients with familial hypobetalipoproteinemia were identified, revealing the potential role of ANGPTL3 in lipid metabolism and atherosclerosis (97). To identify the hypothesis that ANGPTL3 deficiency protects atherogenesis, individuals with loss-of-function mutations as well as Angptl3 knockout mice were both tested for the size of their coronary atherosclerotic lesions, proving its protective role in atherosclerosis (98).

IONIS-ANGPTL3-L_{Rx} is an antisense oligonucleotide targeting hepatic ANGPTL3 mRNA to reduce ANGPTL3 translation, decrease triglycerides and LDL cholesterol in the blood, and eventually slow down atherogenesis. The phase I clinical trial (NCT02709850) to access the safety, effects, kinetics, and pharmacodynamics of IONIS-ANGPTL3-L_{Rx}, as well as animal experiments, have already been completed. A total of 44 volunteers with a higher fasting LDL cholesterol or triglyceride level had received a single-dose or multiple-dose ASO drug for 6 weeks before the indexes for lipid metabolism were tested, revealing a significant reduction in pro-atherogenic lipid in the blood. The results were consistent with those of Apoc3 and Ldlr double-knockout mice which also showed a reduced atherogenesis (99).

AKCEA-APOCIII-L_{Rx}

ApoC-III is a 99-amino acid peptide with a 20 amino acid signal peptide synthesized mostly by the liver. It plays a vital role in the metabolism of triglyceride-rich lipoproteins (TRL) since it helps the assembly of VLDL in the liver, inhibits the intake of TRL in hepatocytes as long, and suppresses the activation of LPL. A high level of plasma ApoC-III is strangely related to hypertriglyceridaemia (100). To figure out its importance on cardiovascular diseases, an exome sequencing for 18,666 genes involving 3,734 participants was launched to find out mutations deactivating ApoC-III. The individuals with the loss-of-function mutations presented lower levels of triglyceride as well as the risk of coronary heart disease (101). Therefore, ApoC-III could be a potential therapeutic target for atherosclerosis treatment.

AKCEA-APOCIII-L_{Rx} is an ASO drug with a triantennary N-acetyl galactosamine ($GalNAc_3$) complex at its 5' terminal for better stability targeting hepatic APOC3 mRNA. The Phase I/IIa clinical trial (NCT02900027) aimed to evaluate its efficacy, pharmacodynamics, and side effects has been conducted. A total of 56 healthy participants with high triglyceride levels were enrolled. After subcutaneous injection of the ASO drug or placebo, every 6 weeks in single-dose cohorts or every 4 weeks in multiple-dose cohorts, the laboratory parameters referred to lipid metabolism were measured 3 months later, resulting in a significant reduction of ApoC-III and an extensive improvement in pro-atherogenic lipid (102). Therefore, further clinical trials

aimed to access the effects on atherosclerotic patients are worthy of launching.

siRNAs

Inclisiran

Proprotein convertase subtilisin-like type 9 (PCSK9) is a 692-amino acid protein located mostly in the liver. It is a key regulator of LDL metabolism as a serine protease that can catalyze the degradation of LDL receptors in the liver (103). Its importance in LDL metabolism was first identified in a family with autosomal dominant hypercholesterolemia, where the gain-of-function missense mutations of PCSK9 caused an increase of low-density lipoprotein cholesterol levels in the blood (104). To further determine the function of PCSK9 in LDL metabolism, the coding regions of PCSK9 in 128 participants with low plasma levels of LDL were sequenced. As expected, two nonsense mutations of PCSK9 were founded, which was consistent with the result above (105). Apart from that, variants in PCSK9 were related to increased LDL cholesterol levels and higher risk for coronary artery disease (106). So PCSK9 is supposed to be an efficient therapeutic target.

Currently, there exist two kinds of drugs targeting PCSK9 recommend by AHA guidelines for patients with high levels of LDL-C, namely the evolocumab and alirocumab (34). Both of them are monoclonal anti-PCSK9 antibodies whose benefits on lowering LDL-C and risk for cardiovascular events were identified in two large clinical trials FOURIER (107) and ODYSSEY (108). Despite its excellent efficacy, two main disadvantages block their wide usage. Firstly, it is likely to be hard to adhere to the antibody treatment since the drugs are required to be injected every 2 weeks. Besides, it is not affordable for everyone because of its high price and frequent injection (109). As a result, inclisiran with lower cost and injection frequency shpuld come out to exist.

Inclisiran is a small interfering RNA targeting PCSK9. Two clinical trials at phage III, named ORION-10 (NCT03399370) and ORION-11 (NCT03400800), were completed to evaluate the benefit of inclisiran on patients with elevated LDL-C despite statin usage. The former one was launched in the United States including 1,561 participants, while the latter one was conducted in Europe and South Africa with 1,617 volunteers involved. In both studies, 300 mg of inclisiran was given to the patients through subcutaneous injections at Day 1, Day 90, and then every 6 months. After a year and a half, the percentage change in LDL-C from baseline was tested. The results showed a reduction of 52.3% in the ORION-10 trial and 49.9% in the ORION-11 trial with a few slight side effects such as injection-site adverse events, revealing the huge therapeutic potential for patients resistant to statin therapy (110).

Cutting-Edge RNA Therapeutics in Atherosclerosis

Conventional RNA therapies treating atherosclerosis have their disadvantages, such as the lack of target specificity, susceptibility to degradation, and massive side effects. Nanotechnology is likely to address these problems (111). Nanomedicine applies nanotechnology for disease imaging, diagnosis, and treatment. The nanoparticles are made up of biological materials such as lipid as well as inorganic nanocrystals like iron oxide, providing a stable environment for the drugs. Equipped with antibodies or antibody fragments targeting specific ligand receptors on the cellular surfaces, the risk for interfering with normal physiological processes in irrelevant cell types declines, reducing the occurrence of adverse effects (112, 113).

Due to of the broad benefits of nanomedicine, more and more studies have focused on exploring nanoparticle strategies targeting atherosclerosis, including nanomedicines containing RNA drugs. siCAM (5) was a nanoparticle-based siRNA drug targeting endothelial cells. It contains five siRNAs separately inhibiting the expression of intercellular adhesion molecules Icam1 and Icam2, Vcam1, E- and P-selectins. *In vivo* experiments showed that monocytes recruitment was significantly decreased in the atherosclerotic lesions in the ApoE-deficient mice, revealing its therapeutic potential (114). SNALP-siApoB was a stable nucleic acid lipid particle containing siRNAs directly targeting ApoB mRNA in the livers, which were not accessible by traditional therapies. The results revealed that this nanoparticle drug could significantly reduce the ApoB expression and serum cholesterol and LDL levels for 11 days in cynomolgus monkeys (115).

CONCLUSION

The above studies have demonstrated that ncRNAs play a vital role during atherogenesis. Atherosclerosis is a complicated disease where different kinds of cell types participated in its development. Among them, three kinds of cells are considered to play important roles in atherogenesis, namely endothelial cells, macrophages, and vascular smooth muscle cells. After lipid retention and oxidation under endothelium of arterials, ECs begin dysfunction, resulting in impaired permeability and overexpression of adhesion molecules. The dysfunction of ECs recruits monocytes from circulation to the lesion, where they differentiate into macrophages. The macrophages take in a mass of ox-LDL underneath the intima, resulting in impaired cholesterol metabolism within the cells, which promotes the formation of foam cells. The accumulation of foam cells forms the necrotic cores in the plaque. During the process, VSMCs continue to migrate from the media to the intima, switch their phenotypes, and produce an extracellular matrix, forming the fibrosis cap. However, their constant loss by apoptosis and necrosis finally leads to plaque rupture. ncRNAs participated in regulating all the mentioned cellular progress.

Apart from regulating the pathophysiological development of atherosclerosis, ncRNAs can also serve as therapeutic tools to treat this disease. The most successful RNA drug in atherosclerosis is Inclisiran, the siRNA drug targeting PCSK9. It has entered phase III clinical trial and showed a strong ability to reduce LDL levels. In addition to traditional RNA therapeutic strategies, advancing technologies are also used to improve the treatment effects. For example, RNA drugs can be encapsulated into nanoparticles to improve their specificity and stability,

revealing the value of research to combine the RNA drugs and nanomedicines together.

AUTHOR CONTRIBUTIONS

YT drafted the manuscript. HL and CC supervised the manuscript. All authors contributed to the article and approved the submitted version.

FUNDING

This work was supported by grants from the National Natural Science Foundation of China (nos. 81822002, 31771264, and 82170273). The funders had no role in the study design, data collection, analysis, manuscript preparation, or decision to publish.

REFERENCES

1. Libby P, Buring JE, Badimon L, Hansson GK, Deanfield J, Bittencourt MS, et al. Atherosclerosis. *Nat Rev Dis Primers.* (2019) 5:56. doi: 10.1038/s41572-019-0106-z
2. Back M, Yurdagul A. Jr., Tabas I, Oorni K, Kovanen PT, Inflammation and its resolution in atherosclerosis: mediators and therapeutic opportunities. *Nat Rev Cardiol.* (2019) 16:389–406. doi: 10.1038/s41569-019-0169-2
3. Nakashima Y, Chen YX, Kinukawa N, Sueishi K. Distributions of diffuse intimal thickening in human arteries: preferential expression in atherosclerosis-prone arteries from an early age. *Virchows Arch.* (2002) 441:279–88. doi: 10.1007/s00428-002-0605-1
4. Nakashima Y, Wight TN, Sueishi K. Early atherosclerosis in humans: role of diffuse intimal thickening and extracellular matrix proteoglycans. *Cardiovasc Res.* (2008) 79:14–23. doi: 10.1093/cvr/cvn099
5. Gimbrone MA. Jr., Garcia-Cardena G, Endothelial Cell Dysfunction and the Pathobiology of Atherosclerosis. *Circ Res.* (2016) 118:620–36. doi: 10.1161/CIRCRESAHA.115.306301
6. Miller YI, Choi SH, Wiesner P, Fang L, Harkewicz R, Hartvigsen K, et al. Oxidation-specific epitopes are danger-associated molecular patterns recognized by pattern recognition receptors of innate immunity. *Circ Res.* (2011) 108:235–48. doi: 10.1161/CIRCRESAHA.110.223875
7. Soehnlein O, Libby P. Targeting inflammation in atherosclerosis - from experimental insights to the clinic. *Nat Rev Drug Discov.* (2021) 20:589–610. doi: 10.1038/s41573-021-00198-1
8. de Nigris F, Lerman LO, Ignarro SW, Sica G, Lerman A, Palinski W, et al. Beneficial effects of antioxidants and L-arginine on oxidation-sensitive gene expression and endothelial NO synthase activity at sites of disturbed shear stress. *Proc Natl Acad Sci U S A.* (2003) 100:1420–5. doi: 10.1073/pnas.0237367100
9. Chao Y, Ye P, Zhu L, Kong X, Qu X, Zhang J, et al. Low shear stress induces endothelial reactive oxygen species via the AT1R/eNOS/NO pathway. *J Cell Physiol.* (2018) 233:1384–95. doi: 10.1002/jcp.26016
10. Morgan MJ, Liu ZG. Crosstalk of reactive oxygen species and NF-kappaB signaling. *Cell Res.* (2011) 21:103–15. doi: 10.1038/cr.2010.178
11. Pober JS, Sessa WC. Evolving functions of endothelial cells in inflammation. *Nat Rev Immunol.* (2007) 7:803–15. doi: 10.1038/nri2171
12. Davies MJ, Gordon JL, Gearing AJ, Pigott R, Woolf N, Katz D, et al. The expression of the adhesion molecules ICAM-1, VCAM-1, PECAM, and E-selectin in human atherosclerosis. *J Pathol.* (1993) 171:223–9. doi: 10.1002/path.1711710311
13. Cybulsky MI, Gimbrone MA. Jr., and Endothelial expression of a mononuclear leukocyte adhesion molecule during atherogenesis. *Science.* (1991) 251:788–91. doi: 10.1126/science.1990440
14. Nagy L, Tontonoz P, Alvarez JG, Chen H, Evans RM, Oxidized LDL. regulates macrophage gene expression through ligand activation of PPARgamma. *Cell.* (1998) 93:229–40. doi: 10.1016/S0092-8674(00)81574-3
15. Tontonoz P, Nagy L, Alvarez JG, Thomazy VA, Evans RM. PPARgamma promotes monocyte/macrophage differentiation and uptake of oxidized LDL. *Cell.* (1998) 93:241–52. doi: 10.1016/S0092-8674(00)81575-5
16. Kunjathoor VV, Febbraio M, Podrez EA, Moore KJ, Andersson L, Koehn S, et al. Scavenger receptors class A-I/II and CD36 are the principal receptors responsible for the uptake of modified low density lipoprotein leading to lipid loading in macrophages. *J Biol Chem.* (2002) 277:49982–8. doi: 10.1074/jbc.M209649200
17. Glass CK, Witztum JL. Atherosclerosis the road ahead. *Cell.* (2001) 104:503–16. doi: 10.1016/S0092-8674(01)00238-0
18. Hsieh V, Kim MJ, Gelissen IC, Brown AJ, Sandoval C, Hallab JC, et al. Cellular cholesterol regulates ubiquitination and degradation of the cholesterol export proteins ABCA1 and ABCG1. *J Biol Chem.* (2014) 289:7524–36. doi: 10.1074/jbc.M113.515890
19. Wang X, Collins HL, Ranalletta M, Fuki IV, Billheimer JT, Rothblat GH, et al. Macrophage ABCA1 and ABCG1, but not SR-BI, promote macrophage reverse cholesterol transport *in vivo*. *J Clin Invest.* (2007) 117:2216–24. doi: 10.1172/JCI32057
20. Yvan-Charvet L, Ranalletta M, Wang N, Han S, Terasaka N, Li R, et al. Combined deficiency of ABCA1 and ABCG1 promotes foam cell accumulation and accelerates atherosclerosis in mice. *J Clin Invest.* (2007) 117:3900–8. doi: 10.1172/JCI33372
21. Ren K, Li H, Zhou HF, Liang Y, Tong M, Chen L, et al. Mangiferin promotes macrophage cholesterol efflux and protects against atherosclerosis by augmenting the expression of ABCA1 and ABCG1. *Aging.* (2019) 11:10992–1009. doi: 10.18632/aging.102498
22. Wang H, Yang Y, Sun X, Tian F, Guo S, Wang W, et al. Sonodynamic therapy-induced foam cells apoptosis activates the phagocytic PPARgamma-LXRalpha-ABCA1/ABCG1 pathway and promotes cholesterol efflux in advanced plaque. *Theranostics.* (2018) 8:4969–84. doi: 10.7150/thno.26193
23. Basatemur GL, Jorgensen HF, Clarke MCH, Bennett MR, Mallat Z. Vascular smooth muscle cells in atherosclerosis. *Nat Rev Cardiol.* (2019) 16:727–44. doi: 10.1038/s41569-019-0227-9
24. Pidkovka NA, Cherepanova OA, Yoshida T, Alexander MR, Deaton RA, Thomas JA, et al. Oxidized phospholipids induce phenotypic switching of vascular smooth muscle cells in vivo and in vitro. *Circ Res.* (2007) 101:792–801. doi: 10.1161/CIRCRESAHA.107.152736
25. Grootaert MOJ, Moulis M, Roth L, Martinet W, Vindis C, Bennett MR, et al. Vascular smooth muscle cell death, autophagy and senescence in atherosclerosis. *Cardiovasc Res.* (2018) 114:622–34. doi: 10.1093/cvr/cvy007
26. Grootaert MO, da Costa Martins PA, Bitsch N, Pintelon I, De Meyer GR, Martinet W, et al. Defective autophagy in vascular smooth muscle cells accelerates senescence and promotes neointima formation and atherogenesis. *Autophagy.* (2015) 11:2014–32. doi: 10.1080/15548627.2015.1096485
27. Gardner SE, Humphry M, Bennett MR, Clarke MC. Senescent vascular smooth muscle cells drive inflammation through an interleukin-1alpha-dependent senescence-associated secretory phenotype. *Arterioscler Thromb Vasc Biol.* (2015) 35:1963–74. doi: 10.1161/ATVBAHA.115.305896
28. Childs BG, Baker DJ, Wijshake T, Conover CA, Campisi J, van Deursen JM. Senescent intimal foam cells are deleterious at all stages of atherosclerosis. *Science.* (2016) 354:472–7. doi: 10.1126/science.aaf6659
29. Lutgens E, de Muinck ED, Kitslaar PJ, Tordoir JH, Wellens HJ, Daemen MJ. Biphasic pattern of cell turnover characterizes the progression from fatty streaks to ruptured human atherosclerotic plaques. *Cardiovasc Res.* (1999) 41:473–9. doi: 10.1016/S0008-6363(98)00311-3
30. Crisby M, Kallin B, Thyberg J, Zhivotovsky B, Orrenius S, Kostulas V, et al. Cell death in human atherosclerotic plaques involves both oncosis and apoptosis. *Atherosclerosis.* (1997) 130:17–27. doi: 10.1016/S0021-9150(96)06037-6
31. Clarke MC, Figg N, Maguire JJ, Davenport AP, Goddard M, Littlewood TD, et al. Apoptosis of vascular smooth muscle cells induces features

of plaque vulnerability in atherosclerosis. *Nat Med.* (2006) 12:1075–80. doi: 10.1038/nm1459
32. Matsui M, Corey DR. Non-coding RNAs as drug targets. *Nat Rev Drug Discov.* (2017) 16:167–79. doi: 10.1038/nrd.2016.117
33. Esteller M. Non-coding RNAs in human disease. *Nat Rev Genet.* (2011) 12:861–74. doi: 10.1038/nrg3074
34. Grundy SM, Stone NJ, Bailey AL, Beam C, Birtcher KK, Blumenthal RS, et al. 2018 AHA/ACC/AACVPR/AAPA/ABC/ACPM/ADA/AGS/APhA/ASPC/NLA/PCNA guideline on the management of blood cholesterol: a report of the American College of Cardiology/American Heart Association Task Force on Clinical Practice Guidelines. *J Am Coll Cardiol.* (2019) 73:e285–350. doi: 10.1016/j.jacc.2018.11.003
35. Poller W, Dimmeler S, Heymans S, Zeller T, Haas J, Karakas M, et al. Non-coding RNAs in cardiovascular diseases: diagnostic and therapeutic perspectives. *Eur Heart J.* (2018) 39:2704–16. doi: 10.1093/eurheartj/ehx165
36. Li CY, Ma L, Yu B, Circular RNA. hsa_circ_0003575 regulates oxLDL induced vascular endothelial cells proliferation and angiogenesis. *Biomed Pharmacother.* (2017) 95:1514–9. doi: 10.1016/j.biopha.2017.09.064
37. Hu YW, Guo FX, Xu YJ Li P, Lu ZF, McVey DG, et al. Long noncoding RNA NEXN-AS1 mitigates atherosclerosis by regulating the actin-binding protein NEXN. *J Clin Invest.* (2019) 129:1115–28. doi: 10.1172/JCI98230
38. Bell RD, Long X, Lin M, Bergmann JH, Nanda V, Cowan SL, et al. Identification and initial functional characterization of a human vascular cell-enriched long noncoding RNA. *Arterioscler Thromb Vasc Biol.* (2014) 34:1249–59. doi: 10.1161/ATVBAHA.114.303240
39. Lyu Q, Xu S, Lyu Y, Choi M, Christie CK, Slivano OJ, et al. SENCR stabilizes vascular endothelial cell adherens junctions through interaction with CKAP4. *Proc Natl Acad Sci U S A.* (2019) 116:546–55. doi: 10.1073/pnas.1810729116
40. Fitzwalter BE, Thorburn A. Recent insights into cell death and autophagy. *FEBS J.* (2015) 282:4279–88. doi: 10.1111/febs.13515
41. Guo FX, Wu Q, Li P, Zheng L, Ye S, Dai XY, et al. The role of the LncRNA-FA2H-2-MLKL pathway in atherosclerosis by regulation of autophagy flux and inflammation through mTOR-dependent signaling. *Cell Death Differ.* (2019) 26:1670–87. doi: 10.1038/s41418-018-0235-z
42. Oni ET, Agatston AS, Blaha MJ, Fialkow J, Cury R, Sposito A, et al. A systematic review: burden and severity of subclinical cardiovascular disease among those with nonalcoholic fatty liver; should we care? *Atherosclerosis.* (2013) 230:258–67. doi: 10.1016/j.atherosclerosis.2013.07.052
43. Su Y, Yuan J, Zhang F, Lei Q, Zhang T, Li K, et al. MicroRNA-181a-5p and microRNA-181a-3p cooperatively restrict vascular inflammation and atherosclerosis. *Cell Death Dis.* (2019) 10:365. doi: 10.1038/s41419-019-1599-9
44. Sun C, Alkhoury K, Wang YI, Foster GA, Radecke CE, Tam K, et al. IRF-1 and miRNA126 modulate VCAM-1 expression in response to a high-fat meal. *Circ Res.* (2012) 111:1054–64. doi: 10.1161/CIRCRESAHA.112.270314
45. Schober A, Nazari-Jahantigh M, Wei Y, Bidzhekov K, Gremse F, Grommes J, et al. MicroRNA-126-5p promotes endothelial proliferation and limits atherosclerosis by suppressing Dlk1. *Nat Med.* (2014) 20:368–76. doi: 10.1038/nm.3487
46. Holdt LM, Beutner F, Scholz M, Gielen S, Gabel G, Bergert H, et al. ANRIL expression is associated with atherosclerosis risk at chromosome 9p21. *Arterioscler Thromb Vasc Biol.* (2010) 30:620–7. doi: 10.1161/ATVBAHA.109.196832
47. Holdt LM, Stahringer A, Sass K, Pichler G, Kulak NA, Wilfert W, et al. Circular non-coding RNA ANRIL modulates ribosomal RNA maturation and atherosclerosis in humans. *Nat Commun.* (2016) 7:12429. doi: 10.1038/ncomms12429
48. Fang J, Pan Z, Wang D, Lv J, Dong Y, Xu R, et al. Multiple Non-coding ANRIL Transcripts Are Associated with Risk of Coronary Artery Disease: a Promising Circulating Biomarker. *J Cardiovasc Transl Res.* (2021) 14:229–37. doi: 10.1007/s12265-020-10053-0
49. Hall IF, Climent M, Quintavalle M, Farina FM, Schorn T, Zani S, et al. Circ_Lrp6, a Circular RNA enriched in vascular smooth muscle cells. Acts as a sponge regulating miRNA-145 function. *Circ Res.* (2019) 124:498–510. doi: 10.1161/CIRCRESAHA.118.314240
50. Weiser-Evans MCM. Smooth muscle differentiation control comes full circle: the circular noncoding RNA, circActa2, functions as a miRNA sponge to fine-tune alpha-SMA expression. *Circ Res.* (2017) 121:591–3. doi: 10.1161/CIRCRESAHA.117.311722
51. Ballantyne MD, Pinel K, Dakin R, Vesey AT, Diver L, Mackenzie R, et al. Smooth muscle enriched long noncoding RNA(SMILR) regulates cell proliferation. *Circulation.* (2016) 133:2050–65. doi: 10.1161/CIRCULATIONAHA.115.021019
52. Mahmoud AD, Ballantyne MD, Miscianinov V, Pinel K, Hung J, Scanlon JP, et al. The human-specific and smooth muscle cell-enriched LncRNA SMILR promotes proliferation by regulating mitotic CENPF mRNA and drives cell-cycle progression which can be targeted to limit vascular remodeling. *Circ Res.* (2019) 125:535–51. doi: 10.1161/CIRCRESAHA.119.314876
53. Dong K, Shen J, He X, Hu G, Wang L, Osman I, et al. CARMN is an evolutionarily conserved smooth muscle cell-specific LncRNA that maintains contractile phenotype by binding myocardin. *Circulation.* (2021) 144:1856–75. doi: 10.1161/CIRCULATIONAHA.121.055949
54. Vacante F, Rodor J, Lalwani MK, Mahmoud AD, Bennett M, De Pace AL, et al. CARMN loss regulates smooth muscle cells and accelerates atherosclerosis in mice. *Circ Res.* (2021) 128:1258–75. doi: 10.1161/CIRCRESAHA.120.318688
55. Zhao H, Wen G, Huang Y, Yu X, Chen Q, Afzal TA, et al. MicroRNA-22 regulates smooth muscle cell differentiation from stem cells by targeting methyl CpG-binding protein 2. *Arterioscler Thromb Vasc Biol.* (2015) 35:918–29. doi: 10.1161/ATVBAHA.114.305212
56. Yang F, Chen Q, He S, Yang M, Maguire EM, An W, et al. miR-22 is a novel mediator of vascular smooth muscle cell phenotypic modulation and neointima formation. *Circulation.* (2018) 137:1824–41. doi: 10.1161/CIRCULATIONAHA.117.027799
57. Farina FM, Hall IF, Serio S, Zani S, Climent M, Salvarani N, et al. miR-128-3p is a novel regulator of vascular smooth muscle cell phenotypic switch and vascular diseases. *Circ Res.* (2020) 126:e120–35. doi: 10.1161/CIRCRESAHA.120.316489
58. Cordes KR, Sheehy NT, White MP, Berry EC, Morton SU, Muth AN, et al. miR-145 and miR-143 regulate smooth muscle cell fate and plasticity. *Nature.* (2009) 460:705–10. doi: 10.1038/nature08195
59. Fichtlscherer S, De Rosa S, Fox H, Schwietz T, Fischer A, Liebetrau C, et al. Circulating microRNAs in patients with coronary artery disease. *Circ Res.* (2010) 107:677–84. doi: 10.1161/CIRCRESAHA.109.215566
60. Lovren F, Pan Y, Quan A, Singh KK, Shukla PC, Gupta N, et al. MicroRNA-145 targeted therapy reduces atherosclerosis. *Circulation.* (2012) 126:S81–90. doi: 10.1161/CIRCULATIONAHA.111.084186
61. Chin DD, Poon C, Wang J, Joo J, Ong V, Jiang Z, et al. miR-145 micelles mitigate atherosclerosis by modulating vascular smooth muscle cell phenotype. *Biomaterials.* (2021) 273:120810. doi: 10.1016/j.biomaterials.2021.120810
62. Gast M, Schroen B, Voigt A, Haas J, Kuehl U, Lassner D, et al. Long noncoding RNA MALAT1-derived mascRNA is involved in cardiovascular innate immunity. *J Mol Cell Biol.* (2016) 8:178–81. doi: 10.1093/jmcb/mjw003
63. Gast M, Rauch BH, Nakagawa S, Haghikia A, Jasina A, Haas J, et al. Immune system-mediated atherosclerosis caused by deficiency of long non-coding RNA MALAT1 in ApoE-/-mice. *Cardiovasc Res.* (2019) 115:302–14. doi: 10.1093/cvr/cvy202
64. Cremer S, Michalik KM, Fischer A, Pfisterer L, Jae N, Winter C, et al. Hematopoietic Deficiency of the Long Noncoding RNA MALAT1 Promotes Atherosclerosis and Plaque Inflammation. *Circulation.* (2019) 139:1320–34. doi: 10.1161/CIRCULATIONAHA.117.029015
65. Wang B, Tontonoz P. Liver X receptors in lipid signalling and membrane homeostasis. *Nat Rev Endocrinol.* (2018) 14:452–63. doi: 10.1038/s41574-018-0037-x
66. Sallam T, Jones M, Thomas BJ, Wu X, Gilliland T, Qian K, et al. Transcriptional regulation of macrophage cholesterol efflux and atherogenesis by a long noncoding RNA. *Nat Med.* (2018) 24:304–12. doi: 10.1038/nm.4479
67. Mazan-Mamczarz K, Galban S, Lopez de. Silanes I, Martindale JL, Atasoy U, Keene JD, et al. RNA-binding protein HuR enhances p53 translation in response to ultraviolet light irradiation. *Proc Natl Acad Sci U S A.* (2003) 100:8354–9. doi: 10.1073/pnas.1432104100

68. Simion V, Zhou H, Haemmig S, Pierce JB, Mendes S, Tesmenitsky Y, et al. A macrophage-specific lncRNA regulates apoptosis and atherosclerosis by tethering HuR in the nucleus. *Nat Commun.* (2020) 11:6135. doi: 10.1038/s41467-020-19664-2
69. Fabunmi RP, Sukhova GK, Sugiyama S, Libby P. Expression of tissue inhibitor of metalloproteinases-3 in human atheroma and regulation in lesion-associated cells: a potential protective mechanism in plaque stability. *Circ Res.* (1998) 83:270–8. doi: 10.1161/01.RES.83.3.270
70. Di Gregoli K, Mohamad Anuar NN, Bianco R, White SJ, Newby AC, George SJ, et al. MicroRNA-181b controls atherosclerosis and aneurysms through regulation of TIMP-3 and elastin. *Circ Res.* (2017) 120:49–65. doi: 10.1161/CIRCRESAHA.116.309321
71. Xu Y, Zalzala M, Xu J, Li Y, Yin L, Zhang Y, et al. A metabolic stress-inducible miR-34a-HNF4alpha pathway regulates lipid and lipoprotein metabolism. *Nat Commun.* (2015) 6:7466. doi: 10.1038/ncomms8466
72. Badi I, Mancinelli L, Polizzotto A, Ferri D, Zeni F, Burba I, et al. miR-34a promotes vascular smooth muscle cell calcification by downregulating SIRT1(Sirtuin 1) and Axl(AXL Receptor Tyrosine Kinase) arterioscler. *Thromb Vasc Biol.* (2018) 38:2079–90. doi: 10.1161/ATVBAHA.118.311298
73. Xu Y, Xu Y, Zhu Y, Sun H, Juguilon C, Li F, et al. Macrophage miR-34a is a key regulator of cholesterol efflux and atherosclerosis. *Mol Ther.* (2020) 28:202–16. doi: 10.1016/j.ymthe.2019.09.008
74. Ceolotto G, Giannella A, Albiero M, Kuppusamy M, Radu C, Simioni P, et al. miR-30c-5p regulates macrophage-mediated inflammation and pro-atherosclerosis pathways. *Cardiovasc Res.* (2017) 113:1627–38. doi: 10.1093/cvr/cvx157
75. Rayner KJ, Suarez Y, Davalos A, Parathath S, Fitzgerald ML, Tamehiro N, et al. Fernandez-Hernando C, MiR-33 contributes to the regulation of cholesterol homeostasis. *Science.* (2010) 328:1570–3. doi: 10.1126/science.1189862
76. Rayner KJ, Sheedy FJ, Esau CC, Hussain FN, Temel RE, Parathath S, et al. Antagonism of miR-33 in mice promotes reverse cholesterol transport and regression of atherosclerosis. *J Clin Invest.* (2011) 121:2921–31. doi: 10.1172/JCI57275
77. Karunakaran D, Thrush AB, Nguyen MA, Richards L, Geoffrion M, Singaravelu R, et al. Macrophage mitochondrial energy status regulates cholesterol efflux and is enhanced by Anti-miR33 in atherosclerosis. *Circ Res.* (2015) 117:266–78. doi: 10.1161/CIRCRESAHA.117.305624
78. Ouimet M, Ediriweera HN, Gundra UM, Sheedy FJ, Ramkhelawon B, Hutchison SB, et al. MicroRNA-33-dependent regulation of macrophage metabolism directs immune cell polarization in atherosclerosis. *J Clin Invest.* (2015) 125:4334–48. doi: 10.1172/JCI81676
79. Ramirez CM, Rotllan N, Vlassov AV, Davalos A, Li M, Goedeke L, et al. Control of cholesterol metabolism and plasma high-density lipoprotein levels by microRNA-144. *Circ Res.* (2013) 112:1592–601. doi: 10.1161/CIRCRESAHA.112.300626
80. de Aguiar Vallim TQ, Tarling EJ, Kim T, Civelek M, Baldan A, Esau C, et al. MicroRNA-144 regulates hepatic ATP binding cassette transporter A1 and plasma high-density lipoprotein after activation of the nuclear receptor farnesoid X receptor. *Circ Res.* (2013) 112:1602–12. doi: 10.1161/CIRCRESAHA.112.300648
81. Hennessy EJ, van Solingen C, Scacalossi KR, Ouimet M, Afonso MS, Prins J, et al. The long noncoding RNA CHROME regulates cholesterol homeostasis in primate. *Nat Metab.* (2019) 1:98–110. doi: 10.1038/s42255-018-0004-9
82. Bushati N, Cohen SM. microRNA functions. *Annu Rev Cell Dev Biol.* (2007) 23:175–205. doi: 10.1146/annurev.cellbio.23.090506.123406
83. Tsai MC, Manor O, Wan Y, Mosammaparast N, Wang JK, Lan F, et al. Long noncoding RNA as modular scaffold of histone modification complexes. *Science.* (2010) 329:689–93. doi: 10.1126/science.1192002
84. Wang KC, Chang HY. Molecular mechanisms of long noncoding RNAs. *Mol Cell.* (2011) 43:904–14. doi: 10.1016/j.molcel.2011.08.018
85. Wilusz JE. A 360 degrees view of circular RNAs: from biogenesis to functions. *Wiley Interdiscip Rev RNA.* (2018) 9:e1478. doi: 10.1002/wrna.1478
86. Jiang F, Chen Q, Wang W, Ling Y, Yan Y, Xia P. Hepatocyte-derived extracellular vesicles promote endothelial inflammation and atherogenesis via microRNA-1. *J Hepatol.* (2020) 72:156–66. doi: 10.1016/j.jhep.2019.09.014
87. Fasolo F, Di Gregoli K, Maegdefessel L, Johnson JL. Non-coding RNAs in cardiovascular cell biology and atherosclerosis. *Cardiovasc Res.* (2019) 115:1732–56. doi: 10.1093/cvr/cvz203
88. Zhou LY, Qin Z, Zhu YH, He ZY, Xu T. Current RNA-based therapeutics in clinical trials. *Curr Gene Ther.* (2019) 19:172–96. doi: 10.2174/1566523219666190719100526
89. Dammes N, Peer D. Paving the road for RNA therapeutics. *Trends Pharmacol Sci.* (2020) 41:755–75. doi: 10.1016/j.tips.2020.08.004
90. Rinaldi C, Wood MJA. Antisense oligonucleotides: the next frontier for treatment of neurological disorders. *Nat Rev Neurol.* (2018) 14:9–21. doi: 10.1038/nrneurol.2017.148
91. Lucas T, Bonauer A, Dimmeler S. RNA therapeutics in cardiovascular disease. *Circ Res.* (2018) 123:205–20. doi: 10.1161/CIRCRESAHA.117.311311
92. Saw PE, Song EW. siRNA therapeutics: a clinical reality. *Sci China Life Sci.* (2020) 63:485–500. doi: 10.1007/s11427-018-9438-y
93. Fang Y, Davies PF. Site-specific microRNA-92a regulation of Kruppel-like factors 4 and 2 in atherosusceptible endothelium. *Arterioscler Thromb Vasc Biol.* (2012) 32:979–87. doi: 10.1161/ATVBAHA.111.244053
94. Loyer X, Potteaux S, Vion AC, Guerin CL, Boulkroun S, Rautou PE, et al. Inhibition of microRNA-92a prevents endothelial dysfunction and atherosclerosis in mice. *Circ Res.* (2014) 114:434–43. doi: 10.1161/CIRCRESAHA.114.302213
95. Abplanalp WT, Fischer A, John D, Zeiher AM, Gosgnach W, Darville H, et al. Efficiency and target derepression of Anti-miR-92a: results of a first in human study. *Nucleic Acid Ther.* (2020) 30:335–45. doi: 10.1089/nat.2020.0871
96. Ruscica M, Zimetti F, Adorni MP, Sirtori CR, Lupo MG, Ferri N. Pharmacological aspects of ANGPTL3 and ANGPTL4 inhibitors: new therapeutic approaches for the treatment of atherogenic dyslipidemia. *Pharmacol Res.* (2020) 153:104653. doi: 10.1016/j.phrs.2020.104653
97. Musunuru K, Pirruccello JP, Do R, Peloso GM, Guiducci C, Sougnez C, et al. Exome sequencing, ANGPTL3 mutations, and familial combined hypolipidemia. *N Engl J Med.* (2010) 363:2220–7. doi: 10.1056/NEJMoa1002926
98. Stitziel NO, Khera AV, Wang X, Bierhals AJ, Vourakis AC, Sperry AE, et al. ANGPTL3 deficiency and protection against coronary artery disease. *J Am Coll Cardiol.* (2017) 69:2054–63. doi: 10.1016/j.jacc.2017.02.030
99. Graham MJ, Lee RG, Brandt TA, Tai LJ, Fu W, Peralta R, et al. Cardiovascular and metabolic effects of ANGPTL3 antisense oligonucleotides. *N Engl J Med.* (2017) 377:222–32. doi: 10.1056/NEJMoa1701329
100. Norata GD, Tsimikas S, Pirillo A, Catapano AL. Apolipoprotein C-III. From pathophysiology to pharmacology. *Trends Pharmacol Sci.* (2015) 36:675–87. doi: 10.1016/j.tips.2015.07.001
101. Tg and Hdl Working Group of the Exome Sequencing Project NHL, Blood I, Crosby J, Peloso GM, Auer PL, Crosslin DR, et al. Loss-of-function mutations in APOC3, triglycerides, and coronary disease. *N Engl J Med.* (2014) 371:22–31. doi: 10.1056/NEJMoa1307095
102. Alexander VJ, Xia S, Hurh E, Hughes SG, O'Dea L, Geary RS, et al. N-acetyl galactosamine-conjugated antisense drug to APOC3 mRNA, triglycerides and atherogenic lipoprotein levels. *Eur Heart J.* (2019) 40:2785–96. doi: 10.1093/eurheartj/ehz209
103. Horton JD, Cohen JC, Hobbs HH. Molecular biology of PCSK9: its role in LDL metabolism. *Trends Biochem Sci.* (2007) 32:71–7. doi: 10.1016/j.tibs.2006.12.008
104. Abifadel M, Varret M, Rabes JP, Allard D, Ouguerram K, Devillers M, et al. Mutations in PCSK9 cause autosomal dominant hypercholesterolemia. *Nat Genet.* (2003) 34:154–6. doi: 10.1038/ng1161
105. Cohen J, Pertsemlidis A, Kotowski IK, Graham R, Garcia CK, Hobbs HH. Low LDL cholesterol in individuals of African descent resulting from frequent nonsense mutations in PCSK9. *Nat Genet.* (2005) 37:161–5. doi: 10.1038/ng1509
106. Willer CJ, Sanna S, Jackson AU, Scuteri A, Bonnycastle LL, Clarke R, et al. Newly identified loci that influence lipid concentrations and risk of coronary artery disease. *Nat Genet.* (2008) 40:161–9. doi: 10.1038/ng.76
107. Sabatine MS, Giugliano RP, Keech AC, Honarpour N, Wiviott SD, Murphy SA, et al. Investigators. Evolocumab and clinical outcomes in

patients with cardiovascular disease. *N Engl J Med.* (2017) 376:1713–22. doi: 10.1056/NEJMoa1615664
108. Schwartz GG, Steg PG, Szarek M, Bhatt DL, Bittner VA, Diaz R, et al. Committees OO, Investigators. Alirocumab and cardiovascular outcomes after acute coronary syndrome. *N Engl J Med.* (2018) 379:2097–107. doi: 10.1056/NEJMoa1801174
109. Katzmann JL, Gouni-Berthold I, Laufs U. PCSK9 inhibition: insights from clinical trials and future prospects. *Front Physiol.* (2020) 11:595819. doi: 10.3389/fphys.2020.595819
110. Ray KK, Wright RS, Kallend D, Koenig W, Leiter LA, Raal FJ, et al. Two Phase 3 trials of inclisiran in patients with elevated LDL cholesterol. *N Engl J Med.* (2020) 382:1507–19. doi: 10.1056/NEJMoa1912387
111. Chen W, Schilperoort M, Cao Y, Shi J, Tabas I, Tao W, Macrophage-targeted nanomedicine for the diagnosis and treatment of atherosclerosis. *Nat Rev Cardiol.* (2021) 19:228–49. doi: 10.1038/s41569-021-00629-x
112. Lobatto ME, Fuster V, Fayad ZA, Mulder WJ. Perspectives and opportunities for nanomedicine in the management of atherosclerosis. *Nat Rev Drug Discov.* (2011) 10:835–52. doi: 10.1038/nrd3578
113. Zia A, Wu Y, Nguyen T, Wang X, Peter K, Ta HT. The choice of targets and ligands for site-specific delivery of nanomedicine to atherosclerosis. *Cardiovasc Res.* (2020) 116:2055–68. doi: 10.1093/cvr/cvaa047
114. Sager HB, Dutta P, Dahlman JE, Hulsmans M, Courties G, Sun Y, et al. Nahrendorf M, RNAi targeting multiple cell adhesion molecules reduces immune cell recruitment and vascular inflammation after myocardial infarction. *Sci Transl Med.* (2016) 8:342ra80. doi: 10.1126/scitranslmed.aaf1435
115. Zimmermann TS, Lee AC, Akinc A, Bramlage B, Bumcrot D, Fedoruk MN, et al. RNAi-mediated gene silencing in non-human primates. *Nature.* (2006) 441:111–4. doi: 10.1038/nature04688

Conflict of Interest: The authors declare that the research was conducted in the absence of any commercial or financial relationships that could be construed as a potential conflict of interest.

Publisher's Note: All claims expressed in this article are solely those of the authors and do not necessarily represent those of their affiliated organizations, or those of the publisher, the editors and the reviewers. Any product that may be evaluated in this article, or claim that may be made by its manufacturer, is not guaranteed or endorsed by the publisher.

frontiers | Frontiers in Cardiovascular Medicine

REVIEW
published: 19 May 2022
doi: 10.3389/fcvm.2022.909480

Role of Catestatin in the Cardiovascular System and Metabolic Disorders

Ewa Zalewska, Piotr Kmieć and Krzysztof Sworczak*

Department of Endocrinology and Internal Medicine, Medical University of Gdansk, Gdansk, Poland

Catestatin is a multifunctional peptide that is involved in the regulation of the cardiovascular and immune systems as well as metabolic homeostatis. It mitigates detrimental, excessive activity of the sympathetic nervous system by inhibiting catecholamine secretion. Based on *in vitro* and *in vivo* studies, catestatin was shown to reduce adipose tissue, inhibit inflammatory response, prevent macrophage-driven atherosclerosis, and regulate cytokine production and release. Clinical studies indicate that catestatin may influence the processes leading to hypertension, affect the course of coronary artery diseases and heart failure. This review presents up-to-date research on catestatin with a particular emphasis on cardiovascular diseases based on a literature search.

Keywords: catestatin, cardiovascular system, hypertension, heart failure, coronary artery disease, immunometabolism, metabolic disorder

OPEN ACCESS

Edited by:
Jian Shi,
University of Leeds, United Kingdom

Reviewed by:
Teresa Pasqua,
University of Calabria, Italy
Geert Van Den Bogaart,
University of Groningen, Netherlands

****Correspondence:***
Piotr Kmieć
piotr.kmiec@gumed.edu.pl

Specialty section:
This article was submitted to Cardiovascular Metabolism, a section of the journal Frontiers in Cardiovascular Medicine

Received: *31 March 2022*
Accepted: *25 April 2022*
Published: *19 May 2022*

Citation:
Zalewska E, Kmieć P and Sworczak K (2022) Role of Catestatin in the Cardiovascular System and Metabolic Disorders. Front. Cardiovasc. Med. 9:909480. doi: 10.3389/fcvm.2022.909480

INTRODUCTION

The sympathetic nervous system is crucial in preserving homeostasis in humans. However, its excessive activity has been recognized to underlie pathologic processes of many cardiovascular diseases (CVDs), which are the leading cause of death globally (1). Among others, upregulated sympathetic nervous system activity has been associated with hypertension (HT), adverse myocardial remodeling, arrhythmias, sudden cardiac death, and overall poor prognosis in patients with heart failure (HF) (2).

Basal and reflex control of the sympathetic activity associated with cardiovascular function occurs in the rostral ventrolateral medulla (3). It sends catecholaminergic projections to the sympathetic preganglionic neurons of the spinal cord. In turn, preganglionic neurons release acetylcholine to activate postganglionic neurons and chromaffin cells of the adrenal medulla, which synthesize and secrete catecholamines (CAs): norepinephrine and epinephrine (stored in sufficient quantities within the cells, which is the reason for a positive chromaffin reaction, and, hence, their name) (3, 4). CAs target α- and β-adrenergic receptors, a family of G protein-coupled receptors. Adrenoceptors are divided into α1, α2, β1, β2, and β3 subtypes. In the smooth muscle cells of blood vessels, there are mainly α1-adrenergic receptors, coupled to stimulatory Gq proteins, which induce constriction by activating phospholipase C. In the heart, the predominant receptor subtype β1 activates the Gs-adenylyl cyclase – adenosine monophosphate – protein kinase A signaling cascade to induce positive inotropic and chronotropic effects (5). α2 receptors are coupled to inhibitory Gi proteins that inactivate adenylyl cyclase and are mainly found in the central nervous system, where their activation lowers arterial blood pressure (BP) (5).

In 1965, Banks and Helle reported that CA secretion from chromaffin granules of the adrenal medulla is associated with the release of soluble proteins (6). In July 1967, Blaschko's group coined the term "chromogranin A" (CgA) for the major component of these proteins (7, 8). In 1988, Simon et al. reported for the first time that proteolytic hydrolysis of CgA, obtained from cultured bovine adrenal medullary chromaffin cells, generated a peptide product that is capable of inhibiting CAs release, a promising and novel mechanism for counteracting the sympathetic outflow (9, 10). However, the exact identity of this functional peptide remained elusive until 1997, when Mahata et al. synthesized 15 peptides spanning ∼80% of the entire CgA molecule and demonstrated that only one, bovine $CgA_{344-364}$ [RSMRLSFRARGYGFRGPGLQL], inhibited CA secretion induced by nicotine (11). They named it "catestatin" (Cts) due to its high capacity to suppress the release of CAs (11).

Cts was initially considered a regulatory peptide that inhibits CA secretion by acting as a noncompetitive mediator of the nicotinic cholinergic stimulation of chromaffin cells and sympathetic neurite outgrowth (11, 12). Further studies showed that Cts inhibits CA release also due to adenylate cyclase-activating polypeptide stimulation and regulates dense core vesicle quanta (13) (**Figure 1**). Moreover, Cts has emerged as a pleiotropic peptide, which – among others – is involved in the regulation of the cardiovascular and immune system, as well as metabolic homeostasis (14, 17, 25–27).

This review presents up-to-date research on the role of Cts in the cardiovascular system and metabolic disorders contributing to CVDs, and Cts as a putative clinical biomarker. It is based on an electronic literature search of PubMed database performed April 20, 2022, using the key term 'catestatin', which yielded 235 results. Papers were included based on screening of titles and abstracts.

CATESTATIN BIOLOGY

Cts (human $CgA_{352-372}$, bovine $CgA_{344-364}$, and rat $CgA_{367-387}$) is a neuroendocrine peptide that is derived from the proteolytic cleavage of its precursor compound CgA. Human chromogranin A (hCgA) consists of nine dibasic sites and is cleaved by prohormone convertases, namely, cathepsin L, plasmin, and kallikrein, which generates: 1) Cts, which is a 21-amino acid, hydrophobic peptide derived from hCgA's C terminal fragment, 2) a dysglycemic peptide pancreastatin (hCgA250–301), 3) a vasodilating, antiadrenergic, and antiangiogenic peptide vasostatin-1 (hCgA1–76), 4) a peptide that acts as an antigen for diabetogenic CD4+ T-cell clones WE14 (hCgA324–337), and, 5) a proadrenergic peptide serpinin (hCgA411–436) (15).

Abbreviations: Akt, Protein kinase B; AMI, acute myocardial infarction; BP, blood pressure; Ca^{2+}, calcium ions; CAD, coronary artery disease; CA, catecholamine; CgA, Chromogranin A; Cts-KO, catestatin knockout; CVD, cardiovascular disease; Chga-KO, Chromogranin knockout; Cts, catestatin; hCgA, human CgA; HF, heart failure; HT, hypertension; I/R injury, ischemia/reperfusion injury; nAChR, nicotinic acetylcholine receptor; NO, nitric oxide; nNOS, neuronal nitric oxide synthase; NYHA, New York Heart Association; OSA, obstructive sleep apnea; PMNs, Polymorphonuclear neutrophils; WT, wild type.

Cts includes a sequence [SSMKLSFRARAYGFRGPGPQL] that is highly conserved across various species and is flanked by proteolytic cleavage sites (11, 28). Five single-nucleotide polymorphisms have been identified in the hCgA gene *(CHGA)* region expressing Cts: Gly364Ser (rs9658667), Pro370Leu (rs965868), Arg374Gln (rs9658669) (29), Tyr363Tyr (rs9658666), and Gly367Val (rs200576557) (15, 30, 31). Intriguingly, a genome-wide association study identified two loci that affect Cts concentrations in regions that include genes encoding kallikrein and Factor XII; these enzymes participating in a proteolytic cascade (Factor XII activates prokallikrein to kallikrein, which activtes FXII) were shown to generate active compounds from chromogranin A and B cleavage *in vivo* and *in vitro* (32). In particular, kallikrein produced a 12-amino-acid CgA-fragment (CgA361-372) with preserved biological activity of 21-amino-acid Cts (32).

Apart from limiting CA secretion, Cts is a potent inhibitor of the release of other chromaffin cell cotransmitters, including neuropeptide Y, adenosine triphosphate, and CgA; it is widely distributed in secretory granules of the chromaffin cells, diffuse neuroendocrine system, neuronal cells, bone-marrow derived cells, the auditory system, and the heart (20, 24, 33, 34) (**Figure 1**). In the latter, processing of CgA can be carried out by extracellular proteases on both cardiomyocyte cell membrane and in the extracellular matrix (33, 35). In a rat model, it was shown that the heart generates intracardiac CgA fragments, including locally derived Cts, in response to hemodynamic and excitatory challenges (36). Moreover, recently, a CgA1-373 fragment that encompasses the Cts domain was found to elicit direct cardiac effects both *in vitro* and *ex vivo* (37).

CATESTATIN AND REGULATION OF BLOOD PRESSURE

In vitro and *in vivo* Animal Studies

In vitro, it was shown Cts binds to α, β, δ, and γ subunits of nicotinic acetylcholine receptors (nAChR) with a high affinity binding site on the β subunit near the membrane surface, which blocks sodium ions' uptake, thus inhibiting membrane depolarization, and blocking the influx of calcium ions (Ca^{2+}) through voltage-gated calcium channels (38, 39). Inhibition of Ca^{2+} influx suppresses both CA release by exocytosis (all-or-none secretion) and *CHGA* transcription through a pathway involving the activation of protein kinase C and mitogen-activated protein kinase (40) (**Figure 1**).

Human Cts polymorphic variants were shown to exhibit varying potency of nAChR inhibition *in vitro* using a rat pheochromocytoma cell line and the human receptor (30, 41, 42). One should bear in mind that lower potency of a Cts variant in this respect does not necessarily translate to higher plasma CAs, since in such a case lower desensitization to CA secretion occurs (i.e., an effect due to repeated exposure of the nAChR to Cts). Further, since Cts blood-lowering effect depends partly on the release of nitric oxide (NO), human Cts Gly364Ser variant (see Clinical Studies) was shown to display lower NO-triggering and

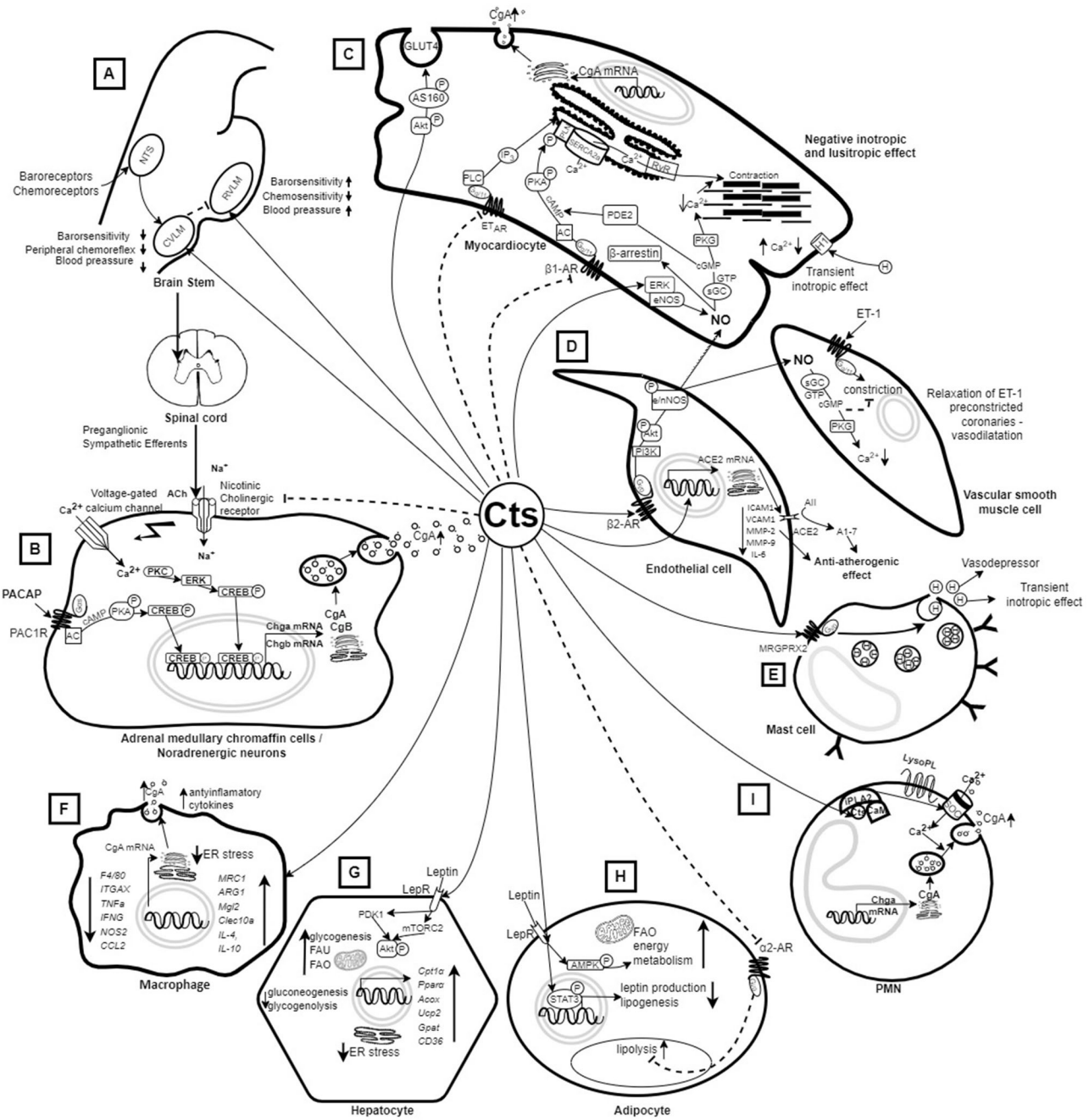

FIGURE 1 | Mechanism of action of catestatin based on *in vitro* and *in vivo* animal studies. **(A)** Injection of Cts into the CVLM or the central amygdala (not shown) of rats decreases sympathetic barosensitivity and attenuates peripheral chemoreflex with consequent hypotension. On the other hand, injection of Cts into the RVLM increases barosensitivity and attenuates chemosensitivity with consequent elevation of blood pressure (14). **(B)** Cts inhibits CA release by binding to nicotinic acetylcholine receptors that block Na^+ uptake (15) as well as due to PACAP stimulation (13). **(C)** Cts inhibits the PKA/PLN signaling pathway and induces NO synthesis in myocardiocytes, and the released NO reduces cellular Ca^{2+}, resulting in decreased cardiac contractility (16) and relaxation of ET-1 preconstricted coronaries (17). Cts also induces glucose uptake and Glut4 translocation (18). **(D)** Cts induces NO synthesis from endothelial cells, and activates ACE2, which has an anti-atherogenic effect (15, 16, 19). **(E)** Cts induces histamine release leading to vasodepression and transient inotropic effect in myocardiocytes (16). **(F)** Treatment with Cts results in polarization of macrophages toward an anti-inflammatory phenotype (20). Macrophages also produce Cts (21). **(G)** Cts up-regulates genes promoting fatty acid oxidation (22) and enhances insulin-induced Akt phosphorylation, which helps in overcoming ER stress and achieving insulin sensitivity (23). **(H)** Cts promotes lipid flux from adipose tissue toward the liver and lowers plasma leptin in Chga-KO mice leading to resensitization of leptin receptors (22). **(I)** PMNs are able to produce and secrete CgA-derived peptides, including Cts, which may penetrate into PMNs and activate the release of innate immune factors (24). A1-7, Angiotensin 1-7; AII, Angiotensin II; AC, Adenylyl cyclase; ACE2, activates angiotensin-converting enzyme-2; Ach, acetylcholine; Acox1, acyl-CoA oxidase 1;

(Continued)

FIGURE 1 | Akt, Protein kinase B; AMPK, AMP-activated protein kinase; ARG1, Arginase 1 gene; β1AR, β1 adrenergic receptors; β2AR, β2 adrenergic receptors; Ca^{2+}, calcium ions; cAMP, adenosine monophosphate; CAs, catecholamines; CCL2, C-C Motif Chemokine Ligand 2; CD36, cluster of differentiation 36; CgA, Chromogranin A; CgB, Chromogranin B; Chga-KO, Chromogranin knockout; cGMP, cyclic guanosine monophosphate; Cpt1α, Carnitine palmitoyltransferase 1α; CREB, cAMP response element-binding protein; Cts, catestatin; CVLM, caudal ventrolateral medulla; DNL, *de novo* lipogenesis; eNOS, endothelial nitric oxide synthase; ER, endoplasmic reticulum; ERK, extracellular signal-regulated kinas; ET-1, endothelin 1; ETAR, Endothelin receptor type A; ETBR, Endothelin receptor type B; FAO, Fatty acid oxidation; FAU, Fatty acid uptake; Gpat4, lipogenic gene glycerol-3-phosphate acyltransferase; GTP, guanosine-5' triphosphate; H, histamine; ICAM1, Intercellular Adhesion Molecule 1; IFNG, Interferon Gamma gene; IL-4, interleukin 4; IL-6, interleukin 6; IL-10, interleukin 10; iPLA2, calcium-independent phospholipase A2; ITGAX, Integrin Subunit Alpha X; LepR, Leptin receptor; LysoPL, lysophospholipids; MMP-2 Matrix Metallopeptidase 2; MMP-9, Matrix metallopeptidase 9; MRC1, Mannose Receptor C-Type 1 gene; MRGPRX2, Mas-Related G Protein-Coupled Receptor-X2; Na+, sodium; NO, nitric oxide; NOS2, Nitric Oxide Synthase 2; nNOS, neuronal nitric oxide synthase; NTS, Nucleus tractus solitarius; P, phosphor; PACAP, Pituitary adenylate cyclase-activating polypeptide; PAC1R, Pituitary adenylate cyclase-activating polypeptide receptor; PDE2, Phosphodiesterase 2; Pi3K, Phosphoinositide 3-kinase; PKA, Protein kinase A; PKC, protein kinase C; PKG, protein kinase G; PLN, phospholamban; PMNs, Polymorphonuclear neutrophils; Pparα, Peroxisome proliferator-activated receptor-α; RVLM, rostral ventrolateral medulla; RyR, Ryanodine receptor; sGC, soluble guanylyl cyclase; SERCA, Sarcoplasmic reticulum Ca-ATPase; SOC, Store-Operated Calcium Channels; STAT3, Signal Transducer And Activator Of Transcription 3; TAG, Triacylglycerols; TNFa, TNF alpha gene; Ucp2, uncoupling protein 2; VCAM1, vascular cell adhesion molecule 1. Dashed arrow – inhibition; continuous arrow – stimulation.

absent anti-adrenergic activity compared to wild-type peptide (WT-Cts) *in vitro* (31, 43).

This *in vitro* research concerning CA release suppression by Cts is supported by *in vivo* studies with genetically modified rodents. First, knockout of the CgA gene region encoding Cts (Cts-KO) in mice resulted in HT, left ventricular hypertrophy, and elevated CAs, yet, high BP was abated by intraperitoneal injection of exogenous Cts (21). Moreover, this strain exhibited marked cardiac and adrenal macrophage infiltration as well as increased proinflammatory cytokine levels, which may trigger CA release and escalate HT (21). Chlodronate depletion of macrophages, and bone marrow transfer between Cts-KO and WT mice demonstrated that immunosuppression of macrophages by Cts partly underlies its antihypertensive and anti-inflammatory effects (21).

Second, ablation of the CgA gene in another mouse model (Chga-KO) led to – among others – high baseline BP and elevated plasma CAs as well as exaggerated pressor and depressor responses to phenylephrine and sodium nitroprusside (44–46). Exogenous Cts replacement selectively diminished stress-induced increments in BP and HR (45) and restored the sensitivity of high-pressure baroreceptors, i.e., attenuation of both reflex tachycardia (due to sodium nitroprusside-induced hypotension) and reflex bradycardia (following phenylephrine-induced HT) occured (45). This indicates Cts functions efficiently as an antihypertensive peptide even under stressful conditions.

Third, in a genomically humanized mice strain expressing insufficient hCgA amounts, increased plasma CA levels as well as elevated systolic and diastolic BP were recorded in comparison to WT controls and a strain with sufficient hCgA expression (47).

However, Kennedy et al. showed Cts did not affect plasma norepinephrine levels and actually significantly (11-fold) increased those of epinephrine following electrical stimulation of male Sprague-Dawley rats, although it did reduce BP increases (even with anti-adrenergic pretreatment) (48). The possible explanation of these results, which contrast with findings from *in vitro* and Cst- and CgA-knockout studies, is that epinephrine release was compensatory to effects triggered by Cts in acute injury by electric stimulation, which could not have been observed *in vitro* (due to study limitations) and in KO mice owing to significant genetic alterations. Mitigation of pressor responses by Cts in the study by Kennedy et al. was attributed to histamine release: it increased 21-fold within 2 min of Cts injection, and the BP lowering effect was abolished by hydroxizine pretreatment, which was also the case for epinephrine elevation (48). Krüger et al. confirmed this hypothesis *in vitro*: Cts lead to histamine release from rat mast cells *via* a peptidergic pathway – by activating the G protein, because this effect was suppressed by the pertussis toxin, a Gi/Go inactivator (49) (**Figure 1**).

Furthermore, although plasma Cts concentrations gradually increased with the progression of HT in spontaneously hypertensive rats, exogenous Cts reduced HR (indicating anti-sympathetic activity) (50), as well as ameliorated vascular, renal and cardiac proliferation (51). *In vitro*, Cts was also reported to act as a potent inhibitor of isoproterenol- and endothelin-1-mediated activities in the frog (52) and rat heart (53). Angelone et al. showed that WT-Cts increased heart rate and decreased left ventricular pressure, rate-pressure product, and, both positive and negative left ventricular contractility. The authors suggested that these negative inotropic and lusitropic effects of WT-Cts may contribute to its hypotensive action (53) (**Figure 1**).

Concerning the central nervous system, Cts plays an important role in cardiorespiratory control (14). Gaede et al. showed that Cts antagonizes both nAChR and β-adrenergic receptors involved in cardiovascular regulation using urethane-anesthetized, vagotomized rats. Cts mitigated the hypertensive effect of nicotine and prevented increased splanchnic sympathetic activity caused by isoproterenol, a non-selective β adrenergic receptor agonist (54). The results of the study indicate Cts may affect BP levels in HT (54). Further, depending on the region of the medulla, Cts exerted sympathoexcitatory or cholinergic effects (3, 55, 56). Injection of Cts into the rostral ventrolateral medulla (a key site for BP control in the brain stem) resulted in increased barosensitivity and attenuation of chemosensitivity with consequent BP elevation (3). On the other hand, injection of Cts into the caudal ventrolateral medulla (55) and the central amygdala (56) (both contain inhibitory neurons of the rostral ventrolateral medulla) of rats resulted in decreased sympathetic barosensitivity and attenuation of the peripheral chemoreflex with consequent hypotension (**Figure 1**).

Effects of Cts based on *in vitro* and *in vivo* experimental studies are presented in **Figure 1**. In summary, Cts may inhibit CA release from chromaffin cells and noradrenergic neurons (11) and induces desensitization of CAs (57); it also exhibits a potent vasodilatory effect mediated – at least in part – by histamine release (48, 49). Moreover, negative inotropic and lusitropic effects of Cts may lower BP (53). Finally, Cts plays a role in central cardiorespiratory control (3, 56). Taken together, experimental studies point to Cts as a novel regulator of BP.

Clinical Studies

On the one hand, similarly to *in vivo* studies on rodents, it was shown that infusion of Cts into the dorsal hand veins of normotensive individuals, after pharmacologic venoconstriction with phenylephrine, resulted in a dose-dependent vasodilation, which was predominantly observed in female subjects (58). On the other, clinical studies generated controversies regarding the association between Cts levels and primary HT.

O'Connor et al. showed that normotensive offspring of patients with HT had significantly lower Cts concentrations compared to normotensive participants with a negative family history of HT (1.32 ± 0.038 vs. 1.5 ± 0.076 ng/mL, $p = 0.024$). Low plasma Cts levels predicted enhanced pressor response to a sympathoadrenal stressor (59). Therefore, reduced Cts levels were postulated to predispose to the development of HT, although categorization by BP status (normotensive vs. hypertensive) did not reveal differences in plasma Cts (1.36 ± 0.03 vs. 1.26 ± 0.06 ng/mL, $p = 0.27$) (59). In line with the result, Durakoglugil et al. showed that the difference in Cts concentrations between previously untreated hypertensive patients and healthy controls was insignificant after adjusting for age, gender, height, and weight (60). However, in another study by the O'Connor group, in a larger cohort (452 normotensives, 215 primary hypertensives), Cts was significantly reduced in HT patients (1.47 ± 0.06 1.26 vs. 1.26 ± 0.08; $p = 0.036$) (61). In contrast, Meng et al. showed that Cts was significantly higher in patients with essential HT than normal controls (1.19 ± 0.74 vs. 1.53 ± 0.72 ng/mL, $p < 0.01$) but found no correlation between Cts and the degree of HT (1.56 ± 0.59 vs. 1.42 ± 0.59 vs. 1.57 ± 0.76 ng/mL, $p > 0.05$) (62). They also suggested Cts level may serve as a prognostic factor for complications of HT, as patients with left ventricular hypertrophy had lower Cts-to-norepinephrine ratios than those without (3.63 ± 1.62 vs. 2.76 ± 0.86, $p < 0.01$) (62). In order to explain the contradictory results concerning Cts levels in normo- and HT, it was hypothesized that Cts decreases in prehypertension, however, sympathetic nervous system activity increases as HT progresses, which contributes to compensatory Cts elevation. Consequently, HT develops when elevated Cts no longer inhibits CA oversecretion (62).

Cts genetic variants exert varying effects on BP (16). The Gly364Ser variant was associated with lower diastolic BP than the Gly364Gly variant (wild type) in two Caucasian hypertensive groups of European ancestry and ca. 1.8% variance of population diastolic BP was attributable to Cts single nucleotide polymorphism (63). Conversely, in Asian populations, Ser-364 allele carriers displayed elevated systolic (up to ≈8 mm Hg; $p = 0.004$) and diastolic (up to ≈6 mm Hg; $p = 0.001$) BP (Indian) (31) as well as systolic BP, pulse pressure and arterial stiffness (Japanese) (64). In line with these, in a normotensive Indian population, Ser-364 allele carriers exhibited much lower plasma CA - by about 40% (consistent with its diminished nAChR desensitization-blocking effect *in vitro*) - than Gly364Gly carriers (30), yet, BP was similar in subjects with different alleles. These contradictory results underscore the necessity of genetic association studies for ethnically different populations.

Processing of CgA to Cts by endoproteolytic enzymes may be involved in the pathogenesis of HT. O'Connor et al. showed that CgA was increased by 117% ($p < 0.001$) in HT patients, whereas Cts reduced by 15% ($p = 0.036$), which suggests diminished conversion of CgA to Cts in HT (normotensives' CgA/Cts ratio of 4.5 ± 0.2 vs. 5.9 ± 0.4 in HT patients, $p = 0.005$) (61). Fung et al. demonstrated that in women compared to men higher plasma Cts (1.30 ± 0.033 vs. 1.14 ± 0.27 nM, $p < 0.001$) combined with lower CgA precursor concentrations (3.89 ± 0.15 vs. 4.65 ± 0.33 nM, $p = 0.006$) may be associated with decreased processing of CgA to Cts in the latter (female vs. male Cts/CgA ratio: 26.3 ± 0.006 vs. 23.1 ± 0.006), which predisposes to HT (58).

Moreover, Biswas et al. showed that *CHGA* variants undergo differential processing to produce Cts in the presence of the endoproteolytic enzyme plasmin (65). Their study indicates that less efficient processing of the Pro370Leu protein (product of one of *CHGA* variants) can contribute to the prevalence of CVDs (65).

CgA variants may also impact target organ damage in HT: black people suffering from end stage renal disease exhibit a common *CHGA* variant (3′-UTR C+87T), which decreased reporter gene expression and subsequently lead to lower Cts levels in this population (2.10 ± 0.88 vs. 3.23 ± 0.29 ng/mL, $p = 0.01$) (66).

Clinical studies concerning Cts in HT are presented in **Table 1**. To summarize, Cts was shown to decrease during prehypertension (59), however, the progression of elevated BP was associated with a compensatory increase in its concentration (62). Moreover, the development of HT may well be connected with diminished conversion of CgA to Cts (58, 61, 65) and depends on different variants of Cts exerting varying effects on BP (16, 63).

CARDIAC FUNCTION OF CATESTATIN

In vitro and *in vivo* Animal Studies

Cts induces NO synthesis from endothelial cells and cardiomyocytes (43, 53). In endothelial cells, NO is acquired from both: (1) the endothelin receptor B – endothelial nitric oxide synthase (eNOS) – NO, and (2) the protein kinase B (Akt) – eNOS/neuronal nitric oxide synthase (nNOS) – NO pathways. In cardiomyocytes, NO release results from the extracellular signal-regulated kinase – eNOS – NO pathway (53) (**Figure 1**). NO reduces inotropism and lusitropism of cardiomyocytes through various pathways (52, 53, 88, 89) (**Figure 1**). It was demonstrated *in vitro* using frog (52), eel (89), and rat (90) heart preparations that higher NO generation due to Cts ameliorates the Frank-Starling response, which is a compensatory mechanism to maintain adequate heart

TABLE 1 | Clinical studies concerning catestatin.

References	Study participants	Main results
	Catestatin and hypertension	
O'Connor et al. (59)	40 normotensives with positive HT family history, 176 normotensives without HT family history, 61 patients with HT	Offspring of HT patients had lower Cts than normotensives without HT family history: 1.32 ± 0.038 vs. 1.5 ± 0.076 ($p = 0.024$) Plasma Cts was not different in normotensives vs. hypertensives (1.36 ± 0.03 vs. 1.26 ± 0.06 ($p = 0.27$)
O'Connor et al. (61)	452 normotensives, 215 patients with HT	Cts was reduced by 15% in hypertensives patients ($p = 0.036$), whereas CgA was increased by 117% ($p < 0.001$); the ratio of CgA/Cts was thus increased by 31% ($p = 0.005$), implying decreased conversion of CgA to Cts in PH.
Salem et al. (66)	Black patients with HT and ESRD ($n = 150$) and black controls ($n = 58$)	ESRD patients had lower Cts: 2.10 ± 0.88 vs. 3.23 ± 0.29 ($p = 0.01$)
Meng et al. (62)	136 HT patients (109 with and 27 without LVH 27) and 61 healthy controls	Cts was higher in hypertensives vs. controls: 1.19 ± 0.74 vs. 1.53 ± 0.72 ($p < 0.01$) There was a non-significant trend toward lower Cts in HT patients with LVH than those without: 1.55 ± 0.7 vs. 1.4 ± 0.53 ($p > 0.05$).
	Catestatin and coronary artery disease	
Wang et al. (67)	50 STEMI patients and 25 non-CAD control patients	STEMI patients had lower plasma Cts on admission than controls: 16.5 ± 5.4 vs. 21.4 ± 6.4 ($p < 0.01$), increased on day 3 to 30.7 ± 12.2 ($p < 0.01$), and on day 7 decreased to levels below than admission (13.8 ± 5.3, $p < 0.01$) in MI
Meng et al. (68)	52 healthy controls 58 STEMI patients, 31 of whom were assessed by echocardiography 3 months later to reveal 7 cases with LVR and 24 without LVR	Plasma Cts on admission higher in patients with AMI than in controls: 1.00 (0.66–1.50) vs. 0.84 (0.56–1.17) ($p < 0.05$) Mean Cts higher on day 3: 1.12 (0.76–1.70) vs. 1.00 (0.66–1.50) ($p < 0.01$) and on day 7.: 1.32 (0.81–1.73) ng/ml vs. 1.00 (0.66–1.50) ($p < 0.01$) Patients with LVR 3 months after AMI vs. those without had higher Cts: -on admission: 2.02 (1.14–5.87) vs. 0.94 (0.39–1.66) ($p = 0.001$), -on day 3: 2.47 (1.10–5.95) vs. 1.16 (0.31–1.95) ($p = 0.006$), and, -on day 7 after STEMI: 3.08 (0.41–6.77) vs. 1.20 (0.30–3.73) ($p = 0.021$)
Liu et al. (69)	30 healthy controls; 15 SAP, 47 UAP, 22 NSTEMI, and 36 STEMI patients	Plasma Cts was higher in CAD patients than controls: 0.41 ± 0.14 vs. SAP patients: 0.72 ± 0.50 ($p < 0.05$) UAP patients 0.88 ± 0.58 ($p < 0.05$) NSTEMI patients 1.05 ± 0.48 ($p < 0.05$) STEMI patients 1.31 ± 0.91 (p < 0.05)
Pei et al. (70)	STEMI patients with MA ($n = 61$) STEMI patients without MA ($n = 64$)	Plasma Cts was higher in patients with STEMI complicated by MA compared with those without MA: 0.083 ± 0.011 vs. 0.076 ± 0.007 ($p < 0.001$)
Zhu et al. (71)	30 non-CAD controls (n = 30) 100 AMI patients including 74 with adverse events on follow-up and 26 without	Cts lower in MI patients on admission vs. controls: 16.7 ± 5.4 vs. 21.8 ± 6.3 ($p <0.0001$), higher on day 3 at 30.9 ± 12.1 ($p < 0.0001$ vs. admission), and again lower on day 7: 13.9 ± 5.2 ($p = 0.0003$ vs. admission) Cts on admission and day 3 in the adverse events group (19.4 ± 6.7 ng/ml, 44.6 ± 13.0, respectively) higher than in the non-adverse events group (15.8 ± 4.5 ($p = 0.003$), 26.1 ± 7.5 ($p < 0.0001$), respectively).
Xu et al. (72)	38 patients with CTO and 38 controls	Cts higher in CTO patients than in controls 1.97 ± 1.01 vs. 1.36 ± 0.97 ($p = 0.009$)
Zhu et al. (73)	72 STEMI patients and 30 control patients without CAD on imaging	Patients with Cts level above median at day 3 (28.71 ng/ml) developed worse ventricular function during the 65 months follow-up ($p < 0.0001$).
Xu et al. (74)	46 STEMI patients, 89, 35 control patients without CAD on imaging	Cts in patients with STEMI (0.80 ± 0.62) and UAP (0.99 ± 0.63) lower than in controls (1.38 ± 0.98; $p = 0.001$).
Kojima et al. (75)	25 CAD patients: 20 with AMI and 5 with UAP; controls: 20 non-CAD patients with mild hypertension and 13 healthy volunteers	Plasma Cts levels were lower in CAD patients (2*) than in non-CAD patients (4*; $p \leq 0.05$).
Chen et al. (19)	204 healthy volunteers 224 CAD patients	CAD patients had lower serum Cts than controls: 1.14 (1.05–1.24) vs. 2.15 (1.92–2.39); $p < 0.001$, and the levels decreased in a stepwise manner with increasing number of diseased vessels: 1.95 (1.83–2.07) vs. 1.57 (1.42–1.73) vs. 1.13 (1.00–1.27), $p <0.001$ (for 1, 2, and 3 vessels, respectively)
	Catestatin and heart failure	
Zhu et al. (76)	300 moderate to severe HF patients:−108 in stage A; 76 in Stage, 116 - Stage C	Cts decreased with higher HF stages and there was a significant difference between stage A and B: 21.29 ± 7.10 vs. 14.61 ± 4.69 ($p < 0.05$).
Liu et al. (77)	172 controls 228 HF patients in NYHA class I – IV	Plasma Cts increased with higher classes, NYHA class III and class IV patients had higher Cts levels than controls: 0.848 (0.664–1.260); 1.54 (0.856–2.432), respectively vs. 0.696 (0.504–0.883) ($p < 0.05$). NYHA class I and class II patients had similar Cts to controls: 0.612 (0.52 −0.844); 0.722 (0.532–1.112), respectively vs. 0.696 (0.504–0.883) ($p > 0.05$)

(Continued)

TABLE 1 | Continued

References	Study participants	Main results
Peng et al. (78)	Cohort of 202 HF patients followed-up for a median of 52.5 months: 143 survived, 59 died – 49 for cardiac causes	Plasma Cts was higher in non-survivors both for all and cardiac causes 1.06 (0.66–1.82) and 1.18 (0.69–1.83), respectively vs. 0.75 (0.58–1.12) in survivors ($p \leq 0.005$)
Wołowiec et al. (79)	Upon a follow-up of 24 months out of 52 HFrEF patients 11 reached the composite endpoint (CE) of unplanned hospitalization and all-cause death 24 healthy volunteers served as controls	Cts lower in HFrEF patients who reached a CE than in those who did not – both before and after exertion: 14.23 (11.05–15.82) vs. 16.86 (14.25–19.46) ($p = 0.03$) and 4.81 (2.20–6.25) vs. 7.82 (5.81–63.48) ($p = 0.002$), respectively; Cts in patients similar to controls: before exertion 15.95 (13.89–18.81) vs. 16.6 (14.75–22.20) ($p = 0.12$), after: 7.04 (4.97–11.08) vs. 9.26 (6.11–140.23) ($p = 0.13$)
Borovac et al. (80)	96 HF patients hospitalized due to an acute worsening of HF, 6 did not survive	Cts was significantly higher among non-survivors than survivors: 19.8 (9.9–28) vs. 5.6 (3.4–9.8) ($p < 0.001$)
	Catestatin and other diseases affecting the cardiovascular system	
Sun et al. (81)	330 controls; 329 hemodialysis patients followed-up for 36 months – 29 died for cardiac and 28 for non-cardiac causes	Cts higher in hemodialysis patients (1.9 ± 0.3) vs. controls (1.2 ± 0.2), $p < 0.001$ Cts higher (2.2 ± 0.1) in patients who died for cardiac causes than in survivors (1.8 ± 0.2) and non-cardiac death non-survivors (1.8 ± 0.3), $p < 0.001$
Izci et al. (82)	97 controls 160 APE patients: 72 with sPESI ≥ 1 and 88< 1	Plasma Cts higher in APE patients than controls: 27.3 ± 5.7 vs. 17.5 ± 6.1 ($p < 0.001$); Cts higher in patients with sPESI ≥ 1 than with sPESI < 1: 37.3 ± 6.1 vs. 24.2 ± 5.3 ($p < 0.001$)
Tüten et al. (83)	100 women with preeclampsia 100 women with uncomplicated pregnancy as controls.	Plasma Cts was significantly increased in the preeclampsia patients compared to the controls: 0.29 ± 0.096 vs. 0.183 ± 0.072 ($p < 0.001$)
Liu et al. (84)	260 healthy workers	Plasma CgA-to-catestatin ratio correlated with effort, reward (negatively), overcommittment, and efford-reward imbalance: $r = 0.218$, -0.249, 0.275, and 0.279, respectively, $p < 0.001$ for all
	Catestatin and metabolic syndrome	
Simunovic et al. (85)	92 obese subjects (BMI Z score >2), age 10-18; 39 controls	Lower plasma Cts concentrations in obese subjects compared to controls: 10.03 ± 5.05 vs. 13.13 ± 6.25 ($p = 0.004$); lower Cts in the subgroup of obese patients with MS: 9.02 ± 4.3 vs. 10.54 ± 5.36 vs. 13.13 ± 6.25 ($p = 0.008$). Cts negatively correlated with DBP ($r = -0.253$, $p = 0.014$), HOMA-IR ($r = -0.215$, $p = 0.037$) and hsCRP ($r = -0.208$, $p = 0.044$).
Kim et al. (86)	85 subjects with mild OSA, 26 with moderate-to-severe OSA, 102 were controls, mean age 7.7 ± 1.4 years	Children with OSA have reduced plasma Cts levels (Log Cts in moderate-to-severe OSA: 0.12 ± 0.22 vs. mild OSA: 0.23 ± 0.20 vs. controls: 0.28 ± 0.19; differences among three groups: $p < 0.01$). Cts levels were inversely correlated with AHI ($r = -0.226$; $p < 0.01$) and with mean arterial BP level ($r = -0.184$; $p < 0.05$).
Borovac et al. (87)	78 OSA patients; 51 controls	Plasma Cts higher in OSA patients compared to controls: 2.9 ± 1.2 vs. 1.5 ± 1.1 ($p < 0.001$). In OSA patients Cts correlated with neck circumference ($r = 0.318$, $p < 0.001$; $\beta = 0.384$, $p < 0.001$) and HDL cholesterol ($r = -0.320$, $p < 0.001$; $\beta = -0.344$, $p < 0.001$).

*Catestatin concentrations are given in ng/mL and the results are shown as median (interquartile range) or mean ± standard deviation; AHA, American Heart Association; AMI, acute myocardial infarction; APE, Acute pulmonary embolism; AWHF, acute worsening of heart failure; BP, blood preassure; CAD, coronary artery disease; CD, Crohn's disease; CE, composite endpoint including unplanned hospitalization and death for all causes; CPET, Cardiopulmonary Exercise Testing (6-minut walk test); Cts, catestatin; CTO, chronic total occlusions; DBP, diastolic blood pressure; ERI, effort, reward imbalance; ESRD, end stage renal disease; HDL, high-density lipoprotein; HF, heart failure; HFrEF, Heart Failure with Reduced Ejection Fraction; HOMA-IR, homeostatic model assessment of insulin resistance; hsCRP, high sensitivity C-reactive protein; HT, hypertension; IBD, inflammatory bowel diseases; LVH, left ventricular hypertrophy; LVR, left ventricular remodeling; MA, malignant arrhythmia; MS, metabolic syndrome; NSTEMI, non-ST segment elevation myocardial infarction; NYHA, New York Heart Association; OSA, obstructive sleep apnea; SAP, stable angina pectoris; STEMI, acute ST- segment elevation myocardial infarction; sPESI, simplified PESI; UAP, unstable angina pectoris; UC, ulcerative colitis. *Mean value (standard deviation was not provided).*

function in response to changes in venous return (90). Moreover, Cts exerts counterregulatory action against β-adrenergic and endothelin-1 stimulation pointing to Cts as a novel, beneficial cardiac modulator (53) (**Figure 1**).

In line with this research, *in vitro*, Cts attenuated norepinephrine-mediated hypertrophic responses in H9c2 cardiac myoblasts and at 10-25 nM signaling was moderated primarily by β1/2-adrenoceptors (91). Interestingly, Bassino et al. observed that a low (5 nM) WT-Cts concentration reduced β-adrenergic stimulation in bovine aortic endothelial cells, although it exhibited no significant effect on myocardial contractility. Higher concentrations (10–50 nM) of Cts induced a transient positive inotropic effect followed by a negative antiadrenergic effect (43). The transient positive effect was probably related to histamine release from mast cells induced by Cts. Histamine exerts a positive inotropic effect on rat ventricular myocardium and H1 histamine receptor antagonist mepyramine blocked the positive effect induced by higher doses of WT-Cts (10 nM). In turn, WT-Cts at a minimal concentration (5 nM) reduced isoproterenol-induced enhancement of papillary muscle contractility via H1 receptor activation without altering basal contractile ability (43).

Several studies point at a cardioprotective role of Cts in ischemia/reperfusion (I/R) injury of the heart in rodent models.

It was apparent for Cts pretreatment (25 nM, 50 nM, and 100 nM infused for 15 min before ischemia) (92) and chronic administration of Cts after MI (0.25 mg/kg/12 h injection intraperitoneally 24 h after AMI for 28 days) (67). Further, infusion of a Cts dose of 75 nM for 20 min at the beginning of reperfusion significantly reduced infarct size, limited post-ischemic contracture, and improved recovery of developed left ventricular pressure (93–96). Protection due to Cts in I/R-injured myocardium was related to salvage of oxidative-stress-induced apoptosis by activation of the β2-adrenergic receptor, and PKB/Akt pathway (96). It must be highlighted that infusion of a higher dose WT-Cts (100 nM) for 120 min during reperfusion caused deleterious effects and did not activate Akt (97). Interestingly, the Gly364Ser variant of Cts at a higher dose (100 nM for 120 min) lowered infarct size, which is probably associated with lower inhibitory activity on the nicotinic cholinergic receptor of the Cts-Gly364Ser variant (97). It is worth underlining that cardioprotection achieved by ischemic preconditioning in wild-type mice was absent in Cts-KOs (21).

Modulation of cardiac glucose metabolism is another cardioprotective mechanism of Cts, in particular, improvement of glucose uptake early during post-ischemic reperfusion (18). In physiological conditions, cardiomyocyte metabolism depends mainly on fatty acid oxidation, although the heart shifts toward glucose metabolism in response to ischemia to ameliorate myocardial contractile efficiency. In isolated rat cardiomyocytes, Cts induced Akt and AS160 phosphorylation and significantly enhanced glucose uptake (18), which may be crucial for recovery of contractile function during post-ischemic reperfusion (98).

A recent study involving an *in vivo* and *in vitro* approach investigated Cts in acute pulmonary embolism (99). Its administration in mice with this pathology increased survival as well as augmented thrombus resolution by attenuating endothelial inflammation (99).

In summary, based on *in vitro* and *in vivo* animal models, it was demonstrated that Cts exhibits a potential cardioprotective effect by acting directly as a cardiodepressing peptide through multiple signaling pathways (52, 53, 88–90), it may also reduce apoptosis of cardiomyocytes induced by oxidative stress (67, 92–96), and is beneficial in acute pulmonary embolism (99). However, more studies are needed in these areas, in particular, regarding Cts in I/R injury of the heart (67, 92–97).

Clinical Studies

Coronary Artery Disease

Wang et al. (100) were the first to investigate Cts in patients with coronary artery disease (CAD) by measuring its plasma concentration in 58 acute myocardial infarction (AMI) patients on admission, day 3 and day 7, and in 25 control subjects who were admitted to the same hospital for atypical chest pain but with normal coronary arteries confirmed by coronary angiography. Compared with controls (21.4 ± 6.4 ng/ml), plasma Cts concentrations were significantly lower on admission due to AMI (16.5 ± 5.4 ng/ml, $p < 0.01$), higher on the third day (30.7 ± 12.2 ng/ml, $p < 0.01$) and again lower on day 7 (13.8 ± 5.3 ng/ml, $p < 0.01$).

Zhu et al. (71) and Xu et al. (74) obtained results consistent with the above: compared to controls, Cts was lower on admission due to AMI, it increased significantly on the third day of hospitalization, but decreased 1 week following AMI. In line with these studies, Kojima et al. showed in small samples of patients that Cts was significantly lower in patients with AMI or unstable angina pectoris than in non-CAD patients (75).

However, Meng et al. (68) and Liu et al. (69) showed that plasma Cts levels at the time of admission were significantly higher in patients with AMI compared to healthy controls. The discrepancy between studies may result from different control groups, which included patients with chest pain without CAD on imaging in studies by Wang et al. (100), Zhu et al. (71) and Xu et al. (74) vs. healthy volunteers in studies by Meng et al. (68) and Liu et al. (69).

In addition, Chen et al. demonstrated serum Cts levels were lower in stable angina pectoris (SAP) patients compared to healthy controls (median (inter-quartile range) 1.14 (1.05–1.24) ng/mL vs. 2.15 (1.92–2.39) ng/mL, $p < 0.001$). Moreover, a stepwise decrease in serum Cts was found when classifying CAD patients according to the number of diseased vessels (19). However, Liu et al. showed that SAP patients ($n = 15$) had significantly higher Cts levels compared to controls (0.41 ± 0.14 ng/mL vs. 0.72 ± 0.50 ng/mL, $p < 0.05$) (69). Divergent findings are difficult to account for, perhaps these depend on disease symptoms in patients of the latter study (Cts increases as CAs are released when pain occurs); small SAP patient sample size in the study by Liu et al. could have biased the results (69).

Further, Xu et al. demonstrated that mean plasma Cts in coronary artery chronic total occlusion patients, who underwent coronary angiography or percutaneous coronary intervention for the first time, were significantly higher than in patients with chest pain but with normal coronary arteries (1.97 ± 1.01 vs. 1.36 ± 0.97 ng/ml, $p = 0.009$) (72).

Of the 58 AMI patients mentioned above, Meng et al. studied 31 by echocardiography 3 months after AMI onset, and diagnosed 7 with left ventricular remodeling (LVR). Interestingly, these patients had significantly higher plasma Cts levels on admission, day 3, and day 7 than those without LVR (68). In line with Meng et al., Dan Zhu et al. found that AMI patients, whose Cts level exceeded the median at day 3 of hospitalization (28.71 ng/ml), exhibited worse left ventricular function in echocardiography 65 months after AMI (73).

In another study performed by Dan Zhu et al., adverse events occurred more frequently in the 65-month follow-up in patients whose Cts level on day 3 exceeded the median as well as in those whose ratios of Cts on day 7 to day 3 were below the median (71). Moreover, plasma Cts level turned out to be an independent prognostic factor for malignant arrhythmia (MA) after AMI, and was significantly higher in patients with AMI complicated by MA (70). However, Xu et al. showed no significant differences in major adverse cardiovascular events, including death from cardiovascular causes, recurrent AMI, or hospital admission for HF, or revascularization between patients with high and low Cts concentrations (72).

Heart Failure

Concerning HF, Dan Zhu et al. showed that the higher the severity stage of HF (according to the American Heart Association, AHA), the lower the Cts level, and that Cts might be a better predictive factor for stage B HF than brain natriuretic peptide, a marker commonly used in clinical practice for HF diagnosis and severity assessment (76). However, according to a study by Liu et al., plasma Cts levels were increasingly higher in patients with growing severity of the New York Heart Association (NYHA) HF classes I to IV, and NYHA class III and IV patients exhibited significantly higher plasma Cts levels than controls, NYHA class I, and class II subjects (77). Seemingly contradictory results may be a consequence of patient enrollment criteria: Zhu et al. recruited asymptomatic chronic patients with stage C HF (76), while NYHA IV patients had resting dyspnea (77). As mentioned before, symptoms that trigger CA release can cause a compensatory increase in Cts levels.

Peng et al. demonstrated that Cts was an independent risk factor for all-cause death (hazard ratio 1.84 (95% CI: 1.02–3.32, $p = 0.042$)) and cardiac death [hazard ratio 2.41 (95% CI: 1.26–4.62, $p = 0.008$)] during a median 52.5-month follow-up (78). In line with their results, in the CATSTAT-HF Study, Cts was found to be an independent and significant predictor of in-hospital death, and its level was significantly higher among non-survivors than survivors (80). However, in the study by Wołowiec et al., patients who reached the composite endpoint of unplanned hospitalization and death for all causes during a 24-month follow-up had lower Cts levels – assessed both before and after physical exertion. Firth coefficient was 6.58 (penalized 95% CI 1.66–21.78, $p = 0.003$) (79). Again, the divergent data could result from different study populations: Wołowiec et al. enrolled only hemodynamically stable patients (79), while in the CATSTAT-HF Study patients with acute decompensation of chronic HF were included (80), and more than half of the patients (55.9%) in the study by Peng et al. study were classified as NYHA III-IV (78).

Catestatin in Other Diseases Affecting the Cardiovascular System

In the scope of CVD, apart from studies on the role of Cts in HT, CAD, and HF, few other have been published.

Sun et al. studied hemodialyzed patients and demonstrated that plasma Cts levels equal to or greater than the mean (1.9 ng/ml) were associated with higher cardiac death risk (RR 6.13, 95% CI 2.54, 18.45) during a 36-month follow-up. Moreover, there was no such association for non-cardiac death (RR 1.29, 95% CI 0.70, 2.85) (81).

Izci et al. showed that plasma Cts levels were higher in patients with acute pulmonary embolism than in control subjects. Also, there was a positive correlation between Cts and right ventricular dysfunction, and between Cts and Simplified Pulmonary Embolism Severity Index(± 0.581, $p < 0.001$), a score used to estimate 30-day mortality in patients diagnosed with non-high-risk acute pulmonary embolism. Furthermore, a Cts cut-off level of 31.2 ng/ml predicted mortality with a sensitivity of 100% and specificity of 52.6% (AUC = 0.883, 95% CI: 0.689–0.921) (82).

In preeclampsia patients, plasma Cts was significantly elevated compared to controls: 0.29 ± 0.096 vs. 0.183 ± 0.072 ($p < 0.001$) (83), and correlated positively with systolic and diastolic BP, urea, creatinine and uric acid levels (83).

Stress may account for- at least in part-, the extent of sympathetic nervous activation, deleteriously affects the immune and coagulation systems, increasing the risk of CVDs. Interestingly, it was demonstrated recently that plasma CgA correlated positively with effort, overcommitment, and effort-reward imbalance ($r = 0.267$, 0.319, and 0.304, respectively, $p < 0.001$ for all three), and negatively with reward ($r = -0.237$, $p < 0.001$). Plasma CgA-to-Cts ratio was also associated with work stress in a manner similar to CgA (84).

Summary of Clinical Studies

Clinical studies regarding Cts in CAD and HF are summarized in **Table 1**. It must be highlighted that CAs release causes an increase in Cts, which changes dynamically. Low levels of Cts may play a pathogenic role in cardiac ischemia (74). Research indicates that Cts is involved in the course of CAD as well as HF, and, possibly, its concentration may be applied in monitoring.

ROLE OF CATESTATIN IN METABOLIC DISORDERS AND ATHEROSCLEROSIS

Metabolic disorders such as obesity, insulin resistance and type 2 diabetes are associated with CVDs. Obesity with an abnormal lipid profile may lead to insulin resistance and is associated with higher cardiovascular risk. In turn, insulin resistance correlates strongly with cardiovascular pathology and is a powerful predictor of future development of type 2 diabetes, an independent risk factor for CVDs (101).

Dysregulated immune system is involved in the pathogenesis of these widely prevalent metabolic disorders. The interdependence of adverse systemic metabolic conditions and immune responses gave rise to the term "immunometabolism," which is currently also used to describe pathologic reprogramming of immune cells not only in the spectrum of metabolic syndrome, but also other diseases (e.g., neoplasms and autoimmunity). Here, the former meaning of immunometabolism was adopted.

In vitro and *in vivo* Animal Studies

Based on *in vitro* and *in vivo* studies with rodent models, Cts plays a role in the crosstalk between the immune and metabolic systems (15), in particular, in the development of atherosclerosis (19). Cts may act as an anti-atherogenic and anti-inflammatory peptide that reduces leukocyte-endothelium interaction by activating angiotensin-converting enzyme-2 and suppressing tumor necrosis factor-α-elicited expression of inflammatory cytokines and adhesion molecules (19); development of atherosclerosis was attenuated by Cts treatment in apolipoprotein E knockout mice fed a high-fat diet (a mouse model of atherosclerosis) (19) (**Figure 1**). Further, after vascular injury, Cts increased the expression of *Mrc1*, a gene encoding an anti-inflammatory peptide, and

prevented macrophage-driven atherosclerosis (75). Presumably, anti-inflammatory actions of Cts partly depend on the regulation of chemotaxis (102). *In vitro* and *in vivo* (rodent models), Cts counteracted chemoattraction of monocytes and neutrophils by inflammatory chemokines (102), likely contributing to reduced immune infiltration in the heart (21, 75). Regulation of chemotaxis by Cts is complex and naturally occurring Cts variants differ in their chemotactic properties (103, 104), which may influence the propensity for CVD.

The liver plays both a critical role in metabolism, and serves as an important site of immune regulation as it contains resident immune cells as well as synthesizes a number of inflammatory proteins (105). Both tissue-resident (Kupffer cells) and recruited macrophages contribute to an inflammatory state of the liver, e.g., in obesity-induced insulin resistance and type 2 diabetes. Using a rodent model, Ying et al. showed that Cts may inhibit the function and infiltration of macrophages in the liver, which suppresses hepatic gluconeogenesis and improves insulin sensitivity (20). Moreover, the authors demonstrated that treatment of diet-induced obese mice with Cts elicited beneficial changes, including decreased plasma lipids and insulin as well as hepatic lipid content, attenuated expression of gluconeogenic and proinflammatory genes, and increased expression of anti-inflammatory genes in both Kupffer cells and recruited monocyte–derived macrophages in the liver (20) (**Figure 1**). Furter *in vivo* research on both diet-induced obese and normal chow diet mice showed that Cts decreased obesity-induced endoplasmic reticulum dilation in hepatocytes and macrophages, and enhanced insulin sensitivity in mammalian cells (106).

Latest research *in vivo* on a rodent Cts-KO model has shown that Cts directly promotes hepatic glycogen synthesis, reduces gluneogenesis and glycogenolysis, as well as enhances downstream insulin signaling (23). Positive effects of Cts were observed in Chga-KO mice too, which – despite regular chow diet - were obese, and had increased plasma CAs, leptin, adiponectin, and ketone bodies at baseline (22). Moreover, compared to WT controls, Chga-KO mice exhibited higher glucose-stimulated insulin secretion, which was likely caused by changes in secretory vesicles and mitochondria observed in CgA-deficient β-cells (107). In this model, treatment with Cts lowered circulating CAs and leptin as well as reduced adipose tissue by about 25% resulting in a lean phenotype, increased lipolysis, enhanced fatty acid oxidation and assimilation into lipids in the liver (**Figure 1**). These beneficial metabolic effects of exogenous Cts were presumed to result from reduction of CA and adiponectin resistance; the effect was mediated by the inhibition of α2 adrenergic signaling (22) (**Figure 1**). In addition, Cts improved leptin signaling (determined by phosphorylation of AMPK and Stat3 in Chga-KO mice) and peripheral leptin sensitivity in both diet-induced obese mice and in leptin-deficient *ob/ob* mice (22) (**Figure 1**). In another model with genetically modified rodents, Cts was found to restore natrium-glucose transporter 1 (SGLT1) expression and abundance as well as intestinal turnover in double knock-out leptin receptor b mice, an experimental model of obesity, type 2 diabetes with hyperleptinemia. The effect was possibly mediated by antagonistic binding of Cts to the leptin receptor a (108).

To sum up, it is increasingly clear that Cts is vital for maintaining metabolic homeostasis, which is partly achieved by affecting the immune system. Based on *in vitro* and *in vivo* experimental studies, Cts may inhibit inflammatory response and leukocyte-endothelial cell interactions (19, 21, 75, 102, 103), prevent macrophage-driven atherosclerosis (19, 75), regulate monocyte migration (103), and cytokine production and release (102–104). As a novel regulator of metabolism, in rodents, Cts was shown to help in achieving insulin sensitivity, overcoming endoplasmic reticulum stress (106), reducing adipose tissue by increasing lipolysis, enhancing oxidation of fatty acids, and their assimilation into lipids (22).

Clinical Studies

So far, only few studies have been conducted in humans on the metabolic role of Cts. Clearly, more research is required in this area.

In a study reported above, O'Connor et al. showed that plasma Cts levels correlated negatively with BMI and plasma leptin concentrations in hypertensive and normotensive subjects (59). Durakoglugil et al. reported that plasma Cts was an independent predictor of high-density lipoprotein cholesterol, and correlated inversely with plasma triglycerides (60). Interestingly, the Ser-364 allele was strongly associated with elevated plasma triglyceride and glucose levels (30).

Simunovic et al. compared plasma Cts levels in 92 obese children and adolescent with those of 39 healthy (normal weight) controls: it levels were significantly lower in the former (10.03 $\pm$ 5.05 vs. 13.13 $\pm$ 6.25 ng/mL, $p = 0.004$) (85), and, in addition, lower in the subgroup of obese patients with metabolic syndrome vs. those without and controls (9.02 $\pm$ 4.3, 10.54 $\pm$ 5.36, and 13.13 $\pm$ 6.25 ng/ml, respectively, $p = 0.008$). Moreover, Cts negatively correlated with diastolic BP ($r = -0.253$, $p = 0.014$), homeostatic model assessment of insulin resistance index ($r = -0.215$, $p = 0.037$), and high sensitivity C-reactive protein ($r = -0.208$, $p = 0.044$) (85) (**Table 1**). In another study, children with obstructive sleep apnea (OSA) had reduced plasma Cts levels (Log Cts in moderate-to-severe OSA: 0.12 $\pm$ 0.22 vs. mild OSA: 0.23 $\pm$ 0.20 vs. controls: 0.28 $\pm$ 0.19; $p < 0.01$) and Cts correlated negatively with apnea-hypopnea index ($r = -0.226$; $p < 0.01$) as well as mean arterial BP ($r = -0.184$; $p < 0.05$) (86) (**Table 1**).

Borovac et al. measured plasma Cts levels in 78 male OSA patients aged 50.3 $\pm$ 8.8 years and 51 age-, sex- and BMI-matched control subjects. They demonstrated that Cts serum levels are higher in the former (2.9 $\pm$ 1.2 vs. 1.5 $\pm$ 1.1 ng/mL, $p < 0.001$) (87). Cts significantly correlated with neck circumference ($r = 0.318$, $p < 0.001$; $\beta = 0.384$, $p < 0.001$) and high-density lipoprotein cholesterol ($r = -0.320$, $p < 0.001$; $\beta = -0.344$, $p < 0.001$), as well as apnea-hypopnea index among non-obese obstructive sleep apnea subjects ($r = 0.466$, $p = 0.016$; $\beta = 0.448$, $p = 0.026$) (87) (**Table 1**).

Evidently, reduced Cts levels seem to be associated with an adverse metabolic profile, including obesity and metabolic syndrome, abnormal lipid concentrations and insulin resistance.

CONCLUSIONS AND PERSPECTIVES

In conclusion, current data indicate that the endogenous bioactive peptide Cts is a vital regulatory factor of cardiovascular and immunometabolic homeostasis. Possibly, in future, Cts can be used in the diagnosis of CVDs and metabolic disorders as a novel biomarker, which may aid in clinical decision-making. Application of Cts in therapy might potentially mitigate detrimental sympathoexcitatory effects, which underlie cardiovascular and metabolic diseases. It should be highlighted that, so far, studies on Cts have been carried out mainly on animal models. More research is required to take advantage of beneficial effects of Cts in clinical practice.

AUTHOR CONTRIBUTIONS

EZ and PK review the literature, and EZ wrote the first draft of the manuscript. PK and EZ wrote sections of the manuscript. KS carried out critical interpretations. All authors contributed to manuscript revision, read, and approved the submitted version.

REFERENCES

1. Gerberding JL. Measuring pandemic impact: vital signs from vital statistics. *Ann Intern Med.* (2020) 173:1022–3. doi: 10.7326/M20-6348
2. Valensi P. Autonomic nervous system activity changes in patients with hypertension and overweight: role and therapeutic implications. *Cardiovasc Diabetol.* (2021) 20:1–12. doi: 10.1186/s12933-021-01356-w
3. Gaede AH, Pilowsky PM. Catestatin in rat RVLM is sympathoexcitatory, increases barosensitivity, and attenuates chemosensitivity and the somatosympathetic reflex. *Am J Physiol Regul Integr Comp Physiol.* (2010) 299:1538–45. doi: 10.1152/ajpregu.00335.2010
4. Callingham BA. The chromaffin cell. *Nature.* (1965) 208:6. doi: 10.1038/208006a0
5. Motiejunaite J, Amar L, Vidal-Petiot E. Adrenergic receptors and cardiovascular effects of catecholamines. *Ann Endocrinol (Paris).* (2021) 82:193–7. doi: 10.1016/j.ando.2020.03.012
6. Banks P, Helle K. The release of protein from the stimulated adrenal medulla. *Biochem J.* (1965) 97:40–1. doi: 10.1042/bj0970040C
7. Blaschko H, Comline RS, Schneider FH, Silver M, Smith AD. Secretion of a chromafafin granule protein, chromogranin, from the adrenal gland after splanchnic stimulation. *Nature.* (1967) 215:58–9. doi: 10.1038/215058a0
8. Schneider FH, Smith AD, Winkler H. Secretion from the adrenal medulla: biochemical evidence for exocytosis. *Br J Pharmacol Chemother.* (1967) 31:94–104. doi: 10.1111/j.1476-5381.1967.tb01980.x
9. Pasqua T, Angelone T, Spena A, Cerra MC. Biological roles of the eclectic chromogranin-a-derived peptide catestatin. *Curr Med Chem.* (2017) 24:3356–72. doi: 10.2174/0929867324666170616104759
10. Simon JP, Bader MF, Aunis D. Secretion from chromaffin cells is controlled by chromogranin A-derived peptides. *Proc Natl Acad Sci U S A.* (1988) 85:1712–6. doi: 10.1073/pnas.85.5.1712
11. Mahata SK, O'Connor DT, Mahata M, Yoo SH, Taupenot L, Wu H, et al. Novel autocrine feedback control of catecholamine release: a discrete chromogranin A fragment is a noncompetitive nicotinic cholinergic antagonist. *J Clin Invest.* (1997) 100:1623–33. doi: 10.1172/JCI119686
12. Biswas N, Gayen J, Mahata M, Su Y, Mahata SK, O'Connor DT. Novel peptide isomer strategy for stable inhibition of catecholamine release: application to hypertension. *Hypertension.* (2012) 60:1552–9. doi: 10.1161/HYPERTENSIONAHA.112.202127
13. Sahu BS, Mahata S, Bandyopadhyay K, Mahata M, Avolio E, Pasqua T, et al. Catestatin regulates vesicular quanta through modulation of cholinergic and peptidergic (PACAPergic) stimulation in PC12 cells. *Cell Tissue Res.* (2019) 376:51–70. doi: 10.1007/s00441-018-2956-1
14. Bozic J, Kumric M, Ticinovic Kurir T, Urlic H, Martinovic D, Vilovic M, et al. Catestatin as a biomarker of cardiovascular diseases: a clinical perspective. *Biomedicines.* (2021) 9:1757. doi: 10.3390/biomedicines9121757
15. Mahata SK, Corti A. Chromogranin a and its fragments in cardiovascular, immunometabolic, and cancer regulation. *Ann N Y Acad Sci.* (2019) 1455:34–58. doi: 10.1111/nyas.14249
16. Zhao Y, Zhu D. Potential applications of catestatin in cardiovascular diseases. *Biomark Med.* (2016) 10:877–88. doi: 10.2217/bmm-2016-0086
17. Pasqua T, Rocca C, Spena A, Angelone T, Cerra MC. Modulation of the coronary tone in the expanding scenario of Chromogranin-A and its derived peptides. *Fut Med Chem.* (2019) 11:1501–11. doi: 10.4155/fmc-2018-0585
18. Gallo MP, Femmino S, Antoniotti S, Querio G, Alloatti G, Levi R. Catestatin induces glucose uptake and GLUT4 trafficking in adult rat cardiomyocytes. *Biomed Res Int.* (2018) 2018:1–7. doi: 10.1155/2018/2086109
19. Chen Y, Wang X, Yang C, Su X, Yang W, Dai Y, et al. Decreased circulating catestatin levels are associated with coronary artery disease: The emerging anti-inflammatory role. *Atherosclerosis.* (2019) 281:78–88. doi: 10.1016/j.atherosclerosis.2018.12.025
20. Ying W, Mahata S, Bandyopadhyay GK, Zhou Z, Wollam J, Vu J, et al. Catestatin inhibits obesity-induced macrophage infiltration and inflammation in the liver and suppresses hepatic glucose production, leading to improved insulin sensitivity. *Diabetes.* (2018) 67:841–8. doi: 10.2337/db17-0788
21. Ying W, Tang K, Avolio E, Schilling JM, Pasqua T, Liu MA, et al. The immunosuppression of macrophages underlies the cardioprotective effects of catestatin (CST). *bioRxiv*. (2021). doi: 10.1101/2020.05.12.092254
22. Bandyopadhyay GK, Vu CU, Gentile S, Lee H, Biswas N, Chi NW, et al. Catestatin (Chromogranin A352-372) and novel effects on mobilization of fat from adipose tissue through regulation of adrenergic and leptin signaling. *J Biol Chem.* (2012) 287:23141–51. doi: 10.1074/jbc.M111.335877
23. Bandyopadhyay G, Tang K, Webster NJG, van den Bogaart G, Mahata SK. Catestatin induces glycogenesis by stimulating the phosphoinositide 3-kinase-AKT pathway. *Acta Physiol (Oxf).* (2022) 235:e13775. doi: 10.1111/apha.13775
24. Zhang D, Shooshtarizadeh P, Laventie BJ, Colin DA, Chich JF, Vidic J, et al. Two chromogranin a-derived peptides induce calcium entry in human neutrophils by calmodulin-regulated calcium independent phospholipase A2. *PLoS ONE.* (2009) 4:e4501. doi: 10.1371/journal.pone.0004501
25. Muntjewerff EM, Dunkel G, Nicolasen MJT, Mahata SK, Van Den Bogaart G. Catestatin as a target for treatment of inflammatory diseases. *Front Immunol.* (2018) 9:1–10. doi: 10.3389/fimmu.2018.02199
26. Bourebaba Y, Mularczyk M, Marycz K, Bourebaba L. Catestatin peptide of chromogranin A as a potential new target for several risk factors management in the course of metabolic syndrome. *Biomed Pharmacother.* (2021) 134:111113. doi: 10.1016/j.biopha.2020.111113
27. Mahata SK, Kiranmayi M, Mahapatra NR. Catestain: a master regulator of cardiovascular functions. *Curr Med Chem.* (2018) 25:1352–74. doi: 10.2174/0929867324666170425100416
28. Taylor C V, Taupenot L, Mahata SK, Mahata M, Wu H, Yasothornsrikul S, et al. Formation of the catecholamine release-inhibitory peptide catestatin from chromogranin A: Determination of proteolytic cleavage sites in hormone storage granules. *J Biol Chem.* (2000) 275:22905–15. doi: 10.1074/jbc.M001232200
29. Wen G, Mahata SK, Cadman P, Mahata M, Ghosh S, Mahapatra NR, et al. Both rare and common polymorphisms contribute functional variation at CHGA, a regulator of catecholamine physiology. *Am J Hum Genet.* (2004) 74:197–207. doi: 10.1086/381399
30. Sahu BS, Obbineni JM, Sahu G, Allu PKR, Subramanian L, Sonawane PJ, et al. Functional genetic variants of the catecholamine-release-inhibitory peptide catestatin in an Indian population: allele-specific effects on metabolic traits. *J Biol Chem.* (2012) 287:43840–52. doi: 10.1074/jbc.M112.407916
31. Kiranmayi M, Chirasani VR, Allu PKR, Subramanian L, Martelli EE, Sahu BS, et al. Catestatin Gly364Ser variant alters systemic blood pressure and the risk for hypertension in human populations

via endothelial nitric oxide pathway. *Hypertension.* (2016) 68:334–47. doi: 10.1161/HYPERTENSIONAHA.116.06568
32. Benyamin B, Maihofer AX, Schork AJ, Hamilton BA, Rao F, Schmid-Schönbein GW, et al. Identification of novel loci affecting circulating chromogranins and related peptides. *Hum Mol Genet.* (2017) 26:233–42. doi: 10.1093/hmg/ddw380
33. Biswas N, Curello E, O'connor DT, Mahata SK. Chromogranin/secretogranin proteins in murine heart: Myocardial production of chromogranin A fragment catestatin (Chga364-384). *Cell Tissue Res.* (2010) 342:353–61. doi: 10.1007/s00441-010-1059-4
34. Mahapatra NR, Mahata M, Mahata SK, O'Connor DT. The chromogranin A fragment catestatin: Specificity, potency and mechanism to inhibit exocytotic secretion of multiple catecholamine storage vesicle co-transmitters. *J Hypertens.* (2006) 24:895–904. doi: 10.1097/01.hjh.0000222760.99852.e0
35. Sugawara M, Resende JM, Marquette A, Chich J, Bechinger B. Membrane structure and interactions of human catestatin by multidimensional solution and solid-state NMR spectroscopy. *FASEB J.* (2010) 24:1737–46. doi: 10.1096/fj.09-142554
36. Pasqua T, Corti A, Gentile S, Pochini L, Bianco M, Metz-Boutigue MH, et al. Full-length human chromogranin-A cardioactivity: myocardial, coronary, and stimulus-induced processing evidence in normotensive and hypertensive male rat hearts. *Endocrinology.* (2013) 154:3353–65. doi: 10.1210/en.2012-2210
37. Rocca C, Grande F, Granieri MC, Colombo B, De Bartolo A, Giordano F, et al. The chromogranin A1-373 fragment reveals how a single change in the protein sequence exerts strong cardioregulatory effects by engaging neuropilin-1. *Acta Physiol.* (2021) 231:e13570. doi: 10.1111/apha.13570
38. Taupenot L, Mahata SK, Mahata M, Parmer RJ, O'Connor DT. Interaction of the catecholamine release-inhibitory peptide catestatin (human chromogranin A352-372) with the chromaffin cell surface and Torpedo electroplax: Implications for nicotinic cholinergic antagonism. *Regul Pept.* (2000) 95:9–17. doi: 10.1016/S0167-0115(00)00135-X
39. Herrero CJ, Alés E, Pintado AJ, López MG, García-Palomero E, Mahata SK, et al. Modulatory mechanism of the endogenous peptide catestatin on neuronal nicotinic acetylcholine receptors and exocytosis. *J Neurosci.* (2002) 22:377–88. doi: 10.1523/JNEUROSCI.22-02-00377.2002
40. Mahata SK, Mahapatra NR, Mahata M, Wang TC, Kennedy BP, Ziegler MG, et al. Catecholamine secretory vesicle stimulus-transcription coupling *in vivo*. Demonstration by a novel transgenic promoter/photoprotein reporter and inhibition of secretion and transcription by the chromogranin A fragment catestatin. *J Biol Chem.* (2003) 278:32058–67. doi: 10.1074/jbc.M305545200
41. Mahata SK, Mahata M, Wen G, Wong WB, Mahapatra NR, Hamilton BA, et al. The catecholamine release-inhibitory "catestatin" fragment of chromogranin A: Naturally occurring human variants with different potencies for multiple chromaffin cell nicotinic cholinergic responses. *Mol Pharmacol.* (2004) 66:1180–91. doi: 10.1124/mol.104.002139
42. Sahu BS, Mohan J, Sahu G, Singh PK, Sonawane PJ, Sasi BK, et al. Molecular interactions of the physiological anti-hypertensive peptide catestatin with the neuronal nicotinic acetylcholine receptor. *J Cell Sci.* (2012) 125:2787. doi: 10.1242/jcs.114389
43. Bassino E, Fornero S, Gallo MP, Ramella R, Mahata SK, Tota B, et al. A novel catestatin-induced antiadrenergic mechanism triggered by the endothelial PI3KeNOS pathway in the myocardium. *Cardiovasc Res.* (2011) 91:617–24. doi: 10.1093/cvr/cvr129
44. Mahapatra NR, O'Connor DT, Vaingankar SM, Sinha Hikim AP, Mahata M, Ray S, et al. Hypertension from targeted ablation of chromogranin A can be rescued by the human ortholog. *J Clin Invest.* (2005) 115:1942–52. doi: 10.1172/JCI24354
45. Gayen JR, Gu Y, O'Connor DT, Mahata SK. Global disturbances in autonomic function yield cardiovascular instability and hypertension in the chromogranin A null mouse. *Endocrinology.* (2009) 150:5027–35. doi: 10.1210/en.2009-0429
46. Gayen JR, Zhang K, RamachandraRao SP, Mahata M, Chen Y, Kim HS, et al. Role of reactive oxygen species in hyperadrenergic hypertension: biochemical, physiological, and pharmacological evidence from targeted ablation of the chromogranin A (Chga) gene. *Circ Cardiovasc Genet.* (2010) 3:414–25. doi: 10.1161/CIRCGENETICS.109.924050
47. Dev NB, Mir SA, Gayen JR, Siddiqui JA, Mustapic M, Vaingankar SM. Cardiac electical activity in a genomically "humanized" chromogranin A monogenic mouse model with hyperadrenergic hypertension. *J Cardiovasc Transl Res.* (2014) 7:483–93. doi: 10.1007/s12265-014-9563-7
48. Kennedy BP, Mahata SK, O'Connor DT, Ziegler MG. Mechanism of cardiovascular actions of the chromogranin A fragment catestatin in vivo. *Peptides.* (1998) 19:1241–8. doi: 10.1016/S0196-9781(98)00086-2
49. Krüger PG, Mahata SK, Helle KB. Catestatin (CgA344-364) stimulates rat mast cell release of histamine in a manner comparable to mastoparan and other cationic charged neuropeptides. *Regul Pept.* (2003) 114:29–35. doi: 10.1016/S0167-0115(03)00069-7
50. Jianqiang G, Li S, Guo J. Effect of catecholamine release-inhibitory peptide catestatin on sympathetic activity of hypertension. *J Am Coll Cardiol.* (2016) 68:C33–4. doi: 10.1016/j.jacc.2016.07.123
51. Liu R, Sun NL, Yang SN, Guo JQ. Catestatin could ameliorate proliferating changes of target organs in spontaneously hypertensive rats. *Chin Med J (Engl).* (2013) 126:2157–62. doi: 10.3760/cma.j.issn.0366-6999.20120757
52. Mazza R, Pasqua T, Gattuso A. Cardiac heterometric response: The interplay between catestatin and nitric oxide deciphered by the frog heart. *Nitric Oxide.* (2012) 27:40–9. doi: 10.1016/j.niox.2012.04.003
53. Angelone T, Quintieri AM, Brar BK, Limchaiyawat PT, Tota B, Mahata SK, et al. The antihypertensive chromogranin A peptide catestatin acts as a novel endocrine/paracrine modulator of cardiac inotropism and lusitropism. *Endocrinology.* (2008) 149:4780–93. doi: 10.1210/en.2008-0318
54. Gaede AH, Lung MSY, Pilowsky PM. Catestatin attenuates the effects of intrathecal nicotine and isoproterenol. *Brain Res.* (2009) 1305:86–95. doi: 10.1016/j.brainres.2009.09.088
55. Gaede AH, Pilowsky PM. Catestatin, a chromogranin A-derived peptide, is sympathoinhibitory and attenuates sympathetic barosensitivity and the chemoreflex in rat CVLM. *Am J Physiol Regul Integr Comp Physiol.* (2012) 302:365–72. doi: 10.1152/ajpregu.00409.2011
56. Avolio E, Mahata SK, Mantuano E, Mele M, Alò R, Facciolo RM, et al. Antihypertensive and neuroprotective effects of catestatin in spontaneously hypertensive rats: Interaction with GABAergic transmission in amygdala and brainstem. *Neuroscience.* (2014) 270:48–57. doi: 10.1016/j.neuroscience.2014.04.001
57. Mahata SK, Mahata M, Parmer RJ, O'Connor DT. Desensitization of Catecholamine Release. *J Biol Chem.* (1999) 274:2920–8. doi: 10.1074/jbc.274.5.2920
58. Fung MM, Salem RM, Mehtani P, Thomas B, Lu CF, Perez B, et al. Direct vasoactive effects of the chromogranin A (CHGA) peptide catestatin in humans *in vivo*. *Clin Exp Hypertens.* (2011) 32:278–87. doi: 10.3109/10641960903265246
59. O'Connor DT, Kailasam MT, Kennedy BP, Ziegler MG, Yanaihara N, Parmer RJ. Early decline in the catecholamine release-inhibitory peptide catestatin in humans at genetic risk of hypertension. *J Hypertens.* (2002) 20:1335–45. doi: 10.1097/00004872-200207000-00020
60. Durakoglugil ME, Ayaz T, Kocaman SA, Kirbaş A, Durakoglugil T, Erdogan T, et al. The relationship of plasma catestatin concentrations with metabolic and vascular parameters in untreated hypertensive patients: Influence on high-density lipoprotein cholesterol. *Anatol J Cardiol.* (2015) 15:577–85. doi: 10.5152/akd.2014.5536
61. O'Connor DT, Zhu G, Rao F, Taupenot L, Fung MM, Das M, et al. Heritability and genome-wide linkage in US and australian twins identify novel genomic regions controlling chromogranin a: implications for secretion and blood pressure. *Circulation.* (2008) 118:247–57. doi: 10.1161/CIRCULATIONAHA.107.709105
62. Meng L, Ye XJ, Ding WH, Yang Y, Di BB, Liu L, et al. Plasma catecholamine release-inhibitory peptide catestatin in patients with essential hypertension. *J Cardiovasc Med.* (2011) 12:643–7. doi: 10.2459/JCM.0b013e328346c142
63. Rao F, Wen G, Gayen JR, Das M, Vaingankar SM, Rana BK, et al. Catecholamine release-inhibitory peptide catestatin (chromogranin A352-372): Naturally occurring amino acid variant Gly364Ser causes profound changes in human autonomic activity and alters risk for hypertension. *Circulation.* (2007) 115:2271–81. doi: 10.1161/CIRCULATIONAHA.106.628859
64. Choi Y, Miura M, Nakata Y, Sugasawa T, Nissato S, Otsuki T, et al. A common genetic variant of the chromogranin A-derived peptide catestatin

is associated with atherogenesis and hypertension in a Japanese population. *Endocr J.* (2015) 62:797–804. doi: 10.1507/endocrj.EJ14-0471
65. Biswas N, Vaingankar SM, Mahata M, Das M, Gayen JR, Taupenot L, et al. Proteolytic cleavage of human chromogranin A containing naturally occurring catestatin variants: Differential processing at catestatin region by plasmin. *Endocrinology.* (2008) 149:749–57. doi: 10.1210/en.2007-0838
66. Salem RM, Cadman PE, Chen Y, Rao F, Wen G, Hamilton BA, et al. Chromogranin A polymorphisms are associated with hypertensive renal disease. *J Am Soc Nephrol.* (2008) 19:600–14. doi: 10.1681/ASN.2007070754
67. Wang D, Liu T, Shi S, Li R, Shan Y, Huang Y, et al. Chronic administration of catestatin improves autonomic function and exerts cardioprotective effects in myocardial infarction rats. *J Cardiovasc Pharmacol Ther.* (2016) 21:526–35. doi: 10.1177/1074248416628676
68. Meng L, Wang J, Ding WH, Han P, Yang Y, Qi LT, et al. Plasma catestatin level in patients with acute myocardial infarction and its correlation with ventricular remodelling. *Postgrad Med J.* (2013) 89:193–6. doi: 10.1136/postgradmedj-2012-131060
69. Liu L, Ding W, Zhao F, Shi L, Pang Y, Tang C. Plasma levels and potential roles of catestatin in patients with coronary heart disease. *Scand Cardiovasc J.* (2013) 47:217–24. doi: 10.3109/14017431.2013.794951
70. Pei Z, Ma D, Ji L, Zhang J, Su J, Xue W, et al. Usefulness of catestatin to predict malignant arrhythmia in patients with acute myocardial infarction. *Peptides.* (2014) 55:131–5. doi: 10.1016/j.peptides.2014.02.016
71. Zhu D, Xie H, Wang X, Liang Y, Yu H, Gao W. Correlation of plasma catestatin level and the prognosis of patients with acute myocardial infarction. *PLoS ONE.* (2015) 10:1–14. doi: 10.1371/journal.pone.0122993
72. Xu W, Yu H, Li W, Gao W, Guo L, Wang G. Plasma catestatin: a useful biomarker for coronary collateral development with chronic myocardial ischemia. *PLoS ONE.* (2016) 11:1–11. doi: 10.1371/journal.pone.0149062
73. Zhu D, Xie H, Wang X, Liang Y, Yu H, Gao W. Catestatin-A novel predictor of left ventricular remodeling after acute myocardial infarction. *Sci Rep.* (2017) 7:44168. doi: 10.1038/srep44168
74. Xu W, Yu H, Wu H, Li S, Chen B, Gao W. Plasma Catestatin in Patients with acute coronary syndrome. *Cardiol.* (2017) 136:164–9. doi: 10.1159/000448987
75. Kojima M, Ozawa N, Mori Y, Takahashi Y, Watanabe-Kominato K, Shirai R, et al. Catestatin prevents macrophage-driven atherosclerosis but not arterial injury-induced neointimal hyperplasia. *Thromb Haemost.* (2018) 118:182–94. doi: 10.1160/TH17-05-0349
76. Zhu D, Wang F, Yu H, Mi L, Gao W. Catestatin is useful in detecting patients with stage B heart failure. *Biomarkers.* (2011) 16:691–7. doi: 10.3109/1354750X.2011.629058
77. Liu L, Ding W, Li R, Ye X, Zhao J, Jiang J, et al. Plasma levels and diagnostic value of catestatin in patients with heart failure. *Peptides.* (2013) 46:20–5. doi: 10.1016/j.peptides.2013.05.003
78. Peng F, Chu S, Ding W, Liu L, Zhao J, Cui X, et al. The predictive value of plasma catestatin for all-cause and cardiac deaths in chronic heart failure patients. *Peptides.* (2016) 86:112–7. doi: 10.1016/j.peptides.2016.10.007
79. Wołowiec Ł, Rogowicz D, Banach J, Gilewski W, Sinkiewicz W, Grzesk G. Catestatin as a new prognostic marker in stable patients with heart failure with reduced ejection fraction in two-year follow-up. *Dis Markers.* (2020) 2020:8847211. doi: 10.1155/2020/8847211
80. Borovac JA, Glavas D, Susilovic Grabovac Z, Supe Domic D, Stanisic L, D'Amario D, et al. Circulating sST2 and catestatin levels in patients with acute worsening of heart failure: a report from the CATSTAT-HF study. *ESC Hear Fail.* (2020) 7:2818–28. doi: 10.1002/ehf2.12882
81. Sun H, Xian W, Geng L, Li E, Peng Z, Tian J. Increased plasma level of catestatin might be associated with poor prognosis in hemodialysis patients. *Int Urol Nephrol.* (2017) 49:1063–9. doi: 10.1007/s11255-017-1528-8
82. Izci S, Acar E, Inanir M. Plasma catestatin level predicts sPESI score and mortality in acute pulmonary embolism. *Arch Med Sci Atheroscler Dis.* (2020) 5:49–56. doi: 10.5114/amsad.2020.95562
83. Tüten N, Güralp O, Gök K, Hamzaoglu K, Oner YO, Makul M, et al. Serum catestatin level is increased in women with preeclampsia. *J Obstet Gynaecol.* (2022) 42:55–60. doi: 10.1080/01443615.2021.1873922
84. Liu X, Dang W, Liu H, Song Y, Li Y, Xu W. Associations between chronic work stress and plasma chromogranin A/catestatin among healthy workers. *J Occup Health.* (2022) 64:e12321. doi: 10.1002/1348-9585.12321
85. Simunovic M, Supe-Domic D, Karin Z, Degoricija M, Paradzik M, Bozic J, et al. Serum catestatin concentrations are decreased in obese children and adolescents. *Pediatr Diabetes.* (2019) 20:549–55. doi: 10.1111/pedi.12825
86. Kim J, Lee S, Bhattacharjee R, Khalyfa A, Kheirandish-Gozal L, Gozal D. Leukocyte telomere length and plasma catestatin and myeloid-related protein 8/14 concentrations in children with obstructive sleep apnea. *Chest.* (2010) 138:91–9. doi: 10.1378/chest.09-2832
87. Borovac JA, Dogas Z, Supe-Domic D, Galic T, Bozic J. Catestatin serum levels are increased in male patients with obstructive sleep apnea. *Sleep Breath.* (2019) 23:473–81. doi: 10.1007/s11325-018-1703-x
88. Angelone T, Quintieri AM, Pasqua T, Gentile S, Tota B, Mahata SK, et al. Phosphodiesterase type-2 and NO-dependent S -nitrosylation mediate the cardioinhibition of the antihypertensive catestatin. *Am J Physiol Circ Physiol.* (2011) 302:H431–H44. doi: 10.1152/ajpheart.00491.2011
89. Imbrogno S, Garofalo F, Cerra MC, Mahata SK, Tota B. The catecholamine release-inhibitory peptide catestatin (chromogranin A344-364) modulates myocardial function in fish. *J Exp Biol.* (2010) 213:3636–43. doi: 10.1242/jeb.045567
90. Angelone T, Quintieri AM, Pasqua T, Filice E, Cantafio P, Scavello F, et al. The NO stimulator, Catestatin, improves the Frank-Starling response in normotensive and hypertensive rat hearts. *Nitric Oxide.* (2015) 50:10–9. doi: 10.1016/j.niox.2015.07.004
91. Alam MJ, Gupta R, Mahapatra NR, Goswami SK. Catestatin reverses the hypertrophic effects of norepinephrine in H9c2 cardiac myoblasts by modulating the adrenergic signaling. *Mol Cell Biochem.* (2019) 464:205–19. doi: 10.1007/s11010-019-03661-1
92. Liao F, Zheng Y, Cai J, Fan J, Wang J, Yang J, et al. Catestatin attenuates endoplasmic reticulum induced cell apoptosis by activation type 2 muscarinic acetylcholine receptor in cardiac ischemia/reperfusion. *Sci Rep.* (2015) 5:16590. doi: 10.1038/srep16590
93. Penna C, Alloatti G, Gallo MP, Cerra MC, Levi R, Tullio F, et al. Catestatin improves post-ischemic left ventricular function and decreases ischemia/reperfusion injury in heart. *Cell Mol Neurobiol.* (2010) 30:1171–9. doi: 10.1007/s10571-010-9598-5
94. Perrelli MG, Tullio F, Angotti C, Cerra MC, Angelone T, Tota B, et al. Catestatin reduces myocardial ischaemia/reperfusion injury: Involvement of PI3K/Akt, PKCs, mitochondrial KATP channels and ROS signalling. *Pflugers Arch.* (2013) 465:1031–40. doi: 10.1007/s00424-013-1217-0
95. Penna C, Pasqua T, Amelio D, Perrelli MG, Angotti C, Tullio F, et al. Catestatin increases the expression of anti-apoptotic and pro-angiogenetic factors in the post-ischemic hypertrophied heart of SHR. *PLoS ONE.* (2014) 9:e102536. doi: 10.1371/journal.pone.0102536
96. Chu SY, Peng F, Wang J, Liu L, Meng L, Zhao J, et al. Catestatin in defense of oxidative-stress-induced apoptosis: a novel mechanism by activating the beta2 adrenergic receptor and PKB/Akt pathway in ischemic-reperfused myocardium. *Peptides.* (2020) 123:170200. doi: 10.1016/j.peptides.2019.170200
97. Brar BK, Helgeland E, Mahata SK, Zhang K, O'Connor DT, Helle KB, et al. Human catestatin peptides differentially regulate infarct size in the ischemic-reperfused rat heart. *Regul Pept.* (2010) 165:63–70. doi: 10.1016/j.regpep.2010.07.153
98. Tamm C, Benzi R, Papageorgiou I, Tardy I, Lerch R. Substrate competition in postischemic myocardium: effect of substrate availability during reperfusion on metabolic and contractile recovery in isolated rat hearts. *Circ Res.* (1994) 75:1103–12. doi: 10.1161/01.RES.75.6.1103
99. Chen H, Liu D, Ge L, Wang T, Ma Z, Han Y, et al. Catestatin prevents endothelial inflammation and promotes thrombus resolution in acute pulmonary embolism in mice. *Biosci Rep.* (2019) 39:1–10. doi: 10.1042/BSR20192236
100. Wang X, Xu S, Liang Y, Zhu D, Mi L, Wang G, et al. Dramatic changes in catestatin are associated with hemodynamics in acute myocardial infarction. *Biomarkers.* (2011) 16:372–7. doi: 10.3109/1354750X.2011.578260
101. Ormazabal V, Nair S, Elfeky O, Aguayo C, Salomon C, Zuñiga FA. Association between insulin resistance and the

development of cardiovascular disease. *Cardiovasc Diabetol.* (2018) 17:1–14. doi: 10.1186/s12933-018-0762-4

102. Muntjewerff EM, Parv K, Mahata SK, van Riessen NK, Phillipson M, Christoffersson G, et al. The anti-inflammatory peptide Catestatin blocks chemotaxis. *J Leukoc Biol.* (2021) 1–6. doi: 10.1002/JLB.3CRA1220-790RR
103. Egger M, Beer AGE, Theurl M, Schgoer W, Hotter B, Tatarczyk T, et al. Monocyte migration: a novel effect and signaling pathways of catestatin. *Eur J Pharmacol.* (2008) 598:104–11. doi: 10.1016/j.ejphar.2008.09.016
104. Aung G, Niyonsaba F, Ushio H, Kajiwara N, Saito H, Ikeda S, et al. Catestatin, a neuroendocrine antimicrobial peptide, induces human mast cell migration, degranulation and production of cytokines and chemokines. *Immunology.* (2011) 132:527–39. doi: 10.1111/j.1365-2567.2010.03395.x
105. Crispe IN. The liver as a lymphoid organ. *Annu Rev Immunol.* (2009) 27:147–63. doi: 10.1146/annurev.immunol.021908.132629
106. Dasgupta A, Bandyopadhyay GK, Ray I, Bandyopadhyay K, Chowdhury N, De RK, et al. Catestatin improves insulin sensitivity by attenuating endoplasmic reticulum stress: In vivo and in silico validation. *Comput Struct Biotechnol J.* (2020) 18:464–81. doi: 10.1016/j.csbj.2020.02.005
107. Wollam J, Mahata S, Riopel M, Hernandez-Carretero A, Biswas A, Bandyopadhyay GK, et al. Chromogranin A regulates vesicle storage and mitochondrial dynamics to influence insulin secretion. *Cell Tissue Res.* (2017) 368:487–501. doi: 10.1007/s00441-017-2580-5
108. Dominguez Rieg JA, Chirasani VR, Koepsell H, Senapati S, Mahata SK, Rieg T. Regulation of intestinal SGLT1 by catestatin in hyperleptinemic type 2 diabetic mice. *Lab Investig.* (2016) 96:98–111. doi: 10.1038/labinvest.2015.129

Conflict of Interest: The authors declare that the research was conducted in the absence of any commercial or financial relationships that could be construed as a potential conflict of interest.

Publisher's Note: All claims expressed in this article are solely those of the authors and do not necessarily represent those of their affiliated organizations, or those of the publisher, the editors and the reviewers. Any product that may be evaluated in this article, or claim that may be made by its manufacturer, is not guaranteed or endorsed by the publisher.

frontiers | Frontiers in Cardiovascular Medicine

REVIEW
published: 26 May 2022
doi: 10.3389/fcvm.2022.904881

Transient Receptor Potential Channels, Natriuretic Peptides, and Angiotensin Receptor-Neprilysin Inhibitors in Patients With Heart Failure

*Kun Ding[1,2], Yang Gui[1,2], Xu Hou[1,2], Lifang Ye[2] and Lihong Wang[2]**

[1] Bengbu Medical College, Bengbu, China, [2] Zhejiang Provincial People's Hospital, Hangzhou, China

OPEN ACCESS

Edited by:
Wei Liu,
The University of Manchester, United Kingdom

Reviewed by:
Nazha Hamdani,
Ruhr University Bochum, Germany
Jian Shi,
University of Leeds, United Kingdom

***Correspondence:**
Lihong Wang
wanglhnew@126.com

Specialty section:
This article was submitted to Cardiovascular Metabolism, a section of the journal Frontiers in Cardiovascular Medicine

Received: *26 March 2022*
Accepted: *26 April 2022*
Published: *26 May 2022*

Citation:
Ding K, Gui Y, Hou X, Ye L and Wang L (2022) Transient Receptor Potential Channels, Natriuretic Peptides, and Angiotensin Receptor-Neprilysin Inhibitors in Patients With Heart Failure. Front. Cardiovasc. Med. 9:904881. doi: 10.3389/fcvm.2022.904881

Heart failure (HF) remains the leading cause of death, morbidity, and medical expenses worldwide. Treatments for HF with reduced ejection fraction have progressed in recent years; however, acute decompensated heart failure remains difficult to treat. The transient receptor potential (TRP) channel family plays roles in various cardiovascular diseases, responding to neurohormonal and mechanical load stimulation. Thus, TRP channels are promising targets for drug discovery, and many studies have evaluated the roles of TRP channels expressed on pain neurons. The natriuretic peptide (NP) family of proteins regulates blood volume, natriuresis, and vasodilation and can antagonize the renin-angiotensin-aldosterone system and participate in the pathogenesis of major cardiovascular diseases, such as HF, coronary atherosclerotic heart disease, and left ventricular hypertrophy. NPs are degraded by neprilysin, and the blood level of NPs has predictive value in the diagnosis and prognostic stratification of HF. In this review, we discuss the relationships between typical TRP family channels (e.g., transient receptor potential cation channel subfamily V member 1 andTRPV1, transient receptor potential cation channel subfamily C member 6) and the NP system (e.g., atrial NP, B-type NP, and C-type NP) and their respective roles in HF. We also discuss novel drugs introduced for the treatment of HF.

Keywords: transient receptor potential cation channel subfamily V member 1, transient receptor potential cation channel subfamily C member 6, natriuretic peptide, heart failure, angiotensin receptor-neprilysin inhibitor (ARNI)

INTRODUCTION

On October 4, 2021, American scientists David Julius and Ardem Patapoutian won the 2021 Nobel Prize in Physiology and Medicine Award owing to their outstanding contributions to the discovery of receptors that sense temperature and touch. In particular, transient

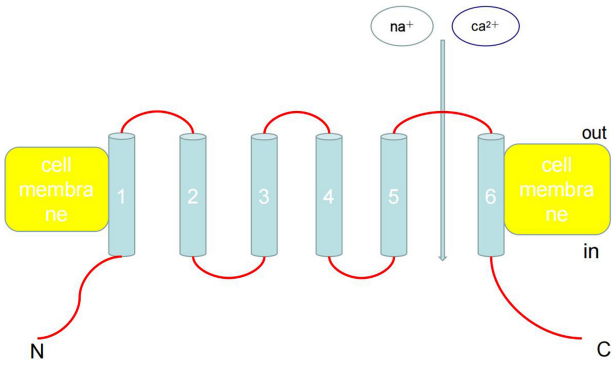

FIGURE 1 | Architecture of TRP channels. TRP can be activated by various physical and chemical stimuli and consist of six transmembrane helices (TM1-6), cytoplasmic N- and C-termini, and a pore area between TM5 and TM6. Ankyrin repeats are found in the amino termini of TRPC and TRPV channels. Currently, the functions and activation mechanisms of TRP family proteins are unclear.

receptor potential (TRP) cation channel subfamily V member 1 (TRPV1) has been shown to act as a receptor for capsaicin. TRP channel proteins can be divided into six families: canonical TRP (TRPC), vanilloid TRP (TRPV), melastatin TRP (TRPM), ankyrin TRP, mucolipin TRP, and polycystin TRP (**Figure 1**). These proteins can be activated by various physical and chemical stimuli and consist of six transmembrane helices (TM1–6), cytoplasmic N- and C-termini, and a pore area between TM5 and TM6 (1, 2). Currently, the functions and activation mechanisms of TRP family proteins are unclear.

The TRPV and TRPC subfamilies are the two most abundant subfamilies and include ion channels that are involved in neuronal pain pathways as well as heat sensing and permeability functions (1). TRP channels are expressed in almost all cardiovascular tissues and are a part of Ca^{2+} entry channels for store-operated channels, receptor-operated channels, stretch-activated channels, and ligand-gated channels. The functional significance of TRP channels may be related to the various gated stimuli that induce Ca^{2+} entry by integrating various variety of physical and chemical factors. Therefore, the participation of TRP channels in cardiovascular disease is uniquely relevant because it provides an opportunity to interfere with the Ca^{2+}-dependent signal transduction process in the cardiovascular system. Although the roles of most TRP channels in cardiovascular diseases are largely unknown, there is no doubt that research linking TRP channel functions with cardiovascular diseases will become an important topic in the medical community in coming years (3).

Natriuretic peptides (NPs) are a group of peptides involved in maintaining the body's water-salt balance, blood pressure, and cardiovascular and kidney function. The NP system is mainly composed of three well-characterized peptides, each of which is a different gene product with a similar structure; atrial NP (ANP) and B-type NP (BNP) are mainly derived from cardiomyocytes (4, 5), whereas C-type NP (CNP) is mainly derived from endothelial cells and kidney cells (6–9). These three peptides protect the heart and kidneys. Notably, BNP is also produced by cardiac fibroblasts and has antifibrotic effects in the heart (10). Muscle cells release ANP and BNP when the cardiac muscle is stretched, whereas endothelial cells release CNP when cytokines and endothelium-dependent agonists, such as acetylcholine, are released. Similar to ANP and BNP, CNP has powerful systemic cardiovascular effects, including reduction of cardiac filling pressure and output, secondary to reduction of vasodilation and venous return, but with minimal renal effects (11). CNPs have the strongest antifibrosis effects among the three natural endogenous NPs. All NPs operate through a second messenger, cGMP. ANP and BNP bind to guanylyl cyclase (GC)-A, whereas CNP binds to GC-B (12). Furthermore, the three NPs are all cleared by the clearance receptor NP receptor (NPR) C (NPR-C), which is unrelated to GCs (13). However, new evidence shows that NPR-C also participates in the antifibrotic effects of NP through a mechanism independent of cGMP activation (14). NPs are also eliminated from circulation by enzymatic degradation of neprilysin (NEP) (12).

Recent studies have demonstrated the roles of NPs, particularly the GC-A agonists ANP and BNP, in metabolic regulation. Among the many potentially beneficial findings, GC-A activation was shown to increase lipid oxidation in transgenic rodents, inhibit fat cell growth, increase oxygen consumption, enhance mitochondrial biogenesis in rodent skeletal muscle, delay gastric emptying, activate adiponectin, convert white adipocytes into brown adipocytes, reduce insulin levels, and improve glucose tolerance (15–23). In addition, a specific human ANP gene mutation, RS5068, increases circulating ANP levels and protects against hypertension and metabolic syndrome (24, 25). Moreover, both hypertension and obesity are related to the reduction of ANP and BNP levels, indicating that the NP system is defective in these cases; therefore, NP treatment is required (26–29). However, owing to the inherent biological properties of NPs, these hormones are now considered to be effective for the treatment of HF and other cardiovascular diseases (such as hypertension) (30–33). Accordingly, in the treatment of human cardiovascular diseases, enhancing the NP system and preventing its degradation by NEP inhibition is a goal worthy of research. The role of NEP inhibition has been explored in animal models and humans, either alone or in combination with the inhibition of other systems involved in cardiovascular disease progression.

In this review, we discuss the relationships between typical TRP family channels and the NP system as well as their respective roles in HF. We also discuss novel drugs introduced for the treatment of HF.

TRANSIENT RECEPTOR POTENTIAL CHANNEL PROTEINS AND ATRIAL NATRIURETIC PEPTIDE

Transient Receptor Potential Cation Channel Subfamily V Member 1 and Atrial Natriuretic Peptide

TRPV1 is a complex component of the ANP cell signaling pathway. The ANP receptor is a guanylate cyclase and antagonist

of the renin-angiotensin-aldosterone system (RAAS). Interaction trap data using the amino and carboxyl termini of intracellular TRPV1 as bait suggested that TRPV1 interacts with NPR1 (GC-A) (13, 34). Activation of the NPR1 and ANP pathway leads to cGMP-dependent stimulation of TRPV1 phosphorylation, thereby inhibiting TRPV1 and reducing the surface current. NPR1-knockout experiments effectively demonstrated the presence of the ANP/NPR1 antihypertrophic pathway in the heart (35). Therefore, the ANP/NPR1/cGMP/protein kinase G (PKG)/TRPV1 linkage mechanism may represent a target for the antifertilization effects of ANP/NPR1. However, further studies are needed to clarify the effects of PKG phosphorylation on TRPV1 (sGC-PKG) because there are two ways to regulate cardiomyocyte function. The PKG pathway, which is regulated by sGC (NO) and pGC (NP), involves PKG phosphorylation, and PKG negatively regulates TRPV1. Data from our recent studies support the negative regulatory effects of NPR1/PKG/TRPV1 phosphorylation; however, in general, compared with protein kinase A and protein kinase C (PKC), the effect of PKG phosphorylation on TRPV1 have not been extensively studied (36–38).

Transient Receptor Potential C6 and Atrial Natriuretic Peptide/B-Type Natriuretic Peptide

In our recent studies, we used an *in vitro* culture system and an *in vivo* genetic engineering model to reveal the functional negative correlations between the ANP/GC-A/cGMP/PKG and TRPC6 calcineurin/fat pathways in cardiomyocytes. ANP directly inhibits the activity of TRPC6 through the cGMP/PKG pathway, thereby blocking the hypertrophic signaling pathway. The selective TRPC inhibitor BTP2 significantly reduces myocardial hypertrophy in GC-A-knockout mice, which are sensitive to the hypertrophic signals caused by TRPC6 overexpression. BTP2 significantly inhibits myocardial hypertrophy caused by chronic infusion of angiotensin II (Ang-II). PKG also inhibits L-type calcium channel (LTCC) activity and calcineurin/nuclear factor of activated T cells (NFAT) signaling (39). In fact, activation of TRPC3/6 has been shown to lead to the activation of LTCC (40), and ANP may inhibit this activation, thereby suppressing calcineurin/NFAT signal transmission. Therefore, the ANP/BNP/cGMP/PKG signaling pathway may inhibit the hypertrophic signaling pathway through multiple steps. ANP and BNP have been used clinically in patients with acute heart failure (31, 41), and the ANP/GC-A/cGMP/PKG signal transduction pathway is a complex pathway involving multiple mechanisms. Therefore, our research shows that inhibition of TRPC6 activity mediates the antihypertrophic effects of ANP/BNP and suggests that inhibition of TRPC6 may prevent pathological effects, providing insights into potential effective treatment strategies for myocardial hypertrophy and remodeling (42).

TRANSIENT RECEPTOR POTENTIAL CHANNEL PROTEINS AND B-TYPE NATRIURETIC PEPTIDE

Among membrane proteins that detect harmful stimuli, sensory neurons (pain receptors) of small and medium diameters express capsaicin (and heat)-sensitive TRP and allicin-1 (TRPV1) channels and/or ATP-gated P2 × 3 subunit receptors (43, 44) to transmit pain. Some studies have shown that TRPV1 is essential for the development of inflammatory heat pain (45–47). The activity of TRPV1 and P2 × 3 receptors is upregulated by endogenous peptides, such as bradykinin, calcitonin gene-related peptide, substance P, and nutritional factors (48–52). The functional effects of these modulators manifest as receptor sensitization, thereby helping to lower the pain threshold and trigger pain, particularly chronic pain.

The NP family, including ANP, BNP, and CNP, are involved in pain sensing. ANP does not affect sensitivity to radiant heat (53) or mechanical ectopic pain (54, 55), whereas CNP is considered an active regulator of chronic pain (56). By contrast, microarray genetic analysis have shown that chronic pain enhances BNP expression and NPR-A, a receptor for BNP, in the rat dorsal root ganglion (DRG). In addition, in a rat model of inflammatory pain, application of BNP reduced the excitability and hyperalgesia of DRG allodynia receptors, suggesting that BNP may have inhibitory roles in chronic pain (57). BNP functions by binding to NPR-A, which is a guanosine cyclase receptor (also sensitive to ANP), and increases intracellular cGMP levels (58, 59). These studies have not explored the molecular mechanisms of GC-A activation and TRPV1 and P2 × 3 receptor changes, and further research is therefore needed to demonstrate whether and how BNP regulates TRPV1 and P2 × 3.

Several intracellular cascades are involved in the trigeminal ganglion (TG). Moreover, TG neurons strongly express NPR-A (in the absence of BNP binding), making TG particularly sensitive to BNP released from various peripheral tissues under physiological and pathological conditions (60). Therefore, the NPR-A system may act as a slow regulator of sensory excitability.

TRANSIENT RECEPTOR POTENTIAL CHANNEL PROTEINS AND C-TYPE NATRIURETIC PEPTIDE

NPR is an enzyme-linked receptor (GC); NPR-A and NPR-B mediate the conduction effects of all NPs in *via* a conventional GC/cGMP/PKG pathway. However, unlike NPR-A and NPR-B, NPR-C lacks the GC kinase domain and therefore acts as an NP clearance receptor (61, 62). Our research shows that functional NPR-A/B/C is expressed in mouse DRG neurons, and CNP and ANP, but not BNP, induce sensitization of TRPV1 channel activity, independent of classic NPR-A/NPR-B/cGMP/PKG signaling. By contrast, NP sensitization of TRPV1 proceeds through atypical NPR-C/Gβγ/phospholipase C (PLC) β/PLC-mediated signaling modules. Specific drugs block these signaling

components, and CNP attenuates the regulation of TRPV1 activity. This modulation of TRPV1 channel activity causes nociceptors to be sensitive to mildly and pathophysiologically related acidic conditions. However, this modulatory mechanism is absent in TRPV1-deficient DRG neurons. In addition, plantar injection of CNP induces thermal hyperalgesia in wild-type mice, but not in TRPV1-deficient mice. Gβγ and TRPV1 inhibitors can be systemically administered to modulate these effects. Overall, these findings indicate that CNP is involved in a novel non-classical Gβγ/PLCβ/PKC/TRPV1 signaling pathway to induce hyperalgesia and thermal hyperalgesia, which may occur under various tissue damage and inflammatory conditions (56).

In general, NPs have substantial effects on inflammatory heat and mechanical allergies. The NPR-A/NPR-B/cGMP/PKG signaling pathway in the central axon of DRG neurons projected to the dorsal horn of the spinal cord promotes mechanical ectopic pain (55, 63, 64), whereas intrathecal BNP induces thermal hyperalgesia and has analgesic effects (57). Our research shows that the PKC/TRPV1 signal in the peripheral afferent nerve is involved in the occurrence of thermal hyperalgesia *via* CNP/Gβγ and NPR-B/NPR-C, which is widely expressed in neurons of all sizes in the DRG. Additionally, the increase in cGMP production in CNP-induced neurons jointly indicates that CNP may be involved in the peripheral sprouting/bifurcation of sensory afferent nerves and induces mechanical effects, including dyskinesia and hyperalgesia. Further studies are required to verify these findings (56).

CNP and ANP have higher affinities for NPR-C than BNP (14, 65). This can explain the lack of BNP-induced TRPV1 currents observed in our work. Based on these findings, we propose a signal module mediated by NPR-C/Gβγ/PLCβ/PLC (56). High concentrations of morphine can directly activate and enhance the TRPV1 currents in mouse DRG neurons (66). Considering that many opioid receptors induce Gαi-coupling downstream signals (67, 68), the sensitization of TRPV1 channel activity by high doses of morphine (66) may involve the Gαi/Gβγ/PLCβ/PKC signaling pathway. This hypothesis still needs to be verified experimentally.

TRANSIENT RECEPTOR POTENTIAL CHANNEL PROTEINS AND HEART FAILURE

Calcium ions participate in many physiological reactions in the human body and play important roles in many cellular reactions. For example, calcium acts as second messenger and blood coagulation factor IV, participates in excitation and contraction coupling, and modulates muscle contraction. Altered intracellular Ca^{2+} helps modulate impaired systolic HF (69, 70). In the myocardium, intracellular Ca^{2+} storage and Ca^{2+} ATP enzymes [sarco endoplasmic reticulum Ca^{2+}-ATPase (SERCA) 2 subtype] play important roles in contraction activation and relaxation. However, in HF, an increase in sodium-calcium exchange (NCX) levels is associated with downregulation of SERCA. In addition, an *in vitro* study using small interfering RNA against myocardial SERCA showed that decreased SERCA2 expression is related to TRPC4, TRPC5, and NCX upregulation, suggesting that deficiency of intracellular storage may be compensated for by entry of Ca^{2+} through the plasma membrane (71). In fact, induced expression of TRPC5 or TRPC6 can be observed in patients with HF (72, 73). The importance of this compensatory mechanism may be related to its universal participation in the Ca^{2+} signaling mechanism, not only for excitation-contraction coupling but also for heart remodeling and hypertrophy.

Myocardial apoptosis is an important process leading to HF; therefore, inhibition of apoptosis is a promising treatment. Apoptosis is induced by various stimuli, including oxidative stress, pro-inflammatory cytokines, catecholamines, and Ang-II (74). Elevated intracellular Ca^{2+} is considered a key initiator of intracellular apoptosis signal transduction (for example, activation of endogenous endonucleases dependent on Ca^{2+}). Currently, there are two reports of TRP channels being involved in myocardial apoptosis in animal models. Activation of the TRPM2 channel and poly (ADP-ribose) polymerase (PARP) is involved in cardiomyocyte death induced by oxidative stress (75, 76). The apoptotic component is caused by activation of the clotrimazle-sensitive NAD^{+}/ADP ribose/PARP-dependent TRPM2 channel, which induces mitochondrial Na^{+} and Ca^{2+} overload, leading to mitochondrial membrane rupture, cytochrome release, and caspase-3-dependent chromatin condensation/fragmentation. Moreover, TRPC7 may be the key initiator of AT1 activation, leading to myocardial apoptosis, and could then participate in the progression of HF (77). Although these findings provide possible strategies for regulating cardiac apoptosis, further research is needed to clarify the complex relationships between TRP and HF.

NATRIURETIC PEPTIDES AND HEART FAILURE

NPs, particularly BNP, play critical roles in the diagnosis of HF. The accuracy of HF severity assessment is directly related to clinical outcomes of treatment in patients. BNP levels are the most commonly used index in clinical practice. The diagnostic roles of NPs in acute and chronic HF have been confirmed. In particular, ANP and BNP levels increase in parallel with the degree of left ventricular dysfunction and hemodynamic pressure, although they are not helpful in distinguishing between systolic and diastolic HF (78). In addition, in cases of acute and chronic HF, the value of NPs as reliable markers for long-term prognostic stratification has been demonstrated. In a study of patients with acute HF, BNP, NT-proBNP, and mid-region (MR) proBNP levels showed significant diagnostic performance, although only MR-proBNP had long-term prognostic value (79). In patients hospitalized due to acute decompensated HF (ADHF), the prognostic performance of NT-proBNP and MR-pro-ANP levels was confirmed by evidence of the increased prognostic value of clinical risk factors for predicting mortality within 1 year of onset (80). In patients with chronic HF, subsequent measurements of BNP or NT-proBNP levels provide independent information about the risk of disease progression, which involves a series

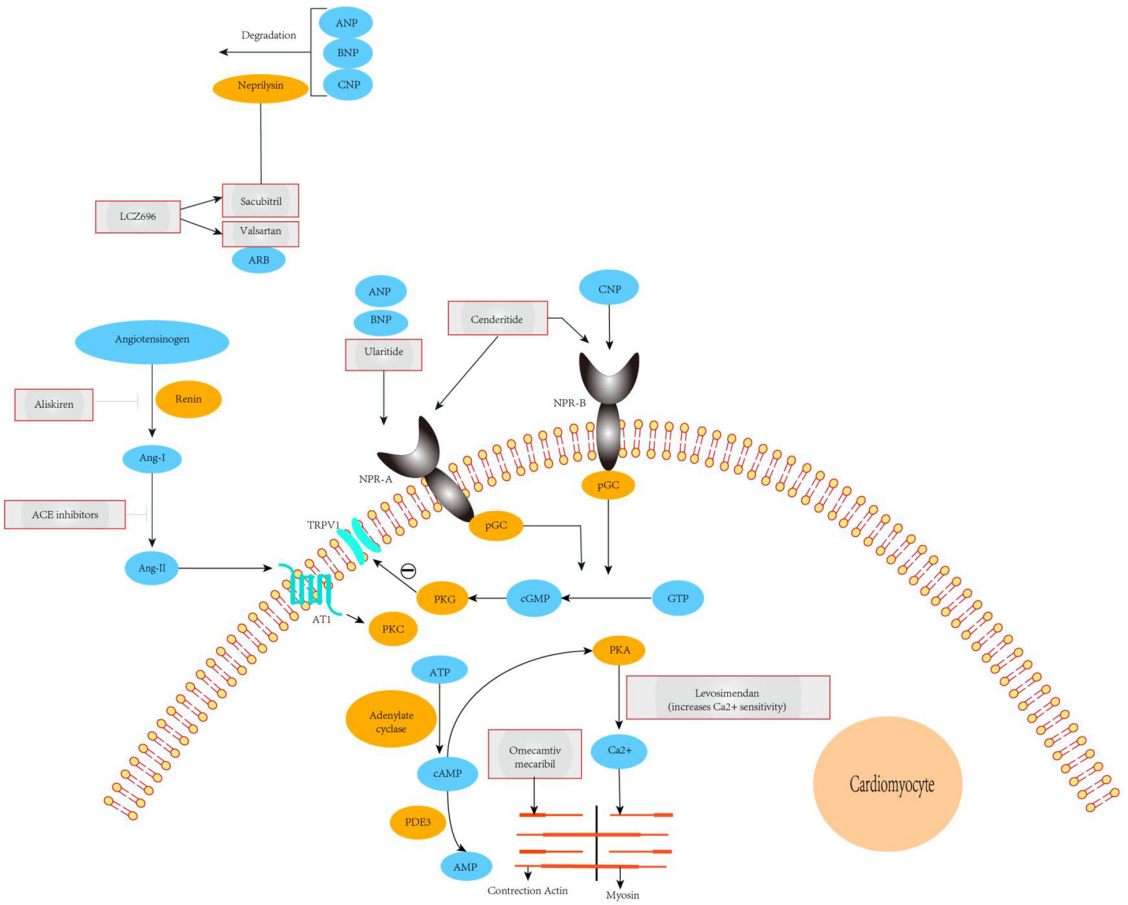

FIGURE 2 | Mechanisms of action of novel therapeutics for heart failure. The ARNi LCZ696 is split into the ARB valsartan and the neprilysin-inhibitor sacubitril. Valsartan abrogates signaling *via* the AT1 receptor, inhibiting deleterious effects mediated by Ang-II such as vasoconstriction, hypertrophy, and fibrosis in major cardiovascular organs. Sacubitril prevents breakdown of endogenous natriuretic peptides (ANP, BNP, and CNP), thereby augmenting their beneficial actions in cardiovascular disease. The overall effects of ARNi are vasodilatation, natriuresis, and diuresis, as well as inhibition of fibrosis and hypertrophy. Ularitide selectively targets NPR-A, whereas cenderitide activates both NPR-A and NPR-B. Both peptides increase intracellular cGMP, which in turn leads to inhibition of the renin-angiotensin-aldosterone system and attenuation of fibrosis, hypertrophy, and vasoconstriction. Our proposed model shows that TRPV1 interacting with NPR-A, activation of the NPR1 and ANP pathway leads to cGMP-dependent stimulation ofTRPV1 phosphorylation. PDE3 antagonists (enoximone, milrinone), calcium sensitizers (levosimendan), and a direct activator of cardiac myosin (omecamtiv mecarbil). ACE, angiotensin-converting enzyme; TRPV1, transient receptor potential cation channel subfamily V member 1; Ang-I/II, angiotensin I/II; ARB, angiotensin-receptor blocker; ARNi, angiotensin receptor-neprilysin inhibitor; AT1, type-1 angiotensin II receptor; ANP, A-type natriuretic peptide; BNP, B-type natriuretic peptide; CNP, C-type natriuretic peptide; NPR-A/B, atrial natriuretic peptide receptor 1/2; PDE3, phosphodiesterase-3; pGC, plasma- membrane-bound guanylate cyclase; PKA, protein kinase A; PKC, protein kinase C; PKG, protein kinase G; pGC, plasma- membrane-bound guanylate cyclase; sGC, soluble guanylate cyclase.

of adverse consequences, including ventricular remodeling, malignant ventricular arrhythmia, HF-related hospitalization, transplantation need, and death (81). In the longest follow-up study of patients with chronic HF, the prognostic ability of multiple biomarkers was evaluated, and the results showed that the plasma ANP level was the strongest long-term predictor of death during all disease stages (82). NPs have prognostic value in patients with HF with reduced ejection fraction (HFrEF) and HF with retention of ejection fraction (HFpEF) (83). Recent studies have shown that screening based on BNP has preventive effects on HF development. In patients with cardiovascular risk factors and those at risk of HF, BNP assessment related to combination therapy reduces the combined incidence of left ventricular systolic dysfunction, diastolic dysfunction, and HF (84).

The clinical significance of NPs in HF indicates that NP level measurement is an effective tools for hormone-guided treatment of HF. In ADHF, BNP measurement improves the accuracy of diagnosis, reduces the hospitalization and admission rates in the intensive care unit, and has beneficial effects on treatment costs and mortality (85). A useful algorithm was developed to treat ADHF guided by BNP (85). Additionally, in chronic HF, NP levels are useful markers for monitoring disease progression related to the benefits of different treatment strategies (86). However, because of uncertainty among studies, the American Heart Association/American College of Cardiology HF guidelines recommend a low level of NP-guided treatment for patients with chronic HF (87). A recent meta-analysis attempted to overcome existing controversies, including randomized

clinical trials, which showed that in patients with chronic HF, NP-guided treatment reduces all-cause mortality and HF-related hospitalization (88).

ANGIOTENSIN RECEPTOR-NEPRILYSIN INHIBITORS AND HEART FAILURE

NEP is a neutral endopeptidase responsible for the degradation of endogenous vasoactive substances in the body, including NPs (ANP, BNP, and CNP), bradykinin, and adrenal medulla hormones. BNP, which is synthesized and secreted by ventricular myocytes, can promote sodium excretion and diuresis and has strong vasodilator effects. The use of pharmacological drugs to reduce the catabolism and elimination of endogenous NPs has been applied in clinical practice. Indeed, sacubitril combined with valsartan to inhibit NEP has been shown to be a successful method for the treatment of arterial hypertension, chronic congestive HF, and myocardial fibrosis. Sacubitril and valsartan sodium are novel types of anti-HF drugs. Valsartan is an angiotensin receptor antagonist that inhibits the RAAS, thereby expanding blood vessels, lowering blood pressure, inhibiting myocardial remodeling, and blocking abnormal activation of the nerve and endocrine system. By contrast, sacubitril is an NEP. The three types of NPs are inactivated by receptor-mediated internalization and lysosomal degradation, followed by enzymatic neutral endopeptidase or NEP degradation. Recent studies have shown that, compared with enalapril, NEP inhibition can moderately increase BNP levels and enhance levels of endogenous brain NP, thereby dilating blood vessels, inducing diuresis, improving myocardial remodeling, and exerting other cardioprotective effects. The combination of the two constitutes sacubitril and valsartan sodium can be used for the treatment of various cardiovascular diseases, including hypertension, HF, and coronary heart disease (**Figure 2**). Sacubitril and valsartan sodium can also inhibit the adverse effects of the RAAS and activate the cardiovascular protective effect of enkephalins. Therefore, drugs involving the combination of both of these components may be suitable for the treatment of patients with HF.

In a prospective study, the effects of angiotensin receptor-neprilysin inhibitors and angiotensin-converting-enzyme inhibitors (ACEIs) on the global mortality and morbidity of heart failure (PARADIGM-HF) were compared. In this multicenter trial, 8,442 patients with reduced ejection fraction and NYHA class II–IV were randomly assigned to the treatment group and received valsartan/sacubitril 200 mg/2 days or enalapril 10 mg/2 days (89–91). After a median follow-up of 27 months, 21.8% of patients in the valsartan/sacubitril group died from cardiovascular causes or were hospitalized for HF compared with 26.5% in the enalapril group; the risk was reduced by 20% ($p < 0.001$) (89). There were no differences between the two groups in the incidence of new-onset atrial fibrillation or decreased renal function. In terms of drug side effects, the incidence of symptomatic hypotension in the valsartan/sacubitril group was higher than that in the enalapril group (14% versus 9.2%, $p < 0.001$), whereas patients in the enalapril treatment group had cough and increased serum creatinine (2.5 mg/dL or higher). Additionally, the incidence of hyperkalemia was significantly higher in the valsartan/sacubitril group than in the enalapril group. During the double-blind treatment, 19 patients in the valsartan/sacubitril group developed angioedema, and 10 patients in the enalapril group developed angioedema. Compared with ACEIs alone, the combined use of ACEIs and the heparanase inhibitor omapatrilat increased the risk of angioedema threefold (92). Thus, valsartan/sacubitril, the first combined ARNI/nephrase inhibitor, can reduce mortality in patients with HFrEF. Ongoing clinical trials will determine its efficacy in other conditions, including hypertension and HFpEF (93).

At present, heart failure is divided into three categories. The first category is heart failure with preserved ejection fraction, the second category is heart failure with reduced ejection fraction, and the third category is heart failure with intermediate ejection fraction. The diagnosis standard needs to be calculated according to 50 and 40%, that is, if the patient's ejection fraction $\geq$50%, it belongs to heart failure with preserved ejection fraction. If the patient's ejection fraction is less than or equal to 40%, it is classified as heart failure with reduced ejection fraction. If the patient's ejection fraction is between 40 and 50%, 50 and 40% are not included, which belong to the heart failure in the middle position of the ejection fraction. Under normal circumstances, the earliest occurrence of heart failure is diastolic dysfunction, and with the gradual decline of diastolic function, it will gradually progress to heart failure with median ejection fraction or heart failure with reduced ejection fraction. Heart failure with preserved ejection fraction refers more to the early stage of heart failure.

For patients with chronic HFrEF, ACEI, ARB, and ARNI can be used as first-line therapy. The PARADIGM-HF study confirmed that ARNI can bring greater benefit to patients with chronic HFrEF than ACEI; but a large number of previous studies have confirmed the efficacy of RAAS inhibitors in patients with HFrEF, but these two types of drugs have poor efficacy in patients with HFpEF, which may be due to the low importance of RAAS system abnormalities in the pathophysiological mechanism of HFpEF. Among them, ARNI can significantly reduce the rate of heart failure hospitalization, but fails to reduce the composite endpoint of cardiovascular death and total heart failure hospitalization in patients with heart failure with LVEF $\geq$ 45% (94).

SUMMARY AND PERSPECTIVES

The TRP family is closely related to the NP family; however, the specific molecular mechanisms remain unclear. TRPs are activated by similar prohypertrophic or profibrotic stimuli and are related to or interact to activate hypertrophy-, fibrosis-, and conduction disorder-related signaling pathways. Unfortunately, common agonists and antagonists used to modulate TRP have not been able to determine which TRP channel proteins may be the correct targets and potential therapeutic tools. Decades of research have outlined the important contributions

of NPs in cardiovascular diseases. In addition to evaluating their diagnostic functions, particularly in HF, TRP channel proteins have important predictive significance for HF and hypertension. Based on the extensive effects of these hormones in the cardiovascular system, NP-derived treatments are currently considered reasonable treatments for cardiovascular diseases. Drugs to treat HF have always been limited and are typically based on RAAS and SNS suppression. In recent years, with the development of ARNI, i.e., sacubitril/valsartan (LCZ696), as the first combined angiotensin receptor antagonist/renal protease inhibitor, the mortality rates in patients with HFrEF have decreased, and its effectiveness and safety have been confirmed. However, the specific mechanisms are still unclear. Moreover, it is still unknown whether the clinical benefit of valsartan/sacubitril is driven by reducing the degradation of NPs or whether other mechanisms function to alleviate symptoms of HF by combining angiotensin receptor antagonists and renin inhibitors. In addition, ARNI is used in patients with clinical HF, and the incidence of angioedema during treatment is still not known. Further studies are needed to address these questions and improve our understanding of clinical HF in order to establish novel treatment strategies in these patients.

AUTHOR CONTRIBUTIONS

KD contributed to ideas, formulation, and evolution of the research goals. XH imagined and made the figures. YG and LY contributed to the preparation of the published work and especially writing the initial part. LW ensured that the descriptions are accurate and agreed by all authors.

REFERENCES

1. Clapham DE, Runnels LW, Strubing C. The TRP ion channel family. *Nat Rev Neurosci.* (2001) 2:387–96.
2. Montell C, Birnbaumer L, Flockerzi V. The TRP channels, a remarkably functional family. *Cell.* (2002) 108:595–8. doi: 10.1016/s0092-8674(02)00670-0
3. Watanabe H, Murakami M, Ohba T, Takahashi Y, Ito H. TRP channel and cardiovascular disease. *Pharmacol Ther.* (2008) 118:337–51. doi: 10.1016/j.pharmthera.2008.03.008
4. de Bold AJ, Borenstein HB, Veress AT, Sonnenberg H. A rapid and potent natriuretic response to intravenous injection of atrial myocardial extract in rats. *Life Sci.* (1981) 28:89–94. doi: 10.1016/0024-3205(81)90370-2
5. Sudoh T, Kangawa K, Minamino N, Matsuo H. A new natriuretic peptide in porcine brain. *Nature.* (1988) 332:78–81. doi: 10.1038/332078a0
6. Heublein DM, Clavell AL, Stingo AJ, Lerman A, Wold L, Burnett JC Jr. C-type natriuretic peptide immunoreactivity in human breast vascular endothelial cells. *Peptides.* (1992) 13:1017–9. doi: 10.1016/0196-9781(92)90065-b
7. Cataliotti A, Giordano M, De Pascale E, Giordano G, Castellino P, Jougasaki M, et al. CNP production in the kidney and effects of protein intake restriction in nephrotic syndrome. *Am J Physiol Renal Physiol.* (2002) 283:F464–72. doi: 10.1152/ajprenal.00372.2001
8. Mukoyama M, Nakao K, Hosoda K, Suga S, Saito Y, Ogawa Y, et al. Brain natriuretic peptide as a novel cardiac hormone in humans. Evidence for an exquisite dual natriuretic peptide system,atrial natriuretic peptide and brain natriuretic peptide. *J Clin Invest.* (1991) 87:1402–12. doi: 10.1172/JCI115146
9. Chen HH, Cataliotti A, Schirger JA, Martin FL, Burnett JC Jr. Equimolar doses of atrial and brain natriuretic peptides and urodilatin have differential renal actions in overt experimental heart failure. *Am J Physiol Regul Integr Comp Physiol.* (2005) 288:R1093–7. doi: 10.1152/ajpregu.00682.2004
10. Tsuruda T, Boerrigter G, Huntley BK, Noser JA, Cataliotti A, Costello-Boerrigter LC, et al. Brain natriuretic peptide is produced in cardiac fibroblasts and induces matrix metalloproteinases. *Circ Res.* (2002) 91:1127–34. doi: 10.1161/01.res.0000046234.73401.70
11. Chen HH, Burnett JC Jr. C-type natriuretic peptide: the endothelial component of the natriuretic peptide system. *J Cardiovasc Pharmacol.* (1998) 32:S22–8.
12. Charles CJ, Espiner EA, Nicholls MG, Richards AM, Yandle TG, Protter A, et al. Clearance receptors and endopeptidase 24.11: equal role in natriuretic peptide metabolism in conscious sheep. *Am J Physiol.* (1996) 271:R373–80. doi: 10.1152/ajpregu.1996.271.2.R373
13. Kuhn M. Molecular physiology of natriuretic peptide signalling. *Basic Res Cardiol.* (2004) 99:76–82. doi: 10.1007/s00395-004-0460-0
14. Anand-Srivastava MB. Natriuretic peptide receptor-C signaling and regulation. *Peptides.* (2005) 26:1044–59. doi: 10.1016/j.peptides.2004.09.023
15. Mitsuishi M, Miyashita K, Itoh H. cGMP rescues mitochondrial dysfunction induced by glucose and insulin in myocytes. *Biochem Biophys Res Commun.* (2008) 367:840–5. doi: 10.1016/j.bbrc.2008.01.017
16. Miyashita K, Itoh H, Tsujimoto H, Tamura N, Fukunaga Y, Sone M, et al. Natriuretic peptides/cGMP/cGMP-dependent protein kinase cascades promote muscle mitochondrial bio-genesis and prevent obesity. *Diabetes.* (2009) 58:2880–92. doi: 10.2337/db09-0393
17. Sarzani R, Marcucci P, Salvi F, Bordicchia M, Espinosa E, Mucci L, et al. Angiotensin II stimulates NEP inhibition in CV disease893 and atrial natriuretic peptide inhibits human visceral adipocyte growth. *Int J Obes.* (2008) 32:259–67. doi: 10.1038/sj.ijo.0803724
18. Bordicchia M, Liu D, Amri EZ, Ailhaud G, Dessi-Fulgheri P, Zhang C, et al. Cardiac natriuretic peptides act via p38 MAPK to induce the brown fat thermogenic program in mouse and human adipocytes. *J Clin Invest.* (2012) 122:1022–36. doi: 10.1172/JCI59701
19. Addisu A, Gower WR Jr., Landon CS, Dietz JR. B-type natriuretic peptide decreases gastric emptying and absorption. *Exp Biol Med.* (2008) 233:475–82. doi: 10.3181/0708-RM-216
20. Meirhaeghe A, Sandhu MS, McCarthy MI, de Groote P, Cottel D, Arveiler D, et al. Association between the T-381C polymorphism of the brain natriuretic peptide gene and risk of type 2 diabetes in human populations. *Hum Mol Genet.* (2007) 16:1343–50. doi: 10.1093/hmg/ddm084
21. Choquet H, Cavalcanti-Proenca C, Lecoeur C, Dina C, Cauchi S, Vaxillaire M, et al. The T-381C SNP in BNP gene may be modestly associated with type 2 diabetes: an updated meta-analysis in 49 279 subjects. *Hum Mol Genet.* (2009) 18:2495–501. doi: 10.1093/hmg/ddp169
22. Tsukamoto O, Fujita M, Kato M, Yamazaki S, Asano Y, Ogai A, et al. Natriuretic peptides enhance the production of adiponectin in human adipocytes and in patients with chronic heart failure. *J Am Coll Cardiol.* (2009) 53:2070–7. doi: 10.1016/j.jacc.2009.02.038
23. Birkenfeld AL, Budziarek P, Boschmann M, Moro C, Adams F, Franke G, et al. Atrial natriuretic peptide induces postprandial lipid oxidation in humans. *Diabetes.* (2008) 57:3199–204. doi: 10.2337/db08-0649
24. Newton-Cheh C, Larson MG, Vasan RS, Levy D, Bloch KD, Surti A, et al. Association of common variants in NPPA and NPPB with circulating natriuretic peptides and blood pressure. *Nat Genet.* (2009) 41:348–53. doi: 10.1038/ng.328
25. Cannone V, Boerrigter G, Cataliotti A, Costello-Boerrigter LC, Olson TM, McKie PM, et al. A genetic variant of the atrial natriuretic peptide gene is associated with cardiometabolic protection in the general community. *J Am Coll Cardiol.* (2011) 58:629–36. doi: 10.1016/j.jacc.2011.05.011
26. Magnusson M, Jujic A, Hedblad B, Engstrom G, Persson M, Struck J, et al. Low plasma level of atrial natriuretic peptide predicts development of diabetes: the prospective Malmo Diet and Cancer study. *J Clin Endocrinol Metab.* (2012) 97:638–45. doi: 10.1210/jc.2011-2425

27. Wang TJ, Larson MG, Levy D, Benjamin EJ, Leip EP, Wilson PW, et al. Impact of obesity on plasma natriuretic peptide levels. *Circulation.* (2004) 109:594–600.
28. Belluardo P, Cataliotti A, Bonaiuto L, Giuffre E, Maugeri E, Noto P, et al. Lack of activation of molecular forms of the BNP system in human grade 1 hypertension and relationship to cardiac hypertrophy. *Am J Physiol Heart Circ Physiol.* (2006) 291:H1529–35. doi: 10.1152/ajpheart.00107.2006
29. Macheret F, Heublein D, Costello-Boerrigter LC, Boerrigter G, McKie P. Human hypertension is characterized by a lack of activation of the anti-hypertensive cardiac hormones ANP and BNP. *J Am Coll Cardiol.* (2011) 57:1386–95.
30. Publication Committee for the VMAC Investigators. Intravenous nesiritide vs nitroglycerin for treatment of decompensated congestive heart failure: a randomized controlled trial. *J Am Med Assoc.* (2002) 287:1531–40. doi: 10.1001/jama.287.12.1531
31. Colucci WS, Elkayam U, Horton DP, Abraham WT, Bourge RC, Johnson AD, et al. Intravenous nesiritide, a natriuretic peptide, in the treatment of decompensated congestive heart failure. Nesiritide Study Group. *N Engl J Med.* (2000) 343:246–53. doi: 10.1056/NEJM200007273430403
32. Hobbs RE, Mills RM, Young JB. An update on nesiritide for treatment of decompensated heart failure. *Expert Opin Investig Drugs.* (2001) 10:935–42. doi: 10.1517/13543784.10.5.935
33. Boerrigter G, Burnett JC Jr. Recent advances in natriuretic peptides in congestive heart failure. *Expert Opin Investig Drugs.* (2004) 13:643–52. doi: 10.1517/13543784.13.6.643
34. Tremblay J, Desjardins R, Hum D, Gutkowska J, Hamet P. Biochemistry and physiology of the natriuretic peptide receptor guanylyl cyclases. *Mol Cell Biochem.* (2002) 230:31–47.
35. Molkentin JD. A friend within the heart: natriuretic peptide receptor signaling. *J Clin Invest.* (2003) 111:1275–7. doi: 10.1172/JCI18389
36. Jin Y, Kim J, Kwak J. Activation of the cGMP/protein kinase G pathway by nitric oxide can decrease TRPV1 activity in cultured rat dorsal root ganglion neurons. *Korean J Physiol Pharmacol.* (2012) 16:211–7. doi: 10.4196/kjpp.2012.16.3.211
37. Bhave G, Hu HJ, Glauner KS, Zhu W, Wang H, Brasier DJ, et al. Protein kinase C phosphorylation sensitizes but does not activate the capsaicin receptor transient receptor potential vanilloid 1 (TRPV1). *Proc Natl Acad Sci USA.* (2003) 100:12480–5. doi: 10.1073/pnas.2032100100
38. Mohapatra DP, Nau C. Regulation of Ca2+-dependent desensitization in the vanilloid receptor TRPV1 by cal- cineurin and cAMP-dependent protein kinase. *J Biol Chem.* (2005) 280:13424–32. doi: 10.1074/jbc.M410917200
39. Fiedler B, Lohmann SM, Smolenski A, Linnemuller S, Pieske B, Schroder F, et al. Inhibition of calcineurin-NFAT hypertrophy signaling by cGMP-dependent protein kinase type I in cardiac myocytes. *Proc Natl Acad Sci USA.* (2002) 99:11363–8. doi: 10.1073/pnas.162100799
40. Onohara N, Nishida M, Inoue R, Kobayashi H, Sumimoto H, Sato Y, et al. TRPC3 and TRPC6 are essential for angiotensin II-induced cardiac hypertrophy. *EMBO J.* (2006) 25:5305–16. doi: 10.1038/sj.emboj.7601417
41. Yoshimura M, Yasue H, Ogawa H. Pathophysiological significance and clinical application of ANP and BNP in patients with heart failure. *Can J Physiol Pharmacol.* (2001) 79:730–5. doi: 10.1139/y01-039
42. Kinoshita H, Kuwahara K, Nishida M, Jian Z, Rong X, Kiyonaka S, et al. Inhibition of TRPC6 channel activity contributes to the antihypertrophic effects of natriuretic peptides-guanylyl cyclase-A signaling in the heart. *Circ Res.* (2010) 106:1849–60. doi: 10.1161/CIRCRESAHA.109.208314
43. Julius D, Basbaum AI. Molecular mechanisms of nociception. *Nature.* (2001) 413:203–10. doi: 10.1038/35093019
44. North RA. The P2X3 subunit: a molecular target in pain therapeutics. *Curr Opin Investig Drugs.* (2003) 4:833–40.
45. Caterina MJ, Leffler A, Malmberg AB, Martin WJ, Trafton J, Petersen-Zeitz KR, et al. Impaired nociception and pain sensation in mice lacking the capsaicin receptor. *Science.* (2000) 288:306–13. doi: 10.1126/science.288.5464.306
46. Davis JB, Gray J, Gunthorpe MJ, Hatcher JP, Davey PT, Overend P, et al. Vanilloid receptor-1 is essential for inflammatory thermal hyperalgesia. *Nature.* (2000) 405:183–7. doi: 10.1038/35012076
47. Gavva NR, Tamir R, Qu Y, Klionsky L, Zhang TJ, Immke D, et al. AMG9810 [(E)-3-(4-t-butylphenyl)-N-(2,3-dihydrobenzo[b][1,4] dioxin-6-yl)acrylamide], a novel vanilloid receptor 1 (TRPV1) antagonist with antihyperalgesic properties. *J Pharmacol Exp Ther.* (2005) 313:474–84. doi: 10.1124/jpet.104.079855
48. Premkumar LS, Abooj M. TRP channels and analgesia. *Life Sci.* (2013) 92:415–24. doi: 10.1016/j.lfs.2012.08.010
49. Park CK, Bae JH, Kim HY, Jo HJ, Kim YH, Jung SJ, et al. Substance Psensitizes P2X3 in nociceptive trigeminal neurons. *J Dent Res.* (2010) 89:1154–9. doi: 10.1177/0022034510377094
50. Giniatullin R, Nistri A, Fabbretti E. Molecular mechanisms of sensitization of pain-transducing P2X3 receptors by the migraine mediators CGRP and NGF. *Mol Neurobiol.* (2008) 37:83–90. doi: 10.1007/s12035-008-8020-5
51. Simonetti M, Giniatullin R, Fabbretti E. Mechanisms mediating the enhanced gene transcription of P2X3 receptor by calcitonin gene- related peptide in trigeminal sensory neurons. *J Biol Chem.* (2008) 283:18743–52. doi: 10.1074/jbc.M800296200
52. Tang H-B, Li Y-S, Miyano K, Nakata Y. Phosphorylation of TRPV1 by neurokinin-1 receptor agonist exaggerates the capsaicin-mediated substance P release from cultured rat dorsal root ganglion neurons. *Neuropharmacology.* (2008) 55:1405–11. doi: 10.1016/j.neuropharm.2008.08.037
53. Azarov AV, Szabó G, Telegdy G. Effects of atrial natriuretic peptide on acute and chronic effects of morphine. *Pharmacol Biochem Behav.* (1992) 43:193–7. doi: 10.1016/0091-3057(92)90657-2
54. Heine S, Michalakis S, Kallenborn-Gerhardt W, Lu R, Lim H-Y. CNGA3: a target of spinal nitric oxide/cGMP signaling and modulator of inflammatory pain hypersensitivity. *J Neurosci.* (2011) 31:11184–92. doi: 10.1523/JNEUROSCI.6159-10.2011
55. Schmidtko A, Gao W, König P, Heine S, Motterlini R, Ruth P, et al. cGMP produced by NO-sensitive guanylyl cyclase essentially contributes to inflammatory and neuropathic pain by using targets different from cGMP-dependent protein kinase I. *J Neurosci.* (2008) 28:8568–76. doi: 10.1523/JNEUROSCI.2128-08.2008
56. Loo L, Shepherd AJ, Mickle AD, Lorca RA, Shutov LP, Usachev YM, et al. The C-type natriuretic peptide induces thermal hyperalgesia through a noncanonical Gβγ-dependent modulation of TRPV1 channel. *J Neurosci.* (2012) 32:11942–55. doi: 10.1523/JNEUROSCI.1330-12.2012
57. Zhang FX, Liu XJ, Gong LQ, Yao JR, Li KC, Li ZY, et al. Inhibitionof inflammatory pain by activating B-type natriuretic peptide signal pathway in nociceptive sensory neurons. *J Neurosci.* (2010) 30:10927–38. doi: 10.1523/JNEUROSCI.0657-10.2010
58. Misono KS. Natriuretic peptide receptor: structure and signaling. *Mol Cell Biochem.* (2002) 230:49–60. doi: 10.1023/A:1014257621362
59. Hofmann F, Feil R, Kleppisch T, Schlossmann J. Function of cGMP-dependent protein kinases as revealed by gene deletion. *Physiol Rev.* (2006) 86:1–23. doi: 10.1152/physrev.00015.2005
60. Potter LR, Yoder AR, Flora DR, Antos LK, Dickey DM. Natriuretic peptides: their structures, receptors, physiologic functions and therapeutic applications. *Handb Exp Pharmacol.* (2009) 191:341–66. doi: 10.1007/978-3-540-68964-5_15
61. Pandey KN. Natriuretic peptides and their receptors. *Peptides.* (2005) 26:899–900. doi: 10.1016/j.peptides.2005.03.055
62. Potter LR, Abbey-Hosch S, Dickey DM. Natriuretic peptides, their receptors, and cyclic guanosine monophosphate-dependent signaling functions. *Endocr Rev.* (2006) 27:47–72. doi: 10.1210/er.2005-0014
63. Schmidtko A, Gao W, Sausbier M, Rauhmeier I, Sausbier U, Niederberger E, et al. Cysteine-rich protein 2, a novel down-stream effector of cGMP/cGMP-dependent protein kinase I-mediated persistent inflammatory pain. *J Neurosci.* (2008) 28:1320–30. doi: 10.1523/JNEUROSCI.5037-07.2008
64. Heine S, Michalakis S, Kallenborn-Gerhardt W, Lu R, Lim HY, Weiland J, et al. CNGA3: a target of spinal nitric oxide/cGMP signaling and modulator of inflammatory pain hypersensitivity. *J Neurosci.* (2011) 31:11184–92.
65. He XI, Chow DC, Martick MM, Garcia KC. Allosteric activation of a spring-loaded natriuretic peptide receptor dimer by hormone. *Science.* (2001) 293:1657–62. doi: 10.1126/science.1062246
66. Forster AB, Reeh PW, Messlinger K, Fischer MJ. High concentrations of morphine sensitize and activate mouse dorsal root ganglia via TRPV1 and TRPA1 receptors. *Mol Pain.* (2009) 5:17. doi: 10.1186/1744-8069-5-17
67. Standifer KM, Pasternak GW. G proteins and opioid receptor-mediated signalling. *Cell Signal.* (1997) 9:237–48. doi: 10.1016/s0898-6568(96)00174-x

68. Stein C. Opioid receptors on peripheral sensory neurons. *Adv Exp Med Biol.* (2003) 521:69–76.
69. Prestle J, Quinn FR, Smith GL. Ca(2+)-handling proteins and heart failure:novel molecular targets?. *Curr Med Chem.* (2003) 10:967–81. doi: 10.2174/0929867033457656
70. Bers DM, Despa S, Bossuyt J. Regulation of Ca2+and Na+in normal and failing cardiac myocytes. *Ann N Y Acad Sci.* (2006) 1080:165–77. doi: 10.1196/annals.1380.015
71. Seth M, Sumbilla C, Mullen SP, Lewis D, Klein MG, Hussain A, et al. Sarco (endo)plasmic reticulum Ca2+ATPase (SERCA) gene silencing and remodeling of the Ca2+signaling mechanism in cardiac myocytes. *Proc Natl Acad Sci USA.* (2004) 101:16683–8. doi: 10.1073/pnas.0407537101
72. Kuwahara K, Wang Y, McAnally J, Richardson JA, Bassel-Duby R, Hill JA, et al. TRPC6 fulfills a calcineurin signaling circuit during pathologic cardiac remodeling. *J Clin Invest.* (2006) 116:3114–26. doi: 10.1172/JCI27702
73. Bush EW, Hood DB, Papst PJ, Chapo JA, Minobe W, Bristow MR, et al. Canonical transient receptor potential channels promote cardiomyocyte hypertrophy through activation of calcineurin signaling. *J Biol Chem.* (2006) 281:33487–96. doi: 10.1074/jbc.M605536200
74. Kang PM, Izumo S. Apoptosis in heart: basic mechanisms and implications in cardiovascular diseases. *Trends Mol Med.* (2003) 9:177–82. doi: 10.1016/s1471-4914(03)00025-x
75. Yang KT, Chang WL, Yang PC, Chien CL, Lai MS, Su MJ, et al. Activation of the transient receptor potential M2 channel and poly(ADP-ribose) polymerase is involved in oxidative stress-induced cardiomyocyte death. *Cell Death Differ.* (2006) 13:1815–26. doi: 10.1038/sj.cdd.4401813
76. Yang XR, Lin MJ, McIntosh LS, Sham JS. Functional expression of transient receptor potential melastatin- and vanilloid-related channels in pulmonary arterial and aortic smooth muscle. *Am J Physiol Lung Cell Mol Physiol.* (2006) 290:L1267–76. doi: 10.1152/ajplung.00515.2005
77. Satoh S, Tanaka H, Ueda Y, Oyama J, Sugano M, Sumimoto H, et al. Transient receptor potential (TRP) protein 7 acts as a G protein-activated Ca2+ channel mediating angiotensin II-induced myocardial apoptosis. *Mol Cell Biochem.* (2007) 294:205–15. doi: 10.1007/s11010-006-9261-0
78. Schrier RW, Abraham WT. Hormones and hemodynamics in heart failure. *N Engl J Med.* (1999) 341:577–85. doi: 10.1056/nejm199908193410806
79. Seronde MF, Gayat E, Logeart D, Lassus J, Laribi S, Boukef R, et al. Comparison of the diagnostic and prognostic values of B-type and atrial-type natriuretic peptides in acute heart failure. *Intern J Cardiol.* (2013) 168:3404–11. doi: 10.1016/j.ijcard.2013.04.164
80. Lassus J, Gayat E, Mueller C, Peacock WF, Spinar J, Harjola V-P, et al. Incremental value of biomarkers to clinical variables for mortality prediction in acutely decompensated heart failure: the Multinational Observational Cohort on Acute Heart Failure (MOCA) study. *Int J Cardiol.* (2013) 168:2186–94. doi: 10.1016/j.ijcard.2013.01.228
81. Boerrigter G, Costello-Boerrigter LC, Burnett JC Jr. Natriuretic peptides in the diagnosis and management of chronic heart failure. *Heart Fail Clin.* (2009) 5:501–14. doi: 10.1016/j.hfc.2009.04.002
82. Volpe M, Francia P, Tocci G, Rubattu S, Cangianiello S, Rao MAE, et al. Prediction of long-term survival in chronic heart failure by multiple biomarker assessment: a 15-year prospective follow-up study. *Clin Cardiol.* (2010) 33:700–7. doi: 10.1002/clc.20813
83. van Veldhuisen DJ, Linssen GC, Jaarsma T, van Gilst WH, Hoes AW, Tijssen JG, et al. B-type natriuretic peptide and prognosis in heart failure patients with preserved and reduced ejection fraction. *J Am Coll Cardiol.* (2013) 61:1498–506. doi: 10.1016/j.jacc.2012.12.044
84. Ledwidge M, Gallagher J, Conlon C, Tallon E, O'Connell E, Dawkins I, et al. Natriuretic peptide-based screening and collaborative care for heart failure: the STOP-HF randomized trial. *JAMA.* (2013) 310:66–74. doi: 10.1001/jama.2013.7588
85. Bhardwaj A, Januzzi JL. Natriuretic peptide-guided management of acutely destabilized heart failure. Rationale and treatment algorithm. *Crit Pathw Cardiol.* (2009) 8:146–50. doi: 10.1097/HPC.0b013e3181c4a0c6
86. Motiwala SR, Januzzi JL. The role of natriuretic peptides as biomarkers for guiding the management of chronic heart failure. *Clin Pharm Ther.* (2013) 93:57–67. doi: 10.1038/clpt.2012.187
87. Jessup M, Abraham WT, Casey DE, Feldman AM, Francis GS, Ganiats TG, et al. 2009 Focused update: ACCF/AHA guidelines for the diagnosis and management of heart failure in adults: a report of the American College of Cardiology Foundation/American Heart Association Task Force on Practice Guidelines: developed in collaboration with the international society for heart and lung transplantation. *Circulation.* (2009) 119:1977–2016. doi: 10.1161/CIRCULATIONAHA.109.192064
88. Savarese G, Trimarco B, Dellegrottaglie S, Prastaro M, Gambardella F, Rengo G, et al. Natriuretic peptide-guided therapy in chronic heart failure: a meta-analysis of 2,686 patients in 12 randomized trials. *PLoS One.* (2013) 8:e58287. doi: 10.1371/journal.pone.0058287
89. McMurray JJ, Packer M, Desai AS, Gong J, Lefkowitz MP, Rizkala AR, et al. Angiotensin-neprilysin inhibition versus enalapril in heart failure. *N Engl J Med.* (2014) 371:993–1004.
90. McMurray JJ, Packer M, Desai AS, Gong J, Lefkowitz MP, Rizkala AR, et al. Dual angiotensin receptor and neprilysin inhibition as an alternative to angiotensin-converting enzyme inhibition in patients with chronic systolic heart failure: rationale for and design of the Prospective comparison of ARNI with ACEI to Determine Impact on Global Mortality and morbidity in Heart Failure trial (PARADIGM-HF). *Eur J Heart Fail.* (2013) 15:1062–73. doi: 10.1093/eurjhf/hft052
91. McMurray JJ, Packer M, Desai AS, Gong J, Lefkowitz M, Rizkala AR, et al. Baseline characteristics and treatment of patients in prospective comparison of ARNI with ACEI to determine impact on global mortality and morbidity in heart failure trial (PARADIGM-HF). *Eur J Heart Fail.* (2014) 16:817–25. doi: 10.1002/ejhf.115
92. Kostis JB, Packer M, Black HR, Schmieder R, Henry D, Levy E. Omapatrilat and enalapril in patients with hypertension: the Omapatrilat Cardiovascular Treatment vs. Enalapril (OCTAVE) trial. *Am J Hypertens.* (2004) 17:103–11. doi: 10.1016/j.amjhyper.2003.09.014
93. Scott A, Hubers MD, Nancy J, Brown MD. Combined angiotensin receptor antagonism and neprilysin inhibition. *Circulation.* (2016) 133:1115–24. doi: 10.1161/circulationaha.115.018622
94. Solomon SD, McMurray JJV, Anand IS, Ge J, Lam CSP, Maggioni AP, et al. Angiotensin-neprilysin inhibition in heart failure with preserved ejection fraction. *N Engl J Med.* (2019) 381:1609–20. doi: 10.1056/NEJMoa1908655

Conflict of Interest: The authors declare that the research was conducted in the absence of any commercial or financial relationships that could be construed as a potential conflict of interest.

frontiers | Frontiers in Cardiovascular Medicine

ORIGINAL RESEARCH
published: 02 June 2022
doi: 10.3389/fcvm.2022.910323

A Tryptophan Metabolite of the Microbiota Improves Neovascularization in Diabetic Limb Ischemia

Xiurui Ma†, Jinjing Yang†, Guanrui Yang, Lei Li, Xiaojun Hao, Guoqin Wang, Jian An and Fei Wang**

Department of Cardiology, Shanxi Cardiovascular Hospital, Taiyuan, China

Diabetes mellitus (DM) is accompanied by a series of macrovascular and microvascular injuries. Critical limb ischemia is the most severe manifestation of peripheral artery disease (PAD) caused by DM and is almost incurable. Therapeutic modulation of angiogenesis holds promise for the prevention of limb ischemia in diabetic patients with PAD. However, no small-molecule drugs are capable of promoting diabetic angiogenesis. An endogenous tryptophan metabolite, indole-3-aldehyde (3-IAld), has been found to have proangiogenic activity in endothelial cells. Nevertheless, the role of 3-IAld in diabetic angiogenesis remains unknown. Here, we found that 3-IAld ameliorated high glucose-induced mitochondrial dysfunction, decreasing oxidative stress and apoptosis and thus improving neovascularization.

Keywords: diabetes mellitus, limb ischemia, indole-3-aldehyde, mitochondrial dysfunction, oxidative stress, apoptosis

OPEN ACCESS

Edited by:
Han Xiao,
Peking University Third Hospital, China

Reviewed by:
Mohammed Abdelsaid, Mercer University, United States
Lu Tie, Peking University, China

****Correspondence:***
Jian An
287716669@qq.com
Fei Wang
wangfxys@163.com

† These authors have contributed equally to this work

Specialty section:
This article was submitted to Cardiovascular Metabolism, a section of the journal Frontiers in Cardiovascular Medicine

Received: *01 April 2022*
Accepted: *16 May 2022*
Published: *02 June 2022*

Citation:
Ma X, Yang J, Yang G, Li L, Hao X, Wang G, An J and Wang F (2022) A Tryptophan Metabolite of the Microbiota Improves Neovascularization in Diabetic Limb Ischemia. Front. Cardiovasc. Med. 9:910323. doi: 10.3389/fcvm.2022.910323

INTRODUCTION

Diabetes mellitus (DM) continues to be an epidemic affecting people worldwide. Globally, nearly 500 million people live with diabetes, and the number is expected to increase by more than 50 percent in the next 25 years (1). DM is a major risk factor for cardiovascular disease, and prolonged diabetes leads to an increased incidence of peripheral artery disease (PAD; 2, 3). Critical limb ischemia (CLI) is a common pathological manifestation of PAD characterized by ischemic rest pain, foot ulcers and gangrene, with a high risk of lower limb amputation and poor prognosis (4). Current therapies, such as surgical revascularization and medication, have limited benefits for CLI patients.

Microbiota-dependent tryptophan catabolites are abundantly produced within the gastrointestinal tract and are known to exert profound effects on host physiology, including the maintenance of epithelial barrier function, endothelial cell (EC) angiogenesis and immune homeostasis (5, 6). Several of the indole derivatives produced by the gut microbiota, including indole-3-aldehyde (3-IAld), are suggested ligands for the aryl hydrocarbon receptor (AHR), a xenobiotic response receptor (7). Notably, endogenous tryptophan metabolism produces several metabolites that are AHR ligands that have been implicated in autoimmunity and cancer (8, 9). Recent analyses suggest that 3-IAld has anti-inflammatory activity and proangiogenic effects, which apparently may involve mechanisms not dependent on AHR (5).

Angiogenesis is critical for the repair of ischemic wounds and tissues (10). Reactive oxygen species (ROS) are a heterogeneous group of highly reactive ions and molecules derived from

molecular oxygen (O_2; 11), and various lines of evidence support the fact that the biological roles of ROS are complex and paradoxical (12, 13). Excessive production of ROS can cause oxidative stress, which may damage cellular lipids, proteins, and DNA (11, 14), thus promoting apoptosis and decreasing cell proliferation, migration and angiogenesis. Therefore, balancing the ROS level is important for regulating cell proliferation, apoptosis, migration, and angiogenesis. Mitochondrial damage is an important source of ROS in most mammalian cells (15). The production of ROS leads to mitochondrial damage in a series of pathological processes and plays an important role in redox signaling (16, 17).

It has been shown that 3-IAId promotes angiogenesis in ECs. Nevertheless, very little is known about the function of tryptophan metabolites, in particular 3-IAId, in diabetic neovascularization. We therefore hypothesized that 3-IAId plays a protective role in diabetic angiogenesis. In this study, we used STZ-induced mice and HG (high glucose)-treated ECs to evaluate the role of 3-IAId in modulating diabetic angiogenesis.

MATERIALS AND METHODS

Animals

Male C57BL/6 mice aged 8 weeks were purchased from Shanghai JieSiJie Laboratory Animal Center (Shanghai, China). As previously described, mice were kept at room temperature on a 12/12 light/dark cycle with free access to water and standard laboratory mouse diets. The animal experiment was approved by the Animal Protection and Utilization Committee of Shanxi Cardiovascular Hospital. Mice were intraperitoneally injected with 50 mg/kg streptozotocin (STZ, Sigma–Aldrich) on 5 consecutive days to induce diabetic hyperglycemia (18). At the 3rd month of DM induction, left hindlimb ischemia (HLI) was induced by femoral artery ligation (19). 3-IAId (Sigma) was dissolved in DMSO and delivered by oral gavage at a dose of 150 mg/kg/day in a final mixture of DMSO (20%), PEG 400 (40%), and citric acid (2%). 3-IAId treatment was started on the 5th day after STZ injection and continued throughout the experiment.

Femoral Artery Ligation

Mice were anesthetized by intraperitoneal injection of 1% pentobarbital sodium. When the mice were unconscious and the muscles were relaxed, the mice were placed supine and fixed on the operative table. Alcohol (75%) was used for skin disinfection. Hair removal cream was used to remove the hair of both lower limbs. The skin was cut near the exposed oval to expose the femoral artery. Then, the accompanying veins and nerves were separated. The femoral artery and vein were ligated with 4–0 silk thread. Then, ophthalmic scissors were used to cut the artery below the ligation line, and the skin was sutured with 6–0 thread.

Laser Doppler Perfusion Imaging

Blood flow restoration was assessed by laser Doppler perfusion imaging (PeriScan PIM 3 system, Perimed, Sweden). Briefly, mice were anesthetized with isoflurane and placed on a heating pad at 37°C. Limb perfusion was detected on Days 1, 3, 7, 14 and 21 after ligation. Blood perfusion was quantified as a percentage of blood flow in the ischemic versus non-ischemic hind limb.

Wound Healing Assay

First, a straight line was drawn on the back of the plate to mark the observation of each area under a mirror. Human umbilical vein endothelial cells (HUVECs) were seeded onto 24-well plates in complete medium until they were 95% confluent. HUVECs were pretreated with or without HG for 24 h. Then, the complete medium was replaced with serum-free medium. Confluent cells were wounded by making a perpendicular scratch with a 200 μL pipette tip. Then, the supernatant was discarded, and fresh serum-free medium was added. The edges of the wound were measured at 0 and 24 h after scratching at the same points according to the markers. ImageJ software was used to calculate the migration distance.

Tube Formation Assay

Human umbilical vein endothelial cells were seeded onto 6-well plates in complete medium and were pretreated with or without HG or 3-IAId for 36 h. Twenty-four-well culture plates were coated with 200 μL of Matrigel (BD Biosciences, San Diego, CA, United States). HUVECs were digested with trypsin, and 1×10^5 cells/well were seeded onto Matrigel. The cells were incubated for an additional 12 h in the absence or presence of high glucose (25 mM; Sigma–Aldrich; 20) or 3-IAId (0.5 mM; Sigma–Aldrich; 5). Images were captured by microscopy (Olympus), and the lengths of the capillary networks were quantified using ImageJ software.

Aortic Ring Sprouting Assay

Aortas were isolated from the mice under sterile conditions and flushed with saline to remove residual blood. Then, aortic tissues were cut into 1 mm × 1 mm pieces. Twenty-four-well culture plates were coated with 200 μL of Matrigel (BD Biosciences, San Diego, CA, United States). The aortic tissue was plated on the surface of the Matrigel, followed by addition of a drop of matrix on the aortic tissue to sandwich the aorta in the middle of the Matrigel. Then, complete culture medium (ECGF, 5 U/ml heparin, 100 U/ml penicillin, 100 μg/ml streptomycin, and 20% fetal calf serum) was added to the 24-well plate. 5 days later, sprouting of the vascular tissue was observed by microscopy (Olympus).

Immunofluorescence Staining

Paraffin-embedded sections (6 μm) of ischemic hind limb skeletal muscle from each group were subjected to Immunofluorescence (IF) staining. The cells were rinsed with PBS 3 times for 5 min each and then blocked with 10% goat serum at 37°C for 1 h. Next, the cells were incubated with an anti-CD31 (AF3628, R&D) antibody at 4°C overnight. Sections were washed three times with PBS and labeled with a secondary antibody (Invitrogen) at 37°C for 1 h. DAPI (Invitrogen) was

used to stain the nuclei. Sections were imaged by confocal fluorescence microscopy (Leica, Germany).

Intracellular and Mitochondrial Reactive Oxygen Species Measurement

The production of ROS was evaluated by analyzing the fluorescence intensity by dihydroethidium (DHE; Invitrogen), DCFDA (Abcam), and MitoSOX (Invitrogen) staining. In brief, frozen musculus gastrocnemius sections were stained with 5 μM DHE at 37°C for 30 min, and then fluorescence intensity was detected by confocal microscopy. HUVECs were stimulated with high glucose (25 mM; Sigma–Aldrich; 20) or 3-IAId (0.5 mM; Sigma–Aldrich; 5) for 24 h, subjected to DCFDA (20 μM), or mitoSOX (5 μM) staining at 37°C for 30 min and then assessed by fluorescence microscopy.

TUNEL Staining

TUNEL staining was performed to detect cellular apoptosis in the gastrocnemius sections after femoral artery ligation according to the TUNEL staining kit manufacturer's instructions (Abcam, Cambridge; United Kingdom; cat no. ab66110). In brief, tissue samples were fixed in 4% paraformaldehyde, embedded in paraffin, and cut into 5 mm transverse sections. Paraffin sections of the aorta were stained with an *in situ* BrdU-Red DNA Fragmentation (TUNEL) Assay Kit (ab66110, Abcam). 4′,6′-Diamidino-2-phenylindole (DAPI) was used for nuclear counterstaining. HUVECs were stimulated with high glucose (25 mM; Sigma–Aldrich; 20) or 3-IAId (0.5 mM; Sigma–Aldrich; 5) for 24 h and then subjected to TUNEL staining at 37°C for 30 min. The number of TUNEL-positive nuclei was analyzed using ImageJ software (NIH, Bethesda, MD, United States). The TUNEL-positive cell number per field for each sample was the average of 6 random fields.

Metabolic Analysis

To characterize metabolic changes in HUVECs from each group, 20,000 cells/well were plated on gelatin-coated 96-well plates for Seahorse analysis 36 h before detection in a 1:1 EGM2 (Promo Cell) and fully supplemented DMEM mixture. A Seahorse XF96 analyzer was used for analysis according to the Agilent protocol (Mito Stress Kit). The metabolic function parameters shown in bars were calculated according to the Agilent protocol: basal respiration: [(final rate before oligomycin treatment) – (minimum rate after rotenone/antimycin A injection) = (non-mitochondrial oxygen consumption)]; ATP production: [(final rate before oligomycin injection) – (minimum rate after oligomycin injection)]; and spare respiratory capacity: [(measurement of maximum rate after injection of FCCP) – (non-mitochondrial respiration)] = [(maximum respiration) – (basal respiration)].

Statistical Analysis

Data were analyzed in GraphPad Prism 9.0 (GraphPad Software, San Diego, CA, United States). Non-normally distributed data were logarithmically converted prior to analysis and represented in the median and quartile ranges. Data are expressed as the mean ± SEM. Statistical significance was assessed by two-way ANOVA with Bonferroni correction for multiple comparisons. $p < 0.05$ was considered statistically significant.

RESULTS

Indole-3-Aldehyde Improves Blood Perfusion and Ischemic Angiogenesis in Diabetic Hindlimb Ischemia

To determine the protective role of 3-IAId against diabetic ischemia, a diabetic model was established by STZ induction, and HLI was induced by femoral artery ligation. Mice in the experimental group were given 3-IAId (150 mg/kg/day) by oral gavage over 21 days. Blood perfusion of the hind limb footpad was evaluated by laser Doppler perfusion imaging technology on Days 1, 3, 7, 14 and 21 after surgery. The results showed that diabetes impaired hind limb blood perfusion recovery in both saline- and 3-IAId-treated mice in a time-dependent manner (**Figures 1A,B**). However, 3-IAId administration in STZ mice promoted greater flow recovery at Days 3–21 after HLI surgery compared with that in diabetic Ctrl mice (**Figures 1A,B**). Furthermore, on Day 21 after femoral artery ligation, the number of necrotic toes in each mouse was counted. Then, mice with different numbers of necrotic toes were classified and quantified, yielding necrotic toe scores. The necrotic degree reflected by the necrotic toe number was considerably lower in 3-IAId and STZ-treated mice than in the corresponding control mice (**Figure 1C**). Consistent with these results, 3-IAId-treated mice with diabetes also had increased capillary density in the gastrocnemius measured 7 and 14 days after HLI compared with that in diabetic Ctrl mice (**Figures 1D–G**). Thus, we conclude that 3-IAId improved blood flow recovery and ameliorated necrosis.

Indole-3-Aldehyde Protects Endothelial Cells From High Glucose-Induced Angiogenic Dysfunction

Endothelial cell migration, sprouting and tube formation are critical processes for angiogenesis, in which the formation of capillary-like tubes by ECs is a crucial step for blood flow recovery *in vivo*. We assessed the contribution of 3-IAId to EC biological functions *in vitro*. Obviously, 3-IAId treatment significantly reversed HG-induced damage to EC tube formation, EC migration and angiogenic sprouting from the aortic vascular wall (**Figures 2A–F**). Taken together, our findings indicate that 3-IAId regulates EC biological functions essential for angiogenesis, including enhanced migration, sprouting and tube formation.

Indole-3-Aldehyde Alleviates Oxidative Stress and Apoptosis in Diabetic Hindlimb Ischemia

Oxidative stress and apoptosis are critical in angiogenesis. Therefore, gastrocnemius sections from each group were

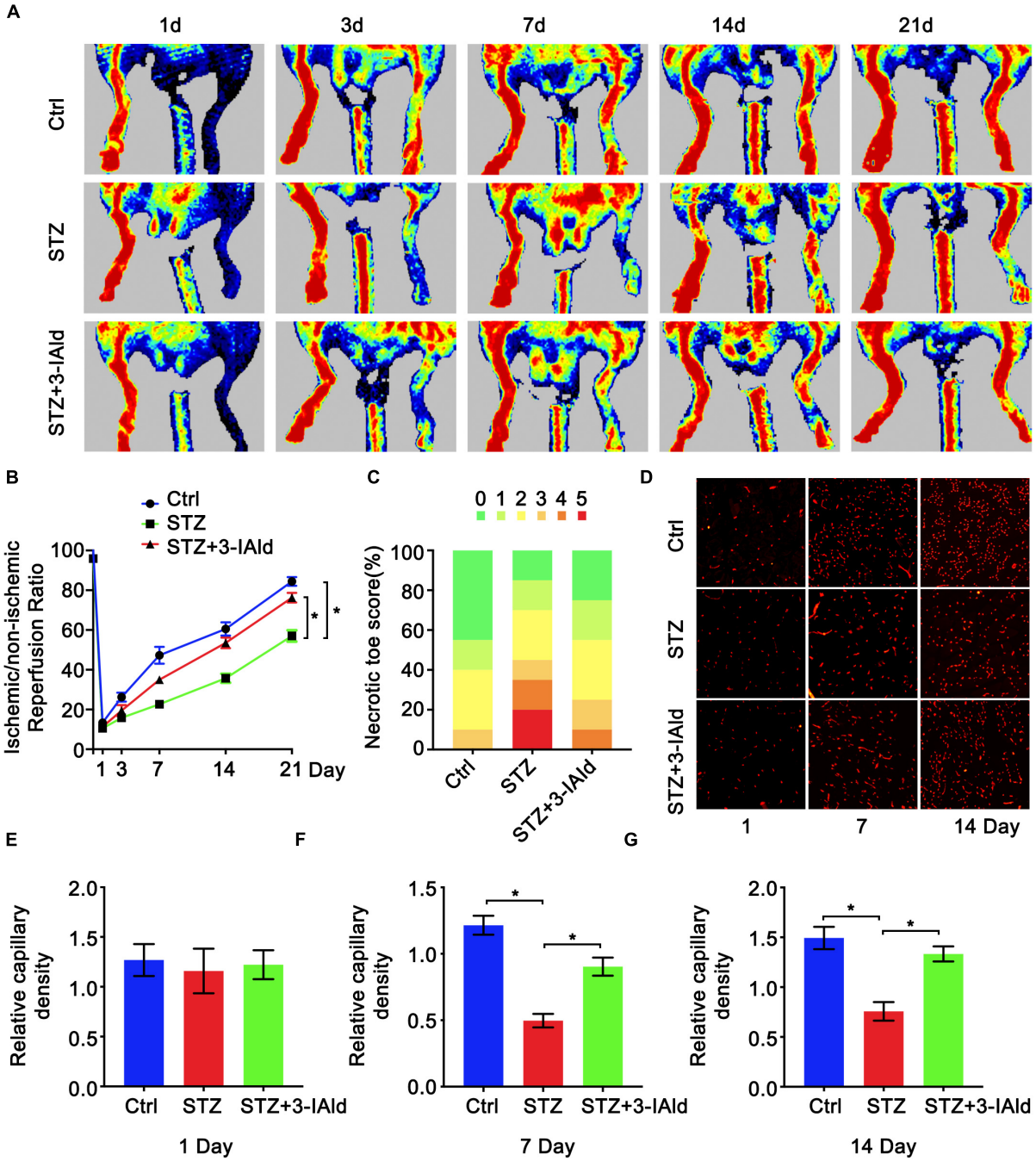

FIGURE 1 | 3-IAld improves blood perfusion and ischemic angiogenesis in diabetic HLI. **(A)** Original laser Doppler perfusion images (LDPIs) displaying hindlimb perfusion in each group at 1, 3, 7, 14, and 21 days after ligation of the femoral artery. **(B)** Perfusion recovery in mice of the control, STZ and STZ + 3-IAld groups at 1, 3, 7, 14, and 21 days after surgery. $n = 10$ for each group. **(C)** Necrotic toe score determined at Day 21 after ischemic injury. $n = 7$ for each group. **(D)** Representative immunofluorescence images showing CD31 density in gastrocnemius muscle at 1 and 14 days after artery ligation. **(E–G)** Capillary density was evaluated as the ratio of capillary number per field; $n = 6$ for each group. Data are presented as the mean ± SEM. $^*P < 0.05$.

subjected to TUNEL staining, and the results showed that STZ treatment exacerbated whereas 3-IAId administration attenuated cell apoptosis (**Figures 3A,B**). Moreover, immunoblot analysis of anti-apoptosis (Bcl2) and pro-apoptosis (Caspase3 and Bax) molecules revealed that the apoptosis exacerbation induced by STZ was rescued by 3-IAId supplementation (**Figures 3C,D**). Additionally, DHE staining of gastrocnemius muscle sections of each group showed that STZ treatment increased cell ROS production (**Figures 3E,F**), while 3-IAId administration reduced cell oxidative stress, which was further proven by

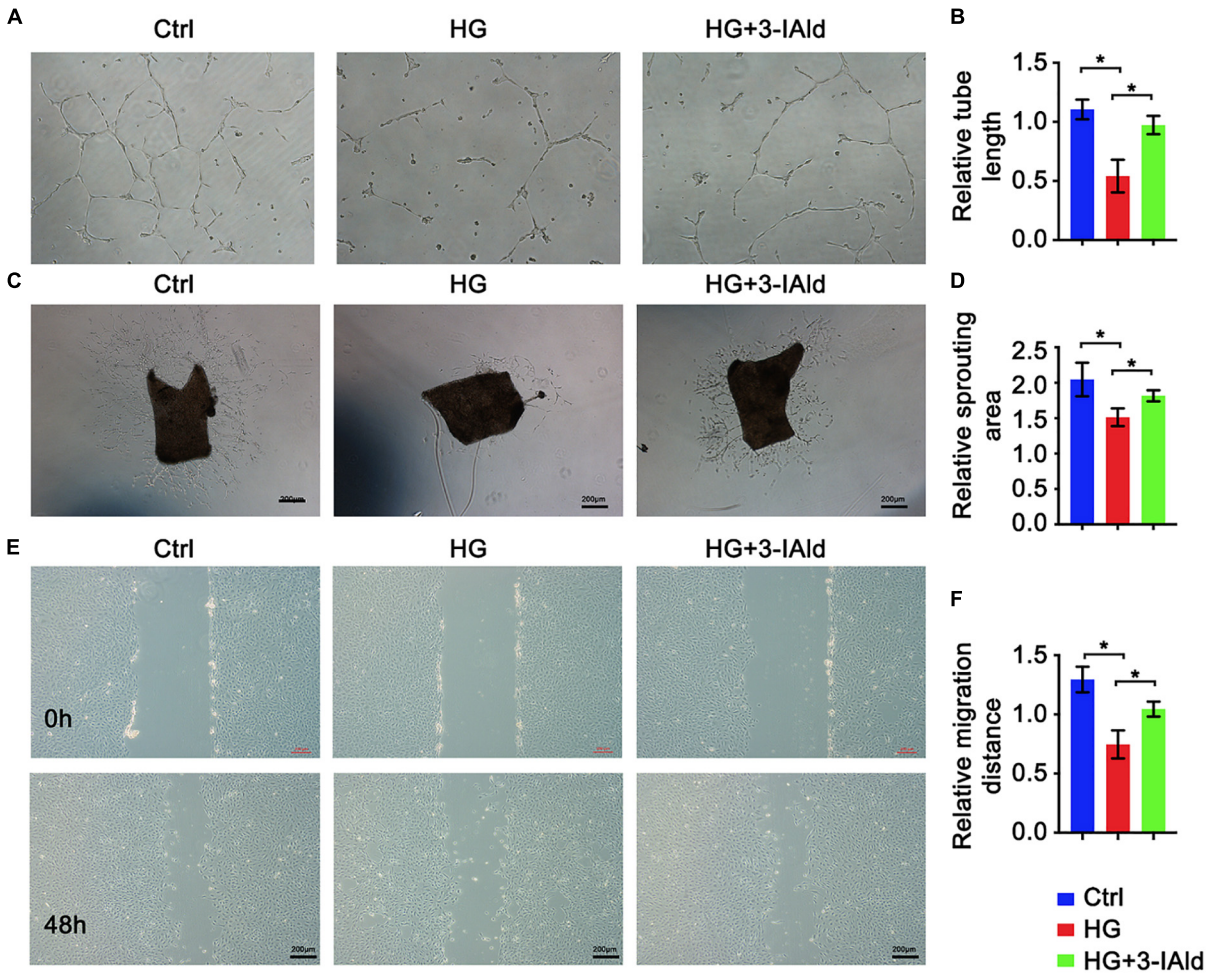

FIGURE 2 | 3-IAld protects ECs from HG-induced angiogenic dysfunction. **(A)** Original micrograph of tube formation in HUVECs in the control, HG and HG + 3-IAld groups; scale bar: 100 μm. **(B)** Quantitative analysis of relative tube length; $n = 6$ for each group. **(C)** Original micrograph of sprouts grown from aortic rings in the control, HG and HG + 3-IAld groups; scale bar: 200 μm. **(D)** Quantitative analysis of the relative sprouting area; $n = 6$ for each group. **(E)** Original micrographs of the wound healing assay; scale bar: 200 μm. **(F)** Quantitative analysis of wound healing assay in control, HG and HG + 3-IAld groups in HUVECs; $n = 6$ for each group. Data are presented as the mean ± SEM. $^*P < 0.05$.

immunoblot analysis (**Figures 3G,H**). Collectively, our data suggest that 3-IAId alleviates STZ-induced ROS production and thus blunts cell apoptosis.

Indole-3-Aldehyde Protects Endothelial Cells From High Glucose-Induced Oxidative Stress and Apoptosis

Furthermore, we validated the antioxidant and anti-apoptotic effects of 3-IAId *ex vivo*. Cultured ECs were treated with HG for oxidative stress and apoptosis induction with or without 3-IAId administration. ECs were subjected to DCFDA staining for ROS detection. In accordance with previous results, 3-IAId was able to attenuate the exacerbated oxidative stress induced by HG stimulation (**Figure 4A**). Immunoblot analysis of oxidant (Cytochrome c, CytoC) and antioxidant (HO-1 and SOD2) molecules revealed that 3-IAId treatment reduced EC oxidative stress (**Figures 4B,C**). TUNEL staining and immunoblot analysis of EC apoptosis also led to the same conclusion as that reached based on the *in vivo* results (**Figures 4D–F**). These findings denote the protective role of 3-IAId in EC oxidative stress and apoptosis.

Indole-3-Aldehyde Attenuates High Glucose-Induced Mitochondrial Dysfunction in Endothelial Cells

Mitochondrial dysfunction promotes ROS production, which exacerbates mitochondrial damage (15, 16). We therefore investigated whether 3-IAId would affect mitochondrial function. Measurement of mitochondrial ROS by MitoSOX staining revealed that 3-IAId significantly alleviated HG-induced mitochondrial ROS production (**Figures 5A,B**). The mitochondrial membrane potential is the central bioenergetic parameter that controls respiratory rate, ATP synthesis and the generation of ROS (21). We further assessed the mitochondrial membrane potential by JC-1 staining. As expected, 3-IAId also played a role in the maintenance of the mitochondrial

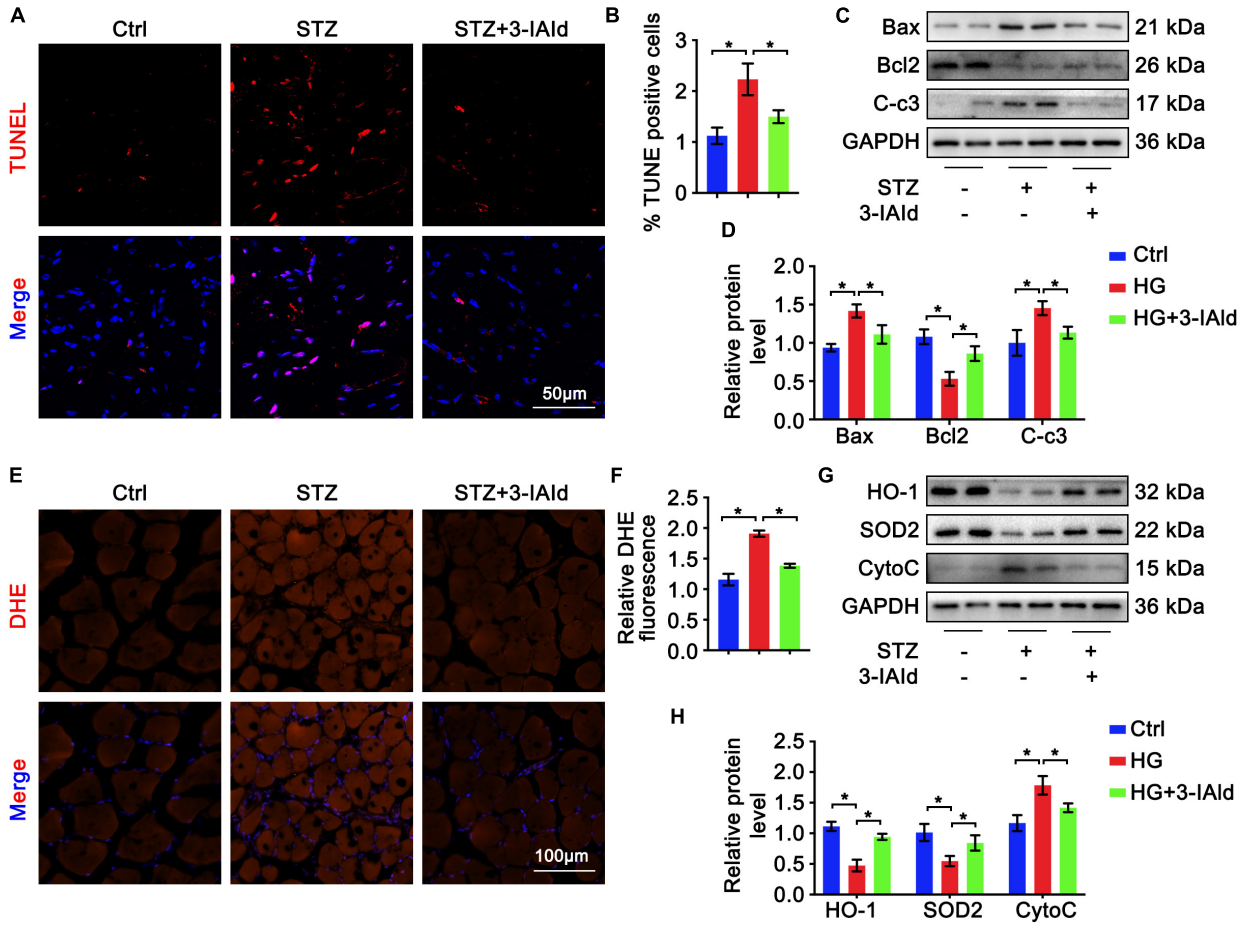

FIGURE 3 | 3-IAld alleviates oxidative stress and apoptosis in diabetic HLI. **(A)** TUNEL staining of diabetic mice in the control, STZ and STZ + 3-IAld groups at 7 days after ligation; scale bar: 50 μm. **(B)** Quantification of TUNEL staining; $n = 6$ for each group. **(C)** Western blot analysis of apoptosis-related molecules in the diabetic mice in the control, STZ and STZ + 3-IAld groups at 7 days after ligation. **(D)** Quantification of relative protein levels; $n = 6$ for each group. **(E)** DHE staining of diabetic mice in the control, STZ and STZ + 3-IAld groups at 7 days after ligation; scale bar: 100 μm. **(F)** Quantification of DHE staining; $n = 6$ for each group. **(G)** Western blot analysis of oxidative stress-related molecules in the diabetic mice in the control, STZ and STZ + 3-IAld groups at 7 days after ligation. **(H)** Quantification of relative protein levels; $n = 6$ for each group. Data are presented as the mean ± SEM. $^*P < 0.05$.

membrane potential (**Figures 5C–E**). For detailed metabolic characterization of ECs in each group, the respiratory capacity of the ECs was assessed using a Seahorse extracellular flux (XF) analyzer. As expected, the oxygen consumption rate (OCR) was drastically reduced in HG-treated ECs, with a significant reduction in the calculated basal and spare respiratory capacities (**Figures 5F,G**). Furthermore, the proportion of basal respiration used to drive ATP production was also dramatically reduced (**Figures 5F,G**). 3-IAId supplementation significantly improved cellular respiration in the mitochondria, as demonstrated by an increased OCR. Collectively, our findings suggest the protective role of 3-IAId in EC mitochondrial dysfunction.

DISCUSSION

The salient findings of our study confirmed for the first time that 3-IAId supplementation improved diabetic angiogenesis and limb perfusion. This finding was supported by data from a limb ischemia model in STZ-induced diabetic mice and *in vitro* experiments in HG-induced HUVECs. Our data further revealed that 3-IAId improved EC migration, tube formation and sprouting. 3-IAId supplementation improved angiogenesis, in part possibly because it reduced apoptosis and oxidative stress. Moreover, we confirmed that the beneficial effects of 3-IAId on EC apoptosis and oxidative stress were due to the improvement of mitochondrial function. This study described both the critical role and potential mechanisms of 3-IAId in diabetic angiogenesis.

Arterial occlusion leads to impaired angiogenesis in response to ischemia, contributing to serious clinical complications in diabetic patients with PAD or CAD (22, 23). The mechanisms that explain impaired angiogenic responses after diabetic ischemia vary, such as vascular degeneration characterized by either endothelial or vascular smooth muscle cell dysfunction (24), the reduced release or functional defects of endothelial progenitor

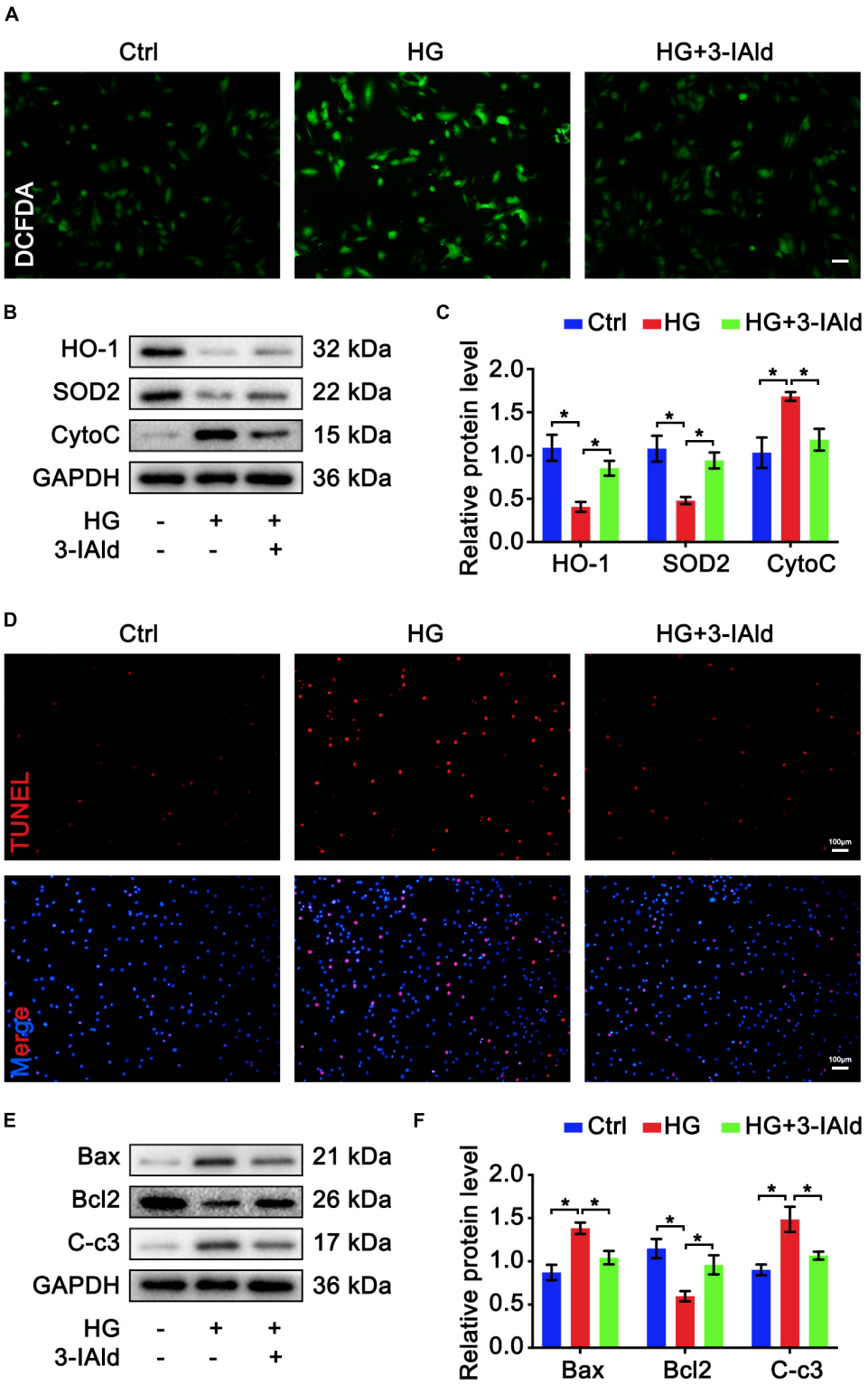

FIGURE 4 | 3-IAld protects ECs from HG-induced oxidative stress and apoptosis. **(A)** DCFDA staining in HUVECs in the control, HG and HG + 3-IAld groups; scale bar: 50 μm. **(B)** Western blot analysis of oxidative stress-related molecules in HUVECs in the control, HG and HG + 3-IAld groups. **(C)** Quantification of relative protein levels; $n = 6$ for each group. **(D)** TUNEL staining in HUVECs in the control, HG and HG + 3-IAld groups; scale bar: 100 μm. **(E)** Western blot analysis of apoptosis-related molecules in HUVECs in the control, HG and HG + 3-IAld groups. **(F)** Quantification of relative protein levels; $n = 6$ for each group. Data are presented as the mean ± SEM. $^*P < 0.05$.

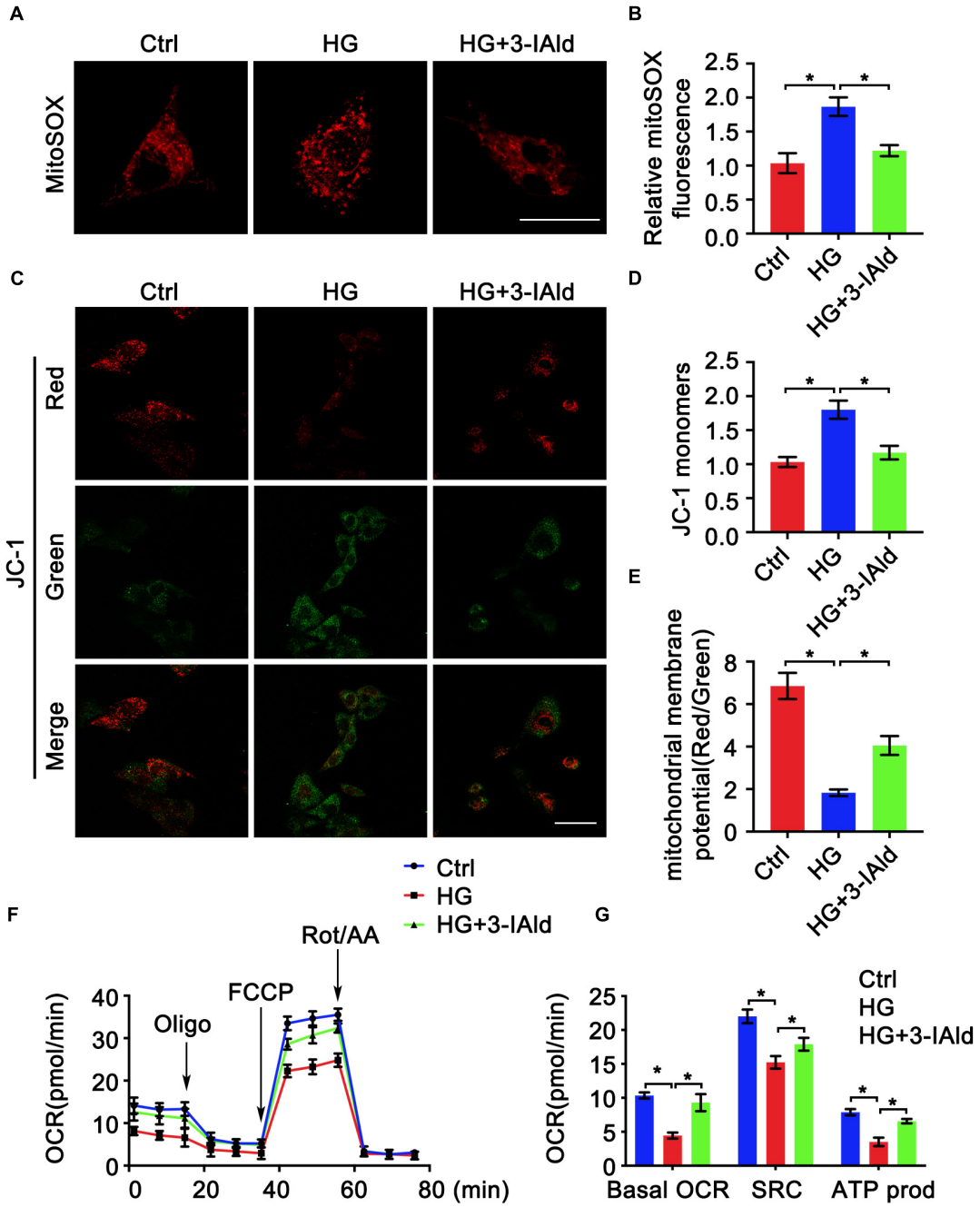

FIGURE 5 | 3-IAld attenuates HG-induced mitochondrial dysfunction in ECs. **(A)** MitoSOX staining in HUVECs in the control, HG and HG + 3-IAld groups, scale bar: 25 μm. **(B)** Quantification of relative MitoSOX fluorescence; $n = 6$ for each group. **(C)** JC-1 staining in HUVECs in the control, HG and HG + 3-IAld groups; scale bar: 50 μm. **(D,E)** Quantification of relative JC-1 monomers and mitochondrial member potential; $n = 6$ for each group. **(F)** Oxygen consumption rates (OCRs) in HUVECs in the control, HG and HG + 3-IAld groups before and after sequential injection of oligomycin, FCCP and a mixture of rotenone/antimycin A, as determined by a Seahorse XF96 Analyzer. **(G)** Corresponding calculated parameters of mitochondrial respiration; $n = 6$ for each group. Data are presented as the mean ± SEM. $^*P < 0.05$.

cells in bone marrow (25), or the dysregulation of vascular growth factor pathways (26). Although various factors have been reported to be responsible for impaired angiogenesis in diabetic ischemia, the microbial metabolites involved in diabetic angiogenesis remain to be explored.

Recently, the microbiome affecting health and the pathogenesis of disease has received extensive attention. One of the modes by which the gut microbiota interacts with the host is by means of metabolites. Microbial metabolites affect immune maturation, immune homeostasis, host energy

metabolism and mucosal integrity maintenance (27). It has been reported that intestinal microbes selectively activate mucosal ECs and mesenchymal cells to promote specific angiogenic responses in a TLR- and Nod-like receptor-dependent manner (28). An array of studies have elucidated that microbial metabolites can regulate tumor angiogenesis. Butyrate, derived from the microbiota, promotes angiogenesis (29). Nicotinic acid effectively resists iodoacetamide-induced colitis by improving pathological angiogenesis and inflammation in a GPR109A-dependent manner (30). Another study demonstrated that a polypeptide of *Escherichia coli* and its tripeptide analogs promoted tumor cell invasion and angiogenesis, thus potentially affecting tumor metastasis (31). Dysregulation of the intestinal flora leads to increased intestinal permeability and chronic inflammation, resulting in increased production of IL-6, IL-1B, TNF-A, and VEGF-A, which ultimately intensifies pathological angiogenesis (32).

Overall, accumulating evidence has implicated the angiogenic process in various microbiota-associated human diseases. Herein, we investigated diabetic angiogenesis influenced by the microbiome, aiming to provide a broad understanding of how angiogenesis is involved in the diabetic state and how the microbiome regulates angiogenesis.

Tryptophan is an indispensable amino acid that can be taken up only *via* the diet. Tryptophan metabolism in different tissues is related to various physiological functions (33). A tryptophan metabolite of the gut microbiota, 3-IAId acid, attenuates inflammation (34). The potential benefits provided by indole derivatives have been highlighted in animal models of colitis and experimental autoimmune encephalomyelitis (35, 36). Moreover, 3-IAId has been found to promote angiogenesis in HUVECs (5). Our observations are consistent with previous studies showing that 3-IAId has proangiogenic properties. A study also showed that 3-IAld could restore epithelial barrier integrity and function, in turn ameliorating the metabolic complications (glucose tolerance and obesity) associated with the intake of a HFD (37). 3-IAId also significantly attenuated skin inflammation in mice with MC903-induced AD-like dermatitis, and this effect was blocked by an AHR antagonist and abolished in AHR-null mice (34). Remarkably, a recent metabolomic study showed that an increased fecal concentration of 3-IAld was associated with resistance to radiation-induced pathology, leading to hematopoietic, gastrointestinal, and cerebrovascular injuries (38). This finding points to a biological function of endogenous 3-IAld and suggests that its administration may provide long-term radioprotection. Studies also indicate that the therapeutic activity of 3-IAld, appropriately delivered through targeted pharmaceutics, may encompass metabolic and organ inflammatory pathology in murine models. Of interest, a pantissue AHR signature has recently highlighted 3-IAld among the metabolites downstream of the L-amino acid oxidase catabolism of Trp that were associated with AHR-driven cancer cell motility and immunosuppression (39). These studies qualify 3-IAld as a potent agent capable of strengthening epithelial barrier function, immune homeostasis and colonization resistance at mucosal and likely distal sites (40). Corresponding with previous studies, our study also demonstrated the protective role of 3-IAId in diabetic limb perfusion.

In conclusion, we have demonstrated that tolerance against severe limb ischemia under hyperglycemia is at least in part attributable to microbial metabolites and that supplementation with 3-IAId is sufficient to improve neoangiogenesis caused by limb ischemia in diabetic mice. We have also shown that this angiogenic response is dependent on mitochondrial function. Therefore, 3-IAId could be an attractive molecule for treating PAD in patients with diabetic vascular complications.

LIMITATIONS

The present study has several limitations. Here, we first confirmed the protective role of 3-IAId in diabetic angiogenesis, as evidenced by improved EC tube formation, alleviated cell apoptosis, reduced ROS production and mitigated mitochondrial dysfunction. However, the potential mechanisms are still elusive and need further study. Additionally, male mice were used in our experiments for the sake of less hormone variability. The outcome in female mice may not be identical to these findings. Furthermore, the effect of 3-IAld on control animals remains unclear and needs to be addressed in future studies. Nevertheless, the findings demonstrate an essential role of 3-IAId in diabetic angiogenesis.

DATA AVAILABILITY STATEMENT

The original contributions presented in the study are included in the article/supplementary material, further inquiries can be directed to the corresponding authors.

ETHICS STATEMENT

The animal study was reviewed and approved by Animal Protection and Utilization Committee of the Shanxi Cardiovascular Hospital.

AUTHOR CONTRIBUTIONS

XM, FW, and JA conceived and designed the study. XM, JY, GY, LL, XH, and GW performed the animal and cell culture experiments. XM, FW, JY, and JA interpreted the data and wrote the manuscript. JA and FW supervised the study and reviewed and edited the manuscript. All authors approved the final manuscript.

FUNDING

This work was supported by the Health Commission of Shanxi Province (2022028) and the Shanxi Province Science Foundation for Youths (202103021223451).

REFERENCES

1. Saeedi P, Petersohn I, Salpea P, Malanda B, Karuranga S, Unwin N, et al. Global and regional diabetes prevalence estimates for 2019 and projections for 2030 and 2045: results from the International Diabetes Federation Diabetes Atlas, 9(th) edition. *Diabetes Res Clin Pract.* (2019) 157:107843. doi: 10.1016/j.diabres.2019.107843
2. Thiruvoipati T, Kielhorn CE, Armstrong EJ. Peripheral artery disease in patients with diabetes: epidemiology, mechanisms, and outcomes. *World J Diabetes.* (2015) 6:961–9. doi: 10.4239/wjd.v6.i7.961
3. Edmonds M. Vascular disease in the lower limb in type 1 diabetes. *Cardiovasc Endocrinol Metab.* (2019) 8:39–46. doi: 10.1097/XCE.0000000000000168
4. Faglia E, Clerici G, Clerissi J, Gabrielli L, Losa S, Mantero M, et al. Early and five-year amputation and survival rate of diabetic patients with critical limb ischemia: data of a cohort study of 564 patients. *Eur J Vasc Endovasc Surg.* (2006) 32:484–90. doi: 10.1016/j.ejvs.2006.03.006
5. Langan D, Perkins DJ, Vogel SN, Moudgil KD. Microbiota-derived metabolites, indole-3-aldehyde and indole-3-acetic acid, differentially modulate innate cytokines and stromal remodeling processes associated with autoimmune arthritis. *Int J Mol Sci.* (2021) 22:2017. doi: 10.3390/ijms22042017
6. Agus A, Planchais J, Sokol H. Gut microbiota regulation of tryptophan metabolism in health and disease. *Cell Host Microbe.* (2018) 23:716–24. doi: 10.1016/j.chom.2018.05.003
7. Roager HM, Licht TR. Microbial tryptophan catabolites in health and disease. *Nat Commun.* (2018) 9:3294. doi: 10.1038/s41467-018-05470-4
8. Kang KY, Lee SH, Jung SM, Park SH, Jung BH, Ju JH. Downregulation of tryptophan-related metabolomic profile in rheumatoid arthritis synovial fluid. *J Rheumatol.* (2015) 42:2003–11. doi: 10.3899/jrheum.141505
9. Platten M, Nollen EAA, Rohrig UF, Fallarino F, Opitz CA. Tryptophan metabolism as a common therapeutic target in cancer, neurodegeneration and beyond. *Nat Rev Drug Discov.* (2019) 18:379–401. doi: 10.1038/s41573-019-0016-5
10. Emanueli C, Van Linthout S, Salis MB, Monopoli A, Del Soldato P, Ongini E, et al. Nitric oxide-releasing aspirin derivative, NCX 4016, promotes reparative angiogenesis and prevents apoptosis and oxidative stress in a mouse model of peripheral ischemia. *Arterioscler Thromb Vasc Biol.* (2004) 24:2082–7. doi: 10.1161/01.ATV.0000144030.39087.3b
11. Schieber M, Chandel NS. ROS function in redox signaling and oxidative stress. *Curr Biol.* (2014) 24:R453–62. doi: 10.1016/j.cub.2014.03.034
12. D'Autreaux B, Toledano MB. ROS as signalling molecules: mechanisms that generate specificity in ROS homeostasis. *Nat Rev Mol Cell Biol.* (2007) 8:813–24. doi: 10.1038/nrm2256
13. Halliwell B. The antioxidant paradox: less paradoxical now? *Br J Clin Pharmacol.* (2013) 75:637–44. doi: 10.1111/j.1365-2125.2012.04272.x
14. Trachootham D, Alexandre J, Huang P. Targeting cancer cells by ROS-mediated mechanisms: a radical therapeutic approach? *Nat Rev Drug Discov.* (2009) 8:579–91. doi: 10.1038/nrd2803
15. Muller F. The nature and mechanism of superoxide production by the electron transport chain: its relevance to aging. *J Am Aging Assoc.* (2000) 23:227–53. doi: 10.1007/s11357-000-0022-9
16. Balaban RS, Nemoto S, Finkel T. Mitochondria, oxidants, and aging. *Cell.* (2005) 120:483–95. doi: 10.1016/j.cell.2005.02.001
17. Droge W. Free radicals in the physiological control of cell function. *Physiol Rev.* (2002) 82:47–95. doi: 10.1152/physrev.00018.2001
18. Biscetti F, Straface G, De Cristofaro R, Lancellotti S, Rizzo P, Arena V, et al. High-mobility group box-1 protein promotes angiogenesis after peripheral ischemia in diabetic mice through a VEGF-dependent mechanism. *Diabetes.* (2010) 59:1496–505.
19. Caporali A, Meloni M, Miller AM, Vierlinger K, Cardinali A, Spinetti G, et al. Soluble ST2 is regulated by p75 neurotrophin receptor and predicts mortality in diabetic patients with critical limb ischemia. *Arterioscler Thromb Vasc Biol.* (2012) 32:e149–60. doi: 10.1161/ATVBAHA.112.300497
20. Khemais-Benkhiat S, Belcastro E, Idris-Khodja N, Park SH, Amoura L, Abbas M, et al. Angiotensin II-induced redox-sensitive SGLT1 and 2 expression promotes high glucose-induced endothelial cell senescence. *J Cell Mol Med.* (2020) 24:2109–22. doi: 10.1111/jcmm.14233
21. Nicholls DG. Mitochondrial membrane potential and aging. *Aging Cell.* (2004) 3:35–40.
22. Al-Delaimy WK, Merchant AT, Rimm EB, Willett WC, Stampfer MJ, Hu FB. Effect of type 2 diabetes and its duration on the risk of peripheral arterial disease among men. *Am J Med.* (2004) 116:236–40. doi: 10.1016/j.amjmed.2003.09.038
23. Hueb W, Gersh BJ, Costa F, Lopes N, Soares PR, Dutra P, et al. Impact of diabetes on five-year outcomes of patients with multivessel coronary artery disease. *Ann Thorac Surg.* (2007) 83:93–9. doi: 10.1016/j.athoracsur.2006.08.050
24. Horvath EM, Benko R, Kiss L, Muranyi M, Pek T, Fekete K, et al. Rapid 'glycaemic swings' induce nitrosative stress, activate poly(ADP-ribose) polymerase and impair endothelial function in a rat model of diabetes mellitus. *Diabetologia.* (2009) 52:952–61. doi: 10.1007/s00125-009-1304-0
25. Loomans CJ, de Koning EJ, Staal FJ, Rookmaaker MB, Verseyden C, de Boer HC, et al. Endothelial progenitor cell dysfunction: a novel concept in the pathogenesis of vascular complications of type 1 diabetes. *Diabetes.* (2004) 53:195–9. doi: 10.2337/diabetes.53.1.195
26. Hazarika S, Dokun AO, Li Y, Popel AS, Kontos CD, Annex BH. Impaired angiogenesis after hindlimb ischemia in type 2 diabetes mellitus: differential regulation of vascular endothelial growth factor receptor 1 and soluble vascular endothelial growth factor receptor 1. *Circ Res.* (2007) 101:948–56. doi: 10.1161/CIRCRESAHA.107.160630
27. Lavelle A, Sokol H. Gut microbiota-derived metabolites as key actors in inflammatory bowel disease. *Nat Rev Gastroenterol Hepatol.* (2020) 17:223–37. doi: 10.1038/s41575-019-0258-z
28. Schirbel A, Kessler S, Rieder F, West G, Rebert N, Asosingh K, et al. Pro-angiogenic activity of TLRs and NLRs: a novel link between gut microbiota and intestinal angiogenesis. *Gastroenterology.* (2013) 144:613–23.e9. doi: 10.1053/j.gastro.2012.11.005
29. Castro PR, Bittencourt LFF, Larochelle S, Andrade SP, Mackay CR, Slevin M, et al. GPR43 regulates sodium butyrate-induced angiogenesis and matrix remodeling. *Am J Physiol Heart Circ Physiol.* (2021) 320:H1066–79. doi: 10.1152/ajpheart.00515.2019
30. Salem HA, Wadie W. Effect of niacin on inflammation and angiogenesis in a murine model of ulcerative colitis. *Sci Rep.* (2017) 7:7139. doi: 10.1038/s41598-017-07280-y
31. De Spiegeleer B, Verbeke F, D'Hondt M, Hendrix A, Van De Wiele C, Burvenich C, et al. The quorum sensing peptides PhrG, CSP and EDF promote angiogenesis and invasion of breast cancer cells in vitro. *PLoS One.* (2015) 10:e0119471. doi: 10.1371/journal.pone.0119471
32. Andriessen EM, Wilson AM, Mawambo G, Dejda A, Miloudi K, Sennlaub F, et al. Gut microbiota influences pathological angiogenesis in obesity-driven choroidal neovascularization. *EMBO Mol Med.* (2016) 8:1366–79. doi: 10.15252/emmm.201606531
33. Le Floc'h N, Otten W, Merlot E. Tryptophan metabolism, from nutrition to potential therapeutic applications. *Amino Acids.* (2011) 41:1195–205. doi: 10.1007/s00726-010-0752-7
34. Yu J, Luo Y, Zhu Z, Zhou Y, Sun L, Gao J, et al. A tryptophan metabolite of the skin microbiota attenuates inflammation in patients with atopic dermatitis through the aryl hydrocarbon receptor. *J Allergy Clin Immunol.* (2019) 143:2108–19.e12. doi: 10.1016/j.jaci.2018.11.036
35. Rothhammer V, Mascanfroni ID, Bunse L, Takenaka MC, Kenison JE, Mayo L, et al. Type I interferons and microbial metabolites of tryptophan modulate astrocyte activity and central nervous system inflammation via the aryl hydrocarbon receptor. *Nat Med.* (2016) 22:586–97. doi: 10.1038/nm.4106
36. Alexeev EE, Lanis JM, Kao DJ, Campbell EL, Kelly CJ, Battista KD, et al. Microbiota-derived indole metabolites promote human and murine intestinal homeostasis through regulation of interleukin-10 receptor. *Am J Pathol.* (2018) 188:1183–94. doi: 10.1016/j.ajpath.2018.01.011
37. Puccetti M, Pariano M, Borghi M, Barola C, Moretti S, Galarini R, et al. Enteric formulated indole-3-carboxaldehyde targets the aryl hydrocarbon receptor for protection in a murine model of metabolic syndrome. *Int J Pharm.* (2021) 602:120610. doi: 10.1016/j.ijpharm.2021.120610
38. Guo H, Chou WC, Lai Y, Liang K, Tam JW, Brickey WJ, et al. Multi-omics analyses of radiation survivors identify radioprotective microbes

and metabolites. *Science.* (2020) 370:eaay9097. doi: 10.1126/science.aay9097

39. Sadik A, Somarribas Patterson LF, Ozturk S, Mohapatra SR, Panitz V, Secker PF, et al. IL4I1 is a metabolic immune checkpoint that activates the AHR and promotes tumor progression. *Cell.* (2020) 182:1252–70.e34. doi: 10.1016/j.cell.2020.07.038
40. Zelante T, Puccetti M, Giovagnoli S, Romani L. Regulation of host physiology and immunity by microbial indole-3-aldehyde. *Curr Opin Immunol.* (2021) 70:27–32. doi: 10.1016/j.coi.2020.12.004

Conflict of Interest: The authors declare that the research was conducted in the absence of any commercial or financial relationships that could be construed as a potential conflict of interest.

Publisher's Note: All claims expressed in this article are solely those of the authors and do not necessarily represent those of their affiliated organizations, or those of the publisher, the editors and the reviewers. Any product that may be evaluated in this article, or claim that may be made by its manufacturer, is not guaranteed or endorsed by the publisher.

frontiers | Frontiers in Cardiovascular Medicine

ORIGINAL RESEARCH
published: 29 June 2022
doi: 10.3389/fcvm.2022.927956

High-Intensity Interval Training Improves Cardiac Function by miR-206 Dependent HSP60 Induction in Diabetic Rats

Maryam Delfan[1], Raheleh Amadeh Juybari[2], Sattar Gorgani-Firuzjaee[3], Jens Høiriis Nielsen[4], Neda Delfan[5], Ismail Laher[6], Ayoub Saeidi[7], Urs Granacher[8]*†‡ and Hassane Zouhal[9,10]*†‡*

[1] Department of Exercise Physiology, Faculty of Sport Sciences, Alzahra University, Tehran, Iran, [2] Department of Exercise Physiology, Faculty of Sport Sciences, Alzahra University, Tehran, Iran, [3] Department of Medical Laboratory Sciences, School of Allied Health Medicine, AJA University of Medical Sciences, Tehran, Iran, [4] Department of Biomedical Sciences, University of Copenhagen, Copenhagen, Denmark, [5] Department of Exercise Physiology, Faculty of Physical Education and Sport Sciences, University of Tehran, Tehran, Iran, [6] Department of Anesthesiology, Pharmacology, and Therapeutics, Faculty of Medicine, University of British Columbia, Vancouver, BC, Canada, [7] Department of Physical Education and Sport Sciences, Faculty of Humanities and Social Sciences, University of Kurdistan, Sanandaj, Iran, [8] Division of Training and Movement Sciences, University of Potsdam, Potsdam, Germany, [9] Movement, Sport, Health and Sciences Laboratory (M2S), UFR-STAPS, University of Rennes 2-ENS Cachan, Av. Charles Tillon, Rennes Cedex, France, [10] Institut International des Sciences du Sport (2IS), Irodouer, France

Objective: A role for microRNAs is implicated in several biological and pathological processes. We investigated the effects of high-intensity interval training (HIIT) and moderate-intensity continuous training (MICT) on molecular markers of diabetic cardiomyopathy in rats.

Methods: Eighteen male Wistar rats (260 ± 10 g; aged 8 weeks) with streptozotocin (STZ)-induced type 1 diabetes mellitus (55 mg/kg, IP) were randomly allocated to three groups: control, MICT, and HIIT. The two different training protocols were performed 5 days each week for 5 weeks. Cardiac performance (end-systolic and end-diastolic dimensions, ejection fraction), the expression of miR-206, HSP60, and markers of apoptosis (cleaved PARP and cytochrome C) were determined at the end of the exercise interventions.

Results: Both exercise interventions (HIIT and MICT) decreased blood glucose levels and improved cardiac performance, with greater changes in the HIIT group ($p < 0.001$, η^2: 0.909). While the expressions of miR-206 and apoptotic markers decreased in both training protocols ($p < 0.001$, η^2: 0.967), HIIT caused greater reductions in apoptotic markers and produced a 20% greater reduction in miR-206 compared with the MICT protocol ($p < 0.001$). Furthermore, both training protocols enhanced the expression of HSP60 ($p < 0.001$, η^2: 0.976), with a nearly 50% greater increase in the HIIT group compared with MICT.

OPEN ACCESS

Edited by:
Jian Shi,
University of Leeds, United Kingdom

Reviewed by:
Dongtak Jeong,
Hanyang Universiy, Erica, South Korea
Shun Yan,
Augusta University, United States
Pingzhu Zhou,
Boston Children's Hospital and Harvard Medical School, United States

****Correspondence:***
Urs Granacher
urs.granacher@uni-potsdam.de
Hassane Zouhal
hassane.zouhal@univ-rennes2.fr
Maryam Delfan
m.delfan@alzahra.ac.ir

†ORCID:
Urs Granacher
orcid.org/0000-0002-7095-813X
Hassane Zouhal
orcid.org/0000-0001-6743-6464

‡These authors share last authorship

Specialty section:
This article was submitted to Cardiovascular Metabolism, a section of the journal Frontiers in Cardiovascular Medicine

Received: *25 April 2022*
Accepted: *13 June 2022*
Published: *29 June 2022*

Citation:
Delfan M, Amadeh Juybari R, Gorgani-Firuzjaee S, Høiriis Nielsen J, Delfan N, Laher I, Saeidi A, Granacher U and Zouhal H (2022) High-Intensity Interval Training Improves Cardiac Function by miR-206 Dependent HSP60 Induction in Diabetic Rats. Front. Cardiovasc. Med. 9:927956. doi: 10.3389/fcvm.2022.927956

Conclusions: Our results indicate that both exercise protocols, HIIT and MICT, have the potential to reduce diabetic cardiomyopathy by modifying the expression of miR-206 and its downstream targets of apoptosis. It seems however that HIIT is even more effective than MICT to modulate these molecular markers.

Keywords: diabetes, apoptosis, miRNAs, exercise, cardiomyopathy

INTRODUCTION

Diabetes mellitus (DM) is a risk factor for cardiovascular disease that is estimated to affect more than 439 million people by 2030 (1). Of note, patients are at increased risk of developing diabetic cardiomyopathy (DCM) which is unrelated to risk factors such as hypertension, coronary artery disease, and valvular heart disease (2). DCM has been associated with disturbances in the myocardial structure and function, involving left ventricular hypertrophy and dysfunction, myocardial fibrosis, and cellular signaling pathway abnormalities, eventually leading to heart failure (3).

The available research suggests that the inhibition of molecular signaling pathways involved in DCM may mitigate the pathological changes in cardiomyocytes of patients with diabetes (2). For instance, high glucose appears to induce early cellular changes, including apoptosis, in cardiomyocytes in DCM (4). Apoptosis and cell survival signals in diabetic cardiomyocytes may be partly mediated by microRNAs (miRNAs) that regulates gene expression post-transcriptionally (5). Cardiac/skeletal muscle-specific miR-206 has been suggested to be involved in apoptotic processes, and over-expression of miR-206 may even accelerate cardiomyocyte apoptosis by ultimately leading to DCM (6, 7). Hyperglycemic conditions up-regulate miR-206 in diabetic heart disease (6). In turn, miR-206 negatively regulates heat shock protein 60 expression (HSP60), which serves as a protective component against diabetes-induced cardiac damage and apoptosis (3).

Physical activity and exercise are effective means to treat diabetes and its cardiovascular adverse effects (8). Recommendations of the World Health Organization (WHO) suggest a minimum weekly dosage of 150 min of moderate to vigorous intensity physical activity (30 min, 5 days per week) to prevent and improve diabetic adverse effects (9). There is evidence however, that large proportions of patients do not meet WHO guidelines (10) and ∼50% of diabetics do not participate in any physical activity, according to a research (11). Accordingly, new intervention strategies are needed that are attractive for individuals and effective in terms of health outcomes at the same time. Patients, especially those with T1DM do not take up exercise due to fear of hypoglycemia and also lack of time (12). Recent evidence indicates that high-intensity interval training (HIIT) has the potential to reduce blood glucose levels (hypoglycemia) which is an established effect for moderate-intensity continuous training (MICT) (13, 14). Moreover, HIIT produces similar or greater improvements in cardiovascular function, hyperglycemia, and other adverse events of diabetes even with 60–80% less exercise time compared with MICT (13, 15). Thus, HIIT may be considered a viable and time-efficient alternative to MICT.

The molecular signaling processes associated with DCM have recently received much attention. While the mechanisms by which hyperglycemia effects cardiomyocytes are not fully elucidated, it has been demonstrated that excessive glucose triggers cellular death by increasing miR-206 expression (6). Accordingly, we examined the effects of different glucose concentrations on C2C12 skeletal muscle cells to examine the differential effects of HIIT and MICT on the expression of miR-206 in DCM by monitoring apoptosis-related markers, HSP60, and cell viability. To better understand the mechanisms underlying apoptosis and exercise-induced cardioprotection against apoptosis, we tested the following hypotheses based on the available literature (6, 16): (1) High glucose concentrations *in vitro* up-regulate the expression of miR-206, leading to decreased HSP60 and increased apoptosis-related markers, (2) Both HIIT and MICT down-regulate the expression of miR-206 and apoptotic markers and up-regulate HSP60 levels, and (3) HIIT produces greater benefits in the molecular and functional markers of DCM.

MATERIALS AND METHODS

Animals

Male Wistar rats (8 weeks old, $n = 18$), weight 260 ± 10 g, were acquired from the Pasteur Institute (Tehran, Iran). The rats were kept in a room with 50% humidity, a temperature of 22°C, a 12 h light/12 h dark cycle, and had access to laboratory chow and water *ad libitum*. All animal procedures were carried out humanely and in accordance with the guidelines of the Tehran University of Medical Sciences' Animal Care Committee (EC-00312).

Induction of Diabetes

Rats received STZ (55 mg/kg IP; Sigma-Aldrich, St. Louis, MO) in a 2% solution of cold 0.1 M citrate buffer (pH 4.5) to induce type 1 diabetes (17, 18). Blood glucose levels were measured using a glucometer (Glucocard 01, Japan) 3 days after STZ treatment to confirm diabetes. Rats were considered to be diabetic when blood glucose concentrations were higher than 300 mg/dL (6, 18).

Training Protocol

Diabetic animals were randomly allocated to three groups ($n = 6$ in each group): control, MICT (Moderate-Intensity Continuous Training), and HIIT (High-Intensity Interval Training). The training was conducted 5 days per week for 5 weeks. After having familiarized the animals to the treadmill, the velocity at VO_{2max}

Abbreviations: HSP60, heat shock protein 60; PARP, poly ADP-ribose polymerase.

TABLE 1 | Intensity of HIIT (in meters per minute) based on vVO_{2max}.

Exercise progression	Main aspects of training			
Training components	Warm up	High intensity	Recovery	Cool down
Time of training	5 min	3 min	1 min	5 min
Intensity of training (% of vVO_{2max})	30–40%	85–90%	30–40%	30–40%
First week (m/min)	4.5–6	12.5–13.5	4.5–6	4.5–6
Second week (m/min)	5.5–7.5	16–17	5.5–7.5	5.5–7.5
Third week (m/min)	6.5–8.5	18.5–20	6.5–8.5	6.5–8.5
Fourth week (m/min)	7–9.5	20.5–21.5	7–9.5	7–9.5
Fifth week (m/min)	8–11	23–24	8–11	8–11

The slope of the treadmill was set at 0° at all stages of training. HIIT, High-Intensity interval training; vVO_{2max}, the velocity at VO_{2max}.

TABLE 2 | Intensity of MICT (in meters per minute) based on vVO_{2max}.

Exercise progression	Warm up	Main part of training	Cool down
Time of training	5 min	30 min	5 min
Intensity of training (% of vVO_{2max})	30–40%	60–65%	30–40%
First week (m/min)	4.5–6	9–9.5	4.5–6
Second week (m/min)	5.5–7.5	11.5–12	5.5–7.5
Third week (m/min)	6–8.5	12.5–13.5	6.85
Fourth week (m/min)	7.5–10	15–16	7.5–10
Fifth week (m/min)	8–10.5	16–17.5	8–10.5

The slope of the treadmill was set at 0° at all stages of training. MICT, Moderate-Intensity continuous training; vVO_{2max}, the velocity at VO_{2max}.

(vVO_{2max}) was assessed every week by using a modified ramp test protocol as previously reported (19, 20).

HIIT

The HIIT program consisted of 5 min of a warm-up with running at 30–40% of vVO_{2max}, followed by the main training session of 3 min of running at 85–90% of vVO_{2max} (the running speed was increased from 12 m/min during the first week to 24 m/min during week five), followed by 1 min of recovery. This cycle was performed four times per session and ended with a 5 min cool-down at 30–40% of vVO_{2max} (**Table 1**).

MICT

The MICT protocol consisted of 40 min of continuous running. Every session included 5 min of a warm-up with running at 30–40% of vVO_{2max}, followed by 30 min of running at 60–65% of vVO_{2max} (the running speed was increased from 9 m/min during the first week to 18 m/min in week 5), and ended with 5 min cool down at 30–40% of vVO_{2max} (**Table 2**). Exercise volume was similar between the intervention groups.

Control

Animals in the control group did not participate in any exercise intervention, but were positioned on a stationary treadmill for 10–15 min daily to simulate the environmental conditions of the exercise protocols.

Echocardiography and Left Ventricular Extraction

Animals were anesthetized with intraperitoneal injections of ketamine (90 mg/kg body mass) and xylazine (10 mg/kg body mass) before investigating cardiac function *in vivo*. After shaving the anterior chest, the animals were positioned in the left lateral decubitus position and a rectal temperature probe was inserted so that the body temperature could be maintained between 37 and 37.5°C using a heating pad. Conventional two-dimensional M-mode echocardiography images (GE Vingmed Ultrasound, Horton, Norway) were obtained to assess markers of cardiac function. Left ventricular end-diastolic dimensions and ejection fractions were assessed using a 10-MHz probe (Horton, Norway) in the short axis (papillary) views. At least three cardiac cycles were used to conduct echocardiographic measurements. All echocardiograms were completed by one operator who was blind to genotype and treatment, using specialized software (EchoPac V113.05, GE Healthcare, Horton, Norway). Blood samples were taken directly from rat hearts, and serum was obtained after centrifugation at 3,000 g for 4 min at 10°C. In addition, left ventricular tissue was removed and washed in saline before promptly frozen in liquid nitrogen.

Cell Culture

A mouse skeletal myoblast cell line (C2C12), which was purchased from Iran's Pasteur Institute, was maintained in Dulbecco's modified Eagle medium (DMEM) supplemented with 20% heat-inactivated fetal bovine serum (FBS) in growth medium (GM) and 1% penicillin-streptomycin. DMEM containing 2% heat-inactivated horse serum (differentiation medium, DM) and 1% penicillin-streptomycin was utilized for myogenic differentiation from myoblasts into myotubes. The MTT assay was used to evaluate cell viability as previously described (21).

microRNA Mimic, and Antisense microRNA Transfection

The miR-206 sequences were transfected into C2C12 cells using RNAiMAX (Invitrogen) according to the manufacturer's instructions. Antisense (2′-*O*-methyl) oligonucleotides in a serum-containing medium were transfected into C2C12 cells. Serum depletion was used to differentiate the cells into muscle cells after 72 h.

miRNA Expression by Real-Time-PCR

MicroRNA was extracted using a miRNeasy mini kit (Qiagen, Hilden, Germany) using the manufacturer's instructions. MiScript II RT kit (Qiagen, Hilden, Germany) was used to synthesize cDNA of the miR-206 genes. Polymerase chain reaction (PCR) was performed using a Real-Time PCR machine (Corbett Rotor-Gene 6000, Qiagen, Hilden, Germany). The Real-Time program for miR-206 (miR-206 miScript Primer Assay, Qiagen, Hilden, Germany) was based on the miScript SYBR Green PCR Kit (Qiagen, Hilden, Germany), which included a cycle of 95°C for 15 min, followed by 40 cycles of 94°C for

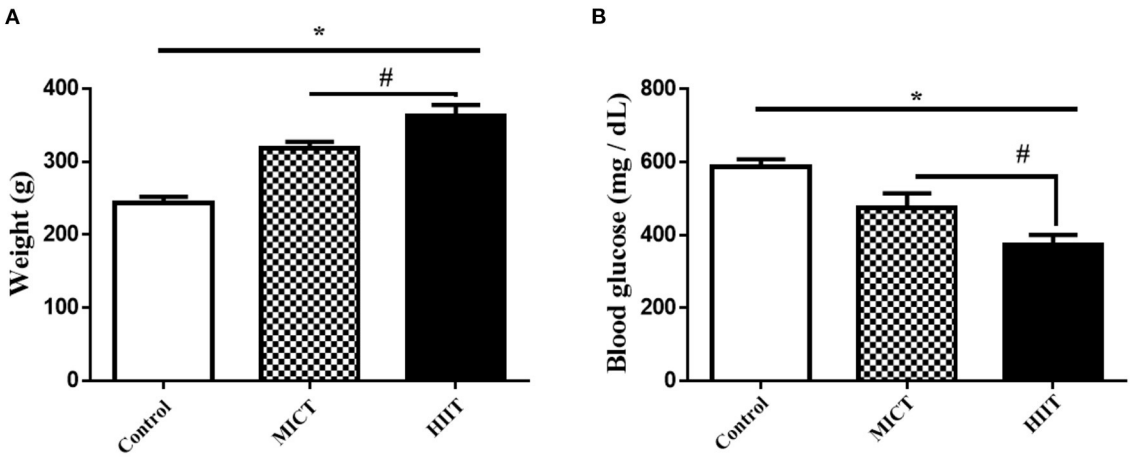

FIGURE 1 | Body mass and fasting blood glucose concentrations in the three experimental groups. **(A)** Body mass **(B)** Blood glucose. Data are presented as means ± standard error of the mean (SEMs). *Significant differences between control and intervention groups, #Significant differences between MICT and HIIT. MICT, moderate-intensity continuous training; HIIT, high-intensity interval training. Rats ($n = 6$ per group) were trained for 5 weeks.

15 s, 55°C for 30 s, and 70°C for 30 s. SNORD-61 (SNORD 61 miScript Primer Assay Qiagen, Hilden, Germany) was used to normalize target gene transcript levels (22). The $2^{-\Delta\Delta CT}$ (delta-delta Ct) method was used to convert real-time CTs to quantitative data.

Western Blot Analysis

Cellular protein was isolated from previously frozen left ventricular tissue by homogenizing 70–100 mg of tissue in a modified RIPA buffer (50 mm Tris–HCl, pH 7.4, 1% Triton X-100, 0.2% sodium deoxycholate, 0.2% SDS, 1 mm Na-EDTA, and 1 mm PMSF) supplemented with protease inhibitor cocktail and PMSF (Roche, Mannheim, Germany). Protein concentration was determined with a Bradford assay, and equivalent amounts of protein were subjected to SDS–PAGE and then transferred onto a PVDF membrane. The membranes were then incubated for 2 h at room temperature in blocking buffer (1: Tris-buffered saline (TBS), 0.5% Tween-20, and 5% non-fat dry milk). Blots were incubated overnight at 4°C with primary antibodies against cleaved PARP, cytochrome C, HSP60 (Cell Signaling Technology, Beverly, MA, USA), and β-actin (Abcam, Cambridge, MA, USA). We utilized an enhanced chemiluminescent substrate (ECL) after incubating with second HRP-conjugated antibodies to visualize protein bands. Densitometry was used to analyze band densities using Image J software.

Statistical Analyses

Results are presented as mean ± SEM (standard error of the mean). The Kolmogorov-Smirnov (KS) test was used to assess data normality. The Levene test was applied to establish variance homogeneity. After confirmation of data normality and homogeneity, a one-way analysis of variance (ANOVA) was conducted to verify significant differences between groups. If ANOVA revealed significant outcomes, the Tukey *post-hoc* test (least significant difference) was computed for pair-wise comparisons to identify the potential difference between three groups. Partial eta-squared (η^2) was used as an effect size measure. The statistical significance level for all comparisons was set at $p < 0.05$. Statistical analysis was carried out using SPSS 19 (IBM SPSS, United Kingdom).

RESULTS

General Characteristics of Animals

The general characteristics of the animals used in this study are shown in **Figure 1**. There were significant differences in body mass between groups ($F_{2,15} = 167.053$, $p < 0.001$, η^2: 0.957), with differences in body mass between the MICT and HIIT groups ($p < 0.003$). There were also significant between group differences in glucose levels ($F_{2,15} = 74.625$, $p < 0.001$, η^2: 0.909). Blood glucose levels were significantly lower in the HIIT and MICT groups compared with the control group (36.5 and 18.9%, respectively, $p < 0.001$). Glucose levels were significantly lower in the HIIT group compared with the MICT group ($p < 0.001$) as shown in **Figure 1B**.

In vivo Left Ventricular Function

The mean left ventricular end-diastolic diameters in control rats were significantly greater than that observed in the MICT and HIIT groups as shown by M-mode echocardiograms (7.56 ± 0.41 vs. 6.20 ± 0.40 and 5.78 ± 0.41 mm, respectively, $p = 0.01$; **Table 3**). Moreover, the mean left ventricular end-systolic diameters in both intervention groups (MICT and HIIT) were significantly lower compared with the control group (3.1 ± 0.17 and 2.90 ± 0.14 vs. 4.49 ± 1.12 mm, $p = 0.002$). In addition, there were differences in ejection fractions between control and exercise animals (66.67 ± 0.93 vs. 75.59 ± 3.71% and 80.38 ± 2.63%; $p = 0.003$). These findings indicate that both exercise protocols (MICT and HIIT) improved heart function in diabetic animals. Further, there were differences in all

electrocardiography parameters (LVESD, LVEDD, and ejection fraction; $p = 0.002$) between the MICT and HIIT groups. Overall, our results indicate that the HIIT protocol enhanced cardiac function more than the MICT protocol.

HIIT Decreases miR-206 Expression

We measured the expression of miRNA in the left ventricular tissue to better understand the potential molecular mechanisms for the beneficial effects of physical exercise on cardiac parameters. Both exercise protocols significantly reduced miR-206 expression compared with control ($F_{2,15} = 222.149$, $p < 0.001$, η^2: 0.967). MICT and HIIT protocols reduced miR-206 expression by 30.3 and 51.3%, respectively. In addition, HIIT showed a 1.7 fold larged reduction in miR-206 expression compared with MICT ($p < 0.001$; **Figure 2A**).

HIIT Enhances HSP60 Expression at the Protein Level

The expression levels of HSP60 protein were determined to investigate potential molecular links between physical exercise and apoptosis in cardiac cells. Both MICT and HIIT protocols enhanced HSP60 expression (1.68- and 2.21-fold, respectively) ($F_{2,15} = 306.781$, $p < 0.001$, η^2: 0.976). HIIT resulted in a ∼50% greater increase in HSP60 expression compared with MICT ($p < 0.001$; **Figure 2B**).

HIIT Program Mitigates Diabetes-Induced Ventricular Apoptosis

We analyzed the protein expression of cleaved PARP and cytochrome C to investigate the effects of the HIIT and MICT on key intermediates of the apoptosis pathway. The expressions of apoptotic marker (PARP and Cyt C) were reduced in both exercise groups ($p<0.001$), with HIIT reducing cleaved PARP ($F_{2,15} = 101.337$, $p < 0.001$, η^2: 0.931) (**Figure 3A**), and cytochrome C protein levels ($F_{2,15} = 129.552$, $p < 0.001$, η^2: 0.945) (**Figure 3B**) more than MICT. Our results indicate that both exercise protocols reduced protein markers of apoptosis in diabetic rat hearts, with greater improvements produced by HIIT compared to MICT.

High Glucose Induces miR-206 Expression and Reduces Cell Viability

We treated C2C12 cell lines with increasing concentrations of glucose (5.5, 11, 22, 33, and 48 mM) to determine a potential role of hyperglycemia on miR-206 expression. Increasing concentrations of glucose enhanced miR-206 expression in a dose-response manner ($F_{4,25} = 339.240$, $p < 0.001$; **Figure 4A**). In addition, the viability of C2C12 cells was evaluated in the presence of different glucose concentrations by using the MTT assay. Increasing concentrations of glucose reduced cell viability in a dose-dependent manner at glucose concentrations greater than 11 mM ($F_{4,25} = 182.212$, $p < 0.001$; **Figure 4B**). We also assessed the effects of different concentrations of glucose on HSP60 and protein markers of apoptosis. Increases in glucose produced concentration-dependent reductions in HSP-60 protein ($F_{4,20} = 107.874$, $p < 0.001$), and increases in cleaved PARP ($F_{4,20} = 533.231$, $p < 0.001$) and cytochrome C ($F_{4,20} = 293.547$, $p < 0.001$) protein expression levels (**Figures 5A–C**).

TABLE 3 | Echocardiographic changes produced by exercise in diabetic rats.

Variable	Control	MICT	HIIT
LVEDD (mm)	7.56 ± 0.41	6.20 ± 0.42*	5.78 ± 0.41*#
LVESD (mm)	4.49 ± 1.12	3.10 ± 0.17*	2.90 ± 0.14*#
Ejection fraction (%)	66.67 ± 0.93	75.59 ± 3.71*	80.38 ± 2.63*#

*Data presented as means ± SEMs *Significant differences between control and exercise groups, #Significant differences between MICT and HIIT. MICT, Moderate-Intensity continuous training; HIIT, High intensity interval training; LVEDD, Left ventricular end-diastolic diameter; LVESD, Left ventricular end-systolic diameter.*

We modulated miR-206 expression and analyzed apoptosis markers to provide additional evidence for the role of miR-206 role in high-glucose-induced myocyte apoptosis. C2C12 cells were transfected with a miR-206 mimic sequence and harvested in the presence of 5.5 and 33 mM of glucose. The miR-206 mimic reduced HSP60 protein expression and induced the protein expression of apoptotic markers in the presence of normal glucose. However, the transfection with the miR-206 antisense sequence (inhibitor) reversed high glucose (33 mM) reduced the expression levels of HSP-60 ($F_{3,16} = 215.402$, $p < 0.001$), and increased cleaved PARP ($F_{3,16} = 1{,}866.64$, $p < 0.001$), and the cytochrome C ($F_{3,16} = 200.5.6$, $p < 0.001$) expression levels (**Figures 5D–F**).

DISCUSSION

Physical exercise has long been considered an effective cardioprotective strategy that improves the anatomical and functional abnormalities of the diabetic heart (8). Our study compared the effects of two different exercise protocols (high intensity interval training [HIIT] vs. moderate-intensity continuous training [MICT]) on cardiac function and apoptosis signaling pathways, focusing on miR-206, HSP60, and apoptosis-related markers. The main findings of this study were that: (1) both HIIT and MICT improved blood glucose levels and cardiac function, with the HIIT protocol producing greater benefits, and (2) both exercise protocols reduced the expression of miR-206 expression and apoptotic markers and increased the expression of HSP60, while HIIT induced greater changes than MICT.

Cardiomyocyte apoptosis is an underlying component of various cardiac diseases, including in high glucose-induced cardiotoxicity (3). MicroRNAs, or small non-coding RNAs regulating gene expression, are potential diagnostic and therapeutic molecules in diabetic individuals with cardiovascular disease. High glucose concentrations increase the expression of miRNAs, such as miR-1 or miR-206, in C2C12 cells and rat cardiac myocytes (4, 23). Our *in vitro* findings suggest that miR-206 may be a destructive miRNA that activates apoptosis signaling pathways. In support of this are the findings of Shan et al. who reported that treatment of cardiomyocytes with 25 mM glucose induced apoptosis via miR-1/miR-206, and moreover, that these microRNAs bind to HSP60, an anti-apoptotic protein,

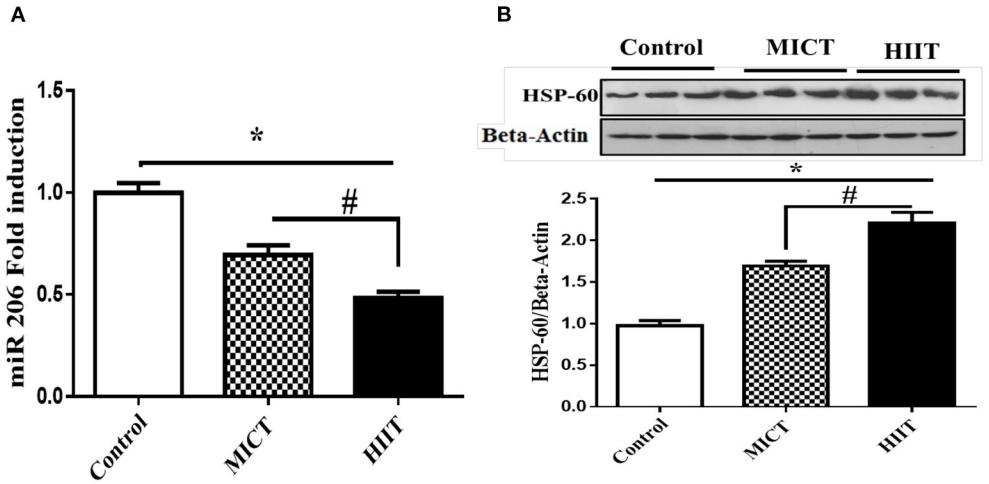

FIGURE 2 | Effects of exercise on miR-206 mRNA. **(A)** HSP60 protein expression. **(B)** Data are presented as means ± standard error of the mean (SEMs). *Significant differences between control and intervention groups, #Significant differences between MICT and HIIT. MICT, moderate-intensity continuous training; HIIT, high-intensity interval training; $n = 6$ and rats trained for 5 weeks.

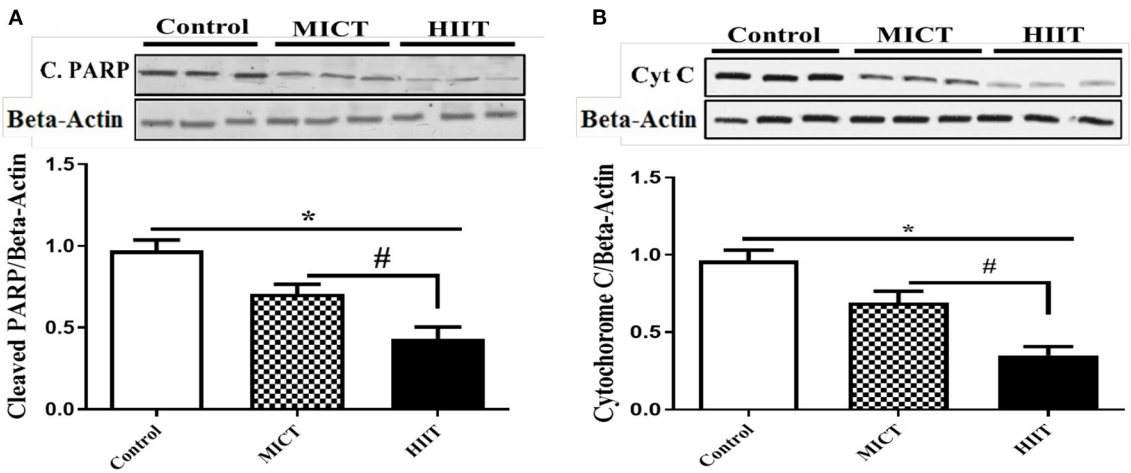

FIGURE 3 | Effects of HIIT and MICT protocol on apoptotic intermediate molecules. **(A)** Cleaved PARP (C.PARP). **(B)** Cytochrome C. Data are presented as means ± standard error of the mean (SEMs). *Significant differences between control and intervention groups, #Significant differences between MICT and HIIT. MICT, moderate-intensity continuous training; HIIT, high-intensity interval training, $n = 6$ and rats trained for 5 weeks.

thereby downregulating HSP60 expression (6). Our findings also suggest that exposure to high glucose concentrations induced miR-206 expression, increased cytochrome C and cleaved PARP protein expression, and inhibited HSP60 protein expression in C2C12 cells. On the other hand, induction of miR-206 with a mimic sequence inhibited the expression of HSP60 at normal glucose concentrations, and the miR-206 antisense sequence reversed the inhibitory effects of a high glucose concentration (33 mM) on HSP60 and promoted HSP60 protein expression.

HSP60 is present in different intracellular compartments, including the cytosol, plasma-cell membrane, extracellular space, mitochondria, and also in the circulation (24). The localization of HSP60 is an important consideration, as extracellular HSP60 can activate the innate immune system *via* Toll-like receptor (TLR)-4 and increase cardiac myocyte apoptosis, while HSP60 acts as an anti-apoptotic factor when present in the cytosol or mitochondria (25). Cytoplasmic HSP60 binds to Bax and Bak (pro-apoptotic proteins) and inhibits their integration into the mitochondrial membrane, thereby indirectly limiting the activation of mitochondrial cytochrome C and the apoptotic cascade (26). Additionally, our findings demonstrate that a miR-206 mimic enhanced protein expression of apoptotic markers at normal glucose concentrations, whereas miR-206 inhibitors decreased the expression of apoptotic markers at higher glucose concentrations. Therefore, miR-206 acts, at least to some extent, targets the expression of cytochrome C and cleaved PARP, two apoptosis-related proteins, and inhibits HSP60 (an anti-apoptotic protein). Our results reinforce the concept that increased

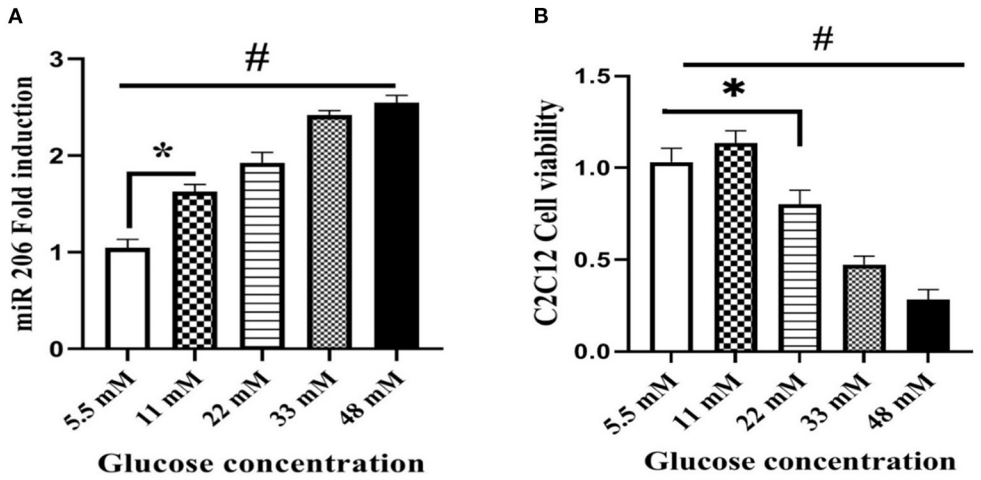

FIGURE 4 | Effect of different glucose concentrations on miR-206 expression and viability of C2C12 cells. **(A)** miR-206 expression **(B)** cell viability. Data are presented as means ± standard error of the mean (SEMs). $n = 6$. C2C12 cells treated for 24 h with high glucose DMEM media, *Significant differences between normal glucose and high glucose, and #significant differences between different glucose concentrations.

miR-206 expression can contribute to high glucose-induced cell death.

The balance between cell survival and cell death signals is complex, particularly in muscle cells. We hypothesized that high glucose concentrations detrimentally impact cell survival; thus, we investigated the adverse effects of high glucose concentrations on cell viability. Concentrations of glucose >11 mM decreased cell viability, which can be attributed to increases in miR-206 and apoptotic-related biomarkers, as well decreases in HSP60 expression. However, cell viability was not affected at 11 mM glucose despite increases in miR-206 and apoptotic markers. Cell viability in 11 mM glucose may be interpreted as a protective mechanism involved in cell survival at lower glucose concentrations, but this remains untested as only a few studies examined the cellular consequences of various concentrations of glucose. Our findings are supported by previous *in vitro* studies indicating that intermittent high glucose concentrations exacerbate oxidative stress and apoptosis in endothelial cells (27).

Our study indicates that HIIT-induced improvements in blood glucose levels and cardiac function were superior than the effects of MICT in STZ-induced diabetic rats. Higher intensity exercise protocols induce greater improvements in glycemic control when compared to moderate-intensity protocols (28, 29). A study by Chavanelle et al. reported that HIIT induced greater insulin-stimulated Akt phosphorylation and muscle glucose transporter 4 (GLUT4) expression than MICT, implying that HIIT is more efficient in improving glucose metabolism (28). The impact of the two different exercise protocols on glycemic control is probably attributed to differences in the effects of the skeletal muscle activity on stimulated glucose transport (30). Moreover, enhanced hepatic glucose production is a key contributor to hyperglycemia, and HIIT reduces hepatic glucose production following exercise more than MICT (31). In addition, high-intensity exercise depletes muscle glycogen concentrations to a greater extent than low-intensity exercise (32). It is probable that exercise-induced glycogen depletion stimulates larger increases in glucose uptake to replenish glycogen stores. Our study confirms these expectations in STZ-induced diabetic rats, where HIIT was superior to MICT in improving blood glucose metabolism (**Figure 1B**). Our results are also consistent with the findings of Terada et al. who reported that HIIT caused greater reductions in blood glucose levels than MICT in patients with type 2 diabetes (T2DM) after 24 h of exercise (33). Similarly, Mendes et al. observed that HIIT had a greater impact on glycemic control than MICT in patients with T2DM treated with metformin (34).

Other noteworthy findings from our study included the down-regulation of miR-206 in the left ventricular tissues of both exercise groups, HIIT reduced miR-206 expression by ∼1.7-fold more times than the effects of MICT (**Figure 2**). Exercise is a powerful regulator of miRNAs expression, whose expression depends on specific training parameters such as intensity, duration, and volume (35). Since high glucose concentrations increased miR-206 expression *in vitro*, it can be inferred that lowering glucose levels, which is a goal of prescribing exercise for patients with diabetes, could also decrease miR-206 following exercise, specifically after high-intensity training. Preliminary studies demonstrated an association between pathological heart conditions and changes in myosin heavy chain (MyHC) proteins, with transformation of the faster α-MyHC isoform to the slower β-MyHC isoform (36). Elevated miR-206 expression correlates with pathologic increases in β-MyHC expression in the left ventricle, and miR-206 deletion leads to conversion of slow to fast muscle MyHC isoforms (37). While the mechanisms by which exercise protects cardiomyocytes from various cardiac insults are unknown, it has been proposed that exercise increases α-MyHC protein expression and suppresses the isoform shift to β-MyHC in the left ventricle, hence aiding in the improvement of cardiac

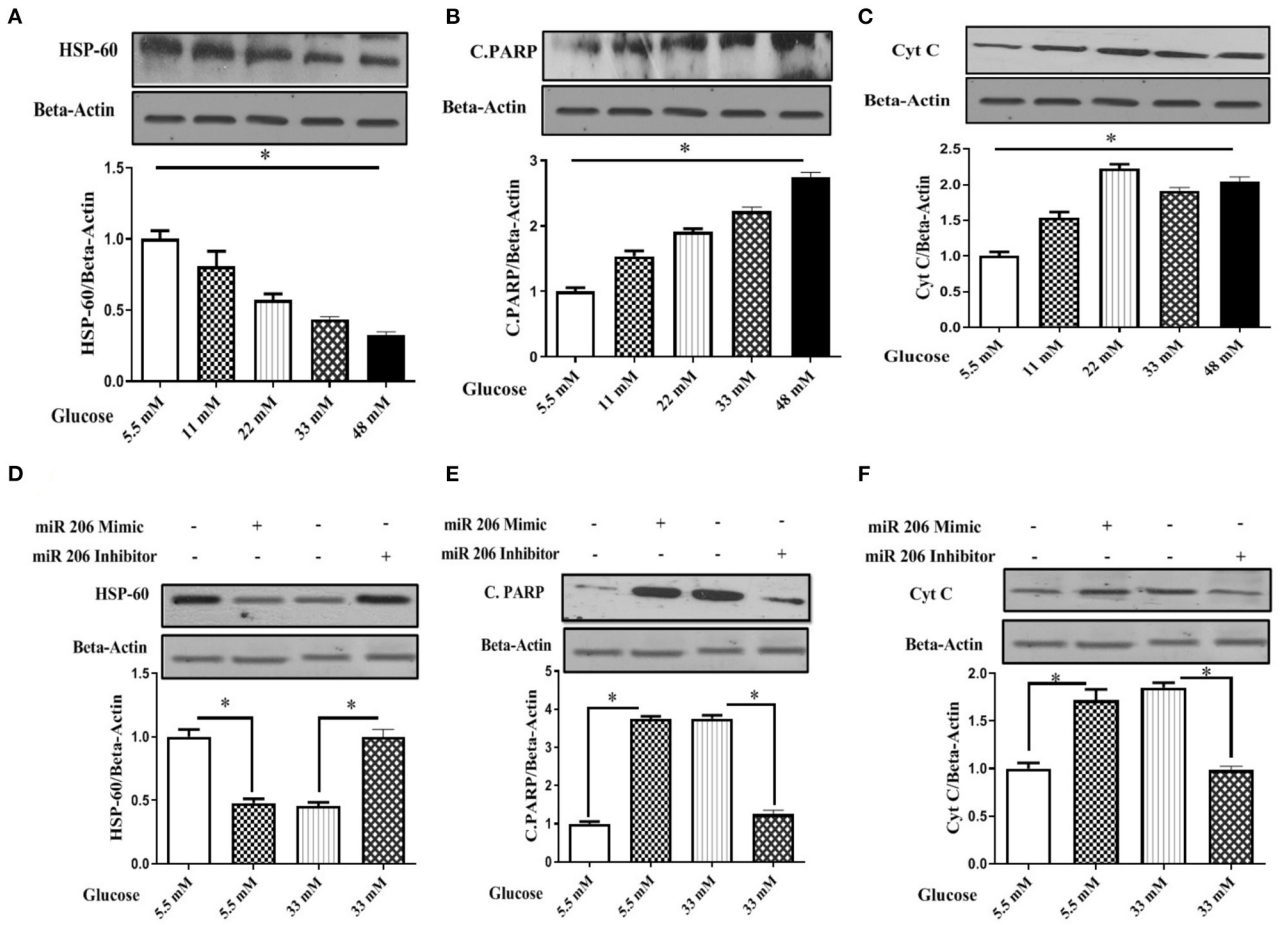

FIGURE 5 | Effect of different glucose concentrations and miR-206 modulation on HSP60 and apoptosis markers in C2C12 cells **(A)** HSP60 protein expression, **(B)** Cleaved PARP (C.PARP) protein expression, **(C)** Cytochrome C protein expression, **(D)** Effects of miR-206 mimic and inhibitor on HSP60 protein expression, **(E)** Effects on miR-206 mimic and inhibitor on C-PARP protein expression, **(F)** Effects of miR-206 mimic and inhibitor on Cytochrome C protein expression. $n = 5$, C2C12 cells treated for 24 h with high glucose DMEM media. *Significant differences.

function (38). It should be noted that a recent study reported no differences in the expression of miR-206 before and after physical exercise (39). This discrepancy in findings could be attributed to the induction of diabetes in the current study, the exercise modes, intensity, and duration of the intervention.

Cardiac and skeletal muscle performance is highly dependent on ATP-generating pathways for energy supply during exercise, and signaling during high-intensity training may be the consequence of alterations in the intracellular environment during training adaptations. For example, the modulated expression of miR-206 can stimulate AMP-activated protein kinase (AMPK), a cellular metabolite-sensing protein kinase (40). The AMPK signaling pathway is activated during physical activity in an intensity-dependent manner in response to fluctuations in the cellular energy states, thereby triggering carbohydrate metabolism to replenish ATP levels (41). Another key finding of our study was that both exercise training protocols enhanced HSP60 expression in the left ventricular tissues, with the HIIT protocol causing a ∼50% greater expression of HSP60 MICT (**Figure 2B**). Overexpression of the chaperone protein HSP60 can boost electron transport chain activity and ATP generation in injured cardiomyocytes (42). HIIT improved the expression of HSP60 more than MICT likely because exercise enhances ATP turnover in an intensity-dependent manner. The main mechanisms driving the effect of exercise on apoptosis may include metabolic perturbations (e.g., oxidative stress, low pH, muscle temperature, ROS, glycogen depletion, and lactate concentration) experienced during the exercise, particularly with HIIT (43). It is likely that these metabolic challenges following training increase the expression of HSP60 as HSPs respond to stress. Another postulated mechanism is that miR-206 contributes to cardiomyocyte apoptosis by post-transcriptional repression of insulin-like growth factor 1 (IGF-1) (16). Additionally, reduced HSP60 suppresses the IGF-1 signaling pathway, resulting in diabetic cardiomyopathy (44). On the other hand, exercise acts enhances the IGFI/PI3K/Akt survival pathway in diabetic hearts (45).

Our findings indicate that the expression of apoptotic markers was reduced in the left ventricular tissues of both training groups, with HIIT decreasing cleaved PARP and cytochrome

C protein levels more than MICT. A growing body of evidence indicates that mitochondrial dysfunction may be a key determinant of oxidative stress and consequently, myocardial apoptotic signaling in pathological conditions (3). In particular, exercise protects against the activation of apoptotic cascades by improving mitochondrial function and structure. For example, Veeranki et al. reported that exercise ameliorates mitochondrial transmembrane potential and prevents cytochrome C leakage into the cytoplasm, reducing cardiomyocyte apoptosis in *db/db* mouse hearts (46). The intensity of exercise influences mitochondrial function (47), suggesting that HIIT may be more effective in improving mitochondrial function and reducing apoptotic markers. Mitochondrial homeostasis requires HSP60, a mitochondrial chaperone protein (24). Increases in HSP60 following HIIT can prevent cardiomyocyte apoptosis by improving mitochondrial function and homeostasis. The effects of miR-206 on its downstream molecular target (HSP60) as well as apoptotic markers suggests that exercise-induced reductions in miR-206 can reduce apoptosis *in vitro*. Our *in vitro* data supports our hypothesis that the exercise-induced decreases in markers of cardiomyocyte apoptosis, and that increases in HSP-60 (especially with HIIT) may be mediated, at least in part, by reductions in miR-206 expression and blood glucose levels.

Diabetes-induced cardiomyopathy includes cardiac functional and morphological abnormalities that are accompanied by myocardial fibrosis, ventricular systolic and diastolic dysfunction, reduced ejection fraction, and impaired cardiomyocyte contractility (2). Regular exercise training promotes cardioprotective adaptations associated with improved cardiac function and structure (8, 13, 14). We used echocardiography to demonstrate that both exercise protocols improved left ventricular function by reducing end-diastolic and end-systolic parameters in STZ-induced diabetic rats. In addition, exercise training also improved ejection fraction in diabetes. Exercise training restores diabetic cardiac abnormalities in an exercise intensity-dependent manner. The superior effect of high-intensity exercise over moderate-intensity exercise on cardiac adaptations is well-documented in both human (48) and animal studies (49).

Hyperglycemia and disrupted energy metabolism are responsible, at least in part, for diabetes-related cardiac abnormalities. Given that both exercise training programs were associated with improvements in cardiac functional and morphological characteristics, it is reasonable to suggest that improvements of blood glucose and underlying cellular modifications induced by both exercise training, particularly HIIT, could improve cardiac function. It has also been suggested that exercise at a high intensity stimulates sympathetic activity, with the greater sympathetic activity in HIIT promoting cardiac contractile capacity and function (50). Our results are supported by findings that HIIT was more effective than moderate exercise training in improving systolic and diastolic function and VO_{2peak} in T2DM (51) and that HIIT improves VO_{2peak} and left ventricular remodeling more than moderate continuous training in patients with prior myocardial infarction and left ventricle systolic dysfunction (52) and also that HIIT improved cardiac structure and function in T2DM patients by increasing left ventricular wall mass, end-diastolic volume, and stroke volume after 12 weeks of exercise (53). In addition, HIIT has a superior effect on vascular endothelial function in patients with diabetes (29). However, some studies reported no differences in VO_{2peak} in patients with T2DM after HIIT and MICT (49). Nevertheless, the majority of studies suggest that the intensity of exercise is an important determinant in improving cardiac function in diabetic patients, and that moderate-intensity exercise may be insufficient to improve myocardial function.

Our study has some limitations that should be acknowledged: (1) We did not assess markers of the apoptotic cascade, such as caspase-9, caspase-3, caspase-8, Bax, Bak and p53. Future research should also measure the influence of different exercise programs on the expression levels of heart failure markers such as ANF, BNP, b-MHC, and (2) We tested LVEDD and LVESD using echocardiography, with no independent confirmation using cardiac tissue sections from the different experimental groups.

In conclusion, our study demonstrates that physical exercise has the potential to reduce plasma glucose levels and miR-206 expression. Suppression of miR-206 and the resulting positive regulation of HSP60 expression leads to improved cardiac function of diabetic rats following physical exercise. Although it has been established previously that MICT provides cardioprotection in diabetes, HIIT appears to stimulate even greater adaptations. Our findings suggest that HIIT should be preferred over MICT if the goal is to treat adverse effects related to diabetes including cardiomyopathy. Moreover, HIIT is a time-efficient exercise protocol compared with MICT.

DATA AVAILABILITY STATEMENT

The original contributions presented in the study are included in the article/supplementary materials, further inquiries can be directed to the corresponding authors.

ETHICS STATEMENT

All animal procedures were carried out humanely and in accordance with the guidelines of Tehran University of Medical Sciences' Animal Care Committee (EC-00312).

AUTHOR CONTRIBUTIONS

MD, RA, AS, SG-F, and HZ participated to the conception and design of the study. MD, SG-F, and RA were responsible for testing. MD, RA, AS, SG-F, JH, and ND were responsible for data collection and statistical analysis. MD, AS, IL, UG, and HZ were responsible for writing and finalization of the manuscript. All authors contributed to manuscript and approved the submitted version.

FUNDING

The authors acknowledge the support of the Deutsche Forschungsgemeinschaft (DFG, German Research Foundation) – Project number 491466077 and Open Access Publishing Fund of the University of Potsdam, Germany. This work was financially supported by Alzahra University.

REFERENCES

1. Shaw JE, Sicree RA, Zimmet PZ. Global estimates of the prevalence of diabetes for 2010 and 2030. *Diabetes Res Clin Pract.* (2010) 87:4–14. doi: 10.1016/j.diabres.2009.10.007
2. Jia G, Hill MA, Sowers JR. Diabetic cardiomyopathy: an update of mechanisms contributing to this clinical entity. *Circ Res.* (2018) 122:624–38. doi: 10.1161/CIRCRESAHA.117.311586
3. Shan Y-X, Liu T-J, Su H-F, Samsamshariat A, Mestril R, Wang PH. Hsp10 and Hsp60 modulate Bcl-2 family and mitochondria apoptosis signaling induced by doxorubicin in cardiac muscle cells. *J Mol Cell Cardiol.* (2003) 35:1135–43. doi: 10.1016/S0022-2828(03)00229-3
4. Yu X-Y, Geng Y-J, Liang J-L, Lin Q-X, Lin S-G, Zhang S, et al. High levels of glucose induce apoptosis in cardiomyocyte via epigenetic regulation of the insulin-like growth factor receptor. *Exp Cell Res.* (2010) 316:2903–9. doi: 10.1016/j.yexcr.2010.07.004
5. Zhao F, Li B, Wei Y-z, Zhou B, Wang H, Chen M, et al. MicroRNA-34a regulates high glucose-induced apoptosis in H9c2 cardiomyocytes. *J Huazhong Univer Sci Technol.* (2013) 33:834–9. doi: 10.1007/s11596-013-1207-7
6. Shan Z-X, Lin Q-X, Deng C-Y, Zhu J-N, Mai L-P, Liu J-L, et al. miR-1/miR-206 regulate Hsp60 expression contributing to glucose-mediated apoptosis in cardiomyocytes. *FEBS Lett.* (2010) 584:3592–600. doi: 10.1016/j.febslet.2010.07.027
7. Mooren FC, Viereck J, Krüger K, Thum T. Circulating microRNAs as potential biomarkers of aerobic exercise capacity. *Am J Physiol Heart Circul Physiol.* (2014) 306:H557–63. doi: 10.1152/ajpheart.00711.2013
8. Piepoli MF, Conraads V, Corra U, Dickstein K, Francis DP, Jaarsma T, et al. Exercise training in heart failure: from theory to practice. A consensus document of the heart failure association and the European association for cardiovascular prevention and rehabilitation. *Eur J Heart Fail.* (2011) 13:347–57. doi: 10.1093/eurjhf/hfr017
9. Colberg SR, Sigal RJ, Yardley JE, Riddell MC, Dunstan DW, Dempsey PC, et al. Physical activity/exercise and diabetes: a position statement of the American diabetes association. *Diabetes Care.* (2016) 39:2065–79. doi: 10.2337/dc16-1728
10. Nelson KM, Reiber G, Boyko EJ. Diet and exercise among adults with type 2 diabetes: findings from the third national health and nutrition examination survey (NHANES III). *Diabetes Care.* (2002) 25:1722–8. doi: 10.2337/diacare.25.10.1722
11. Hays LM, Clark DO. Correlates of physical activity in a sample of older adults with type 2 diabetes. *Diabetes Care.* (1999) 22:706–12. doi: 10.2337/diacare.22.5.706
12. Trost SG, Owen N, Bauman AE, Sallis JF, Brown W. Correlates of adults' participation in physical activity: review and update. *Med Sci Sports Exerc.* (2002) 34:1996–2001. doi: 10.1097/00005768-200212000-00020
13. Boff W, da Silva AM, Farinha JB, Rodrigues-Krause J, Reischak-Oliveira A, Tschiedel B, et al. Superior effects of high-intensity interval vs. moderate-intensity continuous training on endothelial function and cardiorespiratory fitness in patients with type 1 diabetes: a randomized controlled trial. *Front Physiol.* (2019) 10:450. doi: 10.3389/fphys.2019.00450
14. Scott SN, Cocks M, Andrews RC, Narendran P, Purewal TS, Cuthbertson DJ, et al. High-intensity interval training improves aerobic capacity without a detrimental decline in blood glucose in people with type 1 diabetes. *J Clin Endocrinol Metab.* (2019) 104:604–12. doi: 10.1210/jc.2018-01309
15. Jiménez-Maldonado A, García-Suárez PC, Rentería I, Moncada-Jiménez J, Plaisance EP. Impact of high-intensity interval training and sprint interval training on peripheral markers of glycemic control in metabolic syndrome and type 2 diabetes. *Biochim Biophys Acta.* (2020) 1866:165820. doi: 10.1016/j.bbadis.2020.165820
16. Shan Z-X, Lin Q-X, Fu Y-H, Deng C-Y, Zhou Z-L, Zhu J-N, et al. Upregulated expression of miR-1/miR-206 in a rat model of myocardial infarction. *Biochem Biophys Res Commun.* (2009) 381:597–601. doi: 10.1016/j.bbrc.2009.02.097
17. Sato K, Fujita S, Iemitsu M. Acute administration of diosgenin or dioscorea improves hyperglycemia with increases muscular steroidogenesis in STZ-induced type 1 diabetic rats. *J Steroid Biochem Mol Biol.* (2014) 143:152–9. doi: 10.1016/j.jsbmb.2014.02.020
18. Damasceno DC, Netto A, Iessi I, Gallego F, Corvino S, Dallaqua B, et al. Streptozotocin-induced diabetes models: pathophysiological mechanisms and fetal outcomes. *Biomed Res Int.* (2014) 2014:819065. doi: 10.1155/2014/819065
19. Leandro CG, Levada AC, Hirabara SM, Manhães-de-Castro R, De-Castro CB, Curi R, et al. A program of moderate physical training for wistar rats based on maximal oxygen consumption. *J Strength and Cond Res.* (2007) 21:751–6. doi: 10.1519/R-20155.1
20. Høydal MA, Wisløff U, Kemi OJ, Ellingsen Ø. Running speed and maximal oxygen uptake in rats and mice: practical implications for exercise training. *Eur J Prev Cardiol.* (2007) 14:753–60. doi: 10.1097/HJR.0b013e3281eacef1
21. Gorgani-Firuzjaee S, Ahmadi S, Meshkani R. Palmitate induces SHIP2 expression via the ceramide-mediated activation of NF-κB, and JNK in skeletal muscle cells. *Biochem Biophys Res Commun.* (2014) 450:494–9. doi: 10.1016/j.bbrc.2014.06.006
22. Calvano Filho CMC, Calvano-Mendes DC, Carvalho KC, Maciel GA, Ricci MD, Torres AP, et al. Triple-negative and luminal A breast tumors: differential expression of miR-18a-5p, miR-17-5p, and miR-20a-5p. *Tumor Biol.* (2014) 35:7733–41. doi: 10.1007/s13277-014-2025-7
23. Yang B, Lin H, Xiao J, Lu Y, Luo X, Li B, et al. The muscle-specific microRNA miR-1 regulates cardiac arrhythmogenic potential by targeting GJA1 and KCNJ2. *Nat Med.* (2007) 13:486–91. doi: 10.1038/nm1569
24. Meng Q, Li BX, Xiao X. Toward developing chemical modulators of Hsp60 as potential therapeutics. *Front Mol Biosci.* (2018) 5:35. doi: 10.3389/fmolb.2018.00035
25. Malik ZA, Kott KS, Poe AJ, Kuo T, Chen L, Ferrara KW, et al. Cardiac myocyte exosomes: stability, HSP60, and proteomics. *Am J Physiol Heart Circul Physiol.* (2013) 304:H954–65. doi: 10.1152/ajpheart.00835.2012
26. Gupta S, Knowlton AA. HSP60, Bax, apoptosis and the heart. *J Cell Mol Med.* (2005) 9:51–8. doi: 10.1111/j.1582-4934.2005.tb00336.x
27. Risso A, Mercuri F, Quagliaro L, Damante G, Ceriello A. Intermittent high glucose enhances apoptosis in human umbilical vein endothelial cells in culture. *Am J Physiol Endocrinol Metab.* (2001) 281:E924–30. doi: 10.1152/ajpendo.2001.281.5.E924
28. Chavanelle V, Boisseau N, Otero YF, Combaret L, Dardevet D, Montaurier C, et al. Effects of high-intensity interval training and moderate-intensity continuous training on glycaemic control and skeletal muscle mitochondrial function in db/db mice. *Sci Rep.* (2017) 7:204. doi: 10.1038/s41598-017-00276-8
29. Mitranun W, Deerochanawong C, Tanaka H, Suksom D. Continuous vs interval training on glycemic control and macro-and microvascular reactivity in type 2 diabetic patients. *Scand J Med Sci Sports.* (2014) 24:e69–76. doi: 10.1111/sms.12112
30. MacInnis MJ, Zacharewicz E, Martin BJ, Haikalis ME, Skelly LE, Tarnopolsky MA, et al. Superior mitochondrial adaptations in human skeletal muscle after interval compared to continuous single-leg cycling matched for total work. *J Physiol.* (2017) 595:2955–68. doi: 10.1113/JP272570
31. Naufahu J, Elliott B, Markiv A, Dunning-Foreman P, McGrady M, Howard D, et al. High-intensity exercise decreases IP6K1 muscle content and improves insulin sensitivity (SI2*) in glucose-intolerant individuals. *J Clin Endocrinol Metab.* (2018) 103:1479–90. doi: 10.1210/jc.2017-02019
32. Musi N, Hayashi T, Fujii N, Hirshman MF, Witters LA, Goodyear LJ. AMP-activated protein kinase activity and glucose uptake in rat skeletal muscle. *Am J Physiol Endocrinol Metab.* (2001) 280:E677–84. doi: 10.1152/ajpendo.2001.280.5.E677
33. Terada T, Friesen A, Chahal BS, Bell GJ, McCargar LJ, Boulé NG. Exploring the variability in acute glycemic responses to exercise in type 2 diabetes. *J Diabetes Res.* (2013) 2013:591574. doi: 10.1155/2013/591574
34. Mendes R, Sousa N, Themudo-Barata JL, Reis VM. High-intensity interval training versus moderate-intensity continuous training in middle-aged and older patients with type 2 diabetes: a randomized controlled crossover trial of the acute effects of treadmill walking on glycemic control. *Int J Environ Res Public Health.* (2019) 16:4163. doi: 10.3390/ijerph16214163
35. Kirby TJ, McCarthy JJ. MicroRNAs in skeletal muscle biology and exercise adaptation. *Free Rad Biol Med.* (2013) 64:95–105. doi: 10.1016/j.freeradbiomed.2013.07.004
36. Miyata S, Minobe W, Bristow MR, Leinwand LA. Myosin heavy chain isoform expression in the failing and nonfailing human heart. *Circ Res.* (2000) 86:386–90. doi: 10.1161/01.RES.86.4.386

37. Bjorkman KK, Guess MG, Harrison BC, Polmear MM, Peter AK, Leinwand LA. miR-206 enforces a slow muscle phenotype. *J Cell Sci.* (2020) 133:jcs243162. doi: 10.1242/jcs.243162
38. Emter CA, McCune SA, Sparagna GC, Radin MJ, Moore RL. Low-intensity exercise training delays onset of decompensated heart failure in spontaneously hypertensive heart failure rats. *Am J Physiol Heart Circul Physiol.* (2005) 289:H2030–8. doi: 10.1152/ajpheart.00526.2005
39. Yin X, Zhao Y, Zheng YL, Wang JZ, Li W, Lu QJ, et al. Time-course responses of muscle-specific MicroRNAs following acute uphill or downhill exercise in sprague-dawley rats. *Front Physiol.* (2019) 10:1275. doi: 10.3389/fphys.2019.01275
40. Li T, Yu S-S, Zhou C-Y, Wang K, Wan Y-C. MicroRNA-206 inhibition and activation of the AMPK/Nampt signalling pathway enhance sevoflurane post-conditioning-induced amelioration of myocardial ischaemia/reperfusion injury. *J Drug Target.* (2020) 28:80–91. doi: 10.1080/1061186X.2019.1616744
41. Yeo WK, McGee SL, Carey AL, Paton CD, Garnham AP, Hargreaves M, et al. Acute signalling responses to intense endurance training commenced with low or normal muscle glycogen. *Exp Physiol.* (2010) 95:351–8. doi: 10.1113/expphysiol.2009.049353
42. Lin KM, Lin B, Lian IY, Mestril R, Scheffler IE, Dillmann WH. Combined and individual mitochondrial HSP60 and HSP10 expression in cardiac myocytes protects mitochondrial function and prevents apoptotic cell deaths induced by simulated ischemia-reoxygenation. *Circulation.* (2001) 103:1787–92. doi: 10.1161/01.CIR.103.13.1787
43. Fiorenza M, Gunnarsson T, Hostrup M, Iaia F, Schena F, Pilegaard H, et al. Metabolic stress-dependent regulation of the mitochondrial biogenic molecular response to high-intensity exercise in human skeletal muscle. *J Physiol.* (2018) 596:2823–40. doi: 10.1113/JP275972
44. Shan Y-x, Yang T-L, Mestril R, Wang PH. Hsp10 and Hsp60 suppress ubiquitination of insulin-like growth factor-1 receptor and augment insulin-like growth factor-1 receptor signaling in cardiac muscle: implications on decreased myocardial protection in diabetic cardiomyopathy. *J Biol Chem.* (2003) 278:45492–8. doi: 10.1074/jbc.M304498200
45. Cheng S-M, Ho T-J, Yang A-L, Chen I-J, Kao C-L, Wu F-N, et al. Exercise training enhances cardiac IGFI-R/PI3K/Akt and Bcl-2 family associated pro-survival pathways in streptozotocin-induced diabetic rats. *Int J Cardiol.* (2013) 167:478–85. doi: 10.1016/j.ijcard.2012.01.031
46. Veeranki S, Givvimani S, Kundu S, Metreveli N, Pushpakumar S, Tyagi SC. Moderate intensity exercise prevents diabetic cardiomyopathy associated contractile dysfunction through restoration of mitochondrial function and connexin 43 levels in db/db mice. *J Mol Cell Cardiol.* (2016) 92:163–73. doi: 10.1016/j.yjmcc.2016.01.023
47. Granata C, Oliveira RS, Little JP, Renner K, Bishop DJ. Training intensity modulates changes in PGC-1α and p53 protein content and mitochondrial respiration, but not markers of mitochondrial content in human skeletal muscle. *FASEB J.* (2016) 30:959–70. doi: 10.1096/fj.15-276907
48. Rognmo Ø, Hetland E, Helgerud J, Hoff J, Slørdahl SA. High intensity aerobic interval exercise is superior to moderate intensity exercise for increasing aerobic capacity in patients with coronary artery disease. *Euro J Cardiovasc Prev Rehabil.* (2004) 11:216–22. doi: 10.1097/01.hjr.0000131677.96762.0c
49. Kemi OJ, Haram PM, Loennechen JP, Osnes J-B, Skomedal T, Wisløff U, et al. Moderate vs. high exercise intensity: differential effects on aerobic fitness, cardiomyocyte contractility, and endothelial function. *Cardiovasc Res.* (2005) 67:161–72. doi: 10.1016/j.cardiores.2005.03.010
50. Zouhal H, Jacob C, Delamarche P, Gratas-Delamarche A. Catecholamines and the effects of exercise, training and gender. *Sports Med.* (2008) 38:401–23. doi: 10.2165/00007256-200838050-00004
51. Hollekim-Strand SM, Bjørgaas MR, Albrektsen G, Tjønna AE, Wisløff U, Ingul CB. High-intensity interval exercise effectively improves cardiac function in patients with type 2 diabetes mellitus and diastolic dysfunction: a randomized controlled trial. *J Am Coll Cardiol.* (2014) 64:1758–60. doi: 10.1016/j.jacc.2014.07.971
52. Wisløff U, Støylen A, Loennechen JP, Bruvold M, Rognmo Ø, Haram PM, et al. Superior cardiovascular effect of aerobic interval training versus moderate continuous training in heart failure patients: a randomized study. *Circulation.* (2007) 115:3086–94. doi: 10.1161/CIRCULATIONAHA.106.675041
53. Cassidy S, Thoma C, Hallsworth K, Parikh J, Hollingsworth KG, Taylor R, et al. High intensity intermittent exercise improves cardiac structure and function and reduces liver fat in patients with type 2 diabetes: a randomised controlled trial. *Diabetologia.* (2016) 59:56–66. doi: 10.1007/s00125-015-3741-2

Conflict of Interest: The authors declare that the research was conducted in the absence of any commercial or financial relationships that could be construed as a potential conflict of interest.

Publisher's Note: All claims expressed in this article are solely those of the authors and do not necessarily represent those of their affiliated organizations, or those of the publisher, the editors and the reviewers. Any product that may be evaluated in this article, or claim that may be made by its manufacturer, is not guaranteed or endorsed by the publisher.

frontiers | Frontiers in Cardiovascular Medicine

TYPE Mini Review
PUBLISHED 02 August 2022
DOI 10.3389/fcvm.2022.962561

OPEN ACCESS

EDITED BY
Dayoung Oh,
University of Texas Southwestern Medical Center, United States

REVIEWED BY
Hiroya Ohta,
Tokushima Bunri University, Japan
Christy Gliniak,
University of Texas Southwestern Medical Center, United States

*CORRESPONDENCE
Wei Liu
wei.liu@manchester.ac.uk

†These authors have contributed equally to this work

SPECIALTY SECTION
This article was submitted to Cardiovascular Metabolism, a section of the journal Frontiers in Cardiovascular Medicine

RECEIVED 06 June 2022
ACCEPTED 11 July 2022
PUBLISHED 02 August 2022

CITATION
Kaur N, Gare SR, Shen J, Raja R, Fonseka O and Liu W (2022) Multi-organ FGF21-FGFR1 signaling in metabolic health and disease. *Front. Cardiovasc. Med.* 9:962561. doi: 10.3389/fcvm.2022.962561

Multi-organ FGF21-FGFR1 signaling in metabolic health and disease

Namrita Kaur†, Sanskruti Ravindra Gare†, Jiahan Shen, Rida Raja, Oveena Fonseka and Wei Liu*

Division of Cardiovascular Sciences, School of Medical Sciences, Faculty of Biology, Medicine, and Health, The University of Manchester, Manchester, United Kingdom

Metabolic syndrome is a chronic systemic disease that is particularly manifested by obesity, diabetes, and hypertension, affecting multiple organs. The increasing prevalence of metabolic syndrome poses a threat to public health due to its complications, such as liver dysfunction and cardiovascular disease. Impaired adipose tissue plasticity is another factor contributing to metabolic syndrome. Emerging evidence demonstrates that fibroblast growth factors (FGFs) are critical players in organ crosstalk *via* binding to specific FGF receptors (FGFRs) and their co-receptors. FGFRs activation modulates intracellular responses in various cell types under metabolic stress. FGF21, in particular is considered as the key regulator for mediating systemic metabolic effects by binding to receptors FGFR1, FGFR3, and FGFR4. The complex of FGFR1 and beta Klotho (β-KL) facilitates endocrine and paracrine communication networks that physiologically regulate global metabolism. This review will discuss FGF21-mediated FGFR1/β-KL signaling pathways in the liver, adipose, and cardiovascular systems, as well as how this signaling is involved in the interplay of these organs during the metabolic syndrome. Furthermore, the clinical implications and therapeutic strategies for preventing metabolic syndrome and its complications by targeting FGFR1/β-KL are also discussed.

KEYWORDS

diabetes mellitus, metabolic stress, multi-organ signaling, treatment, heart failure

Introduction

FGFR (Fibroblast Growth Factor Receptor) signaling is involved in various stages of human development and metabolic health. In humans, there are 23 distinct fibroblast growth factors (FGFs), 18 of which (FGF1-10 and 16-23) are mitogenic signaling molecules that bind to four high-affinity cell surface receptors, named FGFR1, FGFR2, FGFR3, and FGFR4 (1). The ligand-binding affinity and tissue distribution of these receptors differ across organs (2). FGFR1 is found in a wide range of cell types and tissues and is located on chromosome 8 at position 11.23 in humans (1, 2). Structurally, FGFRs are single-transmembrane proteins that consist of an extracellular ligand-binding domain and a split functional intracellular kinase domain (1). The intracellular domain is responsible for FGFR tyrosine kinase activity, along with phosphorylation or autophosphorylation of the receptor molecule (3). Studies have shown that the binding

of FGFs and FGFRs on the cell membrane induces a variety of biological responses, such as stimulating the formation of new blood vessels, promoting the development and differentiation of embryonic tissues, participating in wound healing and tissue regeneration, neurotrophy and regulation of endocrine effects (3, 4).

Among the FGF family, FGF19, FGF21, and FGF23 act as endocrine hormones that diffuse into circulation to operate on distal tissues (4). Particularly, FGF21 is expressed in numerous organs and is a key regulator in the body upon metabolic or environmental stresses, such as fasting, food overload, autophagy insufficiency, oxidative stress and exercise (5). FGF21 has significant impacts and potential therapeutic applications in several metabolically active tissue organs, including the heart, liver and adipose tissue which are discussed in detail further. Emerging experimental studies highlight the metabolic effects of FGF21 in maintenance of energy homeostasis, glucose and lipid metabolism, and insulin sensitivity (6–8). In addition, FGFRs are diverse in their subtypes and functions. Thus, endocrine FGF21 not only binds to FGFR1 but also with the obligatory co-receptor βeta-Klotho (β-KL) for signaling specificity (9, 10). FGF21-FGFR1/β-KL signaling is therefore involved in a variety of biological functions, including pro-survival signals, anti-apoptotic signals, and cell proliferation and migration stimulation (11, 12). This review discusses the current understanding of the role of FGF21-FGFR1/β-KL signaling pathway across multiple metabolic organs under metabolic health and disease.

FGF21-FGFR1 signaling in liver

FGF21, along with β-KL is upregulated in the liver by nutritional stresses like starvation, amino acid restriction, and high-fat diet (HFD) or ketogenic diets, thereby mediating hepatic response to nutritive stimuli (13–15). Moreover, acute and chronic stress including exercise, oxidative stress and liposaccharides content also increase FGF21 levels (16, 17). Another contributor of hepatic FGF21 expression is hepatic ER stress that is mediated by eukaryotic translation factor 2α-activating transcription factor 4 (eIF2α-ATF4) pathway (18). Many studies have highlighted the key role of FGF21-mediated FGFR1/β-KL activation in the regulation of hepatic lipid and glucose metabolism (15). The overexpression of hepatic FGF21 in mice showed increased ketogenesis, gluconeogenesis, and lipolysis, thereby regulating hepatic metabolism under prolonged fasting (14). Mechanistically, FGF21 induced the expression of peroxisome proliferator-activated receptor gamma coactivator 1α (PGC-1α) and improved β-oxidation of fatty acids, thereby improving adaptive starvation response in the liver in response to prolonged chronic fasting (19). Further, exogenous FGF21 treatment improved liver metabolism (19) and insulin sensitivity (20) in the obese C57BL/6 mice by inducing phosphorylation of downstream pathways, including fibroblast growth factor receptor substrate 2 alpha (FRS2α) and extracellular signal-regulated kinase (ERK) (20). These studies thus indicate the role of FGF21 in improving obesity or prolonged fasting induced metabolic stress. However, there is a low level of endogenous FGFR1 expression in the liver (21), so it is unclear whether the beneficial effects of FGF21-β-KL signaling are mediated directly through FGFR1. Also, FGF21 was shown to have no effect in isolated hepatocytes from mouse and rat (22). This results from insufficient peripheral signals from adipose tissue, modulating the liver's response to FGF21 indirectly. Therefore, a deeper understanding of what extent and how FGF21-FGFR1/β-KL signaling contributes to hepatic metabolic responses needs to be obtained.

FGF21-FGFR1 signaling in adipose tissue

Adipocytes express both β-KL and FGFRs (mainly FGFR1 and FGFR2) and are important targets for FGFs (23). White adipose tissue (WAT) helps in storing energy, whereas brown adipose tissue (BAT) helps in energy expenditure by generating heat through a process called thermogenesis (24). FGF21 expression is induced by exposure to cold or stimulation by β-adrenergic receptors in the adipose tissue (25–28). Multiple genetic and pharmacological studies highlight the role of FGF21-FGFR1/β-KL signaling pathway in regulating adipose tissue metabolism (10, 23, 29, 30). Studies showed that long-term HFD-fed obese mice exhibited hyperglycemia, hyperinsulinemia, and hyperlipidemia, with markedly reduced FGFR1 and β-KL expression in adipose tissue (31). WAT-specific knockout of β-KL/FGFR1 reduced FGF21 response in WAT and eliminated the beneficial effects, such as weight loss and energy expenditure in the obese rodents (31). In addition, Chen et al. found that anti-FGFR1/β-KL bispecific antibody (acting as FGF21 mimetic) stimulated energy expenditure in adipocyte-selective FGFR1-deficient mice, elucidating the indirect role of FGF21 in BAT thermogenesis *via* uncoupling protein 1 (Ucp1) activation (32). Thus, BAT has gained attention as a novel target for treating obesity and Type 2 diabetes due to its "fat-burning" properties (33), mediated by FGF21-FGFR1 signaling (34, 35). BAT-derived FGF21 either functions locally or escapes into the systemic circulation, having an autocrine as well as an endocrine role in thermogenesis *via* PGC-1α, mitogen-activated protein kinase (MAPK) and ERK signaling (27, 28, 36). Moreover, prolonged treatment of FGF21 on brown adipocytes increased glucose consumption (28) and insulin-stimulated glucose uptake *via* hepatic adiponectin secretion in a paracrine manner (22, 37, 38). This suggests a hepatic-adipose crosstalk. However, two groups independently showed that surgical removal of BAT did not alter the effects of FGF21 in obese rodents (7, 39), indicating that BAT activation and

WAT browning alone are not responsible for the systemic metabolic benefits of FGF21 treatment (40). Therefore, further studies, especially clinical trial with existing FGF21 analogs are needed to establish the underlying mechanisms by which FGF21-FGFR1/ β-KL signaling governs systemic metabolism in the adipose tissue.

FGF21-FGFR1 signaling in the heart

Emerging evidence shows that FGF21-FGFR1 signaling is also an important regulator in the heart. For instance, it is stimulated *via* paracrine and endocrine FGFs and exhibits anti-hypertrophic, anti-oxidative and anti-apoptotic properties under physiological and pathological conditions (41–44). Endocrine FGF21 has been shown to have cardiovascular protective effects, specifically in ischemic/reperfusion injury (45), isoproterenol-induced cardiac hypertrophy (46), alcoholic cardiomyopathy (47), and hypertensive heart disease (48). FGF21 activity in the heart is dependent on its binding to FGFR1 and β-KL and induces cell survival *via* anti-oxidative mechanisms and recovery of energy homeostasis in cardiac cells (49). In clinics, myocardial FGF21 is increased in advanced heart failure; however, in a pre-clinical ischemic mouse heart, FGF21 induction is not apparent (43). Nevertheless, FGF21 inhibits cardiac remodeling by activating MAPK signaling in an autocrine manner (41). Following myocardial infarction, FGF21 exerts its cardioprotective action *via* ERK 1/2 and AMP-activated protein kinase (AMPK) in an acute manner and *via* Phosphoinositide 3-kinases (PI3K)/ protein kinase B (Akt) in a sustained fashion (45, 50). Of note, cardiomyocytes can also produce FGF21 in response to disturbances in cellular metabolism (51). An earlier study demonstrated that FGF21 is secreted into the culture media at a basal rate of 0.05 ng/mL per 24 h, thereby establishing FGF21 as a cardiomyokine. The cardiac FGF21 autocrine loop is likely a compensatory mechanism initiated in response to oxidative stress (52). Global FGF21 knockout results in heightened cardiomyocyte inflammatory response *via* increased nuclear factor kappa B activity and upregulation of interleukin 6, concomitant with repressed fatty acid oxidation. Moreover, hypertrophic stimuli induce transcriptional upregulation of cardiac FGF21 *via* Sirtuin 1- PPARα pathway (46). FGF21 directly affects the heart, owing to FGFR1 and β-KL expression in the myocardium (53); however, the molecular basis whereby the FGF21-FGFR1 pathway is involved in cardiac metabolism is elusive.

In streptozotocin (STZ)-induced diabetes, cardiac FGF21 mRNA level is increased significantly (54). FGF21 mediated FGFR1 activation enhanced ERK1/2 phosphorylation, p38 MAPK activity, and AMPK activation, thereby impeding diabetes-induced apoptosis (53). FGF21 global knockout mice are more likely to develop STZ-induced diabetic cardiomyopathy. This is accompanied by severe cardiac dysfunction, structural changes, oxidative stress, and cardiac lipid accumulation *via* cluster of differentiation 36 (CD36) upregulation owing to decreased lipid oxidation, and impaired glucose oxidation. Conversely, using genetic or pharmacological modulation, FGF21 displays cardioprotective properties under dysregulated glucose and lipid metabolism (55–57) FGF21 also promotes lipophagy in mouse cardiomyocytes in obesity-related cardiomyopathy by preventing lipid accumulation (58). In addition, FGF21 protects the heart against Type 2 diabetes by either AMPK-protein kinase B (PKB, also known as AKT)-nuclear factor erythroid 2-related factor 2 (NRF2)-mediated anti-oxidative pathway or acetyl-CoA carboxylase (ACC)-Carnitine palmitoyltransferase I (CPT-1) lipid-lowering pathway, primarily attributable to managing lipotoxicity (59).

Moreover, upon hyperglycemia and hyperlipidemia, endoplasmic reticulum (ER) stress is invoked by oxidative stress, lipid deposition, and abnormal proteins synthesis in cardiomyocytes (60). Maladaptive ER stress eventually disturbs lipid synthesis, calcium homeostasis, protein quality control, leading to cell death (61). FGF21 diminishes ER stress-mediated myocardial apoptosis *via* reduction of ATF4-C/EBP homologous protein (CHOP) pathway (62). Although cardiac-specific overexpression of FGF21 does not play a major role in cardiac energy metabolism under an unstressed-state, FGF21 secretion is activated upon cardiac ER stress altering cardiac glucose oxidation in an autocrine manner (63).

Additionally, FGF21 signaling exerts anti-inflammatory effects by inhibiting PI3K/AKT signaling in the diabetic heart (56) and by promoting AMPK-paraoxonase 1 axis in high-glucose stressed cardiomyocytes (64). On the other hand, FGFR1 signaling is necessary for anti-fibrosis. Endothelial FGFR1 knockout mice showed considerable kidney and heart fibrosis (65). Moreover, FGF21 has anti-oxidative properties *via* AMPK activation in endothelial cells under diabetic stress (66). Furthermore, global β-KL knockout mice show reduced serum levels of adiponectin, known to modulate FGF21 signaling in several organs. Accordingly, global adiponectin knockout mice display diminished cardioprotective effects of FGF21 (67). In general, current research points to the potential importance of further investigating cardiac FGF21-FGFR1/β-KL signaling in metabolic stress.

Multi-organ crosstalk mediated by FGF21

FGF21 response in organs appears to be influenced by tissue-specific interactions (68), summarized in Figure 1. FGF21 stimulates adiponectin secretion from adipocytes, which confers metabolic actions on the other cells/tissue, such as blood vessels (69). The effects of FGF21 are due to

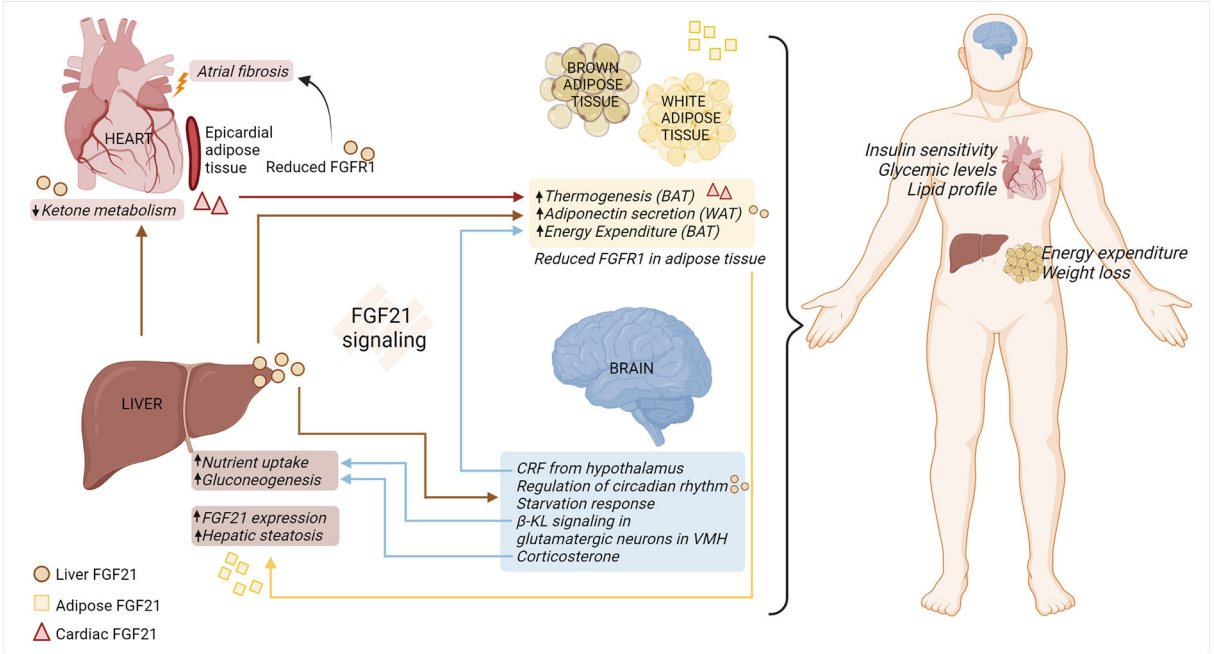

FIGURE 1
FGF21-FGFR1/β-KL regulation of multi-organ crosstalk under metabolic stress. FGF21-FGFR1/β-KL signaling is vital in regulating systemic and organ responses under pathophysiological metabolic stress. Hepatic sourced FGF21 (circle) reduces ketone metabolism in the cardiomyocytes, induces secretion of adiponectin from WAT, and modulates systemic metabolism. Moreover, hepatic sourced FGF21 passes through the blood-brain barrier and is involved in regulation of circadian rhythm and appetite response. In a feedback loop, β-KL signaling in the VMH-specific glutamatergic neurons contributes to modulating hepatic nutrient uptake. The release of CRF and corticosterone from the brain is responsible for regulating energy expenditure in the adipose tissue and liver gluconeogenesis, respectively. Cardiac sourced FGF21 (triangle) promotes thermogenesis in the adipose tissue, thus improving overall metabolic health. Under the adipo-hepatic communication, reduced expression of adipose FGFR1 aggravates hepatic steatosis and adipose FGF21 (square) increases the expression of hepatic FGF21. Hence, multi-organ crosstalk mediated by FGF21-FGFR1/β-KL signaling alleviates metabolic distress by improving insulin sensitivity, glucose, and lipid levels in the body, along with increased energy expenditure in the adipose tissue and weight loss. BAT, brown adipose tissue; β-KL, beta-klotho; CRF, corticotropin releasing factor; FGF21, fibroblast growth factor 21; FGFR1, fibroblast growth factor receptor 1; VMH, ventromedial hypothalamus; WAT, white adipose tissue (created with Biorender.com).

its direct action on hepatocytes or cardiomyocytes, and/or indirect impacts on the brain–hepatic axis. Peripheral signals, along with gastro-intestinal hormones, are responsible for conveying metabolic information to the brain and modulating glucose homeostasis and energy intake in the body (70). Although FGF21 is not expressed in the central nervous system (CNS), it can pass through the blood-brain barrier, allowing communication between peripheral tissues and the CNS (71). It was evidenced by a study utilizing β-KL^{Camk2a} mouse, that lacks β-KL in the hypothalamus and the hindbrain. This model confirmed central FGF21 signaling involved in the regulation of the circadian rhythm and starvation response (72). Additionally, β-KL- glutamatergic knockout mice elucidated that FGF21-FGFR1/β-KL signaling in the ventromedial hypothalamus decreases sucrose consumption/sweet-taste preference, eventually protecting the hepatic metabolism (73). FGF21 is also responsible for stimulating corticotropin-releasing factor and corticosterone in the brain, which subsequently participates in energy expenditure in the BAT (74–76) and hepatic gluconeogenesis, respectively (72, 77). Moreover, a large cohort study conducted by Jiao et al. found that FGFR1 protein in adipose tissue increased in the obese women, and the hypothalamic expression of FGFR1 was increased in the diet-induced obese rats (78). This study thus highlighted FGFR1 as a novel obesity gene that influences adipose tissue and the hypothalamus, thereby initiating obesity and modulating appetite, respectively.

Moreover, the hepatic-cardiac signaling circuit has been documented in human heart failure samples. This study highlights the endocrine action of hepatocyte sourced FGF21, resulting in enhanced binding of FGF21 to diseased cardiomyocytes. This increase in FGF21 binding was associated with reduced ketone metabolism in the heart (11). In addition, cardiac-sourced FGF21 modulates the metabolic phenotype of BAT by promoting

thermogenesis in obese mice with cardiac muscle autophagy deficiency (12). Collectively, further research is needed to explore the role of hepatic- and/or cardiac-sourced FGF21 on FGFR1 signaling across multiple organs under metabolic stress.

Moreover, adipocyte lipolysis releases fatty acids into the bloodstream. These fatty acids subsequently enhance FGF21 expression *via* an indirect mechanism by activating PPARα in hepatocytes (79). Interestingly, one study highlighted that global β-KL knockout increases energy expenditure from BAT, making the mice resistant to obesity (80). Moreover, adipo-hepatic communication was noticed by adipocyte ablation of FGFR1. Adipocyte-specific deletion of FGFR1 aggravates hepatic steatosis (81), indicating the plausible FGFR1 regulation on maintenance of energy homeostasis across multiple organs. Finally, the browning of epicardial adipose tissue (EAT) contributes to atrial fibrillation under diabetic stress. Mechanistically, micro-RNA (miR)-21-3p is significantly upregulated in serum from diabetic patients and participates in atrial fibrosis under hyperglycemia conditions by reducing FGFR1 in EAT (82).

FGF21 resistance in obesity and diabetes

Despite increased serum levels of FGF21 in obesity patients, no metabolic benefits were observed. Therefore, the term "FGF21 resistance" was examined in animal studies, showing reduced FGFR1 and β-KL in adipose tissue in obese mice (83). FGF21 effects on insulin sensitivity is then impeded (84). In addition, FGF21 resistance was also observed post FGF21 administration in obese mice (85). Of note, regarding the role of expression of β-KL in FGF21 resistance in adipose tissue, different results have been reported in obese mice. Although β-KL reduction is not associated with FGF21 resistance (86), its overexpression enhances FGF21 action in adipocytes (87). Additionally, β-KL has been shown to be an integral part of the FGF21 machinery in the liver. In the mice lacking β-KL, FGF21 was defective in regulating lipid and glucose metabolism at the whole organism level in diet-induced obesity (30). Thus, further preclinical and clinical studies are required to determine the molecular basis of FGF21 resistance, particularly in distinct cells.

Recently, serum FGF21 levels were associated with diastolic cardiac dysfunction in humans with cardiovascular diseases, such as dyslipidemic patients with coronary artery disease (50), but only a few reports have examined FGF21's role in heart failure (88). Pre-clinical model shows that FGF21 resistance is likely involved in the impairment of glucose uptake in heart (50). Although there was no discernible difference in FGFR1 levels in hearts from obese and lean rat, β-KL was less expressed in the heart, possibly explaining FGF21 resistance (50). However, exploration of molecular basis and targeting potential of FGF21 resistance in heart is needed for therapeutic implications of heart failure.

Targeting FGF21-FGFR1/β-KL signaling to tackle metabolic stress

It is acknowledged that targeting the FGF21-FGFR1 signaling pathway is advantageous for tackling metabolic stress. Of note, there is an increase in circulating levels of fibroblast activation protein alpha (FAP), a prolyl peptidase related to the dipeptidyl peptidase IV (DPP-IV) enzyme. Increased circulating FAP levels are associated with decreased levels of bioactive to total FGF21, thus impairing its metabolic regulation potential (89). Hence, using long-lasting FGF21 analogs and targeting FGFR1 signaling to combat resistance in several organs could be advantageous. However, the tissue specific effects have not yet been investigated in detail. FGF21 analogs are reported to adjust systemic metabolism in obese and diabetes in clinical trials and pre-clinical studies. For instance, LY2405319, improved dyslipidemia in obese patients with Type 2 diabetes (90) and diabetic monkeys (91, 92). Recently, AKR-001, an Fc-FGF21 analog, also showed beneficial effects on insulin sensitivity and lipoprotein profile in Type 2 diabetes patients (93).

Because pharmacokinetic properties of FGF21 analogs remain the most challenging for balancing therapeutic benefits and mechanism-related toxicity, further research on targeting FGFR1/β-KL signaling is crucial to identify novel therapeutic potentials (94). For instance, endocrine FGF23 bears structural similarity to FGF21 and FGF23 C-terminal alteration to FGF21 C-terminal enhances the ability of scaffold forming of FGF21-like molecule to FGFR1/β-KL complex (95). In addition, one bi-specific avimer for the complex of FGFR1 and β-KL, C3201, improves insulin sensitivity and lipid profiles in male obese cynomolgus monkeys (96). Of note, the FGFR1c/β-KL bispecific antibody, BFKB8488A, demonstrated sustained improvements in cardio-metabolism and weight loss, despite that insulin sensitivity was not consistently improved and lipoprotein responses varied in obese humans (97). However, it is necessary to further investigate the tissue-specific effects of the above-mentioned agents, including on cardiac, liver and adipose tissue function.

Conclusion

FGF21 is an endocrine and cell-autonomous autocrine regulator displaying a varied response across different organs in a stress- and time-dependent manner (43, 98). Most

studies have focused on hepatic sourced FGF21 (endocrine action) in the past. However, adipose- and cardiac muscle-sourced FGF21 require further attention to delineate their paracrine and/or autocrine roles in metabolic diseases. In addition, downstream effectors of the FGF21-FGFR1 signaling cascade in distinct cells also require further investigation. Moreover, the molecular basis underlying FGF21 resistance in organs is undocumented. Finally, the lack of improvement in insulin sensitivity in humans, despite the beneficial effects of FGF21 analogs, necessitates the development of novel therapeutic approaches targeting FGFR1/β-KL signaling in metabolic organs.

Author contributions

NK, SG, and JS collected references, generated, drafted, did revisions, and proofread the manuscript. NK and RR generated the figure. OF proofread the manuscript. NK and WL designed the manuscript. All authors contributed to the article and approved the submitted version.

Funding

This work was supported by grants FS/15/16/31477, FS/18/73/33973, PG/19/66/34600, and FS/19/70/34650 to WL from the British Heart Foundation.

Conflict of interest

The authors declare that the research was conducted in the absence of any commercial or financial relationships that could be construed as a potential conflict of interest.

Publisher's note

References

1. Zhou WY, Zheng H, Du XL, Yang JL. Characterization of FGFR signaling pathway as therapeutic targets for sarcoma patients. *Cancer Biol Med.* (2016) 13:260–8. doi: 10.20892/j.issn.2095-3941.2015.0102

2. Kelleher FC, O'Sullivan H, Smyth E, McDermott R, Viterbo A. Fibroblast growth factor receptors, developmental corruption and malignant disease. *Carcinogenesis.* (2013) 34:2198–205. doi: 10.1093/carcin/bgt254

3. Wang LY, Edenson SP Yu YL, Senderowicz L, Turck CW. A natural kinase-deficient variant of fibroblast growth factor receptor 1. *Biochemistry.* (1996) 35:10134–42. doi: 10.1021/bi952611n

4. Beenken A, Mohammadi M. The FGF family: biology, pathophysiology and therapy. *Nat Rev Drug Discov.* (2009) 8:235–53. doi: 10.1038/nrd2792

5. Kim KH, Lee MS. FGF21 as a stress hormone: the roles of FGF21 in stress adaptation and the treatment of metabolic diseases. *Diabetes Metab J.* (2014) 38:245–51. doi: 10.4093/dmj.2014.38.4.245

6. BonDurant LD, Potthoff MJ. Fibroblast growth factor 21: a versatile regulator of metabolic homeostasis. *Annu Rev Nutr.* (2018) 38:173–96. doi: 10.1146/annurev-nutr-071816-064800

7. Camporez JP, Jornayvaz FR, Petersen MC, Pesta D, Guigni BA, Serr J, et al. Cellular mechanisms by which FGF21 improves insulin sensitivity in male mice. *Endocrinology.* (2013) 154:3099–109. doi: 10.1210/en.2013-1191

8. Huang Z, Xu A, Cheung BMY. The potential role of fibroblast growth factor 21 in lipid metabolism and hypertension. *Curr Hypertens Rep.* (2017) 19:28. doi: 10.1007/s11906-017-0730-5

9. Kurosu H, Choi M, Ogawa Y, Dickson AS, Goetz R, Eliseenkova AV, et al. Tissue-specific expression of betaKlotho and fibroblast growth factor (FGF) receptor isoforms determines metabolic activity of FGF19 and FGF21. *J Biol Chem.* (2007) 282:26687–95. doi: 10.1074/jbc.M704165200

10. Ding X, Boney-Montoya J, Owen BM, Bookout AL, Coate KC, Mangelsdorf DJ, et al. betaKlotho is required for fibroblast growth factor 21 effects on growth and metabolism. *Cell Metab.* (2012) 16:387–93. doi: 10.1016/j.cmet.2012.08.002

11. Sommakia S, Almaw NH, Lee SH, Ramadurai DKA, Taleb I, Kyriakopoulos CP, et al. FGF21 (fibroblast growth factor 21) defines a potential cardiohepatic signaling circuit in end-stage heart failure. *Circ Heart Fail.* (2022) 15:e008910. doi: 10.1161/CIRCHEARTFAILURE.121.008910

12. Yan Z, Kronemberger A, Blomme J, Call JA, Caster HM, Pereira RO, et al. Exercise leads to unfavourable cardiac remodelling and enhanced metabolic homeostasis in obese mice with cardiac and skeletal muscle autophagy deficiency. *Sci Rep.* (2017) 7:7894. doi: 10.1038/s41598-017-08480-2

13. Potthoff MJ. FGF21 and metabolic disease in 2016: a new frontier in FGF21 biology. *Nat Rev Endocrinol.* (2017) 13:74–6. doi: 10.1038/nrendo.2016.206

14. Inagaki T, Dutchak P, Zhao G, Ding X, Gautron L, Parameswara V, et al. Endocrine regulation of the fasting response by PPARalpha-mediated induction of fibroblast growth factor 21. *Cell Metab.* (2007) 5:415–25. doi: 10.1016/j.cmet.2007.05.003

15. Iizuka K, Takeda J, Horikawa Y. Glucose induces FGF21 mRNA expression through ChREBP activation in rat hepatocytes. *FEBS Lett.* (2009) 583:2882–6. doi: 10.1016/j.febslet.2009.07.053

16. Gomez-Samano MA, Grajales-Gomez M, Zuarth-Vazquez JM, Navarro-Flores MF, Martinez-Saavedra M, Juarez-Leon OA, et al. Fibroblast growth factor 21 and its novel association with oxidative stress. *Redox Biol.* (2017) 11:335–41. doi: 10.1016/j.redox.2016.12.024

17. Feingold KR, Grunfeld C, Heuer JG, Gupta A, Cramer M, Zhang T, et al. FGF21 is increased by inflammatory stimuli and protects leptin-deficient ob/ob mice from the toxicity of sepsis. *Endocrinology.* (2012) 153:2689–700. doi: 10.1210/en.2011-1496

18. Kim SH, Kim KH, Kim HK, Kim MJ, Back SH, Konishi M, et al. Fibroblast growth factor 21 participates in adaptation to endoplasmic reticulum stress and attenuates obesity-induced hepatic metabolic stress. *Diabetologia.* (2015) 58:809–18. doi: 10.1007/s00125-014-3475-6

19. Fisher FM, Estall JL, Adams AC, Antonellis PJ, Bina HA, Flier JS, et al. Integrated regulation of hepatic metabolism by fibroblast growth factor 21 (FGF21) *in vivo*. *Endocrinology.* (2011) 152:2996–3004. doi: 10.1210/en.2011-0281

20. Xu J, Lloyd DJ, Hale C, Stanislaus S, Chen M, Sivits G, et al. Fibroblast growth factor 21 reverses hepatic steatosis, increases energy expenditure, and

improves insulin sensitivity in diet-induced obese mice. *Diabetes.* (2009) 58:250–9. doi: 10.2337/db08-0392

21. Yang C, Jin C, Li X, Wang F, McKeehan WL, Luo Y. Differential specificity of endocrine FGF19 and FGF21 to FGFR1 and FGFR4 in complex with KLB. *PLoS ONE.* (2012) 7:e33870. doi: 10.1371/journal.pone.0033870

22. Lin Z, Tian H, Lam KS, Lin S, Hoo RC, Konishi M, et al. Adiponectin mediates the metabolic effects of FGF21 on glucose homeostasis and insulin sensitivity in mice. *Cell Metab.* (2013) 17:779–89. doi: 10.1016/j.cmet.2013.04.005

23. Suzuki M, Uehara Y, Motomura-Matsuzaka K, Oki J, Koyama Y, Kimura M, et al. betaKlotho is required for fibroblast growth factor (FGF) 21 signaling through FGF receptor (FGFR) 1c and FGFR3c. *Mol Endocrinol.* (2008) 22:1006–14. doi: 10.1210/me.2007-0313

24. Rosen ED, Spiegelman BM. What we talk about when we talk about fat. *Cell.* (2014) 156:20–44. doi: 10.1016/j.cell.2013.12.012

25. Fon Tacer K, Bookout AL, Ding X, Kurosu H, John GB, Wang L, et al. Research resource: comprehensive expression atlas of the fibroblast growth factor system in adult mouse. *Mol Endocrinol.* (2010) 24:2050–64. doi: 10.1210/me.2010-0142

26. Chartoumpekis DV, Habeos IG, Ziros PG, Psyrogiannis AI, Kyriazopoulou VE, Papavassiliou AG. Brown adipose tissue responds to cold and adrenergic stimulation by induction of FGF21. *Mol Med.* (2011) 17:736–40. doi: 10.2119/molmed.2011.00075

27. Fisher FM, Kleiner S, Douris N, Fox EC, Mepani RJ, Verdeguer F, et al. FGF21 regulates PGC-1alpha and browning of white adipose tissues in adaptive thermogenesis. *Genes Dev.* (2012) 26:271–81. doi: 10.1101/gad.177857.111

28. Hondares E, Iglesias R, Giralt A, Gonzalez FJ, Giralt M, Mampel T, et al. Thermogenic activation induces FGF21 expression and release in brown adipose tissue. *J Biol Chem.* (2011) 286:12983–90. doi: 10.1074/jbc.M110.215889

29. Ogawa Y, Kurosu H, Yamamoto M, Nandi A, Rosenblatt KP, Goetz R, et al. BetaKlotho is required for metabolic activity of fibroblast growth factor 21. *Proc Natl Acad Sci USA.* (2007) 104:7432–7. doi: 10.1073/pnas.0701600104

30. Adams AC, Cheng CC, Coskun T, Kharitonenkov A. FGF21 requires betaklotho to act *in vivo*. *PLoS ONE.* (2012) 7:e49977. doi: 10.1371/journal.pone.0049977

31. Geng L, Liao B, Jin L, Huang Z, Triggle CR, Ding H, et al. Exercise alleviates obesity-induced metabolic dysfunction *via* enhancing FGF21 sensitivity in adipose tissues. *Cell Rep.* (2019) 26:2738–52 e4. doi: 10.1016/j.celrep.2019.02.014

32. Chen MZ, Chang JC, Zavala-Solorio J, Kates L, Thai M, Ogasawara A, et al. FGF21 mimetic antibody stimulates UCP1-independent brown fat thermogenesis *via* FGFR1/betaKlotho complex in non-adipocytes. *Mol Metab.* (2017) 6:1454–67. doi: 10.1016/j.molmet.2017.09.003

33. Betz MJ, Enerback S. Therapeutic prospects of metabolically active brown adipose tissue in humans. *Front Endocrinol.* (2011) 2:86. doi: 10.3389/fendo.2011.00086

34. Coskun T, Bina HA, Schneider MA, Dunbar JD, Hu CC, Chen Y, et al. Fibroblast growth factor 21 corrects obesity in mice. *Endocrinology.* (2008) 149:6018–27. doi: 10.1210/en.2008-0816

35. Cuevas-Ramos D, Mehta R, Aguilar-Salinas CA. Fibroblast growth factor 21 and browning of white adipose tissue. *Front Physiol.* (2019) 10:37. doi: 10.3389/fphys.2019.00037

36. Zhang Y, Xie C, Wang H, Foss RM, Clare M, George EV, et al. Irisin exerts dual effects on browning and adipogenesis of human white adipocytes. *Am J Physiol Endocrinol Metab.* (2016) 311:E530–41. doi: 10.1152/ajpendo.00094.2016

37. Markan KR, Naber MC, Ameka MK, Anderegg MD, Mangelsdorf DJ, Kliewer SA, et al. Circulating FGF21 is liver derived and enhances glucose uptake during refeeding and overfeeding. *Diabetes.* (2014) 63:4057–63. doi: 10.2337/db14-0595

38. Holland WL, Adams AC, Brozinick JT, Bui HH, Miyauchi Y, Kusminski CM, et al. An FGF21-adiponectin-ceramide axis controls energy expenditure and insulin action in mice. *Cell Metab.* (2013) 17:790–7. doi: 10.1016/j.cmet.2013.03.019

39. Bernardo B, Lu M, Bandyopadhyay G, Li P, Zhou Y, Huang J, et al. FGF21 does not require interscapular brown adipose tissue and improves liver metabolic profile in animal models of obesity and insulin-resistance. *Sci Rep.* (2015) 5:11382. doi: 10.1038/srep11382

40. Veniant MM, Sivits G, Helmering J, Komorowski R, Lee J, Fan W, et al. Pharmacologic effects of FGF21 are independent of the "browning" of white adipose tissue. *Cell Metab.* (2015) 21:731–8. doi: 10.1016/j.cmet.2015.04.019

41. Itoh N, Ohta H. Pathophysiological roles of FGF signaling in the heart. *Front Physiol.* (2013) 4:247. doi: 10.3389/fphys.2013.00247

42. Mima T, Ueno H, Fischman DA, Williams LT, Mikawa T. Fibroblast growth factor receptor is required for *in vivo* cardiac myocyte proliferation at early embryonic stages of heart development. *Proc Natl Acad Sci USA.* (1995) 92:467–71. doi: 10.1073/pnas.92.2.467

43. Kim KH, Lee MS. FGF21 as a mediator of adaptive responses to stress and metabolic benefits of anti-diabetic drugs. *J Endocrinol.* (2015) 226:R1–16. doi: 10.1530/JOE-15-0160

44. Planavila A, Redondo-Angulo I, Ribas F, Garrabou G, Casademont J, Giralt M, et al. Fibroblast growth factor 21 protects the heart from oxidative stress. *Cardiovasc Res.* (2015) 106:19–31. doi: 10.1093/cvr/cvu263

45. Liu SQ, Roberts D, Kharitonenkov A, Zhang B, Hanson SM Li YC, et al. Endocrine protection of ischemic myocardium by FGF21 from the liver and adipose tissue. *Sci Rep.* (2013) 3:2767. doi: 10.1038/srep02767

46. Planavila A, Redondo I, Hondares E, Vinciguerra M, Munts C, Iglesias R, et al. Fibroblast growth factor 21 protects against cardiac hypertrophy in mice. *Nat Commun.* (2013) 4:2019. doi: 10.1038/ncomms3019

47. Ferrer-Curriu G, Guitart-Mampel M, Ruperez C, Zamora M, Crispi F, Villarroya F, et al. The protective effect of fibroblast growth factor-21 in alcoholic cardiomyopathy: a role in protecting cardiac mitochondrial function. *J Pathol.* (2021) 253:198–208. doi: 10.1002/path.5573

48. Ferrer-Curriu G, Redondo-Angulo I, Guitart-Mampel M, Ruperez C, Mas-Stachurska A, Sitges M, et al. Fibroblast growth factor-21 protects against fibrosis in hypertensive heart disease. *J Pathol.* (2019) 248:30–40. doi: 10.1002/path.5226

49. Olejnik A, Franczak A, Krzywonos-Zawadzka A, Kaluzna-Oleksy M, Bil-Lula I. The biological role of klotho protein in the development of cardiovascular diseases. *Biomed Res Int.* (2018) 2018:5171945. doi: 10.1155/2018/5171945

50. Patel V, Adya R, Chen J, Ramanjaneya M, Bari MF, Bhudia SK, et al. Novel insights into the cardio-protective effects of FGF21 in lean and obese rat hearts. *PLoS ONE.* (2014) 9:e87102. doi: 10.1371/journal.pone.0087102

51. Funcke JB, Scherer PE. Beyond adiponectin and leptin: adipose tissue-derived mediators of inter-organ communication. *J Lipid Res.* (2019) 60:1648–84. doi: 10.1194/jlr.R094060

52. Di Lisa F, Itoh N. Cardiac Fgf21 synthesis and release: an autocrine loop for boosting up antioxidant defenses in failing hearts. *Cardiovasc Res.* (2015) 106:1–3. doi: 10.1093/cvr/cvv050

53. Zhang C, Huang Z, Gu J, Yan X, Lu X, Zhou S, et al. Fibroblast growth factor 21 protects the heart from apoptosis in a diabetic mouse model *via* extracellular signal-regulated kinase 1/2-dependent signalling pathway. *Diabetologia.* (2015) 58:1937–48. doi: 10.1007/s00125-015-3630-8

54. Yan X, Chen J, Zhang C, Zhou S, Zhang Z, Chen J, et al. FGF21 deletion exacerbates diabetic cardiomyopathy by aggravating cardiac lipid accumulation. *J Cell Mol Med.* (2015) 19:1557–68. doi: 10.1111/jcmm.12530

55. Tanajak P, Chattipakorn SC, Chattipakorn N. Effects of fibroblast growth factor 21 on the heart. *J Endocrinol.* (2015) 227:R13–30. doi: 10.1530/JOE-15-0289

56. Zhang X, Yang L, Xu X, Tang F, Yi P, Qiu B, et al. A review of fibroblast growth factor 21 in diabetic cardiomyopathy. *Heart Fail Rev.* (2019) 24:1005–17. doi: 10.1007/s10741-019-09809-x

57. Xiao M, Tang Y, Wang S, Wang J, Wang J, Guo Y, et al. The role of fibroblast growth factor 21 in diabetic cardiovascular complications and related epigenetic mechanisms. *Front Endocrinol.* (2021) 12:598008. doi: 10.3389/fendo.2021.598008

58. Ruperez C, Lerin C, Ferrer-Curriu G, Cairo M, Mas-Stachurska A, Sitges M, et al. Autophagic control of cardiac steatosis through FGF21 in obesity-associated cardiomyopathy. *Int J Cardiol.* (2018) 260:163–70. doi: 10.1016/j.ijcard.2018.02.109

59. Yang H, Feng A, Lin S, Yu L, Lin X, Yan X, et al. Fibroblast growth factor-21 prevents diabetic cardiomyopathy *via* AMPK-mediated antioxidation and lipid-lowering effects in the heart. *Cell Death Dis.* (2018) 9:227. doi: 10.1038/s41419-018-0307-5

60. Xu J, Zhou Q, Xu W, Cai L. Endoplasmic reticulum stress and diabetic cardiomyopathy. *Exp Diabetes Res.* (2012) 2012:827971. doi: 10.1155/2012/827971

61. Kaur N, Raja R, Ruiz-Velasco A, Liu W. Cellular protein quality control in diabetic cardiomyopathy: from bench to bedside. *Front Cardiovasc Med.* (2020) 7:585309. doi: 10.3389/fcvm.2020.585309

62. Liang P, Zhong L, Gong L, Wang J, Zhu Y, Liu W, et al. Fibroblast growth factor 21 protects rat cardiomyocytes from endoplasmic reticulum stress by promoting the fibroblast growth factor receptor 1-extracellular signalregulated kinase 1/2 signaling pathway. *Int J Mol Med.* (2017) 40:1477–85. doi: 10.3892/ijmm.2017.3140

63. Brahma MK, Adam RC, Pollak NM, Jaeger D, Zierler KA, Pocher N, et al. Fibroblast growth factor 21 is induced upon cardiac stress and alters cardiac lipid homeostasis. *J Lipid Res.* (2014) 55:2229–41. doi: 10.1194/jlr.M044784

64. Wu F, Wang B, Zhang S, Shi L, Wang Y, Xiong R, et al. FGF21 ameliorates diabetic cardiomyopathy by activating the AMPK-paraoxonase 1 signaling axis in mice. *Clin Sci.* (2017) 131:1877–93. doi: 10.1042/CS20170271

65. Li J, Liu H, Srivastava SP, Hu Q, Gao R, Li S, et al. Endothelial FGFR1 (fibroblast growth factor receptor 1) deficiency contributes differential fibrogenic effects in kidney and heart of diabetic mice. *Hypertension.* (2020) 76:1935–44. doi: 10.1161/HYPERTENSIONAHA.120.15587

66. Ying L, Li N, He Z, Zeng X, Nan Y, Chen J, et al. Fibroblast growth factor 21 Ameliorates diabetes-induced endothelial dysfunction in mouse aorta *via* activation of the CaMKK2/AMPKalpha signaling pathway. *Cell Death Dis.* (2019) 10:665. doi: 10.1038/s41419-019-1893-6

67. Joki Y, Ohashi K, Yuasa D, Shibata R, Ito M, Matsuo K, et al. FGF21 attenuates pathological myocardial remodeling following myocardial infarction through the adiponectin-dependent mechanism. *Biochem Biophys Res Commun.* (2015) 459:124–30. doi: 10.1016/j.bbrc.2015.02.081

68. Spann RA, Morrison CD, den Hartigh LJ. The nuanced metabolic functions of endogenous FGF21 depend on the nature of the stimulus, tissue source, and experimental model. *Front Endocrinol.* (2021) 12:802541. doi: 10.3389/fendo.2021.802541

69. Geng L, Lam KSL, Xu A. The therapeutic potential of FGF21 in metabolic diseases: from bench to clinic. *Nat Rev Endocrinol.* (2020) 16:654–67. doi: 10.1038/s41574-020-0386-0

70. Schwartz MW, Porte D Jr. Diabetes, obesity, and the brain. *Science.* (2005) 307:375–9. doi: 10.1126/science.1104344

71. Hsuchou H, Pan W, Kastin AJ. The fasting polypeptide FGF21 can enter brain from blood. *Peptides.* (2007) 28:2382–6. doi: 10.1016/j.peptides.2007.10.007

72. Bookout AL, de Groot MH, Owen BM, Lee S, Gautron L, Lawrence HL, et al. FGF21 regulates metabolism and circadian behavior by acting on the nervous system. *Nat Med.* (2013) 19:1147–52. doi: 10.1038/nm.3249

73. Jensen-Cody SO, Flippo KH, Claflin KE, Yavuz Y, Sapouckey SA, Walters GC, et al. FGF21 signals to glutamatergic neurons in the ventromedial hypothalamus to suppress carbohydrate intake. *Cell Metab.* (2020) 32:273–86 e6. doi: 10.1016/j.cmet.2020.06.008

74. Sarruf DA, Thaler JP, Morton GJ, German J, Fischer JD, Ogimoto K, et al. Fibroblast growth factor 21 action in the brain increases energy expenditure and insulin sensitivity in obese rats. *Diabetes.* (2010) 59:1817–24. doi: 10.2337/db09-1878

75. Rothwell NJ. Central effects of CRF on metabolism and energy balance. *Neurosci Biobehav Rev.* (1990) 14:263–71. doi: 10.1016/S0149-7634(05)80037-5

76. Owen BM, Ding X, Morgan DA, Coate KC, Bookout AL, Rahmouni K, et al. FGF21 acts centrally to induce sympathetic nerve activity, energy expenditure, and weight loss. *Cell Metab.* (2014) 20:670–7. doi: 10.1016/j.cmet.2014.07.012

77. Patel R, Bookout AL, Magomedova L, Owen BM, Consiglio GP, Shimizu M, et al. Glucocorticoids regulate the metabolic hormone FGF21 in a feed-forward loop. *Mol Endocrinol.* (2015) 29:213–23. doi: 10.1210/me.2014-1259

78. Jiao H, Arner P, Dickson SL, Vidal H, Mejhert N, Henegar C, et al. Genetic association and gene expression analysis identify FGFR1 as a new susceptibility gene for human obesity. *J Clin Endocrinol Metab.* (2011) 96:E962–6. doi: 10.1210/jc.2010-2639

79. Abu-Odeh M, Zhang Y, Reilly SM, Ebadat N, Keinan O, Valentine JM, et al. FGF21 promotes thermogenic gene expression as an autocrine factor in adipocytes. *Cell Rep.* (2021) 35:109331. doi: 10.1016/j.celrep.2021.109331

80. Somm E, Henry H, Bruce SJ, Aeby S, Rosikiewicz M, Sykiotis GP, et al. beta-Klotho deficiency protects against obesity through a crosstalk between liver, microbiota, and brown adipose tissue. *JCI Insight.* (2017) 2:91809. doi: 10.1172/jci.insight.91809

81. Yang C, Wang C, Ye M, Jin C, He W, Wang F, et al. Control of lipid metabolism by adipocyte FGFR1-mediated adipohepatic communication during hepatic stress. *Nutr Metab.* (2012) 9:94. doi: 10.1186/1743-7075-9-94

82. Pan JA, Lin H, Yu JY, Zhang HL, Zhang JF, Wang CQ, et al. MiR-21-3p inhibits adipose browning by targeting FGFR1 and aggravates atrial fibrosis in diabetes. *Oxid Med Cell Longev.* (2021) 2021:9987219. doi: 10.1155/2021/9987219

83. Markan KR. Defining "FGF21 Resistance" during obesity: controversy, criteria and unresolved questions. *F1000Res.* (2018) 7:289. doi: 10.12688/f1000research.14117.1

84. BonDurant LD, Ameka M, Naber MC, Markan KR, Idiga SO, Acevedo MR, et al. FGF21 regulates metabolism through adipose-dependent and -independent mechanisms. *Cell Metab.* (2017) 25:935–44 e4. doi: 10.1016/j.cmet.2017.03.005

85. Hale C, Chen MM, Stanislaus S, Chinookoswong N, Hager T, Wang M, et al. Lack of overt FGF21 resistance in two mouse models of obesity and insulin resistance. *Endocrinology.* (2012) 153:69–80. doi: 10.1210/en.2010-1262

86. Markan KR, Naber MC, Small SM, Peltekian L, Kessler RL, Potthoff MJ. FGF21 resistance is not mediated by downregulation of beta-klotho expression in white adipose tissue. *Mol Metab.* (2017) 6:602–10. doi: 10.1016/j.molmet.2017.03.009

87. Samms RJ, Cheng CC, Kharitonenkov A, Gimeno RE, Adams AC. Overexpression of beta-Klotho in adipose tissue sensitizes male mice to endogenous FGF21 and provides protection from diet-induced obesity. *Endocrinology.* (2016) 157:1467–80. doi: 10.1210/en.2015-1722

88. Chou RH, Huang PH, Hsu CY, Chang CC, Leu HB, Huang CC, et al. Circulating Fibroblast growth factor 21 is associated with diastolic dysfunction in heart failure patients with preserved ejection fraction. *Sci Rep.* (2016) 6:33953. doi: 10.1038/srep33953

89. Tezze C, Romanello V, Sandri M. FGF21 as modulator of metabolism in health and disease. *Front Physiol.* (2019) 10:419. doi: 10.3389/fphys.2019.00419

90. Gaich G, Chien JY, Fu H, Glass LC, Deeg MA, Holland WL, et al. The effects of LY2405319, an FGF21 analog, in obese human subjects with type 2 diabetes. *Cell Metab.* (2013) 18:333–40. doi: 10.1016/j.cmet.2013.08.005

91. Veniant MM, Komorowski R, Chen P, Stanislaus S, Winters K, Hager T, et al. Long-acting FGF21 has enhanced efficacy in diet-induced obese mice and in obese rhesus monkeys. *Endocrinology.* (2012) 153:4192–203. doi: 10.1210/en.2012-1211

92. Stanislaus S, Hecht R, Yie J, Hager T, Hall M, Spahr C, et al. A novel Fc-FGF21 with improved resistance to proteolysis, increased affinity toward beta-Klotho, and enhanced efficacy in mice and cynomolgus monkeys. *Endocrinology.* (2017) 158:1314–27. doi: 10.1210/en.2016-1917

93. Kaufman A, Abuqayyas L, Denney WS, Tillman EJ, Rolph T. AKR-001, an Fc-FGF21 analog, showed sustained pharmacodynamic effects on insulin sensitivity and lipid metabolism in type 2 diabetes patients. *Cell Rep Med.* (2020) 1:100057. doi: 10.1016/j.xcrm.2020.100057

94. Zhang J, Li Y. Fibroblast growth factor 21 analogs for treating metabolic disorders. *Front Endocrinol.* (2015) 6:168. doi: 10.3389/fendo.2015.00168

95. Wu X, Weiszmann J, Ge H, Baribault H, Stevens J, Hawkins N, et al. A unique FGF23 with the ability to activate FGFR signaling through both alphaKlotho and betaKlotho. *J Mol Biol.* (2012) 418:82–9. doi: 10.1016/j.jmb.2012.02.027

96. Smith R, Duguay A, Bakker A, Li P, Weiszmann J, Thomas MR, et al. FGF21 can be mimicked in vitro and in vivo by a novel anti-FGFR1c/beta-Klotho bispecific protein. *PLoS ONE.* (2013) 8:e61432. doi: 10.1371/journal.pone.0061432

97. Baruch A, Wong C, Chinn LW, Vaze A, Sonoda J, Gelzleichter T, et al. Antibody-mediated activation of the FGFR1/Klothobeta complex corrects metabolic dysfunction and alters food preference in obese humans. *Proc Natl Acad Sci USA.* (2020) 117:28992–9000. doi: 10.1073/pnas.2012073117

98. Fan L, Gu L, Yao Y, Ma G. Elevated serum fibroblast growth factor 21 is relevant to heart failure patients with reduced ejection fraction. *Comput Math Methods Med.* (2022) 2022:7138776. doi: 10.1155/2022/7138776

frontiers | Frontiers in Cardiovascular Medicine

TYPE Review
PUBLISHED 08 August 2022
DOI 10.3389/fcvm.2022.964034

OPEN ACCESS

EDITED BY
Jian Shi,
University of Leeds, United Kingdom

REVIEWED BY
Francesca Vinchi,
Lindsley F. Kimball Research Institute, United States
Julie Pires Da Silva,
Université Toulouse III-Paul Sabatier, France
Yue Zheng,
Tianjin Medical University, China

*CORRESPONDENCE
Yue-Jin Yang
yangyjfw@126.com

†These authors have contributed equally to this work

SPECIALTY SECTION
This article was submitted to Cardiovascular Metabolism, a section of the journal Frontiers in Cardiovascular Medicine

RECEIVED 08 June 2022
ACCEPTED 25 July 2022
PUBLISHED 08 August 2022

CITATION
Zhang L-L, Tang R-J and Yang Y-J (2022) The underlying pathological mechanism of ferroptosis in the development of cardiovascular disease.
Front. Cardiovasc. Med. 9:964034.
doi: 10.3389/fcvm.2022.964034

The underlying pathological mechanism of ferroptosis in the development of cardiovascular disease

Li-Li Zhang[1†], Rui-Jie Tang[2†] and Yue-Jin Yang[1*]

[1]State Key Laboratory of Cardiovascular Disease, Department of Cardiology, Fuwai Hospital, National Center for Cardiovascular Diseases, Chinese Academy of Medical Sciences and Peking Union Medical College, Beijing, China, [2]Department of Cardiology, The First Affiliated Hospital of Zhengzhou University, Zhengzhou, China

Cardiovascular diseases (CVDs) have been attracting the attention of academic society for decades. Numerous researchers contributed to figuring out the core mechanisms underlying CVDs. Among those, pathological decompensated cellular loss posed by cell death in different kinds, namely necrosis, apoptosis and necroptosis, was widely regarded to accelerate the pathological development of most heart diseases and deteriorate cardiac function. Recently, apart from programmed cell death revealed previously, ferroptosis, a brand-new cellular death identified by its ferrous-iron-dependent manner, has been demonstrated to govern the occurrence and development of different cardiovascular disorders in many types of research as well. Therefore, clarifying the regulatory function of ferroptosis is conducive to finding out strategies for cardio-protection in different conditions and improving the prognosis of CVDs. Here, molecular mechanisms concerned are summarized systematically and categorized to depict the regulatory network of ferroptosis and point out potential therapeutic targets for diverse cardiovascular disorders.

KEYWORDS

ferroptosis, cardiovascular disease, mechanism, pathology, metabolism

Introduction

Cardiovascular diseases (CVDs) mean an array of diseases, including atherosclerosis, hypertension, acute coronary syndrome, heart failure (HF), cardiomyopathy, arrhythmia, *etc.*, as the major cause of morbidity and mortality in the global population, imposing heavy economic pressure on families and community. Therefore, to prevent the occurrence and development of CVDs, its pathological mechanisms have become the focus of medical research in recent years.

Iron is an essential microelement for multiple life processes, and the imbalance of iron homeostasis can cause many adverse consequences. Iron overload is associated with iron deposition in various tissues including the heart, in 1981, Sullivan et al.

formally proposed the hypothesis of iron-derived heart disease (1). Since then, iron overload was shown to play a pivotal role in the pathogenesis of CVDs and enhance the risk of cardiovascular morbidity (2). Iron overload can induce a novel iron-dependent form of cell death that is neither apoptosis nor necrosis, called ferroptosis (3). Cell death results in the onset and deterioration of acute or chronic disorders, often accompanied by dysregulation of inflammation, cellular dysfunction, and tissue damage. Acute cardiomyocytes (CM) death can cause myocardial infarction (MI) and ischemia-reperfusion (I/R) injury, while chronic progressive CMs death can cause compensatory hypertrophy, eventually leading to HF or cardiomyopathy (4). Ferroptosis is distinguished from other forms of death. And its main feature is the oxidative modification of phospholipid membranes by iron-dependent mechanisms, coupled with a substantial buildup of lipid peroxides. The pathological role of ferroptosis in atherosclerosis, I/R injury, cardiomyopathy, HF and other CVDs has been widely reported, and targeted intervention of ferroptosis effectively prevented the occurrence and development of these diseases (5–9). This review focuses on the underlying pathological mechanism of ferroptosis in CVDs, regarding oxidative stress, inflammation, metabolic disorders and mitochondrial damage, and provides targeted evidence for treatment.

Characteristics of ferroptosis

Dixon et al. (3) showed that the selectively RAS-lethal small molecule erastin not only modulated the mitochondrial voltage-dependent anion channel (VDAC), but also inhibited the function of SLC7A11, an important subunit of the cystine/glutamate reverse transporter system Xc^- (xCT), reducing intracellular glutathione (GSH) synthesis, further increasing the accumulation of iron-dependent lipid peroxide and inducing the death of RAS mutant fibrosarcoma cell lines. They formally named this new form of regulated cell death triggered by erastin as ferroptosis: an iron-dependent non-apoptotic form of cell death caused by the imbalance of intracellular synthesis and degradation of ROS and lipid peroxides (3). Different from typical cell death form, ferroptosis cannot be inhibited by inhibitors of apoptosis and pyroptosis, but can be inhibited by iron chelators (e.g., deferoxamine), antioxidants (e.g., tea polyphenol) (10, 11). Moreover, ferroptosis has unique morphological features and biochemical markers. Morphologically, there was no cell shrinkage, chromatin condensation, formation of apoptotic bodies, or disintegration of the cytoskeleton, but significant shrinkage of mitochondria and reduction of mitochondrial cristae were observed (3). Regarding distinguishing biomarkers, they are associated with the accumulation of intracellular iron ions and ROS accompanied by the decrease in GSH metabolism, as exemplified in **Table 1**.

Mechanisms of ferroptosis

Iron overload is a prerequisite for ferroptosis, and various iron chelators can inhibit ferroptosis. Transferrin receptor 1 (TfR1) can promote the transfer of extracellular iron into cells, and the silencing of its encoding gene prevented ferroptosis caused by erastin. Iron supplementation accelerated erastin-induced ferroptosis (12). Treatment of dopaminergic cells with ferric ammonium citrate to mimic the iron overload showed that ferroptosis occurred before apoptosis and could be rescued by ferroptosis inhibitors (13). These results further demonstrated the necessity of iron overload in the process of ferroptosis.

The accumulation of lipid peroxide is another crucial element in the execution of ferroptosis. Cellular or organelle membranes are especially vulnerable to attack by ROS due to their high polyunsaturated fatty acids, called lipid peroxidation. An important source of ROS in mammalian cells is mitochondria. Among mitochondrial metabolic activities, tricarboxylic acid (TCA) cycle starts with acetyl-CoA from glucose or fatty acid metabolism, and transfers electrons to the electron transport chain (ETC), completing oxidative phosphorylation (OXPHOS). Once the electrons are leaked from ETC complexes I and III, superoxide will be produced and converted to H_2O_2 by superoxide dismutase (SOD) (14). Subsequently, Fe^{2+} released via divalent metal transporter 1 (DMT1) can react with H_2O_2 to yield hydroxyl (·OH) or alkoxy (RO·) radicals, known as "Fenton reaction," resulting in the production of reactive poisonous aldehydes, in the form of 4-hydroxynonenal (4-HNE) and malondialdehyde (MDA) (15–17). In addition, ROS can induce autophagy to accelerate the degradation of ferritin and enhance the expression of TfR1 leading to ferroptosis (18). In turn, ferroptosis can also significantly increase ROS production, disrupt mitochondrial membrane potential, and promote mitochondrial fission (19). Accordingly, mitochondrial damage and energy metabolism disorders exacerbate the vicious cycle between lipid peroxidation and ferroptosis.

As confirmed by Dixon et al., xCT-mediated cystine absorption from extracellular space accompanied by the export of intracellular glutamate could regulate ferroptosis (3). In the cytoplasm, cystine turns into cysteine, a main raw material of GSH synthesis. GSH produced above serves as an electron donor to reduce toxic lipid peroxides into non-toxic alcohols under the enzymolysis of glutathione peroxidase 4 (GPX4) (20). Hence, the xCT-GSH-GPX4 axis conducts the dominant defensive mechanism against cellular ferroptosis. Upregulation of p53 significantly reduced the expression of SLC7A11, which inhibited xCT mediated-cystine uptake and resulted in ferroptosis (21). RSL3, erastin and sulfasalazine are direct targets

TABLE 1 Major regulatory indicators and potential markers of ferroptosis.

Characteristics	Indicators	Key biomarkers
Iron accumulation	Total iron or ferrous ion	Tf, TfR, ferritin, iron-sulfur protein, NCOA4, etc.
Lipid peroxidation	ROS, increased oxidized polyunsaturated fatty acids	NQO1, NOX1, SOD, MDA, NRF2, Arachidonoyl-CoA, PTGS2/COX-2, LOX, ACOT, ACSL, etc.
Decreased GSH metabolism	Ratio of GSH to GSSG	GPX4, GSH, xCT, SLC7A11, SLC3A2, p53, etc.
Mitochondrial dysfunction	Measurement of mitochondrial membrane potential and respiratory function, mtDNA damage	VDAC1, VDAC2, MPTP, ETC complexes, etc.

Tf, transferrin; TfR, transferrin receptor; NCOA4, nuclear receptor coactivator 4; MDA, malondialdehyde; ROS, reactive oxygen species; NQO1, NAD(P)H: quinone oxidoreductase 1; NOX, NADPH oxidase; SOD, superoxide dismutase; NRF2, nuclear factor erythroid 2-related factor 2; GPX4, glutathione peroxidase 4; GSH, glutathione; GSSG, oxidized glutathione; xCT, system Xc-; SLC7A11, solute carrier family 7 member 11; SLC3A2, solute carrier family 3 member 2; VDAC, voltage-dependent anion channel; PTGS2, Prostaglandin G/H synthase-2; COX, cyclooxygenase; LOX, lipoxygenase; ACOT, acyl-CoA thioesterase; ACSL, acyl-CoA synthetases; MPTP, mitochondrial permeablity transition pore; ETC, electron transfer chain.

of GPX4 and make cancer cells more sensitive to ferroptosis (22). It can be inferred that any methods causing xCT inhibition, GSH or GPX4 depletion might promote ferroptosis. In addition, ferroptosis suppressor protein 1 (FSP1), formerly known as apoptosis-inducing factor mitochondria-associated 2, protects cells from GPX4 deletion-induced ferroptosis (23). Treatment of lung cancer cells with iFSP1, an inhibitor of FSP1, potentiated ferroptosis (24). Therefore, antagonism of FSP1 can lead to the occurrence of ferroptosis.

Moreover, ferroptosis as a type of necrotic cell death is mostly accompanied by inflammatory manifestations. Ferroptosis-related necroinflammation was observed in mice with acute kidney injury (25). Ferroptotic cells can release damage-associated molecular patterns (DAMPs) to activate immune cells, which further amplify ferroptosis by releasing inflammatory mediators such as interleukin (IL)-1β and tumor necrosis factor (TNF)-α. In addition, during ferroptosis, polyunsaturated fatty acids, especially arachidonic acids, are prone to peroxidation. The lipoxygenase (LOX) and cyclooxygenase (COX)-generated metabolites of arachidonic acid (hydroxyeicosatetraenoic acid, leukotriene, and prostaglandins) are also involved in inflammatory response (26). The above shows that ferroptosis is closely related to inflammation and immunity, and the persistence of inflammation may form a self-amplifying circuit of ferroptosis.

In sum, oxidative stress, inflammation, metabolic disorders, and mitochondrial damage are the main cellular and molecular pathological mechanisms in ferroptosis.

Pathological mechanism of ferroptosis in cardiovascular diseases

Oxidative stress

Oxidative stress is involved in assorted CVDs like MI, I/R injury, and HF. Excessive production of ROS impairs cellular lipids, resulting in ferroptosis. In the cardiovascular system, the antioxidant system controls intracellular ROS and interacts with biological components to maintain redox equilibrium. This system contains counteroxidant enzymes such as SOD, catalase, GPX, and thioredoxin (Trx), and non-enzymatic antioxidants such as tocopherol and coenzyme Q10 (CoQ10) are shown in **Figure 1**. This system eliminates ROS by chelating metal ions, enhances the production of endogenous antioxidants, and defends against ferroptosis in the cardiac tissues (27–30).

Superoxide dismutase system

Three isoforms of SOD system in mammals are SOD1, SOD2, and SOD3, as the first line of defense against oxygen-derived free radicals in the cardiovascular system. Under the exposure to oxidative stress, they can be rapidly activated to catalyze superoxides into oxygen and H_2O_2. Among three members of SOD family, SOD1, an isoform located in the cytoplasm containing Cu^{2+} and Zn^{2+}, outweighs SOD2 and SOD3 in the expression of abundance. A cohort study showed that SOD1 allelic mutations in the population were linked with an elevated risk of death from cardiovascular complications (sudden death, fatal MI, or stroke) (31). SOD1 deletion promoted the occurrence of ferroptosis (32). Sustained delivery of SOD1 could improve myocardial I/R injury (33). SOD2 is a manganese-containing isoenzyme found in mitochondria, also associated with ferroptosis (34). Deficiency of SOD2 increases ROS in CMs, leading to subsequent overproduction of 4-HNE inside mitochondria and impairment of mitochondrial bioenergy production, which is one of the causes of lethal dilated cardiomyopathy (35). The structure of SOD3 is similar to SOD1, and upregulation of SOD3 is conducive to rid the vascular system of oxidative damage, alleviating the severity of hypertension and coronary arteriosclerosis (36). Therefore, the SOD system may protect from the occurrence of ferroptosis in CVDs by reducing superoxides.

Catalase

Catalase located in the peroxisome varies in different developmental stages of organisms, which is manipulated by peroxisome proliferator-activated receptors (PPARs) and decomposes H_2O_2 into H_2O and oxygen (37). Upregulation

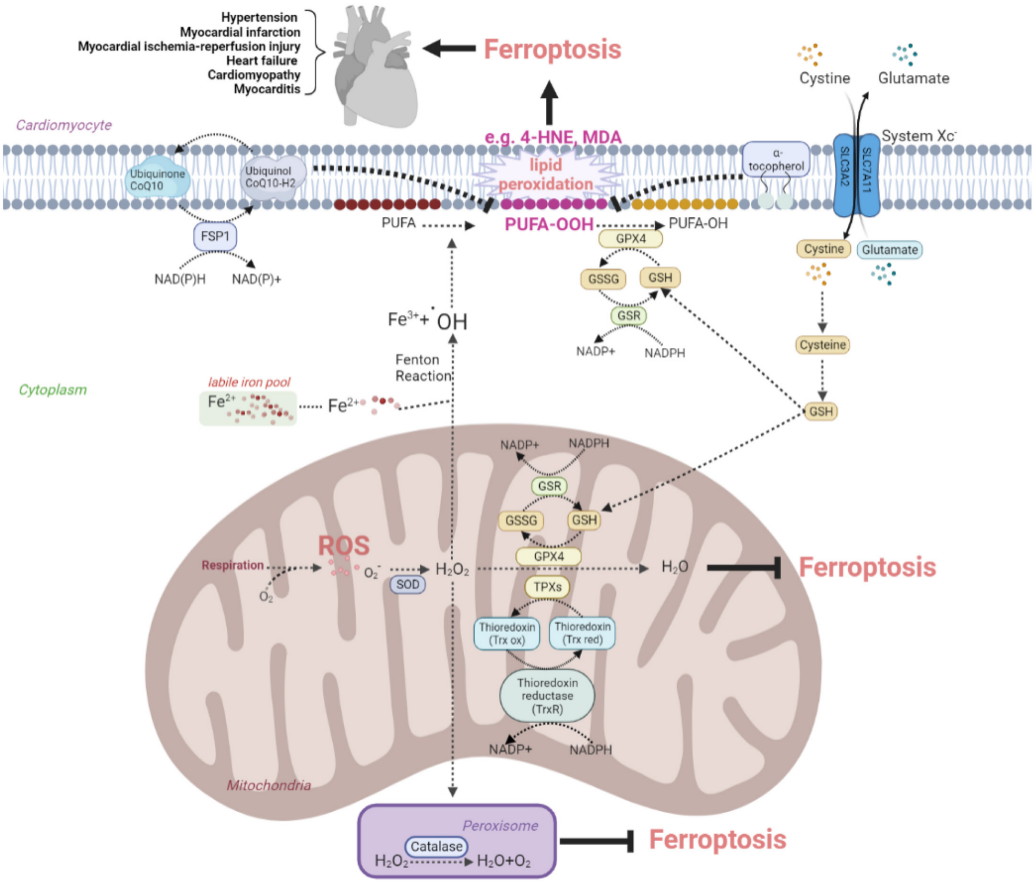

FIGURE 1
The anti-oxidative system inhibits ferroptosis to protect against cardiovascular disease by eliminating oxidative stress. The figure shows the protective effects of the SOD family, catalase, Trx recycles, system Xc^--GSH-GPX4 pathway, FSP1-CoQ10-NAD(P)H pathway, and tocopherol on the elimination of ROS and reducing the conversion to lipid peroxide, such as toxic MDA and 4-HNE. ROS, reactive oxygen species; SOD, superoxide dismutase; FSP, ferroptosis suppressor protein; CoQ, coenzyme Q; GSH, glutathione; GSSG, oxidized glutathione; GSR, glutathione reductase; GPX, glutathione peroxidase; 4-HNE, 4-hydroxynonenal; MDA, malondialdehyde; TPX, thioredoxin peroxidase; Trx red, reduced thioredoxin; Trx ox, oxidized thioredoxin; PUFA, polyunsaturated fatty acid.

of catalase has been reported to increase ferroptosis resistance in xCT-deficient mouse blast fibroblasts. Besides, catalase activation is cardioprotective to H_2O_2-induced stress in myocardial I/R injury by alleviating ferroptosis (38, 39).

Glutathione peroxidase system

Glutathione peroxidase 4 family contain eight members, namely GPX1–GPX8. The similar denominator among diverse GPXs gifts their abilities to reduce H_2O_2 and hydroperoxides to H_2O. GPX4 is unique in the GPXs family which can reduce phospholipid hydroperoxides of membranes using redox equivalents from GSH. A proteomic analysis showed that GPX4 downregulation using specific siRNA or chemical inhibitor RSL3 caused CMs ferroptosis during MI (40). Activation of nuclear factor erythroid 2-related factor 2/xCT/GPX4 signaling pathway attenuates CMs ferroptosis in doxorubicin-induced cardiomyopathy and myocardial I/R injury by inhibiting oxidative stress (41, 42). Besides, the ferroptosis inhibitor ferrostatin-1 markedly prevented pathological myocardial remodeling and fibrosis in angiotensin II-induced hypertensive cardiomyopathy by attenuating the upregulation of ferrous ion levels and lipid peroxidation in mouse microvascular endothelial cells (ECs) through modulating the xCT/GPX4 signaling (43). The Chinese herbal medicine, Tongxinluo, prevented atherosclerosis, and the xanthohumol reduced myocardial I/R injury as well, both through modulating GPX4 expression to decrease ROS (44, 45). Thus, chemicals targeting GPX4 signaling pathway could act as potential drugs to various CVDs by suppressing ferroptosis.

Thioredoxin system

Thioredoxin reductase (TrxR), Trx and NADPH together constitute the Trx system. TrxR is an NADPH-dependent dimeric selenozyme required for reducing and recycling the oxidized Trx1. TrxR was verified to reduce cell sensitivity

to erastin (46). Cardiac-specific TrxR knockout (KO) aged mice were more prone to dilated cardiomyopathy due to increased ROS and dysregulated mitochondrial energy metabolism (47). Additionally, Trx-1 as a small molecule protein participates in redox reactions. Overexpression of Trx-1 could inhibit ferroptosis by increasing GPX4 and GSH (48), which indicated the GSH-Trx cross-talk ensured cell survival. In Trx1 KO mice, increased oxidation of the mammalian target of the rapamycin (mTOR) signaling leads to impaired phosphorylation of substrates and mitochondrial respiratory dysfunction, manifesting as systolic dysfunction in HF (49). The Trx system delivers electrons for thioredoxin peroxidase (TPX), whose function is similar to the GPX to remove ROS by reducing H_2O_2 and hydroperoxides at a rapid reaction rate (50). Thus, it is speculated that the Trx system alleviates ferroptosis to exert cardioprotective effects by modulating the reduction/oxidative balance.

Tocopherol

Vitamin E has eight isomers that inhibit lipid peroxidation by donating phenolic hydrogen to peroxyl radicals, producing inactive tocopherol radicals. Alpha-tocopherol was the most prevalent and physiologically type of vitamin E (51). *In vitro*, alpha-tocopherol was demonstrated to rescue GPX4-deficient cells from ferroptosis, indicating that GPX4 and vitamin E synergistically maintain lipid redox equilibrium (52). Alpha-tocopherol may decrease myeloperoxidase expression, reducing oxidative and inflammatory reactions induced by I/R damage in mice, ultimately, preserving heart function (53). However, Keith et al. conducted a clinical trial showed that vitamin E supplementation significantly elevated alpha-tocopherol plasma concentrations in the treated group but failed to affect any other markers of oxidative stress and prognosis or function in class III or IV advanced HF (54). It is possible that alpha-tocopherol supplementation alone is not sufficient to combat severe oxidative stress and may achieve the desired therapeutic effect in combination with other natural antioxidants.

CoQ10 system

CoQ10 is named because of the mammalian CoQ containing 10 isoprene units. CoQ10 mainly exists in two forms, namely ubiquinone (oxidized form) and ubiquinol (reduced form). Ubiquinone can be transformed into ubiquinol by losing two electrons, and ubiquinol plays the main anti-oxidant role. FSP1 participates in the regulation of CoQ10 antioxidant system to alleviate ferroptosis, in a GSH- and GPX4-independent manner. The N-terminal end of FSP1 containing a typical myristoylation motif can bind to the phospholipid bilayer of cell membrane. The reduced form, ubiquinol, converts to the oxidative form, ubiquinone, after chemically reacting with lipid peroxide radicals released from the metabolism of membrane lipid, and eventually shut down the ferroptosis. Furthermore, under the catalysis of FSP1, ubiquinone can be reduced to ubiquinol in the cell membrane using NAD(P)H (23). Recently, an *in vivo* experiment has proven that FSP1 upregulation alleviates myocardial injury induced by septicemia through inhibition of ferroptosis (54). In short, the FSP1-CoQ10-NAD(P)H axis underlies another indispensable mechanism for myocardium protection under CVDs.

Inflammation

Endogenous damage-associated molecular patterns

Damaged or dead CMs can generate or release host-derived danger signaling molecules DAMPs, which have been identified as endogenous dangerous signals for the innate immune system (55). The high mobility group box 1 (HMGB1) protein is a type of DAMP that can be released by ferroptotic cells. Ferroptosis inducers, erastin, sorafenib and RSL3, all trigger the release of HMGB1, which recruits pro-inflammatory macrophages and microglia via activating receptors for advanced glycation end products (RAGE)-nuclear factor-kappa B (NF-κB) pathway. Upregulation of HMGB1 expression has been shown to contribute to chronic HF and ischemic heart disease (56–59). Besides, inflammasomes are multi-protein complexes involving intracytoplasmic pattern recognition receptors. Inflammasomes were activated by DAMPs, followed by activating pro-inflammatory proteases and producing the corresponding mature cytokines (60, 61). Englestrin, a selective sodium-glucose cotransporter 2 inhibitor, significantly improved cardiac function in adriamycin cardiomyopathy by attenuating CMs ferroptosis through inhibition of the NOD-like receptor thermal protein domain associated protein 3 (NLRP3) inflammasomes related pathways (62). DAMPs are also processed by antigen-presenting cells like dendritic cells (DCs) through Toll-like receptors (TLRs) and presented to T cells to initiate an immune response. Besides, DAMPs released from ferroptotic ECs facilitates neutrophil adhesion to coronary vessels via activating the TLR4/TIR-domain-containing adapter-inducing interferon-β (TRIF)/interferon I (IFN I) pathway, resulting in neutrophil recruitment to the damaged myocardium (63). These discoveries shed light on the contribution of the immune cells activated by DAMPs from ferroptotic cells leading to CVDs, as summarized in **Figure 2**.

Pro-inflammatory factors

Inflammation is tightly associated with oxidative stress, which triggers a range of pro-inflammatory factors such as NF-κB, IL-6, IFN-γ, TNF-α (64–67). Besides, studies have confirmed that the NF-κB pathway and IL-6/JAK2/STAT3 pathway activation could induce ferroptosis (68, 69). IFN-γ could down-regulate the expression of two subunits of xCT, SLC3A2 and SLC7A11, through the ASK1/JNK or JAK1-2/STAT1 pathway, reducing cellular uptake of cystine

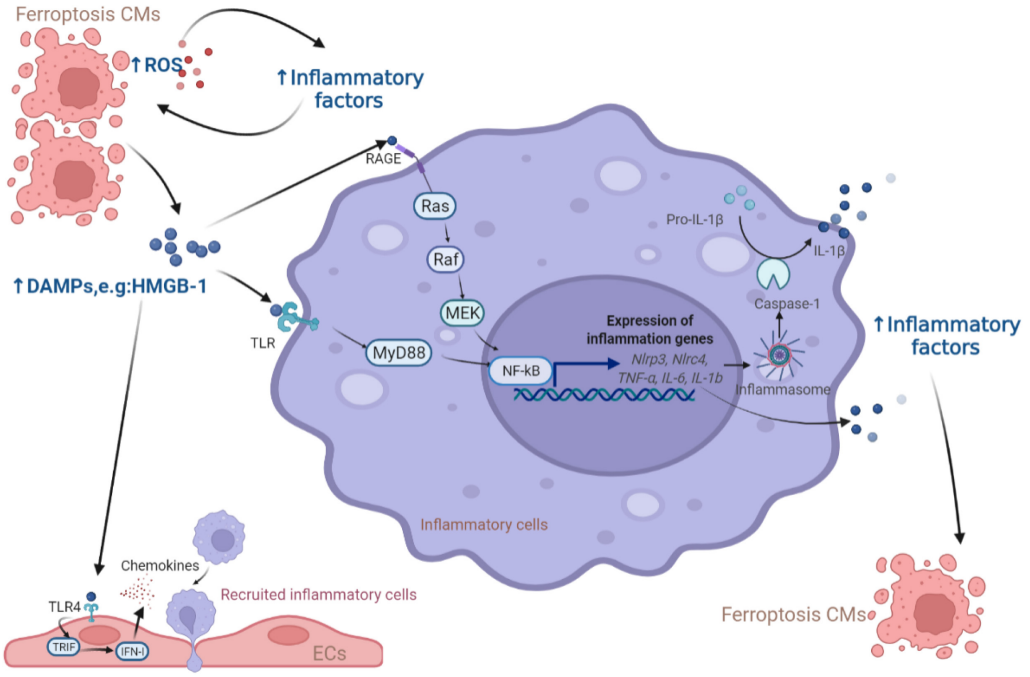

FIGURE 2
The role of DAMPs released from ferroptotic CMs in inflammation. The release of DAMPs from ferroptotic cells activates the downstream NF-κB inflammatory pathway through the TLR and RAGE receptors of inflammatory cells, leading to the production of inflammatory factors (e.g., NF-κB, IL-6, IFN-γ, TNF-α, and IL-1β) which were also produced due to the increase of ROS to induce more CMs ferroptosis. In addition, ECs respond to DAMPs via TLR4 receptors and release chemokines to promote more inflammatory cells entering the myocardial microenvironment. CM, cardiomyocyte; ROS, reactive oxygen species; DAMP, damage-associated molecular pattern; HMGB, high mobility group box; RAGE, receptor for advanced glycation end products; TLR, Toll-like receptors; MEK, mitogen-activated protein kinase kinase; NF-κB, nuclear factor-kappa B; NLRP, NOD-like receptor thermal protein domain associated protein; NLRC, NLR family CARD domain containing; MyD88, myeloid differentiation factor 88; IL, interleukin; TRIF, TIR-domain-containing adapter-inducing interferon-β; IFN, interferon; EC, endothelial cell.

and thus promoting ferroptosis (70, 71). In cardiovascular-related diseases, the inhibition of these inflammatory pathways could rescue the ferroptotic CMs or ECs. For example, the ferroptosis inhibitor ferrostatin-1 improved sepsis-induced cardiac systolic dysfunction partly through alleviating the TLR4/NF-κB signaling pathway and reducing TNF-α and IL-6 (72). A hormone elabela significantly attenuated ferroptosis in hypertensive mice by inhibiting the cardiac IL-6/STAT3 signaling pathway (43). Nevertheless, the involvement of IFN-γ in the occurrence of ferroptosis has not been investigated in CVDs and needs to be further studied.

Furthermore, membrane-bound arachidonic acid was mainly found in the phospholipids of cell membranes and subject to COX, LOX and cytochrome P450 to yield a series of inflammatory mediators, like prostaglandins and leukotrienes, causing aseptic inflammation (73, 74). Reducing intracellular levels of arachidonoyl in CMs blocked neutrophil replenishment and prevented the onset of ferroptosis. Eliminating oxidative productions from arachidonic acid could also inhibit NF-κB pathway activation (75). Thus, agents against metabolites of arachidonic acid can play an anti-inflammatory or cytoprotective role in CVDs caused by ferroptosis.

Immune cells

During myocardial injury, different types of immune cells interact with each other, and with CMs, fibroblasts, and ECs to elicit inflammatory responses. Among these immune cells, the macrophages and T cells are the two most studied types in the cardiovascular field. Here, we focus on the possible effects of these two types of cells on ferroptosis in CVDs, shown in **Figure 3**.

Generally, the first immune cell type to respond to myocardial injury is the tissue-resident macrophages. Tissue-resident C-C motif chemokine receptor 2 $(CCR2)^-$ macrophages originated from the embryonic developmental stage are distinguished from tissue-resident $CCR2^+$ macrophage repopulated by monocytes extravasating into the myocardium. Unlike $CCR2^+$ macrophages, tissue-resident $CCR2^-$ macrophages could inhibit monocyte recruitment (76). Apart from preventing fibrosis and stimulating angiogenesis (77), $CCR2^-$ macrophages also improve cardiac repair via promoting clearance of apoptotic CMs, up-regulating anti-inflammatory mediators IL-10 and TGF-β, and down-regulating pro-inflammatory mediators IL-1β, TNF-α, IL-6 and IFN-γ after MI (78). Consumption of resident $CCR2^-$ macrophages

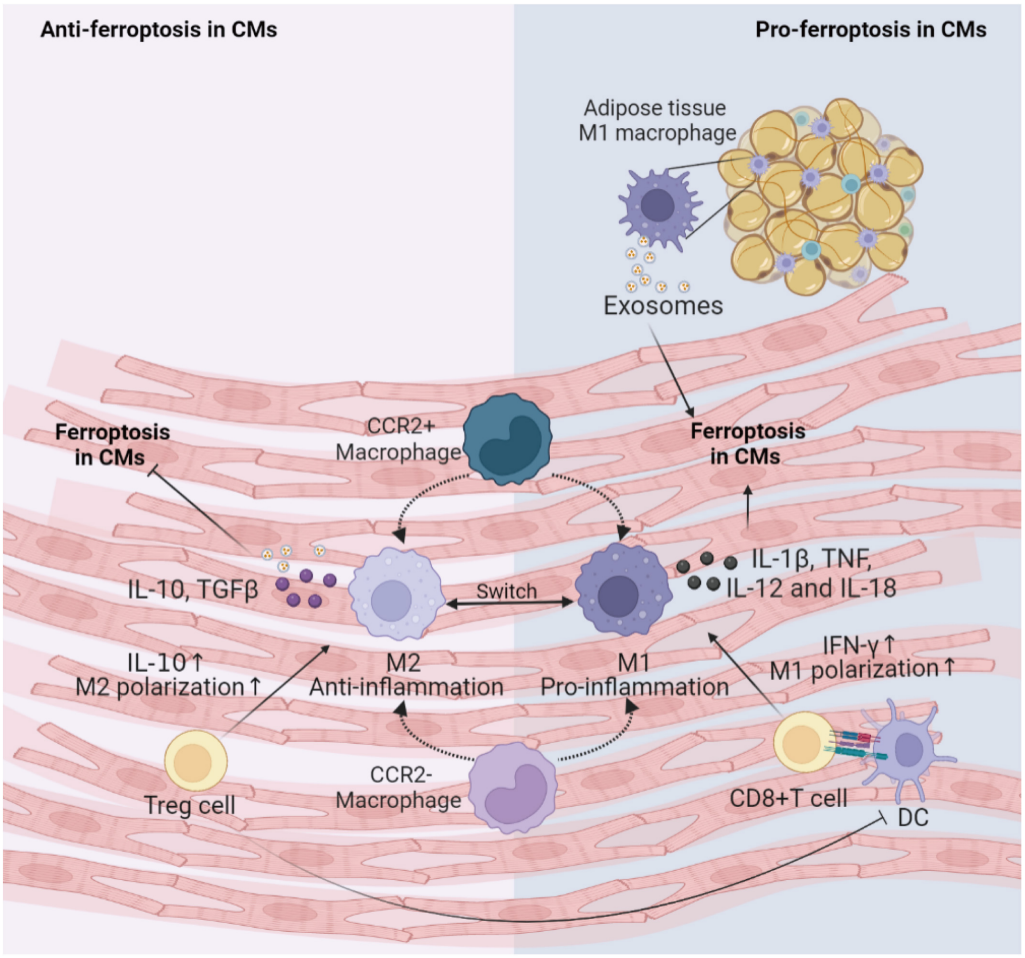

FIGURE 3
Immune cells involved in the regulation of CMs ferroptosis. This figure summarizes macrophages and T cells activity regulating the ferroptosis following cardiac injury. The cross-talk between these immune cells and CMs depends on various inflammatory factors and exosomes. DC, dendritic cell; CM, cardiomyocyte; IL, interleukin; TNF, tumor necrosis factor; IFN, interferon; TGF, transforming growth factor; CCR, C-C motif chemokine receptor 2.

leads to activation of inflammasomes in CMs, abnormal mitochondrial accumulation, and postinfarction ventricular dysfunction (79). It can be inferred that cardiac resident $CCR2^{-}$ macrophages may engulf CMs undergoing ferroptosis and reduce the inflammation to inhibit ferroptosis. Subsequently, the circulating $CCR2^{+}$ mononuclear macrophages infiltrate into the myocardial injury environment in greater number than the $CCR2^{-}$ macrophages and polarize to M1 pro-inflammatory phenotype and M2 reparative phenotype (80). Iron overload promotes polarization of M1 macrophages (81). M1 macrophages are more resistant than M2 macrophages to ferroptosis due to high intracellular levels of inducible nitric oxide synthase and nitric oxide radicals which inhibit lipid peroxidation (82, 83). M1 macrophages secrete large amounts of pro-inflammatory factors such as IL-1β, TNF, IL-12, and IL-18, increase ROS and have the potential to induce ferroptosis in adventitial hypoxic CMs (84, 85). Besides, exosomes derived from M1 macrophages in obese adipose tissue carry miR-140-5p to induce ferroptosis in CMs by targeting xCT to inhibit GSH synthesis, leading to abnormal left ventricular contraction in obese mice (86). While it has been shown that M2 macrophage-derived exosomes inhibit cell ferroptosis (87). Hence, M1 macrophages may be a key inducer of ferroptosis in the microenvironment of myocardial inflammation. Future studies are needed to prove the effects of macrophages on the onset of ferroptosis in CMs.

Infiltrating T cells activated by dendritic cells (DCs) may also regulate the occurrence of ferroptosis in CVDs. Cytotoxic $CD8^{+}$ T cells can lead to poor cardiac remodeling after ischemia, acute hypertensive heart injury, acute rejection of allogeneic heart retransplantation and other CVDs, possibly by inducing CMs ferroptosis through releasing IFN-γ and promoting M1 polarization (88). For $CD4^{+}$ effector T cells, the effects of different subtypes are pleiotropic. T helper (Th)1 cells could

activate cardiac fibroblasts to induce fibrosis; while regulatory Treg cells could reduce the number of myofibroblasts through inhibiting inflammation via anti-inflammatory cytokine IL-10 in hypertension and HF (89–91). Additionally, Treg cells beneficially influenced wound healing after MI by regulating the polarization of M2 macrophages and inhibiting proinflammatory cytokines production (92). Paracrine action of Treg cells also promoted fetal and maternal CMs proliferation to improve the prognosis of MI during pregnancy (93). Thus, Treg cells may alleviate cellular ferroptosis in the myocardial microenvironment by interacting with CMs and inflammatory cells.

Metabolic disorders

Glucose metabolism disorder

As the **Figure 4** shows that under aerobic circumstances, glucose is initially transformed into pyruvate through the glycolytic pathway and subsequently undergoes the TCA cycle and mitochondrial OXPHOS processes to complete metabolism (94, 95). At the initial stage of glycolysis, the glucose molecule is phosphorylated by hexokinase to produce glucose 6-phosphate, which is then further converted to fructose 6-phosphate by glucose 6-phosphate isomerase, to subsequently produce fructose 1,6-diphosphate catalyzed by fructokinase 6-phosphate kinase 1, the main rate-limiting enzyme in the glycolytic process. Simultaneously, fructose 6-phosphate is bypassed by glucose-6-phosphate dehydrogenase and enter the pentose phosphate pathway to produce the essential biosynthetic precursor and NADPH, 60% of which required in animals is produced in this manner. NADPH participates in multiple anabolic reactions, responsible for the recycling of GSH, ubiquinone and Trx, etc., which is crucial for ensuring the redox homeostasis in the body (96). Pyruvate produced by glycolysis enters the mitochondria to generate acetyl-CoA, which enters the TCA cycle to generate NADH, $FADH_2$ coupled with OXPHOS. Mitochondrial OXPHOS is accompanied by the transfer of electrons in the ETC to molecular oxygen, leading to the generation of ROS. Therefore, it can be speculated that glucose metabolism in CMs is closely linked to ferroptosis. Echoing the above hypothesis, appropriate blockade of glycolysis or TCA significantly inhibited ferroptosis induced by erastin, cystine depletion or RSL3 treatment, as manifested by stabilizing

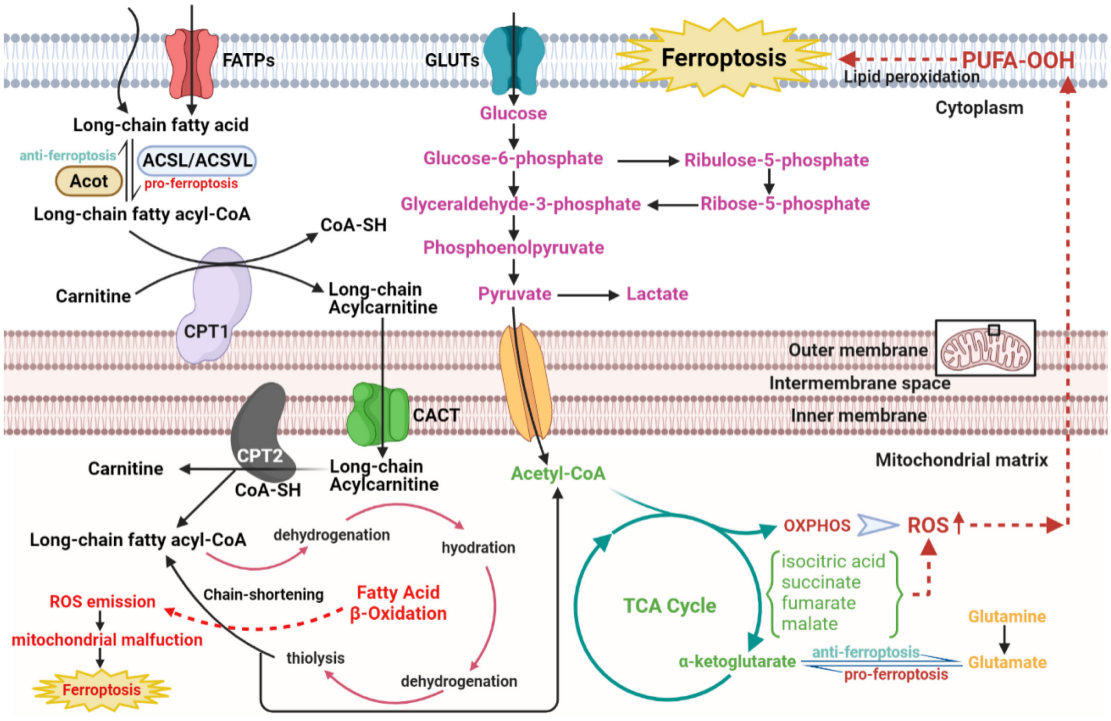

FIGURE 4
The role of glucose and fatty acid metabolic disorders in the regulatory network of ferroptosis of CVDs. The long-chain fatty acid is activated and transformed into long-chain fatty acyl-CoA with the catalytic activity of ACSL/ACSVL. The long-chain fatty acyl-CoA combines with carnitine and enters fatty acid β-oxidation in the mitochondrial matrix with help of CPT1, CPT2, and CACT. Then acetyl-CoA from the β-oxidation cycle, anaerobic glycolysis, and glutaminolysis gather to strengthen the metabolism of the TCA cycle in mitochondrial matrix, which activates downstream OXPHOS and ROS, eventually resulting in cellular ferroptosis. CVDs, cardiovascular diseases; ACSL, long-chain acyl-CoA synthases; ACSVL, very long-chain acyl-CoA synthases; CoA, coenzyme A; CPT1, carnitine palmitoyltransferase1; CPT2, carnitine palmitoyltransferase2; CACT, carnitine-acylcarnitine translocase; OXPHOS, oxidative phosphorylation; ROS, reactive oxygen species.

mitochondrial membrane potential and decreasing lipid peroxides accumulation (97, 98). According to the metabolomic analysis, CMs exposed to the ferroptosis inducer RSL3 showed markedly elevated isocitric acid and ketoglutarate (KG) contents (99). Accumulation of some TCA circulating metabolites, alpha-KG, succinate, fumarate and malate, can all contribute to lipid ROS accumulation and ferroptosis. Additionally, alpha-KG dehydrogenase/succinate/aconitase activity was enhanced during the onset of ferroptosis due to cysteine deprivation (97, 100). In the TCA cycle, glutamine can be catabolized to glutamate by glutaminase, which is further metabolized to alpha-KG for replenishment. The glutamine-fueled intracellular metabolic pathway is required for ferroptosis induced by cysteine deprivation (101). Inhibition of glutamine catabolism reduces cardiac injury triggered by I/R, offering a prospective therapy (102). These results suggest that glucose metabolism products enhance the mitochondrial ROS generation, further amplifying the ferroptosis signal.

Fatty acid metabolism disorder

Given that fatty acids are the core energy source for the myocardium, concerns about lipid metabolism have crucial implications in ferroptosis from CVDs (**Figure 4**). According to the basic perspectives on fatty acid metabolism, three stages are involved in this process, named activation, translocation and β-oxidation. Some biomolecule evolved in the above three stages, either metabolites or relative enzymes, can spark cellular ferroptosis. As the first reaction of fatty acid catabolism, long-chain acyl-CoA synthetases (ACSLs) and very long-chain acyl-CoA synthetases (ACSVLs) converts different kinds of long-chain fatty acid to corresponding fatty acyl-CoA. Among these enzymes, ACSL4 mostly activates the long-chain fatty acids and subsequently enriches cellular membrane with polyunsaturated ones. Specifically, two long-chain fatty acids, arachidonic acid, and adrenoic acid, can be both converted to arachidonoyl-CoA and adrenoyl-CoA via ACSL4 and coenzyme A. Following the activation of long-chain fatty acids, arachidonoyl-CoA and adrenoyl-CoA are used to synthesize phosphatidylethanolamine and phosphatidylinositol, composing negatively charged cell membrane. Phosphatidylethanolamine can often be oxidized, triggering the ferroptosis of cells, particularly under the treatment with RSL3 (103). Consistent with the above findings, ACSL4, iron and MDA level in reperfusion myocardium gradually rose with the prolongation of myocardial ischemic time (104). Serving as the functionally well-matched adversary to ACSLs, Acyl-CoA thioesterases (ACOTs) accelerate fatty acid synthesis with the substrate fatty acyl-CoA, and the balance between ACSLs and ACOTs governs the dynamic equilibrium of fatty acid metabolism. As reported in cardiovascular basic researches, ACOT1, an isoform of ACOTs working in cytoplasm, hydrolyzes fatty acyl-CoAs, varying from short-chain ones to very long-chain ones, to free fatty acids and conenzyme A in myocardium (105, 106). Under the condition of doxorubicin-induced cardiomyopathy, Acot1 knockdown sensitizes CMs to ferroptosis, whereas ACOT1 overexpression poses defensive effect on cellular ferroptosis. This beneficial effect is conducted through ACOTs' function of lipid components alteration and acyl-CoA hydrolysis, evidenced by increased anti-oxidative ω-3 polyunsaturated fatty acids and docosahexaenoic acid abundance in the hearts of ACOT1-overexpressed mice (107). Meanwhile, in the stage of fatty acid activation, the adipokine chemerin deriving from adipose tissue inhibits fatty acid oxidation and maintains fatty acid levels to confer ferroptosis resistance. Chemerin inhibition shuts down the anti-oxidative CoQ system, followed by ROS explosion, additionally, its deficiency remarkably attenuates glycerophospholipid species accumulation, including phosphatidic acid, phosphatidylcholine, phosphatidylglycerol and intact sphingolipids, with an immediate increase in the replenishment of their corresponding oxidative and catabolic products (108, 109). Subsequent to the translocation stage, the substrate, fatty acyl-CoA, enters the β-oxidation cycle in mitochondrial matrix. After every four steps of β-oxidation, the carbon chain of acyl-CoA is shortened by two carbons, with acetyl-CoA released. Then, explosive acetyl-CoA production from fatty acid β-oxidation accelerates downstream TCA cycle and excites ROS-induced ferroptosis. Hence, ideal component remodeling and maintenance of free fatty acids metabolic balance are predicted to improve the sensitivity of CMs to ferroptosis.

Iron metabolism disorder

The balance of iron homeostasis in the body depends on the metabolic regulation of iron absorption, recycling and release. The absorption of dietary iron into the blood is regulated by DMT1 of intestinal epithelial cells. Iron recycling is obtained from senescent red blood cells phagocytosed by reticuloendothelial macrophages. Ferroportin (FP) is the only known mammalian iron exporter capable of releasing iron into the circulation. Hepcidin, a liver-derived hormone, can degrade FP and reduce the release of iron to the circulation. Therefore, in addition to nutritional iron deficiency, the disorders of the process mentioned above such as FP mutation and abnormal hepcidin levels (affected by inflammation, hypoxia, hemochromatosis protein, TfR, and other factors) can lead to the imbalance of iron homeostasis in the body (110).

At the level of individual CMs, the metabolic mechanisms maintaining iron homeostasis are mainly illustrated in **Figure 5**, associated with CMs ferroptosis. The uptake and transport of iron in the CMs mainly depend on TfR1, which takes in the Fe^{3+}-transferrin (Tf) complex into the cytoplasm via endocytosis, and finally Fe^{3+} mainly stores in the form of ferritin and hemosiderin. Ferritin controls the distribution and storage of iron in cells, preventing iron-catalyzed Fenton reaction and free radical production. Ferritin consists of

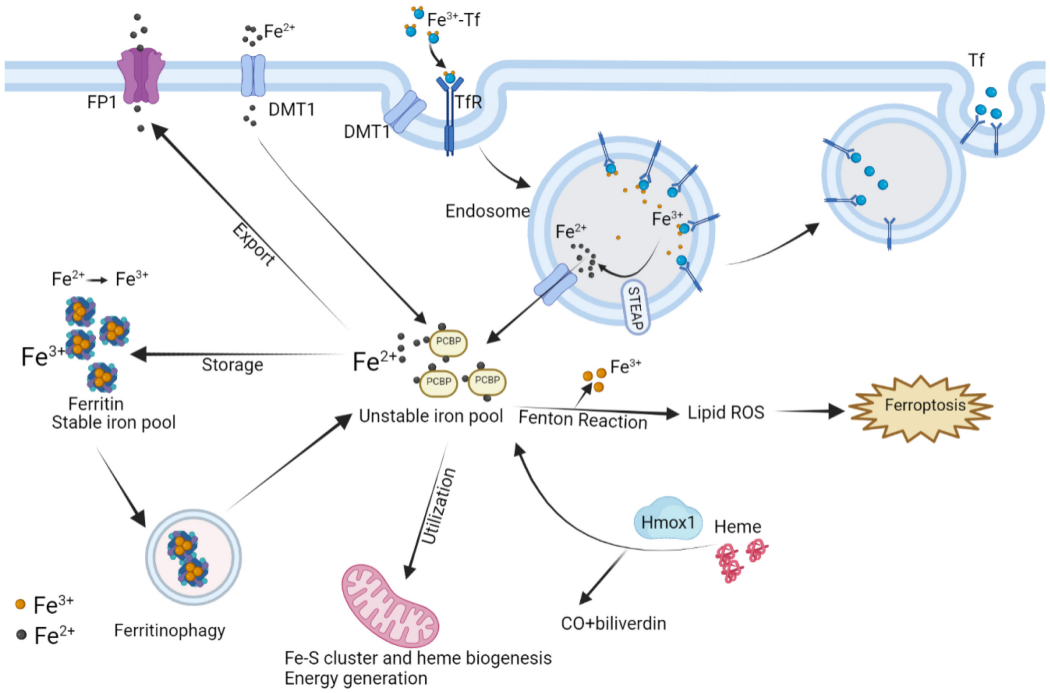

FIGURE 5
Interaction of intracellular iron metabolism and ferroptosis. Fe^{3+} and Tf bind to form Fe^{3+}-Tf complex and enter the cell by means of TfR1 via endocytosis. In endosomes, Fe^{3+} is liberated from Tf and catalyzed by STEAP to Fe^{2+}, while Tf is released extracellularly by exocytosis. The process Fe^{2+} released from endosomes or absorbed into the cells depends on DMT1. In mitochondria, the utilization of Fe^{2+} is mainly the synthesis of Fe–S clusters and heme, which can be degraded by Hmox1 to regenerate Fe^{2+}. Excess Fe^{2+} can store in ferritin by converting into Fe^{3+}, while ferritinophagy can re-release free iron. Intracellular Fe^{2+} can also be exported through FP1. The above processes participate in the regulation of intracellular Fe^{2+} content to control Fenton reaction, thereby regulating the occurrence of ferroptosis. FP1, ferroportin1; DMT1, divalent metal transporter 1; Tf, transferrin; TfR1, transferrin receptor 1; Hmox1, Heme oxygenase 1; STEAP3, six-transmembrane epithelial antigen of the prostate 3.

24 subunits, including ferritin light chain (Ftl), and ferritin heavy chain (Fth), the latter with ferrous oxidase activity can oxidize poly(C)-binding protein (PCBP)-carried Fe^{2+} to Fe^{3+}. In ferritin knock-out mice, ferroptosis induced by decreased xCT expression in CMs predisposed the mice to cardiomyopathy (9). BTB and CNC Homology 1 (BACH1) is a heme-binding transcription factor required for the appropriate regulation of oxidative stress responses and metabolic pathways associated with heme and iron. BACH1 inhibited Fth1 and Ftl1 encoding ferritin, exacerbating MI by promoting ferroptosis (111). Degradation of ferritin, especially Fth1, through nuclear receptor coactivator 4 (NCOA4) –mediated ferritinophagy resulted in the release of ferritin-bound iron to replenish free Fe^{2+} (112). Inhibition of NCOA4-mediated ferritinophagy contributed to myocardial hypertrophy through mitochondrial iron overload (113). Regarding Fe^{2+}, it can be taken up into the CMs by DMT1. Additionally, Fe^{2+} can be transformed by Fe^{3+} deoxygenation under the catalysis of the iron oxide reductase six-transmembrane epithelial antigen of the prostate 3 (STEAP3), followed by releasing from the endosome mediated by DMT1 into the ferroptosis-associated unstable iron pool in the cytoplasm. Furthermore, loss of cardiac iron exporter FP1 rapidly caused an eventual fatal impairment of cardiac function in mice, which is associated with intracellular iron deposition in the myocardium (114). Salvia miltiorrhiza injection decreased cardiac iron deposition and inhibited cardiac oxidation by down-regulating DMT1 and TfR1 expression and up-regulating FP1 protein levels (115). The above evidence suggests that reducing cardiac iron uptake and increasing iron excretion is one of the essential mechanisms for enhancing cardiac function.

Heme oxygenase 1 (Hmox1) is a rate-limiting enzyme in the metabolism of the iron porphyrin compound heme, which is broken down into carbon monoxide, biliverdin, and Fe^{2+}. The myocardium is rich in heme for the synthesis of myoglobin, cytochrome, etc., therefore, Hmox1 plays an important role in the regulation of myocardial iron metabolism. Hmox1 mediates ferroptosis induced by the release of Fe^{2+} from heme and is responsible for adriamycin-induced cardiotoxicity or cardiac injury with sickle cell disease in mice (7, 116). While Hmox1 also regulates intracellular oxidation levels by stabilizing hypoxia-inducible factor 1α to prevent ischemia-mediated injury (117). Consequently, excessive up-regulation of Hmox1 is toxic, while moderate up-regulation of Hmox1 may have a positive cytoprotective effect on the myocardium.

Mitochondrial injury

Apart from serving as the primary organelle for intracellular energy generation, mitochondria also play the central role in utilization, catabolism, and anabolisms for iron. Cellular iron homeostasis and mitochondrial homeostasis are interdependent. Mitochondria must import and incorporate iron ions to form iron–sulfur clusters, heme, and certain mitochondrial proteins that underpin cellular respiration (**Figure 5**) (118–120). While the deficiency in mitochondrial iron-sulfur cluster biosynthesis also triggered intracellular uptake and redistribution of iron (121). The absence of certain RNA-binding proteins in mitochondria can disrupt cellular iron homeostasis and lead to apoptosis (122). Therefore, the following sections elaborated on the association between mitochondria and ferroptosis in CVDs.

The role of ferroptosis in mitochondria

Mitochondrial morphology is an essential judge of cell death. They are generally short rod-shaped or spherical, 1–2 μm long, and consist of double membranes, an outer membrane and an inner membrane with a cristae structure. Ferroptosis is correlated with significant morphological alterations in the mitochondria. After the onset of the ferroptotic stimulus, fragmentation, condensed membrane density, lower volume, reduced or absent cristae and rupture of the outer membrane shortly occurs in the mitochondria (3, 123, 124). The tendency for reduction in mitochondrial membrane potential leads to mitochondrial dysfunction, as evidenced by increased ROS production, mitochondrial membrane hyperpolarization and mitochondrial swelling, ultimately leading to hypertrophy of CMs (113, 125–127). Both Fe^{3+} and Fe^{2+} overload can potentially cause mitochondrial disorders as described above, but Fe^{2+} has been proven to have more destructive effects than Fe^{3+} (128). Tadokoro et al. (129) revealed that excessive accumulation of free Fe^{2+} in mitochondria of CMs in mice with doxorubicin cardiomyopathy or I/R-induced HF, and that chelating Fe^{2+} in mitochondria prevented ferroptosis in CMs. Hence, mitochondrial damage due to Fe^{2+} overload was the main mechanism of cardiac injury (129). On the inner membrane of the mitochondria, the respiratory chain carries out electron transfer via four protein complexes (I, II, III, and IV) to produce ATP, which is the most basic energy metabolism in the organism. Chronic iron overload could additionally inflict damage on mitochondrial DNA and impair the synthesis of respiratory chain subunit complexes I and IV. These results explained chronic progressive cardiac hypertrophy and cardiac insufficiency (130). Treatment with the ferroptosis inhibitor liproxstatin-1 reduced myocardial infarcted size in mice by controlling the entry and exit of mitochondrial ROS via diminishing VDAC1, a pore-like protein in the outer mitochondrial membrane (131). Thus, ferroptosis accounts for impaired cardiac function by causing deterioration of mitochondrial function and interfering with mitochondrial dynamics.

The role of mitochondria in ferroptosis

Mitochondrial metabolism in the pathological state actively facilitates the generation of lipid ROS, and remarkably increases the level of loosely bound unstable iron ions, which is a prerequisite for ferroptosis (132). Mitochondria contains an abundance of GSH, accounting for about 10–15% of total intracellular GSH. Two carrier proteins, mitochondrial dicarboxylate and 2-oxoglutarate, have been identified as GSH transporters (133). Inhibition of these two carrier proteins resulted in the depletion of GSH and ultimately ferroptosis in CMs. In detail, when GSH was depleted rapidly, hyperpolarization of the mitochondrial membrane potential caused the release of cytochrome C and the activation of caspase, thus explaining the role of these two carriers in regulating ferroptosis (97, 134). In mitochondria, there are also organic compounds mitigating ferroptosis. Dihydrolipoic acid acts as an essential cofactor for several mitochondrial enzyme complexes, allowing the direct reduction of pro-ferroptotic peroxidized phospholipids to hydroxyphospholipids and scavenging oxygen radicals (135). It is speculated that more effective pharmacological interventions to protect mitochondria could be new therapeutic targets, improving clinical outcomes in the treatment of CVDs.

Mitophagy and ferroptosis

Mitophagy is a process that selectively scavenges damaged mitochondria and maintains normal mitochondrial activity. Specifically, the serine/threonine kinase PTEN-inducible kinase 1 (PINK1) and the E3 ubiquitin-protein ligase Parkin synergistically sense the functional state of mitochondria and label damaged mitochondria. The damaged mitochondria are encapsulated into autophagosomes and fused with lysosomes, thus completing mitochondrial degradation. Mitophagy was detected to protect against the development of HF, myocardial I/R injury, and obese cardiomyopathy through the Pink1/Parkin pathway (136–138). Mitophagy receptor deficiency can lead to cardiac remodeling and dysfunction through ACSL4-mediated activation of ferroptosis (134). However, overactivation of mitophagy may also induced HF by activating TLR4/NADPH oxidase 4 pathway (8), and mitophagy was also reported to trigger necroptosis and ferroptosis in melanoma cells (139). Therefore, mitophagy has diverse features under different conditions and the regulation of ferroptosis in CMs mediated by mitophagy may need to be further explored.

Several studies have come to the opposite conclusion that mitochondria are dispensable for the execution of ferroptosis induced by GPX4 inhibition, and mitochondria-deficient cell lines show no difference in the susceptibility of ferroptosis from control (3). Possible explanations are that firstly, once GPX4 was eliminated, small amounts of

•O2–, •OH, and H_2O_2 will be quickly magnified by Fenton reaction, causing full-scale ferroptosis whatever the activity of mitochondria, and secondly, there may be some differences in metabolism between cell lines, with varying degree of dependence on mitochondria.

Discussion and conclusion

Rapid advances in current evidence-based medicine for the treatment of CVDs firmly support the effectiveness of several drugs, such as angiotensin-converting enzyme inhibitors, beta-blockers and aldosterone receptor antagonists. Nevertheless, certain adverse side effect of these drugs has caused the administration restricted in specific patients. Recently, targeting iron homeostasis and ferroptosis has become a new direction for clinical treatment of CVDs. Two randomized clinical trials (FAIR-HF and Confirm-HF) have provided clear evidence for the benefit of iron supplementation in patients with chronic HF and iron deficiency. Although oral iron supplementation has no apparent effect, intravenous ferric carboxymaltose can improve hospitalization and mortality from cardiovascular events in iron-deficient HFrEF (LVEF $\leq$ 45%) patients (140). In terms of the secondary prevention of CVDs, a meta-analysis failed to identify participants more likely to derive clinical benefits from iron nutritional supplements in reducing the risk of cardiovascular outcomes (141). The benefit of iron supplementation in patients of acute CVDs without iron deficiency is unclear, and this treatment may exacerbate (I/R) injury. Conversely, administration of deferoxamine which chelates redox-active iron to inhibit ferroptosis has been shown to improve blood oxidative stress markers as an adjunctive therapy for patients with ST-segment elevation MI (142). Intravenous infusion of deferoxamine mesylate at the initiation of thrombolysis was also effective in ischemic stroke patients, with no apparent adverse effects (143). Therefore, pharmacological treatment to maintain iron homeostasis and inhibit ferroptosis may serve as a new therapeutic strategy for CVDs.

Additionally, although indicators of ferroptosis have predictive capacity on the prognosis of amyotrophic lateral sclerosis (144), ferroptosis biomarkers for predicting early diagnosis and prognosis of CVDs have not yet been reported clinically. Classic CVD-related ferroptosis biomarkers validated in animal models include GPX4, ROS, 4-HNE, COX-2, and iron levels, but there are still some limitations of detection (35, 45, 86). First, the activity of ferroptosis metabolites is time-sensitive and should be detected in time after the onset of CVDs. Second, oxidative stress also occurs during necrosis and apoptosis, and simple ROS detection cannot explain the occurrence of CM ferroptosis. Third, the great challenge for COX-2 as a biomarker of ferroptosis is that upregulation of COX-2 has been observed under a variety of inflammatory conditions, except in the case of myocardial ferroptosis. Finally, iron levels may not represent the level of ferroptosis and need to be measured in combination with other indicators. Other potential ferroptosis biomarkers associated with CVDs can be referred to **Table 1**. A recent bioinformatics analysis also determined elevated key genes associated with MI, ferroptosis, and hypoxia, such as Atf3, Socs3, Hspa1b, Cxcl2, and Myd88, which could serve as new biomarkers for MI (145). Thus, indicators of pathophysiology based on ferroptosis may have predictive potential for CVDs in the future, providing better stratification for patient personalized care and resource allocation.

In summary, ferroptosis-related pathological mechanisms such as oxidative stress, inflammation, metabolic disorders and mitochondrial damage are involved in the development of CVDs. As research proceeds, inhibition of ferroptosis may be an effective strategy for the treatment of CVDs.

Author contributions

L-LZ and R-JT determined the topic, wrote the initial manuscript, searched the related literatures, and created the figures of the manuscript. Y-JY supervised the planning and execution of the research activity. All authors have approved to the final version of the manuscript, responsible for the accuracy, and authenticity of the article.

Funding

This study was supported by the National Key Research and Development Program (No. 2017YFC1700503) and the National Natural Science Foundation of China (Nos. 81573957, 81874461, and 82070307).

Conflict of interest

The authors declare that the research was conducted in the absence of any commercial or financial relationships that could be construed as a potential conflict of interest.

Publisher's note

References

1. Sullivan JL. Iron and the sex difference in heart disease risk. *Lancet.* (1981) 1:1293–4. doi: 10.1016/s0140-6736(81)92463-6

2. Oudit GY, Trivieri MG, Khaper N, Husain T, Wilson GJ, Liu P, et al. Taurine supplementation reduces oxidative stress and improves cardiovascular function in an iron-overload murine model. *Circulation.* (2004) 109:1877–85. doi: 10.1161/01.Cir.0000124229.40424.80

3. Dixon SJ, Lemberg KM, Lamprecht MR, Skouta R, Zaitsev EM, Gleason CE, et al. Ferroptosis: An iron-dependent form of nonapoptotic cell death. *Cell.* (2012) 149:1060–72. doi: 10.1016/j.cell.2012.03.042

4. Liu B, Zhao C, Li H, Chen X, Ding Y, Xu S. Puerarin protects against heart failure induced by pressure overload through mitigation of ferroptosis. *Biochem Biophys Res Commun.* (2018) 497:233–40. doi: 10.1016/j.bbrc.2018.02.061

5. Bai T, Li M, Liu Y, Qiao Z, Wang Z. Inhibition of ferroptosis alleviates atherosclerosis through attenuating lipid peroxidation and endothelial dysfunction in mouse aortic endothelial cell. *Free Radic Biol Med.* (2020) 160:92–102. doi: 10.1016/j.freeradbiomed.2020.07.026

6. Wang XD, Kang S. Ferroptosis in myocardial infarction: Not a marker but a maker. *Open Biol.* (2021) 11:200367. doi: 10.1098/rsob.200367

7. Fang X, Wang H, Han D, Xie E, Yang X, Wei J, et al. Ferroptosis as a target for protection against cardiomyopathy. *Proc Natl Acad Sci U.S.A.* (2019) 116:2672–80. doi: 10.1073/pnas.1821022116

8. Chen X, Xu S, Zhao C, Liu B. Role of Tlr4/Nadph oxidase 4 pathway in promoting cell death through autophagy and ferroptosis during heart failure. *Biochem Biophys Res Commun.* (2019) 516:37–43. doi: 10.1016/j.bbrc.2019.06.015

9. Fang X, Cai Z, Wang H, Han D, Cheng Q, Zhang P, et al. Loss of cardiac ferritin h facilitates cardiomyopathy via Slc7a11-mediated ferroptosis. *Circ Res.* (2020) 127:486–501. doi: 10.1161/circresaha.120.316509

10. Yao X, Zhang Y, Hao J, Duan HQ, Zhao CX, Sun C, et al. Deferoxamine promotes recovery of traumatic spinal cord injury by inhibiting ferroptosis. *Neural Regen Res.* (2019) 14:532–41. doi: 10.4103/1673-5374.245480

11. Mu M, Wang Y, Zhao S, Li X, Fan R, Mei L, et al. Engineering a Ph/glutathione-responsive tea polyphenol nanodevice as an apoptosis/ferroptosis-inducing agent. *ACS Appl Bio Mater.* (2020) 3:4128–38. doi: 10.1021/acsabm.0c00225

12. Geng N, Shi BJ, Li SL, Zhong ZY, Li YC, Xua WL, et al. Knockdown of ferroportin accelerates erastin-induced ferroptosis in neuroblastoma cells. *Eur Rev Med Pharmacol Sci.* (2018) 22:3826–36. doi: 10.26355/eurrev_201806_15267

13. Zhang P, Chen L, Zhao Q, Du X, Bi M, Li Y, et al. Ferroptosis was more initial in cell death caused by iron overload and its underlying mechanism in Parkinson's disease. *Free Radic Biol Med.* (2020) 152:227–34. doi: 10.1016/j.freeradbiomed.2020.03.015

14. Ishihara G, Kawamoto K, Komori N, Ishibashi T. Molecular hydrogen suppresses superoxide generation in the mitochondrial complex I and reduced mitochondrial membrane potential. *Biochem Biophys Res Commun.* (2020) 522:965–70. doi: 10.1016/j.bbrc.2019.11.135

15. Winterbourn CC. Toxicity of iron and hydrogen peroxide: The fenton reaction. *Toxicol Lett.* (1995) 82-83:969–74. doi: 10.1016/0378-4274(95)03532-x

16. Shen Z, Liu T, Li Y, Lau J, Yang Z, Fan W, et al. Fenton-reaction-acceleratable magnetic nanoparticles for ferroptosis therapy of orthotopic brain tumors. *ACS Nano.* (2018) 12:11355–65. doi: 10.1021/acsnano.8b06201

17. Liu T, Liu W, Zhang M, Yu W, Gao F, Li C, et al. Ferrous-supply-regeneration nanoengineering for cancer-cell-specific ferroptosis in combination with imaging-guided photodynamic therapy. *ACS Nano.* (2018) 12:12181–92. doi: 10.1021/acsnano.8b05860

18. Park E, Chung SW. Ros-mediated autophagy increases intracellular iron levels and ferroptosis by ferritin and transferrin receptor regulation. *Cell Death Dis.* (2019) 10:822. doi: 10.1038/s41419-019-2064-5

19. Liu M, Fan Y, Li D, Han B, Meng Y, Chen F, et al. Ferroptosis inducer erastin sensitizes nsclc cells to celastrol through activation of the ros-mitochondrial fission-mitophagy axis. *Mol Oncol.* (2021) 15:2084–105. doi: 10.1002/1878-0261.12936

20. Ursini F, Maiorino M, Valente M, Ferri L, Gregolin C. Purification from pig liver of a protein which protects liposomes and biomembranes from peroxidative degradation and exhibits glutathione peroxidase activity on phosphatidylcholine hydroperoxides. *Biochim Biophys Acta.* (1982) 710:197–211. doi: 10.1016/0005-2760(82)90150-3

21. Jiang L, Kon N, Li T, Wang SJ, Su T, Hibshoosh H, et al. Ferroptosis as a P53-mediated activity during tumour suppression. *Nature.* (2015) 520:57–62. doi: 10.1038/nature14344

22. Hangauer MJ, Viswanathan VS, Ryan MJ, Bole D, Eaton JK, Matov A, et al. Drug-tolerant persister cancer cells are vulnerable to Gpx4 inhibition. *Nature.* (2017) 551:247–50. doi: 10.1038/nature24297

23. Bersuker K, Hendricks JM, Li Z, Magtanong L, Ford B, Tang PH, et al. The coq oxidoreductase Fsp1 acts parallel to Gpx4 to inhibit ferroptosis. *Nature.* (2019) 575:688–92. doi: 10.1038/s41586-019-1705-2

24. Jo A, Bae JH, Yoon YJ, Chung TH, Lee EW, Kim YH, et al. Plasma-activated medium induces ferroptosis by depleting Fsp1 in human lung cancer cells. *Cell Death Dis.* (2022) 13:212. doi: 10.1038/s41419-022-04660-9

25. Martin-Sanchez D, Ruiz-Andres O, Poveda J, Carrasco S, Cannata-Ortiz P, Sanchez-Niño MD, et al. Ferroptosis, but not necroptosis, is important in nephrotoxic folic acid-induced aki. *J Am Soc Nephrol.* (2017) 28:218–29. doi: 10.1681/asn.2015121376

26. Kiesel L, Przylipiak A, Rabe T, Przylipiak M, Runnebaum B. Arachidonic acid and its lipoxygenase metabolites stimulate prolactin release in superfused pituitary cells. *Hum Reprod.* (1987) 2:281–5. doi: 10.1093/oxfordjournals.humrep.a136535

27. Zhang J, Wang X, Vikash V, Ye Q, Wu D, Liu Y, et al. Ros and ros-mediated cellular signaling. *Oxid Med Cell Longev.* (2016) 2016:4350965. doi: 10.1155/2016/4350965

28. Lillo-Moya J, Rojas-Solé C, Muñoz-Salamanca D, Panieri E, Saso L, Rodrigo R. Targeting ferroptosis against ischemia/reperfusion cardiac injury. *Antioxidants.* (2021) 10:667. doi: 10.3390/antiox10050667

29. Gasparetto C, Malinverno A, Culacciati D, Gritti D, Prosperini PG, Specchia G, et al. Antioxidant vitamins reduce oxidative stress and ventricular remodeling in patients with acute myocardial infarction. *Int J Immunopathol Pharmacol.* (2005) 18:487–96. doi: 10.1177/039463200501800308

30. Venardos KM, Perkins A, Headrick J, Kaye DM. Myocardial ischemia-reperfusion injury, antioxidant enzyme systems, and selenium: A review. *Curr Med Chem.* (2007) 14:1539–49. doi: 10.2174/092986707780831078

31. Neves AL, Mohammedi K, Emery N, Roussel R, Fumeron F, Marre M, et al. Allelic variations in superoxide dismutase-1 (Sod1) gene and renal and cardiovascular morbidity and mortality in type 2 diabetic subjects. *Mol Genet Metab.* (2012) 106:359–65. doi: 10.1016/j.ymgme.2012.04.023

32. Wang T, Tomas D, Perera ND, Cuic B, Luikinga S, Viden A, et al. Ferroptosis mediates selective motor neuron death in amyotrophic lateral sclerosis. *Cell Death Differ.* (2021) 29:1187–98. doi: 10.1038/s41418-021-00910-z

33. Seshadri G, Sy JC, Brown M, Dikalov S, Yang SC, Murthy N, et al. The delivery of superoxide dismutase encapsulated in polyketal microparticles to rat myocardium and protection from myocardial ischemia-reperfusion injury. *Biomaterials.* (2010) 31:1372–9. doi: 10.1016/j.biomaterials.2009.10.045

34. Chang WT, Bow YD, Fu PJ, Li CY, Wu CY, Chang YH, et al. A marine terpenoid, heteronemin, induces both the apoptosis and ferroptosis of hepatocellular carcinoma cells and involves the ros and mapk pathways. *Oxid Med Cell Longev.* (2021) 2021:7689045. doi: 10.1155/2021/7689045

35. Sharma S, Bhattarai S, Ara H, Sun G, St Clair DK, Bhuiyan MS, et al. Sod2 deficiency in cardiomyocytes defines defective mitochondrial bioenergetics as a cause of lethal dilated cardiomyopathy. *Redox Biol.* (2020) 37:101740. doi: 10.1016/j.redox.2020.101740

36. Decharatchakul N, Settasatian C, Settasatian N, Komanasin N, Kukongviriyapan U, Intharapetch P, et al. Association of combined genetic variations in Sod3, Gpx3, Pon1, and Gstt1 with hypertension and severity of coronary artery disease. *Heart Vessels.* (2020) 35:918–29. doi: 10.1007/s00380-020-01564-6

37. Chen T, Jin X, Crawford BH, Cheng H, Saafir TB, Wagner MB, et al. Cardioprotection from oxidative stress in the newborn heart by activation of Pparγ is mediated by catalase. *Free Radic Biol Med.* (2012) 53:208–15. doi: 10.1016/j.freeradbiomed.2012.05.014

38. Hwang JS, Kim E, Lee HG, Lee WJ, Won JP, Hur J, et al. Peroxisome proliferator-activated receptor δ rescues xct-deficient cells from ferroptosis by targeting peroxisomes. *Biomed Pharmacother.* (2021) 143:112223. doi: 10.1016/j.biopha.2021.112223

39. Liu X, Qi K, Gong Y, Long X, Zhu S, Lu F, et al. Ferulic acid alleviates myocardial ischemia reperfusion injury via upregulating Ampkα2 expression-mediated ferroptosis depression. *J Cardiovasc Pharmacol.* (2021) 79:489–500. doi: 10.1097/fjc.0000000000001199

40. Park TJ, Park JH, Lee GS, Lee JY, Shin JH, Kim MW, et al. Quantitative proteomic analyses reveal that Gpx4 downregulation during myocardial infarction contributes to ferroptosis in cardiomyocytes. *Cell Death Dis.* (2019) 10:835. doi: 10.1038/s41419-019-2061-8

41. Wang Y, Yan S, Liu X, Deng F, Wang P, Yang L, et al. Prmt4 promotes ferroptosis to aggravate doxorubicin-induced cardiomyopathy via inhibition of the Nrf2/Gpx4 pathway. *Cell Death Differ.* (2022). [Onlie ahead of print].

42. Xu S, Wu B, Zhong B, Lin L, Ding Y, Jin X, et al. Naringenin alleviates myocardial ischemia/reperfusion injury by regulating the nuclear factor-erythroid factor 2-related factor 2 (Nrf2) /System Xc-/ glutathione peroxidase 4 (Gpx4) axis to inhibit ferroptosis. *Bioengineered.* (2021) 12:10924–34. doi: 10.1080/21655979.2021.1995994

43. Zhang Z, Tang J, Song J, Xie M, Liu Y, Dong Z, et al. Elabela Alleviates ferroptosis, myocardial remodeling, fibrosis and heart dysfunction in hypertensive mice by modulating the Il-6/Stat3/Gpx4 signaling. *Free Radic Biol Med.* (2022) 181:130–42. doi: 10.1016/j.freeradbiomed.2022.01.020

44. Wang Y, Kuang X, Yin Y, Han N, Chang L, Wang H, et al. Tongxinluo prevents chronic obstructive pulmonary disease complicated with atherosclerosis by inhibiting ferroptosis and protecting against pulmonary microvascular barrier dysfunction. *Biomed Pharmacother.* (2022) 145:112367. doi: 10.1016/j.biopha.2021.112367

45. Lin JH, Yang KT, Lee WS, Ting PC, Luo YP, Lin DJ, et al. Xanthohumol protects the rat myocardium against ischemia/reperfusion injury-induced ferroptosis. *Oxid Med Cell Longev.* (2022) 2022:9523491. doi: 10.1155/2022/9523491

46. Yang Y, Sun S, Xu W, Zhang Y, Yang R, Ma K, et al. Piperlongumine Inhibits thioredoxin reductase 1 by targeting selenocysteine residues and sensitizes cancer cells to erastin. *Antioxidants.* (2022) 11:710. doi: 10.3390/antiox11040710

47. Kiermayer C, Northrup E, Schrewe A, Walch A, de Angelis MH, Schoensiegel F, et al. Heart-specific knockout of the mitochondrial thioredoxin reductase (Txnrd2) induces metabolic and contractile dysfunction in the aging myocardium. *J Am Heart Assoc.* (2015) 4:e002153. doi: 10.1161/jaha.115.002153

48. Bai L, Yan F, Deng R, Gu R, Zhang X, Bai J. Thioredoxin-1 rescues Mpp(+)/Mptp-induced ferroptosis by increasing glutathione peroxidase 4. *Mol Neurobiol.* (2021) 58:3187–97. doi: 10.1007/s12035-021-02320-1

49. Oka SI, Chin A, Park JY, Ikeda S, Mizushima W, Ralda G, et al. Thioredoxin-1 maintains mitochondrial function via mechanistic target of rapamycin signalling in the heart. *Cardiovasc Res.* (2020) 116:1742–55. doi: 10.1093/cvr/cvz251

50. Lu J, Holmgren A. The thioredoxin antioxidant system. *Free Radic Biol Med.* (2014) 66:75–87. doi: 10.1016/j.freeradbiomed.2013.07.036

51. Engin KN. Alpha-tocopherol: Looking beyond an antioxidant. *Mol Vis.* (2009) 15:855–60.

52. Hu Q, Zhang Y, Lou H, Ou Z, Liu J, Duan W, et al. Gpx4 and vitamin E cooperatively protect hematopoietic stem and progenitor cells from lipid peroxidation and ferroptosis. *Cell Death Dis.* (2021) 12:706. doi: 10.1038/s41419-021-04008-9

53. Wallert M, Ziegler M, Wang X, Maluenda A, Xu X, Yap ML, et al. A-tocopherol preserves cardiac function by reducing oxidative stress and inflammation in ischemia/reperfusion injury. *Redox Biol.* (2019) 26:101292. doi: 10.1016/j.redox.2019.101292

54. Keith ME, Jeejeebhoy KN, Langer A, Kurian R, Barr A, O'Kelly B, et al. A controlled clinical trial of vitamin E supplementation in patients with congestive heart failure. *Am J Clin Nutr.* (2001) 73:219–24. doi: 10.1093/ajcn/73.2.219

55. Gong T, Liu L, Jiang W, Zhou R. Damp-sensing receptors in sterile inflammation and inflammatory diseases. *Nat Rev Immunol.* (2020) 20:95–112. doi: 10.1038/s41577-019-0215-7

56. Wen Q, Liu J, Kang R, Zhou B, Tang D. The release and activity of hmgb1 in ferroptosis. *Biochem Biophys Res Commun.* (2019) 510:278–83. doi: 10.1016/j.bbrc.2019.01.090

57. Fan H, Tang HB, Chen Z, Wang HQ, Zhang L, Jiang Y, et al. Inhibiting Hmgb1-rage axis prevents pro-inflammatory macrophages/microglia polarization and affords neuroprotection after spinal cord injury. *J Neuroinflammation.* (2020) 17:295. doi: 10.1186/s12974-020-01973-4

58. Foglio E, Pellegrini L, Germani A, Russo MA, Limana F. Hmgb1-mediated apoptosis and autophagy in ischemic heart diseases. *Vasc Biol.* (2019) 1:H89–96. doi: 10.1530/vb-19-0013

59. Xiao N, Zhang J, Chen C, Wan Y, Wang N, Yang J. Mir-129-5p improves cardiac function in rats with chronic heart failure through targeting Hmgb1. *Mamm Genome.* (2019) 30:276–88. doi: 10.1007/s00335-019-09817-0

60. Son S, Yoon SH, Chae BJ, Hwang I, Shim DW, Choe YH, et al. Neutrophils facilitate prolonged inflammasome response in the damp-rich inflammatory milieu. *Front Immunol.* (2021) 12:746032. doi: 10.3389/fimmu.2021.746032

61. Biasizzo M, Kopitar-Jerala N. Interplay between Nlrp3 inflammasome and autophagy. *Front Immunol.* (2020) 11:591803. doi: 10.3389/fimmu.2020.591803

62. Quagliariello V, De Laurentiis M, Rea D, Barbieri A, Monti MG, Carbone A, et al. The Sglt-2 inhibitor empagliflozin improves myocardial strain, reduces cardiac fibrosis and pro-inflammatory cytokines in non-diabetic mice treated with doxorubicin. *Cardiovasc Diabetol.* (2021) 20:150. doi: 10.1186/s12933-021-01346-y

63. Li W, Feng G, Gauthier JM, Lokshina I, Higashikubo R, Evans S, et al. Ferroptotic cell death and Tlr4/trif signaling initiate neutrophil recruitment after heart transplantation. *J Clin Invest.* (2019) 129:2293–304. doi: 10.1172/jci126428

64. Hori M, Nishida K. Oxidative stress and left ventricular remodelling after myocardial infarction. *Cardiovasc Res.* (2009) 81:457–64. doi: 10.1093/cvr/cvn335

65. Siwik DA, Colucci WS. Regulation of matrix metalloproteinases by cytokines and reactive oxygen/nitrogen species in the myocardium. *Heart Fail Rev.* (2004) 9:43–51. doi: 10.1023/b:Hrev.0000011393.40674.13

66. Peng Y, Yang Q, Gao S, Liu Z, Kong W, Bian X, et al. Il-6 protects cardiomyocytes from oxidative stress at the early stage of lps-induced sepsis. *Biochem Biophys Res Commun.* (2022) 603:144–52. doi: 10.1016/j.bbrc.2022.03.013

67. Emran T, Chowdhury NI, Sarker M, Bepari AK, Hossain M, Rahman GMS, et al. L-carnitine protects cardiac damage by reducing oxidative stress and inflammatory response via inhibition of tumor necrosis factor-alpha and interleukin-1beta against isoproterenol-induced myocardial infarction. *Biomed Pharmacother.* (2021) 143:112139. doi: 10.1016/j.biopha.2021.112139

68. Li S, He Y, Chen K, Sun J, Zhang L, He Y, et al. Rsl3 drives ferroptosis through Nf-Kb pathway activation and Gpx4 depletion in glioblastoma. *Oxid Med Cell Longev.* (2021) 2021:2915019. doi: 10.1155/2021/2915019

69. Zhao Y, Wang C, Yang T, Wang H, Zhao S, Sun N, et al. Chlorogenic acid alleviates chronic stress-induced duodenal ferroptosis via the inhibition of the Il-6/Jak2/Stat3 signaling pathway in rats. *J Agric Food Chem* (2022) 70:4353–61. doi: 10.1021/acs.jafc.2c01196

70. Wei TT, Zhang MY, Zheng XH, Xie TH, Wang W, Zou J, et al. Interferon-Γ induces retinal pigment epithelial cell ferroptosis by a Jak1-2/Stat1/Slc7a11 signaling pathway in age-related macular degeneration. *FEBS J.* (2021) 289:1968–83. doi: 10.1111/febs.16272

71. Zhang H, Jiao W, Cui H, Sun Q, Fan H. Combined exposure of alumina nanoparticles and chronic stress exacerbates hippocampal neuronal ferroptosis via activating Ifn-Γ/Ask1/Jnk signaling pathway in rats. *J Hazard Mater.* (2021) 411:125179. doi: 10.1016/j.jhazmat.2021.125179

72. Xiao Z, Kong B, Fang J, Qin T, Dai C, Shuai W, et al. Ferrostatin-1 alleviates lipopolysaccharide-induced cardiac dysfunction. *Bioengineered.* (2021) 12:9367–76. doi: 10.1080/21655979.2021.2001913

73. Nelson JR, Raskin S. The eicosapentaenoic acid:Arachidonic acid ratio and its clinical utility in cardiovascular disease. *Postgrad Med.* (2019) 131:268–77. doi: 10.1080/00325481.2019.1607414

74. Innes JK, Calder PC. Omega-6 fatty acids and inflammation. *Prostaglandins Leukot Essent Fatty Acids.* (2018) 132:41–8. doi: 10.1016/j.plefa.2018.03.004

75. Li C, Deng X, Xie X, Liu Y, Friedmann Angeli JP, Lai L. Activation of glutathione peroxidase 4 as a novel anti-inflammatory strategy. *Front Pharmacol.* (2018) 9:1120. doi: 10.3389/fphar.2018.01120

76. Bajpai G, Bredemeyer A, Li W, Zaitsev K, Koenig AL, Lokshina I, et al. Tissue resident Ccr2- and Ccr2+ cardiac macrophages differentially orchestrate monocyte recruitment and fate specification following myocardial injury. *Circ Res.* (2019) 124:263–78. doi: 10.1161/circresaha.118.314028

77. Revelo XS, Parthiban P, Chen C, Barrow F, Fredrickson G, Wang H, et al. Cardiac resident macrophages prevent fibrosis and stimulate angiogenesis. *Circ Res.* (2021) 129:1086–101. doi: 10.1161/circresaha.121.319737

78. Jia D, Chen S, Bai P, Luo C, Liu J, Sun A, et al. Cardiac resident macrophage-derived legumain improves cardiac repair by promoting clearance and degradation of apoptotic cardiomyocytes after myocardial infarction. *Circulation.* (2022) 145:1542–56. doi: 10.1161/circulationaha.121.057549

79. Nicolás-Ávila JA, Lechuga-Vieco AV, Esteban-Martínez L, Sánchez-Díaz M, Díaz-García E, Santiago DJ, et al. A network of macrophages supports mitochondrial homeostasis in the heart. *Cell.* (2020) 183:94.e–109.e. doi: 10.1016/j.cell.2020.08.031

80. Lavine KJ, Pinto AR, Epelman S, Kopecky BJ, Clemente-Casares X, Godwin J, et al. The macrophage in cardiac homeostasis and disease: Jacc macrophage in Cvd series (Part 4). *J Am Coll Cardiol.* (2018) 72:2213–30. doi: 10.1016/j.jacc.2018.08.2149

81. Zhou Y, Que KT, Zhang Z, Yi ZJ, Zhao PX, You Y, et al. Iron overloaded polarizes macrophage to proinflammation phenotype through Ros/Acetyl-P53 pathway. *Cancer Med.* (2018) 7:4012–22. doi: 10.1002/cam4.1670

82. Cui Y, Zhang Z, Zhou X, Zhao Z, Zhao R, Xu X, et al. Microglia and macrophage exhibit attenuated inflammatory response and ferroptosis resistance

after Rsl3 stimulation via increasing Nrf2 expression. *J Neuroinflammation.* (2021) 18:249. doi: 10.1186/s12974-021-02231-x

83. Kapralov AA, Yang Q, Dar HH, Tyurina YY, Anthonymuthu TS, Kim R, et al. Redox lipid reprogramming commands susceptibility of macrophages and microglia to ferroptotic death. *Nat Chem Biol.* (2020) 16:278–90. doi: 10.1038/s41589-019-0462-8

84. Wang Y, Qiu Z, Yuan J, Li C, Zhao R, Liu W, et al. Hypoxia-reoxygenation induces macrophage polarization and causes the release of exosomal mir-29a to mediate cardiomyocyte pyroptosis. *Vitro Cell Dev Biol Anim.* (2021) 57:30–41. doi: 10.1007/s11626-020-00524-8

85. Deng Z, Shi F, Zhou Z, Sun F, Sun MH, Sun Q, et al. M1 macrophage mediated increased reactive oxygen species (Ros) influence wound healing via the mapk signaling in vitro and in vivo. *Toxicol Appl Pharmacol.* (2019) 366:83–95. doi: 10.1016/j.taap.2019.01.022

86. Zhao X, Si L, Bian J, Pan C, Guo W, Qin P, et al. Adipose tissue macrophage-derived exosomes induce ferroptosis via glutathione synthesis inhibition by targeting Slc7a11 in obesity-induced cardiac injury. *Free Radic Biol Med.* (2022) 182:232–45. doi: 10.1016/j.freeradbiomed.2022.02.033

87. Xu LC, Cao J, Li WJ, Yang ZM, Zhao R, Zhang JR, et al. [Ferroptosis in laryngeal squamous cell carcinoma and its regulation by M2 macrophage-derived exosomes]. *Zhonghua Er Bi Yan Hou Tou Jing Wai Ke Za Zhi.* (2022) 57:324–32. doi: 10.3760/cma.j.cn115330-20210621-00361

88. Wang W, Green M, Choi JE, Gijón M, Kennedy PD, Johnson JK, et al. Cd8(+) T cells regulate tumour ferroptosis during cancer immunotherapy. *Nature.* (2019) 569:270–4. doi: 10.1038/s41586-019-1170-y

89. Nevers T, Salvador AM, Velazquez F, Ngwenyama N, Carrillo-Salinas FJ, Aronovitz M, et al. Th1 effector T cells selectively orchestrate cardiac fibrosis in nonischemic heart failure. *J Exp Med.* (2017) 214:3311–29. doi: 10.1084/jem.20161791

90. Lu M, Qin X, Yao J, Yang Y, Zhao M, Sun L. Th17/Treg Imbalance modulates rat myocardial fibrosis and heart failure by regulating lox expression. *Acta Physiol.* (2020) 230:e13537. doi: 10.1111/apha.13537

91. Kanellakis P, Dinh TN, Agrotis A, Bobik A. $Cd4^{+}Cd25^{+}Foxp3^{+}$ regulatory t cells suppress cardiac fibrosis in the hypertensive heart. *J Hypertens.* (2011) 29:1820–8. doi: 10.1097/HJH.0b013e328349c62d

92. Weirather J, Hofmann UD, Beyersdorf N, Ramos GC, Vogel B, Frey A, et al. Foxp3+ Cd4+ T cells improve healing after myocardial infarction by modulating monocyte/macrophage differentiation. *Circ Res.* (2014) 115:55–67. doi: 10.1161/circresaha.115.303895

93. Zacchigna S, Martinelli V, Moimas S, Colliva A, Anzini M, Nordio A, et al. Paracrine effect of regulatory T cells promotes cardiomyocyte proliferation during pregnancy and after myocardial infarction. *Nat Commun.* (2018) 9:2432. doi: 10.1038/s41467-018-04908-z

94. Hui S, Ghergurovich JM, Morscher RJ, Jang C, Teng X, Lu W, et al. Glucose feeds the tca cycle via circulating lactate. *Nature.* (2017) 551:115–8. doi: 10.1038/nature24057

95. Yao X, Li W, Fang D, Xiao C, Wu X, Li M, et al. Emerging roles of energy metabolism in ferroptosis regulation of tumor cells. *Adv Sci.* (2021) 8:e2100997. doi: 10.1002/advs.202100997

96. Fan J, Ye J, Kamphorst JJ, Shlomi T, Thompson CB, Rabinowitz JD. Quantitative flux analysis reveals folate-dependent nadph production. *Nature.* (2014) 510:298–302. doi: 10.1038/nature13236

97. Gao M, Yi J, Zhu J, Minikes AM, Monian P, Thompson CB, et al. Role of mitochondria in ferroptosis. *Mol Cell.* (2019) 73:354.e–63.e. doi: 10.1016/j.molcel.2018.10.042

98. Lee H, Zandkarimi F, Zhang Y, Meena JK, Kim J, Zhuang L, et al. Energy-Stress-mediated ampk activation inhibits ferroptosis. *Nat Cell Biol.* (2020) 22:225–34. doi: 10.1038/s41556-020-0461-8

99. Rodríguez-Graciani KM, Chapa-Dubocq XR, Ayala-Arroyo EJ, Chaves-Negrón I, Jang S, Chorna N, et al. Effects of ferroptosis on the metabolome in cardiac cells: The role of glutaminolysis. *Antioxidants.* (2022) 11:278. doi: 10.3390/antiox11020278

100. Shin D, Lee J, You JH, Kim D, Roh JL. Dihydrolipoamide dehydrogenase regulates cystine deprivation-induced ferroptosis in head and neck cancer. *Redox Biol.* (2020) 30:101418. doi: 10.1016/j.redox.2019.101418

101. Luo M, Wu L, Zhang K, Wang H, Zhang T, Gutierrez L, et al. Mir-137 regulates ferroptosis by targeting glutamine transporter Slc1a5 in melanoma. *Cell Death Differ.* (2018) 25:1457–72. doi: 10.1038/s41418-017-0053-8

102. Gao M, Monian P, Quadri N, Ramasamy R, Jiang X. Glutaminolysis and transferrin regulate ferroptosis. *Mol Cell.* (2015) 59:298–308. doi: 10.1016/j.molcel.2015.06.011

103. Doll S, Proneth B, Tyurina YY, Panzilius E, Kobayashi S, Ingold I, et al. Acsl4 Dictates ferroptosis sensitivity by shaping cellular lipid composition. *Nat Chem Biol.* (2017) 13:91–8. doi: 10.1038/nchembio.2239

104. Tang LJ, Luo XJ, Tu H, Chen H, Xiong XM, Li NS, et al. Ferroptosis Occurs in phase of reperfusion but not ischemia in rat heart following ischemia or ischemia/reperfusion. *Naunyn Schmiedebergs Arch Pharmacol.* (2021) 394:401–10. doi: 10.1007/s00210-020-01932-z

105. Franklin MP, Sathyanarayan A, Mashek DG. Acyl-Coa thioesterase 1 (Acot1) regulates Pparα to couple fatty acid flux with oxidative capacity during fasting. *Diabetes.* (2017) 66:2112–23. doi: 10.2337/db16-1519

106. Cavalli M, Diamanti K, Dang Y, Xing P, Pan G, Chen X, et al. The thioesterase Acot1 as a regulator of lipid metabolism in type 2 diabetes detected in a multi-omics study of human liver. *Omics.* (2021) 25:652–9. doi: 10.1089/omi.2021.0093

107. Liu Y, Zeng L, Yang Y, Chen C, Wang D, Wang H. Acyl-Coa thioesterase 1 prevents cardiomyocytes from doxorubicin-induced ferroptosis via shaping the lipid composition. *Cell Death Dis.* (2020) 11:756. doi: 10.1038/s41419-020-02948-2

108. Tan SK, Mahmud I, Fontanesi F, Puchowicz M, Neumann CKA, Griswold AJ, et al. Obesity-dependent adipokine chemerin suppresses fatty acid oxidation to confer ferroptosis resistance. *Cancer Discov.* (2021) 11:2072–93. doi: 10.1158/2159-8290.Cd-20-1453

109. Thayyullathil F, Cheratta AR, Alakkal A, Subburayan K, Pallichankandy S, Hannun YA, et al. Acid sphingomyelinase-dependent autophagic degradation of Gpx4 is critical for the execution of ferroptosis. *Cell Death Dis.* (2021) 12:26. doi: 10.1038/s41419-020-03297-w

110. Lakhal-Littleton S. Mechanisms of cardiac iron homeostasis and their importance to heart function. *Free Radic Biol Med.* (2019) 133:234–7. doi: 10.1016/j.freeradbiomed.2018.08.010

111. Nishizawa H, Matsumoto M, Shindo T, Saigusa D, Kato H, Suzuki K, et al. Ferroptosis is controlled by the coordinated transcriptional regulation of glutathione and labile iron metabolism by the transcription factor Bach1. *J Biol Chem.* (2020) 295:69–82. doi: 10.1074/jbc.RA119.009548

112. Qin X, Zhang J, Wang B, Xu G, Yang X, Zou Z, et al. Ferritinophagy is involved in the zinc oxide nanoparticles-induced ferroptosis of vascular endothelial cells. *Autophagy.* (2021) 17:4266–85. doi: 10.1080/15548627.2021.1911016

113. Tang M, Huang Z, Luo X, Liu M, Wang L, Qi Z, et al. Ferritinophagy activation and sideroflexin1-dependent mitochondria iron overload is involved in apelin-13-induced cardiomyocytes hypertrophy. *Free Radic Biol Med.* (2019) 134:445–57. doi: 10.1016/j.freeradbiomed.2019.01.052

114. Lakhal-Littleton S, Wolna M, Carr CA, Miller JJ, Christian HC, Ball V, et al. Cardiac ferroportin regulates cellular iron homeostasis and is important for cardiac function. *Proc Natl Acad Sci U.S.A.* (2015) 112:3164–9. doi: 10.1073/pnas.1422373112

115. Zhang Y, Xue Y, Zheng B, Han X, Ma D, Ma Z, et al. Salvia miltiorrhiza (Sm) injection ameliorates iron overload-associated cardiac dysfunction by regulating the expression of Dmt1, Tfr1, and Fp1 in rats. *Evid Based Complement Alternat Med.* (2021) 2021:6864723. doi: 10.1155/2021/6864723

116. Menon AV, Liu J, Tsai HP, Zeng L, Yang S, Asnani A, et al. Excess Heme upregulates heme oxygenase 1 and promotes cardiac ferroptosis in mice with sickle cell disease. *Blood.* (2022) 139:936–41. doi: 10.1182/blood.2020008455

117. Dunn LL, Kong SMY, Tumanov S, Chen W, Cantley J, Ayer A, et al. Hmox1 (heme oxygenase-1) protects against ischemia-mediated injury via stabilization of Hif-1α (hypoxia-inducible factor-1α). *Arterioscler Thromb Vasc Biol.* (2021) 41:317–30. doi: 10.1161/atvbaha.120.315393

118. Alfadhel M, Nashabat M, Abu Ali Q, Hundallah K. Mitochondrial iron-sulfur cluster biogenesis from molecular understanding to clinical disease. *Neurosciences.* (2017) 22:4–13. doi: 10.17712/nsj.2017.1.20160542

119. Misslinger M, Lechner BE, Bacher K, Haas H. Iron-sensing is governed by mitochondrial, not by cytosolic iron-sulfur cluster biogenesis in aspergillus fumigatus. *Metallomics.* (2018) 10:1687–700. doi: 10.1039/c8mt00263k

120. Sandoval-Acuña C, Torrealba N, Tomkova V, Jadhav SB, Blazkova K, Merta L, et al. Targeting Mitochondrial iron metabolism suppresses tumor growth and metastasis by inducing mitochondrial dysfunction and mitophagy. *Cancer Res.* (2021) 81:2289–303. doi: 10.1158/0008-5472.Can-20-1628

121. Dietz JV, Fox JL, Khalimonchuk O. Down the iron path: Mitochondrial iron homeostasis and beyond. *Cells* (2021) 10:2198. doi: 10.3390/cells10092198

122. Su Y, Yang Y, Huang Y. Loss of Ppr3, Ppr4, Ppr6, or Ppr10 Perturbs iron homeostasis and leads to apoptotic cell death in schizosaccharomyces pombe. *FEBS J.* (2017) 284:324–37. doi: 10.1111/febs.13978

123. Sedlackova L, Korolchuk VI. Mitochondrial quality control as a key determinant of cell survival. *Biochim Biophys Acta Mol Cell Res.* (2019) 1866:575–87. doi: 10.1016/j.bbamcr.2018.12.012

124. DeHart DN, Fang D, Heslop K, Li L, Lemasters JJ, Maldonado EN. Opening of voltage dependent anion channels promotes reactive oxygen species generation, mitochondrial dysfunction and cell death in cancer cells. *Biochem Pharmacol.* (2018) 148:155–62. doi: 10.1016/j.bcp.2017.12.022

125. Kumfu S, Chattipakorn S, Fucharoen S, Chattipakorn N. Mitochondrial calcium uniporter blocker prevents cardiac mitochondrial dysfunction induced by iron overload in thalassemic mice. *Biometals.* (2012) 25:1167–75. doi: 10.1007/s10534-012-9579-x

126. Kim M, Kim J, Cheon CI, Cho DH, Park JH, Kim KI, et al. Increased expression of the F(1)F(O) Atp synthase in response to iron in heart mitochondria. *BMB Rep.* (2008) 41:153–7. doi: 10.5483/bmbrep.2008.41.2.153

127. Sripetchwandee J, KenKnight SB, Sanit J, Chattipakorn S, Chattipakorn N. Blockade of mitochondrial calcium uniporter prevents cardiac mitochondrial dysfunction caused by iron overload. *Acta Physiol.* (2014) 210:330–41. doi: 10.1111/apha.12162

128. Chen MP, Cabantchik ZI, Chan S, Chan GC, Cheung YF. Iron overload and apoptosis of Hl-1 cardiomyocytes: Effects of calcium channel blockade. *PLoS One.* (2014) 9:e112915. doi: 10.1371/journal.pone.0112915

129. Tadokoro T, Ikeda M, Ide T, Deguchi H, Ikeda S, Okabe K, et al. Mitochondria-dependent ferroptosis plays a pivotal role in doxorubicin cardiotoxicity. *JCI Insight.* (2020) 5:e132747. doi: 10.1172/jci.insight.132747

130. Gao X, Qian M, Campian JL, Marshall J, Zhou Z, Roberts AM, et al. Mitochondrial dysfunction may explain the cardiomyopathy of chronic iron overload. *Free Radic Biol Med.* (2010) 49:401–7. doi: 10.1016/j.freeradbiomed.2010.04.033

131. Feng Y, Madungwe NB, Imam Aliagan AD, Tombo N, Bopassa JC. Liproxstatin-1 protects the mouse myocardium against ischemia/reperfusion injury by decreasing Vdac1 levels and restoring Gpx4 levels. *Biochem Biophys Res Commun.* (2019) 520:606–11. doi: 10.1016/j.bbrc.2019.10.006

132. Ibrahim WH, Habib HM, Kamal H, St Clair DK, Chow CK. Mitochondrial superoxide mediates labile iron level: Evidence from Mn-Sod-transgenic mice and heterozygous knockout mice and isolated rat liver mitochondria. *Free Radic Biol Med.* (2013) 65:143–9. doi: 10.1016/j.freeradbiomed.2013.06.026

133. Chen Z, Lash LH. Evidence for mitochondrial uptake of glutathione by dicarboxylate and 2-oxoglutarate carriers. *J Pharmacol Exp Ther.* (1998) 285:608–18.

134. Pei Z, Liu Y, Liu S, Jin W, Luo Y, Sun M, et al. Fundc1 insufficiency sensitizes high fat diet intake-induced cardiac remodeling and contractile anomaly through Acsl4-mediated ferroptosis. *Metabolism.* (2021) 122:154840. doi: 10.1016/j.metabol.2021.154840

135. Jang S, Chapa-Dubocq XR, Tyurina YY, St Croix CM, Kapralov AA, Tyurin VA, et al. Elucidating the contribution of mitochondrial glutathione to ferroptosis in cardiomyocytes. *Redox Biol.* (2021) 45:102021. doi: 10.1016/j.redox.2021.102021

136. Wang B, Nie J, Wu L, Hu Y, Wen Z, Dong L, et al. Ampkα2 protects against the development of heart failure by enhancing mitophagy via Pink1 phosphorylation. *Circ Res.* (2018) 122:712–29. doi: 10.1161/circresaha.117.312317

137. Yao L, Chen H, Wu Q, Xie K. Hydrogen-rich saline alleviates inflammation and apoptosis in myocardial I/R injury Via pink-mediated autophagy. *Int J Mol Med.* (2019) 44:1048–62. doi: 10.3892/ijmm.2019.4264

138. Wang SH, Zhu XL, Wang F, Chen SX, Chen ZT, Qiu Q, et al. Lncrna H19 governs mitophagy and restores mitochondrial respiration in the heart through Pink1/parkin signaling during obesity. *Cell Death Dis.* (2021) 12:557. doi: 10.1038/s41419-021-03821-6

139. Basit F, van Oppen LM, Schöckel L, Bossenbroek HM, van Emst-de Vries SE, Hermeling JC, et al. Mitochondrial complex I inhibition triggers a mitophagy-dependent ros increase leading to necroptosis and ferroptosis in melanoma cells. *Cell Death Dis.* (2017) 8:e2716. doi: 10.1038/cddis.2017.133

140. Jankowska EA, Drozd M, Ponikowski P. Iron deficiency treatment in patients with heart failure. *Handb Exp Pharmacol.* (2017) 243:561–76. doi: 10.1007/164_2017_30

141. Khan SU, Khan MU, Riaz H, Valavoor S, Zhao D, Vaughan L, et al. Effects of nutritional supplements and dietary interventions on cardiovascular outcomes: An umbrella review and evidence map. *Ann Intern Med.* (2019) 171:190–8. doi: 10.7326/m19-0341

142. Chan W, Taylor AJ, Ellims AH, Lefkovits L, Wong C, Kingwell BA, et al. Effect of iron chelation on myocardial infarct size and oxidative stress in st-elevation-myocardial infarction. *Circ Cardiovasc Interv.* (2012) 5:270–8. doi: 10.1161/circinterventions.111.966226

143. Millán M, DeGregorio-Rocasolano N, Pérez de la Ossa N, Reverté S, Costa J, Giner P, et al. Targeting pro-oxidant iron with deferoxamine as a treatment for ischemic stroke: Safety and optimal dose selection in a randomized clinical trial. *Antioxidants.* (2021) 10:1270. doi: 10.3390/antiox10081270

144. Devos D, Moreau C, Kyheng M, Garçon G, Rolland AS, Blasco H, et al. A ferroptosis-based panel of prognostic biomarkers for amyotrophic lateral sclerosis. *Sci Rep.* (2019) 9:2918. doi: 10.1038/s41598-019-39739-5

145. Liu K, Chen S, Lu R. Identification of important genes related to ferroptosis and hypoxia in acute myocardial infarction based on Wgcna. *Bioengineered.* (2021) 12:7950–63. doi: 10.1080/21655979.2021.1984004

frontiers | Frontiers in Cardiovascular Medicine

TYPE Mini Review
PUBLISHED 02 September 2022
DOI 10.3389/fcvm.2022.999044

OPEN ACCESS

EDITED BY
Xiaoqiang Tang,
Sichuan University, China

REVIEWED BY
Juan Feng,
Peking University, China
Jun Ren,
Fudan University, China

*CORRESPONDENCE
Wei Liu
wei.liu@manchester.ac.uk
Andrea-Ruiz-Velasco
andrea.ruiz@manchester.ac.uk

SPECIALTY SECTION
This article was submitted to Cardiovascular Metabolism, a section of the journal Frontiers in Cardiovascular Medicine

RECEIVED 20 July 2022
ACCEPTED 15 August 2022
PUBLISHED 02 September 2022

CITATION
Raja R, Fonseka O, Ganenthiran H, Ruiz-Velasco A and Liu W (2022) The multifaceted roles of ER and Golgi in metabolic cardiomyopathy. *Front. Cardiovasc. Med.* 9:999044. doi: 10.3389/fcvm.2022.999044

The multifaceted roles of ER and Golgi in metabolic cardiomyopathy

Rida Raja, Oveena Fonseka, Haresh Ganenthiran, Andrea-Ruiz-Velasco* and Wei Liu*

Faculty of Biology, Medicine, and Health, The University of Manchester, Manchester, United Kingdom

Metabolic cardiomyopathy is a significant global financial and health challenge; however, pathophysiological mechanisms governing this entity remain poorly understood. Among the main features of metabolic cardiomyopathy, the changes to cellular lipid metabolism have been studied and targeted for the discovery of novel treatment strategies obtaining contrasting results. The endoplasmic reticulum (ER) and Golgi apparatus (GA) carry out protein modification, sorting, and secretion activities that are more commonly studied from the perspective of protein quality control; however, they also drive the maintenance of lipid homeostasis. In response to metabolic stress, ER and GA regulate the expression of genes involved in cardiac lipid biogenesis and participate in lipid droplet formation and degradation. Due to the varied roles these organelles play, this review will focus on recapitulating the alterations and crosstalk between ER, GA, and lipid metabolism in cardiac metabolic syndrome.

KEYWORDS

metabolic syndrome, metabolic cardiomyopathy, cardiac lipid metabolism, endoplasmic reticulum, Golgi apparatus

Introduction

In the past five decades, the global prevalence of obesity, diabetes, and hypertension has reached epidemic dimensions (1, 2). These disorders, collectively termed metabolic syndrome, confer substantial morbidity and mortality of cardiovascular disease (3, 4). At the same time, they are high-risk factors for the development of cardiomyopathy (5). The metabolic syndrome encompasses a diverse set of conditions that exert chronic stress on cellular functions, such as systemic dyslipidemia, hyperglycemia, and insulin resistance. The pathophysiological changes induced in the heart by these stressors are termed metabolic cardiomyopathy. Clinically, patients with metabolic cardiomyopathy initially present diastolic dysfunction, followed by late-onset systolic dysfunction and, ultimately, heart failure (HF) (6). Along with adverse structural remodeling and increased presence of reactive oxygen species, cell death, and inflammation (7, 8), metabolic cardiomyopathy features cardiac energetic impairment (9, 10). Lipid mishandling and subsequent lipotoxicity are prominent effects of this alteration (11, 12). Efficacious therapeutic options targeting cardiac lipid derangements are lacking, therefore advanced

understanding of the pathogenesis is necessary. The endoplasmic reticulum (ER) and the Golgi apparatus (GA) are essential for lipid homeostasis, hosting and processing proteins involved in triacylglycerol (TG) synthesis and lipolysis. Previous reviews have focused on the central role the mitochondria play in lipid oxidation in metabolic cardiomyopathy (13–16); however, the role of the ER and GA in lipid metabolism in the heart under metabolic stress remains poorly defined.

Cardiac lipid metabolism

Fatty acids (FAs) account for approximately 70% of the energy sources required for ATP synthesis in cardiomyocytes. In circulation, FAs are commonly found as triacylglycerols (TGs) associated with lipoproteins or chylomicrons or as free FAs bound to albumin. TGs are hydrolyzed by lipoprotein lipase (LpL) Cardiomyocytes take up extracellular FAs by passive diffusion across the plasma membrane or by surface receptors such as protein cluster of differentiation 36 (CD36), fatty acid transport protein 1, and fatty acid binding protein (17). Once in the cytoplasm, FAs are shuttled into the mitochondria for β-oxidation resulting in high energy molecules required for cardiac function (18). Excessive FAs are converted back to TGs by diacylglycerol acyltransferase (DGAT) and stored in lipid droplets (LD). When required, FAs are released from LDs by adipocyte triglyceride lipase (ATGL) and hormone-sensitive lipase (HSL) (19). Lipid homeostasis also requires the participation of other organelles. For example, peroxisomes manage very long-chain fatty acid breakdown and β-oxidation, lysosomes carry out lipid catabolism, and ER and GA handle LD formation (20). It is widely accepted that in metabolic syndrome the myocardium experiences an increase in lipid consumption (9, 21), meaning that different organelles activate stress responses to manage different stages of lipid homeostasis.

Lipotoxicity in cardiomyopathy

Cardiac lipotoxicity develops due to a build-up of FAs and lipid intermediates that disrupt β-oxidation homeostasis. Among such intermediates are ceramides and di-acyl glycerol (DAG). In a mouse model of lipid-induced dilated cardiomyopathy by LpL cardiac-overexpression, ceramides were found to regulate substrate utilization, where inhibition of ceramide biosynthesis normalized FAs and glucose oxidation and improved survival. In addition, ceramides induce various pathological processes that promote lipotoxicity, for instance, insulin resistance, inflammation, and apoptosis (22).

Similarly, DAG induces apoptosis via mitochondrial apoptotic pathways. It also impairs insulin signaling, an effect that can be accelerated due to the reactive oxygen species production (ROS) by free FAs (19). These pathological processes associated with toxic lipid intermediates contribute to the development of metabolic cardiomyopathy; therefore, it is important to study the mechanisms available in the cell to counteract such conditions.

ER stress response and UPR

The ER is involved in protein quality control (PQC), calcium homeostasis, and lipid metabolism. Chronic metabolic stress can perturb ER homeostasis leading to ER stress and proteotoxicity that consist of protein misfolding and protein accumulation. Protein quality is vital to sustain cardiac function and in metabolic cardiomyopathy it has been identified as an inducer of cell death (23). ER stress triggers an adaptive signal transduction pathway known as the unfolded protein response (UPR) which neutralizes ER stress and sustains cellular function. Three transmembrane proteins maintain ER homeostasis; inositol-requiring enzyme 1α (IRE1α), protein kinase RNA-like ER kinase (PERK), and activating transcription factor 6 (ATF6) initiate the UPR (24). Under basal conditions, these sensor proteins are associated with chaperone GRP78/Bip, rendering them inactive (25). When proteostasis is disrupted, GRP78/Bip detaches and these become active (26). IRE1α processes the transcription factor X-box binding protein 1 (XBP1), forming the transcriptionally active spliced-XBP1 (XBP1s) (25, 27). XBP1s binds to a set of UPR-target genes that upregulate organelle biosynthesis, PQC, and ER-associated degradation (ERAD) (28). PERK phosphorylates the eukaryotic translation initiating factor 2α (elf2α), attenuating protein synthesis (27, 29). In turn, elf2α also induces the translation of ATF4, which regulates the expression of genes involved in autophagy, apoptosis, antioxidant response, and the transcription factor DNA damage-inducible 34 (GADD34). GADD34 can restore protein synthesis by binding to protein phosphatase 1C (PP1C), which dephosphorylates elf2α (27). PERK upregulates the proapoptotic transcription factor CHOP/GADD153. Finally, ATF6's transcriptional activity induces the expression of ERAD and XBP1 genes (24). These transcriptional events act in a well-choreographed manner to maintain ER equilibrium.

ER regulation of lipid metabolism

In addition to its protein-centric role, the UPR is an essential nutrient sensing ER apparatus critical for maintaining lipid homeostasis (30, 31). Palmitate activates the PERK-eIF2α-CHOP pathway and decreases Bip expression in HepG2 liver cells. Accordingly, Bip overexpression reduced CHOP levels and attenuated palmitate-induced ER stress and apoptosis (32). Moreover, GADD34-mediated dephosphorylation of eIF2α reduces hepatosteatosis in *Alb::GC* transgenic mice upon high-fat diet (HFD) feeding (33). Following this, depletion of ATF4, the downstream effector of the PERK-eIF2α pathway, protects mice against hepatic steatosis and hypertriglyceridemia in

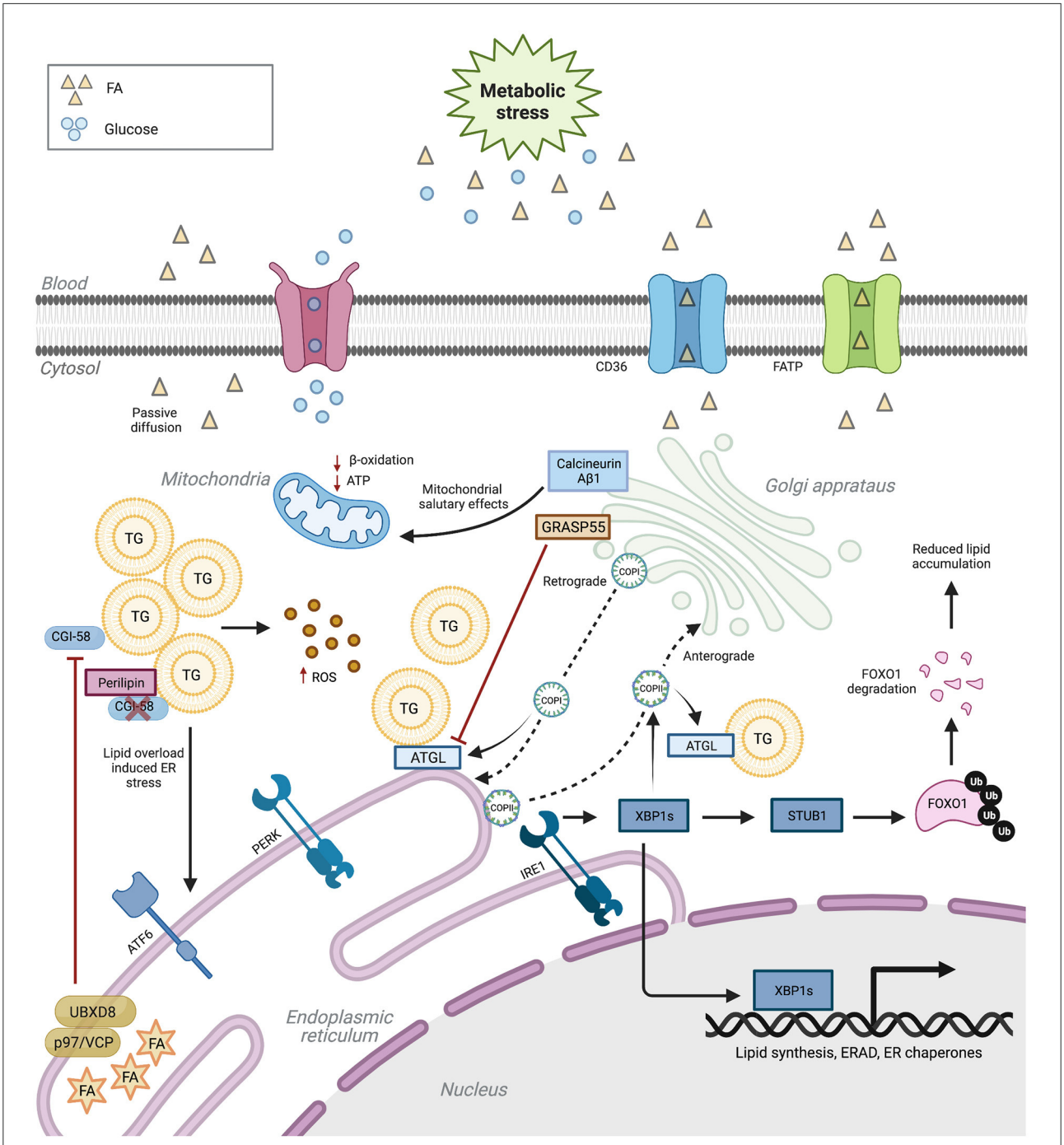

FIGURE 1
ER and Golgi regulation of lipid metabolism. ER and Golgi functions are paramount for lipid metabolism. Aberrant ER and Golgi function induce cellular lipid disequilibrium. In turn, lipotoxicity negatively regulates the function of these two organelles. Upon metabolic stress, ER dysfunction inhibits TG degradation, eventually leading to oxidative stress. ER stress also reduces genes participating in ER function and lipid metabolism. Impaired Golgi proteins or COPI/II pathways damage lipogenesis and lipolysis balance. CD36 (cluster of differentiation 36), FATP (fatty acid transport protein), TG (triacylglycerol), FA (fatty acid), ROS (reactive oxygen species), ATGL (adipose triglyceride lipase), XBP1s (spliced X-box binding protein 1), FoxO1 (Forkhead box protein O1), COPI (coat protein complex I) and COPII (coat protein complex II). Created with Biorender.com.

response to high-fructose diet feeding (34), suggesting that the PERK pathway regulates lipogenesis in hepatocytes. Similarly, PERK depletion inhibits lipogenesis during the differentiation of mouse embryonic fibroblasts to adipocytes (35) (Figure 1).

The IRE1α-XBP1 branch of the UPR is also a critical regulator of metabolic-stress-induced lipid disequilibrium (36). Adipocyte Xbp1s overexpression prevents obesity in HFD-fed mice and leptin-deficient *ob/ob* mice via increased uridine biosynthesis (37). Added to this, ectopic adipocyte Xbp1s expression promotes systemic glucose homeostasis in both lean and *ob/ob* mice by increasing adiponectin serum levels (38). XBP1 deletion reduces hepatic steatosis and improves insulin sensitivity in mice fed a high-fructose diet despite increased ER stress (39). In accordance, Lee et al. (40) demonstrated that XBP1 regulates lipogenesis. Finally, ATF6 modulates lipid metabolism in an XBP1-independent manner (41). ATF6α-knockout mice administered the pharmacological ER-stress inducer tunicamycin exhibit liver dysfunction and steatosis, ensued from aberrant ß-oxidation and suppression of very-low-density lipoproteins (VLDLs) formation. However, these abnormalities are obliterated by ATF6 overexpression (42). A similar account is observed in ATF6α deficient hepatocytes following a high-fat and high-sucrose diet feeding (43). During adipogenesis, ATF6α deficiency reduces the expression of key audiogenic genes needed for adipocyte differentiation (44). These studies highlight the importance of the ER stress response regulating lipid homeostasis in metabolically active peripheral tissues, such as adipose and liver. The crosstalk between such tissues and the heart is a major subject of study and their influence in the development of metabolic cardiomyopathy has been reported (45, 46). However, the amount of evidence also suggests that similar mechanisms could be present in the heart and be worth exploring for a better understanding of the disease.

ERAD factors' involvement in lipid metabolism

ERAD is an integral part of the ER stress response. It recognizes and labels abnormal proteins in the ER directing them to the cytosol for proteasomal degradation. Cell-type-specific ERAD mouse model studies are limited. Adipocyte-specific Sel1L deficient mice are resistant to HFD-induced obesity, developing postprandial hypertriglyceridemia and displaying hepatic steatosis (47). Here, in the absence of Sel1L, LPL is retained in the ER in the form of ERAD-resistant aggregates. Similar observations were made on other LPL-expressing cells, including cardiomyocytes and macrophages (47). Hepatocyte-specific ER degradation enhancing alpha-mannosidase-like protein 3 (EDEM3) knockdown mice had increased LRP1 expression leading to enhanced VLDL uptake, thereby reducing plasma TG levels (48). Concurrently, data obtained from Gan et al. (49) showed that ischemic heart-derived small extracellular vesicles (sEVs) carrying miR-23-27-24 suppress adiponectin biosynthesis by downregulating EDEM3. This pathological communication causes adipocyte ER stress and endocrine dysfunction, which contributed to post-MI metabolic disorders.

Furthermore, Choi et al. (50) reported that depletion of the ER membrane-anchored E3 ligase gp78 stabilized DGAT2 in hepatic cells, which increased LD levels. UBXD8 is a protein that interacts with p97 during ERAD to facilitate proteasomal degradation of ubiquitinated proteins; however, UBXD8 has also emerged as a critical determinant of fatty acid (FA) metabolism and TG storage (51–54). UBXD8 acts as an unsaturated FA sensor. In FA-depleted cultured cells, UBXD8 inhibits the conversion of DAGs to TGs; this effect is reversed upon exposure to unsaturated FAs (53). Mechanistically, UBXD8 negatively regulates ATGL by promoting the dissociation of its activator CGI-58 (51). Therefore, FAs increase TG content by inactivating UBXD8. In line with this, UBXD8 depletion in murine hepatocytes leads to periportal steatosis upon HFD feeding (55). Whilst there is a vast body of literature evidencing ERAD involvement in lipid metabolism, the role of ERAD proteins in metabolic cardiomyopathy remains unexplored.

ER stress and cardiac lipid metabolism

ER stress has been identified as a crucial pathophysiological driver of cardiovascular disease in preclinical and clinical studies (23). ER stress is implicated in cardiac lipotoxicity (56–58); however, the mechanisms by which ER disruptions contribute to lipotoxic alterations in cardiomyocytes are unclear. Recently, Schiattarella et al. (59) reported that cardiomyocyte-specific overexpression of Xbp1s ameliorates cardiac dysfunction and reduces myocardial steatosis in a preclinical model of HF with preserved ejection fraction. Further investigations revealed that Xbp1s promotes the ubiquitination and degradation of Forkhead box protein O1 (FoxO1) via E3 ubiquitin ligase STUB1. FoxO1 is a vital transcriptional regulator of genes involved in cellular metabolism and its transcriptional activity is increased in obese and diabetic animal models (60, 61). In cardiac muscle cells, FoxO1 orchestrates lipid accumulation; the sequential events underpining this accumulation remain unknown. Conversley, FoxO1 overexpression inhibits lipid accumulation in hepatocytes by mediating ATGL-dependent lipolysis (62). CGI-58 is an LD-associated protein that plays a vital role in TG hydrolysis by activating ATGL (63). it is decreased in failing human hearts (64). CGI-58-deficient mice display adverse cardiac remodeling accompanied by accentuated cardiac TG levels, ROS production, and inflammation when after HFD feeding (65). The chemical chaperone 4-PBA attenuated HFD-induced cardiac remodeling and dysfunction; alleviated mitochondrial dissonance, oxidative stress, and lipid accumulation in cardiac-specific CGI58- knockout mice (65). Moreover, inhibiting

calpains, calcium-activated proteases, prevents lipotoxicity-associated myocardial injury in HFD-challenged mice by attenuating ER stress, thereby improving cardiac function (66). These studies suggest ER stress regulates cardiac lipid homeostasis and acts as a potential therapeutic target for metabolic cardiomyopathy.

While ER stress alters lipid metabolism, FAs can also induce ER stress in a bidirectional loop, creating a vicious cycle (67). Saturated fatty acids instigate lipotoxic injury in cardiomyocytes via ER stress-mediated apoptosis pathways (68–70). Cardiomyocyte-specific PPARβ/δ deletion perturbed myocardial fatty acid oxidation, induced ER stress, and lead to cardiac steatosis, hypertrophy, and congestive HF in a preclinical mouse model (71, 72). The PPARβ/δ agonist, GW501516, attenuated palmitate-induced ER-stress in AC16 cells, underscoring the therapeutic potential of PPARβ/δ for ER-stress mediated cardiac lipotoxicity (72). Moreover, CTRP9, a highly conserved paralog of adiponectin, has also been reported to regulate lipid metabolism. CTRP9-knockout mice displayed augmented ER-stressed induced apoptosis; nevertheless, recombinant CTRP9 treatment exerted anti-ER-stress-related apoptotic effects and anti-oxidative stress effects to abate lipotoxicity in neonatal rat cardiomyocytes (73).

The physiological function of the GA

The GA comprises a series of stacked membranes that process ER proteins and lipids. Its main functions include protein glycosylation, sorting and secretion, and phospholipid and sphingomyelin synthesis. The GA network can be divided into the cis and trans components. While the cis network is responsible for receiving cargo from the ER, the trans-Golgi network (TGN), on the other end, regulates cargo exit from the Golgi. The cargo is carried in transport vesicles formed by protein complexes that regulate their content and direction. From the ER exit sites, coat protein complex II (COPII) vesicles travel through the ER-Golgi intermediate compartment (ERGIC) to the cis-component via anterograde transport. In retrograde transport, COPI-coated vesicles recycle ER-resident proteins. Finally, cargo directed to other organelles or the plasma membrane exit the TGN in clathrin-covered vesicles (74). Like the ER, the GA can experience stress when unable to keep up with the flux of proteins and lipids, leading to the activation of the Golgi stress response. Even though this response has not been as well-characterized as the UPR in the heart, pathways such as transcription factor binding to IGHM enhancer 3 (TFE3), CAMP responsive element binding protein 3 (CREB3), and heat shock protein 47 (HSP47) have been found to regulate GA structure and functions (75).

GA regulation of lipid metabolism

The GA is mainly known for its role in lysosomal, transmembrane, and secretory protein glycosylation and trafficking activities. In addition to its protein processing activities, its contributions to lysosomal function and membrane dynamics are vital for lipid recycling, lysosomal lipid signaling, and membrane composition, all of which are key to lipid metabolism in the setting of metabolic disease (76–78). Presently, manifestations of direct GA involvement in lipid signaling and metabolism not associated to membrane dynamics that have not been clearly defined will be discussed. Recent observations from Fan et al. (79) demonstrated that hyperglycemia affects myocardial GA protein expression and causes fragmentation in a preclinical model of type 1 diabetes. Proofs of how this could impair lipid metabolism have been found in different animal models or cell lines. For instance, the membrane lipid transporter CD36 is processed in the GA before its transport to the plasmatic membrane. A mutation that blunted its passing through the GA resulted in ER accumulation and low lipid uptake (80).

Knocking down COPI subunits in flies (81) and Hep62 (82) cells showed they are required for lipolysis activation. They regulate LD surface proteins that inhibit lipolysis, such as Perilipins 2 and 3, and promote the formation of ER-LD bridges through which ATGL is transferred to the LDs. The deletion of oxysterol binding protein-like 2 (OSBPL2), an intracellular lipid receptor, disrupted LD localization of the subunit COPBI, leading to lipid accumulation in larger LDs and hypercholesterolemia in zebrafish (82). Furthermore, genetic or chemical interference with the ADP-ribosylation factor (ARF1)-COPI pathway at different stages gave similar results. Golgi-specific brefeldin A-resistance guanine nucleotide exchange factor 1 (GBF1) interacts directly with ATGL (83), and its deletion hindered ATGL transport to nascent LDs, inducing the lipase's proteasomal degradation (84). In addition, impeding the function of the COPII complex also disrupted lipolysis, but the effect was smaller than that of COPI. In different cells, knockdown of ARF1, a COPI complex initiator, showed that this machinery has the ability to form nano-buds from the LD membranes and target TG synthesis enzyme to the LD membrane (85), suggesting that it affects LD composition as well as degradation.

Similar to the observations above, deletion of GRASP55, another Golgi-resident protein, impaired the trafficking of ATGL and MGL to LDs, impairing lipolysis. In mice, this systemic deletion conferred resistance to HFD-induced obesity due to a decreased formation and secretion of chylomicrons and VLDLs from enterocytes resulting in low lipid uptake (86). Hepatic deletion of the initiator of COPII complex GTP-binding protein SAR1b (SAR1) in mice showed increased accumulation of TGs and cholesterol in the liver with reduced lipid plasma

levels protecting them from atherosclerosis (87). In this study, Wang et al. (87) identified surfeit locus protein 4 (SURF4) as a receptor for specific VLDL secretion downstream of the COPII pathway and as a protein with a COPI sorting signal for recycling. Comparable effects were observed in liver-specific IRE1 knockout mice where COPII transport was reduced. In this case, XBP1 overexpression restored COPII gene expression and trafficking, resolving the fatty liver and hypolipidemia (88). The significance of the GA transport role in lipoprotein secretion was confirmed by a report showing eight different mutations of *SARA2* (coding SAR1 protein) in patients with severe fat absorption disorders (89). These results indicate that the ER-GA transport network can be targeted for the systemic regulation of metabolic diseases.

Finally, in addition to its role in protein and LD processing, the GA is involved in metabolic and cell death signaling. In the heart, activating an alternative isoform of calcineurin presenting a new Golgi-localization signal was found to regulate metabolism through AKT phosphorylation, reducing mitochondrial dysfunction and preventing myocardial remodeling following transaortic constriction (90). AKT signaling is impaired in the hearts of obese mice (91), and this pathway inhibits cardiac lipolysis (92). Furthermore, GA stress pathways have been found to promote apoptosis, particularly in neurological diseases, by modulating caspase cleavage and calcium influx (93). In Hela cells, the ferroptosis pathway was also activated by inducers of GA stress (94). Ferroptosis is an iron-dependent cell death process driven by lipid peroxidation, making these observations relevant for the study of GA and metabolic stress. There is clear evidence that the GA regulates lipid metabolism and that it responds to stress in relevant metabolically active tissues. However, the specific links involved in metabolic cardiomyopathy, particularly taking place in the myocardium, need further study to identify better potential therapeutic targets.

Conclusion

The ER and GA regulation of lipid metabolism are complex and largely unexplored. Both organelles have a clear role in sustaining protein synthesis and processing during metabolic stress conditions, which is essential for preventing HF. However, their part goes beyond protein quality control; they are deeply involved in different stages of lipid metabolism, from synthesis to storage and catabolism, by processing lipids and governing lipid droplet dynamics. Moreover, their sensing abilities trigger signaling pathways that coordinate their own functional capacity and that of other organelles. In metabolic cardiomyopathy, these tasks become even more critical due to the altered lipid profile state and the high lipotoxicity risks. Therefore, it follows that further studying and targeting ER and GA homeostasis for the treatment of metabolic cardiomyopathy could provide opportunities for the prevention of HF.

Author contributions

RR, OF, and AR-V collected references, drafted, and proofread the manuscript. RR and HG generated the figure. AR-V and WL designed the manuscript. All authors contributed to the article and approved the submitted version.

Funding

This work as supported by grants FS/15/16/31477, FS/18/73/33973, PG/19/66/34600, and FS/19/70/34650 to WL from the British Heart Foundation.

Conflict of interest

The authors declare that the research was conducted in the absence of any commercial or financial relationships that could be construed as a potential conflict of interest.

Publisher's note

References

1. Lee IM, Shiroma EJ, Lobelo F, Puska P, Blair SN, Katzmarzyk PT, et al. Effect of physical inactivity on major non-communicable diseases worldwide: an analysis of burden of disease and life expectancy. *Lancet.* (2012) 380:219–29. doi: 10.1016/S0140-6736(12)61031-9

2. Lim SS, Vos T, Flaxman AD, Danaei G, Shibuya K, Adair-Rohani H, et al. A comparative risk assessment of burden of disease and injury attributable to 67 risk factors and risk factor clusters in 21 regions, 1990–2010: a systematic analysis for the global burden of disease study 2010. *Lancet.* (2012) 380:2224–60. doi: 10.1016/S0140-6736(12)61766-8

3. Bozkurt B, Aguilar D, Deswal A, Dunbar SB, Francis GS, Horwich T, et al. Contributory risk and management of comorbidities of hypertension, obesity, diabetes mellitus, hyperlipidemia, and metabolic syndrome in chronic heart failure:

a scientific statement from the American heart association. *Circulation.* (2016) 134:e535–e78. doi: 10.1161/CIR.0000000000000450

4. Low Wang CC, Hess CN, Hiatt WR, Goldfine AB. Clinical update: cardiovascular disease in diabetes mellitus: atherosclerotic cardiovascular disease and heart failure in type 2 diabetes mellitus - mechanisms, management, and clinical considerations. *Circulation.* (2016) 133:2459–502. doi: 10.1161/CIRCULATIONAHA.116.022194

5. Jia G, Demarco V, Sowers Jr. Insulin resistance and hyperinsulinaemia in diabetic cardiomyopathy. *Nat Rev Endocrinol.* (2016) 12:144–53. doi: 10.1038/nrendo.2015.216

6. Tan Y, Zhang Z, Zheng C, Wintergerst KA, Keller BB, Cai L. Mechanisms of diabetic cardiomyopathy and potential therapeutic strategies: preclinical and clinical evidence. *Nat Rev Cardiol.* (2020) 17:585–607. doi: 10.1038/s41569-020-0339-2

7. Miki T, Yuda S, Kouzu H, Miura T. Diabetic cardiomyopathy: pathophysiology and clinical features. *Heart Fail Rev.* (2013) 18:149–66. doi: 10.1007/s10741-012-9313-3

8. Wong C, Marwick TH. Obesity cardiomyopathy: diagnosis and therapeutic implications. *Nat Clin Pract Cardiovasc Med.* (2007) 4:480–90. doi: 10.1038/ncpcardio0964

9. Liu W, Ruiz-Velasco A, Wang S, Khan S, Zi M, Jungmann A, et al. Metabolic stress-induced cardiomyopathy is caused by mitochondrial dysfunction due to attenuated Erk5 signaling. *Nat Commun.* (2017) 8:494. doi: 10.1038/s41467-017-00664-8

10. Buchanan J, Mazumder PK, Hu P, Chakrabarti G, Roberts MW, Yun UJ, et al. Reduced cardiac efficiency and altered substrate metabolism precedes the onset of hyperglycemia and contractile dysfunction in two mouse models of insulin resistance and obesity. *Endocrinology.* (2005) 146:5341–9. doi: 10.1210/en.2005-0938

11. Bugger H, Abel ED. Molecular mechanisms of diabetic cardiomyopathy. *Diabetologia.* (2014) 57:660–71. doi: 10.1007/s00125-014-3171-6

12. Abel ED, Litwin SE, Sweeney G. Cardiac remodeling in obesity. *Physiol Rev.* (2008) 88:389–419. doi: 10.1152/physrev.00017.2007

13. Nguyen BY, Ruiz-Velasco A, Bui T, Collins L, Wang X, Liu W. Mitochondrial function in the heart: the insight into mechanisms and therapeutic potentials. *Br J Pharmacol.* (2019) 176:4302–18. doi: 10.1111/bph.14431

14. Bugger H, Abel ED. Mitochondria in the diabetic heart. *Cardiovasc Res.* (2010) 88:229–40. doi: 10.1093/cvr/cvq239

15. Galloway CA, Yoon Y. Mitochondrial dynamics in diabetic cardiomyopathy. *Antioxid Redox Signal.* (2015) 22:1545–62. doi: 10.1089/ars.2015.6293

16. Chen YR, Zweier JL. Cardiac mitochondria and reactive oxygen species generation. *Circ Res.* (2014) 114:524–37. doi: 10.1161/CIRCRESAHA.114.300559

17. Lopaschuk GD, Ussher JR, Folmes CD, Jaswal JS, Stanley WC. Myocardial fatty acid metabolism in health and disease. *Physiol Rev.* (2010) 90:207–58. doi: 10.1152/physrev.00015.2009

18. Fillmore N MJ, Lopaschuk GD. Mitochondrial fatty acid oxidation alterations in heart failure, ischaemic heart disease and diabetic cardiomyopathy. *Br J Pharmacol.* (2014) 171:2080–90. doi: 10.1111/bph.12475

19. Drosatos K, Schulze PC. Cardiac lipotoxicity: molecular pathways and therapeutic implications. *Curr Heart Fail Rep.* (2013) 10:109–21. doi: 10.1007/s11897-013-0133-0

20. Gordaliza-Alaguero I, Canto C, Zorzano A. Metabolic implications of organelle-mitochondria communication. *EMBO Rep.* (2019) 20:e47928. doi: 10.15252/embr.201947928

21. Jia AG, Hill RM, Sowers RJ. Diabetic cardiomyopathy: an update of mechanisms contributing to this clinical entity. *Circ Res.* (2018) 122:624–38. doi: 10.1161/CIRCRESAHA.117.311586

22. D'Souza K, Nzirorera C, Kienesberger PC. Lipid metabolism and signaling in cardiac lipotoxicity. *Biochim Biophys Acta.* (2016) 1861:1513–24. doi: 10.1016/j.bbalip.2016.02.016

23. Kaur N, Raja R, Ruiz-Velasco A, Liu W. Cellular protein quality control in diabetic cardiomyopathy: from bench to bedside. *Front Cardiovasc Med.* (2020) 7:5309. doi: 10.3389/fcvm.2020.585309

24. Hetz C. The unfolded protein response: controlling cell fate decisions under ER stress and beyond. *Nat Rev Mol Cell Biol.* (2012) 13:89–102. doi: 10.1038/nrm3270

25. Wang S, Binder P, Fang Q, Wang Z, Xiao W, Liu W, et al. Endoplasmic reticulum stress in the heart: insights into mechanisms and drug targets. *Br J Pharmacol.* (2018) 175:1293–304. doi: 10.1111/bph.13888

26. Bertolotti A, Zhang Y, Hendershot LM, Harding HP, Ron D. Dynamic interaction of BiP and ER stress transducers in the unfolded-protein response. *Nat Cell Biol.* (2000) 2:326–32. doi: 10.1038/35014014

27. Hetz C, Chevet E, Harding HP. Targeting the unfolded protein response in disease. *Nat Rev Drug Discov.* (2013) 12:703–19. doi: 10.1038/nrd3976

28. Hetz C, Papa FR. The Unfolded Protein Response and Cell Fate Control. *Mol Cell.* (2018) 69:169–81. doi: 10.1016/j.molcel.2017.06.017

29. Claudio H. The unfolded protein response: controlling cell fate decisions under ER stress and beyond. *Nat Rev Mol Cell Biol.* (2012) 13:89.

30. Basseri S, Austin RC. Endoplasmic reticulum stress and lipid metabolism: mechanisms and therapeutic potential. *Biochem Res Int.* (2012) 2012:841362. doi: 10.1155/2012/841362

31. Han J, Kaufman RJ. The role of ER stress in lipid metabolism and lipotoxicity. *J Lipid Res.* (2016) 57:1329–38. doi: 10.1194/jlr.R067595

32. Gu X, Li K, Laybutt DR, He ML, Zhao HL, Chan JC, et al. Bip overexpression, but not CHOP inhibition, attenuates fatty-acid-induced endoplasmic reticulum stress and apoptosis in HepG2 liver cells. *Life Sci.* (2010) 87:724–32. doi: 10.1016/j.lfs.2010.10.012

33. Oyadomari S, Harding HP, Zhang Y, Oyadomari M, Ron D. Dephosphorylation of translation initiation factor 2alpha enhances glucose tolerance and attenuates hepatosteatosis in mice. *Cell Metab.* (2008) 7:520–32. doi: 10.1016/j.cmet.2008.04.011

34. Xiao F, Deng J, Guo Y, Niu Y, Yuan F, Yu J, et al. BTG1 ameliorates liver steatosis by decreasing stearoyl-CoA desaturase 1 (SCD1) abundance and altering hepatic lipid metabolism. *Sci Signal.* (2016) 9:ra50. doi: 10.1126/scisignal.aad8581

35. Bobrovnikova-Marjon E, Hatzivassiliou G, Grigoriadou C, Romero M, Cavener DR, Thompson CB, et al. PERK-dependent regulation of lipogenesis during mouse mammary gland development and adipocyte differentiation. *Proc Natl Acad Sci USA.* (2008) 105:16314–9. doi: 10.1073/pnas.0808517105

36. Sha H, He Y, Chen H, Wang C, Zenno A, Shi H, et al. The IRE1alpha-XBP1 pathway of the unfolded protein response is required for adipogenesis. *Cell Metab.* (2009) 9:556–64. doi: 10.1016/j.cmet.2009.04.009

37. Deng Y, Wang ZV, Gordillo R, Zhu Y, Ali A, Zhang C, et al. Adipocyte Xbp1s overexpression drives uridine production and reduces obesity. *Mol Metab.* (2018) 11:1–17. doi: 10.1016/j.molmet.2018.02.013

38. Sha H, Yang L, Liu M, Xia S, Liu Y, Liu F, et al. Adipocyte spliced form of X-box-binding protein 1 promotes adiponectin multimerization and systemic glucose homeostasis. *Diabetes.* (2014) 63:867–79. doi: 10.2337/db13-1067

39. Jurczak MJ, Lee AH, Jornayvaz FR, Lee HY, Birkenfeld AL, Guigni BA, et al. Dissociation of inositol-requiring enzyme (IRE1alpha)-mediated c-Jun N-terminal kinase activation from hepatic insulin resistance in conditional X-box-binding protein-1 (XBP1) knock-out mice. *J Biol Chem.* (2012) 287:2558–67. doi: 10.1074/jbc.M111.316760

40. Lee AH, Scapa EF, Cohen DE, Glimcher LH. Regulation of hepatic lipogenesis by the transcription factor XBP1. *Science.* (2008) 320:1492–6. doi: 10.1126/science.1158042

41. Bommiasamy H, Back SH, Fagone P, Lee K, Meshinchi S, Vink E, et al. ATF6alpha induces XBP1-independent expansion of the endoplasmic reticulum. *J Cell Sci.* (2009) 122(Pt 10):1626–36. doi: 10.1242/jcs.045625

42. Yamamoto K, Takahara K, Oyadomari S, Okada T, Sato T, Harada A, et al. Induction of liver steatosis and lipid droplet formation in ATF6alpha-knockout mice burdened with pharmacological endoplasmic reticulum stress. *Mol Biol Cell.* (2010) 21:2975–86. doi: 10.1091/mbc.e09-02-0133

43. Chen X, Zhang F, Gong Q, Cui A, Zhuo S, Hu Z, et al. Hepatic ATF6 increases fatty acid oxidation to attenuate hepatic steatosis in mice through peroxisome proliferator-activated receptor alpha. *Diabetes.* (2016) 65:1904–15. doi: 10.2337/db15-1637

44. Lowe CE, Dennis RJ, Obi U, O'Rahilly S, Rochford JJ. Investigating the involvement of the ATF6alpha pathway of the unfolded protein response in adipogenesis. *Int J Obes.* (2012) 36:1248–51. doi: 10.1038/ijo.2011.233

45. Kim JB. Dynamic cross talk between metabolic organs in obesity and metabolic diseases. *Exp Mol Med.* (2016) 48:e214. doi: 10.1038/emm.2015.119

46. Jahng JW, Song E, Sweeney G. Crosstalk between the heart and peripheral organs in heart failure. *Exp Mol Med.* (2016) 48:e217. doi: 10.1038/emm.2016.20

47. Sha H, Sun S, Francisco AB, Ehrhardt N, Xue Z, Liu L, et al. The ER-associated degradation adaptor protein Sel1L regulates LPL secretion and lipid metabolism. *Cell Metab.* (2014) 20:458–70. doi: 10.1016/j.cmet.2014.06.015

48. Xu YX, Peloso GM, Nagai TH, Mizoguchi T, Deik A, Bullock K, et al. EDEM3 modulates plasma triglyceride level through its regulation of LRP1 expression. *iScience.* (2020) 23:100973. doi: 10.1016/j.isci.2020.100973

49. Gan L, Liu D, Xie D, Bond Lau W, Liu J, Christopher TA, et al. Ischemic Heart-Derived Small Extracellular Vesicles Impair Adipocyte Function. *Circ Res.* (2022) 130:48–66. doi: 10.1161/CIRCRESAHA.121.320157

50. Choi K, Kim H, Kang H, Lee SY, Lee SJ, Back SH, et al. Regulation of diacylglycerol acyltransferase 2 protein stability by gp78-associated endoplasmic-reticulum-associated degradation. *FEBS J.* (2014) 281:3048–60. doi: 10.1111/febs.12841

51. Olzmann JA, Richter CM, Kopito RR. Spatial regulation of UBXD8 and p97/VCP controls ATGL-mediated lipid droplet turnover. *Proc Natl Acad Sci USA.* (2013) 110:1345–50. doi: 10.1073/pnas.1213738110

52. Suzuki M, Otsuka T, Ohsaki Y, Cheng J, Taniguchi T, Hashimoto H, et al. Derlin-1 and UBXD8 are engaged in dislocation and degradation of lipidated ApoB-100 at lipid droplets. *Mol Biol Cell.* (2012) 23:800–10. doi: 10.1091/mbc.e11-11-0950

53. Lee JN, Kim H, Yao H, Chen Y, Weng K, Ye J. Identification of Ubxd8 protein as a sensor for unsaturated fatty acids and regulator of triglyceride synthesis. *Proc Natl Acad Sci U S A.* (2010) 107:21424–9. doi: 10.1073/pnas.1011859107

54. Wang CW, Lee SC. The ubiquitin-like (UBX)-domain-containing protein Ubx2/Ubxd8 regulates lipid droplet homeostasis. *J Cell Sci.* (2012) 125(Pt 12):2930–9. doi: 10.1242/jcs.100230

55. Imai N, Suzuki M, Hayashi K, Ishigami M, Hirooka Y, Abe T, et al. Hepatocyte-specific depletion of UBXD8 induces periportal steatosis in mice fed a high-fat diet. *PLoS ONE.* (2015) 10:e0127114. doi: 10.1371/journal.pone.0127114

56. Bosma M, Dapito DH, Drosatos-Tampakaki Z, Huiping-Son N, Huang LS, Kersten S, et al. Sequestration of fatty acids in triglycerides prevents endoplasmic reticulum stress in an in vitro model of cardiomyocyte lipotoxicity. *Biochim Biophys Acta.* (2014) 1841:1648–55. doi: 10.1016/j.bbalip.2014.09.012

57. Park SY, Cho YR, Finck BN, Kim HJ, Higashimori T, Hong EG, et al. Cardiac-specific overexpression of peroxisome proliferator-activated receptor-alpha causes insulin resistance in heart and liver. *Diabetes.* (2005) 54:2514–24. doi: 10.2337/diabetes.54.9.2514

58. Ljubkovic M, Gressette M, Bulat C, Cavar M, Bakovic D, Fabijanic D, et al. Disturbed fatty acid oxidation, endoplasmic reticulum stress, and apoptosis in left ventricle of patients with type 2 diabetes. *Diabetes.* (2019) 68:1924–33. doi: 10.2337/db19-0423

59. Schiattarella GG, Altamirano F, Kim SY, Tong D, Ferdous A, Piristine H, et al. Xbp1s-FoxO1 axis governs lipid accumulation and contractile performance in heart failure with preserved ejection fraction. *Nat Commun.* (2021) 12:1684. doi: 10.1038/s41467-021-21931-9

60. Kim JJ Li P, Huntley J, Chang JP, Arden KC, Olefsky JM. FoxO1 haploinsufficiency protects against high-fat diet-induced insulin resistance with enhanced peroxisome proliferator-activated receptor gamma activation in adipose tissue. *Diabetes.* (2009) 58:1275–82. doi: 10.2337/db08-1001

61. Behl Y, Krothapalli P, Desta T, Roy S, Graves DT. FOXO1 plays an important role in enhanced microvascular cell apoptosis and microvascular cell loss in type 1 and type 2 diabetic rats. *Diabetes.* (2009) 58:917–25. doi: 10.2337/db08-0537

62. Zhao N, Tan H, Wang L, Han L, Cheng Y, Feng Y, et al. Palmitate induces fat accumulation via repressing FoxO1-mediated ATGL-dependent lipolysis in HepG2 hepatocytes. *PLoS ONE.* (2021) 16:e0243938. doi: 10.1371/journal.pone.0243938

63. Lu X, Yang X, Liu J. Differential control of ATGL-mediated lipid droplet degradation by CGI-58 and G0S2. *Cell Cycle.* (2010) 9:2719–25. doi: 10.4161/cc.9.14.12181

64. Jebessa ZH, Shanmukha KD, Dewenter M, Lehmann LH, Xu C, Schreiter F, et al. The lipid droplet-associated protein ABHD5 protects the heart through proteolysis of HDAC4. *Nat Metab.* (2019) 1:1157–67. doi: 10.1038/s42255-019-0138-4

65. Xie X, Tie YF, Lai S, Zhang YL Li HH, Liu Y. Cardiac-specific CGI-58 deficiency activates the ER stress pathway to promote heart failure in mice. *Cell Death Dis.* (2021) 12:1003. doi: 10.1038/s41419-021-04282-7

66. Li S, Zhang L, Ni R, Cao T, Zheng D, Xiong S, et al. Disruption of calpain reduces lipotoxicity-induced cardiac injury by preventing endoplasmic reticulum stress. *Biochim Biophys Acta.* (2016) 1862:2023–33. doi: 10.1016/j.bbadis.2016.08.005

67. Otoda T, Takamura T, Misu H, Ota T, Murata S, Hayashi H, et al. Proteasome dysfunction mediates obesity-induced endoplasmic reticulum stress and insulin resistance in the liver. *Diabetes.* (2013) 62:811–24. doi: 10.2337/db11-1652

68. Akoumi A, Haffar T, Mousterji M, Kiss RS, Bousette N. Palmitate mediated diacylglycerol accumulation causes endoplasmic reticulum stress, Plin2 degradation, and cell death in H9C2 cardiomyoblasts. *Exp Cell Res.* (2017) 354:85–94. doi: 10.1016/j.yexcr.2017.03.032

69. Zou L, Li X, Wu N, Jia P, Liu C, Jia D. Palmitate induces myocardial lipotoxic injury via the endoplasmic reticulum stressmediated apoptosis pathway. *Mol Med Rep.* (2017) 16:6934–9. doi: 10.3892/mmr.2017.7404

70. Park M, Sabetski A, Kwan Chan Y, Turdi S, Sweeney G. Palmitate induces ER stress and autophagy in H9c2 cells: implications for apoptosis and adiponectin resistance. *J Cell Physiol.* (2015) 230:630–9. doi: 10.1002/jcp.24781

71. Cheng L, Ding G, Qin Q, Huang Y, Lewis W, He N, et al. Cardiomyocyte-restricted peroxisome proliferator-activated receptor-delta deletion perturbs myocardial fatty acid oxidation and leads to cardiomyopathy. *Nat Med.* (2004) 10:1245–50. doi: 10.1038/nm1116

72. Palomer X, Capdevila-Busquets E, Botteri G, Salvado L, Barroso E, Davidson MM, et al. PPARbeta/delta attenuates palmitate-induced endoplasmic reticulum stress and induces autophagic markers in human cardiac cells. *Int J Cardiol.* (2014) 174:110–8. doi: 10.1016/j.ijcard.2014.03.176

73. Zuo A, Zhao X, Li T, Li J, Lei S, Chen J, et al. CTRP9 knockout exaggerates lipotoxicity in cardiac myocytes and high-fat diet-induced cardiac hypertrophy through inhibiting the LKB1/AMPK pathway. *J Cell Mol Med.* (2020) 24:2635–47. doi: 10.1111/jcmm.14982

74. De Matteis MA, Luini A. Exiting the Golgi complex. *Nat Rev Mol Cell Biol.* (2008) 9:273–84. doi: 10.1038/nrm2378

75. Sasaki K, Yoshida H. Golgi stress response and organelle zones. *FEBS Lett.* (2019) 593:2330–40. doi: 10.1002/1873-3468.13554

76. Xu J, Huang X. Lipid metabolism at membrane contacts: dynamics and functions beyond lipid homeostasis. *Front Cell Dev Biol.* (2020) 8:615856. doi: 10.3389/fcell.2020.615856

77. Thelen AM, Zoncu R. Emerging roles for the lysosome in lipid metabolism. *Trends Cell Biol.* (2017) 27:833–50. doi: 10.1016/j.tcb.2017.07.006

78. Bankaitis VA, Garcia-Mata R, Mousley CJ. Golgi membrane dynamics and lipid metabolism. *Curr Biol.* (2012) 22:R414–24. doi: 10.1016/j.cub.2012.03.004

79. Fan YQ, Wang YH, Shao YY, Shao XT, Hu J, Xu CQ, et al. [Exogenous spermine alleviates myocardial injury induced by hyperglycemia by inhibiting golgi stress]. *Zhongguo Ying Yong Sheng Li Xue Za Zhi.* (2019) 35:385–9. doi: 10.12047/j.cjap.5795.2019.082

80. Thorne RF, Ralston KJ, de Bock CE, Mhaidat NM, Zhang XD, Boyd AW, et al. Palmitoylation of CD36/FAT regulates the rate of its post-transcriptional processing in the endoplasmic reticulum. *Biochim Biophys Acta.* (2010) 1803:1298–307. doi: 10.1016/j.bbamcr.2010.07.002

81. Beller M, Sztalryd C, Southall N, Bell M, Jackle H, Auld DS, et al. COPI complex is a regulator of lipid homeostasis. *PLoS Biol.* (2008) 6:e292. doi: 10.1371/journal.pbio.0060292

82. Wang T, Wei Q, Liang L, Tang X, Yao J, Lu Y, et al. OSBPL2 Is Required for the BInding of COPB1 to ATGL and the regulation of lipid droplet lipolysis. *iScience.* (2020) 23:101252. doi: 10.1016/j.isci.2020.101252

83. Ellong EN, Soni KG, Bui QT, Sougrat R, Golinelli-Cohen MP, Jackson CL. Interaction between the triglyceride lipase ATGL and the Arf1 activator GBF1. *PLoS One.* (2011) 6:e21889. doi: 10.1371/journal.pone.0021889

84. Soni KG, Mardones GA, Sougrat R, Smirnova E, Jackson CL, Bonifacino JS. Coatomer-dependent protein delivery to lipid droplets. *J Cell Sci.* (2009) 122(Pt 11):1834-41. doi: 10.1242/jcs.045849

85. Wilfling F, Thiam AR, Olarte MJ, Wang J, Beck R, Gould TJ, et al. Arf1/COPI machinery acts directly on lipid droplets and enables their connection to the ER for protein targeting. *Elife.* (2014) 3:e01607. doi: 10.7554/eLife.01607

86. Kim J, Kim H, Noh SH, Jang DG, Park SY, Min D, et al. Grasp55(-/-) mice display impaired fat absorption and resistance to high-fat diet-induced obesity. *Nat Commun.* (2020) 11:1418. doi: 10.1038/s41467-020-14912-x

87. Wang X, Wang H, Xu B, Huang D, Nie C, Pu L, et al. Receptor-mediated ER export of lipoproteins controls lipid homeostasis in mice and humans. *Cell Metab.* (2021) 33:350–66. doi: 10.1016/j.cmet.2020.10.020

88. Liu L, Cai J, Wang H, Liang X, Zhou Q, Ding C, et al. Coupling of COPII vesicle trafficking to nutrient availability by the IRE1alpha-XBP1s axis. *Proc Natl Acad Sci USA.* (2019) 116:11776–85. doi: 10.1073/pnas.1814480116

89. Jones B, Jones EL, Bonney SA, Patel HN, Mensenkamp AR, Eichenbaum-Voline S, et al. Mutations in a Sar1 GTPase of COPII vesicles are associated with lipid absorption disorders. *Nat Genet.* (2003) 34:29–31. doi: 10.1038/ng1145

90. Padron-Barthe L, Villalba-Orero M, Gomez-Salinero JM, Acin-Perez R, Cogliati S, Lopez-Olaneta M, et al. Activation of serine one-carbon metabolism by calcineurin abeta1 reduces myocardial hypertrophy and improves ventricular function. *J Am Coll Cardiol.* (2018) 71:654–67. doi: 10.1016/j.jacc.2017.11.067

91. Zhang L, Ussher JR, Oka T, Cadete VJ, Wagg C, Lopaschuk GD. Cardiac diacylglycerol accumulation in high fat-fed mice is associated with

impaired insulin-stimulated glucose oxidation. *Cardiovasc Res.* (2011) 89:148–56. doi: 10.1093/cvr/cvq266

92. Zheng P, Xie Z, Yuan Y, Sui W, Wang C, Gao X, et al. Plin5 alleviates myocardial ischaemia/reperfusion injury by reducing oxidative stress through inhibiting the lipolysis of lipid droplets. *Sci Rep.* (2017) 7:42574. doi: 10.1038/srep42574

93. He Q, Liu H, Deng S, Chen X, Li D, Jiang X, et al. The golgi apparatus may be a potential therapeutic target for apoptosis-related neurological diseases. *Front Cell Dev Biol.* (2020) 8:830. doi: 10.3389/fcell.2020.00830

94. Alborzinia H, Ignashkova TI, Dejure FR, Gendarme M, Theobald J, Wolfl S, et al. Golgi stress mediates redox imbalance and ferroptosis in human cells. *Commun Biol.* (2018) 1:210. doi: 10.1038/s42003-018-0212-6

frontiers | Frontiers in Cardiovascular Medicine

TYPE Original Research
PUBLISHED 13 October 2022
DOI 10.3389/fcvm.2022.965995

OPEN ACCESS

EDITED BY
Wei Liu,
The University of Manchester,
United Kingdom

REVIEWED BY
Giuseppe Mandraffino,
University of Messina, Italy
Jin Liu,
Duke-NUS Medical School, Singapore

*CORRESPONDENCE
Yi-Da Tang
tangyida@bjmu.edu.cn

†These authors have contributed equally to this work and share first authorship

SPECIALTY SECTION
This article was submitted to Cardiovascular Metabolism, a section of the journal Frontiers in Cardiovascular Medicine

RECEIVED 10 June 2022
ACCEPTED 20 September 2022
PUBLISHED 13 October 2022

CITATION
Chen K, Zheng J, Shao C, Zhou Q, Yang J, Huang T and Tang Y-D (2022) Causal effects of genetically predicted type 2 diabetes mellitus on blood lipid profiles and concentration of particle-size-determined lipoprotein subclasses: A two-sample Mendelian randomization study.
Front. Cardiovasc. Med. 9:965995.
doi: 10.3389/fcvm.2022.965995

Causal effects of genetically predicted type 2 diabetes mellitus on blood lipid profiles and concentration of particle-size-determined lipoprotein subclasses: A two-sample Mendelian randomization study

Ken Chen[1,2†], Jilin Zheng[1†], Chunli Shao[1,3,4], Qing Zhou[3,4], Jie Yang[3,4], Tao Huang[1,5,6,7] and Yi-Da Tang[1,3,4*]

[1]Key Laboratory of Molecular Cardiovascular Sciences, Department of Cardiology, Institute of Vascular Medicine, Ministry of Education, Peking University Third Hospital, Beijing, China, [2]Department of Cardiology, Xinhua Hospital, Shanghai Jiaotong University School of Medicine, Shanghai, China, [3]Department of Cardiology, State Key Laboratory of Cardiovascular Disease, Fuwai Hospital, National Center for Cardiovascular Diseases, Chinese Academy of Medical Sciences and Peking Union Medical College, Beijing, China, [4]Graduate School of Peking Union Medical College, Chinese Academy of Medical Sciences and Peking Union Medical College, Beijing, China, [5]Department of Epidemiology and Biostatistics, School of Public Health, Peking University, Beijing, China, [6]Department of Global Health, School of Public Health, Peking University, Beijing, China, [7]Center for Intelligent Public Health, Institute for Artificial Intelligence, Peking University, Beijing, China

Background: Observational studies have shown inconsistent results of the associations between type 2 diabetes mellitus (T2DM) and blood lipid profiles, while there is also a lack of evidence from randomized controlled trials (RCTs) for the causal effects of T2DM on blood lipid profiles and lipoprotein subclasses.

Objectives: Our study aimed at investigating the causal effects of T2DM on blood lipid profiles and concentration of particle-size-determined lipoprotein subclasses by using the two-sample Mendelian randomization (MR) method.

Methods: We obtained genetic variants for T2DM and blood lipid profiles including high-density lipoprotein-cholesterol (HDL-C), low-density lipoprotein-cholesterol (LDL-C), triglycerides (TG), and total cholesterol (TC) from international genome-wide association studies (GWASs). Two-sample MR method was applied to explore the potential causal effects of genetically predicted T2DM on blood lipid profiles based on different databases, respectively, and results from each MR analysis were further meta-analyzed to obtain the summary results. The causal effects of genetically predicted T2DM on the concentration of different subclasses of lipoproteins that are determined by particle size were also involved in MR analysis.

Results: Genetically predicted 1-unit higher log odds of T2DM had a significant causal effect on a higher level of TG (estimated β coefficient: 0.03, 95% confidence interval [CI]: 0.00 to 0.06) and lower level of HDL-C (estimated β coefficient: −0.09, 95% CI: −0.11 to −0.06). The causality of T2DM on the level of TC or LDL-C was not found (estimated β coefficient: −0.01, 95% CI: −0.02 to 0.01 for TC and estimated β coefficient: 0.01, 95% CI: −0.01 to 0.02 for LDL-C). For different sizes of lipoprotein particles, 1-unit higher log odds of T2DM was causally associated with higher level of small LDL particles, and lower level of medium HDL particles, large HDL particles, and very large HDL particles.

Conclusion: Evidence from our present study showed causal effects of T2DM on the level of TG, HDL-C, and concentration of different particle sizes of lipoprotein subclasses comprehensively, which might be particularly helpful in illustrating dyslipidemia experienced by patients with T2DM, and further indicate new treatment targets for these patients to prevent subsequent excessive cardiovascular events from a genetic point of view.

KEYWORDS

type-2 diabetes, dyslipidemia, cardiovascular disease, Mendelian randomization, triglyceride, high-density lipoprotein (HDL)

Introduction

Type 2 diabetes mellitus (T2DM), a global serious condition with reduced quality of life and life expectancy, is expected to reach 550 million people by 2030 (1), and the estimated global health expenditure on T2DM will be $490 billion in 2030 (2). The mortality of cardiovascular disease (CVD) in patients with T2DM was 2–4 times higher compared with non-diabetic population (3, 4). These observational studies arouse the recognition of T2DM as an essential risk factor for CVD.

Dyslipidemia, one of the key cardiometabolic risk factors, was found to be associated with excessive CVD risk in patients with T2DM (5). Dyslipidemia included disorders of high-density lipoprotein-cholesterol (HDL-C), low-density lipoprotein-cholesterol (LDL-C), very low-density lipoprotein-cholesterol (VLDL-C), triglycerides (TG) and total cholesterol (TC). Among these blood lipid profiles, LDL-C was proved to be a major atherogenic lipoprotein which was also a key risk factor for CVD. Reducing the level of LDL-C of patients with T2DM showed significant benefit in CVD risk reduction according to previous randomized controlled trials (RCTs) (6, 7), while evidence supporting the benefits of control of other blood lipid profiles was inadequate. Only LDL-C lowering treatment was recommended by current guidelines to reduce the excessive risk of CVD among patients with T2DM (8–10). However, the Framingham Heart Study found no statistically significant difference in the level of LDL-C and TC in patients with T2DM compared to those without T2DM. Significantly higher level of TG and lower level of HDL-C were found among patients with T2DM compared to patients with non-diabetes instead (11), which were further supported by subsequent observational studies (12–15). The above studies indicated that the efficacy of lowering LDL-C to attenuate excessive CVD risk among patients with T2DM still needs to be reconfirmed, while potential effects of other types of lipid profiles on excessive CVD risk should be taken into consideration seriously. In addition, as the technology of lipoprotein profiling advanced in recent years, measuring the concentration of lipoprotein particles and sub-particles that are related to cardiometabolic risks might provide better predictors of CVD risks among patients with T2DM than traditional lipid panels (16–18). However, the previous observational studies only displayed the associations of T2DM with alterations of blood lipid profiles, without uncovering the causal effects of T2DM on various blood lipid profiles and different sizes of lipoproteins sub-particles remained largely unexamined.

Mendelian randomization (MR) is a genetic epidemiological method to explore the causality of an exposure on an outcome using genetic variants as instrumental variables (19). Unlike observational studies which are more prone to be biased by reverse causality, measurement error, and other confounding factors, the genetic variants used in MR were determined at conception which had lifelong influence and thus could largely avoid reverse causality and other confounding factors. MR could provide efficient and robust results that closely resemble those of RCTs as nature's randomized trials as there is currently a lack of well-conducted, high-quality RCTs through which to investigate the causal relationships of T2DM and blood lipid profiles.

Therefore, to provide more efficient and precise treatment strategies to reduce the excessive CVD risk in patients with T2DM, we conducted a two-sample MR study by analyzing genome-wide association studies (GWASs) summary statistics from international genetic consortia to further explore the

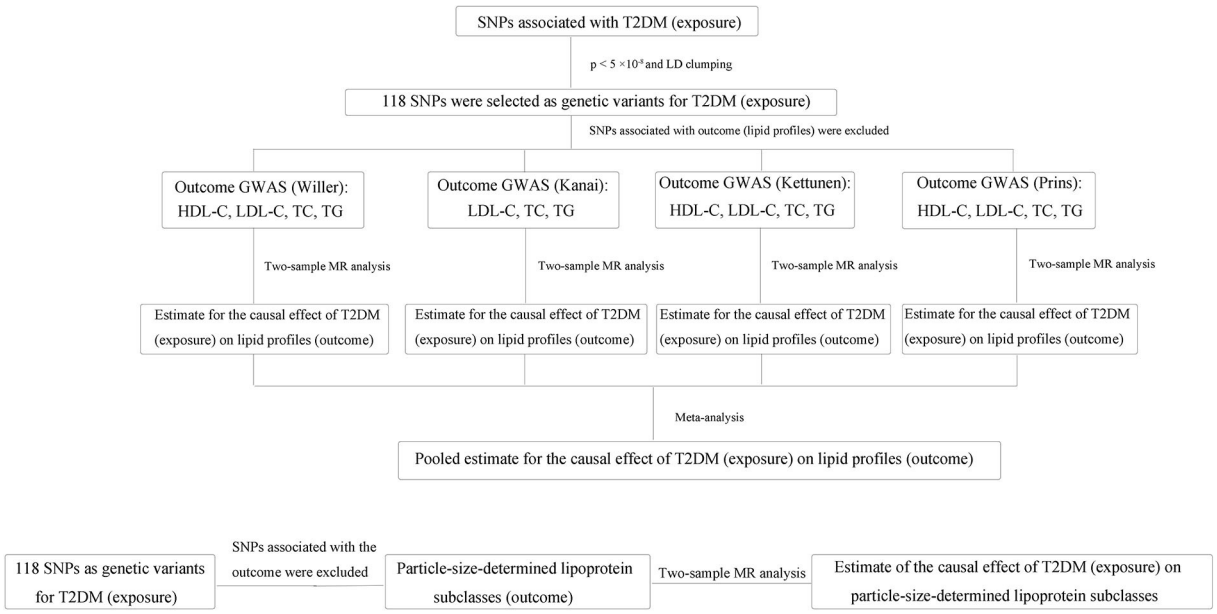

FIGURE 1
Flow diagram of the overview of our study design. First, we conducted a two-sample MR study to investigate the potential causal effects of genetically predicted T2DM on genetically predicted blood lipid profiles according to different large GWAS data resources, respectively. Then, we performed the overall meta-analysis to obtain the summary results by meta-analyzing each MR result to determine those causal effects more comprehensively across different data sources. In addition, the estimates of the causal effect of T2DM on each particle-size-determined lipoprotein subclass were also made via the two-sample MR method. SNP, single-nucleotide polymorphism; T2DM, type 2 diabetes mellitus; GWAS, genome-wide association study; HDL, high-density lipoprotein; LDL, low-density lipoprotein; TC, total cholesterol; TG, triglycerides; MR, Mendelian randomization.

potential causal effects of genetically predicted T2DM on genetically predicted various blood lipid profiles as well as genetically determined different particle sizes of lipoproteins.

Methods

Overall study design

First, we conducted a two-sample MR study by using genetic instrumental variables as proxies for T2DM and blood lipid profiles to investigate the potential causal effects of genetically predicted T2DM on genetically predicted blood lipid profiles according to different large GWAS data resources, respectively. Then, we performed an overall meta-analysis to obtain the summary results by meta-analyzing each MR result to determine those causal effects more comprehensively across different data sources. An overview of our study design is shown in Figure 1.

Data sources

Genetic instrumental variable for T2DM

We searched GWAS summarized data and extracted 143 single-nucleotide polymorphisms (SNPs) from the latest analysis including 62,892 patients with T2DM and 596,424 controls of European ancestry (20). Among these SNPs, 118 were finally used for genetic variants for T2DM which met the standard of genome-wide significance (p-value$<5 \times 10^{-8}$) and not in linkage disequilibrium ($r^2 < 0.001$). The analysis we selected was larger in scale than previous studies and explained 10% of the heritability of T2DM (20) which was almost two times than previous GWAS (21–23). Genetic variants used as proxies for T2DM in our study are shown in Supplementary Table 1.

GWAS summary statistics for blood lipid profiles

Genome-wide association studies' summary statistics for HDL-C, LDL-C, TC, and TG were obtained from various sources including: (1) a GWAS including 1,88,578 European ancestry individuals and 7,898 non-European ancestry individuals (24); (2) 24,925 European ancestry participants from a GWAS (25); (3) 9,961 European ancestry individuals from the UK Household Longitudinal Study (26); and (4) a GWAS including 1,62,255 Asian ancestry individuals (27). The GWAS including 24,925 individuals further categorized LDL and HDL according to the particle size of lipoproteins, and we took each category

TABLE 1 Summary information of GWAS for blood lipid profiles.

	Author	Sample size	Ancestry
1	Willer et al. (24)	18,8,578	Mostly European
2	Kettunen et al. (25)	24,925	European
3	Prins et al. (26)	9,961	European
4	Kanai et al. (27)	1,62,255	European

TABLE 2 Genetic association for the causal effect of T2DM on blood lipid profiles using IVW method in each data source.

Author		β	SE	*P*-value
Willer	HDL-C	−0.07	0.02	<0.001
	LDL-C	0.01	0.01	0.418
	TC	6.04×10^{-04}	0.02	0.969
	TG	0.05	0.03	0.09
Kettunen	HDL-C	−0.08	0.02	<0.001
	LDL-C	0.02	0.02	0.146
	TC	5.25×10^{-03}	0.02	0.782
	TG	0.06	0.03	0.02
Prins	HDL-C	−0.15	0.03	<0.001
	LDL-C	−0.07	0.03	0.008
	TC	−0.06	0.03	0.025
	TG	0.14	0.03	<0.001
Kanai	LDL-C	3.00×10^{-04}	0.01	0.974
	TC	-4.89×10^{-03}	0.01	0.625
	TG	−0.02	0.03	0.41

T2DM, Type 2 diabetes mellitus; IVW, inverse variance weighted; HDL, high-density lipoprotein; LDL, low-density lipoprotein; TC, total cholesterol; TG, triglycerides; SE, standard error.

(e.g., small LDL, medium LDL, and large LDL) into subsequent subgroup analysis. Summary information of the GWAS sources for outcomes in our study are shown in Table 1.

Statistical analysis

All the analyses in our study were performed by using R version 4.0.3 (The R Foundation for Statistical Computing) through TwoSampleMR and Meta package.

Mendelian randomization

The MR method used in our study was based on three assumptions: (1) the genetic variants used as instrumental variables are associated with the exposure; (2) the genetic variants are not associated with other confounders; and (3) the genetic variants are only associated with the outcome through the exposure (28). In addition, estimated SNPs were used to calculate the causal effects of exposure (genetically predicted T2DM) on the outcome (genetically predicted level of blood lipid profiles and concentration of particle-size-determined lipoprotein subclasses) using an inverse-variance weighted (IVW) which combined the estimates from each SNP based on summarized GWAS database. For binary exposure (T2DM), MR estimates are odds ratios (ORs) per genetically predicted unit difference in log odds of having the relevant exposure (T2DM). Thus, causal estimates are presented as the association of one unit genetically predicted higher log odds of T2DM with genetically predicted levels of various blood lipid profiles and concentration of particle-size-determined lipoprotein subclasses. We scaled genetically predicted effect size of the genetic variant of exposure (T2DM) on the continuous outcome (levels of various blood lipid profiles and concentrations of particle-size-determined lipoprotein subclasses) as one copy addition of the effect allele of exposure on standard deviation units difference in outcome according to the database resources we referred to. IVW method was applied as the main analysis because of its efficiency, but it must satisfy all three assumptions for MR (29). Results of IVW were expressed as estimated β coefficient, standard error, 95% confidence interval (CI) keeping two decimals and *p*-value. *P*-value <0.05 indicates statistical significance. It is noteworthy that even one invalid genetic instrument may cause bias for IVW results (29). In addition, if the strength of genetic variants is not strong enough, this "weak instrument bias" may also cause bias. Besides, horizontal pleiotropy may also greatly influence the results of IVW. Therefore, we applied multiple sensitivity analyses to evaluate those possible biases.

MR sensitivity analysis

We performed various MR sensitivity analyses to testify whether our results were influenced by the violation of the three assumptions of MR. F-statistic for each SNP was calculated to examine whether weak instrument bias might influence IVW results. F-statistic larger than 10 indicates less prone to weak instrument bias (30). Simple median estimator and weighted median estimator analysis were also performed and the estimated results would be consistent with IVW if at least more than half of the genetic variants were valid. Briefly speaking, a simple median can be regarded as a certain situation that weighted median estimators have equal weights (31). We applied the weighted median method to explore whether the results of IVW were influenced by an invalid instrument. The *p*-value of both IVW and weighted median was <0.05, indicating that the result of IVW was not likely to be influenced by invalid instrument bias. MR-Egger regression and the intercept of MR-Egger estimates the horizontal pleiotropy which is the main source of bias for MR studies (32). The *p*-value of MR-Egger regression larger than 0.05 indicated

horizontal pleiotropy, and the *p*-value of MR-Egger intercept suggested whether such pleiotropy was statistically significant. Mendelian randomization pleiotropy residual sum and outlier (MR-PRESSO) was designed to detect and correct for pervasive horizontal pleiotropy (33). A unique test in MR-PRESSO called "the distortion test" allows it to evaluate whether the difference between the causal estimate before and after the removal of outliers is significant. Whether our results were influenced by horizontal pleiotropy was carefully examined according to the results of MR-Egger regression, MR-Egger intercept, and MR-PRESSO. Besides, we still applied single-SNP analysis to identify the association between each genetic variant and the outcome and leave-one-out analysis to explore whether the causality of the exposure on the outcome is mainly credited to a certain genetic variant. All the MR analyses were performed in the "TwoSampleMR" package in R software.

Meta-analysis of the estimates from various outcome sources

We performed MR analyses to identify the causality of T2DM on each blood lipid profile according to each outcome source, respectively, and these results were further meta-analyzed to obtain the pooled estimates for the causality of T2DM on each blood lipid profile. I^2 statistics were calculated to quantify the heterogeneity between estimates from different outcome sources. All meta-analyses were performed using the "Meta" package in R software.

Results

Pooled estimate of the causal effect of T2DM on blood lipid profiles

Estimate of the causal effect of T2DM on each data source was made individually and details are shown in Supplementary Tables 2–16, and genetic association for the causal effect of T2DM on blood lipid profiles using the IVW method in each data source is shown in Table 2. Pooled β for HDL-C, LDL-C, TC, and TG per unit increase in log odds of T2DM was −0.09 (95% CI: −0.11 to −0.06, I^2 = 62%, *p*-value = 0.07), 0.00 (95% CI: −0.03 to 0.02, I^2 = 67%, *p*-value = 0.03), −0.01 (95% CI: −0.02 to 0.01, I^2 = 35%, *p*-value = 0.20), and 0.06 (95% CI: −0.01 to 0.12, I^2 = 80%, *p*-value < 0.01), respectively (Figure 2). Random-effect model meta-analyses were used due to the heterogeneity across databases in terms of LDL-C and TG when pooling the primary analyses results using the IVW method. Fix-effect model meta-analyses were used because the heterogeneity in terms of HDL-C and

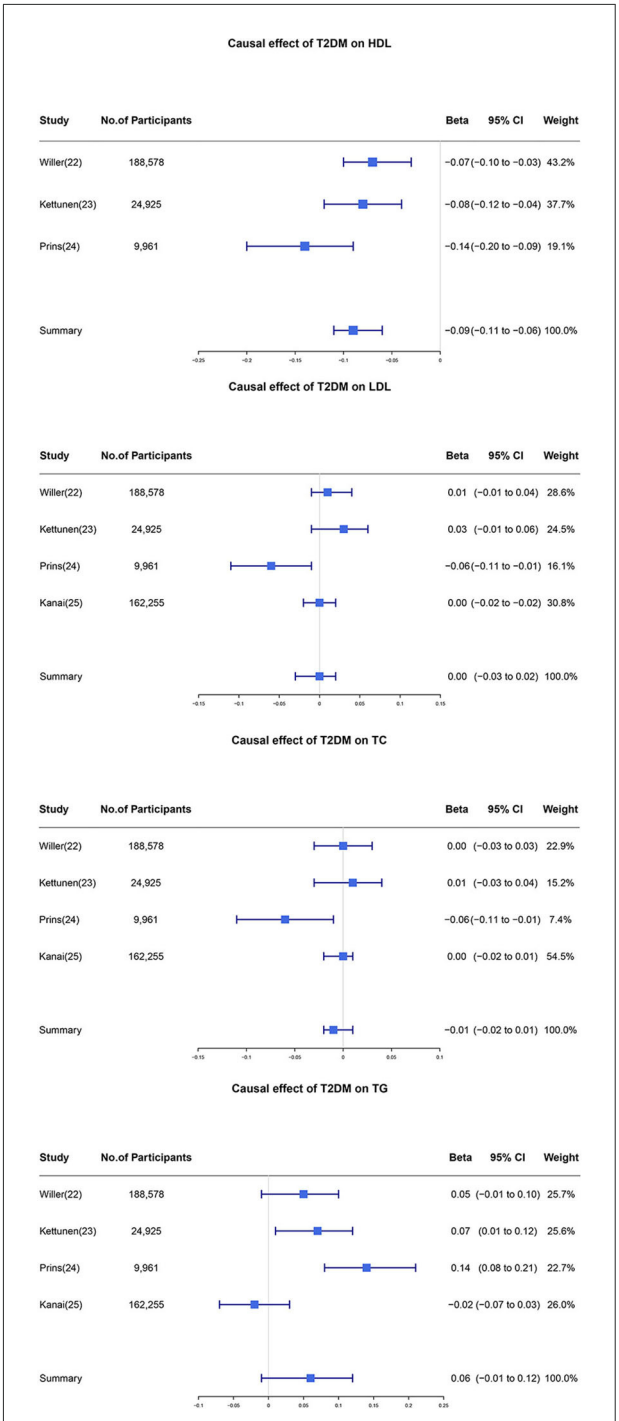

FIGURE 2
Individual and pooled estimate of the causal effect of T2DM on each blood lipid profile. Firstly we applied the two-sample MR method to estimate the causal effect of T2DM on each blood lipid profile. Then these individual estimates were further meta-analyzed to obtain the pooled results. T2DM, type 2 diabetes mellitus; HDL, high-density lipoprotein; LDL, low-density lipoprotein; TC, total cholesterol; TG, triglycerides; CI, confidence interval.

TC was minor across databases when the primary analyses were pooled using the IVW method.

Sensitivity analysis for heterogeneity

We noticed that the I^2 statistics for pooled β in regard to LDL-C and TG were larger than 50% with a p-value <0.05. After performing the senstivity analysis, we identified that the source of heterogeneity was mainly from the UK Household Longitudinal Study. After removing the data from the UK Household Longitudinal Study, pooled β for LDL-C and TG were 0.01 (95% CI: −0.01 to 0.02, I^2 = 0%, p-value = 0.44) and 0.03 (95% CI: 0.00 to 0.06, I^2 = 66%, p-value = 0.06), respectively (Figure 3). Overall, our results showed that one unit higher log odds of T2DM was associated with lower level of HDL-C and higher level of TG. Pooled β did not support the causality of T2DM on TC and LDL-C levels.

Estimate of the causal effect of T2DM on different sizes of HDL and LDL particles

Our study further categorized HDL particles and LDL particles into subgroups to investigate whether T2DM had different causal effects on the levels of different particle sizes. Results showed that T2DM had causal effects on the level of medium HDL particles (β: −0.04, 95% CI: −0.08 to −0.01, p-value = 0.019), large HDL particles (β: −0.09, 95% CI: −0.13 to −0.05, p-value < 0.001), and very large HDL particles (β: −0.05, 95% CI: −0.08 to −0.01, p-value = 0.016). In addition, the causality of T2DM on the level of small LDL particles was also found (β: 0.04, 95% CI: 0.00 to 0.08, p-value = 0.048). However, the causal effects of T2DM on the level of small HDL particles or large LDL or medium LDL-C particles were not found (p-value > 0.05) (Figure 4).

MR sensitivity analyses

In MR sensitivity analyses, F-statistics of genetic variants for T2DM in our study was larger than 10 which indicated that genetic variants included in our study were strong enough to avoid weak instrument bias.

For the estimate of the causality of T2DM on the level of HDL-C (data source: Kettunen et.al), the MR-Egger intercept was non-zero with a p-value larger than 0.05, and the p-value for the distortion test of MR-PRESSO was larger than 0.05, which both indicated that the influence of horizontal pleiotropy was not statistically significant, and the difference between before and after removing outliers which caused horizontal pleiotropy was also not statistically significant either. In addition, the p-value for weighted median was <0.05 which was also consistent with the IVW method. Thus, we reckon that the estimate of the causal effect of T2DM on the level of HDL-C (data source: Kettunen) based on IVW results was robust.

Likewise, for the estimate of the causality of T2DM on the level of LDL-C (data source: Kanai, Kettunen, Willer), TC (data source: Kanai, Kettunen, Willer), TG (data source:Kanai, Willer), results of MR sensitivity analyses showed no horizontal pleiotropy, while for the estimate of the causality of T2DM on the level of LDL-C (data source: Prins), TC (data source: Prins), TG (data source: Kettunen, Prins), and MR sensitivity analyses indicated that the influence of horizontal pleiotropy on our results was not statistically significant either.

Results of single-SNP analyses and leave-one-out analyses were also consistent with our main analyses. The only exception was the estimate of the causality of T2DM on the level of HDL-C (data source: Prins), for the p-value of MR-Egger regression and distortion test in MR-PRESSO was both <0.05, thus we reckon that IVW results might be influenced by horizontal pleiotropy which we further discussed in the limitation part. Details of MR sensitivity analyses are shown in Supplementary Tables 24–69.

Discussion

In the present study, we explored the causal effect of T2DM on blood lipid profiles and found that one additional unit of log odds of T2DM was causally associated with a 4% higher level of TG, 8% lower level of HDL-C, and also had significant causality on the concentration of different sizes of HDL and LDL lipoprotein particles. The above blood lipid profiles causally influenced by T2DM might be more specifically responsible for the excessive CVD risk among patients with T2DM, and new treatments may be developed to target these blood lipid alterations to further reduce secondary CVD risk among patients with T2DM.

As MR studies that explored the potential causal effects of T2DM on blood lipid profiles were lacking and RCTs were also scarce due to the difficulties in design and ethics, thus previous research which illustrated the relationship between T2DM and blood lipid profiles was mainly observational. Results of our study showed that T2DM had a positive causal effect on TG, and a negative causal effect on HDL-C, which were consistent with previous studies (11, 12, 15, 34–36). The causal relationship between T2DM and TC level was not found in our study which was also proved by the Framingham study (11), but there were also opposite results from comparative studies with 8-year follow-up claiming that TC levels of patients with T2DM were higher than non-diabetic participants (men: 5.84 ±

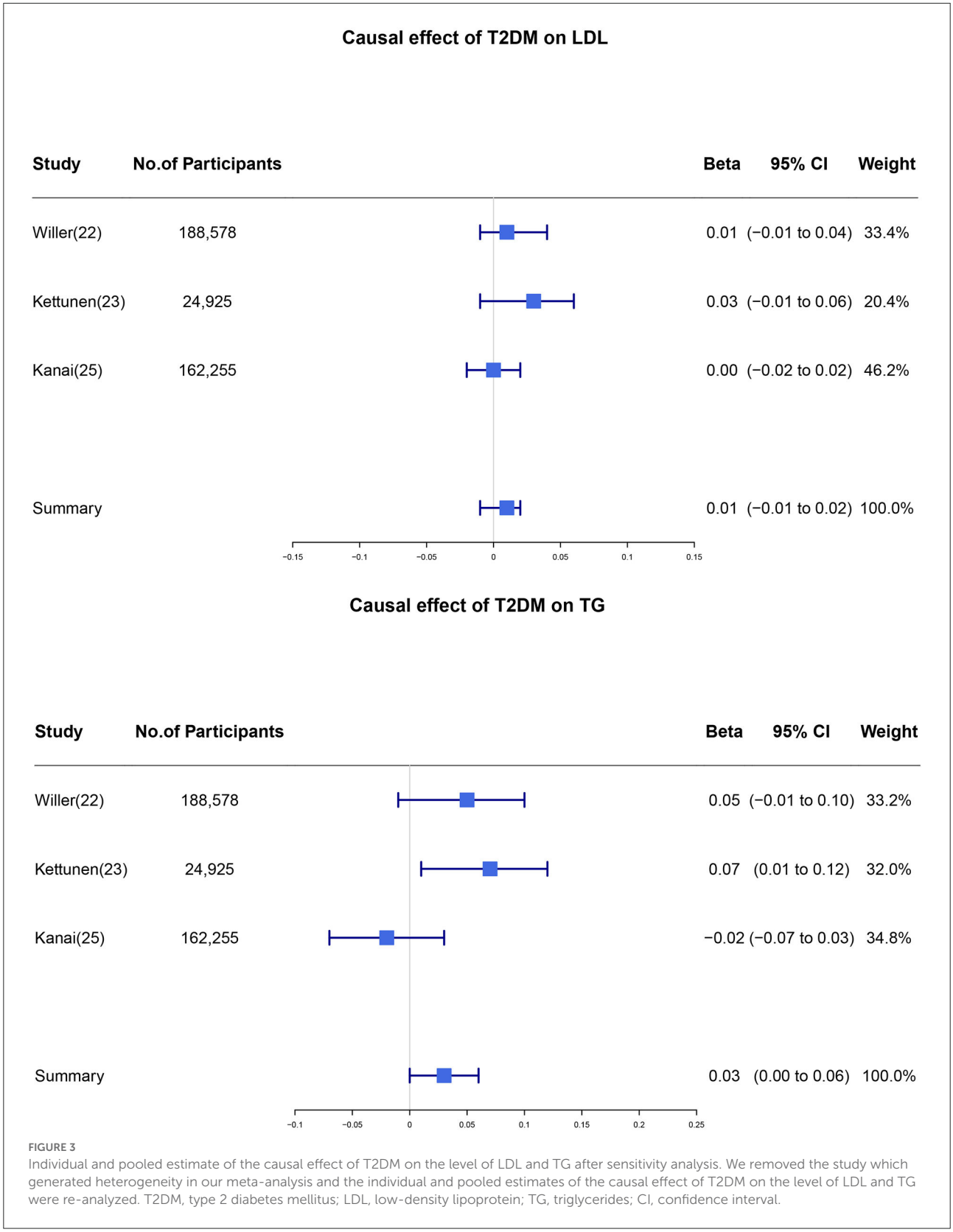

FIGURE 3
Individual and pooled estimate of the causal effect of T2DM on the level of LDL and TG after sensitivity analysis. We removed the study which generated heterogeneity in our meta-analysis and the individual and pooled estimates of the causal effect of T2DM on the level of LDL and TG were re-analyzed. T2DM, type 2 diabetes mellitus; LDL, low-density lipoprotein; TG, triglycerides; CI, confidence interval.

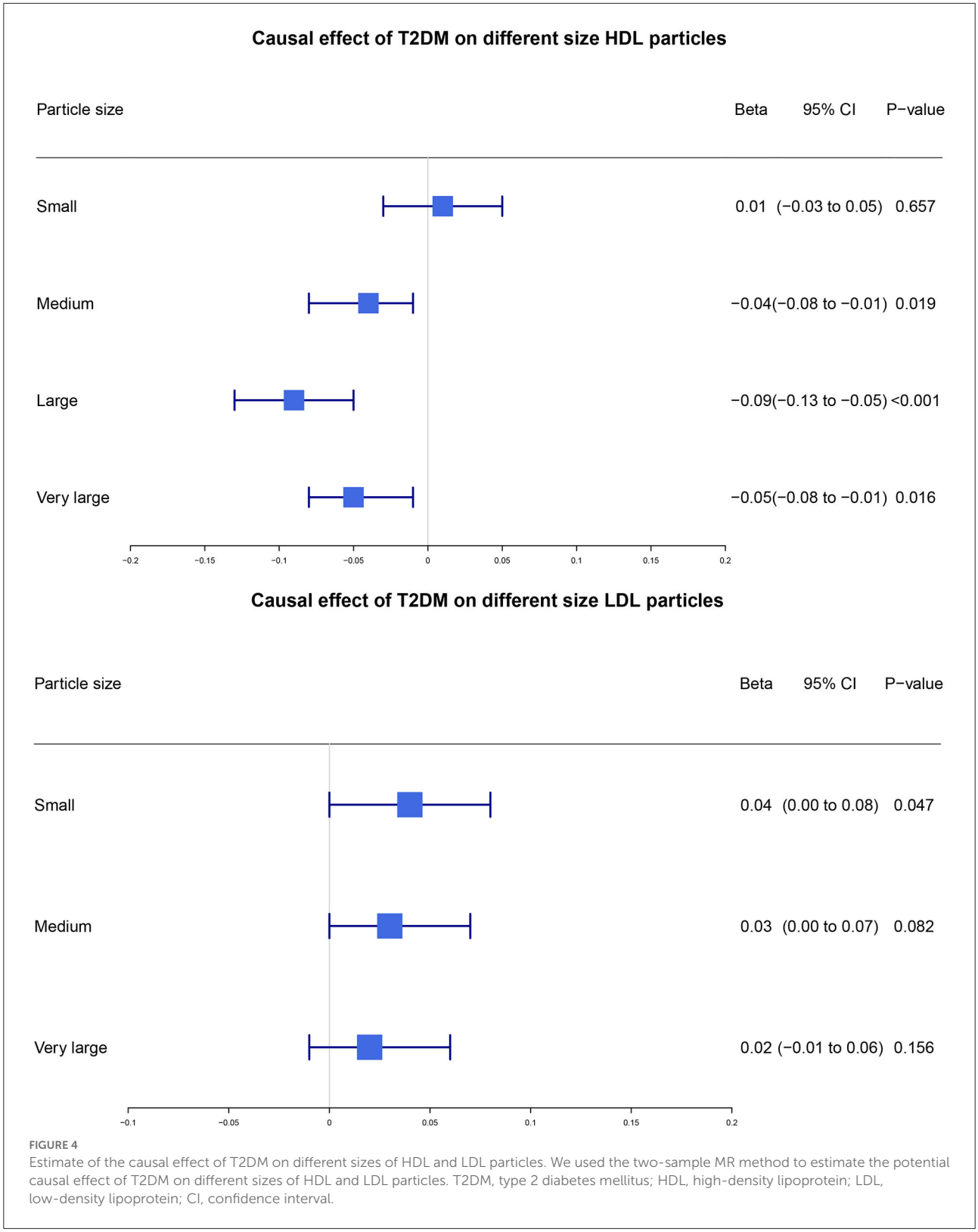

FIGURE 4
Estimate of the causal effect of T2DM on different sizes of HDL and LDL particles. We used the two-sample MR method to estimate the potential causal effect of T2DM on different sizes of HDL and LDL particles. T2DM, type 2 diabetes mellitus; HDL, high-density lipoprotein; LDL, low-density lipoprotein; CI, confidence interval.

0.18 mmol/L, women: 5.84 ± 0.18 mmol/L vs. men: 5.55 ± 0.05 mmol/L, women: 5.20 ± 0.05 mmol/L, p-value = 0.002) (12). However, this difference may be due to the limited number of participants (17 males and 26 females). Most previous studies showed normal LDL-C levels among patients with T2DM (14, 36–38). A more recent study "PROCAM" also found little difference in the occurrence of high LDL levels between patients with T2DM and non-diabetic participants (22.7 vs. 21.7%) (15).

It is particularly noteworthy that the increasing number of studies in recent years illustrated that there were little differences in LDL-C levels between diabetic and non-diabetic population; however, the level of small dense LDL particles was found to increase instead (39–44) which were in accordance with our MR results. As the increasing number of small dense LDL is the consequence of lipolysis of increasing TG-rich VLDL particles (44), it is rational to observe both the increase of small LDL particles and TG levels in our study. Recent studies have shown that increasing levels of small LDL particles were closely associated with increased risk of CVD (45, 46) and a statement also suggested that cardiovascular disease risk may be more closely related to the number of atherogenic lipoprotein particles than to LDL cholesterol (47). Thus, our MR results which further indicated significant causal effects of genetically predicted T2DM on the subclass of lipoprotein particles could provide more robust evidence for better predictors of future CVD risks than the traditional lipid panel, especially in subjects with cardiometabolic diseases such as T2DM when traditional lipid panel is relatively normal. In addition, previous observational studies also showed that medium and large HDL particles were associated with T2DM (44, 48) which is consistent with the estimated β coefficient for genetically predicted medium, large, and very large HDL particles in our study. Due to the close relationship of atherogenic lipoprotein subclass particles with non-alcoholic fatty liver disease (NAFLD) and subsequent CVD events (49–51), our results may explain the excessive CVD risk among patients with T2DM.

Including data from the UK Household Longitudinal Study in meta-analyzing pooled β for TG and LDL-C could originate significant heterogeneity in our study. After comparing with other GWAS, we found patients taking statins and other lipid-lowering treatments were excluded except for the UK Household Longitudinal Study. Therefore, it might partly explain the lower estimated β coefficient for HDL-C and higher for TG using data from the UK Household Longitudinal Study, and lower estimated β coefficient for LDL-C might be due to statin intake.

Strengths

First, to the best of our knowledge, the present study is the first MR study to identify the potential causality of T2DM on blood lipid profiles. MR studies can largely avoid bias from reverse causation, measurement error, and other unknown confoundings which are responsible for less conclusive results from observational studies. Besides, MR studies are less time-consuming, less expensive, easier to design, and with lifelong exposure compared with RCTs. Therefore, the uniqueness of MR studies makes them an effective method to explore the possible causal effect. Our MR study illustrated that T2DM had causal effects on certain types of blood lipid profiles which might provide help in exploring the complex mechanism of dyslipidemia in patients with T2DM.

Second, using MR-based statistics, we further conducted a meta-analysis to integrate different causal effects of T2DM on blood lipid profiles across distinct data resources to provide a more consolidated and desirable conclusion.

Third, the number of genetic variants used as proxies for each blood lipid profile in the present study is considerable and sensitivity analyses have confirmed the results of MR main analyses are less prone to be biased by weak instruments and less significant influence by horizontal pleiotropy, thus adding to the robustness of MR estimates. In addition, genetic variants for T2DM in the present study were identified from the latest GWAS which was larger in scale and also explained double heritability of T2DM than previous GWAS. Besides, data sources for outcomes were thoroughly searched and carefully checked for consistency, which further contributes to less heterogeneity and more reliability for final pooled MR estimates.

In addition, we further involved MR analysis for genetically predicted HDL and LDL into different subgroups according to the genetically determined size of lipoprotein particles. MR results showed the causal relationship between genetically predicted T2DM with a higher level of small LDL particles, and lower level of medium, large and very large HDL particles, which shed new light on the treatment targets to reduce the CVD risk of patients with T2DM despite the relatively normal level of LDL-C.

Last but not least, the present study design is different from normal MR studies that our individual estimates of the estimated β coefficient for each blood lipid profile were subsequently meta-analyzed to obtain a pooled estimated β coefficient from various data sources which made our results more persuasive.

Limitations

There are several limitations of our study. First of all, the number of GWAS included for each blood lipid profile is not large enough and the sample size of some GWAS was also moderate. For example, the largest GWAS included in the present study recruited 1,88,578 participants, while the sample size of the UK Household Longitudinal Study was <10,000 and the sample size of another GWAS included was merely over 20,000. Second, although the number of genetic variants used in the present study was from the latest GWAS and was far more than previous studies, they could

only explain a small proportion of T2DM heritability, leaving almost 90% unexplained. Besides, MR studies can avoid most biases affecting observational studies, but bias from horizontal pleiotropy should always be considered. Horizontal pleiotropy was generated when there were other pathways for the exposure to influence the outcome and the assumption of MR studies was violated, thus resulting in bias for MR main analysis. We have examined that most of our results were robust, while the estimate of the causal effect of T2DM on the level of HDL-C (data source: Prins) might be biased. In addition, restricted by the contradiction between the format of our data sources and the R software codes, we did not perform MR analyses that could detect correlated horizontal pleiotropy including Genome-wide mR Analysis under Pervasive PLEiotropy (GRAPPLE) (52) or Causal Analysis Using Summary Effect Estimates (CAUSE) (53). Future investigators are encouraged to apply more sensitivity analyses to detect both correlated and uncorrelated horizontal pleiotropy in order to minimize bias. Lastly, inspite of the large sample sizes of GWAS included in our study, the effect size of LDL-C and TC was rather small; thus, we could not completely rule out the causality of T2DM on LDL-C and TC. More large-scale GWAS and well-conducted observational studies are expected in future to provide more supportive evidence.

Clinical and public implications

The causal effect of T2DM on LDL-C is still unclear and results from observational studies indicated an increase of small dense LDL-C in patients with T2DM. Results of our study were in accordance with previous studies and also found lower level of very large HDL, large HDL, and medium HDL, which might be indicative of the excessvie CVD risk of patients with T2DM. Besides, statin treatment for lowering LDL-C is widely recommended by various dyslipidemia guidelines for patients with T2DM. The 2016 ESC/EAS Guidelines for the Management of Dyslipidaemias regarded LDL-C as the primary target of lipid-lowering treatment among patients with T2DM (54). However, whether treatment for diabetic patients with higher TG and lower HDL-C is beneficial for CVD risk reduction remains controversial. These might be ascribable to the negative effects on reducing major cardiovascular events by using fenofibrate on patients with T2DM reported by FIELD and ACCORD studies (55, 56). The present study which was conducted in an MR framework indicated that patients with T2DM were more inclined to experience higher level of TG and lower level of HDL-C despite the relatively normal level of LDL-C. Moreover, our MR analysis also uncovered the causal effects of genetically predicted T2DM on genetically predicted atherogenic lipoprotein sub-particles. As the atherogenic lipoprotein sub-particles were closely related to cardiometabolic diseases such as NAFLD and increased subsequent risk of CVD, our results might provide new ideas for future RCTs to evaluate the impact of targeting the concentration of atherogenic lipoproteins sub-particles to attenuate CVD risk among patients with T2DM.

Conclusion

Evidence from our study supported higher level of TG and lower level of HDL-C among patients with T2DM. Moreover, T2DM was also causally associated with higher level of small LDL particles, and lower level of medium, large, and very large HDL particles. New evidence from a genetic point of view for the causality of T2DM on these blood lipid profiles and lipoprotein subclass particles based on our study might be constructive for developing new therapeutic strategies to reduce the excessive CVD risk experienced by patients with T2DM.

Data availability statement

The datasets presented in this study can be found in online repositories. The names of the repository/repositories and accession number(s) can be found in the article/Supplementary material.

Author contributions

KC and JZ contributed equally to this manuscript, performed data analysis, and wrote the manuscript. KC and Y-DT designed this study, also took responsibility for the integrity, accuracy of data analysis in this study, and are the guarantors. CS, QZ, JY, TH, and Y-DT reviewed and revised the manuscript. All authors had access to data in this study and contributed to statistical analysis and reviewing of the manuscript. All listed authors meet authorship criteria. All authors contributed to the article and approved the submitted version.

Funding

This work was supported by (1) National Key R&D Program of China (2020YFC2004700). (2) Research Unit of Medical Science Research Management/Basic and Clinical Research of Metabolic Cardiovascular Diseases from Chinese Academy of Medical Sciences (2021RU003). (3) National Natural Program (81825003). (4) Science and Technology Project of Xicheng District Finance (XCSTS-SD2021-01). (5) Basic research funds of the Central Public Welfare Research Institutes of the Chinese Academy of Medical Sciences (2018PT32032, 2018RC320014-2, and 3332019044).

Conflict of interest

The authors declare that the research was conducted in the absence of any commercial or financial relationships that could be construed as a potential conflict of interest.

Publisher's note

All claims expressed in this article are solely those of the authors and do not necessarily represent those of their affiliated organizations, or those of the publisher, the editors and the reviewers. Any product that may be evaluated in this article, or claim that may be made by its manufacturer, is not guaranteed or endorsed by the publisher.

Supplementary material

The Supplementary Material for this article can be found online at: https://www.frontiersin.org/articles/10.3389/fcvm.2022.965995/full#supplementary-material

References

1. Zimmet PZ, Magliano DJ, Herman WH, Shaw JE. Diabetes: a 21st century challenge. *Lancet Diabetes Endocrinol.* (2014) 2:56–64. doi: 10.1016/S2213-8587(13)70112-8

2. Zhang P, Zhang X, Brown J, Vistisen D, Sicree R, Shaw J, et al. Global healthcare expenditure on diabetes for 2010 and 2030. *Diabetes Res Clin Pract.* (2010) 87:293–301. doi: 10.1016/j.diabres.2010.01.026

3. Sarwar N, Gao P, Seshasai SR, Gobin R, Kaptoge S, Di Angelantonio E, et al. Diabetes mellitus, fasting blood glucose concentration, and risk of vascular disease: a collaborative meta-analysis of 102 prospective studies. *Lancet.* (2010) 375:2215–22. doi: 10.1016/S0140-6736(10)60484-9

4. Coutinho M, Gerstein HC, Wang Y, Yusuf S. The relationship between glucose and incident cardiovascular events. A metaregression analysis of published data from 20 studies of 95,783 individuals followed for 124 years. *Diabetes Care.* (1999) 22:233–40. doi: 10.2337/diacare.22.2.233

5. Lu W, Resnick HE, Jablonski KA, Jones KL, Jain AK, Howard WJ, et al. Non-HDL cholesterol as a predictor of cardiovascular disease in type 2 diabetes: the strong heart study. *Diabetes Care.* (2003) 26:16–23. doi: 10.2337/diacare.26.1.16

6. Costa J, Borges M, David C, Vaz Carneiro A. Efficacy of lipid lowering drug treatment for diabetic and non-diabetic patients: meta-analysis of randomised controlled trials. *BMJ.* (2006) 332:1115–24. doi: 10.1136/bmj.38793.468449.AE

7. Kearney PM, Blackwell L, Collins R, Keech A, Simes J, Peto R, et al. Efficacy of cholesterol-lowering therapy in 18,686 people with diabetes in 14 randomised trials of statins: a meta-analysis. *Lancet.* (2008) 371:117–25. doi: 10.1016/S0140-6736(08)60104-X

8. Detection E. And treatment of high blood cholesterol in adults (Adult Treatment Panel III). *Jama.* (2001) 285:2486–97. doi: 10.1001/jama.285.19.2486

9. Graham I, Atar D, Borch-Johnsen K, Boysen G, Burell G, Cifkova R, et al. European guidelines on cardiovascular disease prevention in clinical practice: executive summary: Fourth joint task force of the european society of cardiology and other societies on cardiovascular disease prevention in clinical practice (constituted by representatives of nine societies and by invited experts). *Eur Heart J.* (2007) 28:2375–414. doi: 10.1093/eurheartj/ehm316

10. Rydén L, Standl E, Bartnik M, Van den Berghe G, Betteridge J, de Boer MJ, et al. Guidelines on diabetes, pre-diabetes, and cardiovascular diseases: executive summary. The task force on diabetes and cardiovascular diseases of the European society of cardiology (ESC) and of the European association for the study of diabetes (EASD). *Eur Heart J.* (2007) 28:88–136. doi: 10.1093/eurheartjehl260

11. Kannel WB, McGee DL. Diabetes and glucose tolerance as risk factors for cardiovascular disease: the Framingham study. *Diabetes Care.* (1979) 2:120–6. doi: 10.2337/diacare.2.2.120

12. Haffner SM, Stern MP, Hazuda HP, Mitchell BD, Patterson JK. Cardiovascular risk factors in confirmed prediabetic individuals. Does the clock for coronary heart disease start ticking before the onset of clinical diabetes? *Jama.* (1990) 263:2893–8. doi: 10.1001/jama.1990.03440210043030

13. Tan CE, Chew LS, Chio LF, Tai ES, Lim HS, Lim SC, et al. Cardiovascular risk factors and LDL subfraction profile in type 2 diabetes mellitus subjects with good glycaemic control. *Diabetes Res Clin Pract.* (2001) 51:107–14. doi: 10.1016/S0168-8227(00)00211-4

14. Taskinen MR. Quantitative and qualitative lipoprotein abnormalities in diabetes mellitus. *Diabetes.* (1992) 41 Suppl 2:12–7. doi: 10.2337/diab.41.2.S12

15. Assmann G, Cullen P, Schulte H. Simple scoring scheme for calculating the risk of acute coronary events based on the 10-year follow-up of the prospective cardiovascular Münster (PROCAM) study. *Circulation.* (2002) 105:310–5. doi: 10.1161/hc0302.102575

16. Cromwell WC, Otvos JD, Keyes MJ, Pencina MJ, Sullivan L, Vasan RS, et al. LDL particle number and risk of future cardiovascular disease in the framingham offspring study—implications for LDL management. *J Clin Lipidol.* (2007) 1:583–92. doi: 10.1016/j.jacl.2007.10.001

17. Ai M, Otokozawa S, Asztalos BF, Ito Y, Nakajima K, White CC, et al. Small dense LDL cholesterol and coronary heart disease: results from the Framingham Offspring Study. *Clin Chem.* (2010) 56:967–76. doi: 10.1373/clinchem.2009.137489

18. Koba S, Hirano T, Ito Y, Tsunoda F, Yokota Y, Ban Y, et al. Significance of small dense low-density lipoprotein-cholesterol concentrations in relation to the severity of coronary heart diseases. *Atherosclerosis.* (2006) 189:206–14. doi: 10.1016/j.atherosclerosis.2005.12.002

19. Lawlor DA, Harbord RM, Sterne JA, Timpson N, Davey Smith G. Mendelian randomization: using genes as instruments for making causal inferences in epidemiology. *Stat Med.* (2008) 27:1133–63. doi: 10.1002/sim.3034

20. Xue A, Wu Y, Zhu Z, Zhang F, Kemper KE, Zheng Z, et al. Genome-wide association analyses identify 143 risk variants and putative regulatory mechanisms for type 2 diabetes. *Nat Commun.* (2018) 9:2941. doi: 10.1038/s41467-018-04951-w

21. Ahmad OS, Morris JA, Mujammami M, Forgetta V, Leong A, Li R, et al. A Mendelian randomization study of the effect of type-2 diabetes on coronary heart disease. *Nat Commun.* (2015) 6:7060. doi: 10.1038/ncomms8060

22. Larsson SC, Scott RA, Traylor M, Langenberg CC, Hindy G, Melander O, et al. Type 2 diabetes, glucose, insulin, BMI, and ischemic stroke subtypes: Mendelian randomization study. *Neurology.* (2017) 89:454–60. doi: 10.1212/WNL.0000000000004173

23. Ross S, Gerstein HC, Eikelboom J, Anand SS, Yusuf S, Paré G. Mendelian randomization analysis supports the causal role of dysglycaemia and diabetes in the risk of coronary artery disease. *Eur Heart J.* (2015) 36:1454–62. doi: 10.1093/eurheartj/ehv083

24. Willer CJ, Schmidt EM, Sengupta S, Peloso GM, Gustafsson S, Kanoni S, et al. Discovery and refinement of loci associated with lipid levels. *Nat Genet.* (2013) 45:1274–83. doi: 10.1038/ng.2797

25. Kettunen J, Demirkan A, Würtz P, Draisma HH, Haller T, Rawal R, et al. Genome-wide study for circulating metabolites identifies 62 loci and reveals novel systemic effects of LPA. *Nat Commun.* (2016) 7:11122. doi: 10.1038/ncomms11122

26. Prins BP, Kuchenbaecker KB, Bao Y, Smart M, Zabaneh D, Fatemifar G, et al. Genome-wide analysis of health-related biomarkers in the UK Household Longitudinal Study reveals novel associations. *Sci Rep.* (2017) 7:11008. doi: 10.1038/s41598-017-10812-1

27. Kanai M, Akiyama M, Takahashi A, Matoba N, Momozawa Y, Ikeda M, et al. Genetic analysis of quantitative traits in the Japanese population links cell types to complex human diseases. *Nat Genet.* (2018) 50:390–400. doi: 10.1038/s41588-018-0047-6

28. Burgess S, Thompson SG. Interpreting findings from Mendelian randomization using the MR-Egger method. *Eur J Epidemiol.* (2017) 32:377–89. doi: 10.1007/s10654-017-0255-x

29. Burgess S, Butterworth A, Thompson SG. Mendelian randomization analysis with multiple genetic variants using summarized data. *Genet Epidemiol.* (2013) 37:658–65. doi: 10.1002/gepi.21758

30. Burgess S, Thompson SG. Avoiding bias from weak instruments in Mendelian randomization studies. *Int J Epidemiol.* (2011) 40:755–64. doi: 10.1093/ije/dyr036

31. Bowden J, Davey Smith G, Haycock PC, Burgess S. Consistent estimation in Mendelian randomization with some invalid instruments using a weighted median estimator. *Genet Epidemiol.* (2016) 40:304–14. doi: 10.1002/gepi.21965

32. Bowden J, Davey Smith G, Burgess S. Mendelian randomization with invalid instruments: effect estimation and bias detection through Egger regression. *Int J Epidemiol.* (2015) 44:512–25. doi: 10.1093/ije/dyv080

33. Verbanck M, Chen CY, Neale B, Do R. Detection of widespread horizontal pleiotropy in causal relationships inferred from Mendelian randomization between complex traits and diseases. *Nat Genet.* (2018) 50:693–8. doi: 10.1038/s41588-018-0099-7

34. Monami M, Vitale V, Ambrosio ML, Bartoli N, Toffanello G, Ragghianti B, et al. Effects on lipid profile of dipeptidyl peptidase 4 inhibitors, pioglitazone, acarbose, and sulfonylureas: meta-analysis of placebo-controlled trials. *Adv Ther.* (2012) 29:736–46. doi: 10.1007/s12325-012-0045-5

35. Duvillard L, Pont F, Florentin E, Galland-Jos C, Gambert P, Vergès B. Metabolic abnormalities of apolipoprotein B-containing lipoproteins in non-insulin-dependent diabetes: a stable isotope kinetic study. *Eur J Clin Invest.* (2000) 30:685–94. doi: 10.1046/j.1365-2362.2000.00702.x

36. Taskinen MR, Nikkilä EA, Ollus A. Serum lipids and lipoproteins in insulin-dependent diabetic subjects during high-carbohydrate, high-fiber diet. *Diabetes Care.* (1983) 6:224–30. doi: 10.2337/diacare.6.3.224

37. BV H. Lipoprotein metabolism in diabetes mellitus. *J Lipid Res.* (1987) 28:613–28. doi: 10.1016/S0022-2275(20)38659-4

38. GM. R. Abnormal lipoprotein metabolism in non-insulin-dependent diabetes mellitus. Pathogenesis and treatment. *Am J Med.* (1987) 83:31-40. doi: 10.1016/0002-9343(87)90801-1

39. Garvey WT, Kwon S, Zheng D, Shaughnessy S, Wallace P, Hutto A, et al. Effects of insulin resistance and type 2 diabetes on lipoprotein subclass particle size and concentration determined by nuclear magnetic resonance. *Diabetes.* (2003) 52:453–62. doi: 10.2337/diabetes.52.2.453

40. Siegel RD, Cupples A, Schaefer EJ, Wilson PW. Lipoproteins, apolipoproteins, and low-density lipoprotein size among diabetics in the Framingham offspring study. *Metabolism.* (1996) 45:1267–72.

41. Festa A, Williams K, Hanley AJ, Otvos JD, Goff DC, Wagenknecht LE, et al. Nuclear magnetic resonance lipoprotein abnormalities in prediabetic subjects in the Insulin Resistance Atherosclerosis Study. *Circulation.* (2005) 111:3465–72. doi: 10.1161/CIRCULATIONAHA.104.512079

42. Goff DC, D'Agostino RB, Haffner SM, Otvos JD. Insulin resistance and adiposity influence lipoprotein size and subclass concentrations results from the insulin resistance atherosclerosis study. *Metabolism.* (2005) 54:264–70. doi: 10.1016/j.metabol.2004.09.002

43. Hodge AM, Jenkins AJ, English DR, O'Dea K, Giles GG. NMR-determined lipoprotein subclass profile predicts type 2 diabetes. *Diabetes Res Clin Pract.* (2009) 83:132–9. doi: 10.1016/j.diabres.2008.11.007

44. Mora S, Otvos JD, Rosenson RS, Pradhan A, Buring JE, Ridker PM. Lipoprotein particle size and concentration by nuclear magnetic resonance and incident type 2 diabetes in women. *Diabetes.* (2010) 59:1153–60. doi: 10.2337/db09-1114

45. Duran EK, Aday AW, Cook NR, Buring JE, Ridker PM, Pradhan AD. Triglyceride-rich lipoprotein cholesterol, small dense LDL cholesterol, and incident cardiovascular disease. *J Am Coll Cardiol.* (2020) 75:2122–35. doi: 10.1016/j.jacc.2020.02.059

46. Rizvi AA, Stoian AP, Janez A, Rizzo M. Lipoproteins and cardiovascular disease: an update on the clinical significance of atherogenic small, dense LDL and new therapeutical options. *Biomedicines.* (2021) 9:1579. doi: 10.3390/biomedicines9111579

47. Mora S, Otvos JD, Rifai N, Rosenson RS, Buring JE, Ridker PM. Lipoprotein particle profiles by nuclear magnetic resonance compared with standard lipids and apolipoproteins in predicting incident cardiovascular disease in women. *Circulation.* (2009) 119:931–9. doi: 10.1161/CIRCULATIONAHA.108.816181

48. Delgado-Velandia M, Gonzalez-Marrachelli V, Domingo-Relloso A, Galvez-Fernandez M, Grau-Perez M, Olmedo P, et al. Healthy lifestyle, metabolomics and incident type 2 diabetes in a population-based cohort from Spain. *Int J Behav Nutr Phys Act.* (2022) 19:8. doi: 10.1186/s12966-021-01219-3

49. Ekstedt M, Franzén LE, Mathiesen UL, Thorelius L, Holmqvist M, Bodemar G, et al. Long-term follow-up of patients with NAFLD and elevated liver enzymes. *Hepatology.* (2006) 44:865–73. doi: 10.1002/hep.21327

50. Siddiqui MS, Sterling RK, Luketic VA, Puri P, Stravitz RT, Bouneva I, et al. Association between high-normal levels of alanine aminotransferase and risk factors for atherogenesis. *Gastroenterology.* 2013;145:1271-9.e1–3. doi: 10.1053/j.gastro.2013.08.036

51. Siddiqui MS, Fuchs M, Idowu MO, Luketic VA, Boyett S, Sargeant C, et al. Severity of nonalcoholic fatty liver disease and progression to cirrhosis are associated with atherogenic lipoprotein profile. Clin Gastroenterol Hepatol. (2015) 13:1000-8.e3. doi: 10.1016/j.cgh.2014.10.008

52. Wang J, Zhao Q, Bowden J, Hemani G, Davey Smith G, Small DS, et al. Causal inference for heritable phenotypic risk factors using heterogeneous genetic instruments. *PLoS Genet.* (2021) 17:e1009575. doi: 10.1371/journal.pgen.1009575

53. Morrison J, Knoblauch N, Marcus JH, Stephens M, He X. Mendelian randomization accounting for correlated and uncorrelated pleiotropic effects using genome-wide summary statistics. *Nat Genet.* (2020) 52:740–7. doi: 10.1038/s41588-020-0631-4

54. Catapano AL, Graham I, De Backer G, Wiklund O, Chapman MJ, Drexel H, et al. 2016 ESC/EAS guidelines for the management of dyslipidaemias. *Eur Heart J.* (2016) 37:2999–3058. doi: 10.1093/eurheartj/ehw272

55. Ginsberg HN, Elam MB, Lovato LC, Crouse JR. 3rd, Leiter LA, Linz P, et al. Effects of combination lipid therapy in type 2 diabetes mellitus. *New Eng J Med.* (2010) 362:1563–74. doi: 10.1056/NEJMoa1001282

56. Keech A, Simes RJ, Barter P, Best J, Scott R, Taskinen MR, et al. Effects of long-term fenofibrate therapy on cardiovascular events in 9,795 people with type 2 diabetes mellitus (the FIELD study): randomised controlled trial. *Lancet.* (2005) 366:1849–61. doi: 10.1016/S0140-6736(05)67667-2

Frontiers in
Cardiovascular Medicine

Innovations and improvements in cardiovascular treatment and practice

Focuses on research that challenges the status quo of cardiovascular care, or facilitates the translation of advances into new therapies and diagnostic tools.

Discover the latest Research Topics

See more →

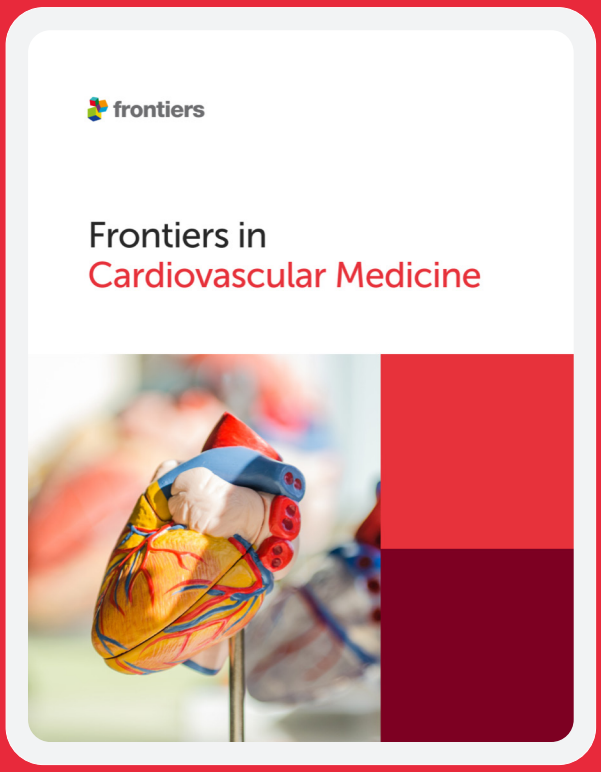

Frontiers

Avenue du Tribunal-Fédéral 34
1005 Lausanne, Switzerland
frontiersin.org

Contact us

+41 (0)21 510 17 00
frontiersin.org/about/contact